



Delft University of Technology

Proceedings of the 9th PowerSKIN Conference

Auer, Thomas; Knaack, U.; Schneider, Jens

DOI

[10.47982/BookRxiv.27](https://doi.org/10.47982/BookRxiv.27)

Publication date

2021

Document Version

Final published version

Citation (APA)

Auer, T., Knaack, U., & Schneider, J. (Eds.) (2021). *Proceedings of the 9th PowerSKIN Conference*. TU Delft OPEN. <https://doi.org/10.47982/BookRxiv.27>

Important note

To cite this publication, please use the final published version (if applicable). Please check the document version above.

Copyright

Other than for strictly personal use, it is not permitted to download, forward or distribute the text or part of it, without the consent of the author(s) and/or copyright holder(s), unless the work is under an open content license such as Creative Commons.

Takedown policy

Please contact us and provide details if you believe this document breaches copyrights. We will remove access to the work immediately and investigate your claim.

APRIL 9TH 2021 – MUNICH

POWERSKIN CONFERENCE

PROCEEDINGS

APRIL 9TH 2021 – MUNICH

POWERSKIN CONFERENCE

PROCEEDINGS

APRIL 9TH 2021 – MUNICH

POWERSKIN CONFERENCE

The building skin has evolved enormously over the past decades. The energy performance and environmental quality of both the interior and exterior of buildings are largely determined by the building envelope. The façade has experienced a change in its role as an adaptive climate control system that leverages the synergies between form, material, mechanical and energy systems towards an architectural integration of energy generation.

The PowerSKIN Conference aims to address the role of building skins to accomplish a carbon neutral building stock. Topics such as building operation, embodied energy, energy generation and storage in context of envelope, energy and environment are considered.

The focus of the PowerSKIN issue 2021 deals with the question of whether simplicity and robustness stay in contradiction to good performance of buildings skins or whether they even complement each other: **simplicity vs. performance?**

As an international scientific event - usually held at the BAU trade fair in Munich - the PowerSKIN Conference builds a bridge between science and practice, between research and construction, and between the latest developments and innovations for the façade of the future.

The Technical University of Munich, Prof. Dipl.-Ing. Thomas Auer, **TU Darmstadt**, Prof. Dr.-Ing. Jens Schneider and **TU Delft**, Prof. Dr.-Ing. Ulrich Knaack, are hosting the PowerSKIN Conference. It is the third event of a biennial series: April 9th 2021, architects, engineers, and scientists present their latest developments and research projects for public discussion and reflection. For the first time the conference will be a virtual event. On the one hand, this is a pity, as conferences are also about meeting people and social interaction; on the other hand, it offers the possibility that we can reach more people who connect from all over the world.

Publisher

TU Delft Open
TU Delft / Faculty of Architecture and the Built Environment
Julianalaan 134, 2628 BL Delft, The Netherlands

Editors

Thomas Auer, TUM
Ulrich Knaack, TU Delft
Jens Schneider, TU Darmstadt

Editorial office

Roman Ficht, TUM
Laura Franke, TUM
Uta Stettner, TUM

Design & layout

Usch Engelmann
Véro Crickx, Sirene Ontwerpers
Franklin van der Hoeven, TU Delft

Cover image

Louisiana Museum of Modern Art, Photo by Philipp Vohlidka

CC-BY-4.0

ISBN 978-9463664066



Contents

- 006 **PREFACE**
- 007 **CONFERENCE HOSTS**
- 008 **SCIENTIFIC COMMITTEE**
- 010 **KEYNOTES**
- 013 **PART 1 // ENVELOPE**
- 015 **Comparison of Health Effects Caused by Fire and Noise on the Façade Considering the Years of Life Lost**
Daniel Herzog, Anica Mayer
- 025 **Smart Textile Sun-Shading: Development of Functional ADAPTEX Prototypes**
Paul-Rouven Denz, Christiane Sauer, Ebba Fransén Waldhör,
Maxie Schneider, Puttakhun Vongsingha
- 027 **Responsive Skins: Complexity vs Simplicity**
Katia Gasparini, Alessandro Premier
- 037 **Ge³TEX – Multifunctional Monomaterials Made from Foamed Glass-, Basalt- or PET-based 3D Textiles**
Claudia Lüling, Petra Rucker-Gramm, Agnes Weilandt, Johanna Beuscher,
Dominik Nagel, Jens Schneider, Andreas Maier, Hans-Jürgen Bauder, Timo Weimer
- 051 **Additive Manufacturing of Thermally Enhanced Lightweight Concrete Wall Elements with Closed Cellular Structures**
Gido Dielemans, David Briels, Fabian Jaugstetter, Klaudius Henke, Kathrin Dörfler
- 053 **Evaluating the Real Performance of Brick Masonry with Dynamic U-Values**
Dr.-Ing. Sabine Kuehnast
- 063 **Skin Metrics: The Wicked Problem of Façade System Assessment**
Keith Boswell, Stéphane Hoffman, Stephen Selkowitz, Mic Patterson
- 065 **3D Printed Future Façade – Experimental Testing of a 3D-Printed Building Envelope**
Moritz Mungenast

- 091 **PAOSS - Pneumatically Actuated Origami Sun Shading**
Christina Eisenbarth, Walter Haase, Yves Klett, Lucio Blandini, Werner Sobek
- 093 **Use of Vacuum Glass (VG) in the Implementation of Transparent and Translucent Exterior Wall Systems with Very High Thermal Insulation**
Luis Ocanto
- 109 **PART 2 // ENVIRONMENT**
- 111 **Study on the Interaction of Room Design, Material, Ventilation and User Behaviour Towards a Robust Building Operation**
Laura Franke, Tilmann Jarmer, Thomas Auer
- 125 **A Full Performance Paper House**
Rebecca Bach, Alexander Wolf, Martin Wilfinger, Nihat Kiziltoprak, Ulrich Knaack
- 127 **Multi-Criteria Design and Decision Support for Solar and Green Envelopes**
Elisabeth Fassbender, Claudia Hemmerle, Natalie Muhr
- 141 **Design Model for Dry-Stacked and Demountable Masonry Blocks**
Gelen Gael Chew Ngapeya, Danièle Waldmann
- 153 **Eco-Construction for Sustainable Development: Concept of a Material and Component Bank**
Laddu Bhagya Jayasinghe, Daniele Waldmann
- 165 **A Definition of Essential Characteristics for a Method to Measure Circularity Potential in Architectural Design**
Charlotte Heesbeen, Magdalena Zabek, Linda Hildebrand
- 175 **Sustainability in Façade Design: Approaches and Outlooks from Design Practitioners**
Alejandro Prieto, Mimi Oldenhave
- 187 **Fibrous Interfaces for Indoor Temperature Modulation Based on Phase Change Materials**
Iva Rešetar, Christiane Sauer
- 199 **Mono-Material Wood Wall: Digital Fabrication of Performative Wood Envelopes**
Oliver Bucklin, Prof. Achim Menges, Oliver Krieg, Hans Drexler, Angela Rohr
- 201 **Exploring the Possibility of Using Bioreceptive Concrete in Building Façades**
M. Veeger, A. Prieto, M. Ottelé
- 203 **State of the Art and Potentials of Additive Manufactured Earth (AME)**
Elisabeth Endres, Jan Mehnert, Linda Hildebrand, Marcel Schweiker, Eike Roswag-Klinge, Ulrich Knaack

- 213 **Carbon Conscious!
The Impact of Embodied Emissions on Design Decisions for Building Envelopes**
Tania Cortes Vargas, Linda Hildebrand, Lisa Rammig, Andrea Zani
- 225 **PART 3 // ENERGY**
- 227 **Holistic Design Explorations of Building Envelopes
Supported by Machine Learning**
Federico Bertagna, Pierluigi D'Acunto, Ole Patrick Ohlbrock, Vahid Moosavi
- 229 **Simple versus Complex: Comparing the Accuracy of Cooling Energy
Demands for Complex Fenestration Systems using BSDF and SHGC**
Christiane Wermke, Brian Cody
- 243 **Comparison of BSDF, Climate-based SHGC and Annual SHGC**
Deepak Singh Dhama, Daniel Arzmann
- 257 **Effects of Phase Change Materials on Heat Flows Through Double Skin Façades**
Thomas Wüest, Lars O. Grobe, Andreas Luible
- 259 **Effects of Heat Transfer Systems on Comfort and Energy Demand**
David Bewersdorff, Carina da Silva, Ulrich Knaack
- 271 **Robust Renovation of Buildings: Enhancing Energy Efficiency and Flexibility**
Martin Gabriel, Manuel de-Borja-Torrejon
- 283 **Potential of Façade-Integrated PVT with Radiant Heating and Cooling Panel
Supported by a Thermal Storage for Temperature Stability and Energy Efficiency**
Mohannad Bayoumi
- 285 **Simplicity and Performance | Area-Efficient Super-Insulating Façades**
David Schenke, Dipl. Ing. LEED AP
- 297 **Effect of Energy Management and Influencing Parameters in Local PV Use**
Lea Bogischef, Manuel de-Borja-Torrejon, Claudia Hemmerle
- 313 **Internal Shading Systems Analysis for High-
Performance Façades – Do More With Less**
Alessandro Baldini, Anna Ioannidou-Kati
- 325 **Photovoltaic Warm Façades
with Phase Change Materials in European Climates**
Christian Popp, Dirk Weiß, Katja Tribulowski, Bernhard Weller
- 327 **Design of Moveable Façade Elements for Energy Harvesting and Vibration
Control of Super Slender Tall Buildings under Wind Excitation**
Yangwen Zhang, Thomas Schauer, Laurenz Wernicke, Apostolos Vrontos,
Michael Engelmann, Wulf Wulff, Achim Bleicher

PREFACE

The building skin has evolved enormously over the past decades. The energy performance and environmental quality of both the interior and exterior of buildings are primarily determined by the building envelope. The façade has experienced a change in its role as an adaptive climate control system that leverages the synergies between form, material, mechanical and energy systems towards an architectural integration of energy generation.

The PowerSKIN Conference aims to address the role of building skins to accomplish a carbon-neutral building stock. The focus of the PowerSKIN issue 2021 deals with the question of whether simplicity and robustness stay in contradiction to good performance of buildings skins or whether they even complement each other: simplicity vs performance?

As an international scientific event - usually held at the BAU trade fair in Munich - the PowerSKIN Conference builds a bridge between science and practice, between research and construction, and between the latest developments and innovations for the façade of the future. Topics such as building operation, embodied energy, energy generation and storage in the context of the three conference sessions envelope, energy and environment are considered:

- Envelope: The building envelope as an interface for the interaction between indoor and outdoor environment. This topic is focused on function, technical development and material properties.
- Energy: New concepts, accomplished projects, and visions for the interaction between building structure, envelope and energy technologies.
- Environment: Façades or elements of façades, which aim to provide highly comfortable surroundings where environmental control strategies as well as energy generation and/or storage are an integrated part of an active skin.

The Technical University of Munich, TU Darmstadt, and TU Delft are signing responsible for the organisation of the conference. It is the third event of a biennial series: April 9th 2021, architects, engineers, and scientists present their latest developments and research projects for public discussion and reflection. For the first time, the conference will be a virtual event. On the one hand, this is a pity, as conferences are also about meeting people and social interaction; on the other hand, it offers the possibility that we can reach more people who connect from all over the world.

We have to thank the authors, speakers and keynote speakers for their contribution and our teams for doing such a good job in organising this event. Finally, we have to thank our sponsors for their support and the Technical University of Munich, which is so kind to support this virtual conference with their broadcasting technology and other amenities.

*Thomas Auer,
Ulrich Knaack,
Jens Schneider,*

the conference hosts.

CONFERENCE HOSTS



Prof. Dipl.-Ing. Thomas Auer

Trained as a Process Engineer at the Technical University in Stuttgart, Thomas is a partner and managing director of Transsolar GmbH, a German engineering firm specialized in energy efficient building design and environmental quality with offices in Stuttgart, Munich, Paris and New York. In January of 2014 Thomas became Professor for building technology and climate responsive design at TUM. Thomas collaborated with world known architecture firms on numerous international design projects and competitions. A specialist in the fields of integrated building systems and energy efficiency in buildings as well as sustainable urban design, Thomas has developed concepts for projects around the world noted for their innovative design and energy performance – an integral part of signature architecture. The office tower for Manitoba Hydro in down-town Winnipeg, Canada, is considered one of the most energy efficient high-rise buildings in North America. Lower Don Lands, Toronto, is going to be among the first carbon neutral districts in North America. Outside of Transsolar, Thomas taught at Yale University and was a visiting professor at the ESA in Paris and other Universities. He speaks frequently at conferences and symposia. In 2010 Thomas received the Treehugger “best of green” award as “best engineer”.



Prof. Dr.-Ing. Ulrich Knaack

Ulrich was trained as an architect at the RWTH Aachen University, Germany. After earning his degree he worked at the university as a researcher in the field of structural use of glass and completed his studies with a PhD. In his professional career Ulrich worked as an architect and general planner in Düsseldorf, Germany, succeeding in national and international competitions. His projects include high-rise and office buildings, commercial buildings and stadiums. In his academic career Ulrich was professor for Design and Construction at the Hochschule OWL, Germany. He also was and still is appointed professor for Design of Construction at the Delft University of Technology / Faculty of Architecture, Netherlands, where he developed the Façade Research Group. In parallel Ulrich is professor for Façade Technology at the TU Darmstadt / Faculty of Civil engineering in Germany where he participates in the Institute of Structural Mechanics + Design. Ulrich organizes interdisciplinary design workshops and symposiums in the field of façades and is author of several well-known reference books, articles and lectures.



Prof. Dr.-Ing. Jens Schneider

Jens is a full professor for structural engineering at the Institute of Structural Mechanics and Design, TU Darmstadt, Germany. After his studies in civil engineering in Darmstadt and Coimbra, Portugal, Jens received his PhD from TU Darmstadt in 2001 in a topic about structural glass design and impact loading. From 2001-2005, Jens worked at the engineering office Schlaich, Bergermann and Partner where he was involved in the structural design of complex steel, glass and concrete structures. In 2006, Jens was appointed as an authorized sworn expert on glass structures, in 2007 to the position of a professor for structural engineering in Frankfurt. and in 2009 to his current position at TU Darmstadt, where Jens is currently Vice President for Transfer and International Affairs. Since 2011, Jens is also partner in his engineering office SGS GmbH in Heusenstamm in Frankfurt, Germany. Since 2015, Jens leads the European project group for the preparation of the new Eurocode 11 „Structural Glass”. Jens is specialized in structural mechanics of glass & polymers, façade structures, structural design and synergetic, energy-efficient design of façades and buildings.

SCIENTIFIC COMMITTEE



Prof. Thomas Auer
Technical University of Munich



Prof. Paulo Cruz, PhD
University of Minho



Prof. Dr. sc. ETH Kathrin Dörfler
Technical University of Munich



Prof. Deborah Hauptmann, PhD
Iowa State University



Prof. Dr.-Ing. Tillmann Klein
Delft University of Technology



Prof. Dr.-Ing. Ulrich Knaack
Delft University of Technology



Prof. Dr. ir. Christian Louter
Technical University of Dresden



Prof. Dr. Andreas Luible
Lucerne University of Applied Sciences
and Arts



Prof. Dipl.-Ing. Claudia Lüling
Frankfurt University of Applied
Sciences



Prof. Dr. Madjid Madjidi
University of Applied Science Munich



Katia Perini, PhD
University of Genoa



Prof. Marco Perino, PhD
Polytechnic University of Turin



Prof. Dr.-Ing. Uta Pottgiesser
Delft University of Technology



Prof. Dr.-Ing. Jens Schneider
Technical University of Darmstadt



Prof. Dipl.-Ing. Christiane Sauer
weißensee school of art and design Berlin
photo by Michelle Mantel



Assc. Prof. Claudio Vásquez Zaldívar
Pontifical Catholic University of Chile



Prof. Dr.-Ing. Frank Wellershoff
HafenCity University Hamburg

KEYNOTES

PROF. ALMUT GRÜNTUCH-ERNST



Prof. Almut Grüntuch-Ernst, architect and partner of Grüntuch Ernst Architects, heads the IDAS (Institute for Design and Architectural Strategies) at the TU Braunschweig, where she builds up research at the intersections of architecture, biology, and technology in order to transfer the knowledge gained to the design of buildings. She introduces the topic and advances the awareness and expertise needed to develop a nature-based urban architecture with projects, ideas and experiences of international experts who have exchanged ideas at three symposia at the TU Braunschweig.

HORTITECTURE – MORE NATURE WITHIN THE ARTEFACT

Plants and architecture: two seemingly opposite elements. How can we combine them to plan future cities that are closer to nature? What synergies can we explore? Hortitecture (from the Latin “hortus” for garden and the English “architecture”) seeks to discover the creative and constructive potential of vital plant material, and explores its applications in ecosystem services and urban food production.

With the increasing density of cities, new buildings should maximise bio-active surfaces that could effectively enhance wellbeing and reduce our footprint on the built environment. Nature-based architectural strategies aim for more urban vitality - they aim to activate surface areas in the city - between, around and on buildings to offer direct access to a maximum of private, collective and public outdoor spaces. Current projects by Grüntuch Ernst architects illustrate the conceptual approach of how to integrate and activate biodiversity within office buildings.

PROF. FLORIAN NAGLER



Prof. Florian Nagler, architect and founder of Nagler Architekten, heads the Chair of Design and Construction at the Faculty of Architecture, Technical University of Munich. After an apprenticeship as a carpenter, Florian Nagler studied architecture at the University of Kaiserslautern. Visiting and substitute professorships took him to the Gesamthochschule Wuppertal, the Royal Danish Academy in Copenhagen and the Hochschule für Technik in Stuttgart. Florian Nagler is a founding member of the Stiftung Baukultur and has been a member of the Akademie der Künste, Baukunst section in Berlin, and the Bayerische Akademie der schönen Künste since 2010.

POWER YES — SKIN NO

Florian Nagler's chair is primarily concerned with the connection between design and construction and the direct implementation of analytical studies in designs. The research work revolves around the theme of "simply build" and attempts to contribute to a new building culture – the simplification of building and buildings operation.

The principles based on calculations and simulations, such as reasonable room geometry, sufficient window areas for natural lighting, but above all a monolithic and simple construction method, are tested in practice. The concept is mainly driven by combining resource-friendly preparation, reasonable costs and a long-lasting operation phase with a low maintenance effort. Energy efficiency regarding the HVAC systems and excellent reuse and recycling capabilities are further aspects.

PART 1 // ENVELOPE

Comparison of Health Effects Caused by Fire and Noise on the Façade Considering the Years of Life Lost

Daniel Herzog¹, Anica Mayer²

Chair of Building Physics, Department of Civil Engineering, Technical University of Munich, Germany

1 Daniel Herzog, M.Sc, Lst Bauphysik, Arcisstraße 21, 80333 München, daniel.herzog@tum.de

2 Anica Mayer, M.Sc, Lst Bauphysik, Arcisstraße 21, 80333 München, anica.mayer@tum.de
[Equal Contributors]

Abstract

Façades are designed with the purpose of protecting their residents from all environmental influences, but is the health protection against every hazard on the same level? This paper describes a method to examine and compare health hazards in urban areas caused by smoke, fire and flames and traffic noise. To obtain a comparable data basis, statistical values of health data of people affected by noise or fire were converted into the unit years of life lost as defined by the World Health Organisation (WHO). As an example, it was found that noise-induced ischemic heart disease (IHD) in Munich costs, on average, more than twice as many years of life lost than dwelling fires. These results can be extended by other city-specific health hazards, such as smog and sick building syndromes, to optimise the requirements for façades in their entirety by a multi-criteria optimisation. In addition, this paper shows that the legal regulations in the area of noise are significantly lower than those for fire protection.

Keywords

Comparison, health, YLLs, noise, ischemic heart disease, fire, façade

1 INTRODUCTION

Anthropogenic climate change is scientifically proven, and today, society is experiencing the first serious consequences, such as increased average annual temperatures combined with an increase in extreme weather events. Furthermore, the United Nations predicts that by the year 2050, two of three people of the world's population will live in cities. As a result, the number of megacities (more than 10 million inhabitants) will also increase. (United Nations, 2018) The suppression of nature in urban areas through intensive land sealing intensifies the consequences of climate change and leads to, among other things, the heat island effect and negative effects on both the physical and mental health of the inhabitants.

Buildings, and especially their façades, are designed with the purpose of protecting their residents from all environmental influences, like weather, fire and wild animals, or strangers. Moreover, there are city-specific health impairments like smog, noise and the sick building syndrome, which must be counteracted. Based on this, requirements are defined for each hazard; however, these requirements neglect upcoming interdependencies and health hazards that aren't as obvious as an apartment on fire. In this paper exemplary, the health effects of noise and fire exposure are compared. The selection of these two exposures is arbitrary and could also be done with other exposures, shown in Figure 1. In Germany, on the outside of a residential house, a maximum of 59 dB by day is requested to prevent the health hazard of noise. (BImSchV, 2020) But is this limit as safe for health as the requirements of structural fire protection? Further, does this limit prevent the noise of a multi-lane street (a higher risk) to the same degree as fire regulations protect residents from a dwelling fire spreading over the façade? And if so, what is the optimum construction of a façade to protect the citizens, under the premise that the different requirements affect each other? For example, a green façade filters air pollutants and can reduce noise but is inherently flammable therefore, inferior to a concrete wall. (Engel & Noder, 2020) In contrast, a common concrete wall has no positive effect on air and noise pollution, but it's incombustible. In order to determine the protection and the required level of protection of the local façade in the best possible way, in the first step, the actual acting health risks must be quantified. Therefore, this paper investigates one initial approach to compare the health impact of the different requirements.

2 METHODOLOGY

2.1 LITERATURE

The literature review on noise, especially traffic noise and cardiovascular health effects, was performed by conducting a systematic, keyword-based research in the database Web of Science (Keywords: transportation, traffic noise, health effect) and adding a systematic snowball review of the mentioned literature. Furthermore, founded meta-analyses comparing traffic noise in German cities and the impact of the cardiovascular health of the citizens were used to define the level of disease. Other noise exposures, like airplane or recreational noise, were sorted out because of the small group of affected people and the discontinuity of the exposure. In order to quantify the effects, they must be combined with statistical surveys. The required data for fire deaths, (International Classification of Disease ICD 10: X00-X09) myocardial infarction (ICD 10: I20-I25) and life expectations are based on statistical inquiry of the "Statistisches Bundesamt" and the local, annual statistics of the City of Berlin, Hamburg and Munich.

2.2 TRANSFORMATION

To compare the data, they were transformed into the unit DALYs (disability-adjusted life years), defined by Murray and Lopez. (Murray & Lopez, 1990) DALYs consist of the summation of two terms YLLs (Years of Life Lost) and YLD (Years lived with disability). For this paper, only the YLLs were used because there is no data basis for YLDs caused by fire. YLLs are calculated by the age of death of a person and the statistical related life expectation by birth year of the person. The existing data only gives a range of years for the deaths by fire and myocardial infarction, (e.g. 30-45 Years, 320 deaths) so the lowest value of age, (in the example 30 years) leading to the most YLLs were used for the calculations. Furthermore, the odd ratio, the variance, the p-value and the CI were calculated for the statistical series from 2005 to 2016 to eliminate confounding effects.

This is just a small part of the ongoing PHD method shown in Figure 1. The highlighted sections represent the topics discussed in this paper.

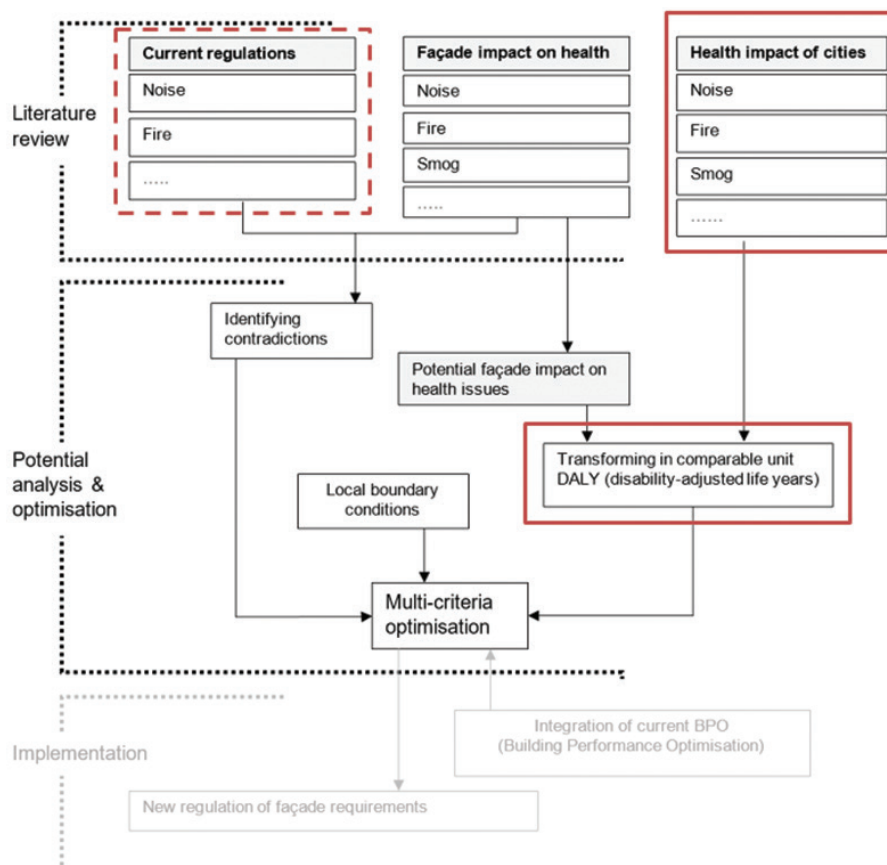


FIG. 1 Schematic methodology followed to solve optimisation

3 RISK CALCULATION AND CURRENT REGULATIONS

3.1 NOISE EXPOSURE RISK

To clarify the differences between fire and noise exposure, only the ischemic heart diseases (IHD) leading to premature death were considered in this publication. It should be noted that there are other noise-induced premature deaths, such as the consequences of permanent sleep disorders, which are not considered in this study. The results of the environmental noise guidelines for the European region, published in 2018 by the WHO, are based on different meta-studies that determined the exposure-response relationship between noise exposure to road traffic noise and IHD under consideration of confounders. (WHO, 2018) The relative risk of adverse health, which indicates the relation of a risk between a noise-exposed and a non-exposed control group, was found to be 1.08 (CI: 95%: 1.01 – 1.15) per 10 dB increase. This pooled value is based on seven studies and a total of 67,224 participants. (van Kempen, Casas, & Pershagen, 2018) This leads to the exposure-response function shown in Figure 2.

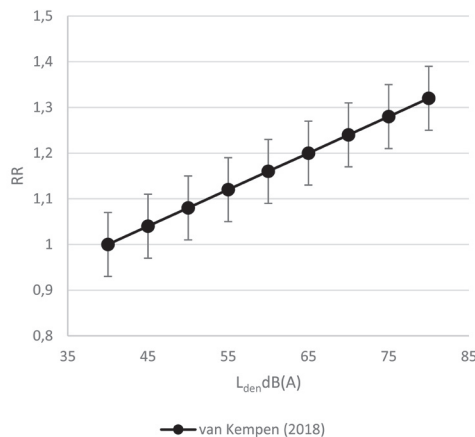


FIG. 2 Exposure-response curve between traffic noise and the relative risk for an incidence of ischemic heart disease, (van Kempen 2018)

The approach of Prüss-Üstün et al. is used to calculate the population-attributable fraction (PAF), which specifies the percentage of IHD that can be attributed to noise exposure in a country. (Prüss-Üstün et al., 2003) As an example, the attributable fraction, the percentage of people who are affected by traffic noise, is derived from a report by the Bavarian Environment Agency (LfU) in 2019. (LfU, 2019) According to this source, 12 % of the population in Munich is affected by a noise level Lden of 55-60 dB(A), 8.5 % by 60-65 dB(A), 8.5% by 65-70 dB(A) and more than 3% by noise levels over 70 dB(A). In total, 32.2% of the Munich population is affected by traffic noise. Unlike the RR calculation, the impairment starts at 55 dB(A) instead of 50 dB(A). Therefore, the non-affected percentage determined by the LfU are attributed to a RR of 1.0. The impairment is thereby probably even higher than the calculation yields. The PAF is calculated to 5.0%. A similar calculation was undertaken by Babisch and Kim, estimating a PAF for the German population in 1991 of 2.9%, whereby the relative risk was lower and the hazard threshold started at a Lday level of 60 dB(A). (Babisch & Kim, 2006)

$$PAF = \frac{(0.12 \cdot 0.12 + 0.16 \cdot 0.085 + 0.20 \cdot 0.085 + 0.24 \cdot 0.029 + 0.28 \cdot 0.002)}{1 + (0.12 \cdot 0.12 + 0.16 \cdot 0.085 + 0.20 \cdot 0.085 + 0.24 \cdot 0.029 + 0.28 \cdot 0.002)} = 0.05$$

L_{DAY} (DB(A))	PERCENTAGE EXPOSED [%]	RELATIVE RISK
< 50	67.8	1.00
50-55		1.08
55-60	12.0	1.12
60-65	8.5	1.16
65-70	8.5	1.20
70-75	2.9	1.24
>75	0.19	1.28

TABLE 1 Exposure of road traffic noise in Munich 2019 and the relative risk (LfU, 2019) (van Kempen et al., 2018)

For example, if the PAF is set as an estimate for Munich, Germany and multiplied with the number of deaths by IHD in Munich for the year 2016 according to the age group, it leads to a total number of 44 people who died by IHD due to the exposure to noise. That are three deaths per 100,000 inhabitants. To transform the results in DALYs only the fatal IHD are examined. The calculated number of deaths for IHD at the certain age group is multiplied by the life expectancy at each age. (Bundesamt für Statistik, 2020) Therefore, as mentioned in chapter 2, the lowest age, per age group was used for the determination of the YLLs, so the result indicates the worst condition. To reduce confounders, a five-year (2012 – 2016) average is used for the YLLs. Years lost due to disability (YLDs) are neglected to be comparable with the fire deaths. The results per age group are visualised in Figure 3. It shows the number of noise attributable YLL of the respective year as well as the attributed deaths. The 5-year average is plotted with the data results. It can be summarised that the five-year average of all age groups leads to a total of 531 YLLs due to 45 deaths caused by IHD per year assignable to traffic noise.

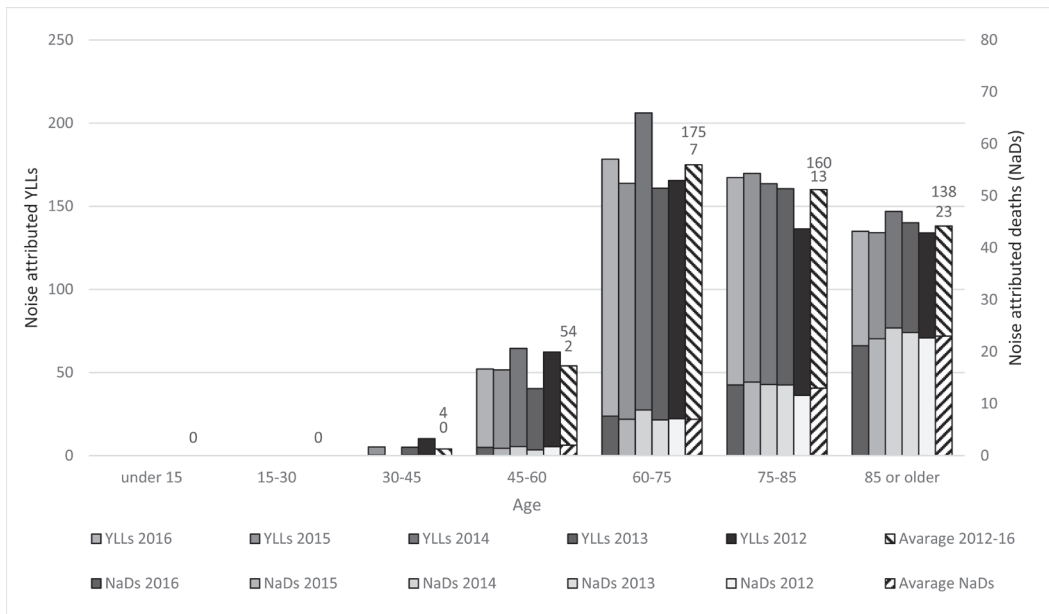


FIG. 3 Noise attributed YLLs and noise attributed death per age group 2012-2016

3.2 CURRENT REGULATION ON NOISE PROTECTION

In Germany, traffic noise is regulated by the "Bundesimmissionsschutzverordnung" (BImSchV). In housing areas and small settlements, a level of 59 dB(A) by day and 49 dB(A) by night is

mandatory. For central areas in cities and mixed zones (business and dwelling), the limit is 5 dB(A) higher. (BImSchV, 2020) These values are far above the advice given by the WHO (50 dB(A) by day and 40 dB(A) by night). (WHO, 2011) Furthermore, the technical building regulations demand graded acoustic insulation for exterior walls depending on the ambient noise. Starting with a minimum evaluated building acoustic insulation (R_w') of 30 dB by an ambient noise level of maximum 55 dB and reaching up to an R_w' of 50 dB by 80 dB ambient noise. If there is a noise level over 80 dB outside, individual measures must be adopted. (DIN, 2018) This regulation can, of course, only ensure the health of the resident if the windows are closed. As soon as the windows are open for ventilation, the acoustic insulation is ineffective. Therefore, the noise limit on the outside façade surface is decisive for noise, respectively health protection.

3.3 FIRE EXPOSURE RISK

Similar to noise exposure risk, fire exposure risk depends on a variety of different factors. The fire risk is a function of multiple variables; these can be summarised as social, technical, and natural factors. Further, these terms are caused by another variety of variables like alcohol and tobacco consumption, energy consumption level, frequency of thunderstorm and so on. (Nokolay et al., 2010) To quantify these factors and transform them into the unit DALY, long term statistics were used to calculate the risk. For the example in this paper, the data from Germany, respectively Munich, is used. In Germany, an average of 2.34 fires is counted on 100,000 inhabitants for the year 2000 and 1.92 for 2005. Statically 0.31 people die in 100 fires, which leads to 0.59 fire deaths per 100,000 inhabitants for the year 2005. (Nokolay et al., 2010) To ensure the transferability to current surveys and to validate the data, it was compared with current statics. The arithmetic average over the past 13 years (2005-2017) is 0.5 deaths [D] per 100,000 inhabitants [I] per year [a] $[D/(103 \cdot I \cdot a)]$ in Munich. (Variance [v] = 0.07, standard deviation [SD] = 0.26). For a 15-year average (2005-2019), the same calculation leads to 0.86 (v = 0.02, SD = 0.13) $[D/(103 \cdot I \cdot a)]$ for Berlin and 0.75 (v = 0.04, SD = 0.19) $[D/(103 \cdot I \cdot a)]$ for Hamburg. The average, over the last 15 years, of the three biggest cities in Germany is 0.7 $[D/(103 \cdot I \cdot a)]$ and close to the total average of 0.59 for 2005, which shows that the data can be taken as valid.

2015 five people and 2016 seven people died due to fire in Munich. The associated number of inhabitants in Munich was 1,450 (2015) and 1,464 (2016) millions, which leads to a result of 0.34 and 0.48 fire deaths per 100,000 inhabitants. (StAM, 2019) Taking a closer look at the fire victims of 2015 and 2016 leads to the age-depending statistic of Table 2. By combining these values with the average life expectancy at the corresponding age, the YLLs can be obtained.

EXPOSURE	YEAR	TOTAL DEATHS	OF WHICH AT THE AGE OF ... TO UNDER ...						
			UNDER 15	15-30	30-45	45-60	60-75	75-85	85 OR MORE
SMOKE, FIRE, FLAME	2016	7	1	2	1	1	2	0	0
	2015	5	0	0	1	0	1	2	1

TABLE 2 Fire deaths per age (StAM, 2019)

	YEAR	AGE								
		0	15	30	45	60	75	85	90	100
AVERAGE LIFE EXPECTANCY	2016	80.875	66.2	51.5	37.0	23.5	12.1	6.0	4.0	1..
	2015	80,77	66.1	51.4	36.9	23.5	12.0	5.9	4.0	2.0

TABLE 3 Average life expectancy Germany 2016 (Statista, 2020)

To calculate the YLLs, the lower age limits are used, so the results represent the worst-case scenario, equal to the YLLs caused by noise-induced IHD. This results in a total number of 355.5 YLLs by smoke, fire and flame for the year 2016 and 104.8 YLLs for 2015 in Munich. To compare this data with the noise induced deaths, it is also important to investigate the location of fire deaths, thus, for example, fire deaths caused by forest fires can be excluded. Wagner of the CTIF claims that 95% of fire deaths can be attributed to fires in buildings and traffic. (Wagner et al., 2020) Based on press reports, 6 of 7 fire deaths in 2016 could be clearly assigned to residential fires. (Stadtmagazin-München24, 2016 a-f) Furthermore, it could be proven that none of the fire fatalities of 2015 and 2016 was caused by a flashover over the façade. For this reason, it can be assumed that the fire protection requirements for façades are sufficient. The total results are shown in Figure 4.

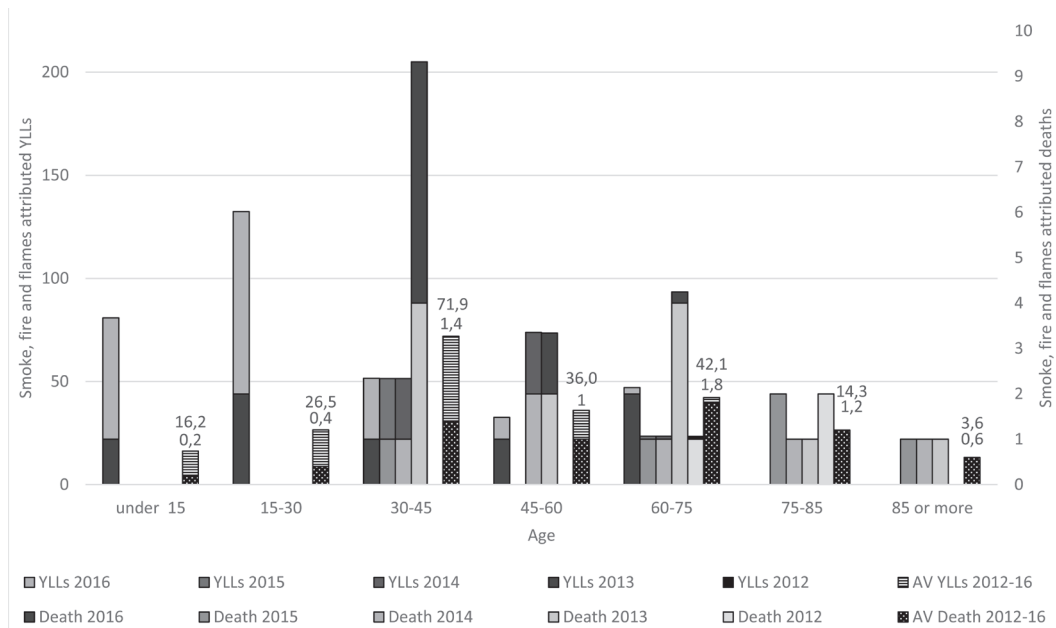


FIG. 4 YLLs and Deaths caused by Fire, Smoke and Flame 2012-2016

3.4 CURRENT REGULATION ON FIRE PROTECTION

The fire risk is a specific value for a country, respectively for a city, depending on local building legislation, fire brigade strength and so on. The comparison of the local building legislations for skyscrapers in New York City (USA) and Munich (Germany) shows that the requirements for fire protection in some cases are higher in NYC than in Munich. For example, the fire-resistance rating of bearing walls for a 50 m high building is 180 minutes (NYC-BC) compared to 90 minutes in Munich. (BayBO, 2020) (NYC-BC, 2014) For this reason, the fire risk must always be determined for the local conditions. The fire protection legislation in Germany is a state matter. Each state has its own regulations for constructions.

Most of them adhere to the "Musterbauordnung", a draft legislation, developed by the working group of the heads of the professional fire departments in the Federal Republic of Germany (AGBF). The requirements for exterior walls are principally defined as follows "External walls and parts of external walls such as parapets and aprons must be designed in such a way that the spread of fire on and in these components is limited for a sufficiently long time" (MBO, 2019, p. 22) It is generally possible to vary this requirement but only with a compensation, so the protection aim, to confine the fire in the fire-affected dwelling and the dwelling above, for up to 20 minutes is given. (Simon &

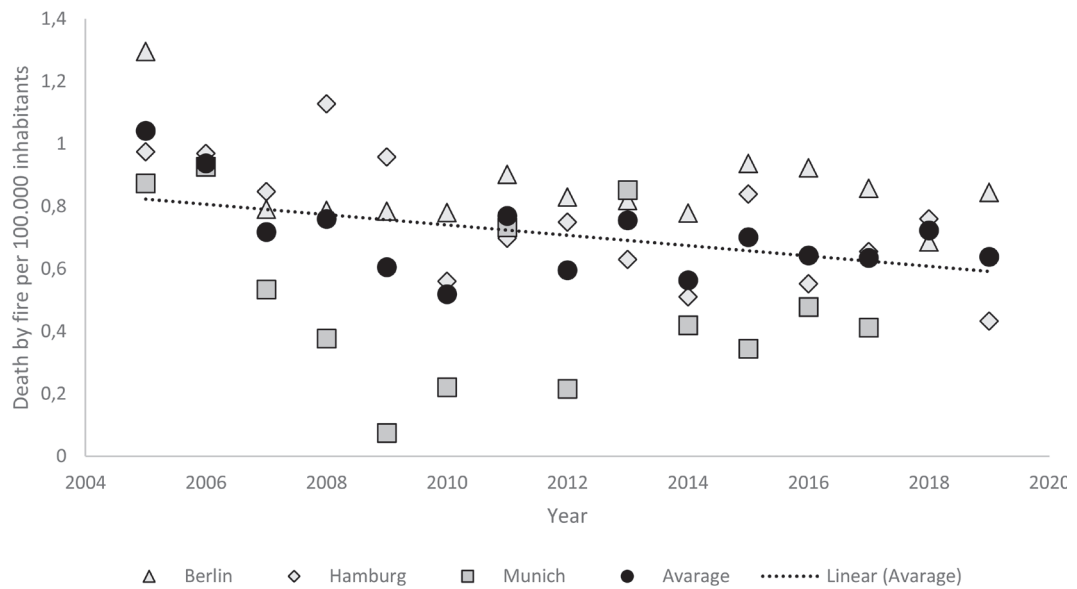


FIG. 5 Fire deaths per 100.000 inhabitants

Busse, 2020) The consequences of disregarding the protection aim of the façade could horrifyingly be seen at the fire of the Grenfell Tower in 2017, where 72 people lost their life to smoke and flames. (Davies, 2018) This illustrates, among other things, the indispensability of this protection aim. As seen in Figure 5, the linear regression of the average of deaths caused by fire, smoke and flames, in the Cities Berlin, Hamburg and Munich, decreased from about 0.8 to 0.6 deaths per 100.000 inhabitants. The laws of fire protection have hardly changed in the last 15 years, which reflects the socially accepted risk of dying in case of fire. In other words, society considers the legislation to be sufficiently safe. Furthermore, it is assumed that a further tightening of the legislation would not have a positive influence on fire deaths. This consideration is currently being investigated by the Munich Fire Department. (Engel, 2020)

4 COMPARISON

To compare the data, the calculations are combined in Figure 6. For the year 2016 in Munich, 44 deaths by IHD caused by traffic noise are compared to seven early deaths caused by fire, smoke and flames. In 2015 the ratio was 45 to five. For the period 2012-2016, the annual average ratio was 45 to 7. Observing the YLLs leads to the conclusion that noise-induced deaths do not occur until old age but are increased there. In comparison, fire deaths are distributed evenly across the age groups. Especially the age group from 60 to 75 is strongly affected by noise. Although on average, only seven people (15%) in this age group die from the effects of noise-induced IHD, this leads to 175 (33%) of all YLLs in this category.

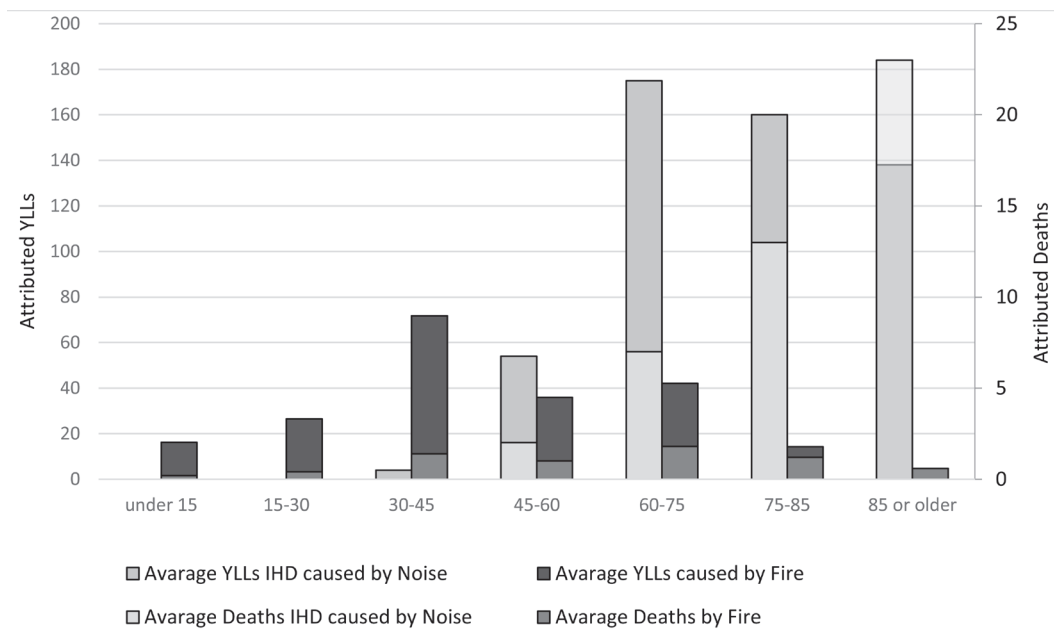


FIG. 6 Average YLL and death by IHD (noise affected) and fire 2012-2016

The chance to die between 45 and 60 years in a fire is 1 to 100,000. Whereas traffic noise affected IHD claims 2 of 100,000 people's lives. This means the probability of dying from a noise-induced IHD is twice as high as burning to death in a building. Overall, it can be seen that the noise-induced YLLs (531) far exceed those of smoke, fire and flames (211). In the legislative field, it can be summarised that the fire protection requirements provide reliable protection for people and are sufficiently defined. In the area of noise protection, the regulations and their implementation are much less stringent.

5 CONCLUSION

In this paper, a method was presented to compare the health risk of fire to the risk of noise-induced IHD. The comparison of the collected respectively calculated data shows the vast impact of traffic noise on the health of inhabitants of cities. It should also be mentioned that only the IHD caused by noise were considered, as mentioned in 3.1. Health impairments such as sleep disturbances etc. can also represent a mortality risk as a result of noise. The current regulations are not as sufficient as the fire protection regulations to counter the negative impact of noise. As an example, the permitted noise level of 64 dB(A) in central areas increases the relative risk of dying earlier than expected to 1.19. On the one hand, it directly shows the necessity to tighten regulations to the WHO suggested legal limits of 50 dB, this is hardly viable, especially in existing city structures. On the other hand, it shows the chance for architects and engineers to make a contribution to reduce traffic noise by optimising the surface of façades. It could not be proven what direct influence the fire protection requirements have on the façade, but the low number of fatalities clearly shows that the protective measures are sufficiently effective. Noise protection requirements are set for the indoor environment, but the data shows that they are insufficient to protect people from the negative effects of traffic noise. Here, the façade surface can help to reduce indirect noise, for example by absorbing a part of the traffic-induced noise. It is necessary to succeed in combining the protection goals of fire protection with an adequate level of noise protection. In addition, the health impairments caused by other health hazards such as smog or the sick building syndrome must be identified. The approach presented in this paper can as well be used to compare the health hazards and to

integrate them into the optimisation of the façade, as shown in Figure 1. Further considerations must be made, for example, whether the health hazards for the resident should be assessed and compared directly on the façade (micro view) or for a quarter (meso view). The comparison of quarters also allows other urban areas to be used to reduce health hazards. In this way, local accumulations of health hazards could be identified, necessary countermeasures prioritised, and the urban space as a whole optimised.

The term safety expresses the condition of being protected from any danger. So it is not allowed to focus the protection just on one specific aspect, it is necessary to evaluate the prevalent risks and find solutions to safe the affected inhabitants.

References

- United Nations. (2018). The World's Cities in 2018. Retrieved from: https://www.un.org/en/development/desa/population/publications/pdf/urbanization/the_worlds_cities_in_2018_data_booklet.pdf Access date: 7.08.2020
- Bundesministerium für Umwelt, Naturschutz und nukleare Sicherheit (2020). Sechzehnte Verordnung zur Durchführung des Bundes-Immissionsschutzgesetzes (Verkehrslärmschutzverordnung - 16.BImSchV)
- Engel, T., Noder, J. (2020). Begrünte Fassaden aus brandschutztechnischer Sicht. München: Bautechnik, Vol 8.
- Murray, C. J., Lopez, A. D. (1990). The global burden of disease: A comprehensive assessment of mortality and disability from diseases, injuries, and risk factors in 1990 and projected to 2020. Boston: World Health Organization, World Bank & Harvard School of Public Health.
- WHO (2018). Environmental Noise Guidelines for the European Region: WHO Regional Office for Europe.
- van Kempen, E., Casas, M. & Pershagen, G. (2018). WHO Environmental Noise Guidelines for the European Region: A Systematic Review on Environmental Noise and Cardiovascular and Metabolic Effects: A Summary. International Journal of Environmental Research and Public Health(15), 59.
- Prüss-Üstün, A., et al. (2003). Introduction and methods: assessing the environmental burden of disease at national and local levels. (Vol. 1). Geneva: World Health Organization
- Bayerisches Landesamt für Umwelt (LfU) (2019). Kartierung des Ballungsraumes München. Retrieved from: https://www.lfu.bayern.de/laerm/eg_umgebungslaermrichtlinie/kartierung/doc/ballungsraum_muenchen_betroffenenstatistik.pdf Access date: 08.07.2020
- Babisch, W. & Kim, R. (2006). The burden of cardiovascular diseases due to road traffic noise. The Journal of the Acoustical Society of America, 120(5), 3239-3239.
- Bundesamt für Statistik (2020). Entwicklung der Einwohnerzahl in München (kreisfreie Stadt) von 1995 bis 2019. Retrieved from: genesis.destatis.de Access date: 10.08.2020
- WHO (2011). Burden of disease from environmental noise - Quantification of healthy life years lost in Europe: WHO Regional Office for Europe
- Deutsches Institut für Normung e. V (2018). DIN 4109-1 Schallschutz im Hochbau - Teil 1: Mindestanforderungen (pp. 30). Beuth Verlag GmbH
- Brushlinsky, N., Sokolov, S. & Wagner, P. (2010) Humanity and Fire Leipzig: Interschutz 2010
- Statistisches Amt der Landeshauptstadt München (StAM) (2019). Statistisches Jahrbuch 2019. München: Statistisches Amt der Landeshauptstadt München.
- Statistische Ämter des Bundes und der Länder (2020) Sterbetafeln. Ergebnisse aus der laufenden Berechnung von Periodensterbetafeln für Deutschland und die Bundesländer. Wiesbaden
- https://www.statistischebibliothek.de/mir/receive/DESerie_mods_00003028 Access date: 17.09.2020
- Wagner P, & Sokolov S (2020). Wold fire Statistics (Vol. 25): CTIF
- Stadtmagazin-München24 (2020)
- a) www.stadtmagazin-muenchen24.de/muenchen-mann-stirbt-bei-brand-in-seinem-appartement-22969, 10.08.2020
 - b) www.stadtmagazin-muenchen24.de/zimmerbrand-in-wohnheim-mann-verbrennt-im-bett-21509, 10.08.2020
 - c) www.muenchen.tv/26-jaehriger-stirbt-bei-wohnungsbrand-in-obersending-170735, 10.08.2020
 - d) www.stadtmagazin-muenchen24.de/muenchen-hoelzernes-treppenhaus-brennt-in-wohnhaus-in-dachauer-strasse-dreitote-29909, 10.08.2020
- Bayerisches Staatsministerium für Wohnen, Bau und Verkehr (2020) Bayerische Bauordnung (BayBO) in der Fassung der Bekanntmachung vom 14. August 2007 zuletzt geändert am 24. Juli 2020 (GVBl. S. 381)
- New York City Department of Buildings (2014) New York City Building Code (NYC-BC)
- Bauministerkonferenz (2020), Musterbauordnung (MBO) Fassung November 2002 zuletzt geändert durch Beschluss der Bauministerkonferenz vom 22.02.2019, p. 22
- Simon A & Busse J (2020). Bayerische Bauordnung - Kommentar (Vol. 136) München: Beck
- Davies, H. (2018). What Can We Learn From the Grenfell Tower Disaster?: Priorities for Sustainable Change. Journal of Sustainable Design & Applied Research, 6(1).
- Engel, T. (2020). Masterarbeit zum Thema: Evaluierung der Maßnahmen des vorbeugenden Brand- und Gefahrenschutzes. Retrieved from https://www.bgu.tum.de/fileadmin/w00blj/hb/03_Lehre/Abschlussarbeiten/Masterarbeiten/Themen/Ausschreibung_TUM_Masterarbeit_Branddirektion_Muenchen_Abt_Einsatzvorbeugung_20180202_Wam.pdf. Access date 17.06.2020

Smart Textile Sun-Shading Development of Functional ADAPTEX Prototypes



**Paul-Rouven Denz^{*1}, Christiane Sauer², Ebba Fransén Waldhör², Maxie Schneider²,
Puttakhun Vongsingha¹**

* Corresponding author

1 Priedemann Façade-Lab, Germany/Delft University of Technology, Architecture and the Built Environment, Netherlands,
paul.denz@priedemann.net

2 weißensee academy of art berlin, Textile and Surface Design, Germany

Abstract

The research project ADAPTEX pursues the goal of developing adaptive, energy-efficient textile sunshading systems using the smart material Shape Memory Alloy (SMA). Within this approach lies a high potential for novel sun-protection systems demanding little energy or even self-sufficiently adapting to external stimuli while reducing operation and maintenance costs and at the same time offering solutions to tackle growing demand for sun and glare protection. A Design Categories Matrix is presented bringing together various involved fields from textile design, façade construction to smart material development.

Based on this, two concepts have been further elaborated: ADAPTEX Wave and Mesh. Both incorporating SMA into textile structures but expressing different design and performance potential by changing the geometry and openness factor of the surface area. For further evaluation various functional prototypes scaling up from 0.2 x 0.2 m to 1.35 x 2.80 m are developed and reviewed. Verifying the buildability and functionality of SMA driven textile sun-shading systems incorporating requirements from the various involved fields. Parallel ADAPTEX Wave's and Mesh' feasibility was assessed comparing its performance to state-of-the-art sun shading systems. Subsequently optimizing and scaling the technological ideas up in various cycles for follow-up testing at indoor and outdoor environment.

Keywords

Adaptive sun-shading, textile building envelope, smart materials, autarkic operation and control mechanism, Shape Memory Alloy (SMA)

DOI 10.7480/jfde.2021.1.5539

Responsive Skins: Complexity vs Simplicity

Katia Gasparini¹, Alessandro Premier²

- 1 Iuav University of Venice, Santa Croce, 191, 30135 Venice (IT) , tel. no. +393803576774, katia.gasparini@iuav.it
- 2 The University of Auckland, Future Cities Research Hub, School of Architecture and Planning, Building 421E, 26 Symonds Street, 1010, Auckland, New Zealand, +6499233848, alessandro.premier@auckland.ac.nz

Abstract

Responsive skins are often considered complex hi-tech systems. The results of previous researches led the authors to reflect on the actual implications of kinetic responsive skins having a high impact from the visual point of view but presenting higher issues of durability and maintenance. This new research investigates the latest trends on responsive skins to better understand their evolving role in the current global scenario. The aim of the research is to give an overview of the impact of contemporary materials and technologies on this special topic. A set of case studies have been investigated according to the adopted technologies and materials. The central role of environmental design seems to correspond to an increased simplicity of the systems, where the role of passive strategies and emerging technologies is essential. The results seem to show that generative design is transforming responsive skins, with an increasing importance of digital fabrication. Emerging materials are being tested to better understand their reliability, while parametric design seems to be more related to the generation of static surfaces working on the environmental response and communication.

Keywords

Responsive skins, responsive architecture, kinetic façade, media façade

1 INTRODUCTION: THE COMPLEXITY OF SYSTEMS

Façades design today requires a multidisciplinary approach because contemporary architectural surfaces are made by several components and technologies that usually come from mechanical, electrical or ICT engineering. Therefore, contemporary façades can be considered complex systems because they are made with complex technologies derived from sectors other than the traditional building and construction industry. In this sense the broader definition of AEC industry seems more appropriate.

What is the meaning and what are the functions of complex systems in architecture? The concept of “complex system” is common in different scientific and cultural fields. The concept of “system” in the building and construction industry and in particular relating to façades, include a series of relationships and links, even very complex, between elements and information of very different origin, of material and technologies (Knaack & Klein, 2008).

In this context it seems very useful to remember the Systems Theory - already applied in many fields of research - that studies the relationships between the actors of a whole (e.g. the façade's components) and puts them in relationship with the construction (e.g. the building) and the environment. Generally, we can consider the meaning of “system” provided by Miller (1978) as a “a set of interactive units that are related to each other”. In technical terms, a system can be conceived as a “structured set of interdependent solid parts, acting as a whole [...]. Systems can be divided into elementary and complex” (Ciribini, 1979).

As a consequence, the balance of a simple or complex system is ensured by the continuous interaction between the parts (Miller, 1978). According to Kant (1871) a system can be considered as the unity of multiple knowledge under one idea which, in our field of research, should be ensured by the design of architectural elements.

We can therefore argue that complexity in architectural façades can be identified in a network of physical relationships between their components, as the temporal mutations (rotation, inclination, connection, etc.) and in their actions along the 24 hours of a day (daylight, shading, communication, etc.). These relationships and the actions that derive from them define the façade functions and its changeability and adaptability to different conditions (responsive façade). The term “responsive architecture” was introduced by Nicholas Negroponte in the late nineteen sixties. According to Negroponte (1975) a “responsive architecture is the natural product of the integration of computing power into built spaces and structures. He also extends this belief to include the concepts of recognition, intention, contextual variation, and meaning into computed responses and their successful and ubiquitous integration into architecture” (d'Estrée Sterk, 2003). Today, despite there is no consistent definition of façade responsiveness (Romano et al., 2018), we usually consider responsive skins as those that measure actual environmental conditions to be able to adapt their form, shape, colour or character responsively. Often, the term adaptive façade is used to refer to the same type of systems (Aelenei et al., 2015).

Responsive façades can be made with several components and technologies (mechanical, electrical, ICT, etc.). These technologies have been experimented, studied and tested in their specific industrial sectors, but there are no studies about the reliability of these technologies in buildings. Thus, managing and carrying out maintenance on these skins is increasingly complicated and the solutions that are usually pursued in new designs involve the reduction of mechanical devices in favor of chemical technologies and digital technologies. In general, passive technologies are preferred over active ones, in order to reduce operational energy as well as maintenance

costs. These aspects and the incidence of innovative and emerging technologies have been investigated in this research.

2 RESPONSIVE SKINS: PROSPECTS OF RELIABILITY

Responsive surfaces are the result of a complex combination of technologies, components and materials. Thanks to advanced chemical and electronic technologies, it is possible to modify and stimulate the chemical and physical performances of materials and assemble them into complex components in order to obtain different patterns of responsiveness. These innovations also involve traditional materials and their use – with new formulations – made by mechanical, electrical or lighting technologies. The aim of these new responsive surfaces is always to create a form of interaction between the building and the user, while providing new visions in the urban landscape (media responsiveness). Ironically, to build these façades, designers use electronic and mechanical components, which are tested and used in sectors other than the building and construction industry (technology transfer). These devices are often the outcome of studies with accurate data and results. Some examples are digital cards or LED components.

However, how reliable are these results when these devices are applied on a different scale, such as the façade of a building? A responsive façade must be designed as a system integrated with all the other architectural components, and - according to the Systems Theory - it can be considered a complex system. We know very well that the greater sophistication of the solutions means reduced life cycles and a greater need for control and service maintenance (Zennaro, 2000). At the building scale, this increased level of complexity has led some researchers to identify a number of issues in the operational and maintenance phase, with a final impact on the overall reliability of the building (Zomorodian and Tahsildoost, 2018); (Favoino et al., 2013). On the other hand, these interactions between process innovation and the use of components from other sectors may be interpreted as tools to develop an increased level of reliability and maintenance scheduling of the whole system.

A previous research led by the authors investigated the problem of maintenance of responsive skins (Gasparini and Premier, 2019). In particular we tried to understand if it is possible (and acceptable) to keep these architectures efficient with timely and accurate maintenance. This research was based on the available literature as well as on the experience of trained professionals. We proposed a vision in which the responsive surface is interpreted as a 'machine' and, in this way, it should be conceived as a device, which has been tested for working within a very precise time frame and conditions. Technological evolution means that the project team becomes complex in relation to the complexity of the construction itself. In the same way, the operations that must be programmed over time for scheduled maintenance (or for the replacement of parts of the system) are complex and articulated. These are, however, systems with a short and programmed lifespan – definitely shorter than the historical thresholds we are used to. Results showed that if a building is not designed to be durable and is a temporary investment, the problem of maintenance and durability does not exist. Otherwise, if a responsive façade is considered to be an historical example, it will be preserved over time. In addition, in this scenario the role of the designer is rapidly changing: professionals involved in the project team are increasingly trained in the fields of engineering and electronics, as well as in ICT and chemistry.

Comparing the data of two researches conducted by the authors on media façades and responsive surfaces and on smart materials for solar shading, interesting results have been achieved. In the first research (Gasparini, 2009), on 100 case studies, combined technologies (i.e. complex systems) (Fig.1) were used over 40%, while the impact of information technology on these category was at least 80%. Emerging materials were applied only in a few cases. Similarly, the research on smart

materials (Premier, 2019) demonstrated that, among 51 case studies, only colour-changing materials and photovoltaic technologies were implemented in products available on the market, while all the solutions dealing with shape memory materials were still experimental or at the prototype stage (Fig. 2). These two researches have been cited to demonstrate the evolution of technologies in a 10-year time frame. Thus, in order to better understand the current evolution of technologies related to responsive architecture, we decided to analyse buildings and projects (case studies) developed in the last 15 years.

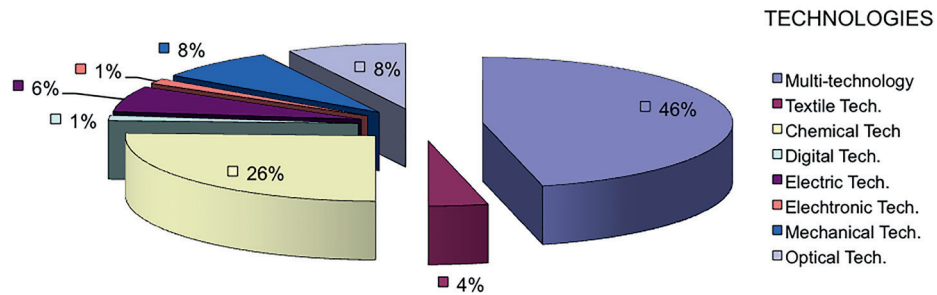


FIG. 1 Technologies for media architecture (K. Gasparini)

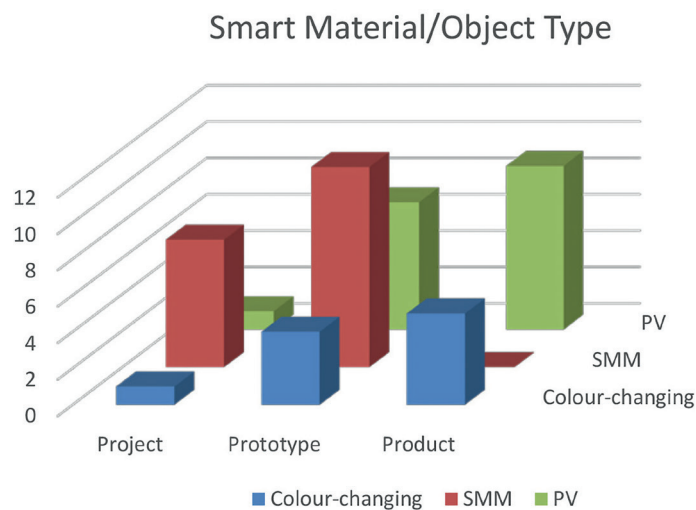


FIG. 2 Smart materials for solar shading (A. Premier)

3 METHODOLOGY

In order to achieve the predefined objectives, the research process has been developed as follows:

- Introduction of the concepts of complex and simple responsive skins (3.1);
- Definition of the criteria for the analysis of case studies (3.2);
- Review of the objectives of responsiveness and design and fabrication tools (3.3);
- Selection and analysis of case studies of responsive skins (3.4);
- Comparison of the results of the analysis (4).

3.1 COMPLEX AND SIMPLE RESPONSIVE SKINS

According to the classification proposed by Matin & Eydgahi, responsive surfaces are characterized by active and passive technologies (Fig 3). Active technologies involve: mechanical technology (M); electro-mechanical technology (EM), information technology (IT). Passive technologies involve material-based technology (MB) and natural agent-based technology (NAB) (Matin & Eydgahi, 2019). In our research, complex systems are related to active technologies while simple systems are related to passive technologies. All complex façade systems feature a sensing phase, a control phase and an actuating phase (Matin & Eydgahi, 2019). In the mechanical systems the sensing phase is determined by the user's requirements, the system is hand operated and the actuators are cables, gears and so on. In the electro-mechanical systems the sensing phase involves sensors, the control phase is run by a logic unit and the actuators can be pneumatic, hydraulic, electrical, motor-based. In the information technology system a network of sensors and micro-controllers control the whole apparatus, while the actuators can be electro-mechanical or material based. Simple façade systems can be material-based, composed by smart materials (emerging materials) which combine the three phases (sensing, control and actuation) in a single device or component (Ritter, 2006). Another option is based on autonomous structures with no sensors or controlling technology, acting according to natural phenomena like moisture, wind or sunlight (natural agent systems).

3.2 OTHER ANALYSIS CRITERIA

Apart from the distinction between complex and simple systems, the criteria (Fig. 4) applied for the analysis of the case studies were:

- State of the case study: project or built. Built examples involves also prototypes and temporary constructions.
- Year of construction or design. The selected time frame included projects and buildings designed and/or built between the years 2008 and 2020.
- Type of responsiveness: active or passive according to Matin & Eydgahi classification (2019).
- Objective of responsiveness: environmental or media (communication). See section 3.3.
- Design and fabrication tools: traditional or generative. See section 3.3.

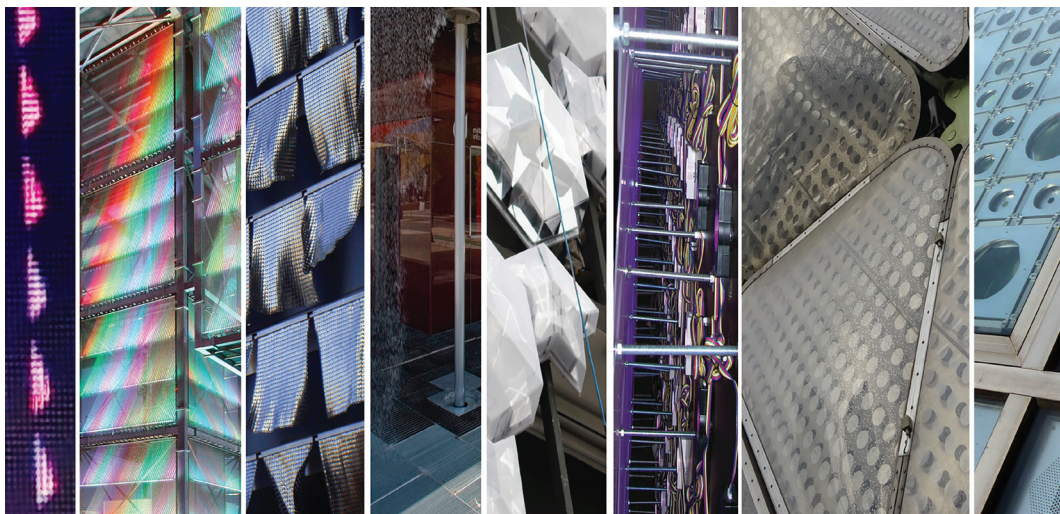


FIG. 3 Collage with examples of active and passive responsive skins (K. Gasparini)

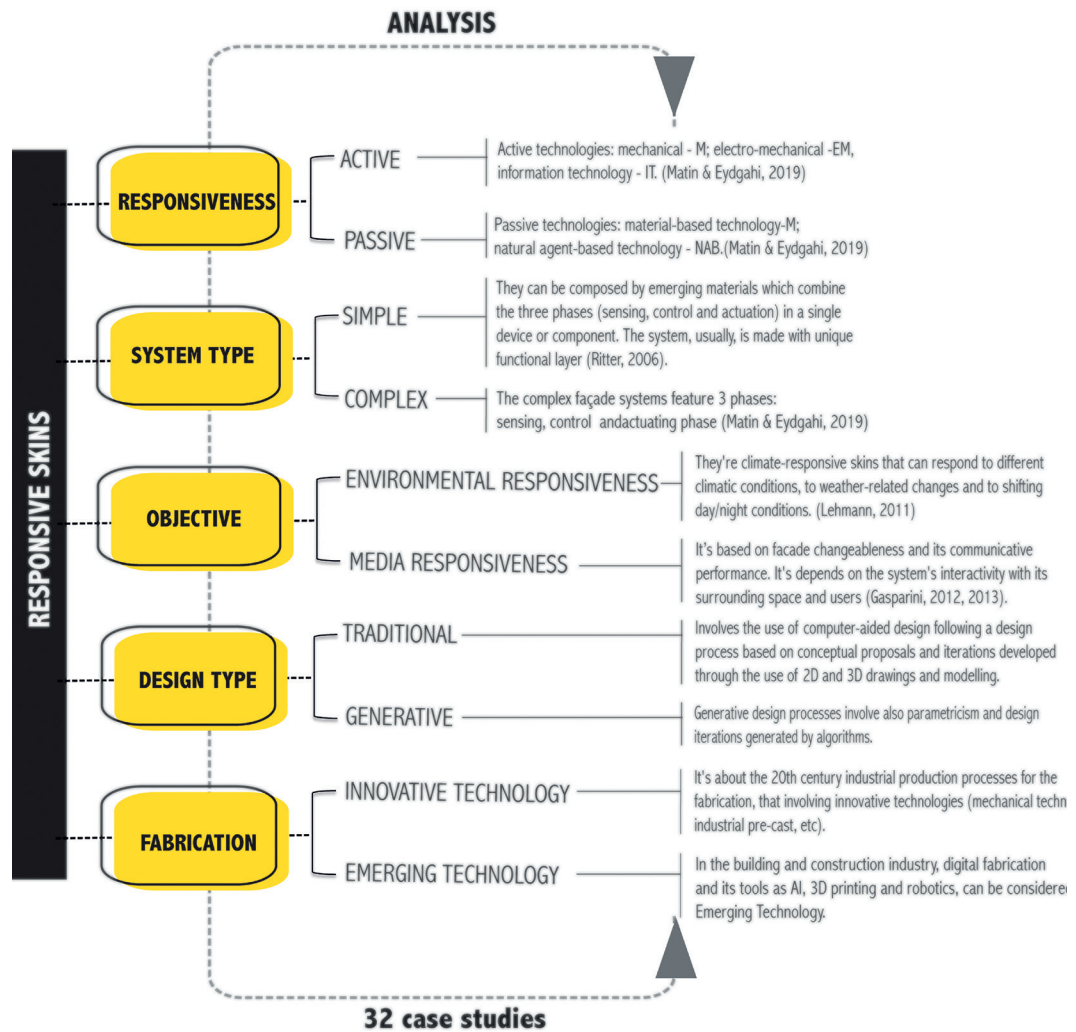


FIG. 4 Research criteria

3.3 OBJECTIVES AND DESIGN PROCESSES

There seems to be two main approaches towards responsive architecture: the so-called climate-responsive architecture which is focused more on the environmental approach and media architecture which is focused more on communication and/or human interaction. According to Lehmann (2011) "Climate-responsive" means that the building's façade and systems can respond to different climatic conditions, to weather-related changes and to shifting day/night conditions. One of the fundamental principles is to design buildings 'low tech', where passive strategies are employed before active ones". Media responsiveness is based on the media value of the building and the interactivity with its surrounding space and users: a visual as well as physical and cultural interactivity, often combined with artistic or socially valuable contents. In other words, the building project's main aim is to communicate, through urban screens, lighting surfaces, changeable shapes, etc. All the other functional and spatial requirements become less important compared to this (Gasparini, 2012, 2013). Both objectives can be achieved through a traditional design process or a generative design process. Traditional design process involves the use of computer aided design following a design process based on conceptual proposals and iterations developed through the use of 2D and 3D drawings and modelling. Generative design processes involve also parametricism and design iterations generated by algorithms. The traditional process is based mainly on computer aided design (CAD) and technical drawings for the design stage and on the 20th century industrial

production processes for the fabrication, thus involving innovative technologies. The generative process usually involves digital fabrication, including the use of AI, 3D printing and robotics. The generative design process use algorithms to explore the variants of a design beyond what is currently possible using the traditional design process. Mimicking nature evolutionary approach, generative design uses parameters and goals to rapidly explore thousands of design variants to find the best solution (McKnight, 2016). The generative process usually involves digital fabrication, including the use of AI, 3D printing and robotics, that in this research are considered as Emerging Technologies (industry 4.0). Technology is defined as Emerging (ET) when it causes a radical change to business, industry, or society. Technology is considered as Emerging in a particular context (domain, place, or application) but it can be identified elsewhere. Emerging Technology has no limited or predetermined lifespan (Halaweh, 2013). In the building and construction industry, digital fabrication and its tools can be considered an Emerging Technology.

3.4 SELECTION OF THE CASE STUDIES

The applied methodology involved a selection of 32 case studies of responsive building skins (Table 1). The identified case studies are located mainly in Europe (13), Asia (10) and USA (8). Only one is located in Oceania (Australia). This confirms the results of other research related to responsive and adaptive façades (Premier, 2019) and indicates that major investments in research within this topic are made in those countries. Case studies have been selected through a review of literature carried out on architecture magazines (digital and printed), books, journal articles and research reports. The following keywords have been used: responsive architecture, responsive skins, kinetic façades, adaptive façades. Design or construction date was an essential criteria for the selection in order to achieve a set of case studies built in the last 15 years (the actual timeframe is the last 12 years) and, at the same time, to reduce the number of buildings and prototypes already studied in previous research by the authors. Responsiveness was the other essential criteria and each project should have responded to at least one of the two identified types of responsiveness: environmental or media.

CASTE STUDY	STATUS	DESIGNER	PLACE	YEAR
NEVSEHIR MUSEUM OF MODERN ART	Project	Burak Celik	Turkey	2017
DYNAMIC ETFE FAÇADE	Built	John Ronan Architects	Chicago	2017
INVERT AUTO-SHADING WINDOWS	Built	Do Su Studio	Los Angeles	2017
SNAPPING FAÇADE	Project	Jin Young Song	Buffalo	2017
FLUID MORPHOLOGY	Project	Research Lab of TUM	München	2017
V ON SHENTON	Built	UNStudio	Singapore	2018
HEERIM KINETIC Façade HRKF	Built	Heerim Architects	Seoul	2018
ADAPTIVE SOLAR Façade ASF	Built	Arno Schlueter	Zürich	2018
THE SHED	Built	Diller Scofidio + Renfro	New York	2019
SCOTT SPORTS HEADQUARTERS	Built	IttenBrechtbühl	Givisiez, CH	2019
RESPONSIVE FAÇADE	Project	Boutros Bou-Nahra Architect	Miami, Florida	2020

TABLE 1 Case studies of the research

4 RESULTS AND DISCUSSION

According to the survey carried out on the selected case studies, environmental responsiveness seems to prevail over media responsiveness. Over the years, media responsiveness has lost importance. The environmental approach is fundamentally linked to traditional design and industrialized manufacturing (innovative technologies) (Fig. 5). This is more evident if we consider

the projects characterized by “Active responsiveness” and built with “Complex systems”, where the environmental objective is 42%.

Almost half of the projects (14 out of 32) seem to be generated through parametric design. Amongst those, at least 2/3 refer to complex and active systems. Generative design is strictly linked to digital fabrication and emerging technologies (Davis et al, 2011). There seems to be a direct proportion between these two categories.

Summarizing these results, 1/3 of the projects seem to be made with emerging technologies (3D printing and robotics) and almost all of them seem to be designed through parametricism (75%). Emerging technologies seem to be applied to both simple and complex systems, indifferently to active and passive responsive skins.

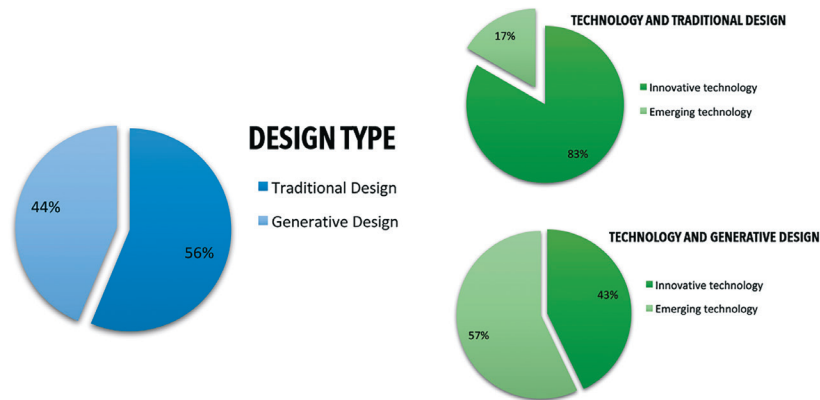


FIG. 5 Design type and related technologies

An example of passive responsiveness and simple system is represented by the “HygroSkin-Meteorosensitive” case study, a climate-responsive pavilion with kinetic apertures. It is an example of climate-responsive architecture whose modular wooden skin detect weather changes. The response is a contraction or expansion of its apertures that are mad of thin wooden diaphragms. These diaphragms respond to the surrounding environment, adjusting to changes in relative humidity. The climatic changes enable the material-innate movement which creates continuous modifications of the natural illumination of the internal space (Azzarello, 2013).

Innovative technologies (based on 20th century industry standards) are applied on 2/3 of the case studies (20 out of 32). It seems particularly interesting to observe the difference between the adopted technology in comparison with the design type (Fig. 6): the traditional design approach seems to be linked to the use of innovative technology (83%), instead, generative design seems to be linked to emerging technology (57%).

An interesting example of the application of innovative technologies is represented by the “Responsive façade” project, designed by Boutros Bou-Nahra Architect (2020). The project has been classified as an example of active responsiveness and it represents a complex skin system. The design type is originated by parametric design tools. The surface was conceived for a climate and daylight control, but it is interesting also for the changeable configuration of its skin. According to Boutros Bou-Nahra Architect, goal of the project was to maximize views (fenestration) but minimize solar heat gain. This goal is achieved by implementing a responsive façade that is closed by default but senses when there is movement in close proximity and opens up to reveal a view. Each panel of the façade is individually operated by a sensor and an actuator. Based on the distance of the

people passing by, the actuators open accordingly and allows for a trail like effect. The façade panels consist of a lightweight wood frame wrapped in cured fiberglass (Fig. 6).

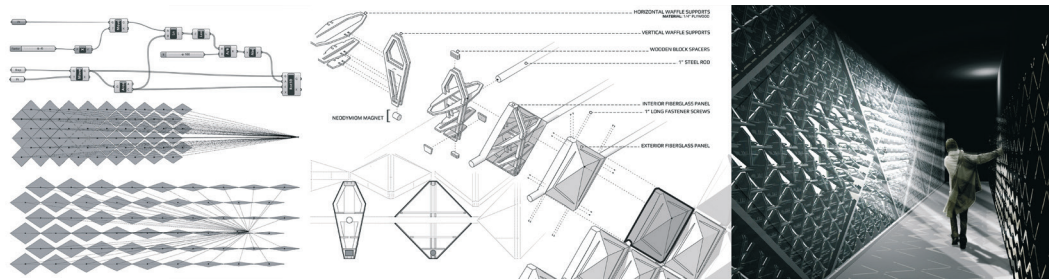


FIG. 6 Type of responsiveness. Courtesy of Boutros Bou-Nahra Architect. <https://boutrosbounahra.com>

In the selected case studies, traditional design deals almost equally with simple and complex systems, but mostly with active systems (twice as much as passive ones). The case studies are almost equally divided between built and projects (17 vs 15). From the analysis, we argued that, in the built case studies, the adoption of complex or simple systems is equally distributed, while in the case studies still in the design or prototype phase, there is a great predisposition to the use of complex systems (80%). Therefore, simple systems with a passive type of responsiveness seem more feasible, reliable and accepted. However, we also found that the case studies that are still in the prototype stage are the more experimental ones, where 60% are designed with generative design tools and the technologies adopted are equally distributed between emerging and innovative. Instead, the 80% of the built case studies has been designed through traditional designing processes and built using innovative technologies.

5 CONCLUSIONS

The research involved the analysis of 32 case studies of responsive building skins. Case studies have been investigated according to a set of criteria including: the type of responsiveness (active or passive); the complexity of the system; the use of innovative or emerging technologies and their relationship with the design process (traditional or generative); the objective of the project (focus on environmental or media responsiveness).

From the statistical analysis, we argued that emerging technologies are entering the AEC industry very slowly, a little too late compared to the use of parametric design tools. However, their application mainly allows for the construction of passive and simple responsive skins. This leads to the design of buildings with a high degree of sustainability and reliability. Parametric design in conjunction with emerging technologies can change the design paradigm already in the heuristic phase, linking it to an industrial-type approach, closer to product design and customized design, with a high degree of adaptability to the environmental conditions and based on a human-centred approach. The reproducibility of the components, and the reduction of their complexity, increase the overall reliability of the system and the possibility of maintenance and replacement over time.

In conclusion, we might affirm that emerging technologies and parametric design need to be developed and used more in the design process because they are customized for each project and not derived from technology transfer. Therefore, they generate mainly simple and passive systems. These technologies are currently used on prototypes, small buildings or architectural elements and art installations (e.g. 3D printed mock-ups). This represents the future of design and fabrication where the focus is not on the durability of innovative technologies.

Acknowledgements

This research has been conducted by the authors at the 'Eterotopie. Colour, Light and Communication' Research Centre in Italy and at the Future Cities Research Hub of the University of Auckland, New Zealand.

References

- Aelenei, L., Brzezicki, M., Knaack, U., Luible, A., Perino, M., & Wellershoff, F. (2015). "COST Action TU1403 - Adaptive Façades Network", in Aelenei, L., Brzezicki, M., Knaack U., Luible, A., Perino, M., & Wellershoff, F., Adaptive façade network - Europe. Delft: TU Delft Open
- Azzarello, N. (2013). "hygroskin: a climate-responsive kinetic sculpture", in Designboom.com (02.09.2020)
- Ciribini, G. (1979). *Introduzione alla tecnologia del design: metodi e strumenti logici per la progettazione dell'ambiente costruito*. Milan: Franco Angeli.
- Davis, D., Salim, F., Burry, J. (2011). "Designing responsive architecture. Mediating analogue and digital modelling in studio", in Herr, C.M., Gu, N., Roudavski, S., Schnabel, M.A., *Circuit Bending, Breaking and Mending: Proceedings of the 16th International Conference on Computer-Aided Architectural Design Research in Asia*, 155–164. Hong Kong: CAADRIA.
- d'Estrée Sterk, T. (2003). "Building Upon Negroponte: A Hybridized Model Of Control Suitable For Responsive Architecture", in *Proceedings eCAADe 21 digital design*, 407-414. Graz, Austria: Graz University of Technology.
- Favoino, F., Goia, F., Perino, M., Serra, V. (2013). "Experimental assessment of the energy performance of an advanced responsive multifunctional façade module, in *Energy and Buildings*, ELSEVIER BV. <https://doi.org/10.1016/j.enbuild.2013.08.066>
- Gasparini, K. (2012). *Schermi Urbani (Urban screen)*. Milan: Wolters Kluwer
- Gasparini, K. (2013). "Media architecture: origin, synonyms and interpretations", in *Screenicity journal*, n.1 jan-april 2013, ISSN 2281-1516
- Gasparini, K., Premier, A. (2019). "The future of Responsive Surfaces in the Liquid Modernity", in *Future Talks 019. Surfaces - Lectures and workshops on technology and conservation of the modern*, November 11 to 13, 2019. Munich, Germany: The Design Museum (in print)
- Halaweh, M. (2013). "Emerging Technology:What is it?", *J.Technol. Manag. Innov.* 2013,Volume 8, Issue 3, ISSN: 0718-2724
- Kant, I. (1781). *Critik der reinen Vernunft*. Riga: Johann Friedrich Hartknoch
- Knaack, U., & Klein, T. (2008). *The Future Envelope 1: A Multidisciplinary Approach*. Amsterdam: IOS Press
- Lehmann, S. (2011). "Energy-Efficient Building Design: Towards Climate-Responsive Architecture", in *Built Environment, UNESCO, Encyclopedia of Life Support Systems (EOLSS)*.
- Matin N.H., Eydgahi A., (2019). "Technologies used in responsive façade systems: a comparative study", in *Intelligent Buildings International*, Taylor & Francis. <https://doi.org/10.1080/17508975.2019.1577213>
- McNight M. (2016), "Generative Design: What it is? How is it Being Used? Why it's a Game Changer!", in *DesTech Conference Proceedings*, KnE Publishing, DOI: 10.18502/keg.v2i2.612
- Miller, J.G. (1978). *Living Systems*. New York: Mc Graw-Hill
- Negroponte, N. (1975). *Soft Architecture Machines*. Cambridge, MA: MIT Press
- Premier, A. (2019). "Solar shading devices integrating smart materials: an overview of projects, prototypes and products for advanced façade design", in *Architectural Science Review*, Taylor & Francis. <https://doi.org/10.1080/00038628.2019.1653259>
- Ritter, A. (2006). *Smart Materials in Architecture, Interior Architecture and Design*, Basel: Birkhäuser
- Romano, R., Aelenei, L., Aelenei, D., Mazzucchelli, E.S., (2018), "What is an Adaptive Façade? Analysis of Recent Terms and Definitions from an International Perspective", in *Journal of Façade Design and Engineering*, Delft: TU Delft Open, Vol.6., No.3, pp. 65-76. DOI: 10.7480/jfde.2018.3.2478
- Zennaro, P. (2000). *La qualità rarefatta. Considerazioni sull'influenza del vuoto nella costruzione dell'architettura*. Milan: Franco Angeli
- Zomorodian, Z.S., Tahsildoost, M., (2018), "Energy and carbon analysis of double skin façades in the hot and dry climate", in *Journal of Cleaner Production*, ELSEVIER BV. <https://doi.org/10.1016/j.jclepro.2018.06.178>

Ge³TEX – Multifunctional Monomaterials Made from Foamed Glass-, Basalt- or PET-based 3D Textiles

**Claudia Lüling¹, Petra Rucker-Gramm¹, Agnes Weilandt¹, Johanna Beuscher¹, Dominik Nagel¹,
Jens Schneider², Andreas Maier², Hans-Jürgen Bauder³, Timo Weimer³**

- 1 FFin Frankfurter Forschungsinstitut, FRA-UAS (Frankfurt University of Applied Sciences), Nibelungenplatz 1, 60318 Frankfurt, tel. +49 69 1533 2768, fax. +49 69 1533 2374, mail clue@fb1.fra-uas.de
- 2 Technische Universität Darmstadt, Institute of Structural Mechanics and Design, Franziska-Braun-Str. 3, 64287 Darmstadt, tel +49 6151 1623018, fax +49 6151 162338, mail maier@ismd.tu-darmstadt.de
- 3 Deutsche Institute für Textil- und Faserforschung Denkendorf, Körschtalstrasse 26, 73770 Denkendorf, tel +49 711 9340 254, fax +49 711 93 40 311, mail hans-juergen.bauder@ditf.de

Abstract

Ge³TEX's focus is on monomaterials for lightweight, architectural applications, based on spacer fabrics. The project explores three material combinations for new composite components, two of them mineral based and one polymer based. The spacer fabrics are used in three variations as lost formwork for foamed fillings as well as structural elements for tension forces:

- *basalt fibre-based spacer fabrics in combination with foamed concrete;*
- *glass fibre-based spacer fabrics in combination with foamed glass from recycling resources;*
- *spacer fabrics made from PET-fibres from recycling in combination with PET-based particle foams, also from recycling material.*

The project is supported by the Federal Ministry of the Interior, Building and Community and is coordinated by Frankfurt University of Applied Sciences. The academic partners are the DITF Denkendorf for woven spacer fabrics, Technical University Darmstadt for foamed concrete, and industrial partners such as Poraver Service GmbH & Co. KG (foamed glass) and others. The industrial partners involved cover the full range of textile and building expertise required. The project aims are:

- *to establish and improve fibre and foam materials in order to improve the bond between the foamed and textile materials;*
- *to investigate appropriate textile technologies and geometries, depending on different applications in the building skin, e.g. wall and roof elements;*
- *to design and build demonstrators from each of the three envisioned monomaterials in a 1:1 scale.*

The initial tests show promising results. Foamed glass has been combined with a special glass-based matrix, and first mock-ups combining E glass and AR glass have been produced. A demonstrator, made initially from PE fibres, was able to be bent after filling, thereby becoming a lightweight and form-active building element. Form-active elements are under development also using foamed concrete and spacer-fabrics from basalt fibre. Here the DITF developed not only conventional plane-parallel spacer fabrics but also for the first time double-curved fabric structures from basalt rovings. Basalt rovings have been developed that can be woven and which have equally sufficient alkali resistance. As for polymer, ongoing research has proven that possibilities exist for in-situ foaming from PET-particle foams in PET-spacer fabrics, in combination with folding strategies to achieve form-active roof and wall elements.

The aim: lightweight, form-active building elements, made in-situ with additional textile-based functions such as low-tech absorption and release of thermal energy and passive lighting.

Keywords

Lightweight design, textile building, multifunctional monomaterial, lost formwork

1 INTRODUCTION

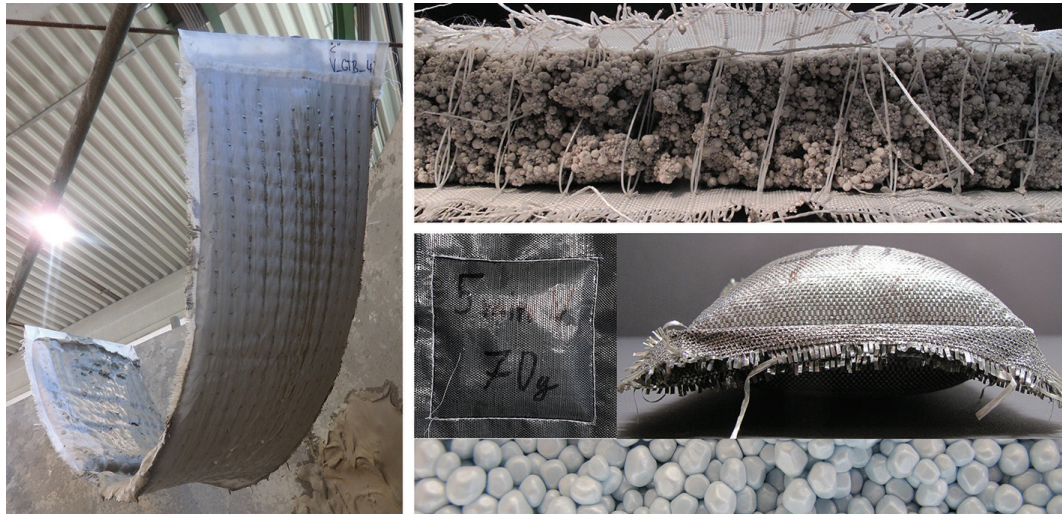


FIG. 1 Left: filling test, woven spacer fabric filled with foam concrete for form-active building elements

FIG. 2 Top right: filling test, woven spacer fabric filled with glass foam

FIG. 3 Bottom: filling test, fabric from PET fibres filled, foamed and formed with PET particle foam

Lightweight construction is a fundamental cross-sectional technology not only in the automotive sector. Less material, multifunctionality, the highest possible prefabrication of highly functional (semi-)finished parts and the manufacture of robust, recyclable components are also future challenges for the construction industry.

In the "Ge³TEX" project, new lightweight components for the building envelope are being developed based on the "3dTEX – lightweight wall element" preliminary project. Specifically, the focus here is on two mineral-based and one polymer-based variant: basalt fibres and foam concrete, glass fibres and expanded glass as well as recycled PET fibres and PET foam. The aim is to develop structure-differentiated monomaterials with gradient potential for foamed lightweight construction elements made of three-dimensional textiles (spacer textiles). Very good recycling options and synergies are expected in terms of load transfer, insulation, weather protection and fire protection. To this end, the mechanical and structural functionalities of each material group are first of all optimized in Ge³TEX. On the one hand, the adhesion between the respective foam and the associated fibre material is important, as is the interaction between the fibres and foam to form a supporting and insulating gradient material. On the other, the focus is on the textile geometries of the 3D textiles, including for the first time also 3D basalt textiles. The textile as lost formwork has a decisive shaping effect. It also serves as weather protection and functionally for the load transfer of tensile forces and the optimisation of shear force transfer. The ultimate objective are demonstrators for the wall and roof area, which convince with form-giving and functional textile geometries and the integration of defined functions. In direct connection with the production process and with the highest possible degree of prefabrication, textile-based (self-)unfolding or self-curvature mechanisms for form-active supporting structures for stabilisation are also being investigated; structural joining points are being developed and the implementation of PCM materials, heat-conducting and light-conducting fibres is being evaluated.

1.1 METHODOLOGY

In an iterative and experimental research strategy, the three groups of materials mentioned above are initially investigated separately. Here the focus is on individual requirements for the fibres (finishing/coating etc.) as well as on the optimisation of the foam formulations and their interaction with the textile in terms of adhesion and filling processes. Finally, the material, manufacturing process, functionality and sustainability of the realised demonstrators are compared in a cross-comparison. Figures 4 and 5 show the methodological structure.

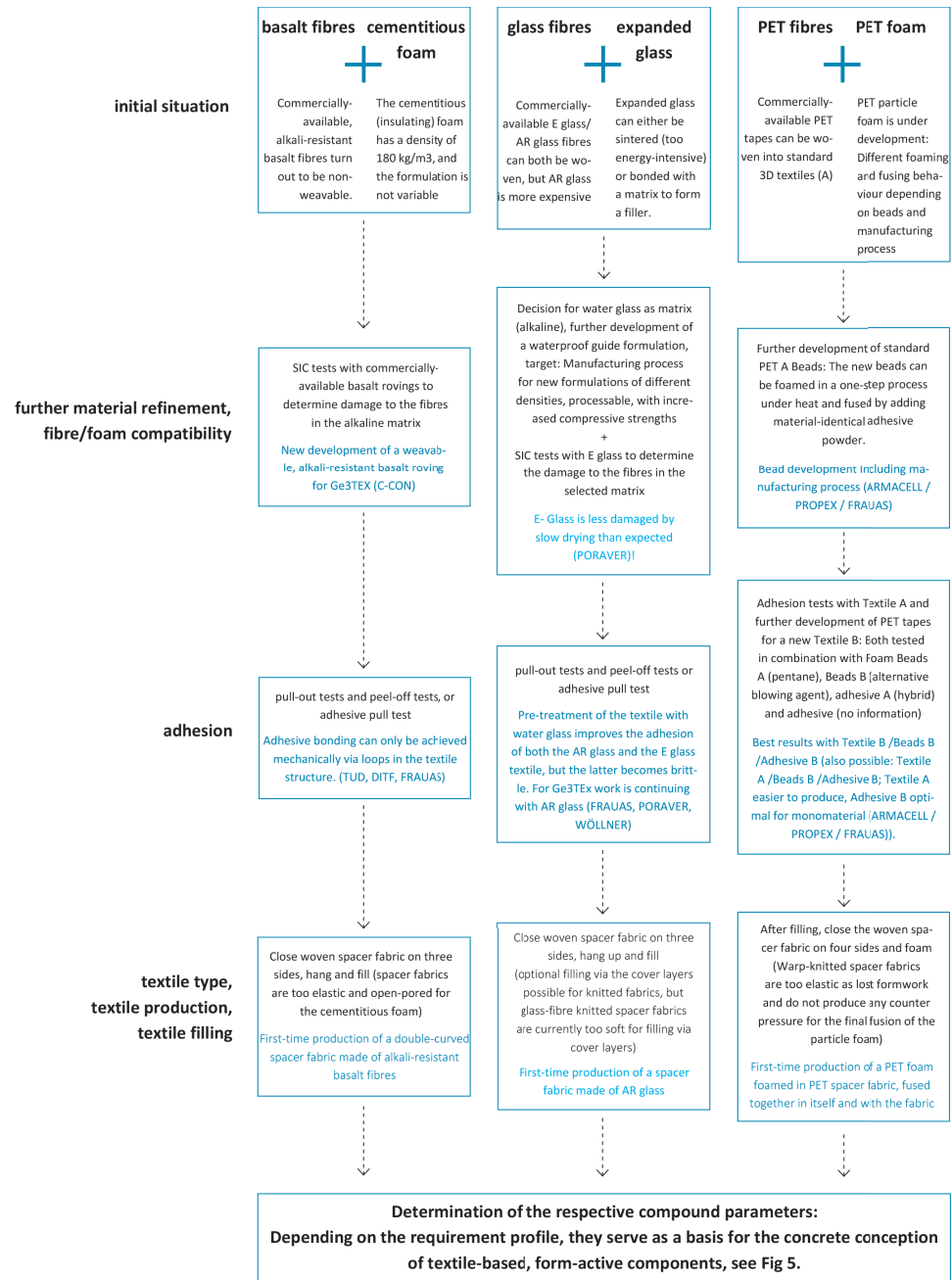


FIG. 4 Development of structure-differentiated monomaterials made of fibres and foam of the same material groups (mineral- and polymer-based variants)

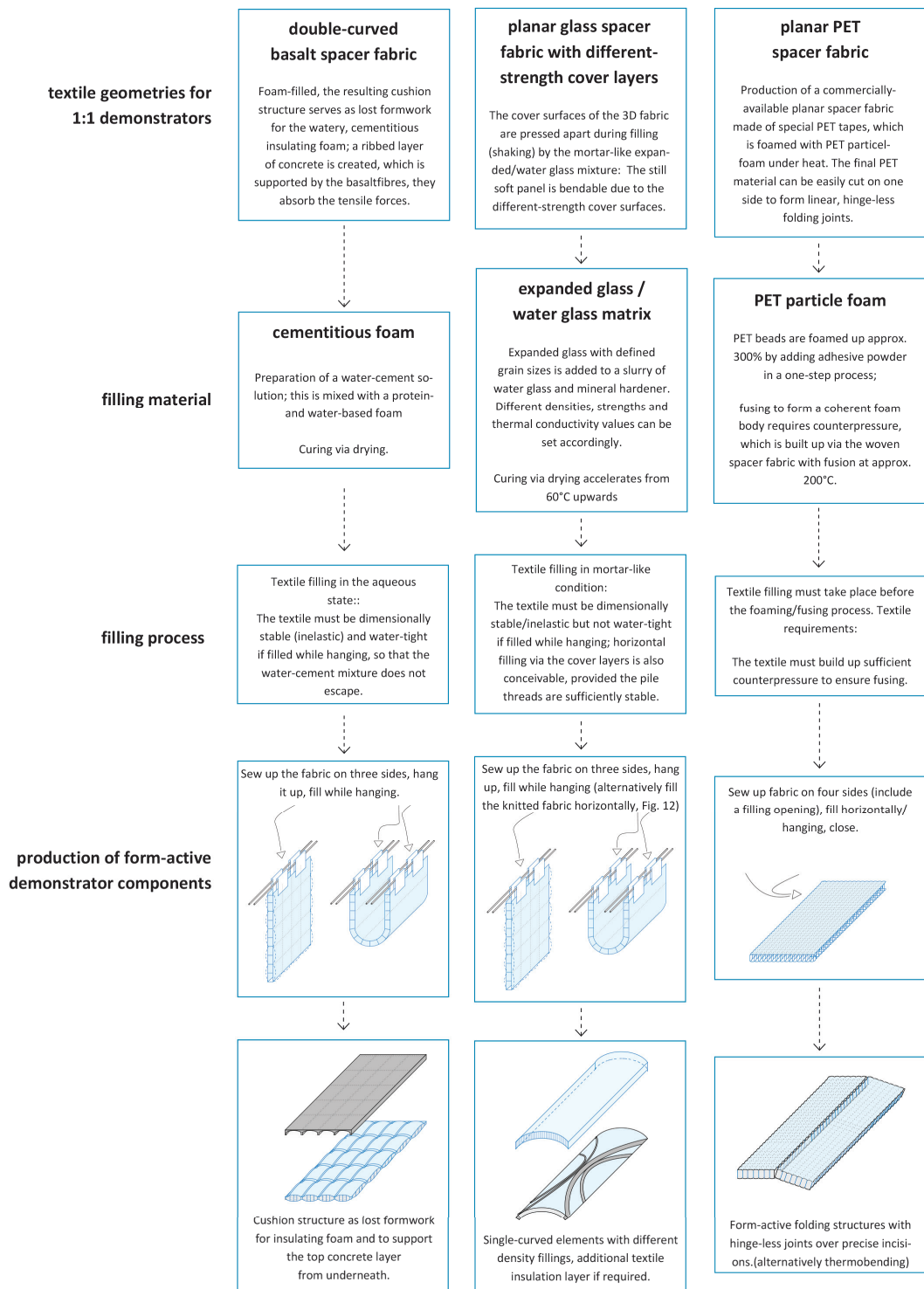


FIG. 5 Development of form-active lightweight components from structure-differentiated monomaterials depending on the material and process

2 EXPERIMENTAL RESEARCH, EXPERIMENTS

2.1 SPACER FABRICS

The manufacture of mineral-based spacer textiles, which are intended to serve as lost formwork and to absorb tensile forces, poses the following challenges:

The mineral rovings consist of a large number of fibres that must not fray or break during processing. Despite their brittleness, they must be sufficiently bendable, so that in particular the pile threads from the cover layers can be woven or knitted into the opposite side (Fig. 6). In addition, the glass or basalt rovings must be protected with coatings against the alkaline environment to which they are exposed. The thicker the coatings, the more alkali-resistant they are, which further limits their processability. In Ge³Tex, 14 commercially-available basalt rovings and eight E glass rovings were first of all tested for their alkali resistance and processability. In addition, two AR glass rovings (640tex, 1,200tex) were also tested for their processability and evaluated.

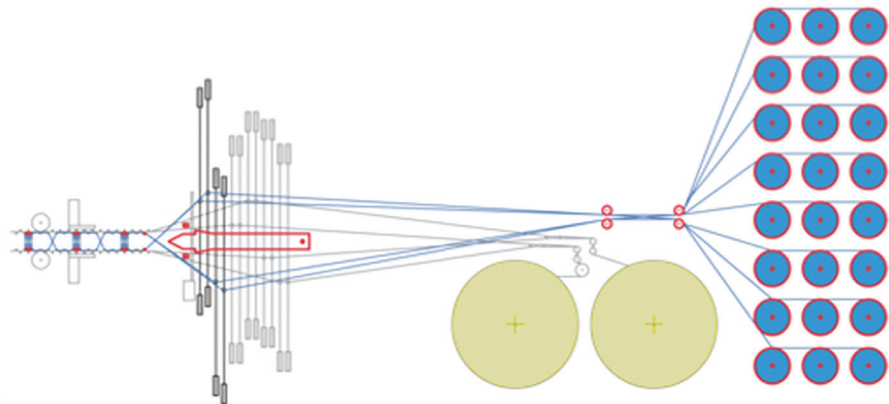


FIG. 6 Spacer weaving machine with lancet technology and tangential withdrawal of the spacer threads from the creel

In contrast to mineral-based textiles, the production of spacer textiles from PET monofilaments or PET tapes does not pose a problem per se. Here the challenge is a different one. The melting points of the PET textile and the ideal expansion temperature of the PET beads, which lie in a very narrow temperature range, must be reconciled with each other. The PET textile must not melt under heat when the used particle foam is foamed and must also build up sufficient counterpressure so that the foamed foam particles fuse together. The particle foam in turn needs sufficient heat to fuse. A standard PET textile was tested and a PET tape developed specifically for the project was woven into single-layer test fabrics for further trials.

2.2 BASALT FIBRES AND CONCRETE FOAM

Together with the involved industrial partner, the basalt rovings were individually poured into the cementitious foam matrix and tested for alkali resistance in accordance with DIN EN ISO 2062 and DIN EN 14649 (SIC test) for damage. The manufacturer's cementitious foam has a density of 180 kg/cbm. The adhesion of the individual rovings was checked in pull-out tests (Fig. 7 left). These rovings were also poured in according to the subsequent position of the pile threads between the cover layers and in the cementitious foam. In addition, the rovings were woven into single-layer

textile fabrics. Their adhesion was investigated in peel-off tests according to the subsequent position of the cover layers on or next to the cement foam (Fig. 7 right). Filling tests were only carried out with woven fabrics due to the rather fluid structure of the cement foam. Knitted fabrics are too porous and too elastic to be used as lost formwork.



FIG. 7 Single rovings in form-work for pull-out tests



FIG. 8 Single-layer basalt fabric, test setup – peel-off test

2.3 GLASS FIBRES AND FOAMED GLASS

Expanded glass made of recycled material can be bonded either by sintering (energy-intensive, in-situ unsuitable) or by using a suitable matrix to form a pore-based filler for filling spacer fabrics. Water glass was chosen as the matrix for the development of a solid monomaterial.

In contrast to the existing formulation for the cementitious foam, see 3.2, existing standard formulations for the production of waterproof expanded glass and water glass mixtures must be tested and adapted for Ge³TEX (Fig. 8). The aim of the tests was to develop a processable, as light as possible, but equally pressure-stable expanded glass/water glass mixture - or to provide a number of formulations that are partially available for filling depending on the textile geometry and load case or insulation requirements. The test series had the following parameters: density of the expanded glass granules, mixing ratio of the water glass and mineral hardener, drying temperature, drying time, and waiting time until the mechanical and structural parameters are measured.

As with the basalt rovings, the eight E glass rovings were subjected to SIC tests to check for fibre damage. Together with the two AR glass rovings, pull-out tests, peel-off tests and adhesive pull tests were also carried out. In addition, the strength of the formulation was tested again after prolonged exposure to water. In contrast to the rather liquid, cementitious foam, the expanded/water glass matrix has a mortar-like structure. Filling tests were accordingly carried out with woven fabrics from the side and knitted fabrics over the cover layers.



FIG. 9 Preparation of a water-proof expanded glass/water glass mixture; standard formulation: slurry consisting of two parts by weight water glass (potassium silicate) and one part powdery, mineral hardener; ratio of slurry/expanded glass approx. 80/20, drying at approx. 150°C.

2.4 PET FIBRES AND PET FOAM

Corporate partners were acquired for the project that use raw material from the recycling for the PET tape material used for the production of spacer fabrics and for the PET particle foam. Both products can also be returned to the recycling chain. Together with both corporate partners, both the PET tapes and the selected PET particle foam were developed further.

The two PET tape or strapping materials mentioned under 3.1 (Standard Material A, new material B with better adhesion options) were tested as textile A and textile B with standard particle foam A and a likewise newly-developed particle foam B with greater expansion capacity A (Fig. 9). For the test, PET pouches were alternatively filled with unfoamed and prefoamed beads and the expansion behaviour and the fusion of the expanded beads with each other was examined in different processes (oven, microwave, infrared, radio wave). In addition, two different adhesives were used to help the particles adhere to each other – a hybrid powder and an adhesive powder more appropriate for the planned mono-material.

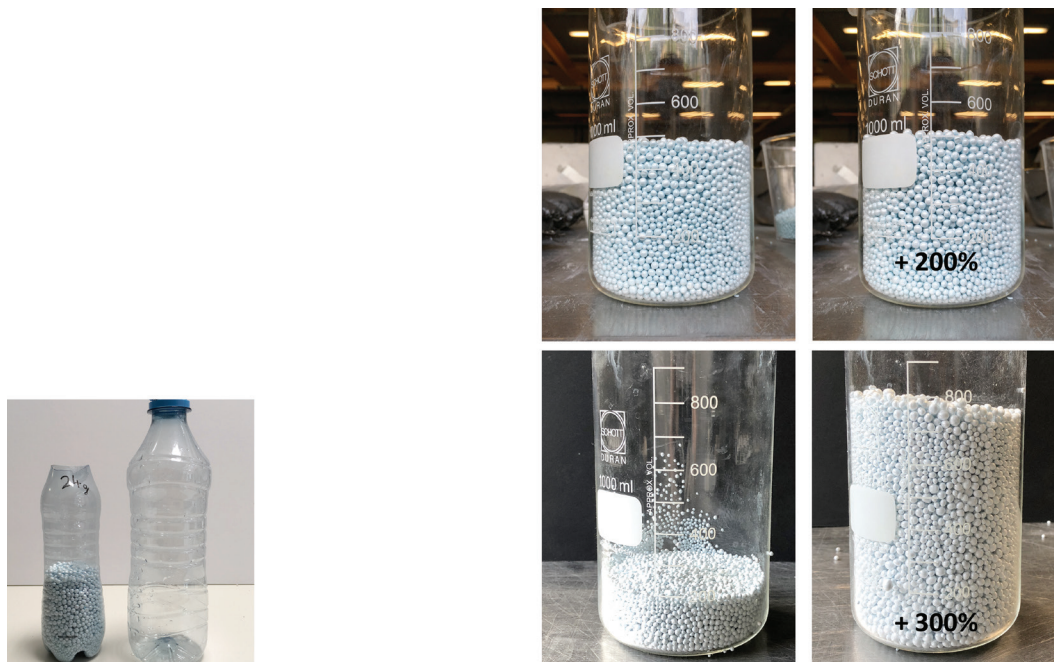


FIG. 10 Left: shrinking behaviour of PET under heat; right upper row – standard PET beads (A), lower row – new PET beads (B), foaming behaviour under 150°C

3 RESULTS

3.1 COMPONENT MANUFACTURE FROM SPACER TEXTILES MADE OF BASALT ROVINGS AND CEMENTITIOUS FOAM – RESULTS

- For Ge³TEX, special, alkali-resistant and processable rovings have been developed; standard alkali-resistant basalt rovings are not processable.
- The new rovings were used to produce 2-layer woven spacer fabrics for the first time at the DITF. Due to their elasticity and porosity, warp-knitted spacer fabrics are unsuitable as lost formwork for the aqueous cement foam.
- Adhesion of the new rovings with the cement foam could not be proven, nor could adhesion of the single-layer textile surfaces made from them (Fig. 10 left).
- The woven spacer fabrics could be modified in such a way that loops formed on the inside lead to sufficient mechanical adhesion (Fig. 10 right).
- Due to the low density of the cement foam, it can only be used for insulation purposes. For lightweight, pressure- and tension-stable insulated components, geometries have been developed for initially single- and subsequently double-curved cushion structures made of basalt fabric. The cementitious foam cushion structure (Fig. 11) serves as lost formwork for a ultra high performance top concrete layer. This results in a concrete-ribbed structure which is also supported horizontally underneath by the layer of filled basalt textile in the area of the crossing points, see Fig. 5 bottom left and Fig. 11. The basalt fibres underneath absorb the tensile forces.



FIG. 11 Pull-out test to determine the adhesion of basalt roving / cementitious foam



FIG. 12 First-time production of a double-curved spacer fabric made of basalt rovings

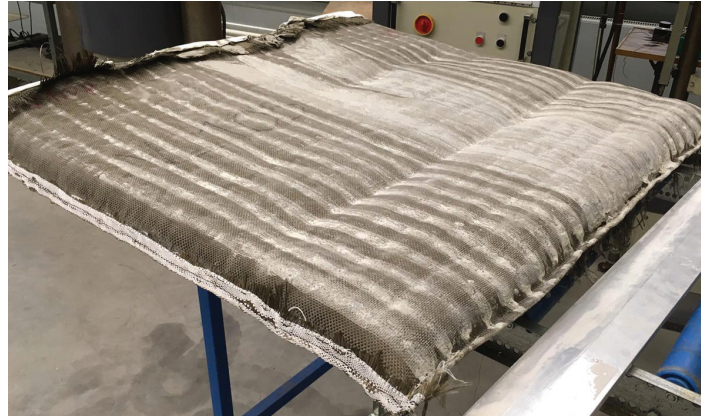


FIG. 13 First demonstrator made of single-curved basalt spacer fabric

3.2 COMPONENT MANUFACTURE FROM SPACER TEXTILES MADE OF GLASS ROVINGS AND A WATER-RESISTANT EXPANDED AND WATER GLASS MATRIX – RESULTS

- Unlike the basalt rovings, all commercially available E glass rovings can be processed. Only two showed strong filamentation and are not suitable for the warp or for use as pile threads
- The first SIC tests show the longer the duration of the drying process, the less damage is done to the E glass rovings by the expanded glass/water glass mixture. Here it must be evaluated how the ratio of cost savings when using E glass compares to the longer times for component production.
- The adhesion of single-layer fabrics made of E glass such as AR glass could only be achieved satisfactorily by pre-treatment and impregnation of the fabric.
- Structurally dense mixtures as well as single-grain mixtures of expanded glass of different grain sizes were tested – the former on the assumption that they require less binder, because the spaces between them are filled by the smaller grains themselves rather than by the binder. The result shows that the optimised, dense mixture shows no added value in terms of strength and water glass content compared to a single-corn mixture of the same density.
- The mortar-like structure of the expanded water glass mixture enables warp-knitted spacer fabrics to be filled by applying the mixture with a squeegee over the cover surfaces (Fig. 12). The filling of an initial PE warp-knitted spacer fabric and subsequent drying over a mould shows very good results. Research is still underway into the production of warp-knitted spacer fabrics made of glass rovings. For reasons of processability, it will probably not be possible to produce a stable pile yarn structure with the resilience needed for the squeegeeing process from glass rovings – a disadvantage as regards the desired monomateriality.

- For the first time, woven spacer fabrics made of AR glass were manufactured for the production of final demonstrators. Initial tests for the vertical filling of PE spacer fabrics were successfully carried out.

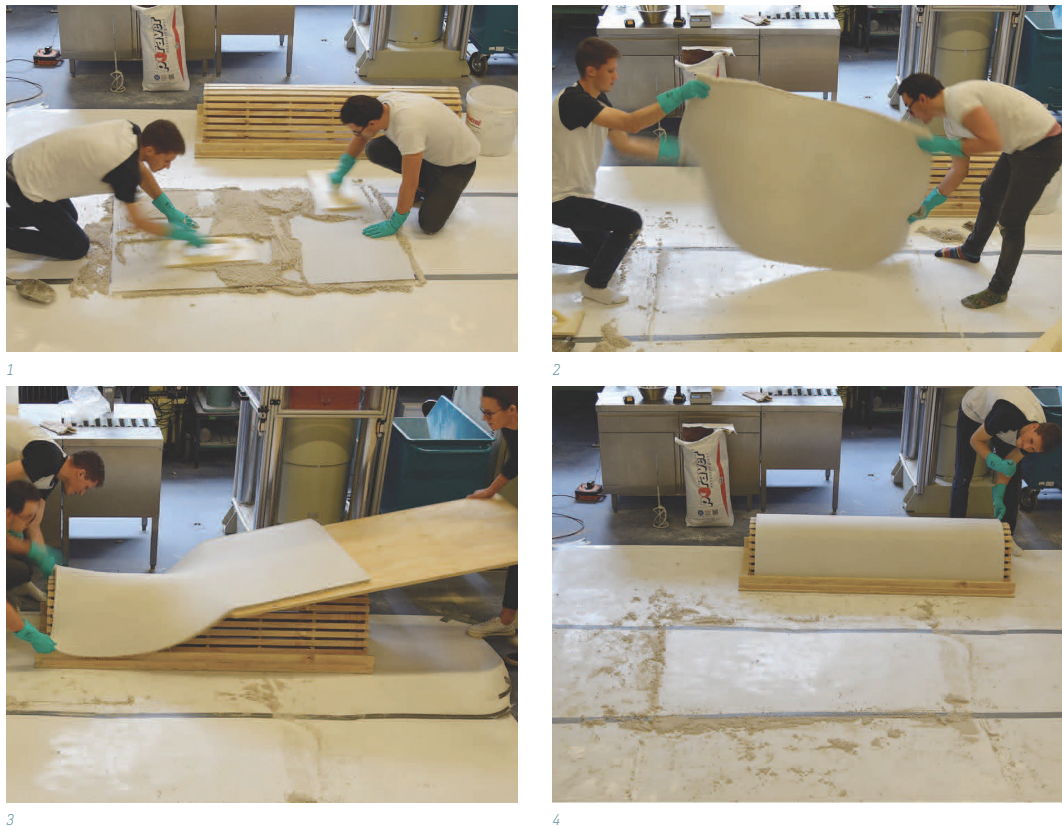


FIG. 14 Production of a form-active, single-curved component comprising an expanded glass/water glass matrix and a warp-knitted spacer fabric made of PE material: apply the material with a squeegee on one side of the cover surface, turn over, repeat the procedure on the other side; subsequent drying over a moulded part (alternatively, drying in a hanging position possible)

3.3 COMPONENT MANUFACTURING FROM SPACER TEXTILES MADE OF PET TAPES AND PET PARTICLE FOAM – RESULTS

- The shrinking behaviour of the PET textile has a positive effect compared to the expanding particle foam. In various test series, the optimal filling volume in relation to the shrinking textile volume could be determined. All combinations of Textiles A and B with Beads A and B were tested. The new Beads B are optimal, and the adhesion to the textile itself works best when using Textile B.
- In further test series with and without prefoaming, robust fusion of the foamed beads with each other was not achieved. Only by using adhesive powder, which is added to the unfoamed beads, is it possible to produce a cut-resistant foam material from the foamed beads in a one-step process (Fig. 13).

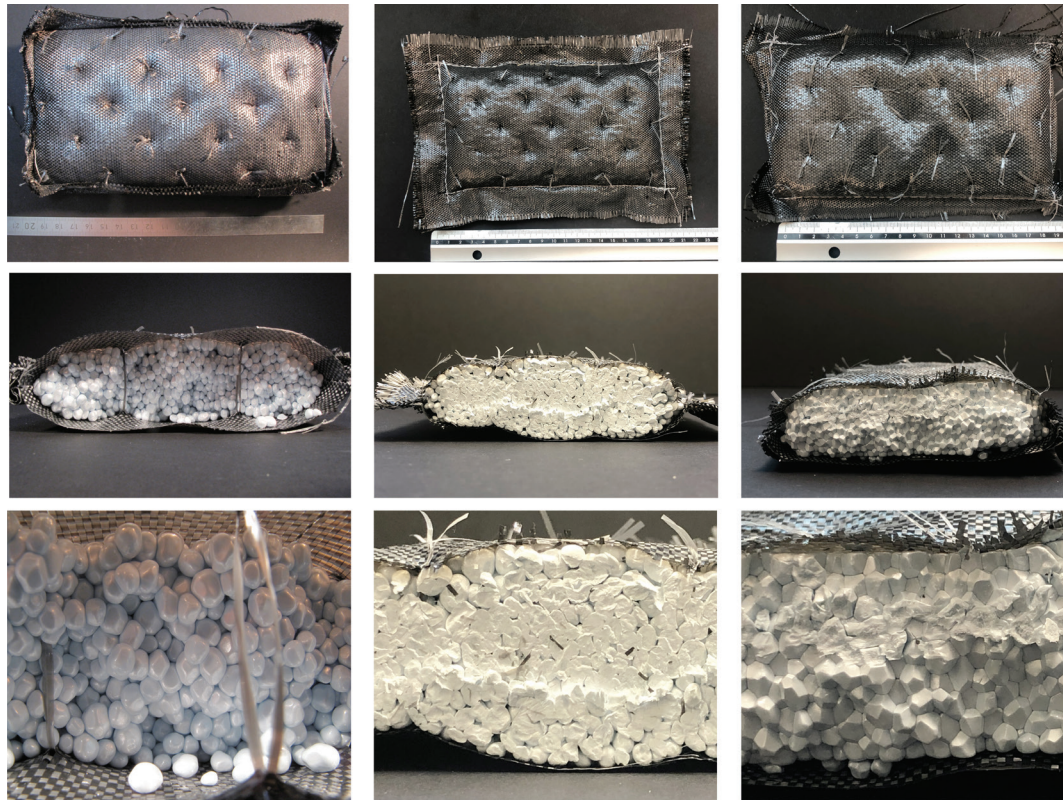


FIG. 15 PET spacer fabric as lost formwork for PET particle foam: left column – two-stage oven process, pre-foaming and fusion of Beads A and Textile B; middle column – one-stage oven process, Textile A and Beads B with Adhesive Powder A; right column – radio-frequency process – Textile A and Beads A

4 CONCLUSIONS

The aim of Ge³Tex is the production of light, self-supporting and insulating building components for the building envelope, that have the lowest-possible transport volume, dispense with formwork, can be easily assembled on site as highly functional semi-finished parts from one material group, and are part of recycling cycles. The results so far are very promising. Fig.14 shows the advantages and disadvantages in each case. For the individual material groups, depending on the parameters the results are as follows:

- Monomaterial / recyclability: The combination of basalt textile and cementitious foam can be shredded like all concrete materials and used in downcycling (e.g. road construction). There is no need for the separation of individual materials as with reinforced concrete. The combination of glass textile and foam glass can be melted down and recycled, and the expanded glass is obtained from recycled material. For the PET material group, both the textile and the foam can be obtained from recycled material and reprocessed into recyclate.
- Manufacturing process: Fig. 14 shows a comparative presentation of the material groups. The process steps are compared, e.g. seven steps in the production of a basalt fibre/cement foam element: Weave textile, sew up on three sides incl. mounting loops, hang up, fill, cut to size, make four-sided formwork, apply top concrete layer. For the glass fibre/blown glass element there are six steps: weave textile, sew up on three sides including mounting loops, hang up, fill, cut to size, apply insulation. With the PET Element there are four steps: weave textile, sew up on four sides including filling opening, fill, one-stage foaming process under heat.

- Strengths: For the basalt textile/cementitious foam combination, an additional, denser concrete must be used for the load transfer of compressive forces. In Ge³TEX, a two-layer spacer textile made of basalt was produced for the first time. In the future, pressure-active zones could be filled in a three-layer textile without any additional formwork costs. For the glass textile/foamed glass combination it is the other way round, due to the higher densities of the expanded/water glass formulation. Here, either expanded-glass zones of different densities are required depending on the mechanical and structural requirements, or with a three-layer textile an outer textile layer takes over in this case the insulation. For the PET textile/PET foam combination, strength and insulating capacity can be used in several layers according to the controllable density of the foams, e.g. with a three-layer textile. Alternatively, different foam densities can be used side by side in a single layer textile.
- Fire protection: Both mineral variants are generally classified in building material group A. The PET textile can reach B1 quality when treated with additives. A B1 quality is currently being developed for the PET particle foam.

Initial applications for the building envelope are currently being developed.. First half-shell-shaped demonstrators for roof or façade applications (Fig. 14 middle left, Fig 15) made of glass-based monomaterial were already shown at Bautec 2020. Fig. 16 shows the production of large-format cement foamed 3D basalt fabric from 3.80 m height, according to the concept shown in Fig. 14 on the left. A startup from FRA-UAS uses the research results from the PET area for self-supporting, insulated temporary buildings, see > zelthaus.com. The design is based on the folding mechanism shown in the lower left corner of Fig. 14 and Fig 17. Functional supplements are currently being investigated for all variants. This includes the integration of light- and heat-conducting fibres (Fig. 18) and the use of PCM material. The TU Darmstadt has already produced initial results for the cement-based foam in combination with PCM.

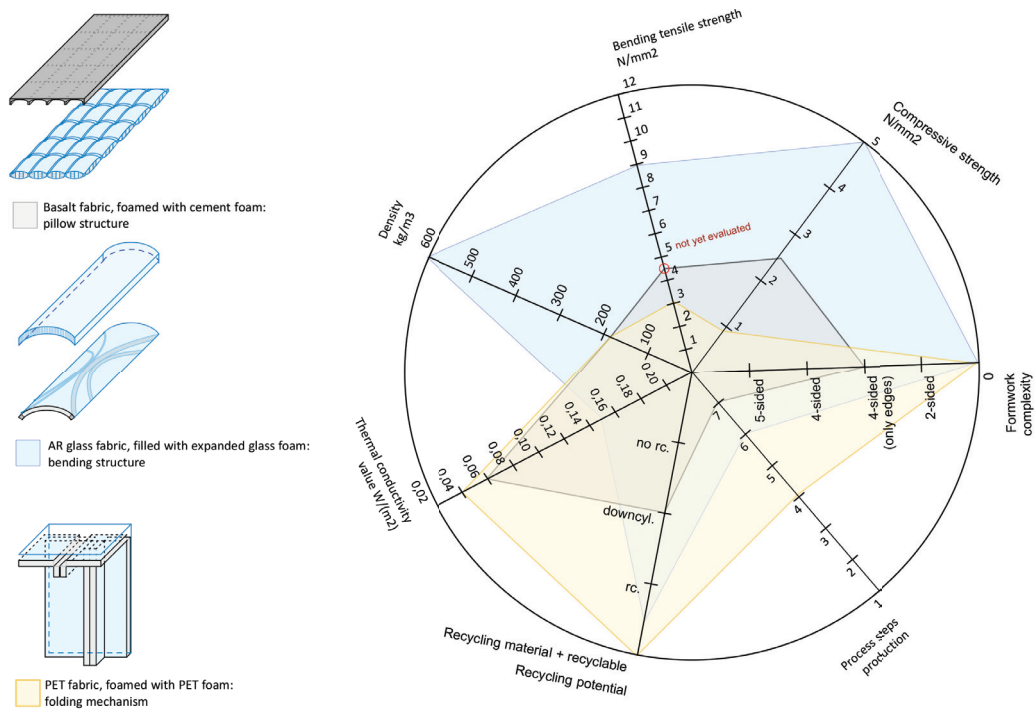


FIG. 16 Comparative presentation of textile-based, foamed components made of monomaterial materials; grey basalt fibres and cementitious foam, blue glass fibres and expanded glass, yellow PET fibres and PET particle foam



FIG. 17 bautec 2020, half-shell-shaped façade elements made from foamed glass and 3D textile, height 2m



FIG. 18 In the background, large-format basalt fabric, foamed with cement foam, height 3.80 m, section of the element in front



FIG. 19 Student seminar "Light Light", additional functionalisation of spacer fabrics, Luminale Frankfurt 2020

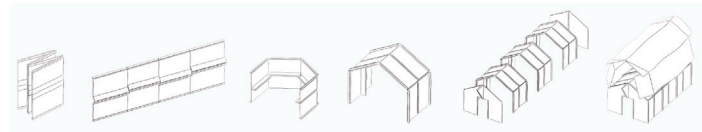


FIG. 20 zelthaus.com, research results from the PET area are used for self-supporting, insulated temporary buildings

Acknowledgements

Forschungsinitiative Zukunft Bau (an initiative of the Federal Ministry of the Interior, Building and Community (BMI), Federal Institute for Research on Building, Urban Affairs and Spatial Development (BBSR) in the Federal Office for Building and Regional Planning (BBR)) and to all our innovative industrial partners that are supporting the project: C-Con GmbH & Co. KG, Gustav Gerster GmbH & Co. KG, MAGEBA Tex Maschinen GmbH & Co. KG, Johns Manville Slovakia a.s., Nippon Electric Glass Europe GmbH, Po-raver Service GmbH & Co. KG, Propex Fabrics GmbH & Co. KG, Wilhelm Röser Söhne GmbH & Co. KG Betonwerk, E. Schoepf GmbH & Co. KG, Ultima Deutschland GmbH (Armacell Group)

References

- Aldridge, D. (2005) Introduction to foamed concrete: what, why, how? University of Dundee
- Bauder, H.-J., Wolfrum, J., Caliskan, M., Gresser, G. (2015) Entwicklung gewebter Abstandsstrukturen für gekrümmte Bauteile, Melliland Newsletter 10/2015
- Gilka-Bötzow, A. (2015) Stabilität von ultraleichtem Schaumbeton - Betrachtung instationärer Zustände. TU Darmstadt
- Gries, T., Veit D., Wulfhorst, B. (2019) Textile Fertigungsverfahren: Eine Einführung, Hrsg. Carl Hanser Verlag, 3. Aufl., München
- Koch, A., Lüling A. (2017) BasFlair - Basaltfasern als ökologische Bewehrung für Textilbeton, Abschlussbericht des Projektpartners RWTH Aachen – ITA im Rahmen des Zentralen Innovationsprogramms Mittelstand (ZIM)
- Kulas, C.H. (2013) Zum Tragverhalten getränkter textiler Bewehrungselemente für Betonbauteile, Dissertation Fakultät Bauingenieurwesen, RWTH Aachen
- Lüling, C., Richter, I., (2018) Architecture Fully Fashioned - Exploration of foamed spacer fabrics for textile based building skins. Delft: Journal of Façade Design and Engineering, 1/2017, pp. 77-92, doi: <https://doi.org/10.7480/>
- Lüling, C., (2019) Architecture Fully Fashioned - Abstandstextilien in der Architektur Melliland Newsletter Online Ausgabe 9/2019
- Rybin, V., Utkin, A. & Baklanova, N. (2012) Alkali resistance, microstructural and mechanical performance of zirconia-coated basalt-fibers. Institute of Solid State Chemistry and Mechanochemistr, Novosibirsk
- Wolfrum, J., Bauder, H.-J., Caliskan, M., Gresser, G., Toma, B., Wendel, R., Rosenberg, P., Henning, F. (2017) Aus einem anderen Blickwinkel – ORW-Verfahren für RTM-Strukturbauteile, Kunststoff 2/2017

Additive Manufacturing of Thermally Enhanced Lightweight Concrete Wall Elements with Closed Cellular Structures



Gido Dielemans^{1*}, David Briels², Fabian Jaugstetter¹, Klaudius Henke³, Kathrin Dörfler¹

* Corresponding author

1 TT Professorship Digital Fabrication, Department of Architecture, Technical University of Munich, Munich, Germany, gido.dielemans@tum.de

2 Chair of Building Technology and Climate Responsive Design, Department of Architecture, Technical University of Munich, Munich, Germany

3 Chair of Timber Structures and Building Construction, Department of Civil, Geo and Environmental Engineering, Technical University of Munich, Munich, Germany

Abstract

Building envelopes incorporate a multitude of functions, such as structure, room enclosure, insulation, and aesthetic appeal, typically resulting in multi-material layered constructions. With the technology of additive manufacturing, geometrical freedom can instead be utilised to integrate functional requirements into mono-material building components. In this research, the additive manufacturing method of lightweight concrete extrusion and its potential for thermal performance via geometric customisation is explored. It investigates whether the insulating performance of wall components can be increased through the creation of closed cellular structures, and further, whether these performance features can be functionally graded by locally adapting the geometric properties. A design tool for closed-cell wall geometries is created, which integrates lightweight concrete extrusion related fabrication constraints and takes into account thermal and structural performance considerations. Through the simulation of heat transfer, generated wall geometries are analysed for their thermal performance. By calculating the layer cycle times and determining the overhang during extrusion, the structural capacity during printing is validated. Finally, experimental manufacturing of 1:1 scale architectural prototypes is executed to test the feasibility of the concept.

Keywords

Additive manufacturing, lightweight concrete extrusion, computational design, thermal performance, functionally graded materials

DOI 10.7480/jfde.2021.1.5418538

Evaluating the Real Performance of Brick Masonry with Dynamic U-Values

Dr.-Ing. Sabine Kuehnast

Hellkamp 70, 20255 Hamburg, +49 175 146 7433, sabine.kuehnast@gmail.com

Abstract

Central point of the dissertation is the cavity wall with air gap (acc. to Eurocode 6) combining bricks with high bulk densities such as clinker and bricks with low bulk densities (light perforated bricks). In contrary to insulated cavity walls, in this cavity wall the transmission of sun energy occurs from exterior to interior, so that the transmission heat losses during the heating period in winter can be partially compensated. So far, the transmission heat gains through sun energy in winter has not been examined. This research follows two goals: First, the factors influencing the transmission heat gains are examined. The focus is set on properties that have a big impact on architecture: clinker colour, orientation/height of the building and the thickness of the masonry wall. Secondly, dynamic U-values are determined with different combinations of those influencing factors.

It will be shown that the combination of two types of clay brick without additional insulation layer (mineral etc.) achieves extremely good performance with very low dynamic U-values.

Keywords

Brick masonry, dynamic U-Value, transmission heat gain

1 INTRODUCTION

Central point of the dissertation (Kuehnast, S., 2016) is the cavity wall with air gap (acc. to Eurocode 6) combining bricks with high bulk densities such as clinker and bricks with low bulk densities (light perforated bricks). In contrary to insulated cavity walls, in this cavity wall the transmission of sun energy occurs from exterior to interior, so that transmission heat losses during the heating period in winter can be partially compensated.

In reality, complex energy and material transports take place on an outer wall that separates the inside of the building from the outside. Fig. 1 shows these transport processes schematically. These processes are subject to daily and seasonal fluctuations and changes of direction and are therefore referred to as transient or dynamic (Sedlbauer, K.P., Künzel, H.M., 2015). For example solar energy in the form of heat is absorbed by the wall during the day and this heat is released again at night. The transport of substances such as moisture is also subject to the daily and seasonal rhythm. With the dynamic hygro-thermal approach, the real moisture and heat transports are mapped.

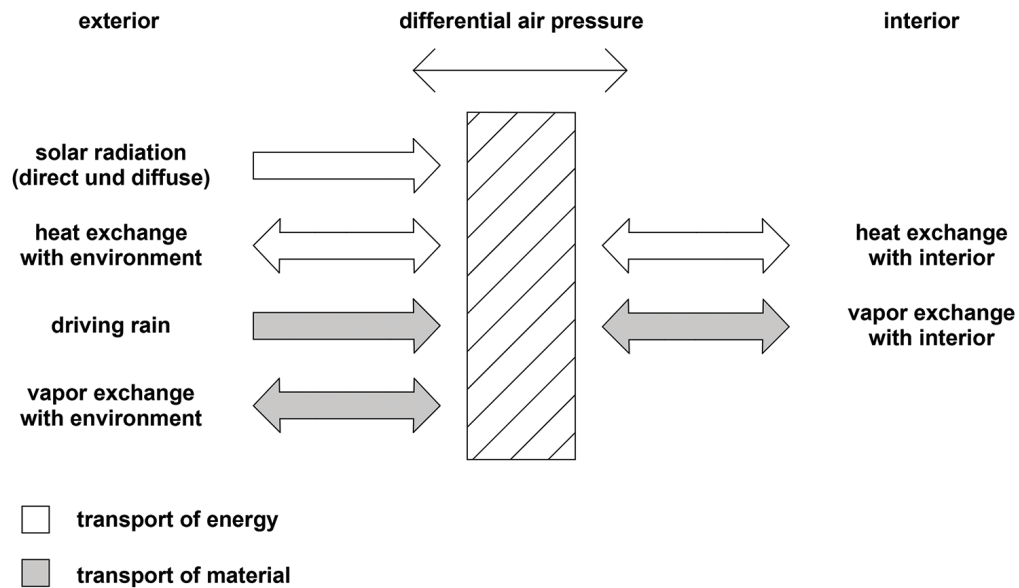


FIG. 1 Energy and mass transport on external walls

The potential transmission heat gains through sun energy in winter are examined as follows with two goals: First, the factors influencing the transmission heat gains are examined. The focus is set on properties that have a big impact on architecture: clinker colour, orientation/height of the building and the thickness of the masonry wall. Secondly, dynamic U-values are detected with different combinations of those influencing factors. It will be shown that the combination of two types of brick without additional insulation layer (mineral, etc.) achieves extremely good performance = very low dynamic U-values.

The aim of the research is to examine the possible variations of clay products – be they of an aesthetic nature (brick colour or technical nature (physical properties) – for an important question in the building industry: that of the energetic behaviour as an individual component, as a construction type and as a building. For this purpose, using thermal and hygric material parameters, five different types of facing brick constructions in two types of structure are checked under complex realistic conditions with regard to the following questions:

- Does the colour design and the alignment of the construction lead to different energetic behaviour? (see 4.1)
- Are the two typical types of construction (with insulating brick or with insulating mineral wool) better characterized in terms of their energetic behaviour by dynamic U-values than with stationary U-values? (see 4.2)
- Architecture: How does the extensive and consistent application of dynamic U-values affect technology and the quality of expression for a free-standing building with a uniform U-value. (see 4.3)

The development from full masonry to double-shell exposed brickwork took place in the period from 1860 to 1950. Characteristic for the developments was the successive separation into a front wall and a back wall. This began as early as the 19th century to introduce an insulating layer (the air layer) in rain-rich areas. (Fleischinger, A. F; Becker, W. A., 1859) Initially, the two layers were interlocked with an embedding brick and formed a bond. (Breymann, G. A., 1860). In the 20th century, the functional separation into two shells was accomplished with thin wire anchors. This resulted in a clear separation of functions from a building physics and structural planning point of view.

The two typical double-shell designs are described in German Industrial Standards DIN. While the two-layer masonry with insulation is a widespread construction, in the course of the dissertation only two buildings could be found in the German-speaking area that corresponded to the masonry with a layer of air: The rectory in Landshut by Neumeister Parringer Architects, however, had a mortar-mortared shell joint. Numrich Klump Architects' Atelier B. had an air layer between the two bricks and thus complies with DIN. The building 2226 by the architects was erected with two layers of light hollow bricks. As it had no outer shell made from coloured facing bricks, it was not included in the summary of buildings.

2 METHODOLOGY

A simulation program that can simulate the processes in multilayer, porous structures is used for the realistic dynamic calculation of the coupled one-dimensional heat and moisture transport within fair-faced brickwork. WUFI© Pro was developed at the University of Stuttgart (Kuenzel, H. M., 1994) and is now available in the sixth version (early 2016). When calculating the heat transport, the following transport mechanisms are taken into account:

- Heat conduction,
- Enthalpy flows through vapour diffusion with phase change,
- Short-wave solar radiation,
- Long-wave nocturnal radiation.

When calculating the steam transport, WUFI© Pro 5 takes the following transport mechanisms into account:

- Vapour diffusion,
- Solution diffusion,
- To calculate the liquid transport: capillary conduction and surface diffusion.

The simulation process is carried out as a finite volume process, which means that the laws of mass and energy conservation are better mapped than in the finite element process. It is the standard procedure in the field of building physics. The simple geometries of the building physics are adequately mapped and the advantage of the finite element method - to approximate complicated geometries more precisely - is not necessary.

The program WUFI® Pro (Fraunhofer Institute for Building Physics) uses a multitude of material properties, the orientation of buildings and the weather data from Hanover/Germany for the simulation of the dynamic U-Value. The average dynamic U-Value is created by using the results of the heating period October to April. Steady U-Values are calculated as usual using the thermal conductivity and the thickness of the layers of construction. The dynamic and the steady U-Value are compared to evaluate the difference between the results. The dynamic U-value is chosen as a benchmark to compare the results on the level of the construction to continue later with whole buildings.

3 SIMULATION

3.1 EXAMINED BRICKS

The bricks considered in this work have gross densities of 850 kg/m³ for the inner, load-bearing and insulating brick layer and 1,800 kg/m³ for the outer facing bricks. Bricks can be distinguished according to a variety of properties (Backe, H.; Hiese, W., Möhring, R., 2009). The following table shows that the division of the two-shell masonry - inside and outside - creates both optimal and less optimal properties. The low susceptibility of the outer tile to weather has an advantageous effect in this layered division. This is due to the low water absorption capacity and the low water absorption capacity, which are the result of the low porosity. In the case of clinker bricks, it is particularly low because they are sintered on the surface due to a higher firing temperature. The outer layer is therefore optimized with high density bricks, while the inner layer is subject to the paradox of good insulation properties as well as a good load bearing capacity. These two properties are directly dependent on one another: the better the brick insulates, the lower its gross density and the lower its load-bearing capacity.

MATERIAL PROPERTY	INNER BRICK ρ [850 KG/M ³]	Facing Brick ρ [850 kg/m ³]
Compressive strength	low	high
Bulk density	low	high
Heat storage capacity	low	high
Thermal conductivity	low	high
Thermal expansion	low	high
Water absorbency	high	low
Porosity	very high	low
Frost resistance	low	high
Load capacity	medium	high

TABLE 1 Material properties from bricks depending from the bulk density ρ [850 kg/m³]

Today bricks are being developed as load-bearing bricks, particularly with regard to their low thermal conductivity. In particular, since the international oil crisis in 1973, five measures have been successively introduced to reduce thermal conductivity (Fig. 2):

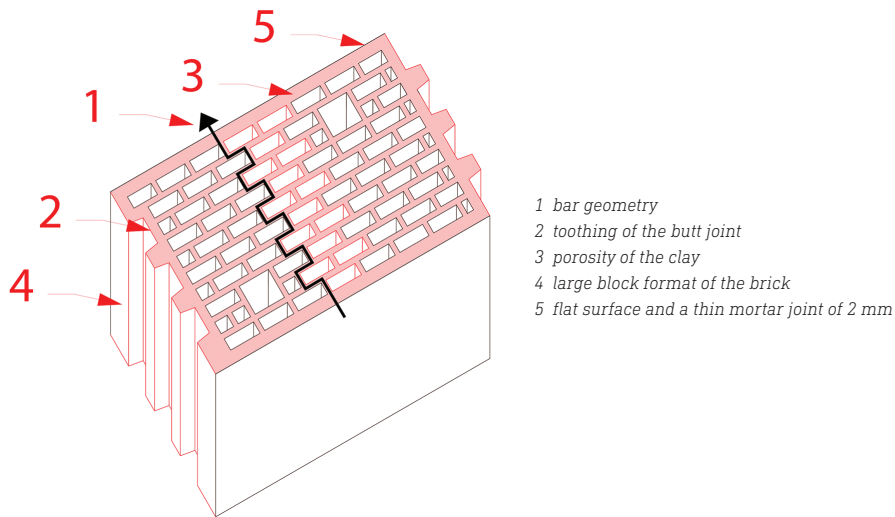


FIG. 2 Five measures to reduce thermal conductivity

Grouting can be dispensed with when interlocking the butt joint. Mortar has a higher thermal conductivity than the body. When a web geometry is formed, cavities are offset so that the heat conduction path is lengthened. At the same time, the cavities are made as small as possible. As a consequence, the number of webs increases and thus, in turn, the heat conduction path. The webs are also minimized in width. In particularly small cavities, thermal radiation makes an ever greater contribution to the transport of heat, but the advantages of the small cavities outweigh this. The total cross-section of the holes is around 50% today. The examined brick has a λ -value of 0.11 W/mK and can be used for buildings up to six storeys.

At the end of the observation period in 2013, the end of the technical possibility of further reducing the thermal conductivity of bricks: the lowest λ -value at 0.075 W/mK for two-storey houses.

3.2 TWO-SHELL CONSTRUCTION TYPES MADE OF BRICKS

If you look at the production methods for bricks and then fan out the commercially available brick products, the following possible combinations result that can be built into masonry:

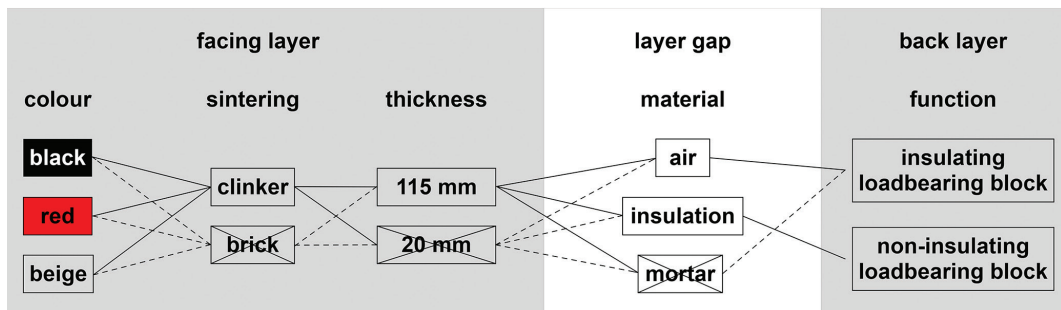


FIG. 3 Combination of commercially available brick products

From the large number of possible variations, two types of construction are selected as research objects, which are mapped in German industrial standards:

NO	TOTAL THICKNESS [mm]	LAYERS [mm]			
1	540	115 clinker	40 air	365 LHB	15 rendering
3	600	115 clinker	40 air	425 LHB	15 rendering
5	660	115 clinker	40 air	490 LHB	15 rendering

TABLE 2 Type A: Wall with insulating light hollow bricks [LHB]

NO	TOTAL THICKNESS [mm]	LAYERS [mm]				
1	520	115 clinker	20 air	140 MI	240 CB	15 rendering
3	560	115 clinker	20 air	180 MI	240 CB	15 rendering

TABLE 3 Type B: Wall with mineral insulation [MI] and clay block work [CB]

The type of heat and moisture transmission in the space between the bowls will reveal the decisive difference in the hygro-thermal behaviour. At this point, heat and moisture can pass into the back wall, which is mainly responsible for the heat-insulating function. The buildings examined were constructed with walls made of two different bricks. The bricks used were a facing brick and a lighter back brick, which had an insulating effect due to its low bulk density. Nevertheless, the division of tasks of these bricks or the shells cannot be clearly identified for the disciplines of building physics and the structure.

The structure of the masonry to be examined was determined with simulations in advance. The aim was to keep the water content in the masonry low, as this would lead to an increase in the U-value. Therefore, clinker and not brick is used: clinker is burned at higher temperatures up to the sintering limit and therefore has a lower water absorption coefficient than brick.

There is an air layer of 4 cm between the facing wall and the supporting shell. This ensures that any water that may enter is not transferred into the insulating supporting brick. Earlier constructions with shell joints mortared out meant that more water was transferred into the interior.

3.3 DATA FOR THE SIMULATION

In the following the modelling method and procedure are explained, according to which the simulations of the constructions for the determination of the dynamic values UD are carried out under complex realistic conditions. These can be categorized as follows:

- Architecture: absorption coefficient (clay colour of the outer facing bricks), orientation, height of the building
- Construction: layers of building materials
- Material properties: bulk density, porosity, heat capacity dry, 10°C, water vapour diffusion resistance, reference moisture content, free water saturation, water absorption coefficient, thermal conductivity surcharge, moisture, thermal conductivity surcharge, temp. moisture storage function
- German Weather Data for Hanover (hourly data for a complete year): Outside temperature, solar radiation (absorption of solar energy as heat), wind (dissipation of heat from the outside surfaces), precipitation (moisture penetration of the construction)

4 RESULTS

4.1 INVESTIGATION TO DETERMINE THE GENERAL DEPENDENCIES

The architectural properties are first examined, and the following statements can be made:

- Cardinal directions: The dynamic U-values depends on cardinal directions. While the values in the north and east are almost identical, they are lowest in the south and highest in the west. The west is also referred to as the weather side, since in Central Europe the wind mainly comes from the west and with it the main precipitation takes place, which has an effect on an increase in the dynamic U-value.
- Height of the building: also reflects the influence of the weather: the higher the area investigated, the higher the dynamic U-value, as both wind and rain increase with the height.
- Colour of the clinker: The colour of the clinker has the following effects: The higher the absorption coefficient, the lower the dynamic U-value.

4.2 COMPARISON OF THE INSULATED MASONRY WITH THE MASONRY CONTAINING ONLY CLAY PRODUCTS

The following question is in the foreground in this investigation: Due to this influence, the constructions 1, 3 and 5 are more likely to be mapped with U-value ranges than with specific values. In principle, the dynamic U-values are below the stationary ones, namely up to $0.07 \text{ W/m}^2\text{K}$. The constructions with $\alpha = 0.36$ are an exception: Here the mean value of the range corresponds to the stationary U-value.

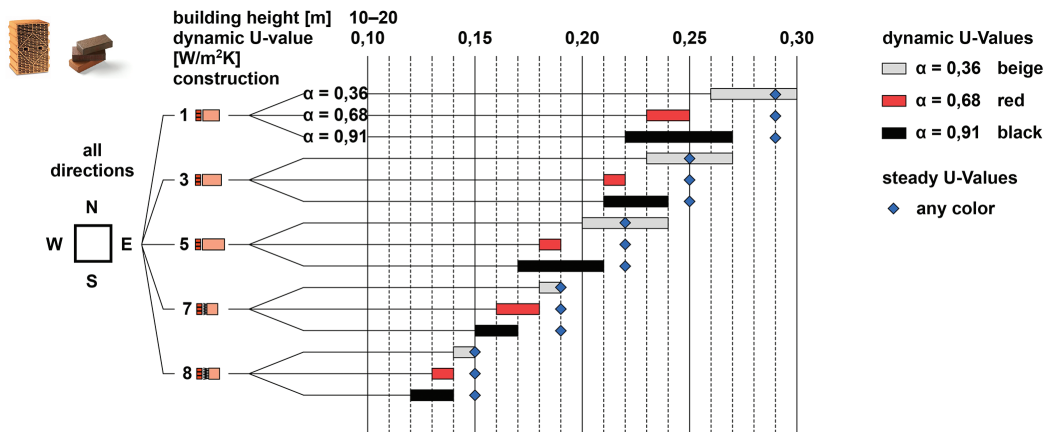


FIG. 4 Comparison: Dynamic U-values in $\text{W/m}^2\text{K}$ of walls 1, 3, 5, 7 and 8 with stationary U-values (heights of 10-20m)

Furthermore, it was investigated to what extent masonry with insulation between the load-bearing brick and the facing wall can be reproduced with dynamic U-values. It was shown that with a wall with insulation materials almost independent of the boundary conditions orientation, weather, and colour of clinker. This is because the absorbed solar energy is not conducted into the interior, as it is interrupted by the insulation, just like the reverse path from the inside to the outside. Therefore, the dynamic U-values of the insulated masonry correspond approximately to the stationary U-values.

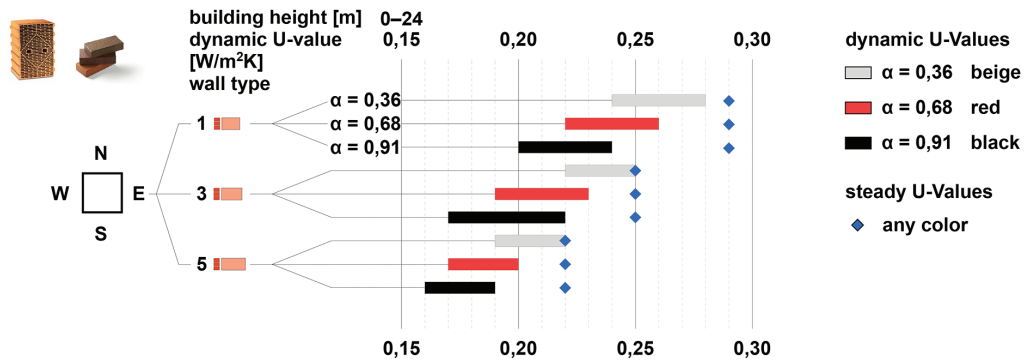


FIG. 5 Comparison: Dynamic U-values in W/m^2K of walls 1, 3, and 5, with stationary U-values (heights of 0-24m)

Constructions 1, 3 and 5 are not precisely mapped by the stationary U-value. Both the development of a range of dynamic U-values and the deviation from the stationary U-value are very large. The brightest stone with the stationary U-value is most likely to be shown. It is therefore advisable to use dynamic U-values for these constructions.

4.3 ILLUSTRATION OF THE U-VALUES ON A PROTOTYPE BUILDING

In the case of wall structures with insulating bricks, it is shown that they do not have a uniform U-value, but rather U-value ranges that depend on the brick colour, the direction of the compass, the building height and, of course, the wall thickness of the insulating brick.

The following shows how these areas can be made visible by reversing the question. With the help of a visualization of prototypical buildings with the dimensions $24m \times 24m \times 24m$, the visual effects of the investigation are shown. The following assumptions are made:

- Three height ranges are used (as specified by WUFI© Pro): 0-10m, 10-20m, 20-24m
- Every building should have a U-value between $0.18-0.19 W/m^2K$.
- The thinnest construction 3 is not used in the two lower height ranges 0–10 m and 10–20 m, unless construction 3 or 1 is available in the areas above. (Principle of tectonics)

In order to determine the variations in the façade developments for the low U-value range of $0.18-0.19 W/m^2K$, the following steps are required to create colour and construction variants:

First creation of combinations for the respective height ranges 0–10m, 10–20 m and > 20 m, second creation of combinations of floor-by-floor combination of the first combinations.

By combining four façade developments in the low storey area (0-10 m) with four others in the middle storey area (10-20m) and two in the upper storey area (> 20m), 32 different façade developments could be created. Each of the 32 combinations for the U-value range $0.18-0.19 W/m^2K$ consists of twelve façade surfaces, so that there are 384 individual façade surfaces. The qualitative evaluation shows that areas with the absorption coefficient $\alpha = 0.91$ have a share of 55.2% and the areas with the absorption coefficient $\alpha = 0.68$ a share of 37.5%. Those with the absorption coefficient $\alpha = 0.36$, however, only have a share of 7.3%. Construction 3 can only be used on the south sides and only in the absorption coefficient $\alpha = 0.91$ and 0.68 .

The 32 different façade developments are each placed as a building cubature with an edge length of 24m in an urban planning scheme. The experiment is checked using a south-east perspective and a north-west perspective.

Figures 6 and 7 show the consistent application of dynamic U-values. The south-east perspective spreads out the spectrum of eight different façade combinations, while the north-west perspective offers only four variations and only in the colours red and black.



FIG. 6 Buildings seen from south-east, $U=0.18-0.19$ W/m²K



FIG. 7 Buildings seen from north-west, $U=0.18-0.19$ W/m²K

5 CONCLUSIONS

For exterior walls with slightly high-perforated bricks: Dynamic U-Values are up to 30% lower than the stationary U-Values. The lowest dynamic U-Value is 0.16 instead of the steady U-Value of 0.22 W/

m²K for the lightest brick. For black bricks the difference is even higher: U-Value is 0.2 instead of the steady U-Value of 0.29 W/m²K.

These more realistic values are important for today's buildings but also for the existing buildings:

- 1 New Buildings can be better rated energetically and are equivalent to the highly insulated houses. However, this depends on the urban situation and the shading. Basically, it is a robust design that is very durable on the one hand and is much simpler in terms of details than the double-shell masonry with insulation on the other.
- 2 For existing buildings, low dynamic U-Values may help to prevent from external layers of insulation. The renewal of windows and building technology will be sufficient to meet the energy requirements. Here, solar radiation is particularly advantageous in the looser development of the 20th century. The building culture value of a dynamic assessment of clinker buildings should not be underestimated, especially for secular buildings.

This research demonstrates the huge advantage of robust constructions. Their simplicity makes advantage of heat transfers which was not seen since the development of functional layers for an exterior wall.

Acknowledgements

Fraunhofer Institut für Bauphysik Stuttgart, Universität der Künste Berlin, be Architekten, Neumeister Parringer Architekten, Numrich Albrecht Klumpp Architekten.

References

- Backe, H.; Hiese, W., Möhring, R. (2009). Baustoffkunde für Ausbildung und Praxis. Köln: Werner Verlag.
- Breymann, G. A. (1860): Allgemeine Bau-Konstruktions-Lehre mit besonderer Beziehung auf das Hochbauwesen. Stuttgart: J.M.Gebhardt's Verlag.
- Fleischinger, A. F; Becker, W. A. (1859): Die Mauer-Verbände: Die Mauerwerks- und Stein-Constructionen. Berlin: Verlag von Ernst & Korn.
- Kuehnast, S. (2016). Sichtziegelmauerwerk: Bauten, Konstruktionen und hygro-thermische Eigenschaften unter komplexen realistischen Bedingungen. Berlin: Dissertation Universität der Künste Berlin.
- Sedlbauer, K.P., Künzel, H.M. (2015). Feuchteschutzbeurteilung durch hygrothermische Bauteilsimulation. Bauphysik Kalender 2015, pp. 161–187.
- Künzel, H. M. (1994). Verfahren zur ein- und zweidimensionalen Berechnung des gekoppelten Wärme- und Feuchtetransports in Bauteilen mit einfachen Kennwerten, Stuttgart: Dissertation Universität Stuttgart 1994.

Skin Metrics: The Wicked Problem of Façade System Assessment



Keith Boswell¹, Stéphane Hoffman², Stephen Selkowitz³, Mic Patterson⁴

- 1 Skidmore, Owings & Merrill
- 2 Morrison Hershfield,
- 3 Lawrence Berkeley National Laboratory
- 4 Façade Tectonics Institute,

Abstract

Building façades are key to the building systems integration necessary to realize critical health, carbon, resilience and sustainability goals in buildings and urban habitat. In addition, façade system design and delivery may be the most rapidly developing building technology, with novel materials, assemblies and techniques introduced in the marketplace frequently. Yet these developments are occurring in the long-running absence of an appropriate framework for façade system performance evaluation. There has been no general convergence on the assessment criteria or, for the most part, metrics to accompany those criteria. The convergence of myriad and often competing variables that characterize the building façade mark the development of a comprehensive integrative assessment framework as a wicked problem. But the lack of such a framework inhibits meaningful development and adoption of innovative façade technology, leaving aesthetic considerations to drive application and compromising the evolution of performative system behaviour. It prohibits a meaningful comparison between façade systems, or of new techniques with prior applications. Adoption of new façade technology is constrained as designers, building owners and, most importantly, authorities with jurisdiction at the level of city government, are unable to accurately value its performative contribution to occupants, to a building project or to the urban environment.

Very early efforts and thinking in the development of a comprehensive Integrative Façade Assessment Framework by the Façade Metrics Working Group of the Façade Tectonics Institute are documented here. A preliminary review of existing façade system metrics and assessment strategies reveals they are fragmented, too narrowly focused and lack the comprehensive integration to provide an accurate evaluation. With a strong focus on energy performance in new buildings, deep and vital considerations like retrofit and renovation strategies, passive survivability, durability and service life, and resilience are often neglected entirely. We outline some new directions that begin to address these gaps and suggest a data-rich, visual framework and knowledge-sharing platform to advance progress with enhanced metrics and façade systems evaluation and comparison.

Keywords

Façades, building skin, curtain wall, building envelope, façade performance metrics, façade performance, sustainable façade systems, building resilience

DOI 10.7480/jfde.2021.1.5538

3D Printed Future Façade – Experimental Testing of a 3D-Printed Building Envelope

Moritz Mungenast

Chair of Building Technology and Climate Responsive Design, Technical University of Munich (TUM), Germany,
+49 (0)89 289 28486, moritz.mungenast@tum.de

Abstract

3D printing offers new architectural potentials in fabrication and prototyping. Small series in the small scale are already competitive and the digital chain (from digital design to final product) is closed by using less resources.

The majority of buildings are prototypes, which means their building envelope differs in size, function, orientation and climate-zone. However, how can the advantages of additive manufacturing be adapted to the macro scale, to architecture? What is the architectural outcome? 'Circular Economy', new façade materials, material savings, process optimization and energy savings are urgent topics in the building industry.

The focus of this research project is the development of a 3D-printed, translucent and functional-integrated building envelope. The objective is to evaluate the do ability of printing prototypes, which meet the quality standards and architectural design requirements. Experimental testing explores the outcome in regard of the design decisions and assumptions made in the research process.

Exerted method for the development of the first façade prototype is research by design additionally informed by façade functions, 3D-printing process restrictions of FDM process, material properties and constructive dependency. The production is an essential part of the research project to identify production problems on machine-, material- and ambient atmosphere level and to gain significant experience in the material behaviour and process technology. The experimental testing is divided into three different categories: Material testing (tension and compression), component testing (bending, U- and g-value and fire) and comparable testing (day-light-factor, self-shading and illumination) with an existing façade product to verify the overall performance and to re-feed the results in the next evolution and simulation programs.

The results of this research project led to an application of a first project at the Deutsches Museum in Munich, where the next evolution of the 3D-Printed Future Façade was designed, which passed the technical building requirements for ZiE (Zustimmung im Einzelfall). The new challenge besides performance and durability and closed material cycle is 'up-scaling' in regard of façade volume and production process and installation.

Keywords

Functional geometry, additive manufacturing, 3D printed architecture, digital fabrication, integrated façade technology, building envelope, functional integration, circular economy

PRELIMINARY REMARKS

Part 3 of the dissertation 'Development, prototyping and experimental investigation of a 3D printed, translucent and functionally integrated building envelope' by Dr.-Ing. Moritz Mungenast presents the results of part 2, the development of a functionally integrated façade element (Tomorrow-Element). Part 3 contains the following topics for the creation of the digital 3D model basis for the production and the experimental investigations:

- 1 Prototype creation: knowledge gained during the production of the façade prototype using the FDM printing process of the Tomorrow element to generate a basic knowledge of the production process for future investigations. Up to now, no component of this size and complexity has been realized with this process and material.
- 2 Component relevant tests: Various investigations of the static, building physics and fire engineering properties of the geometry development of the single element 'Tomorrow' (compression and tension and bending, U-value, g-value and fire behaviour).
- 3 Experimental comparative measurements: comparative measurements of the two elements 'Today' and 'Tomorrow' on the solar station (self-shading, luminance daylight quotient and façade surface temperature).
- 4 Long-term test: Observation of the weather influences on the surface quality.

The aim of the large number of tests in part 3 is to get first estimates of the different requirements in order to generate new knowledge for further developments. A 3D-printer from the Chair of Design and Building Envelopes at TUM is used to produce the 'Tomorrow-Element'.

The test facilities for these investigations are the façade test stand at the TUM solar station for long-term tests of the effects of weathering and for comparative measurements of the façade elements 'Today' and 'Tomorrow', the TUM wood research laboratory for compression, tensile and bending tests, the Holzforstalt Holzforschung TUM for fire tests to determine the building material class and the IFT Rosenheim for the U-value / g-value determination. The investigations at the solar station of the TUM are to be understood as potential estimations. This is related to the limited measuring equipment available and leads to an exemplary assessment within the scope of this doctoral thesis. The results shall serve to identify areas for further scientific investigations. The results and evaluations of part 3 will either confirm the hypothesis of this dissertation or point out further research foci to be investigated.

Deviations in the preparation of the test elements

After the results of part 2 showed that it is not possible to print transparent areas, the integration of the window was abandoned when creating the Today element. The ventilation openings in the Today element were also not implemented, since the test facility for comparative measurements at the solar station does not have any facilities for air exchange testing.

Research questions of part 3:

- Is it possible to produce the 3D-printed façade element on a scale of 1:1?
- What is the deviation from the 3D CAD model?
- What are the material properties of a 3D-printed component?
- Does the inherent shading function work as determined by the simulation?

In order to carry out a 1:1 scale examination of a façade element (tomorrows element) that is very complex in its geometry, it is important to select a reference façade (today element) in order to be able to produce comparative measurements.

1 PROTOTYPE CREATION

1.1 MANUFACTURING OF THE COMMERCIALY AVAILABLE TODAY-ELEMENTS, 1:1

The Today element with the dimensions 2.80 m height and 1.60 m width was manufactured according to the Rodeca system assembly instructions. The aluminium profiles were mitred and screwed together with aluminium angles. The sealing lip was clamped at the back and the Rodeca light construction elements PC-2560, d = 60mm, transparent, were shortened to the length of 2.70 m. The three light construction elements were plugged together at the vertical joints, sealed at the top and bottom with steam pressure permeable adhesive tape and placed in the frame. Aluminium clamping profiles were inserted and the sealing lip was attached. The element was fastened to the test equipment by means of aluminium brackets.

Element data: Weight without frame: 33 kg > approx. 7.5 kg/m² Total weight: 39 kg

1.2 MANUFACTURING OF THE FUNCTIONALLY INTEGRATED FAÇADE ELEMENT (TOMORROW ELEMENTS), 1:1

The production of the element was realized with commercially available material (filament) and 3D printer. In order to print the 280 x 160 cm façade element, it is necessary to segment the format according to the installation space of the 3D printer used. The maximum width of the installation space for an element with a depth of about 20 cm is about 80 cm for the Delta Tower, which also reduces the height to about 90 cm. To keep the number of joints as small as possible, a maximum size of the individual element of 74 cm width and 90 cm height was chosen. This results in six single elements for the production. The segments were connected to each other by a tongue-and-groove connection and the connecting tail was integrated into the 3D model. The individual segments were plugged in and glued and sealed with silicone. The complete façade element was then inserted into an aluminium frame identical in construction to the Rodeca element, fastened with the same clamping strips and sealed with the same sealing lips.

FDM Printer

The Delta Tower 900 was used with a cylindrical single extruder, a diameter of 90 cm and a maximum height of 100 cm.

Material

PETG was used as a transparent material, as the production of the previous cut-out models had shown that this material is easier to process than polycarbonate, but has approximately the same properties. 10 kg filament rolls were used to print one element with only one change.

Print files of the 3D models

The stl-files exported from Rhino (3D CAD program) were sliced by the Simplify slicing program into a G-code, a readable file form, for controlling the 3D printer.

1.3 PRINTING RESULTS

The print results are very heterogeneous. All six sub-elements have larger or smaller deviations. Listed in detail below is the comparison of the final element-weight with the production data by Simplify and specification of the deformations during production.

Single element 1 (bottom left) is listed here as an example:

- Size: 90cm / 65cm d = ca. 4-6cm
- Printing time: 10 days 11 hours (251 hours) as estimated
- Weight: 10.1 kg (Simplify target: 11.2 kg)
- Deformation: Very small, 3-4 mm in Z-axis at bottom left corner and bottom right
- Nozzle diameter: 1 mm, Layer height: 0.35 mm, Printing Temperature: 245 °C

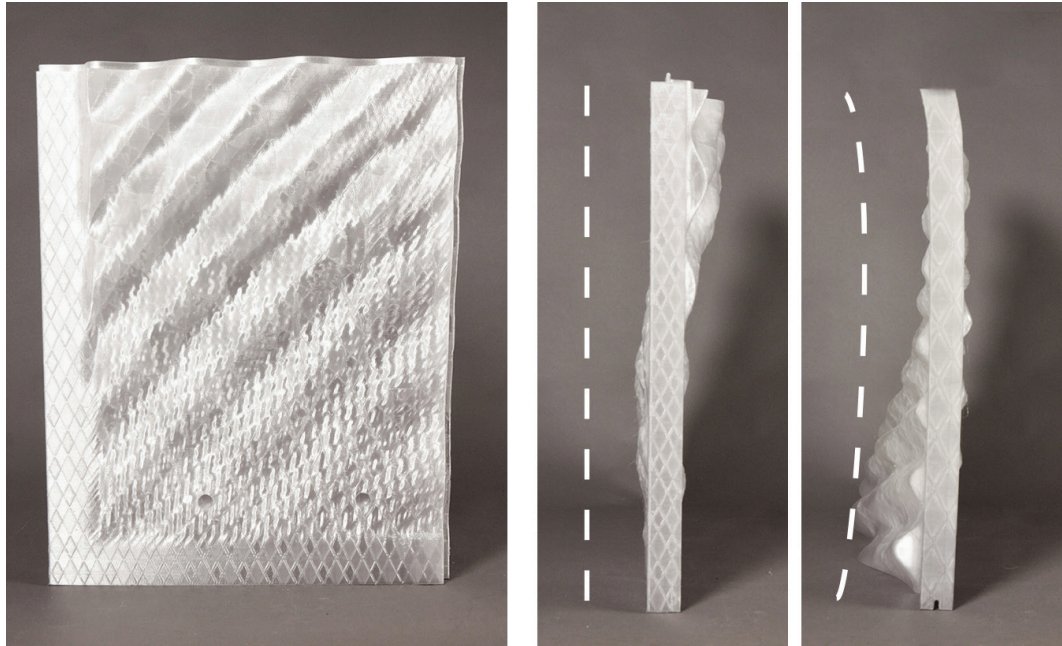


FIG. 1 Left: 3D-printed façade element M 1:1, centre: straight element, right: heavily deformed element

Conclusion

Surfaces - The quality of the surface with regard to the unity (connection) of the individual layers and the degree of reflection is very good.

Deformation - The main problem is deformation of the plastic when the printed layers cool down. In this case, these deformations are greater when more material is printed and the shape of the element has higher differences (projections). In terms of process technology, this is also due to the lack of containment and the uncontrolled ambient temperature. Small changes in the ambient temperature and air movements have a high influence on the deformation. Elements that show a low deformation could be assembled directly. In the case of more severe deformations, reworking by means of a hand milling machine was necessary.

Colour - Material differences in the colour of different batches have led to an uneven appearance of the individual elements. This is a major problem from an aesthetic point of view, as the colour spectrum is a very important issue in a translucent façade and must be controlled.

1.4 ASSEMBLY OF THE TOMORROW ELEMENT

The individual parts of the Tomorrow element were assembled in two assembly steps. The tongue and groove connection makes this necessary.

Element properties: Weight of all individual elements (without aluminium frame): 72 kg; corresponds to an average of 16 kg/m². Total weight: 78 kg



FIG. 2 Assembled façade elements M 1:1, left: Tomorrow element, right: Today element

2 COMPONENT RELEVANT TESTS

2.1 MATERIAL TESTS: TENSILE AND COMPRESSION TEST

Tensile and compression tests were carried out to investigate the material behaviour of 3D-printed PETG plastic in order to obtain an indication of its strength. The following questions had to be answered: What influence does the layer-by-layer application of the additive manufacturing method have on the tensile strength parallel or orthogonal to the tensile direction? Which compressive forces can be absorbed? Are the breaking points oriented to the layers of the additive manufacturing method?

2.1.1 Tensile Test

Test body tensile test (DIN 527): Dimensions: 20-10 mm x 6 mm x 150 mm (w x h x l),

Cross section: 10 x 6 mm = 60 mm², Weight: 15 g, (Fig. 3 + 4)

Test result tensile strength

- Orthogonal to the direction of tension: Maximum force F_{max}: 1950 N (195 kg)
- Cross section: 60 mm² Tensile strength R: 32,67 N/mm²
- Parallel to the pulling direction: Maximum force F_{max}: 2650 N (265 kg)

- Cross section: 60 mm²
- Tensile strength R: 44.17 N/mm² = 36 % additional load

[Attachment 01] Test report of the tensile test

Conclusion tensile strength

An important result was that the alignment of the layers had less influence on the strength than expected. The connection of the individual layers is very good due to the melt layer process, especially considering the advantage of material purity for recycling. The layers running orthogonal to the direction of tension can only take 36% less load.

Layer-by-layer structure: The alignment of the layers has an influence on the type of failure. With orthogonal alignment to the tensile direction, there was a fracture failure (test bodies 1 + 2) and with parallel alignment there was a strain failure (test bodies 3).

2.1.2 Pressure test

Test body compression test (Fig. 3 + 4): Dimensions: 60 mm x 60 mm x 100 mm (w x l x h), Weight: 161 g.

The compression test is the reversal of the tensile test when viewed from the direction of force. The force test is used to test building materials. In this test, the rectangular specimens (cross-sectional area 60 x 60 mm) are loaded with a continuously increasing force between two parallel compression plates. The load is increased until brittle materials break. The force applied is determined and from this the compressive strength in N/mm² is determined. The stress-strain diagram is the result of the compression test. The technical material parameters such as the compressive strength N/mm² can be read off this diagram. In order to be able to represent the compressive strength of the 3D printed façade structure, the volume of the test bodies was printed with the inner cell structure of the Tomorrow element.



FIG. 3 3D printed test specimen tensile test

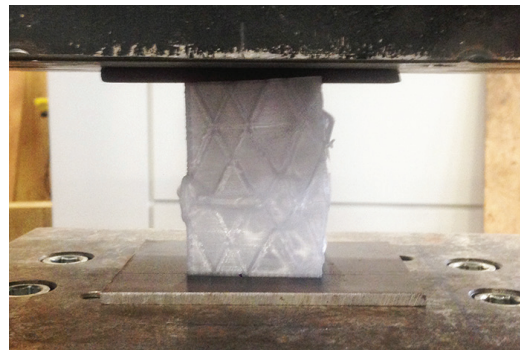


FIG. 4 3D printed test specimen compression test

[Attachment 02] Test report of the compression test

Test result Compressive strength

The test specimens withstood an average force (F_{max}) of 45,500 N (4,550 kg) before breaking. The deviation is 1.8 %.

Conclusion Compressive strength

Despite the internal cell structure, which reduces the test body to a weight of only 161 g, it is very resilient.

Layer-by-layer structure: The fracture pattern on failure shows individual fragments that come loose. Their geometry is independent of the layer pattern of the additive manufacturing method of the test body, which suggests anisotropic material properties.

The following conclusion can be drawn from these two results of the tensile and compression tests: Despite the isotropic arrangement of the layers, anisotropic material properties can be detected. This would be an advantage of the FDM process compared to other deposition processes such as paste extrusion and binding processes such as powder-binder processes, since isotropic material properties are obtained here.

2.2 COMPONENT INVESTIGATIONS

Various component tests are carried out, since the complex geometry of the façade elements makes calculations too complicated or impossible with current methods. Real tests also have the advantage that the process can be observed and new insights can be gained.

2.2.1 Bending test

The bending test is a method of destructive material testing. There are different types of bending test, the procedure is similar and they differ in the way the specimen is stored and the number of load introductions. From the recorded bending force and deflection values, different material characteristics and the stress-strain curve of the bending stress can be determined. Here the 3-point bending test is applied. The test sample is positioned on two supports and loaded in the middle with a test stamp. In the bending test, the component is examined for compression, tensile and shear forces. This arrangement of the test sample is intended to simulate the wind load or impact load on the façade. Five test specimens are tested in order to obtain a loadable average value.

Test result bending test

The test specimens withstood an average force (F_{max}) of 6180 N (618 kg) before breaking. The deviation is 3.2 %. After four tests, the test was terminated, as all four test bodies behaved approximately the same.

Conclusion bending test

Due to the internal cell structure, the component is very resilient at a weight of only 2340g.

Layer-by-layer structure: The fracture pattern on failure shows individual fragments that come loose. Their geometry is independent of the layer pattern of the test body, which suggests anisotropic material properties.



FIG. 5 Design of the experimental unit with test specimen, distributor plate and support forms

[Attachment 03] Test report of the bending test

2.2.2 Heat transfer coefficient (U-value) and total energy transmittance (g-value)

By computational methods, it was not possible to determine the U-value and g-value in advance because the irregularity of the geometry and the size of the test element of 90 x 74cm (HxW) could not be mapped by digital methods. In order to nevertheless obtain an estimation of the insulation behaviour and the energy transmission of the heterogeneous geometry of the 'Tomorrow' element, a U-value and g-value determination was commissioned from IFT-Rosenheim.

The test element for determining the U-value and the g-value is element (top right) with the outer dimensions of 74 cm width and 90 cm height. This element has different cell sizes of the inner insulation structure, which is exemplary for the determination of an average value as result for the U-value. Furthermore, this element has a pronounced wave geometry for self-shading, from which different values for the g-value can be determined.

Heat transfer coefficient (U-value)

Definition: The U-value (heat transfer coefficient) indicates the heat transfer of exterior wall constructions in W/m²K. The U-value is a specific characteristic value of a building component. It is mainly determined by the thermal conductivity and thickness of the materials used, but also by thermal radiation and convection at the surfaces. The heat transfer coefficient depends on the heat transfer coefficients between the solid body and the fluids as well as the thermal conductivity and geometry of the solid body. [1] (Wikipedia, heat transfer coefficient)

Test result

The test element achieved a U-value of: 1.6 W/(m²K) (for testing, see the IFT Rosenheim verification annex)

Classification of the result: U-values of transparent components

- Acrylic glass (plexiglass) d=5 mm: 5.3 W/m²K
- Single window d=4 mm: 5,9 W/m²K
- Insulating glazing d=2.4 cm: 2.8-3.0 W/m²K
- Heat insulation glazing d=2.4 cm: approx. 1.3 W/m²K
- Triple thermal insulation glazing: 1.1 W/m²K
- Lighting component polycarbonate clear d=6 cm: approx. 0.83 W/m²K
- Windows in passive house standard: 0,5-0,8 W/m²K

[1] (Wikipedia, heat transfer coefficient)

[Attachment 04] Cover sheet of the IFT Rosenheim heat transfer coefficient certificate

Total energy transmittance g-value

Definition: The g-value (energy transmittance) is a measure of the energy transmittance of transparent components. It indicates the percentage of energy that can reach the inside of the building, e.g. through solar radiation, where it contributes to heating. The g-value as total energy transmittance is the sum of the direct transmission of solar radiation and the secondary heat dissipation to the inside by radiation and convection. Loss is caused by reflection or absorption from or on the transparent component. The g-value takes values between 0 and 1. A g-value of 0.7 indicates that 70% of the incident energy is transmitted. [2] (Wikipedia, energy transmittance) Test result: The test element achieved a g-value of: irradiation angle 0° = 0.29; irradiation angle 60° = 0.26 (for testing see annexes proof IFT Rosenheim)

Classification of the result: g-values of glazings

- Usual single glazing: g = 0.75 - 0.87
- 3-pane composite window or 2-pane insulating glass with coating: g = 0.60
- Glass blocks or wired glass: g = 0.60
- 3-pane insulating glazing with coating: g = 0.5-0.55
- Special sun protection glass: g = 0.3-0.5
- Lighting component polycarbonate clear: g = 0.42

[2] (Wikipedia, energy transmittance)

[Attachment 05]) Cover sheet of the IFT Rosenheim total energy transmittance certificate

Result

At 1.6 W/m²K, the result of the examination of the heat transfer coefficient (U-value) just misses the requirements of the EnEV 2014/2016, which requires averaged U-values of 1.5 W/m²K for transparent exterior components and curtain walls for non-residential buildings from 2016. The result of the total energy transmittance (g-value) of 0.29 at an irradiation angle of 0° and 0.26 at an irradiation angle of 60° shows the dependence of the g-value on the position of the sun and the geometry used.

Conclusion

These results show the first important basic values, which were determined on the basis of the investigation on a prototype on a scale of 1:1 and thus form the basis for further developments of the geometry with regard to necessary insulation and sun protection requirements.

2.2.3 Fire testing

After the first tests on fire behaviour, a verification of the fire behaviour according to DIN 4102-1:1998 of the building material class B1 was carried out at the test and certification area Fire of the Wood Research Institute of the TUM. In this test, besides the material, the geometry is an important parameter for the test. For this purpose, specimens of PETG and the underlying internal structure of the 'Tomorrow' façade element were produced. The aim of this test is to find out which influence the inner geometry has on the fire behaviour and thus also on the building material class. In the course of the fire shaft test, four test specimens with the dimensions 100cm x 19cm x 6cm are directly exposed to a fire source for 10 minutes. After the fire test, the remaining length of the samples is measured, the dripping behaviour (burning/non-burning), the resulting smoke density and smoke gas temperature are analysed.

Test result fire shaft test

The test samples have a residual length of 100%, no burning dripping took place, the smoke density was with 12% very low as well as the smoke gas temperature with maximum 111°C.

Conclusion fire test

The tested elements meet the requirements of DIN 4102-1, building material class B1. The high residual length, the low smoke density and the smoke gas temperature were positive in this test. Another disadvantage is the dripping of the molten plastic, although it does not drip in a burning state. However, constructive precautions must be taken when using this material so that no persons can be injured in the event of fire.



FIG. 6 Specimens lined up after the test for determining the residual length

3 COMPARISON TEST TODAY AND TOMORROW ELEMENT ON THE SOLAR STATION

In order to carry out measurements, both façade elements, "Today" and "Tomorrow", were mounted as planned on the solar station of the TU Munich. The interior is highly insulated, and separate rooms are arranged behind each façade element to carry out independent comparative measurements. The Today element served as a reference object for the measurements on the Tomorrow element.

These measurements are intended to serve as an indicator for estimating the potential of further developments and have model character.

3.1 SELF-SHADING

Thermal Comfort - Shading of the façade is an important component of functional integration to ensure protection against overheating of translucent façades in the summer months and is thus a partial aspect of thermal comfort. The inherent shading in the summer should show the advantage of the geometry compared to the reference façade. The aim is to verify the simulated results of the self-shading for the creation of functional geometry under real conditions.

Proofs will be provided by two investigations:

- 1 a thermal imaging camera is used to compare the heat input from the inside. Thermal imaging camera: SEEK
- 2 a photographic documentation of the sun-path on a summer day shows the self-shadowing in an exemplary way.

Investigation 1

Comparison of the solar radiation in the interior of the two façade elements (Today- and Tomorrow-Element) by means of a thermal imaging camera. This investigation serves as an exemplary examination of the different geometries with regard to the reduction of solar radiation in the interior. The temperature curve on the inside of the façade elements will be investigated on a sunny summer day (June 11, 2018). The 'Tomorrow' façade element has a heterogeneous inner cell structure and the self-shading geometry is also differently shaped in some areas, which reveals different qualities of the different geometry combinations.

These can be divided into four groups: G1 (Small cell structures with self-shading), G2 (Small cell structures without self-shading), G3 (Large cell structures with inherent shading) and G4 (Large cell structures without self-shading). The 'Today' façade element is homogeneous in its geometry.

Result

Due to the projections and the resulting shading, the surface temperature in these areas is lower. The thermal images show a difference of 2 to 3°C.

Conclusion

Although the same solar radiation hits the same area of the façade made of transparent material, the geometry developed shows that the absorbed heat is not transferred in equal parts to the inner surface. The larger number of cells in the solar control area insulate better towards the interior. The more translucent areas where more solar radiation can penetrate have a lower cell count to allow more daylight in. However, these cells are shaded by the sun protection geometry in summer. The chosen approach shows the desired results as well as the potential to further develop this strategy.

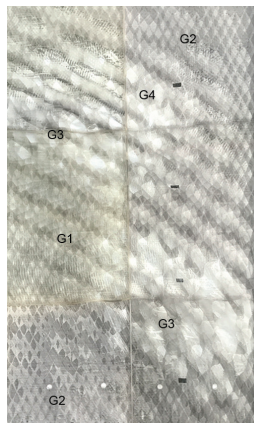


FIG. 7 Tomorrow-Element heterogeneous façade geometry
 Left: Image interior view of different areas of interior structure G1-G4
 Right: Image of surface temperature inside

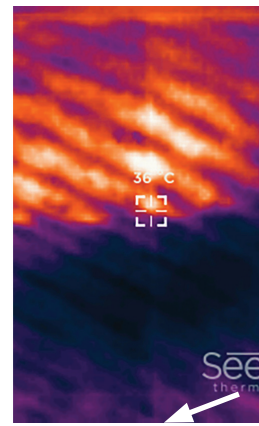
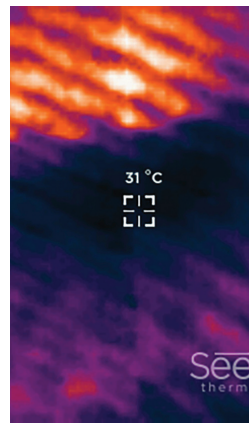
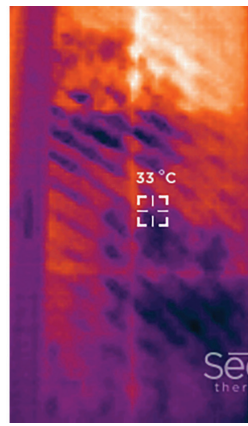


FIG. 8 Close-up of self-shading
 Thermal images of the surface in the inner area of the shading geometry
 Left: Shading range surface temp. 31°C ;
 Right: Exposure range surface temp. 36°C

Result

The images of the thermal imaging camera show the maximum heat input in the area G4 (large cell structures without self-shading) followed by G2 (small cell structures without self-shading). G1 and G3 (large and small cell structures with self-shadowing) have the lowest heat input. Shading is achieved by the protrusions of the wave geometry, and the higher number of cells in the inner structure allows better absorption of solar radiation due to the increased mass. Therefore the surface temperature in these areas is lower than in the other areas. The thermal images show a temperature difference of 2 to 5°C between shaded and unshaded areas.

Conclusion

Although the same solar radiation hits the same area of the façade made of transparent material, the geometry developed shows that the absorbed heat is not transferred in equal parts to the inner surface. The larger number of cells in the solar control area insulate better towards the interior. The more translucent areas, where more solar radiation can penetrate, have a lower cell count to allow more daylight in. However, these cells are shaded by their own shading geometry in summer. The chosen approach shows the desired results and the potential for further development of this strategy. However, the wave geometry could still be used in larger areas to achieve more effective shading. The choice to use a radial (curved) wave geometry also proves to be advantageous because a larger period of self-shading is covered than with a linear geometry. Nevertheless, the self-shading geometry would also have to be applied in the sub-areas whose geometry is flattened in order to achieve the maximum shading. This would have to be considered individually and adapted to the requirements of the respective use.

3.2 FAÇADE SURFACE TEMPERATURE ON THE INSIDE

Thermal Comfort - The surface temperature of the façade in the interior is part of the thermal comfort. Surfaces that have a high difference to the room temperature are perceived as disturbing, especially in summer they contribute to increased heat sensation, similar to a radiator. In winter, cold surfaces create a drop in air and thus drafts. This study shows the surface temperature differences of the two elements.

Measurement setup

The surface temperature is measured 20 cm from the vertical centre axis of the façade from bottom to top at intervals of 50 cm. The average temperature of the surface is calculated from the individual

results. This is especially necessary because the 'Tomorrow' element has a heterogeneous structure and therefore temperature differences occur. The outside surface temperature was also recorded simultaneously with the same method.

Records were recorded on several sunny and cloudy days and then the average values were calculated to obtain representative results. This study is to be understood as a model, since only a relatively short period of time was available for the measurements. Measurements to determine the operative temperature and collect it over a long period of time would be the next step.

Recording period: 16.04. - 04.05.2018, Measuring device for surface temperatures: Voltcraft Dual Laser IR-SCAN-350RH/2The

Examination 1: 'sunny'

The temperature difference in favour of the façade surface on the inside is on sunny days:

09:00 h = 2.3 °C; 13:00 h = 5.1 °C; 17:00 h = 2.8 °C

The interior temperature difference is: 09:00 h = 1.4 °C; 13:00 h = 1.3 °C; 17:00 h = 2.5 °C

Examination 2: 'cloudy'

The temperature difference of the façade surface on the inside is on cloudy days:

09:00 h = 0.8 °C; 13:00 h = 1.8 °C; 17:00 h = 1.8 °C

The interior temperature difference is: 09:00 h = 0.4 °C; 13:00 h = 1.0 °C; 17:00 h = 0.8 °C

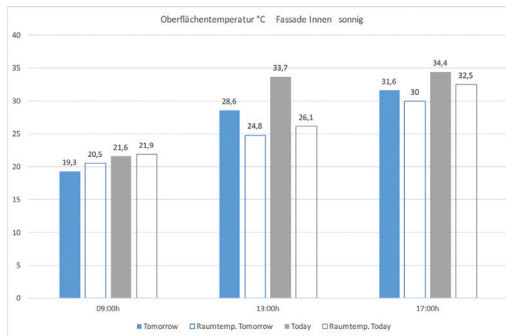


FIG. 9 Examination 1, surface temperature comparison test Tomorrow and Today element; average temperature value of the inner surface of the façade in sunshine

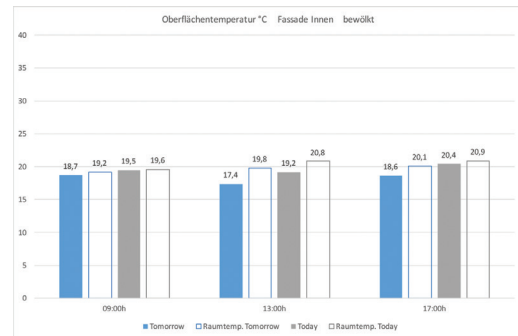


FIG. 10 Examination 2, surface temperature comparison test of Tomorrow and Today element; average temperature value of the inner surface of the façade under cloudy conditions

Result

The temperature of the Tomorrow element is on average 2.8 °C lower than the Today element. On sunny days the temperature difference of 5.1°C was measured on the façade surface. There is a significant effect on the room temperature of 2.5°C difference at 17:00. On cloudy days this temperature difference is lower and is 1.8°C at noon and afternoon.

Conclusion

This temperature difference shows that the Tomorrow element emits less solar radiation to the interior. However, one should not forget that the mass of the Tomorrow element is twice as high as that of the Today element. The inherent shading of the Tomorrow element during the radiation-intensive period from 12 to 15 o'clock also suggests a positive effect, as shown by the thermal imaging camera.

3.3 ILLUMINANCE

Visual Comfort - The aim is to achieve visual comfort by evenly illuminating the interior. The 'Tomorrow' element is translucent despite the use of a transparent material. This means that light can enter but cannot be seen out as with transparent glazing - it is characteristically a "frosted glass pane". Characteristic values for visual comfort are, for example, 300 lux illuminance as a minimum for computer workstations, 500 lux for workstations with normal office activity. The upper limit of illuminance is approx. 4000 lux, then we speak of glare, which must be prevented. Visual comfort depends on many parameters and is also subject to the subjective perception of the individual user.

The 'Today' element, although also made of the transparent material polycarbonate, is also not transparent. According to the manufacturer, it has a light transmission of 41%. Due to the homogeneity of the Rodeca façade, the light transmission is evenly distributed over the entire element. This does not apply to the Tomorrow element, as its diameter and internal structure are heterogeneous. Simulations for such a geometry are currently still too complex. In order to obtain realistic results, measurements of the façade element are necessary. The illuminance is measured at different measuring points, which are positioned on the floor in steps of 50 cm orthogonal to the façade (Fig. below). The results of this investigation have model character and shall show the potential for further investigations.

Measurement setup of the investigation of the illuminance in the interior

- Recording period: 16.04. - 04.05.2018
- Measuring interval: morning 9:00 h; noon 13:00 h; evening 17:00 h
- Interior measurement: The measuring points for recording the illuminance are placed orthogonally on the floor at 0.5 m intervals in the centre of the façade.
- Exterior measurement: Horizontal 1 m distance to the façade at a height of 1 m
- Measuring instrument: Hand-held illuminance meter Voltcraft MS-200LE

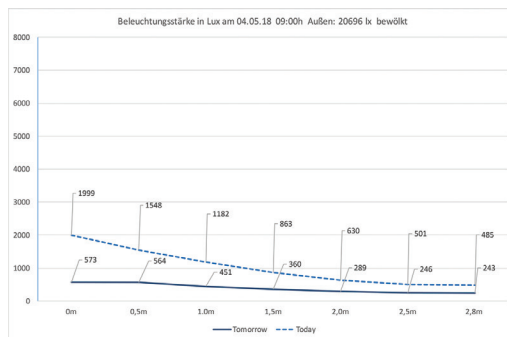


FIG. 11 Illuminance comparison test Tomorrow and Today element 09:00 a.m. under cloud cover

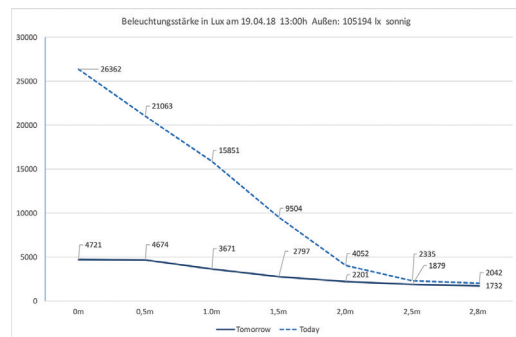


FIG. 12 Illuminance comparison test Tomorrow and Today element 13:00 a.m. in sunshine

Result

The tests show that the Tomorrow element allows less daylight to enter the interior compared to the Today element. This is also clearly visible when comparing the daylight quotient (see following paragraph).

Conclusion

The Tomorrow element buffers extreme light input compared to the Today element. You can see from the diagrams that the 'Tomorrow' element illuminates the room more evenly and prevents high solar gain in the interior. In measurement results 4 and 6, the 'Today' element far exceeds the unpleasant

illumination levels that occur in sunshine when the sun is shining, which occur from about 4000 lux upwards. The values for the Tomorrow element, on the other hand, are in the permissible or comfort range. The disadvantage of the 'Tomorrow' element is that it falls below 500 lx in the range from 2 m distance under cloudy skies and in the morning (see measurements 1, 2 and 3).

The daylight quotient is given in percent without unit and generates values that make different systems comparable by referring to the external illuminance. DIN 5034 requires a minimum daylight quotient TQ of 0.75% to 1% in living and working spaces, DIN 5034. Definition: The daylight quotient (TQ) sets the level of internal illuminance in relation to the external horizontal illuminance in an unshaded position.

The Tomorrow element has a two-thirds lower daylight quotient compared to the Today element. The result is above the minimum requirements of [3] DIN 5034.

- Calculation: $TQ = (E_p / E_a) * 100 (\%)$
- E_a Outdoor illuminance on 05/04/2018: $E_a = 20696 \text{ lx}$
- E_p Illuminance inside:
- **Tomorrow element: $E_p = 370 \text{ lx} > TQ = 1.8$**
- Today element: $E_p = 1277 \text{ lx} > TQ = 6.2$

Conclusion

Additive manufacturing enables the production of translucent façade elements with a sufficient daylight quotient. The exact adaptation to the different requirements can be adjusted via the geometry, the inner structure and the diameter of the façade element.

4 LONG-TERM TESTS ON THE SOLAR STATION

4.1 WEATHER AND UV RESISTANCE PETG TEST PIECE

In order to obtain a reliable assessment of the UV resistance (yellowing) and soiling of the surface, a test body was exposed to the open weather for nine months at the solar station. For comparison, two test bodies were produced in one production process. The second test specimen was not exposed to UV radiation during these nine months.

Test setup - Location: Solar station TU Munich, south facing, fully weathered; Duration: 2017-09-14 - 2018-06-12

Result

Test body 1 showed a strong yellowing due to UV radiation. Contamination of any kind, such as algae or lichen formation or residues of dust cannot be detected. The surface is still highly reflective.

Conclusion

In order to achieve a satisfactory long-term effect of the 3D printed surface of PETG, UV protection must be integrated. An examination of embrittlement, which can lead to static impairments, was not covered by this test.

4.2 CONDENSATION AND CONTAMINATION TOMORROW ELEMENT

Measurement setup: Location: Solar station TU Munich, SSW-alignment, fully weathered; Duration: 21.03.2018 - 04.04.2019

Condensation was observed in the early morning hours of both test elements (today and tomorrow element) (Fig. 13 + 14). Polycarbonate and PETG are both diffusion-open plastics. In the 'Today' element, the condensate can drain off downwards through the arrangement of the vertical tubes of the inner structure. The cell structure of the 'Tomorrow' element does not allow condensation to drain off. It can be seen that the condensate is only produced in the cells which have direct contact to the outer surface. No condensate can be seen in the inner cells.

Due to the constant moisture development in the outer cells, soiling or algae formation can be seen in some areas of individual elements. It is unclear, however, why in some cells no algae formation or contamination occurs despite the loss of condensation water as in single element E3, E4 and E6. A possible answer can easily be found in the production quality and processing environment. Trapped dust particles or pollen etc. could contribute to algae formation and contamination when exposed to moisture. These different contamination states V1 – V3 (Fig. 15) can be seen in the figures on the left. However, the formation of condensation has not led to visible impairments of the 3D-printed surface. No cracks or chipping caused by freezing condensation water occurred.



FIG. 13 Today-Element condensation

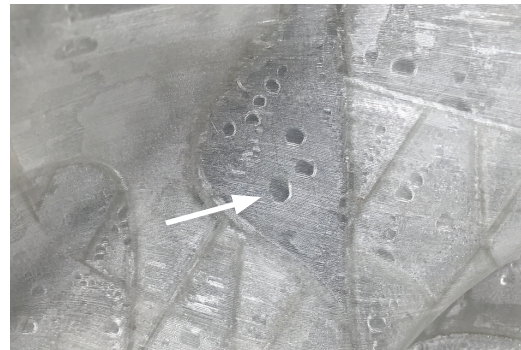


FIG. 14 Tomorrow-Element condensation in the cells with direct contact to the outer surface



FIG. 15 Left, middle, right: Tomorrow-Element contamination / Algae formation through condensation in the cells

Conclusion

This problem of condensation formation can lead to problems especially in the winter months when the condensate freezes. In general, the internal contamination due to algae formation is to be seen very critically, since cleaning is not possible.

5 EVALUATION MATRIX OF THE EXEMPLARILY TESTED PROPERTIES FROM PART 3

In order to be able to carry out an overview of the various investigations and an evaluation, this matrix shows the various test and investigation results.

Legend (evaluation parameters of the results): + = good o = satisfactory - = unsatisfactory

* Test specimens of the Rodeca light building element were placed in the same test facility, the test specimens proved to be too flexible to withstand the loads introduced.

INVESTIGATIONS	TOMORROW ELEMENT	TODAY ELEMENT
Material testing		
Tension	+	xxxx
Compression	+	(-)*
Transparency	-	(o)*
Building component testing		
Bending	+	(-)*
U-Value	-	+
g-Value	+	-
Fire resistance	+	++
Comparative measurements		
Self -Shading	+	-
Surface temperature	+	-
Illuminance	o	o
Daylight quotient	o	o
Long-term testing		
UV-resistance	-	+
Condensation	-	+

TABLE 4 Evaluation matrix of the test and investigation results

6 RESULT

Mechanical testing - The 'Tomorrow' element shows good static properties in the compression test compared to the 'Today' element. The disadvantages of the layer-by-layer structure through additive manufacturing are minor, because the fracture patterns are not based on the layers.

Building components testing - In the bending test, the 'Tomorrow' element shows surprisingly good values, which can be explained by the internal cell structure and the double-curved surfaces. The determined U_p -value (U-value only for the panel) of the 'Tomorrow' element is $1.6 \text{ W} / \text{m}^2\text{K}$ and is thus significantly worse than the 'Today' element with a value of $0,71 - 0,77 \text{ W} / \text{m}^2\text{K}$ (manufacturer information). On the part of the 'Tomorrow' element, this is related to the sometimes relatively large cells of the internal structure.

The g-value (energy transmittance) is significantly lower for the 'Tomorrow' element, although both versions are made from a transparent base material. This is the result of the various production methods, with the 'Tomorrow' element the light is refracted several times due to the layered structure. Here, depending on the angle of incidence from 45 to 60° , the value is approx. 20% and for the "Today" element approx. 42%.

The fire behaviour of both materials is similar, the PETG used for the 'Tomorrow' element is more easily flammable and drips, but nevertheless achieved building material class B1 in the fire test according to DIN 4102.3.

Comparative-measurements - The self-shading of the 'morning' element leads to a different façade surface temperature inside and to a different illuminance. This is also reflected in the daylight quotient. The results of the investigation of the illuminance in the interior have shown advantages and disadvantages for both elements. The 'Tomorrow' element leads to an equal illumination of the interior, but shows lower values (below 500 lx) according to ASR in the interior in the event of low sun exposure. Opposite behaviour is investigated to the values of the 'Today' element, since there is glare on sunny days, but the correct values of the ASR are reached at low sun exposure.

Long-Term testing - UV resistance / condensation: the 'Today' element does not have any problems in terms of UV resistance and condensation drainage, the weak points of the 'Tomorrow' element belong to these topics.

7 CONCLUSION AND OUTLOOK

The central question of this work "Can a functionally integrated building envelope be developed by using additive manufacturing?" can be answered as follows:

The integration of different façade functions such as solar shading, insulation, wind and dead load transfer, ventilation, day-lighting and acoustic dispersion was possible and could even be implemented using a transparent material. The results in the implementation of the individual functions can be evaluated differently. Positively can be noted, that the strengths of the additively manufactured components were better than expected due to the FDM printing process, especially in the bending-test. Self-shading was found to be feasible and effective. The reduction of room temperature and façade surface temperature inside in summer when the sun is shining can be attributed to it. Satisfactory are the insulation properties and illumination have confirmed assumptions, but still show room for improvement. Negatively has to be stated the production of transparent surfaces for visual connection between the interior and exterior is not possible with this method at this stage, even with post-processing. Another negative outcome, the formation of condensation cannot be avoided with this type of façade and, in the cellular variant, leads to soiling and algae formation over longer periods. Effective solutions must be found for this. The functional areas of acoustic scattering and natural ventilation could be integrated but not yet investigated in this study.

In general, the results of the investigation show that the achievement of the four comfort parameters for an efficient façade - thermal comfort, acoustic comfort, visual comfort and the supply of fresh air - can be achieved by an additively manufactured building envelope.

Process reliability - When it comes to manufacturing the façade elements, in terms of execution quality and manufacturing time, the problem of non-uniform material properties and low process reliability is still a risk factor for process reliability that should not be underestimated. The use of the FDM-Delta system was sufficient for the production of a prototype, but is not target-oriented for further development in this design.

Material - The change from polycarbonate to PETG has proved to be a sensible move, as it has simplified processing during manufacture. UV resistance, fire behaviour and vapour diffusion openness are problem areas that still need to be solved.

Architectural design -The freedom that additive manufacturing brings to the development of new architectural design possibilities was exemplified here. Despite some limitations, the design potential cannot be dismissed out of hand.

The methodology 'Research by Design' used has proven to be purposeful and has led to satisfactory results that can be used as a basis for further developments.

The previously established hypothesis of this dissertation thesis "Additively manufactured and functionally integrated building envelopes make, with the same performance, the technical façade equipment superfluous" cannot yet be confirmed for all functions after this investigation. However, the results of the investigation suggest that it is possible to reduce the use of technical façade components. It has been proven that additive manufacturing can be used to produce complex functional geometries for façade applications. These can be implemented in one manufacturing step and with one material. This confirms the predicted potential for the building envelope.

The exemplary investigations show the potential and the function which still need to be improved of the 'To-morrow' element. In the field of mechanical properties, reaction to fire, one can be confident to generate the required properties. The building physics properties can be improved through the adaptation of the geometry as required. The negative results in the field the long-term tests of this first prototypes can be found in regard of UV resistance and the problem of condensation, already found solutions of the 'Today' element classify these problems as solvable.

Future challenges - In order to contribute to the implementation of Agenda 2030, further development is strongly dependent on material and process development. Manufacturing time and material properties, such as durability and fire behaviour are essential factors in the development of a marketable building product.

Design tools also need to be further developed. The simulation of complex functional geometries and their integration into function-integrated façades will initially only be possible by means of studies on real models in order to generate basic data that will in turn allow the future simulation of the desired functions. This is necessary to make full and effective use of this type of façade planning and execution of 'design to product'.

The development for new certification tools for 3D Printed Building-Components on national and international standards not only to certify a single design and function but to certify a certain range of a building product where the freedom of design and functionality can be fully exploited without having to pass each time a new certification process.

The search for new architectural expressions in ornamental and functional applications will be a future journey yet to be heavily explored and closely linked to the new developments of AM-processes, materials and environmental influences.

Prospect – Research-project in industrial scale. The results of this research project led to an application of a first-project at the Deutsches Museum in Munich, where the next evolution of the 3D-Printed Future Façade was designed (design by 3F Studio), which passed the technical building requirements for ZiE (Zustimmung im Einzelfall). The new challenge besides performance and durability and closed material cycle is 'up-scaling' in regard of façade volume and production process and installation.



FIG. 16 Final Prototype of 3D Printed Future Façade



FIG. 17 Research project – Façade of the Future Deutsches Museum (Façade-design by 3F Studio)

References

- [1] (Wikipedia, Wärmedurchgangskoeffizient) <https://de.wikipedia.org/wiki/Wärmedurchgangskoeffizient>
- [2] (Wikipedia, Energiedurchlassgrad) <https://de.wikipedia.org/wiki/Energiedurchlassgrad>
- [3] DIN 5034: „Tageslicht in Innenräumen“

Literature list

- Ferry, J. D. (1980). Viscoelastic properties of polymers, 3rd Ed. New York: Wiley.
- Knaack, U., Klein, T., Bilow, M., & Auer, T. (2014). Façades, Principles of construction. Basel: Birkhäuser Verlag GmbH.
- Kuntsche, J., & Schneider, J. (2014). Experimental and numerical investigation of the mechanical behaviour of explosion resistant glazing. Proceedings of engineered transparency 2014, pp. 219-225.
- Young, R. F. (2007). Crossing boundaries in urban ecology: Pathways to sustainable cities (Doctoral thesis). Retrieved from ProQuest Dissertations Thesis database. (UMI No. 327681). For more information see: <http://www.library.cornell.edu/resrch/citmanage/apa>
- Badarnah, L., & Kadri, U. (2015). A methodology for the generation of biomimetic design concepts. Architectural Science Review, 58(2)
- Strauss, H. (2013). AM Envelope – the potencial of Additive Manufacturing of façade construction. TU Delft, (Dissertation)
- Nachtigall, W. (2005). Biologisches Design Systematische KAtatlog fü bionisches Gestalten. Springer, (Book)
- Knippers, J., Gabler, M., & Lienhard, J. (2010). Atlas Kunststoffe+Membranen. Basel: Birkhäuser Verlag Edition Detail, (Book)
- Herzog, T., Krippner, R., & Lang, W. (2004). Fassaden Atlas. Basel: Birkhäuser Verlag Edition Detail, (Book)

Acknowledgement

The following student was part of the production and testing team: Luc Morrioni

Figure credits

Fig. 2 + 16 TUM / Heddergott

Fig. 17 Visualization by nuur

All other figures by the author

Appendix

- Attachment A Test report of the tensile test
- Attachment B Test report of the compression test
- Attachment C Test report of the bending test
- Attachment D Cover sheet of the IFT Rosenheim heat transfer coefficient certificate
- Attachment E Cover sheet of the IFT Rosenheim total energy transmittance certificate
- Attachment F 2.1.1 Material Test: Material, dimensions and production of test specimens
- Attachment G 2.2.1 Bending Test: Material, dimensions and production of test specimens



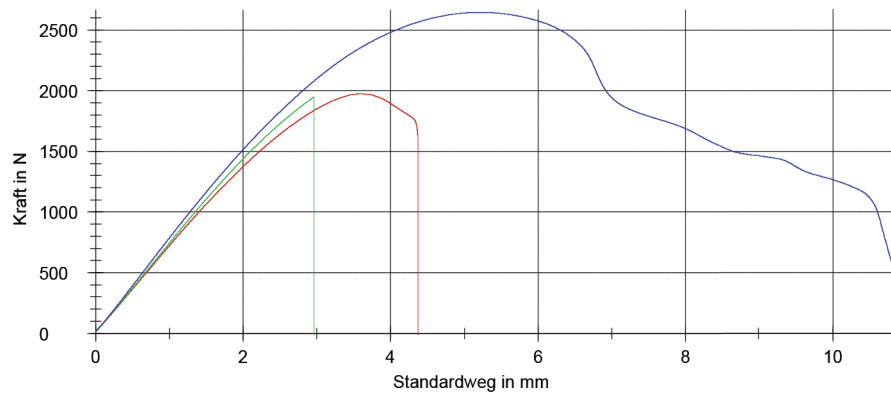
Prüfprotokoll

Vorkraft : 5 N
 Prüfgeschwindigkeit : 0,6 mm/min

Prüfergebnisse:

Nr	F _{max} N	dL bei F _{max} mm	F _{Bruch} N	dL bei Bruch mm
1	1970	3,6	1560	4,4
2	1950	3,0	1950	3,0
3	2650	5,2	529	10,8

Seriengrafik:



Statistik:

Serie	F _{max} N	dL bei F _{max} mm	F _{Bruch} N	dL bei Bruch mm
n = 3				
\bar{x}	2190	3,9	1340	6,1
s	396	1,2	733	4,2
v [%]	18,06	29,79	54,52	69,29



13.06.17

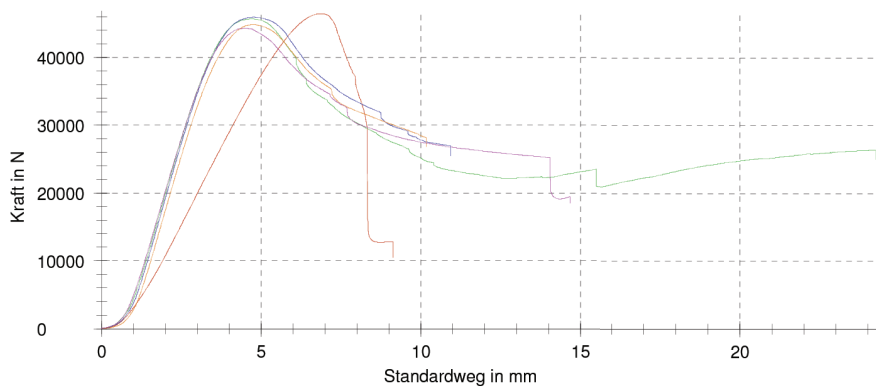
Prüfprotokoll

Vorkraft : 20 N
 Prüfgeschwindigkeit : 5 mm/min

Prüfergebnisse:

Nr	F _{max} N	dL bei F _{max} mm
1	46500	6,9
2	45700	4,7
3	45900	4,8
4	44900	4,8
5	44300	4,5

Seriengrafik:



Statistik:

Serie n = 5	F _{max} N	dL bei F _{max} mm
\bar{x}	45500	5,1
s	854	1,0
V [%]	1,88	19,34



03.05.18

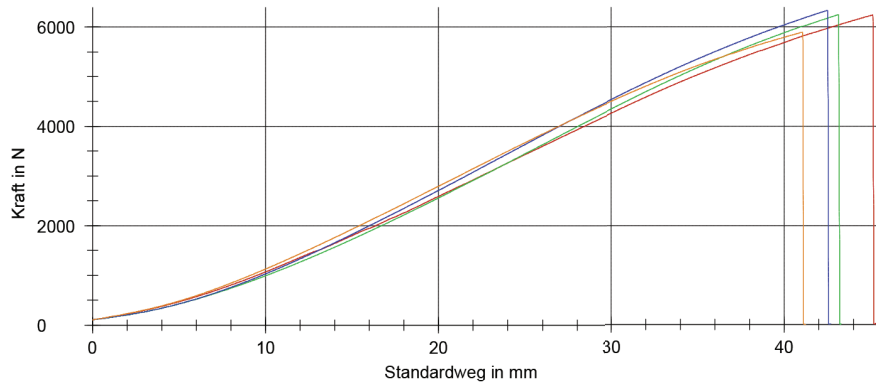
Prüfprotokoll

Kunde : Probentyp :
 Auftrags-Nr. : Vorbehandlung :
 Prüfnorm : Prüfer :
 Art und Bezeichnung : Bemerkung :
 Werkstoff : Maschinendaten :
 Probenentnahme :
 Vorkraft : 100 N
 Prüfgeschwindigkeit : 0,5 mm/s

Prüfergebnisse:

Legende	Nr	F _{max} N	dL bei F _{max} mm	F bei Bruch N	dL bei Bruch mm
	1	6240	45,1	6080	45,1
	2	6250	43,1	6060	43,2
	3	6330	42,5	6330	42,5
	4	5890	41,1	5730	41,1
	ϕ 5	4560	44,8	-	-

Seriengrafik:



Statistik:

Serie n = 4	F _{max} N	dL bei F _{max} mm	F bei Bruch N	dL bei Bruch mm
\bar{x}	6180	43,0	6050	43,0
s	195	1,7	246	1,7
v [%]	3,16	3,92	4,06	3,92

APPENDIX D COVER SHEET OF THE IFT ROSENHEIM HEAT TRANSFER COEFFICIENT CERTIFICATE

Nachweis Wärmedurchgangskoeffizient

Prüfbericht
Nr. 18-002496-PR07
(PB 01-H07-06-de-01)



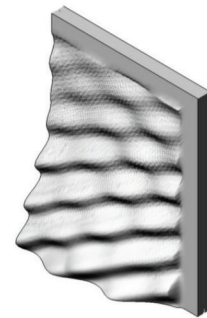
Auftraggeber Technische Universität München
Fakultät für Architektur
Professur für Entwerfen und Gebäudehülle
Arcisstr. 21
80333 München
Deutschland

Grundlagen *)

EN ISO 12567-1:2010-07

*) und entsprechende nationale Fassungen (z.B. DIN EN)

Darstellung



Weitere Darstellungen siehe Anlage 1.

Produkt **Panel**

Bezeichnung Bauobjekt: Eingangsbereich des Deutschen Museums München

Leistungsrelevante Produktdetails Abmessungen; Breite in mm 704; Länge in mm 896; Gesamtdicke in mm ca. 60 am Paneelrand (2 Kanten); Aufbau Dreidimensional geformtes Paneel mit strukturierter Deckschicht und Hohlkammern (weitere Informationen siehe Anlage 1); Material Polyethylene - Terephthalate - Glycol „extrudr PETG“; Flächengewicht in kg/m² 22,0 (Messwert)

Besonderheiten --

Ergebnis

Wärmedurchgangskoeffizient in Anlehnung an
EN ISO 12567-1:2010-07



$$U = 1,6 \text{ W/(m}^2\text{K)}$$

Verwendungshinweise

Die ermittelten Ergebnisse können für den Nachweis entsprechend den oben angegebenen Grundlagen verwendet werden.

Gültigkeit

Die genannten Daten und Einzelergebnisse beziehen sich ausschließlich auf den geprüften/beschriebenen Probekörper. Diese Prüfung/Bewertung ermöglicht keine Aussage über weitere leistungs-/qualitätsbestimmende Eigenschaften des Produkts; insbesondere Witterungs- und Alterungseinflüsse wurden nicht berücksichtigt.

Veröffentlichungshinweise

Es gilt das "Merkblatt zur Benutzung von ift-Prüfdokumentationen". Das Deckblatt kann als Kurzfassung verwendet werden.

Inhalt

Der Nachweis umfasst insgesamt 5 Seiten und Anlagen (3 Seiten).

ift Rosenheim
20.08.2019

Konrad Huber, Dipl.-Ing. (FH)
Prüfstellenleiter
Bauphysik

Stefan Junker, Dipl.-Ing. (FH)
Prüfingenieur
Bauphysik

Ve-PB0-1190-de ()

ift Rosenheim GmbH
Theodor-Giell-Str. 7-9
D-83026 Rosenheim

Kontakt
Tel. +49 8031 261-0
Fax +49 8031 261-290
www.ift-rosenheim.de

Prüfung und Kalibrierung – EN ISO/IEC 17025
Inspektion – EN ISO/IEC 17020
Zertifizierung Produkte – EN ISO/IEC 17065
Zertifizierung Managementsysteme – EN ISO/IEC 17021

Notified Body 0757
PUZ-Stelle: BAY 18



APPENDIX E COVER SHEET OF THE IFT ROSENHEIM TOTAL ENERGY TRANSMITTANCE CERTIFICATE

Nachweis

Gesamtenergiedurchlassgrad

Prüfbericht

Nr. 18-002496-PR07

(PB02-H07-07-de-01)

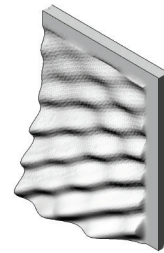


Auftraggeber **Technische Universität München
Fakultät für Architektur
Professur für Entwerfen und Gebäudehülle
Arcisstr. 21
80333 München
Deutschland**

Grundlagen

Hausverfahren „Kalorimetrische Bestimmung des Gesamtenergiedurchlassgrades g“ 2002-06

Darstellung



Verwendungshinweise

Dieser Prüfbericht dient zum Nachweis des Gesamtenergiedurchlassgrades g bzw. g_{total} des Probekörpers. Hierbei handelt es sich um den „center-of-glazing“-Wert. Einflüsse des Randverbundes wurden nicht berücksichtigt. Die Werte beziehen sich auf direkten Strahlungseinfall, diffuse Strahlung ist gesondert zu berücksichtigen.

Produkt	Panel
Bezeichnung	Bauobjekt: Eingangsbereich des Deutschen Museums München
Leistungsrelevante Produktdetails	Abmessungen; Breite in mm 704; Länge in mm 896; Gesamtdicke in mm ca. 60 am Paneelrand (2 Kanten); Aufbau Dreidimensional geformtes Panel mit strukturierter Deckschicht und Hohlkammern (weitere Informationen siehe Anlage 1); Material Polyethylene - Terephthalate - Glycol „extrudr PETG“; Flächengewicht in kg/m ² 20,0 (Messwert)
Besonderheiten	--

Gesamtenergiedurchlassgrad g



Einstrahlwinkel	0°	60°
g	0,29 ± 0,05	0,26 ± 0,05

ift Rosenheim
20.08.2019

Manuel Demel, M.BP, Dipl.-Ing. (FH)
Stv. Prüfstellenleiter
Bauphysik

Konrad Huber, Dipl.-Ing. (FH)
Prüfingenieur
Bauphysik

Gültigkeit

Die genannten Daten und Ergebnisse beziehen sich ausschließlich auf den geprüften und beschriebenen Gegenstand.

Die Prüfung der strahlungsphysikalischen Kenngrößen ermöglicht keine Aussage über weitere Leistungs- und qualitätsbestimmenden Eigenschaften der vorliegenden Konstruktion.

Veröffentlichungshinweise

Es gilt das ift-Merkblatt „Bedingungen und Hinweise zur Benutzung von ift-Prüfdokumentationen“. Das Dokument kann nur vollständig verwendet werden.

Inhalt

Der Nachweis umfasst insgesamt 8 Seiten

- 1 Gegenstand
- 2 Durchführung
- 3 Einzelergebnisse

ift Rosenheim GmbH
Theodor-Gietl-Str. 7-9
D-83029 Rosenheim
Kontakt
Tel. +49 8031 281-0
Fax +49 8031 281-290
www.ift-rosenheim.de

Prüfung und Kalibrierung – EN ISO/IEC 17025
Inspektion – EN ISO/IEC 17020
Zertifizierung Produkte – EN ISO/IEC 17065
Zertifizierung Managementsysteme – EN ISO/IEC 17021

Notified Body 0757
PTZ-Stelle BAY 18



Deutsche
Akreditungsgesellschaft
D-PL 11149 01 09

APPENDIX F 2.1.1 MATERIAL TEST: MATERIAL, DIMENSIONS AND PRODUCTION OF THE TEST SPECIMEN

Material data

- Filament: COLORFABB_XT CLAER
- Material: ColorFabb_XT, PETG
- Diameter tolerance: ± 0.05 mm
- Density: 1.27 g/cm³
- Glass transition temperature: 75°C

Printer settings

- 3D Printer: Ultimaker2
- Layer height: 0.3 mm
- Shell thickness: 2 mm (2 layers with 1 mm nozzle)
- Top thickness: 1,8 mm
- Bottom thickness: 1.2 mm
- Nozzle: 1 mm
- Dual extrusion overlap: 0.15 mm
- Initial layer width: 125%.
- Fan: 100 %
- Combing: on
- Print temp.: 250 °C
- Print-Bed temp.: 70 °C

APPENDIX G 2.2.1 BENDING TEST: MATERIAL, DIMENSIONS AND PRODUCTION OF THE TEST SPECIMEN

The same pressure settings were used to produce the test specimens as for the production of the façade elements.

- Filament: extruded, completely transparent
- Material: PETG
- Diameter tolerance: ± 0.05 mm
- Density: 1.27 g/cm³
- Glass transition temperature: 75 °C
- Test body bending test:
- Dimensions: 180 mm x 60-80 mm x 700 mm (h x w x l), weight: 2340 g

Printer settings:

- 3-D printer: Delta Tower 900
- Layer height: 0.35 mm
- Shell thickness: 2 mm (2 layers with 1 mm nozzle), top thickness :1.8 mm, bottom thickness: 1.2 mm
- Nozzle: 1 mm
- Dual extrusion overlap: 0.15 mm
- Initial layer width: 125%.
- Fan: 100 %
- Combing: on
- Print temp.: 245 °C
- Bed temp.: 77 °C

PAOSS - Pneumatically Actuated Origami Sun Shading



Christina Eisenbarth¹, Walter Haase¹, Yves Klett¹, Lucio Blandini^{1,3}, Werner Sobek^{1,3}

* Corresponding author

- 1 ILEK Institute for Lightweight Structures and Conceptual Design, Faculty 2: Civil and Environmental Engineering, University of Stuttgart, Germany, christina.eisenbarth@ilek.uni-stuttgart.de
- 2 IFB Institute of Aircraft Design, Faculty 6: Aerospace Engineering and Geodesy, University of Stuttgart, Germany
- 3 Werner Sobek AG, Stuttgart, Germany

Abstract

This paper describes the development of an innovative, material and energy efficient façade concept: a pneumatically actuated Origami sun shading system - abbreviated "PAOSS" - which combines the aesthetic and material-immanent qualities of textile materials with the functional aspects of a controlled and targeted light transmission regulation by means of integrated active pneumatic components (FIG. 1). Due to the possibility of reducing a given surface to a minimal form, textile-based folding structures are highly suitable for selective sun and glare protection systems, in order to optimise energy consumption and increase user comfort. For astrophysical purposes, the American space agency (NASA) developed an Origami folding geometry called "Starshade", which is characterised by a particularly high difference between its closed and open state. Inspired by NASA's "Starshade", an adaptive, pneumatically actuated sun and glare protection system was designed and developed to be embedded in the cavity of pneumatically supported multi-layer ETFE cushion façades. By implementing active components, one can obtain a targeted, partial or full-surface regulation of light and radiation transmission as well as the back-reflection properties of the façade. Within the scope of the research project "Adaptive Membrane Façades" funded by the research initiative Zukunft Bau, the PAOSS will be prototypically built in a scale of 1:1 and implemented at one storey of the demonstration high-rise building of the Collaborative Research Centre 1244 entitled "Adaptive Skins and Structures for the Built Environment of Tomorrow". The goal is the system validation and the monitoring of the reliability and efficiency, especially in terms of building physics and daylight performance under real weather conditions.

Keywords

Adaptivity, textile, pneumatic cushion, sun shading, glare protection, origami folding, façade

DOI 10.7480/jfde.2021.1.5535

Use of Vacuum Glass (VG) in the Implementation of Transparent and Translucent Exterior Wall Systems with Very High Thermal Insulation

Luis Ocanto

- 1 Dortmund University of Applied Sciences and Arts, Dept. of Architecture, Chair of Building Materials Technology
Emil-Figge-Str. 40. 44227 Dortmund tel. 0231 9112 4434 fax 0231 9112 4466 e-mail: luis.ocanto@fh-dortmund.de

Abstract

In order to implement the goals of the energy transition in the intended period, energy-efficient solutions must be developed both for new buildings, and especially for the energy-efficient renovation of existing buildings. The vision of the VG_WALL project is the development of a transparent and translucent glass wall in a façade system that is efficient and adaptable to the needs of the user and at the same time proposes efficient and sophisticated architectural concepts, considering the latest production techniques and material developments. VG_WALL is a research project that aims to design and develop a multifunctional building module for the building envelope, consisting primarily of vacuum glass (thermal insulation, sound insulation) that can be modelled with selected translucent and transparent building materials depending on the requirements. The vacuum glass is to be regarded as functional, transparent insulation and sound insulation. From the knowledge gained in previous projects it follows that the constructive covering of the glass edge bond from the vacuum glass can solve the thermal bridge problem in this area. In the context of this research project, translucent and transparent glass elements are being developed as hybrid structures for façades. The adaptation of conceived glass hybrid structures to conventional façade systems such as: mullion-transom constructions, direct bonding of point-fixed façade constructions in new and existing buildings (retrofits) are also goals of this research project. Innovative façade concepts for element and all-glass façades are also examined. The conceived façade concepts are: glass wall module (Concept 01) and glass bricks and channel glass module (Concept 02). They are developed and tested with respective demonstrators, which should convince through design and function-related properties in the building envelope. The structure of the new glass module (Concept 01 glass wall module) creates e.g. two parallel, continuous levels of vacuum glass, U_g value of $0.4 \text{ W} / \text{m}^2\text{K}$ or less, and superimpose one another in the area of the edge seal in order to avoid thermal bridges. In the second system concept (Concept 02) with new glass bricks and channel glass elements, the construction is designed in such a way that an energy-efficient exterior wall can be built using the quick construction method with as few components as possible. The VG_WALL research project is funded by the Zukunft Bau research initiative, Federal Institute for Building, Urban and Spatial Research (BBSR).

Keywords

Vacuum glass, energy efficiency, adaptive 1: climate, adaptive 2: lifespan & life cycles, material in material

1 INTRODUCTION

All translucent and transparent components and systems available in the building sector can only be installed to a limited extent or not at all in accordance with the EnEV (Energy Saving Ordinance) - glass construction walls are currently only used in industrial and commercial buildings. The research project "VG-WALL" there-fore aims to develop two novel highly insulated transparent or translucent exterior wall concepts/systems that can also be used for residential construction. The aim is to achieve a previously unattainable thermal insulation for transparent and translucent components. This will enable aesthetically pleasing new construction and renovation projects to be realized by taking up design elements such as "glass brick", "glass wall" and "channel glass", which are very popular with architects but are outdated in terms of energy.

The heat-insulating functional level in both cases is vacuum glass (VG), which is supplemented by float and special glass to form a wall system. This is an additive, highly flexible building system made of glass, which should be very dynamically adaptable to user behaviour and building context. From the building physics knowledge gained in previous projects it follows that the constructive covering of the glass edge seal of vacuum glass can solve the thermal bridge problem in this area.

The construction of the new glass module, (concept 01) multilayer glass module, creates e.g. two parallel, continuous levels in the building envelope once, the vacuum glass level, which alone has a U_g -value of $0.58 \text{ W/m}^2\text{K}$ or less, and a second level of transparent or translucent materials. In the structural design concept, the VG layer of the glass modules is enclosed on the outside by functional layers (special glasses, foils) and on the room side by load-bearing layers (float glass, TVG, ESG or VSG). In this way, a layered structure is created in which component properties can be adjusted simply by installing the appropriate layers.

In the second system concept (Concept 02) with new solid glass bricks or channel glass elements, the construction is designed in such a way that an exterior wall can be completed with as few components as possible in quick construction. The glass clinkers are laminated by direct bonding to the VG layer. The channel glass elements are mounted to the VG panes or held together by thermally separated aluminium or GRP profiles at the edges of the modules thus created. Air-filled spaces and GRP hollow profiles provide the thermally necessary edge cover of the vacuum glazing and can be used as media channels as required.

As could be pointed out in the previous projects "Ultraslim", "Ultralight" and "VG-Façade", the very low U_g -values of vacuum glazing in the middle of the pane ($0.3 - 0.7 \text{ W/m}^2\text{K}$) are opposed to a glass edge compound of glass solder, which forms a thermal weak point of the system. Investigations in the above-mentioned re-search projects showed that a few centimetres of overlap are sufficient to eliminate thermal bridges and thus the accumulation of condensate. In addition, the new VG wall constructions must meet all static and building physics requirements that are placed on opaque exterior walls. Cost-efficient building systems can be created thanks to the high system flexibility with a minimum number of components. These new systems should be particularly applicable in existing situations and make it possible to carry out energy-efficient building renovations quickly and while retaining the visual appearance.

Vacuum glass, state of the art

Vacuum glass technology is still young, but is developing rapidly in the Asian region. Due to the tightening of energy laws in Asia, the demand for VG there has grown enormously. In Europe and Germany, changes are traditionally extremely slow in the construction industry. Despite the interesting results of various research projects and on the basis of buildings realized in Europe and

Germany, vacuum glass is considered a marginal phenomenon or niche product. At the beginning of the millennium, for a few years it looked as if vacuum insulation glass (VIG) could become the product of the future. After intensive efforts by machine manufacturers, together with research institutes from 2005 to 2014, the topic was rather marginalized in Europe. This was due to the European market with its individual design of very different window sizes and types as well as the lack of test certificates with reliable statements on durability.

At present, the trade press (Huber, Lieb 2019) has repeatedly reported on vacuum glass and its advantages and potential. However, attention is also drawn to the aspects of VG glazing in terms of building law. The well-known European regulations for assessing the durability of multiple-glazed insulating glass (MIG) in the EN 1279 series of standards explicitly exclude the product vacuum insulation glass in its new versions. This seems to make sense, the marginal loads in MIG are mainly determined by the enclosed gas volume. VG is exposed to the same effects for use in windows and façades and should have a usability over the service life of the component (durability). Therefore, VG is still an unregulated and not a harmonized construction product in Europe. CE marking is not possible, proof of the usability of construction products is necessary (early approval in individual cases, ZiE). The building law situation of the VG still has to be regulated, that will come. In this research project, this situation is viewed with confidence, as the latest developments in the field of vacuum glasses show heat transfer coefficients which are equal to or better than the U_g -values of today's standard triple-glazed insulating glasses. As already mentioned, VG has already been installed in selected building projects in Europe. A practical implementation has therefore already been tested and implemented. The experience gained with VG in these building projects and in research projects will have a decisive influence on the further positive development of VG (Hohenstein 2019). Since there is also a production in Belgium since April 2019, the building law situation as well as the delivery situation should also improve in the future.

Research project, status

This is an ongoing research project. The project is not yet completed and thermal insulation studies and simulations are still being carried out. Direct bonding and linear bonding are still to be investigated. The construction of the demonstrators is planned for spring 2021. Thus, the first results of the investigations on the prototypes will be available in spring summer 2021. In order to determine the type of construction of the demonstrators and their compositions, FEM simulations of various design proposals were carried out. First results of the FEM-simulations on the topic of thermal insulation (moisture-technical and heat-technical) were evaluated.

2 METHODOLOGY

Building construction and building physics approach.

The aim is the conception and development of a multifunctional building module for the building envelope consisting primarily of vacuum glass (thermal insulation, sound insulation), which can be modelled according to requirements with selected translucent and transparent building materials. Fields of application: residential and commercial construction.

In the research project two concepts are investigated: Concept 01 is mainly composed of VG and transparent and translucent materials. Concept 02 is composed of a) VG and solid glass bricks and b) VG and channel glass. The glass structures are adapted to existing façade systems or adapted to the structural design. The thermal performance of the glass structures on the façade system is evaluated by means of FEM simulations. The lamination of the glass parts is examined in two different processes: direct bonding over the entire surface and line bonding at the edges of the glazing

with spacers. This is followed by the production of prototypes for load and climate tests. Finally, demonstrators on a scale of 1:1 are built for exhibition purposes as wall and façade samples. Due to its high level of detail, the study is only carried out at the level of the fixed glazing of the façade.

Methodology of the study

- 1 Determination of the current requirements for transparent exterior walls. Updating the legal requirements for glass and load-bearing exterior walls and curtain walls. Research and sounding out the possible products with new material properties.
- 2 Selection of suitable materials (glazing, adaptive foils, control systems, adhesives/sealants, etc.) by preliminary tests for material and façade system determination, consideration of economic and sustainable factors in cooperation with the company partners.
- 3 Conception of the modular layer structure for the glass module construction system (Concept 01). Development of a system for wall constructions from new VG glass modules, taking into account all system components
- 4 Design of a solid glass bricks system and a channel glass system (concept 02) with a minimum number of components, taking into account all system components
- 5 Adaptation and structural adjustment of the developed glass structures to selected façade systems: type mullion and transom and structural glazing system
- 6 Evaluation of solution approaches for new VG glass hybrid components on the basis of FEM simulations of the thermal component behaviour and optimisation of the systems.
- 7 Concept 01: Preliminary bonding tests for bonding translucent, transparent selected material sheets, functional foils and other elements to the vacuum glass.
 - 7.1 7.1 Load and climate tests on prototypes of the new glass module system (Concept 01), if necessary optimization and adaptation of the system. Construction of 1:1 functional prototypes based on the results of the preliminary tests and simulations. Load and differential climate tests on functional prototypes. Construction and testing of sample wall sections (assembly, air and water tightness, impact tests, decomposability) Tests to adjust the degree of transparency over films and pane layers.
- 8 Concept 02: Design and construction of prototypes of the new solid glass bricks and channel glass system, (1:1) Adhesive pretests on different glazing packages. Trials to find a suitable material for the butt joints and in particular for the bedding joints of the solid glass bricks; the starting point are silicones with mineral additives to achieve a permanently high compressive strength. Tests on a sample wall cut-out (assembly, air and water tightness, impact tests, decomposability).
- 9 8.1 Load and climate tests on prototypes of the new channel glass system, if necessary optimization and adaptation of the system. Material and know-how will be provided by the partner companies Dow and Raico and test series on adhesive and sealant finding will be carried out.

3 EXPERIMENT / RESEARCH

3.1 EDGE SEAL PROBLEM OF VACUUM GLAZING STUDY CASES AND THE SPECIAL PROPERTIES OF VACUUM GLAZING

If one compares vacuum glass and conventional - i.e. filled with inert gases - multiple thermal insulation glazing, there are two main differences with regard to the thermal component behaviour

- U_g in the middle of the pane is much lower with VG (also compared to krypton - triple)
- Edge seal 0.1-0.2 mm glass solder or metal with comparatively high thermal conductivity

Modern multiple thermal insulation glazing has a thermal edge structure in the area of the glass edge seal, which ensures thermal separation (Fig. 1).

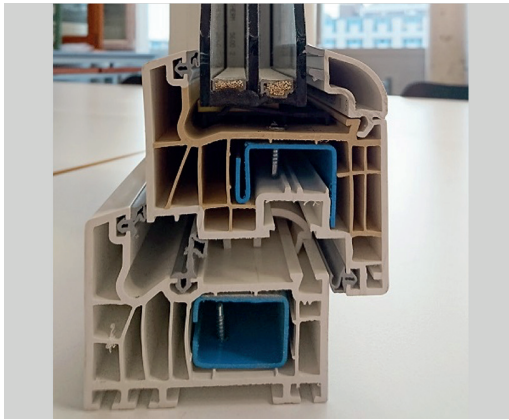


FIG. 1 Section through a gas-filled triple glazing 4/12/4/12/4 from Pilkington



FIG. 2 Spacers enlarged 20 times

The desiccant, which is always necessary for gas-filled glazing, is here present in a hollow profile made of plastic, which has a low thermal conductivity. Thin metal foils are applied on the outside to create a gas-tight seal. Sealing is achieved in the upper area by butyl elastomers, in the lower area by polysulfide or silicone. In contrast to this, the construction of the glass edge seal is much easier in vacuum glazing ("edge seal"), as no desiccant is required here. The two panes are directly connected to each other by glass solder in order to ensure a permanent high vacuum in the space between the panes (Fig. 3, 4).

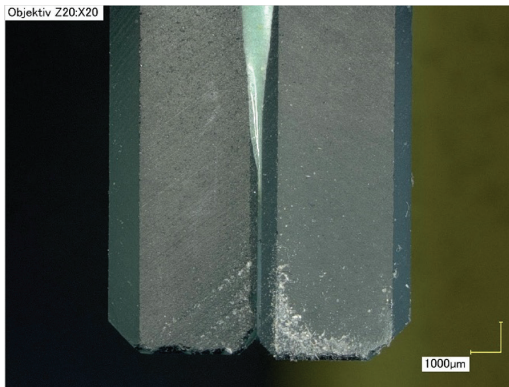


FIG. 3 Section through a gas-filled triple glazing 4/12/4/12/4 from Pilkington



FIG. 4 Spacers enlarged 20 times

As can be seen in a simple FEM simulation of the heat flow, vacuum glazing behaves similarly to single glazing in the area of the edge seal, since the connection from outside to inside is completely connected via the glass (Fig. 4).

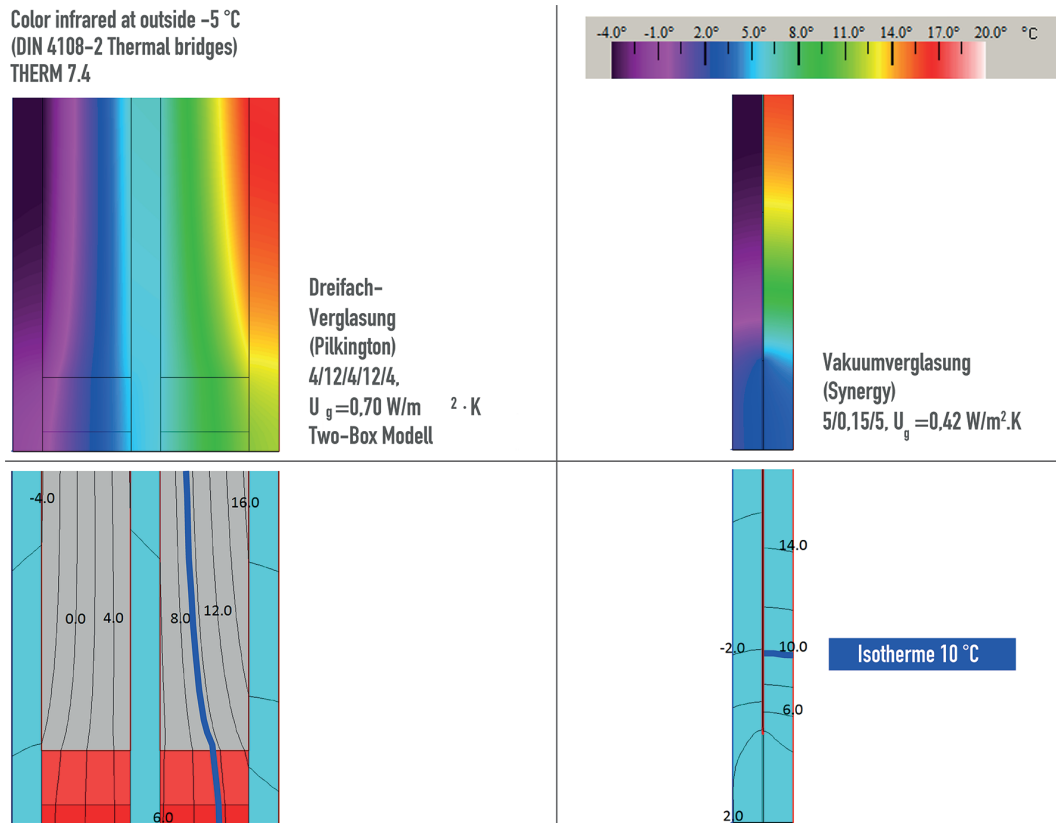


FIG. 5 Simulated temperature profile (THERM) at -5° C outside and 20° C inside for triple thermal insulation glazing 4/12/4/12/4 with $U_g = 0.70 \text{ W / m}^2\text{K}$ (left) and vacuum glazing 4 / 0.15 / 4 with $U_g = 0.42 \text{ W / m}^2\text{K}$ (right)

The edge seal is the weak point of the glass laminate with vacuum glass and is treated differently depending on the façade system. In façade systems in which the edge seal is concealed (mullion and transom façade) or framed, the statics, thermal bridge problems and drainage or sealing are different from those of all-glass façade systems (structural glazing). Without appropriate constructional measures, the room-side surface temperatures in the area of the edge seal would be so low that in winter, a strong accumulation of condensation water would have to be expected. A challenge in terms of building physics in the VG_WALL research project was to compensate for this thermal weakness in such a way that the excellent U_g -values of the glazing are not impaired.

3.2 CONCEPTION OF THE GLASS COMPOSITION, MATERIAL SELECTION

When designing the glass structures, materials with translucent or transparent properties were primarily selected. Translucent building products could be used in façades by planners and designers, but due to their poor thermal insulation, they are not suitable for façades or exterior walls. The following materials were selected: cast glass, structured glass, switchable and laminated glass, light concrete, glass ceramics, metal mesh, solid glass bricks. Nine glass structures as composite material were developed and six representative structures were selected for the investigations. The six abutments differ in function, structure, degree of translucency and transparency, density and thickness:

1) cast glass/structured glass, 2) laminated glass with switchable coating, 3) light concrete, 4) glass ceramic, 5) channel glass and 6) solid glass bricks.

Each structure should fulfil certain properties and functions when used on the façade system, see Fig. 06.

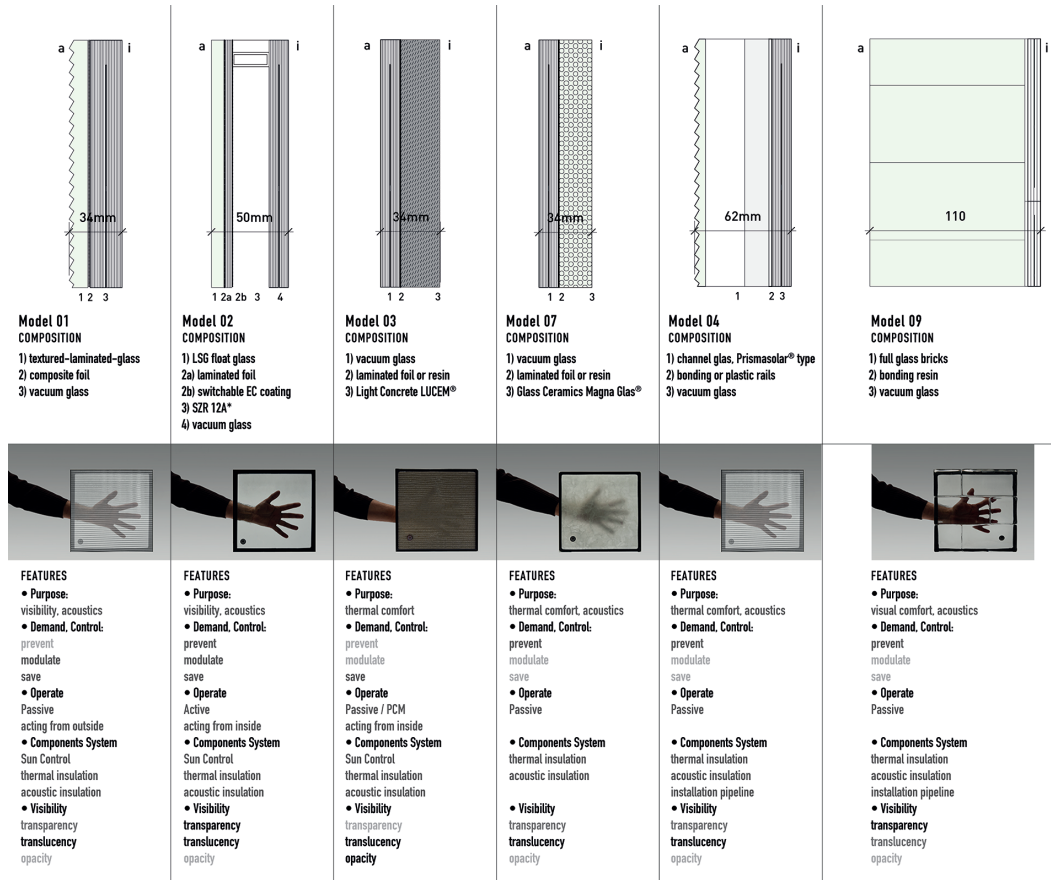


FIG. 6 VG Compositions, structure and features, selection

3.3 MATERIAL PROPERTIES

Characteristics of the VG-glazing to be used in the research project VG_WALL (standard): The data of the material properties of the vacuum glass are given by the South Korean manufacturer EAGON Windows & Doors, EAGON Industrial Co. Seoul / South Korea see Fig. 5

Composition Float Glass 5 mm	Vacuum layer	Pillar centre distance	Edge sealing with lead-glass solder	Wind pressure resistance [in Pascal]	U_g [W/m ² K]	Light transmission T_L [in %]	Solar factor g-Value EN 410 [in %]	R_w (C.Ctr) Value [dB]	Weight [Kg/m ²]
TL5-V-T5 10,25 mm	0,25 mm	40 mm	10 mm	3.400	0,48	81,63	60,90	37	20

T = tempered, L = low emission film, V = vacuum,

FIG. 7 Vacuum glass properties

Each material used in the research project is considered according to the relevant literature with regard to "common" values from practice (see Fig.8). This should not distort the results of

the comparison with standard façades. The adaptation of the material properties and thus the improvement of the façade performance are topics for further investigations.

MATERIAL	λ [W/(m·K)]	ρ [kg/m ³]	ϵ [-]
AL I Aluminium 10456 Ar18 in 50 mm U 0.52	160	2700	0,06
STAINLESS STEEL	17	7800	0,08
GLASS	0,8	2490	0,92-0,94
CONCRETE	>2,0 bis 2,6	>2000 bis 2600	0,94
Plastic fiber	0,25-0,35	1150	0,900
Glass Ceramics	1,04	2400	0,92
Channel Glas	1,0	2490	0,92
EPDM	0,25	0,250	0,900
Silicone-Standard	0,30-0,40	1250-1900	0,900
Warm-Edge-Silicone	0,19	1250-1900	0,900
Thermally conductive silicone	2,0	1250-1900	0,900
Gas filling	0,034	–	
Gas filling, Argon	0,021	–	
Vacuum (air)	0,0000040525	–	
Aerogel board (Slentite®)	0,0017	130	0,900
Swisspacer Ultimate Box 2	0,14		0,900
Polyvinyl Chloride PVC-U hart	0,17	1390	0,900
Polyvinyl Chloride PVC-P weich	0,14	1200	0,900
Polyurethane (PU)	0,40	1500	0,900
Polychloropene (PCP) z.B. Neopren	0,23	1240	0,900

FIG. 8 Material properties

3.4 GENERAL CONDITIONS

The developed glass structures as well as the suitable façade systems are first examined in FEM simulations under the following criteria and parameters

For all façade systems:

- In residential construction: a θ_{si} room-side surface temperature [°C] lower than 13° C, at an outside temperature of -10° C and +20° C in the interior at a relative humidity > 50% should be avoided (DIN 4108-2)
- In commercial buildings: a θ_{si} room-side surface temperature [°C] lower than 10.5° C, at an outside temperature of -10° C and +20° C in the interior at a relative humidity of 40% should be avoided.
- Play off façade concepts: For façade openings: box-type windows, box-type window façade, all-glass façade, double-skin façade, pivot elements
- Parametrization of the façade design according to the location or cardinal point of the façade in order to vary and test finishing such as screen printing, foliation.

The following constructional measures are taken during the simulation models, see Tab. 01

FOR CURTAIN WALLS: MULLION/TRANSOM SYSTEM	FOR DIRECT BONDING: STRUCTURE GLAZING, POINT HOLDER
- Change installation position or:	- Variation of the depth of the glass recess
- Variation of the depth of the glass recess	- Simplify and rationalize glass fixing
- Position of glazing with additional insulation of the frame from the outside	- Filigree sealing or narrower joints due to external heat-insulating seal
- External insertion of seals made of heat-insulating materials	- Room-side installation of collectors and seals made of heat-conducting materials
- Room-side installation of collectors and seals made of heat-conducting materials	- Point support should be checked depending on the position of the VG (statics)
- Attachment of a thin ESG with spacer "warm edge"	- Optimization of the auxiliary frame (substructure), use of alternative materials with lower thermal conductivity e.g. GFK, CFK.
- Insulating layers of different thickness and thermal conductivity	
- Reduction of the width of the VG edge seal, VG with 5mm edge seal (ideal).	
- Increase of the frame depth (window systems)	
- Variation or increase of the system width, more scope for the depth of the glass recess and accommodation of necessary technology e.g. with adaptive glazing (mullion-transom)	

TABLE 1 - Constructional measures, criteria and parameters of the depth of the glass recess

3.5 THERMAL PERFORMANCE

As it could be pointed out in the previous projects "Ultraslim", "Ultralight" or "VG-Façade", a special consideration of the edge seal between glazing and the façade construction is necessary to achieve an optimal thermal performance of the vacuum glass. The dependence of this connection point is essentially determined by the length of the edge seal and the glass recess. In order to show the thermal performance of the glazing with the associated façade construction, numerical thermal bridge simulation was used, as in the VG-Façade research project. For the studies, simplified calculation models of the design proposals with vacuum glass were carried out using the software FLIXO 8.0, THERM, WINDOW 7.5 and Grasshopper.

Thermal simulation using FEM software, thermal bridge simulation.

In order to be able to evaluate the performance of the conceived constructions, the experiences of the research project VG-Façade regarding FEM-simulations were used. In detail the software FLIXO 8.0 and the software WINDOWS 7.5 was used for this purpose. Detail connections (horizontal and vertical sections) of the different compositions and the connections to the façade systems were made in 2D and 3D models in CAD drawings and imported into the simulation program. Configured with the material parameters, the corresponding simulations were then carried out.

Among the most important performance indicators that can be determined in this way are

- Temperatures and heat flows in the constructions and on the surfaces of the constructions. These can be expressed as thermal coupling coefficients, but can also be described with simple indicators such as the f_{Rsi} value.

- Even if the PSI-value has only a low significance regarding the thermal quality of building components, these values can be used quite well to compare constructions without vacuum glass (i.e. with conventional glass or insulating glass) and those with vacuum glass.
- Water vapour diffusion in the building components as well as possible corrosion, condensation and mould growth can be described by means of the simulation.

3.6 FAÇADE SYSTEMS, ADAPTATION AND CUSTOMIZATION

The proposed glass structures were adapted and simulated on an existing façade system of the project partner:

RAICO GmbH. The selected Raico system program is the THERM+ A-I system. In order to be able to better guide the isotherms, great importance was attached to using a profile with the largest possible screw channel. For this reason, a profile from the RAICO THERM+ A-I series (aluminium "I-Façade") was selected as the supporting profile. These profiles have a larger screw channel (18.5 instead of 13 mm) compared to the V-version. A further advantage of the "I-façade" is that the height of the inner gasket is 13.5 mm instead of 9.5 mm for the V-variant, which means that the surface temperatures in the critical areas in particular will be lower, see Fig. 9.

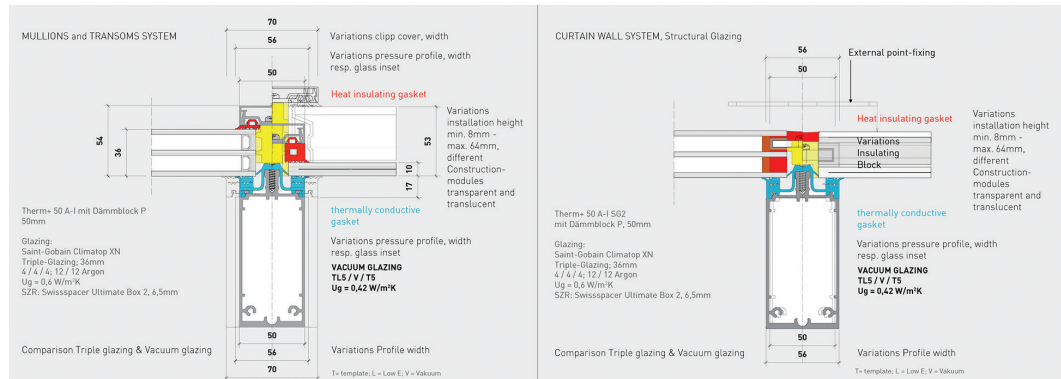


FIG. 9 Façade system Raico Therm+ A_I mullion-transom (left) and structural glazing (right) Building construction measures for investigation, comparison with triple glazing

3.7 SEALS AND DIRECT BONDING

New types of silicones are used in the current research project: Heat-insulating silicone on the seal of the outside of the construction and heat-conducting silicone on the seal of the inside of the construction. Our calculations show that further improvements of the thermal component behaviour are possible if the thermal conductivities of the outer and room-side covering of the glass edge seal (gaskets) are optimised.

In the research project "VG-WALL" the following assumption was investigated: If, in the most advantageous configuration, heat is conducted on the room side to the critical glazing frame junction point and material with the lowest possible thermal conductivity is applied on the outside to cover it. In this way, the aluminium profile can be used effectively as a collector and the edge seal of the vacuum glazing can be heated in a targeted manner to prevent the formation of condensation without losing a lot of energy to the outside. In this way, the aluminium profile can be used effectively as a collector and the edge seal of the vacuum glazing can be tempered to prevent the formation of condensation. In this way, especially in combination with the vacuum glazing with reduced glass edge seal examined in the research project, the thermal insulation of mullion-transom and all-glass

façades with vacuum glazing can be significantly improved once again. On the room side, more heat-conducting materials are used and on the outside, more heat-insulating materials are used.

The new compositions developed are basically designed as laminated glass. The intermediate layer is laminated either with foil or cast resin, depending on the material properties. The use of foils is more suitable for mirror-smooth materials such as glass ceramic, float glass and light concrete. For irregular surfaces such as cast glass and solid glass bricks, a liquid compound is more suitable.

The Concept 01 part A of the research project VG_WALL provides for direct bonding. As a production process, direct bonding is relatively uncomplicated and the result is effective and efficient. This type of bonding proves to be disadvantageous if it is to be dismantled. The separation or dismantling of the components of the glass composite is complex. The components are separated mechanically for the first time and the residues resulting from the separation are washed out or dissolved. After this process, components and waste material are sorted again and prepared for recycling.

In view of this problem, a variant in concept 01 has been proposed to simplify the dismantling of the glass structures.

The Concept 01 part B of the research project VG_WALL provides for a line bonding and is less invasive than a direct bonding to deconstruct the glass composite more easily and environmentally friendly. As with the insulating glass, a linear bonding of the edges of the glazing components (various glass structures VG + translucent materials) was considered. This concept also favours an improvement of the thermal insulation in the edge area. The translucent materials of the developed glass structures (translucent concrete, glass ceramic and solid glass bricks) have a thickness of 25 mm to 50 mm. The resulting glass compositions with vacuum glass are almost as thick as bullet-proof or fire protection glass. The bonding of the vacuum glass slides and the selected translucent materials should be fixed by means of a spacer. This creates a space between the panes. The resulting cavity or SZR should protect against dirt and water ingress and be permanently sealed.

In Concept 02, the solid glass bricks and the VG are laminated by direct bonding, the channel glass construction elements are mechanically fixed to the profiles of the façades without direct bonding, only the joint between the channel glass construction elements is sealed with silicone to withstand the weather.

3.8 SIMULATIONS ON FAÇADE SYSTEM, CONCEPT 01 AND CONCEPT 02

As described in point 3.5, detail connections of the glass structures on mullion-transom façades and all-glass façades Structural Glazing of concept 01 were simulated. In this context, the different compositions were examined with the design measures and parameters (see Tab. 01). The type of bonding in combination with the façade construction mullion-transom or structural glazing influences the thermal behaviour of the compositions and, as a consequence, the edge seal.

In the case of Concept 01, VG glazing in combination, two sub-concepts are differentiated: Part A, compositions in direct bonding of the composite layers on mullion-transom façades and Part B, linear bonding of the composite layers at the edges with SZR (spacer). Here, all components of the glazing are brought together on only one level. In the resulting module, the laminated glass panes and functional layers permanently insulate the interior climate from the exterior climate. With the concept 01 - part A, the dismantling of all glass structures is possible by mechanical separation of the glass and foil layers, but is costly. A re-installation of the newly developed glass modules after dismantling makes more sense thanks to its long service life. In Concept 01 - Part B, line bonding with inter-pane space and valves for pressure equalization ensures that the glass modules

are bonded together and at the same time promotes dismantling or recycling by separating the individual components.

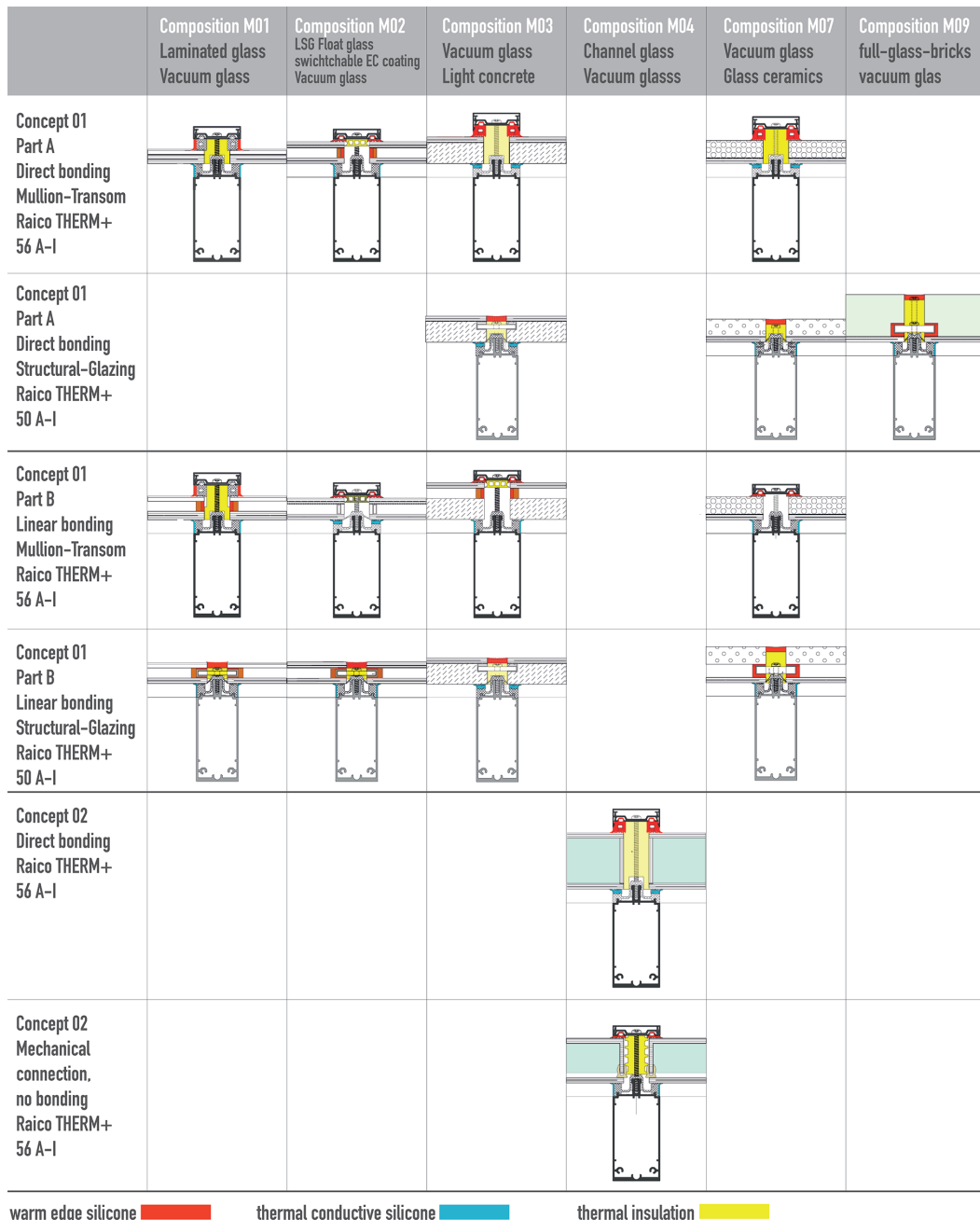


FIG. 10 Therm+ A-I and SG façade system with selected VG – compositions, overview

In Concept 02, the glass construction 09 full glass clinker with VG in direct bonding is only simulated on structural glazing façades, because in the mullion-transom façade system Raico Therm+ A-I the construction depth of the construction exceeds the depth of the fastening, construction depth only up to 64 mm. The M04 structure - channel glass with a flange height of 40 mm fits into the Raico Therm+ A-I mullion-transom system. In structural glazing systems the structure 04 - channel glass is not adapted. An overview of the compositions and the subdivision of the concepts according to façade type is shown in Fig. 10.

The building physical properties of the developed compositions were checked with FEM simulations. The thermal insulation is guaranteed by the vacuum glass. With the exception of the combination with light concrete, the position of the vacuum glazing is generally on the inside of the glass compositions. Depending on the formulation, concrete is an excellent heat accumulator. At the same time, this glass structure acts like a Trombe wall and provides thermal comfort indoors, especially in the cold seasons. Partial results of the simulations are explained in Chapter 4 Results.

After completion of the investigated simulations, the prototypes of the demonstrators will be built. Each demonstrator will be built on a 1:1 scale. The demonstrators consist of a glass composite and a frame construction as a post and beam or as a structural glazing system depending on the nature of the composite, see also Fig.06. The demonstrators have dimensions of: 1500 mm x 500 mm. This dimension is determined by the size of the translucent concrete panels, which have a maximum size of 620 mm x 1600 mm during production. The demonstrator of the channel glass is a wider version and has a dimension of 1500 mm x 750 mm. The demonstrators are examined and tested in a differential climate chamber.

4 RESULTS

In order to prevent condensation and to ensure optimum guidance of the isotherms in the construction, the installation position, glass recess, outer and inner seal of the glazing must be examined more closely. To prevent condensation, no part of the surface of window profiles or glass surfaces should be exposed to temperatures below 10 °C. To also avoid the problem of mould growth, it is also advantageous if no temperatures < 13 °C occur on the interior surfaces. The critical range for the lowest surface temperature on profiles is usually in the case of the inner glass seal in the transition to the glass in the frame corner area.

For this reason, some isothermal calculations were performed with the Flixo software, experimenting with different installation positions of the glazing. The risk of condensation and mould growth is determined by the surface temperature humidity that is generated. As a result of these calculations, correlations are to be derived in order to determine the optimal installation position. The findings from these calculations will optimize and improve the design proposals.

First findings from the investigations:

The first results (01), see Fig. 11, of the examined constructions show a relatively bad performance of the suggested seals. The problem of the edge seal is not satisfactorily solved with the proposed measures. The heat and moisture protection values are achieved with the SZR (pane gap) or spacer construction.

The position of the heat-conducting silicone is decisive for the explanation of the deficits of the inner surface temperatures. The silicone layer is placed parallel to the VG, where the temperatures are low, resulting in a thermal bridge or a disturbance of the isothermal curve. Conceptual corrections have been made to the designs, the gaskets with heat-conducting or heat-protecting qualities have been combined with conventional EPDM gaskets. The silicone gaskets are applied as a coating perpendicular to the EPDM gaskets.

VG_WALL Results 01 Façade-System mullion-transom & Structural Glazing RAICO THERM+ A-I Vacuum glazing $U_g = 0,42 \text{ W/m}^2\text{K}$ Edge seal = 9 mm		Material GASKET outside $\lambda \text{ [W/m}^2\text{K]}$	GLASS – inset in mm	Material INSULATING BLOCK $\lambda \text{ [W/m}^2\text{K]}$	Material GASKET inside $\lambda \text{ [W/m}^2\text{K]}$	Temperature factor f_{Rsi} – value	θ_{si} inside room surface temperature outside $\theta_e = -5^\circ \text{C}$
REFERENCE VG_W_R_PFS6_M00 Vacuum glazing pure		Warm Edge Silicone $\lambda = 0,19 \text{ W/m}^2\text{K}$	13	Aerogel- Platte BASF Slentite® $\lambda = 0,0171 \text{ W/m}^2\text{K}$	thermal conductive silicone $\lambda = 2,0 \text{ W/m}^2\text{K}$ EPDM $\lambda = 0,25 \text{ W/m}^2\text{K}$	0,65	11,3
Composition 01 Mullion-Transom VG_W_R_PFS6_M01 Prism glass + vacuum glazing		Warm Edge Silicone $\lambda = 0,19 \text{ W/m}^2\text{K}$	13	Aerogel- Platte BASF Slentite® $\lambda = 0,0171 \text{ W/m}^2\text{K}$	thermal conductive silicone $\lambda = 2,0 \text{ W/m}^2\text{K}$ EPDM $\lambda = 0,25 \text{ W/m}^2\text{K}$	0,62	10,6
Composition 02 Pforsten-Riegel VG_W_R_PFS6_M02 Switchable glass + SZR + vacuum glazing		Warm Edge Silicone $\lambda = 0,19 \text{ W/m}^2\text{K}$	13	Aerogel- Platte BASF Slentite® $\lambda = 0,0171 \text{ W/m}^2\text{K}$	thermal conductive silicone $\lambda = 2,0 \text{ W/m}^2\text{K}$ EPDM $\lambda = 0,25 \text{ W/m}^2\text{K}$	0,78	14,6
Composition 03 Mullion-Transom VG_W_R_PFS6_M03 Vacuum glazing + light concrete		Warm Edge Silicone $\lambda = 0,19 \text{ W/m}^2\text{K}$	13	Aerogel- Platte BASF Slentite® $\lambda = 0,0171 \text{ W/m}^2\text{K}$	thermal conductive silicone $\lambda = 2,0 \text{ W/m}^2\text{K}$ EPDM $\lambda = 0,25 \text{ W/m}^2\text{K}$	0,79	14,9
Composition 04 Mullion-Transom VG_W_R_PFS6_M04 Channel glas + vacuum glazing		Warm Edge Silicone $\lambda = 0,19 \text{ W/m}^2\text{K}$	13	Aerogel- Platte BASF Slentite® $\lambda = 0,0171 \text{ W/m}^2\text{K}$	thermal conductive silicone $\lambda = 2,0 \text{ W/m}^2\text{K}$ EPDM $\lambda = 0,25 \text{ W/m}^2\text{K}$	0,59	9,9
Composition 05 Mullion-Transom VG_W_R_PFS6_M07 Glass ceramic + vacuum glazing		Warm Edge Silicone $\lambda = 0,19 \text{ W/m}^2\text{K}$	13	Aerogel- Platte BASF Slentite® $\lambda = 0,0171 \text{ W/m}^2\text{K}$	thermal conductive silicone $\lambda = 2,0 \text{ W/m}^2\text{K}$ EPDM $\lambda = 0,25 \text{ W/m}^2\text{K}$	0,59	9,8
Composition 02 Structural Glazing VG_W_R_SG50_M02 Switchable glass + SZR + vacuum glazing		Warm Edge Silicone $\lambda = 0,19 \text{ W/m}^2\text{K}$	12	Aerogel- Platte BASF Slentite® $\lambda = 0,0171 \text{ W/m}^2\text{K}$	thermal conductive silicone $\lambda = 5,0 \text{ W/m}^2\text{K}$ EPDM $\lambda = 0,25 \text{ W/m}^2\text{K}$	0,59	9,8
Composition 03 Mullion-Transom VG_W_R_SG50_M03 Vacuum glazing + light concrete		Warm Edge Silicone $\lambda = 0,19 \text{ W/m}^2\text{K}$	12	Aerogel- Platte BASF Slentite® $\lambda = 0,0171 \text{ W/m}^2\text{K}$	thermal conductive silicone $\lambda = 5,0 \text{ W/m}^2\text{K}$ EPDM $\lambda = 0,25 \text{ W/m}^2\text{K}$	0,71 ⁵	12,9

warm edge silicone ■ thermal conductive silicone ■ thermal insulation ■

FIG. 11 Results 01 FEM-Simulation Construction Glass Compositions

The other results (02) are much better, see Fig. 12. The new design of the seals and the use also on the spacers show optimal results. The compositions with only VG or VG in combination with cast glass are to be further optimized. In this context, a widening of the glass inlet is certainly a suitable measure to increase θ_{si} (interior surface temperature) and to bring the temperature factor f_{Rsi} to the minimum values of DIN 4108-2 (thermal insulation and energy saving in buildings; Supplement 2: Thermal bridges) or better.

VG_WALL Results 02 Façade-System mullion-transom & Structural Glazing RAICO THERM+ A-I Vacuum glazing $U_g = 0.42 \text{ W/m}^2\text{K}$ Edge seal = 9 mm		Material GASKET outside λ [W/m·K]	GLASS – inset in mm	Material INSULATING BLOCK λ [W/m·K]	Material GASKET inside λ [W/m·K]	Temperature factor f_{Rsi} – value	θ_{si} inside room surface temperature at outside $\theta_e: -5^\circ \text{C}$
REFERENCE 01 VG_W_R_PFS6_CTxn Triple-Glazing Glazing: Saint-Gobain Climatop XN Triple-Glazing: 36mm 4 / 4 / 4, 12 / 12 mm SZR: SwisspacerUltimate Box 2, 6,5mm		Warm Edge Silicone $\lambda = 0,19 \text{ W/m}^2\text{K}$	15	PE-insulation block $\lambda = 0,040 \text{ W/m}^2\text{K}$	thermal conductive silicone $\lambda = 2,0 \text{ W/m}^2\text{K}$ EPDM $\lambda = 0,25 \text{ W/m}^2\text{K}$	0,88	17,1
REFERENCE 02 Mullion-transom VG_W_R_PFS6_M00 Vakuumglas pur		Warm Edge Silicone $\lambda = 0,19 \text{ W/m}^2\text{K}$ EPDM $\lambda = 0,25 \text{ W/m}^2\text{K}$	13	Aerogel- Plate BASF Slentite® $\lambda = 0,0171 \text{ W/m}^2\text{K}$	thermal conductive silicone $\lambda = 2,0 \text{ W/m}^2\text{K}$ EPDM $\lambda = 0,25 \text{ W/m}^2\text{K}$	0,69	12,3
Construction 01 Mullion-transom VG_W_R_PFS6_M01 Prism glass + Vacuum glazing		Warm Edge Silicone $\lambda = 0,19 \text{ W/m}^2\text{K}$ EPDM $\lambda = 0,25 \text{ W/m}^2\text{K}$	13	Aerogel- Plate BASF Slentite® $\lambda = 0,0171 \text{ W/m}^2\text{K}$	thermal conductive silicone $\lambda = 2,0 \text{ W/m}^2\text{K}$ EPDM $\lambda = 0,25 \text{ W/m}^2\text{K}$	0,66	11,6
Construction 02a Pfosten-Riegel VG_W_R_PFS6_M02 Switchable glass + SZR + Vacuum glazing		Warm Edge Silicone $\lambda = 0,19 \text{ W/m}^2\text{K}$	13	EPDM insulation block $\lambda = 0,05 \text{ W/m}^2\text{K}$ Swisspacer Ultimate Box 2 $\lambda = 0,14 \text{ W/m}^2\text{K}$	thermal conductive silicone $\lambda = 2,0 \text{ W/m}^2\text{K}$ EPDM $\lambda = 0,25 \text{ W/m}^2\text{K}$	0,83	15,8
Construction 02b Structural Glazing VG_W_R_SG50_M02 Switchable glass + SZR + Vacuum glazing with gap		Warm Edge Silicone $\lambda = 0,19 \text{ W/m}^2\text{K}$	13	Aerogel-Plate BASF Slentite® $\lambda = 0,017 \text{ W/m}^2\text{K}$ Swisspacer Ultimate Box 2 $\lambda = 0,14 \text{ W/m}^2\text{K}$	thermal conductive silicone $\lambda = 2,0 \text{ W/m}^2\text{K}$ EPDM $\lambda = 0,25 \text{ W/m}^2\text{K}$	0,77	14,3
Construction 02b Structural Glazing VG_W_R_SG50_M02 Schaltbares Glas + SZR + VG without gap		Warm Edge Silicone $\lambda = 0,19 \text{ W/m}^2\text{K}$	13	Aerogel-Plate BASF Slentite® $\lambda = 0,017 \text{ W/m}^2\text{K}$ Swisspacer Ultimate Box 2 $\lambda = 0,14 \text{ W/m}^2\text{K}$	thermal conductive silicone $\lambda = 2,0 \text{ W/m}^2\text{K}$ EPDM $\lambda = 0,25 \text{ W/m}^2\text{K}$	0,81 ⁵	15,4
Construction 03 Structural Glazing VG_W_R_SG50_M03 Vacuum glazing + Light concrete with gap		Warm Edge Silicone $\lambda = 0,19 \text{ W/m}^2\text{K}$	12	Aerogel- Plate BASF Slentite® $\lambda = 0,0171 \text{ W/m}^2\text{K}$	thermal conductive silicone $\lambda = 2,0 \text{ W/m}^2\text{K}$ EPDM $\lambda = 0,25 \text{ W/m}^2\text{K}$	0,78	14,5

FIG. 12 Results 02 FEM-Simulation Construction Glass Composites

5 CONCLUSIONS

The use of vacuum glass as heat protection or "transparent thermal insulation" is an efficient, intelligent and at the same time aesthetic measure to optimize the energy efficiency of transparent and translucent materials on façades. Transparent and translucent materials, which due to their good thermal conductivity do not meet today's energy saving standards, are improved in this way in order to make efficient use on building envelopes. The construction models with vacuum glass that have been investigated in the research project to date lead to a promising future for vacuum glass. Demonstrators will be used to test and investigate the limits of the models and systems. A topic that is also considered in the research project is the dismantling of the used components

and building materials from the construction models with VG. The requirements for the dismantling and recyclability of glass in composites are composed of logistical, technical and economic factors as well as quality requirements. A concrete statement on deconstruction is currently only possible to a limited extent and is usually decided on a case-by-case basis. In the research project, a suitable answer to this topic is sought.

Acknowledgements

This paper is based on a research project supported by the "Forschungsinitiative ZukunftBAU" in Bundesinstitut für Bau-, Stadt- und Raumforschung (BBSR).

References

- PILKINGTON DEUTSCHLAND AG (2014). Pilkington Spacia vacuum glazing Product information, as of PILKINGTON DEUTSCHLAND AG: unpublished communication
- BEIJING SYNERGY VACUUM GLAZING TECHNOLOGY CO., LTD (2015). World Pioneer of Vacuum Glazing. Product information.
- COLLINS, R.E. ; FISCHER-CRIPPS, A.C. ; TANG, J.-Z (1992). Transparent evacuated insulation In: Solar Energy 49 (5), pp. 333-350
- SIMKO, T.M. ; BECK, F.A., COLLINS, R.E., ARASTEH, D (1994). Edge conduction in vacuum glazing. In: THERMAL ENVELOPES VI (Heat Transfer in Fenestration II - Principles), pp. 601-611
- GLASER, SIEGFRIED ET AL (2007). Vacuum Insulating Glass (VIG) Research Report BMWi, Project Management PtJ, Funding Number 0327366 A to G
- GLASER, SIEGFRIED ET AL (2011). Highly heat-insulating window and façade systems (HWFF) Research report BMWi, Project Management PtJ, grant number 0327654 Abis H
- GLASER, SIEGFRIED ET AL (2012). Production techniques for vacuum insulating glass (ProVIG) / Research report BMWi, Project Management PtJ, funding number 0327419 A to G
- HOHENSTEIN, HELMUT (2014). Market Study of the Global Vacuum Glass Status in Practice Market Study, Marl
- HOHENSTEIN, HELMUT (2017). Vacuum Glass Status Report - Energy efficient building skins with Vacuum Glass Market Study, Marl
- HOHENSTEIN, HELMUT (2019): Historical development, market situation and applications of vacuum glass (VG); activities and requirements for further development, especially for façade and window systems for the research project "VG façade", status report, Marl
- HUBER, KONRAD; LIEB, KARIN: Technical article "Gebäude Energieberater" edition 04 / 2019

PART 2 // ENVIRONMENT

Study on the Interaction of Room Design, Material, Ventilation and User Behaviour Towards a Robust Building Operation

Laura Franke¹, Tilmann Jarmer², Thomas Auer³

- 1 Technical University of Munich, Department of Architecture, Chair of Building Technology and Climate Responsive Design, Arcisstraße 21, 80333 Munich, Germany, phone: 0049 89 289 22403, mail: laura.franke@tum.de
- 2 Technical University of Munich, Department of Architecture, Chair of Design and Construction, Arcisstraße 21, 80333 Munich, Germany, phone: 0049 89 289 23881, mail: tilmann.jarmer@tum.de
- 3 Technical University of Munich, Department of Architecture, Chair of Building Technology and Climate Responsive Design, Arcisstraße 21, 80333 Munich, Germany, phone: 0049 89 289 22475, mail: thomas.auer@tum.de

Abstract

Recent studies on residential buildings show a significant gap between the actual energy consumption and the calculated energy demand. It can be suspected that user behaviour in interaction with the building and the technical systems account for the gap between theory and practice. On the other hand, there are buildings today that require little to no additional energy for heating by utilizing internal gains coupled with reduced ventilation, effective thermal mass and reduced heat loss through the façade. Understanding the interaction between user, building and ventilation technology is crucial for a robust reduction of the overall energy consumption by residential buildings (hypothesis).

The authors compared every possible combination of input conditions on a room design level – such as geometry, construction material and ventilation – using thermal-dynamic building simulation. The variations can be considered as extreme scenarios, chosen to span the maximum range each parameter can have. Conducting the method resulted in 448 different investigation scenarios, evaluated according to energy demand and thermal comfort.

The results show that the energy demand for heating ranges from almost zero up to 90 kWh/m²a. The summery discomfort caused by overheat hours spans from around 100 up to over 3400 Kh/a. The dataset of results the authors used to examine the interaction of the different input conditions and their strengthening or balancing effect.

Conclusion 1: The energy demand of the simulated variants is strongly driven by the effect of the user's ventilation behaviour. This explains a significant share of the gap between the actual energy consumption and the calculated energy demand since past calculations usually assume the user behaviour to be fixed. It is a strong argument to focus on user behaviour in the energy demand calculation of residential buildings. However, results show that e.g. the insulating effect of the building envelope recedes far into the background compared to the user behaviour.

Conclusion 2: As known, high internal gains and minimal air exchange rate reduce the energy demand significantly. In combination, it is possible to keep a room temperature within the comfortable range in winter, without using a heating system. This suggest changing our perception of the heating system towards a temporary backup system since it is obsolete during most time of the year.

Conclusion 3: Appropriate window sizes with triple glazing combined with high thermal mass content of the room structure ensure a high level of room comfort in summer, balancing out even high internal gains and eliminating the need for movable sun shading or active cooling systems.

"Simply Build" constructions respecting these conclusions as a design guideline result in buildings that require little heating energy and do not overheat in summer.

Keywords

Robust optimization, user behaviour, ventilation behaviour, room design, simply built

1 INTRODUCTION

For decades, efforts to reduce the energy consumption of our buildings have been intensified. Particularly with regard to the insulating properties of the building envelope - i.e. façade and roof - the German legislation sets strict regulations. Building owners must prove to the authorities that the specifications have been met (§79 GEG). Experts with the help of defined calculation models provide the proof. These models use standardized boundary parameters, concerning e.g. outdoor climate, user behaviour or technical installations. This method guarantees fair and comparable energy certificates. However, it is not suitable for accurately predicting the energy consumption of buildings in practice.

This discrepancy between theory and practice has been investigated in detail. The German Institute for Housing and the Environment, "Institut für Wohnen und Umwelt" (IWU), which conducted the study on behalf of the federal government, selected 2856 data sets from a large number of data sets and compared the calculated energy demand with the measured energy consumption. The proposed model illustrates the relationship between energy consumption and energy demand according to DIN V 4108-6 / 4701-10. In Fig. 1, the dashed line shows the estimated value of consumption, the grey area shows the uncertainty of the estimate for an individual building. The area reference is the heated living space, service systems run on combined operation for heating and hot water without using additional heat generators. The system energy sources are natural gas and district heating. (IWU, 2019)

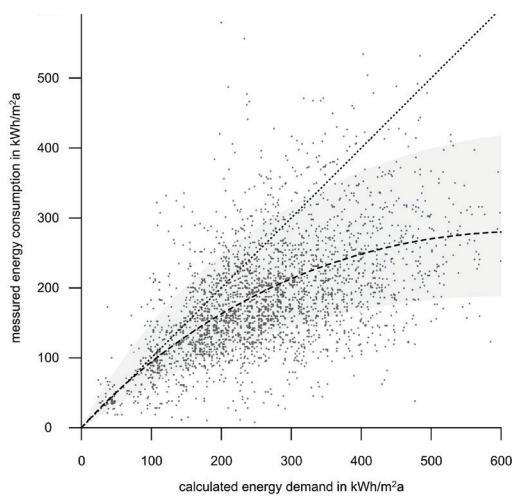


FIG. 1 Relationship between energy consumption and energy demand according to DIN V 4108-6 / 4701-10 (IWU, 2019)

In the described scientific study, the authors provide a formula for converting the theoretically calculated energy demand to the actual consumption to be expected. However, the point cloud in the graph on which the formula is based on depicts the buildings under consideration and clearly shows that the formula can only give an estimate.

While this meta-study from IWU looks at a wide variety of buildings, the Munich housing association GEWOFAG takes a different approach: For six new buildings of the same size and orientation, the energy consumption was measured over a period of three years. All buildings were occupied, while certain components were varied in each case (Fig. 2, building description 1 to 6). (GEWOFAG, 2020).

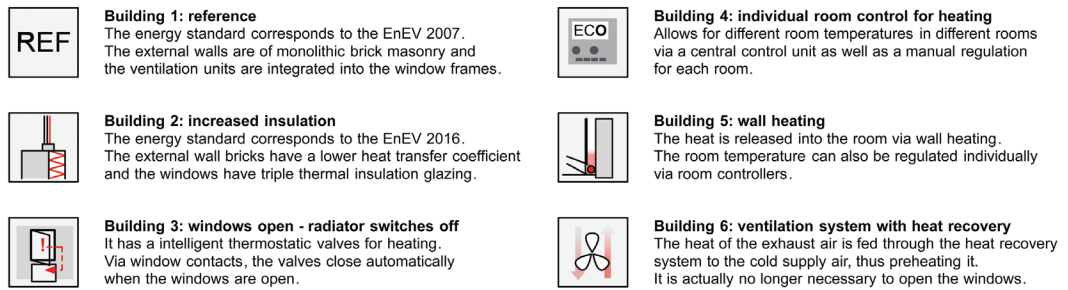


FIG. 2 Different equipment features of the six GEWOFAG research houses (GEWOFAG, 2020)

Building 1 was constructed by GEWOFAG according to the usual standard, representing the reference building. The other five buildings differ in one detail each. Building 2, for example, has a better insulation standard and Building 6 has a ventilation system. Fig. 3 describes the differences between the six otherwise identically constructed research houses. The results are surprising. With the exception of Building 3, no other measure can achieve real savings in energy consumption. This suggests that no further optimization is possible in building and technology, unless the occupants are influenced to more economical behaviour at the same time.

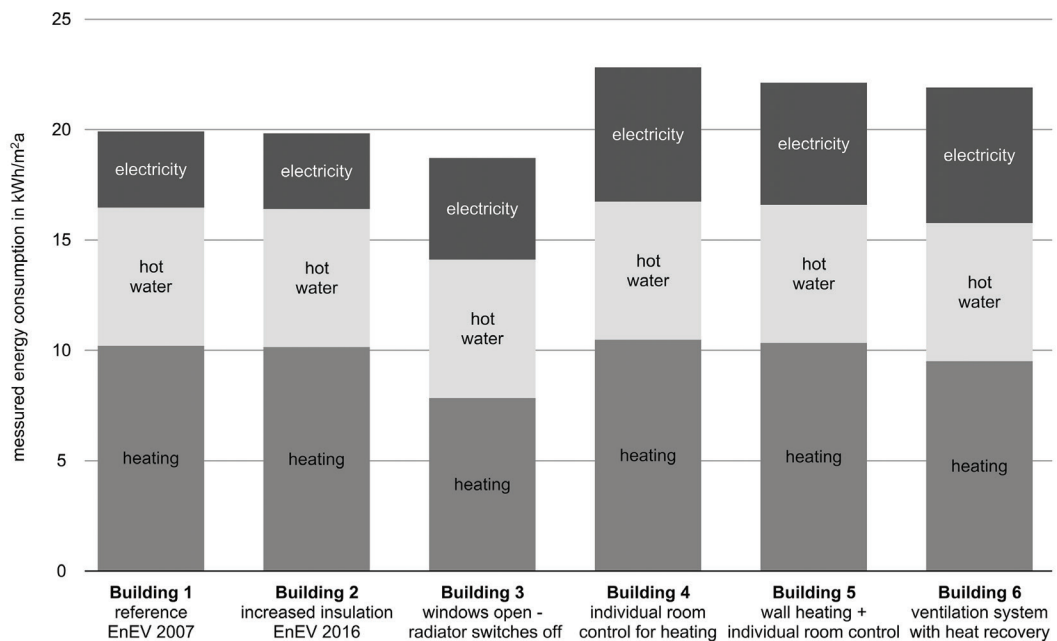


FIG. 3 Measured primary energy consumption. Electricity indicates the consumption for the operation of the heating and ventilation systems (GEWOFAG, 2020)

On this matter, Project 2226 in Lustenau is encouraging. The office building has neither HVAC nor heating system. Instead, waste heat from people and equipment is used to the maximum. The building mass functions as thermal storage. Motors open the windows depending on air temperature and CO2 level in the room. In winter, the exchange with outside air is reduced to the necessary amount, minimizing the heat loss of the building. In summer, the windows are set to open for night-time cooling. As a result, indoor air temperatures remain pleasant during a warm summer day (Eberle et al., 2016). In residential construction, the gains from waste heat are naturally lower than in an office building, where office equipment is used intensively. Nevertheless, this concept has

now also been applied to residential construction; the residential studio house in Erlenmatt Ost in Basel by the architect Heinrich Degelo.

The examples above show: It is difficult but possible to construct buildings that require little heating energy and do not overheat in summer. To understand how these buildings should look like in concrete terms, we have to look at material, construction, technical systems, user behaviour and outdoor conditions – all at once.

Which influence have room design, material, ventilation and user behaviour? Do they interact with each other and thus have a strengthening or balancing effect? This study aims to answer these questions in a fundamental and comprehensible manner.

2 METHODOLOGY

The authors compared input conditions combinations on a room design level, using parametric thermal-dynamic building simulation, and evaluated them according to energy demand and thermal comfort. The variations can be considered as extreme scenarios, chosen to span the maximum range of the effect each parameter can have. Conducting the method resulted in 448 different investigation scenarios; the variant combinations are based on the choice of construction material and technical service system, orientation, room geometry including window size and type of glass, as well as climate conditions and user behaviour (Fig. 4).

3 SIMULATION SETTINGS

The simulation was conducted on a room model level, using the Rhinoceros/Grasshopper® environment with the plug-in TRNLizard and the calculation kernel of the software TRNSYS 18. The room model has a room floor area of 18 m². The room is located between two building floors and surrounded by identical student rooms and a corridor. One external wall with window connects the room to outside climate conditions. The parameters of the base case's room model can be seen in Fig. 4, as well as the parameters for construction material, technical service system, and orientation. The room is occupied by one person, describing the standard situation of a student dorm room. Following paragraphs describe the additional parameters concerning the climate conditions and user ventilation behaviour.

Outdoor climate

To assess the impact of the climate conditions, the study compares two extreme weather data sets of the present (2010x) and its meteorological prognosis for 2035 (2035x) in Munich, using the data sets for "typical reference year" (TRY) of the German Weather Service (DWD, 2020).

Sun shading

The effect of an external, movable sun shading (factor 0.8) is simulated for the construction types "timber EB", "standard EnEV" and "low energy building". For those variants, the extreme situation of a defective sun shading (no shading) throughout the year was modelled in order to examine the maximum impact this parameter has as a worst-case scenario.

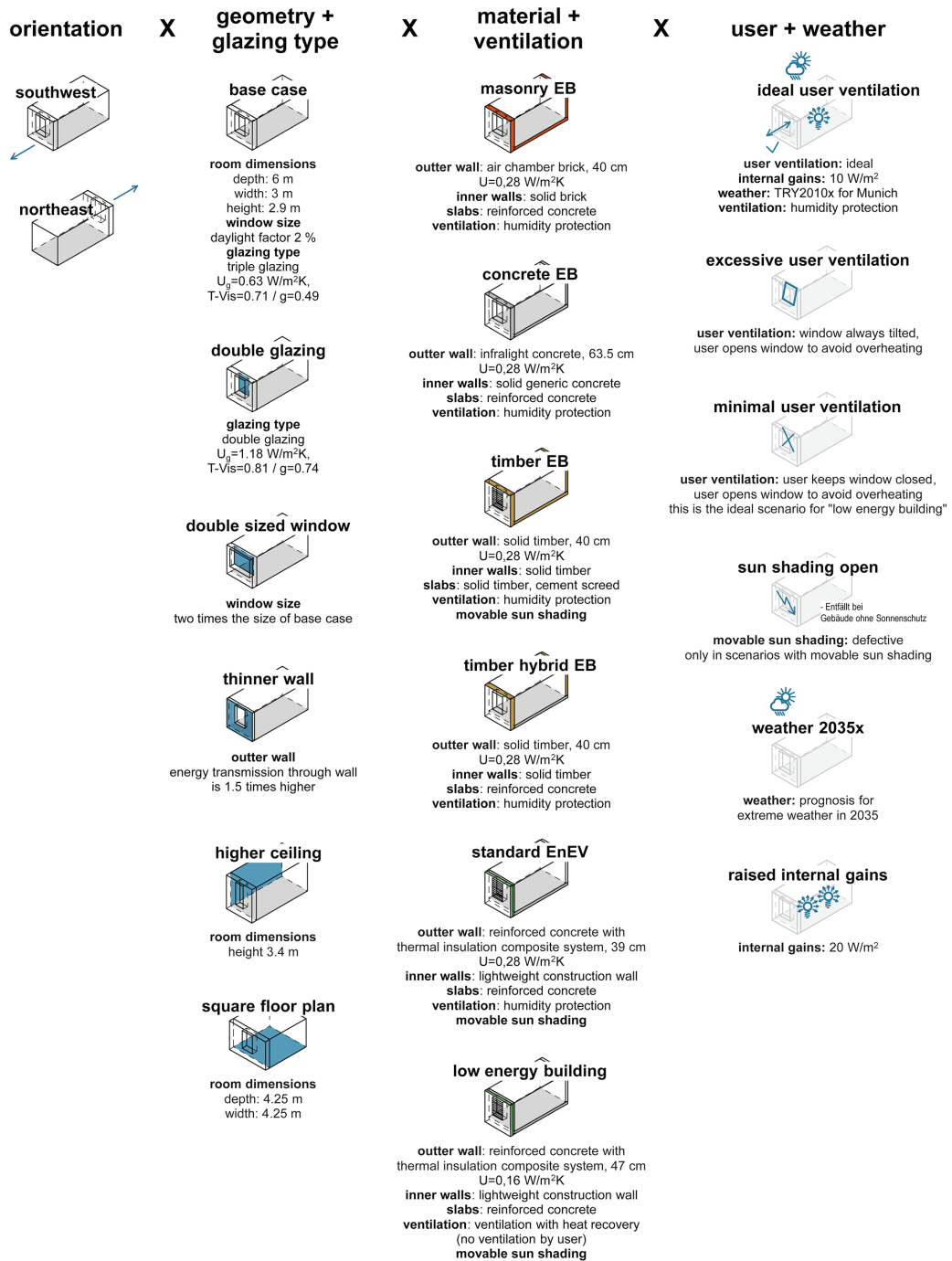


FIG. 4 Parameters of each scenario with a total variant amount of combinations of 448

Raised internal gains

In addition to the heat gains from solar radiation and the human body (75 W), the internal gains for equipment and artificial lighting are summed up to 10 W/m^2 room floor area for the base case. This value is doubled to 20 W/m^2 for the scenario "raised internal gains". In the simulation, the internal gains for equipment are linked to the occupancy schedule of the user.

Ideal user ventilation

In all ventilation scenarios, the fresh air infiltration rate is set to provide humidity protection and is established by a window rebate slot in combination with an exhaust fan in the bathroom. The ideal ventilation scenario assumes that the user provides hygienic minimum air exchange of $1.25 \text{ m}^3/(\text{h}\cdot\text{m}^2)$ at all times of occupancy. Additionally, the user ideally ventilates to avoid overheating from 24 to 22 degrees room air temperature. The fresh air rate is calculated depending on the window height and opening area, as well as the delta in air temperature indoors and outdoors. The maximum air change rate, including the hygienic minimum rate, is limited to 3/h at day and 4/h at night.

Minimal user ventilation

This scenario assumes that the user never opens the window, except to avoid intense overheat situations. The user ventilates from 26 to 24 degrees room air temperature during day and night. This leads to a constant minimal air exchange in form of the infiltration rate, increased by the additional window ventilation with maximum air change rates (no hygienic minimum rate!) limited to 3/h at day and 4/h at night.

Excessive user ventilation

For the opposite worst case of user ventilation, the window is constantly tilted by the user, even in winter. This leads to unnaturally high energy demands. However, the study method at this point is to span the maximum range of the impact of each so-called unpredictable boundary condition. Built examples confirm excessive heating energy demands that are attributed to the user's ventilation behaviour (Schneider, 2015). This user profile assumes a constant increased fresh air change rate of $2.25 \text{ m}^3/(\text{h}\cdot\text{m}^2)$ with overheat ventilation from 24 to 22 degrees room air temperature. The total maximum air change rate, including the permanent ventilation, is limited to 3/h at day and 4/h at night.

For the standard EnEV scenario, the same ventilation profiles are used. However, the low energy building contains a mechanical ventilation system of constant air exchange with heat recovery according to DIN EN 13053, meeting the requirements for minimum hygienic ventilation. The three user ventilation profiles are applied to the running system.

Evaluation criteria

The authors choose two criteria to cover both the building's performance in winter and in summer. The heating energy demand is used as performance criterion for winter, whereas overheating in form of accumulated Kelvin hours above the adaptive comfort range according to DIN 15251 is the performance criterion for summer period.

4 RESULTS AND DISCUSSION

The results show the effects on overheat hours and energy demand depending on the choice of variation from the base case. The following point cloud gives an overview of all runs simulated in order to show the overall span concerning energy demand and summery overheat hours, ranging from almost zero up to $90 \text{ kWh/m}^2\text{a}$ and from approximately 100 up to over 3400 Kh/a (Fig. 5).

The overview clearly depicts sub-groups within the point cloud, which can be linked to the effect of the parameters examined in the present study. In order to find the parameters behind the sub-clouds, the authors designed graphs that highlight the base case and its five variants in different colours: "ideal user ventilation" (base case), "excessive user ventilation", "minimal user ventilation", "raised internal gains", "weather 2035x", and "sun shading open" (Fig. 6).

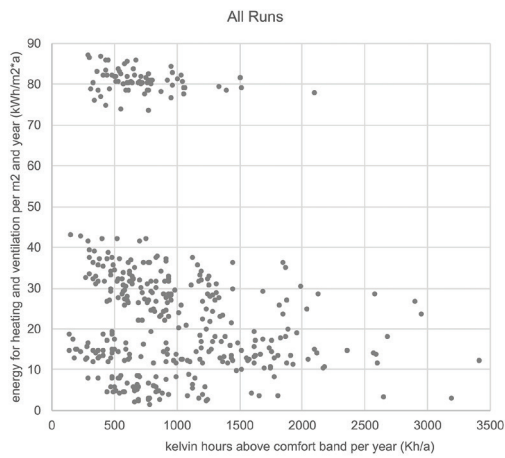


FIG. 5 Point cloud of all simulation runs accordingly to the criteria energy demand and summery overheate hours per year

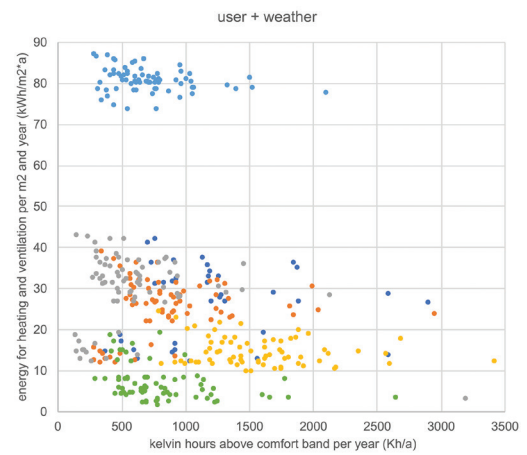


FIG. 6 Point cloud of all simulation runs coloured accordingly to six scenarios

The results show the expected significance of user behaviour concerning ventilation. The effect of future climate conditions shows a reduced energy demand – due to milder outside air temperature in winter – and a greater overheating – due to more frequent sequences of hot days and nights in summer. The climate not being the overall key aspect in the discussion is due to the small chosen future time span of the year 2035 and the fact that the DWD data prognosis does not show extreme future climate conditions.

However, the results show that raised internal gains have the highest impact on overheating in summer, whereas the ventilation behaviour of the user is the overall key parameter concerning the energy demand.

In the further discussion, conclusions are drawn on the observed results. Before looking at the building construction types, the study starts with the geometrical properties of the room (Fig. 7). In this way, the authors discuss each of the characteristics examined individually.

Constellation by geometry

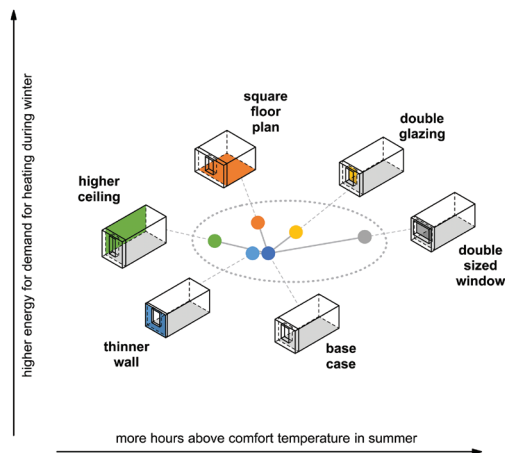


FIG. 7 Constellation of the geometrical variants related to overheating in summer and heating energy demand.

Thinner wall

The smallest deviation from the "base case" can be found in the variant with reduced outer wall thickness. Thereby, several effects overlap each other; The reduced wall thickness also reduces the insulation value of the outer wall, which in turn increases the heat transmission through the outer wall, provided there is a temperature difference between room temperature and outside air temperature. At the same time, the reduced thickness of the wall increases the intake of light through the window. This means that a slightly smaller window is also sufficient, providing the same amount of daylight, which reduces heat loss through the windows in winter. In the overall balance, the superposition of these effects on the outside wall and window mildly reduces in almost all variants the overheat in summer and the energy demand in winter.

Square floor plan

A stronger deviation from the "base case" can be observed in the variant with squared footprint. Due to the changed spatial form "width x depth" of 4.25 m x 4.25 m instead of 3 m x 6 m, the proportion of the outer wall in particular increases, which increases the heat transmission. The inner wall surface decreases accordingly. This changes the thermal storage mass depending on the material. Due to a smaller room depth, the window can be slightly smaller, providing the same amount of daylight. In the overall balance, the energy demand increases in winter. The overheating in summer is reduced compared to the "base case".

High Ceilings

The strongest improvement regarding overheating in summer is achieved by this variant with a greater room height of 3.4 m instead of the 2.9 m of the base case. The height of the room increases the area of the outer and inner walls accordingly. This, in turn, increases the thermal storage mass depending on the material. For the room models, the dimensions of the window were initially specified to remain constant, with a parapet height of 0.9 m and a lintel height of 0.2 m. The height of the window therefore changes accordingly with the room height. Due to the increased height of the window, a greater exchange of air is also assumed for natural night ventilation on cool summer nights (Fitzner, 2012). The width of the window is approximately the same in order to maintain the assumed daylight supply. All in all, the window area is slightly larger. Compared to the base case, an increase in the energy demand can usually be observed. It can be assumed that in addition to the slightly larger windows, the storage masses in combination with the night setback of the heating system also lead to this result (Tersluisen et al., 2017).

Double glazing

In this variant, the three-pane glazing of the base case window was replaced by a double-glazing. This increases both the daylight and the solar gains through transmission. In all scenarios, a stronger overheating in summer can be observed. The total energy demand remains almost the same, respectively is slightly increased or reduced.

Double sized window

The window area with this variant is twice as large as in the base-case. This increases both the daylight and solar gains through transmission. In the overall balance, the energy demand remains almost the same, respectively is slightly increased or reduced. In comparison to the base case, this variant causes the strongest over-heating in summer.

In the following, the authors lead through the variants that result from the different materials and ventilation behaviour individually.

Masonry EB (Simply Build)

Both investigated orientations show similar results (Fig 8). The room facing northeast has a slightly higher energy demand in winter and a lower overheating in summer. Surprisingly, even in the

northeast orientation several variants are above the comfort limit for overheating in summer of 1200 Kelvin hours per year. Especially concerning the variants with increased internal gains – representing e.g. a “home office room”. In general, for the “simply build” method of the massive construction “masonry EB” the following applies: with large windows and high internal gains, overheating in summer can be assumed, regardless of the other factors.

On the other hand, higher internal gains lead to a strong reduction of energy demand. The effect on energy demand is only exceeded by the natural ventilation behaviour of the user. If the user ventilates minimally, this strongly reduces the energy demand. If the user keeps the window tilted, the energy demand rises significantly. Already at this point, it is possible to give an answer to the research questions asked:

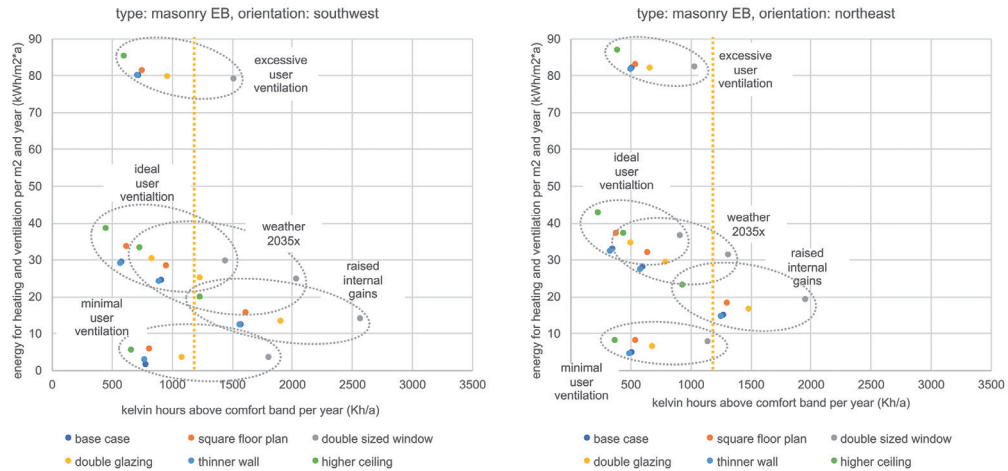


FIG. 8 Performance of the “masonry EB” construction method in relation to overheating and heating energy demand

- 1 The gap between the actual energy consumption and the calculated energy demand is strongly driven by the effect of the user’s ventilation behaviour.
- 2 High internal gains and minimal ventilation reduce the energy demand significantly. In combination, it is very likely to keep a room in the comfortable range in winter, without using a heating system. It is to note that restrictions in air quality (CO2 level) are to be tolerated.

Concrete EB (Simply Build)

The results of the “concrete EB” construction method are very similar to those of “masonry EB” (Fig. 9). Overall, the summery overheating is lower, which can be linked to the high thermal storage mass of this construction method. The variant with increased room height has an especially high thermal storage mass and more effective night cooling through natural ventilation. This variant is always in the comfortable range, independent of user behaviour or climate conditions, and is therefore particularly robust with regard to over-heating in summer.

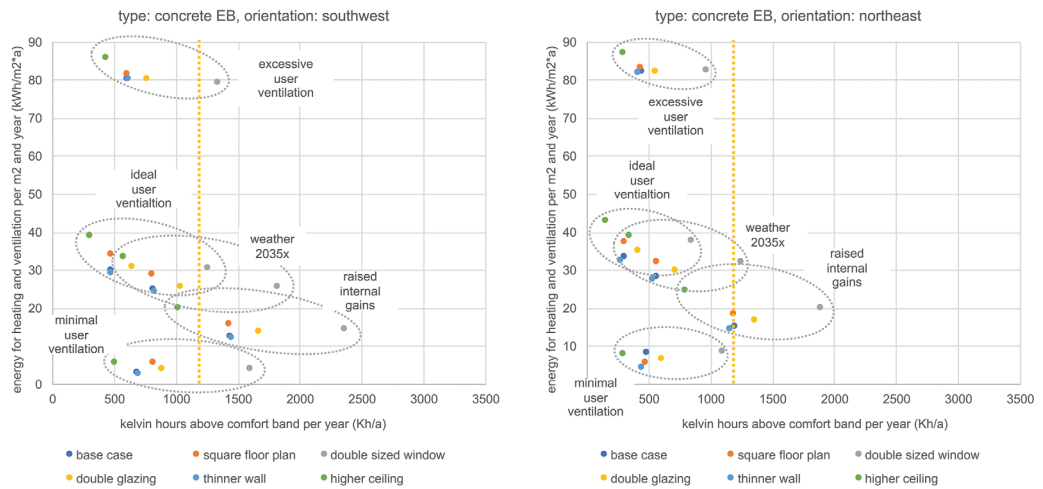


FIG. 9 Performance of the "concrete EB" construction method in relation to overheating and heating energy demand

Timber EB (Simply Build)

The massive construction method "timber EB" is, in contrast to the previous versions, equipped with a movable, external sun shading. Previous investigations by the authors observed that this base case variant is robustly protected against overheating in summer (Nagler et al., 2019). Even less overheating compared to "masonry EB" and "concrete EB" proves that this measure is effective. However, this does not apply to the timber variants with increased internal gains. Endres et al. already identified the thermal storage mass as a positive effect on room comfort, provided the use of the room causes high internal heat gains (Endres et al., 2018). Without sufficient thermal storage mass, overheating can only be avoided with active technical measures. In the present study, the authors simulated the case without external movable sun shading. Particularly in connection with the double-sized window, overheating in summer is evident. Only the variant with increased room height and correspondingly larger thermal mass and more effective night cooling lies within in the comfortable range, regardless of the building's orientation (Fig. 10).

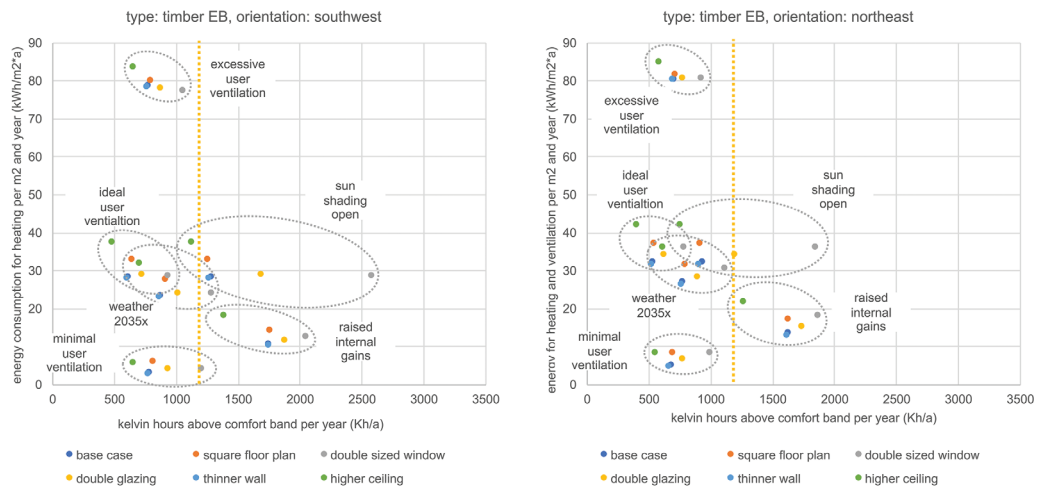


FIG. 10 Performance of the "timber EB" construction method in relation to overheating and heating energy demand

Timber hybrid EB (Simply Build)

The "timber hybrid EB" variant consists of solid wood walls and a reinforced concrete slab. This set of variants is investigated to test whether this material combination can be sufficiently robust against overheating in summer, even without an external movable sun shading. The test turned out to be successful for many parameter combinations (Fig 11). The test was not successful for all variants with doubled window size and increased internal heat gains. For the orientation southwest, all variants with double-glazing, minimal ventilation rate and extremely hot climate conditions result in summery overheating. The variant with increased room height is always within the comfortable range regardless of climate, orientation and ventilation behaviour of the user, excluding the case of raised internal gains.

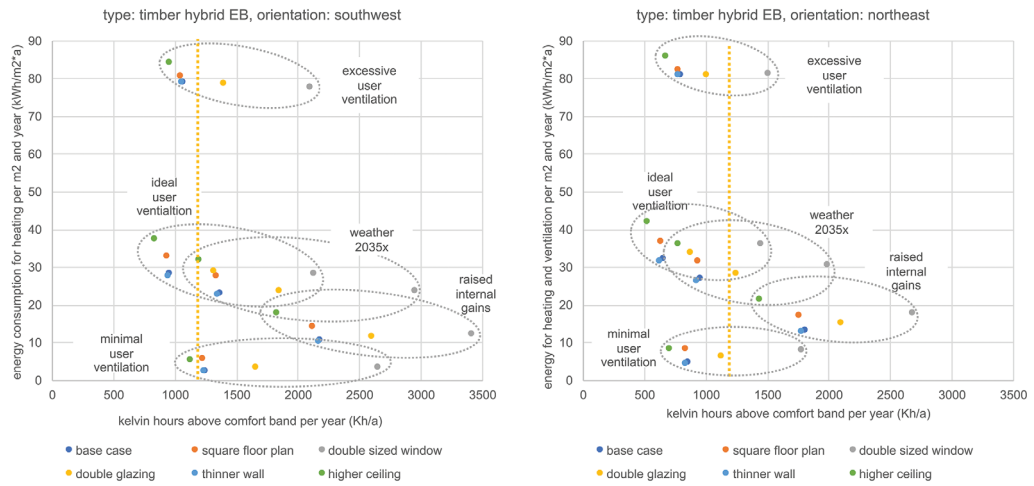


FIG. 11 Performance of the "timber hybrid EB" construction method in relation to overheating and heating energy demand

Standard EnEV

In this room variant, the outer wall consists of reinforced concrete and external insulation. The floor slabs are also made of reinforced concrete. The inner walls are designed as metal stud walls with lightweight panels. The window is equipped with an external, movable sun shading. The results are almost identical to the results of "timber EB" (Fig. 12). Overall, the overheating is minimally reduced. Within this batch simulation, the squared-floor-plan-variant performs well concerning thermal comfort in summer. This shows that the reinforced concrete of the outer wall contributes strongly to the thermal inertia of the system. Overall, the conclusions equal those of the "timber EB" variant.

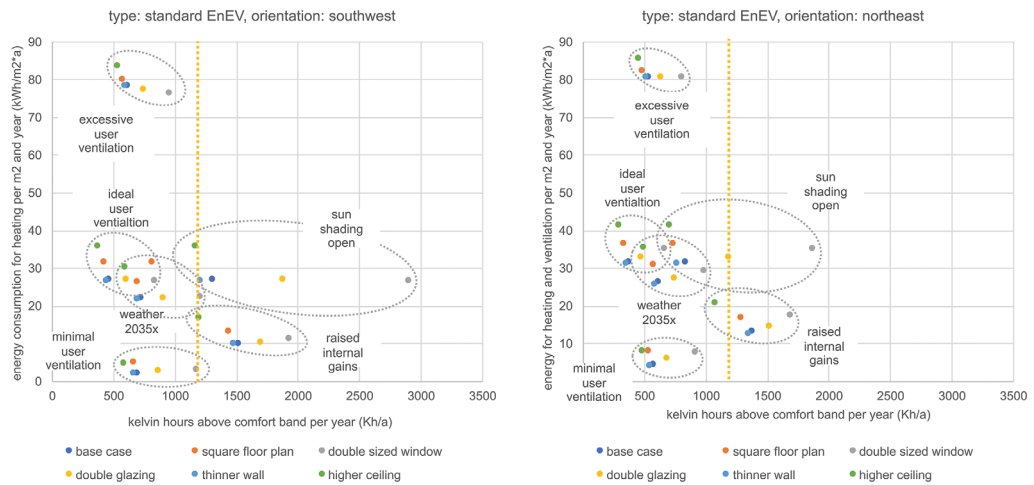


FIG. 12 Performance of the "standard EnEV" construction method in relation to overheating and heating energy demand

Low energy building

This variant is similar to the "standard EnEV" variant in terms of its design but has a thicker insulation layer on the outer wall as well as a mechanical room ventilation with heat recovery. The room air is constantly exchanged by the ventilation system in order to meet the requirements for air temperature and hygienic air conditions. Therefore, the user should keep the windows closed, to ensure that the heat recovery system performs at its highest efficiency. In winter, it reduces heat losses, which would occur through the exchange of room air with the fresh air. The results reflect this effect (Fig. 13): The energy demand is approximately half compared to the "standard EnEV" variant. The increased demand for operating energy for ventilation is already included. The model also scores well in the simulation for thermal comfort in summer. Only the variants with double sized windows or doubled glazing in combination with malfunctioning sun shading or increased internal heat gains exceed the comfort limit for overheating in summer. The energy demand increases rapidly in winter, when the user tilts the window in addition to the mechanical ventilation. This is in line with the results of the GEWOFAG study, where only 7% savings in operation were achieved instead of the theoretically determined 30% savings (GEWOFAG, 2020). A similar study by the Baugenossenschaft Hagenbrünneli in Zurich even measured a mere 2 % savings in heat demand compared to a reference building without mechanical room ventilation. The authors of this study state: "[...] it was clearly shown for a specific residential property that a central ventilation system with heat recovery is neither ecologically nor financially worthwhile compared to uncontrolled window ventilation with exhaust air." (Knecht Sigrist, 2019).

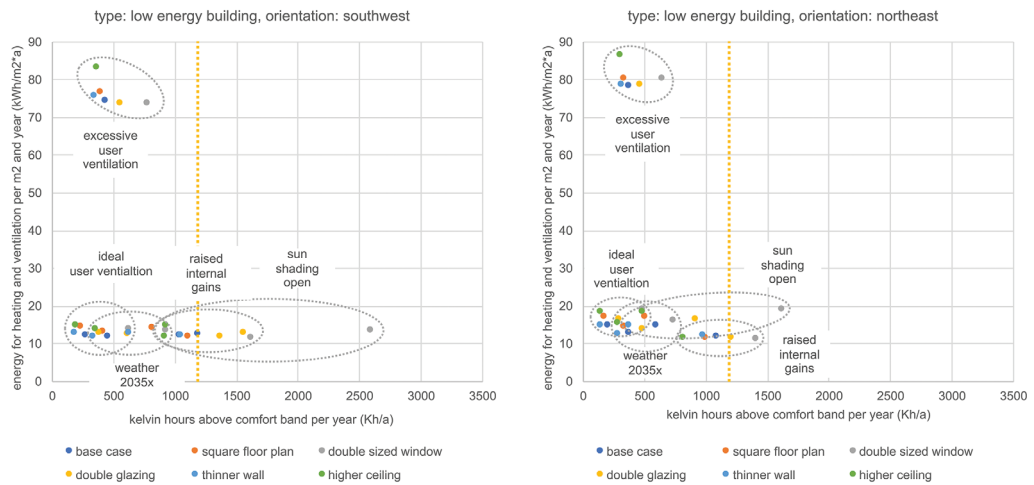


FIG. 13 Performance of the "low energy building" construction method in relation to overheating and heating energy demand

The observations of this variant reinforce that the gap between the actual energy consumption and the theoretically calculated energy demand is strongly influenced by the ventilation behaviour of the user. Deviations of the ventilation system's theoretical performance – e.g. due to poor maintenance – are not yet included here.

5 CONCLUSIONS

Construction methods with high thermal storage mass content in combination with appropriate window sizes and triple glazing ensure a high level of room comfort in summer. In winter, an optimized utilization of internal heat gains combined with an energy-efficient ventilation behaviour of the user results in only little to no energy for heating. On a long-term perspective, monolithic façades rank on a par with standard EnEV and low-energy building façades.

The "Simply Build" strategy reduces the complexity of building construction, creating buildings through material- and climate-friendly design that require little heating energy and do not overheat in summer. In this way, the necessary building technology can be reduced to a few robust systems. Wherever possible, single-layer components made of natural and renewable raw materials protect the environment over the entire life cycle of the building. To give an outlook on the study matter, research is being carried out at the Technical University of Munich in an interdisciplinary research group called "Einfach Bauen" (Nagler et al., 2019). Residential buildings on which the "Simply Build" strategy is being tested in practice are already under construction (Fig. 14), others are being planned. Further information on the research buildings can be found at www.einfach-bauen.net.



FIG. 14 The "Simply Build" research buildings in infra-light concrete, massive timber and masonry construction; Bad Aibling, Germany; @sebastianschels

References

- §79 GEG. Gesetz zur Einsparung von Energie und zur Nutzung erneuerbarer Energien zur Wärme- und Kälteerzeugung in Gebäuden (Gebäudeenergiegesetz - GEG) § 79 Grundsätze des Energieausweises
- DWD. (02. 09. 2020). Testreferenzjahre (TRY). Von <https://www.dwd.de/DE/leistungen/testreferenzjahre/testreferenzjahre.html> abgerufen
- Eberle et al. (2016). Die Temperatur der Architektur: Be 2226; Portrait eines energieoptimierten Hauses. Basel: Birkhäuser.
- Endres et al. (2018). Parameterstudie Low-Tech Bürogebäude. Endbericht. Technische Universität München. BBSR Bonn: Fraunhofer IRB Verlag.
- Fitzner. (2012). Lüftungsregeln für freie Lüftung. Dortmund/Berlin/Dresden.
- GEWOFAG. (06. 04. 2020). Forschungshäuser Riem (2016). Von [https://www.gewofag.de/web.nsf/id/8-seiter-forschungshaeuser-riem-gewofag/\\$file/8-Seiter_Forschungshaeuser_Riem.pdf](https://www.gewofag.de/web.nsf/id/8-seiter-forschungshaeuser-riem-gewofag/$file/8-Seiter_Forschungshaeuser_Riem.pdf) abgerufen
- IWU. (2019). Berücksichtigung des Nutzerverhaltens bei energetischen Verbesserungen. Bonn: BBSR-Online-Publikation Nr. 04/2019.
- Knecht Sigrist (2019). Vergleich der beiden Lüftungskonzepte der Siedlung Klee bezüglich Ökologie und Ökonomie, s3 GmbH, Dübendorf
- Nagler et al. (2019). Einfach Bauen. Ganzheitliche Strategien für energieeffizientes, einfaches Bauen - Untersuchung der Wechselwirkung von Raum, Technik, Material und Konstruktion. BBSR Bonn: Fraunhofer IRB Verlag.
- Schneider. (2015). Nutzerverhalten bei Sanierungen berücksichtigen. RWTH Aachen Universität. E.ON Energy Research Centre. BINE Informationsdienst. Projektinfo 02/2015.
- Terluisen et al. (2017). Untersuchung zeitgemäßer, monolithischer Wandaufbauten hinsichtlich bauphysikalischer, ökologischer und ökonomischer Eigenschaften. Kaiserslautern: BBSR AZ 10.08.18.07-15.34.

A Full Performance Paper House



**Rebecca Bach*¹, Alexander Wolf¹, Martin Wilfinger¹,
Nihat Kiziltoprak¹, Ulrich Knaack¹**

* Corresponding author

¹ TU Darmstadt Institute of Structural Mechanics and Design ISM+D

Abstract

According to the UNHCR, in 2019 there were 70,8 million refugees worldwide. Due to war, catastrophes and emergency situations a great demand for temporary accommodation occurred within the last couple of years. The main requirements for these shelters are protection for the inhabitants, easy transportability and quick construction. In addition, in terms of resource efficiency, the recyclability of the construction materials is of great importance. Paper materials have a high potential for this, due to their strong structure, cost-effective production and optimized recycling processes.

The following paper presents a case study of a prototype for a temporary paper house that meets the static and technical requirements for a comfortable and hygienic living space by the combination of different paper materials.

The overall objective of this research was the constructive development of building elements made of paper materials, that meet the requirements for a temporary residential use over a period of at least 3 years. The main advantages of using paper materials for this purpose are easy processing, cost-effective production and a high probability for its sustainable disposal after usage. The main challenges of the material are fire protection and moisture protection, which affect the recyclability as well as the gluing and joining techniques. An overview of possible solutions for these disadvantages and their applicability will be demonstrated and discussed.

The paper aims to emphasize that simplicity and performance do not need to be diametrically opposed. The envelope, which provides all the functions required of a modern building through its multi-layered structure, represents the performance of this project. Transportation, construction and joining, on the other hand, were kept as simple as possible in order to make assembly possible even by unskilled workers and under very basic conditions.

It is divided into four sections. At first the technical and regulatory requirements for temporary emergency shelters as well as the decisive characteristics of paper materials are described and analysed. Within the second part the architectural design and the construction typology are defined. The third part focusses on the elaboration and evaluation of building elements with regard to joining technologies, statics, building physics and production technologies. In the end the results of the prototype and their transferability are presented and discussed.

Keywords

Paper, construction, building with paper, prototype, emergency shelter, full performance paper house

DOI 10.7480/jfde.2021.1.5533

Multi-Criteria Design and Decision Support for Solar and Green Envelopes

Elisabeth Fassbender¹, Claudia Hemmerle², Natalie Muhr³

- 1 Technical University of Munich, Chair of Building Technology and Climate Responsive Design, Arcisstraße 21, 80333 Munich, Germany, +49 89 289-23980, elisabeth.fassbender@tum.de
- 2 Technical University of Munich, Chair of Building Technology and Climate Responsive Design, Arcisstraße 21, 80333 Munich, Germany, +49 89 289-22964, claudia.hemmerle@tum.de
- 3 Technical University of Munich, Chair of Building Technology and Climate Responsive Design, Arcisstraße 21, 80333 Munich, Germany, +49 89 289-23980, natalie.muhr@tum.de

Abstract

Cities play a key role in facing the challenges of climate change and building envelopes serve as the representative face of the built environment while simultaneously offering opportunities to integrate climate and energy active technologies such as solar energy or building greenery. Thus, they are able to contribute to climate protection as well as to climate adaptation and liveability. To exploit these potentials, the district scale has proven to be effective and manageable, benefiting from synergies among buildings and infrastructures. However, district development and renovation needs to cope with limited urban surfaces and a variety of civil-society, political and economic stakeholders with partially conflicting objectives and claims. Thus, a balancing and prioritization of different technological measures and design options for building envelopes is required, considering urban planning, architectural, energy, climate, biodiversity and other aspects beyond the envelope context. This research work develops a holistic, district-scale design and decision support in early design stages to promote high performance and resilient building envelope solutions. The methodology is based on a multi-criteria decision analysis (MCDA) approach in order to account for the complexity of design decisions. It provides a transparent and structured process to systematically evaluate and compare different envelope designs in five categories. A modular structure allows the adaptation of the decision support system according to individual decision contexts and criteria as well as to the assessment scale from a single building up to a whole district. Based on a default decision context, a wide target system and associated criteria were derived and the evaluation and aggregation principles were developed. To offer intuitive application, the theoretical concept was implemented into a user-friendly digital tool. In conclusion, the tool offers support to investors and developers, architects and urban planners as well as municipal and private business decision makers in objectively comparing and communicating different design scenarios in a structured work flow to make robust implementation, investment or funding decisions. Used during early design stages, it can promote district concepts with high energy and climate performance and resilience and reduce reservations about the architectural quality of solar and greening systems and their integration in sensitive urban environments. Perspectively, a more sophisticated MCDA method will be applied in order to use the full potential of MCDA to model and display various stakeholder perspectives as default option in the framework of a case study.

Keywords

Solar energy, greenery, decision support, district-scale performance, energy and climate resilience, architectural quality

1 INTRODUCTION

Cities play a key role in facing the challenges of climate change. Increasing heat stress in cities enhances the demand for climate adaptation measures to increase climate resilience of the urban living environment. Climate protection measures to reduce carbon emissions and mitigate climate change are closely linked to energy saving and the promotion of renewable sources and therefore to buildings as major energy consuming sector. The carbon positive transformation of buildings should pay particular attention to building envelopes and their different functions. They serve as the representative face of the built environment while simultaneously offering opportunities to integrate climate and energy active technologies such as solar energy or building greenery. Thus, they are able to contribute to climate protection as well as to climate adaptation and liveability.

Solar energy and greenery systems in building envelopes only will achieve broad acceptance if they are accompanied by an adequate aesthetic expression and, especially when applied to existing buildings, respect the built environment with its architectural and urban context and characteristics. Deficient design quality in favour of climate or energy activation may turn out counterproductive for further dissemination. In other words, the “quest for a sustainable architecture should never be an excuse for compromising quality of design.” (Foster, 2010). Yet, the integration of both technologies into building envelopes presents new a planning and design task resulting in a demand for design support in developing solutions with high architectural quality.

To exploit the potentials of climate and energy activated envelopes, the district scale has proven to be effective and manageable, benefiting from synergies among buildings and infrastructures without having to take into account the complexity of a whole city. However, district development and renovation needs to cope with limited urban surfaces and a variety of civil-society, political and economic stakeholders involved. The fact that it is not always possible to resolve their sometimes conflicting objectives and claims often leads to dissatisfaction regarding the planning and implementation process (Brohmann et al., 2020). Therefore, a decision support is required to set soundly-based priorities. Within the research project TRASIQ, an interactive evaluation tool for planning staff and residents, allowing a first quick assessment of different planning alternatives in terms of sustainable living criteria, has proven to be an appropriate instrument (Brohmann et al., 2020). In the case of competing technological measures for building envelopes, the balancing has to consider urban, architectural and energy concepts of the whole district.

Such complex decision tasks with multiple and conflicting objectives and dimensions can be addressed by means of a multi-criteria decision analysis (MCDA), integrating multiple perspectives and constraints, and considering multiple relevant, but sometimes unclear consequences (Cinelli et al., 2020; Geldermann & Lerche, 2014). MCDA is widely used to support decision making in domains like energy technologies and systems evaluations, urban regeneration planning, resilience and sustainability assessment, comparison of policy options (Cinelli et al., 2020; Wilkens, 2012) and helpful to compare and select investment projects from public services to technological solutions for buildings systems (Andes, 2019; Rosasco & Perini, 2019).

Few studies already applied MCDA to solve decision tasks concerning design and planning processes. Vullo et al. (2018) have identified a lack of criteria in tender procedures to evaluate the effects of diverse properties of façade components on the overall building performance and described a general need for easily usable methods and tools giving immediate feedback on the impact of various design variations to assist less-experienced decision makers. Therefore, they developed a new multi-criteria approach and performance evaluation tool for designers and contracting authorities in public procurement processes during early design phases with a focus on façade retrofitting. They have concluded that the tool sensitizes designers and initiators, offers

support in making informed and performance based design decisions by all stakeholders and drives awarding design variations with the best overall performance. Moghtadernejad et al. (2020) provide a systematic approach for designers to balance design objectives and select desirable, high performance façade alternatives based on multi criteria optimization and decision support tools, stating that the application of MCDA methods in façade design procedures is useful but not yet completely mature. These approaches, however, refer to the single building scale without taking into consideration interactions with the urban environment at district scale.

In recent years, sustainability certification systems such as the German DGNB (Deutsche Gesellschaft für Nachhaltiges Bauen) and the US American LEED (Leadership in Energy and Environmental Design) systems enlarged their assessment scale from single buildings up to neighbourhoods and urban districts including criteria treating climate resilience aspects (Berardi, 2015; Deutsche Gesellschaft für Nachhaltiges Bauen e.V., 2020). Yet, these systems are too complex to provide specific decision support for the selection of building envelope solutions. Moreover, various aspects described above are not represented, especially the individual integration of diverging perspectives and preferences of the involved decision-makers and stakeholders or policy goals of the respective city.

Thus, this research work aims to develop a concept to support design and decision processes of solar technology and greenery solutions as climate protection and climate adaptation measures in the building envelope, considering district scale interactions with the urban environment and allowing to include multiple players' objectives and needs. By means of adapting existing evaluation systems and methodological approaches to the specific analysis objective and scale, the proposed concept evaluates functional qualities in terms of performance, resilience and feasibility as well as ecological, liveability and economic aspects and addresses relevant factors influencing the decision to implement greening and solar technologies in buildings. The theoretical concept is based on the framework of MCDA and is transferred into a digital, interactive tool to facilitate an intuitive application and to motivate architects, urban planners and project developers to use the tool as design and decision support in early design stages. It is meant to quickly visualize the effects of design decisions and raise awareness – in the first place why to apply solar and green systems and secondly to understand the complex issues and to create high quality integration and in the third place to communicate design proposals to owners and investors, to financing, tendering or approval bodies and to the civil society.

2 METHODOLOGY

The research procedure is literature based, comprising a review of the structural elements and the potential of MCDA to integrate sustainability and resilience assessment methods as well as multiple perspectives and constraints. The development of the concept for design and decision support condenses and adapts the findings of a broad literature review including 1) approaches, criteria and aspects to define, enhance and evaluate design and integration quality for the design support part and 2) sustainability rating systems and indicators for the evaluation and decision support part.

2.1 MCDA FRAMEWORK

The MCDA concept provides a systematic process to explore and structure a decision-making problem, to elicit decision makers' and stakeholders' preferences and to analysis benefits and disadvantages regarding multiple evaluation aspects. It results in a transparent and documented identification of the most advantageous alternative, in the most acceptable compromise or

in a ranking of the solutions according to the agreed criteria. Hereby, MCDA techniques can combine the assessment of

- Effects measured in monetary terms (cost flows),
- Physically quantifiable effects like energy and material flows or micro-climate effects (which might be transferred into monetary terms) and
- Non-monetisable effects in terms of design, user acceptance or competing installations.

These features qualify MCDA approaches as methodological basis for the complex decision task to choose or rate urban building envelope solutions and distinguish them from disciplinary and mono-criteria assessment methods like cost benefit analysis typically used to support investment decisions and can lead to the selection of options with poor performance in other dimensions and poor balancing of interests.

Literature describes various series of structured process steps to carry out a MCDA, which are very similar in essential points. Yet, it is pointed out that in practice, the method is not a rigid, linear process, but an iterative, feedback-based procedure. The steps may be combined or adjusted in their order and reflections in subsequent steps may refine or complement previous steps. (Dhar et al., 2015; Geldermann & Lerche, 2014; Wilkens, 2012) Our concept relies on the process structure shown in Fig. 1.

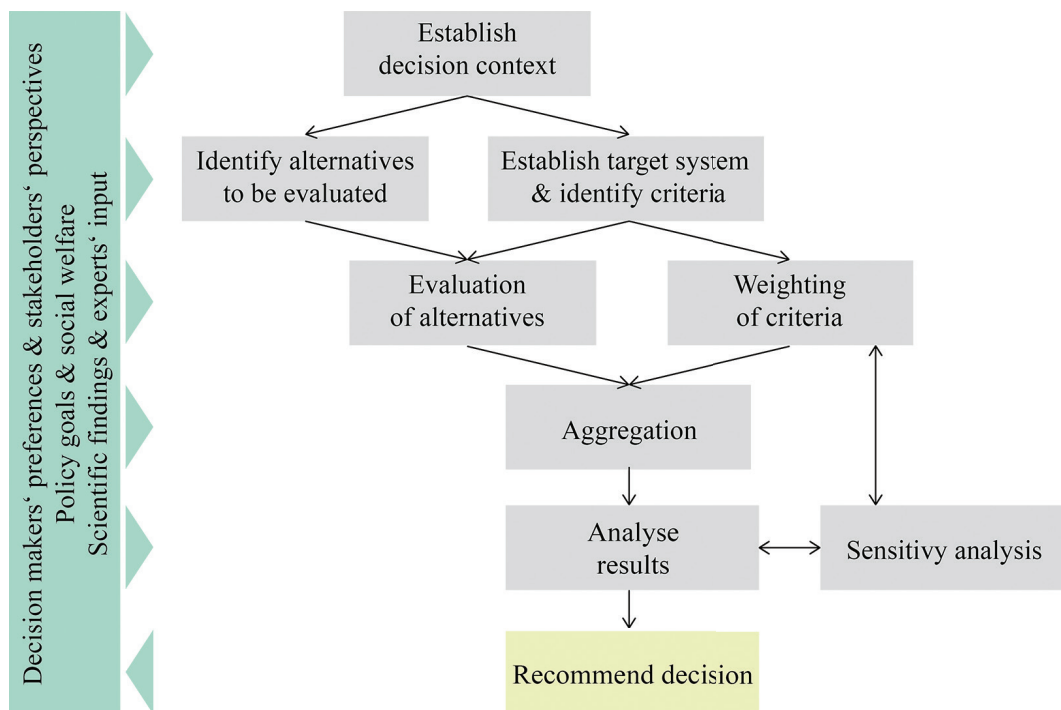


FIG. 1 MCDA process steps and potential integration of varying concerns and available information based on (Dhar et al., 2015)

The decision context describes the aim of the decision process and its structure. The identification of the players includes both the decision makers who take on responsibility for the decision and the relevant stakeholders who are affected by the decision or have an interest in it, and reveals goal conflicts resulting from their divergent interests. The subject of the comparison, the alternatives, are various compilations of façade and roof design proposals integrating solar PV and / or greenery elements throughout the district. At this point, the proposed concept provides a design module to support in developing alternative options and specifies the relevant characteristics for the later

evaluation according to the evaluation criteria established in the following step: the hierarchical target system. The target system breaks down the rather abstract objective into more specific sub-targets. These are finally translated into measurable evaluation criteria for each sub-target.

The evaluation step assesses each alternative against each criterion. As the focus is on the building envelope, impacts of other building components are excluded and the evaluation does not consider urban morphology nor green and open spaces nor district energy infrastructures. Yet, positive effects of renewable energy production in the envelope and energy balancing of individual buildings within the district will be reflected. Any evaluation methods can be selected to determine the performance of the alternatives using different physical or monetary units (quantitative data) or relative scales (qualitative data), as the performance values are subsequently normalized to one common scale. This allows integrating established methods like life-cycle assessment. Weighting takes into account how important one criterion is for the decision problem in relation to the other criteria.

Using more or less complex mathematical algorithms, aggregation combines the normalized evaluation scores and the criterion weights to provide one overall score for each alternative. The final decision recommendation is based on an examination and discussion of the aggregated results including a sensitivity analysis to reflect the stability and consistency of results. The sensitivity analysis particularly addresses the criterion weights, but is also recommended to reflect different opinions on performance judgements or different climate scenarios or time scales (Geldermann & Rentz, 2005; Trærup & Bakkegaard, 2015).

MCDA offers a variety of inputs and participatory elements throughout the process steps. The decision context and target system may respond to local or national policy goals, funding programs or marketing strategies. Decision makers' preferences are considered when identifying alternatives and criteria, and particularly represented in the performance levels (e. g. reference values) and criteria weighting. Wilkens (2012) considers active stakeholder participation appropriate and viable in a workshop setting for the development of criteria, criteria weighting and discussion of results, whereas evaluation and aggregation should be carried out by analysts and experts. Criteria weighting may also serve to analyse a decision from various perspectives. (Hermann et al., 2007) developed three sets of weights based on local, regional and national perspectives to take into account different relevance of environmental impacts on these scales. A Spanish research project presented a methodology to assess residential energy retrofitting options where the weighting was established by a team of psychologists based on user surveys (Lizana et al., 2016); and a study on the design decision of choosing green roof systems involved a panel of experts to identify the criteria and perform the evaluation from the perspectives of designers and academics respectively (Rosasco & Perini, 2019).

2.2 DEVELOPMENT OF THE CONCEPT

Following the process steps in Fig. 1, the research documented in section 3 started with the description of a default decision context. A design support module has been worked out to guide architects to create design proposals of high quality. While the evaluation of design quality of building related solar energy systems could refer to existing approaches and principles in literature, the greening part was specially developed. Based on the decision context, a wide target system and associated criteria were derived. The selected evaluation categories and criteria are oriented towards the planning tasks of early design stages in order to achieve a close connection to the design process and to simplify the application of the evaluation system. The target system serves as modular structure of the evaluation from which the relevant criteria can be selected in a given decision context. An evaluation and aggregation principle was designed to consider different scales from a single building skin up to a whole district. Following the approach of established sustainability

rating systems in Germany, benefit analysis served as MCDA method. As a preliminary mode, equal weighting was applied, but can be adjusted by the decision maker.

2.3 DEVELOPMENT OF THE TOOL

The concept for multi-criteria design and decision support was operationalised into a digital and interactive tool in order to intuitively support architects and planners in making informed design decisions in early planning stages. The primary requirements for the evaluation tool are a clear design and intuitive application along with a comprehensible presentation of evaluation results. Thus, a software tool named SoGreEn (Solar Energy – Greening – Envelope) was implemented and tested in MS Excel featuring plain structure (see section 4).

3 RESEARCH

3.1 DECISION CONTEXT

The overarching objective to promote the application and integration quality of solar energy and greenery systems as climate and energy activated building envelopes in urban district (re) development projects concerns a wide range of potential decision makers and stakeholders. Simply due to their visual influence on the cityscape, solar and green façades are a matter of urban planning. Moreover, the overall district concept usually affects a variety of residential, infrastructural, economic, energy, climate, biodiversity and other aspects of urban development. Thus, the municipal administration is a relevant decision maker in its role as planning and approval authority or as funding body. Other key decision makers are owners and property developers or investors who finance the project or measurements related to single buildings or residential complexes. The group of owners in particular shows a great variety from private owner occupiers and owner communities to private or public housing societies and redevelopment agencies. Architects and planners as contractors of the owners and investors play a consulting role in the decision and can use the analysis tool to develop and optimize their envelope designs.

Stakeholders include the residents with potentially different needs and basic orientation according to their age, economic and social situation; implementers like craftspeople, companies and energy consultants; local or national energy supply companies or energy service companies; and the general public as visitors in the district or ideally involved civil society organizations like owners' and tenants' associations or climate activists.

Goal conflicts arise between individual, mostly economically driven interests of owners or companies and collective interests which are to be represented by municipalities following the concept of public services. The latter also includes climate change mitigation and adaptation as general objectives. Further conflict potential lies in the mismatch of time horizons of long-term oriented urban planning and short-term oriented investment decisions. As fundamental design decisions are taken in early planning phases and the early inter-disciplinary coordination of measures and technologies in the planning process is essential for achieving high integration quality, the evaluation system is explicitly designed for the initial planning phases comprising the services establishment of planning parameters, preliminary planning and conceptual design.

3.2 DEFINITION OF ALTERNATIVES: DESIGN PROPOSALS

The universal acceptance of solar energy and greenery systems integrated into building skins requires architectural solutions with high design quality. However, the identification of high-quality design proposals proves to be challenging as design is a quality that cannot be measured in quantitative terms and subjective perceptions inevitably affect the design process. Therefore, this research strives to offer guidance in making design decisions based on criteria for high design quality derived from relevant studies discussing formal integration quality and taking cultural heritage concerns into consideration. To account for varying needs concerning the level of detail, the criteria are divided into the two sub-categories 'Urban design' and 'Architectural design'. Fig. 2 lists the identified criteria for both sub-categories.

Research reveals a broad consensus regarding the perception of high-quality architectural design and the existence of implicit criteria that are shared by the architectural community (Kaan & Reijenga, 2004; Munari Probst & Roecker, 2007, 2016). The acknowledgment of solar modules as an integral part of a building requires coherence of formal aspects of solar energy systems such as geometry, material and module as well as field size and form with the building design. Reference of solar modules to further parts of the building envelope as well as coplanarity with the building surface is requested (Munari Probst & Roecker, 2012).

For the application of building greenery, such criteria do not yet exist. However, different criteria such as changes in appearance throughout the year, colour of foliage and leaf coverage are inherent to greenery and thus become significant for architectural appearance and design quality. To account for the complexity of seasonal changes of greenery and its impact on building design the planner first needs to set a design objective: The design can either strive to be a monochrome or a polychrome design featuring colour changes throughout the year. Then, an objective function needs to be defined: The greenery can either act as a seasonal shading, as blinds or sight protection or the vegetation can be mounted in front of an opaque building envelope. Only in the context of these objectives the different appearances of greenery can be played on adequately thus achieving high architectural design quality.

Design strategies		
Urban Design	Architectural Design	
Integrity of historic building stock	Geometry	Seasonal changes
Ensemble effect	Materiality	Coverage
Reference to the surroundings	Modular grid	Quality of integration
	Reference to further building envelopes	
	Coplanarity	

FIG. 2 Criteria for high design quality of climate (green) and energy (yellow) activated façades

The review of design proposals based on the mentioned criteria allows a pre-selection of alternatives meeting high demands on design quality. The alternatives can subsequently be assessed according to the evaluation categories and criteria explained in 3.3.

3.3 TARGET SYSTEM AND EVALUATION CRITERIA

The primary objective to achieve high integration quality of solar energy and greenery systems in building envelopes at district scale reflecting various decision makers' and stakeholders' perspectives set the direction for specifying the target and criteria tree in a top-down-approach. The definition of sub-targets started from the basic aims of the research project Cleanvelope in the context of which the analysis takes place: to balance climate protection and climate change adaptation measurements, to guarantee cultural integrity of the built urban environment and to identify financially affordable solutions. To analyse climate and energy activated envelopes in a holistic way, the dimensions of established sustainability assessment systems were involved, including environmental impacts and technological quality. Generally, the guiding principle was to include the most relevant factors that motivate or keep designers, developers, owners or municipalities from choosing solar or green envelopes instead of inactive solutions.

The identified sub-targets (categories) shown in Fig. 3 cover all aspects required for a holistic evaluation of active building skins. They are derived from the existing assessment system DGNB (Deutsche Gesellschaft für Nachhaltiges Bauen e.V., 2020) and the research project 'Multielement II' (Schuetze et al., 2015), but focus on the performance and contribution to urban resilience of climate and energy activated envelopes.

Thus, the category Climate protection & Energy emphasizes the climate activation of building envelopes by means of photovoltaics and the local production of renewable energy, while the category Climate resilience spotlights the climate adaptation potential achieved by greenery and its effects on the urban micro-climate. In the sub-target Environment the environmental impact of the design proposals and their use or resources is analysed. The category Functionality & Technology puts emphasis on the process quality and the category Economy allows a financial comparison in order to find financially affordable solutions. Due to the preceding guided definition of alternatives high design quality in the design proposals is taken for granted.

By means of specific analysis criteria for each category, it can be determined to what extent the alternatives meet the sub-target contributes in achieving the objective. To obtain meaningful results, the criteria have to fulfil the following requirements (Kühnapfel, 2019):

- Completeness: All criteria relevant for the decision problem need to be considered
- Assessability: Each criterion needs to be assessable by the decision-maker
- Relevance: Each criterion needs to be meaningful for the decision problem
- Reproducibility: The results must not be dependent on the time the assessment is performed

Fig. 3 displays the resulting sub-targets (categories) and the associated criteria. To minimize the expenditure of time while receiving significant results, a balance between the number of analysis criteria and the level of detail of each analysis step with the required time expenditure is striven for. In all categories, the criteria are limited to effects directly caused by the building skin. Thus, effects caused by redensification of districts in the course of energetic restoration as well as criteria concerning the use of open spaces are not taken in to account. Functional requirements such as fire safety, sound insulation or thermal insulation are considered as mandatory and therefore are excluded.

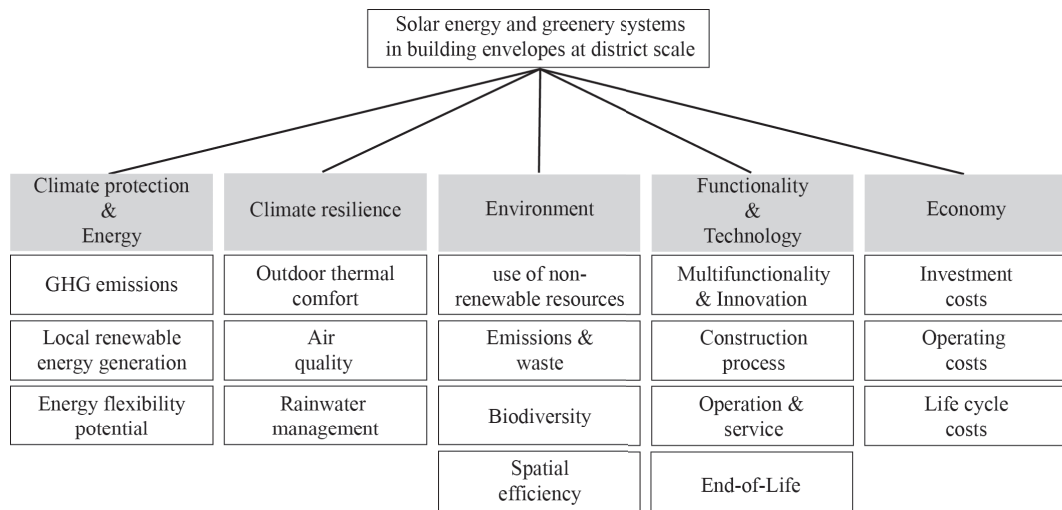


FIG. 3 Target system with primary and secondary objectives

Many cities have developed climate change strategies or concepts. The suggested evaluation criteria and their later weighting can be adjusted to be in line with the overarching objectives of these or of other urban development strategies and plans. Thus, the district's development can be integrated into the overall city perspective.

3.4 EVALUATION, WEIGHTING AND AGGREGATION

Analysing climate and energy activated envelopes at district scale presents a particular challenge in terms of different analysis levels. Some criteria describe effects on the entire district. Other criteria, however, are related to single building envelopes or even parts of building envelopes and thus need to be considered on a more detailed scale. Yet, assessing each single envelope would be very time-consuming. The solution found is to introduce three levels of analysis:

- A Analysis at district scale: One evaluation score for the whole district
- B Analysis according to technologies: Solar and greenery systems of the same technology and installation type also are subject to pooled evaluation, based on default characteristics of common types
- C Analysis according to system groups: Systems of the same superordinate system group (e.g. photovoltaic or greenery) are subject to pooled evaluation

Each criterion requires a specific evaluation method to determine the corresponding performance of an alternative. Quantitative criteria result in numeric values and quantitative criteria are indicated via classification in categories or using rating scales. The rating is based on verbal explanations. Fact sheets for each criterion provide assistance in the evaluation. Similar to the BNB and DGNB certification systems which use a benefit analysis approach (Andes, 2019), the evaluations of both qualitative and quantitative criteria are transformed into normalized scores on a rating scale ranging from 0 to 10, where 0 indicates "unsatisfied", 1 the minimum level, 5 and average and 10 the best possible performance (Deutsche Gesellschaft für Nachhaltiges Bauen e.V., 2020).

According to the nature of the criteria and the three analysis levels described above, some criteria rely on a single feature and others combine the mean values of several entities or systems or comprise several partial criteria.

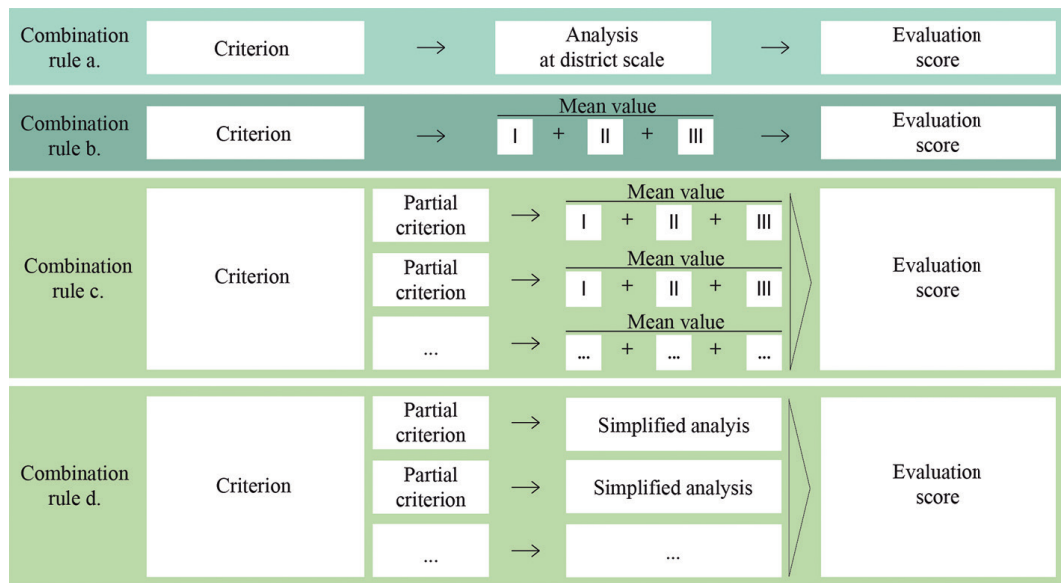


FIG. 4 Combination rules for repeatedly applied envelope technologies and for partial criteria

The total evaluation score per criterion may be calculated in four different ways (see Fig. 4):

- A District wide score: One evaluation score for district scale criteria (according to analysis level A.)
- B Mean values: The building envelopes/parts of building envelopes are pooled according design principle (analysis level B.) or technology types (analysis level C.). The evaluation score is the mean value of all included types, weighted according to the respective envelope area of each design principle or technology
- C Partial criteria I: One criterion is composed of several partial criteria. The partial criteria are combined according to combination rule b, the evaluation score is the mean value of the scores of all partial criteria
- D Partial criteria II: One criterion is composed of several partial criteria. The partial criteria are analysed in a simplified way depending on the applied system group, the evaluation score is the mean value of the scores of all partial criteria

An evaluation matrix for each design proposal summarizes the evaluation scores over all categories and assigns the weighting factors to the criteria. The weighting factors add up to 100 % and are multiplied with the evaluation scores. For the time being, no specific weighing is considered, all criteria are seen as equivalent. However, the system allows to customize weighting of criteria depending on the political context and the stakeholders' interests in the individual district.

The following step of the MCDA process, the aggregation, totals the weighted evaluation scores and results in the overall value of benefit. As a sub-result, the system also calculates the value of benefit per category in order to show the performance of a design proposal with regard to the sub-targets climate protection & energy, climate resilience, environment, functionality & technology and economy. To calculate this category performance, the weighted evaluation scores of each category are normalized to 100 %.

4 RESULTS: ANALYSIS TOOL SoGreEn

The analysis tool SoGreEn (Solar Energy – Greening – Envelope) is structured into two parts (Fig. 5): The informative part offers guidance in making design decisions based on design strategies and in

documenting the alternatives to evaluate (see 3.2). The second part involves the evaluation of the identified design proposals according to the evaluation categories and criteria shown in Fig. 3.

The informative and documentary part, the design module, requests the decision-maker to qualitatively debate the design proposal at hand. He is supposed to comment the alternatives according to the identified design criteria (see Fig. 2) and to describe the pursued design strategies and the underlying design objectives. To support the documentation, supplementary information such as examples of high- or low-quality architectural integration are given by the tool as reference and assistance in documenting the design proposal at hand. As each user has a different need for information, the supplementary information are retrievable via interactive buttons and the underlying database is expandable. Thus, the level of information is adaptable without compromising the compactness of the tool's graphical user interface.

After the identification and documentation of alternatives, each design proposal is evaluated separately in two sheets each. The first sheet is the input sheet to define and select the elements and features and conduct the analysis. The second one summarizes the analysis results in an evaluation matrix. The final sheet displays the analysis results of all alternatives and allows to draw comparisons between the analysed design proposals.

The analysis sheets provide the user with several analysis approaches associated to the respective criteria. The analysis of system-dependent criteria is performed automatically based on the selection of the applied technology and occupied area via an integrated database with system-typical information. Further criteria like 'Multifunctionality' are analysed at district scale by means of ticking check boxes. The number of e.g. existent functionalities covering an area larger than 50 m² is translated into an evaluation score.

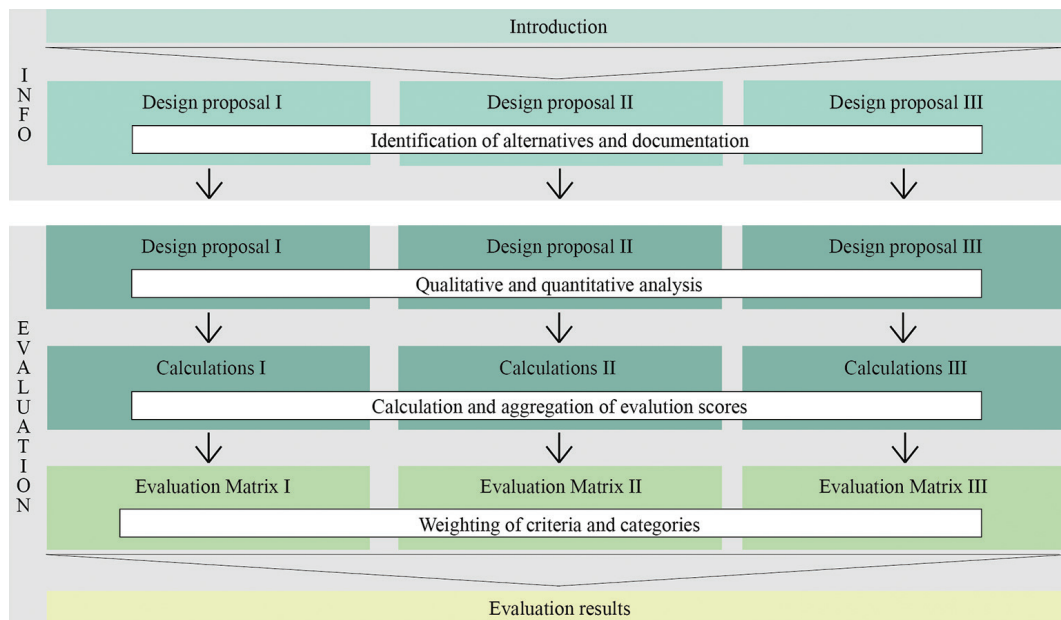


FIG. 5 Structure of the software tool SoGreEn

The evaluation scores are calculated and aggregated according to the analysis methods explained in 3.4 in hidden sheets and transmitted into the result sheet. Here, the total evaluation results appear as a bar chart while a summarizing display of results as a radar chart allows the intuitive comparison of different design proposals with regard to all analysis categories (see Fig. 6). Furthermore, a

detailed and colour-coded display of resulting scores for all analysis categories and criteria allows a focused interpretation of results and identification of potentials for improvement.

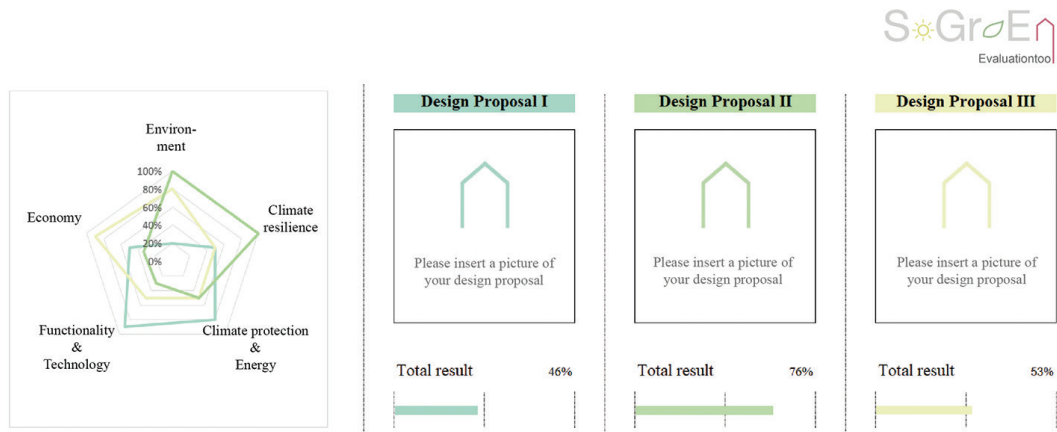


FIG. 6 Display of results of the evaluation tool SoGreEn

5 CONCLUSIONS

Due to their specific aesthetic features and specific benefits in different dimensions and scales, e. g. contributions to global climate change mitigation and climate change resilience of urban districts, deciding upon solar and / or greening systems in the envelope of buildings requires the evaluation of different alternatives in early planning phases. This paper presents the conceptual development of an analysis concept to support design decisions in the urban district (re)development context and to assess different design proposals for building envelopes under consideration of relevant aspects. Several analysis scales from the envelope of a single building skin up to the entire district have been balanced leading to the conceptual approach.

The concept is divided into an informative and an evaluative part. The informative part, the design module, offers guidance in making design decisions in early planning phases based on criteria for high design quality. Literature already provides approaches to define architectural integration quality of solar systems and this work adds criteria for high design quality of greenery systems. As the aim is to support the user's decision, the main benefit lies in providing knowledge and inspiration to guide and empower the argumentation and decision.

The evaluative part of the concept is based on an MCDA approach and provides a transparent and structured process to systematically evaluate and compare different envelope designs in five categories: climate protection & energy, climate resilience, environment, functionality & technology and economy. According to these categories, the system comprises five evaluation modules and suggests three to five evaluation criteria per module including the corresponding evaluation method. The modular structure allows to adapt the evaluation according to individual decision contexts as well as to adjust the assessment scale from a single building up to an entire district.

Calculation methods were described to combine qualitative and quantitative data, to cope with different evaluation levels from single building skins to the whole district as well as to aggregate the evaluations within the individual criteria and within the categories. The calculations were implemented into a user-friendly, Excel based tool. Instead of a final overall score and ranking of

the analysed alternatives, the tool visualizes the aggregation results per category in order to reveal strengths and weaknesses as well as optimization potentials of each design proposal.

In conclusion, the tool offers support to investors and developers, architects and urban planners as well as municipal and private business decision makers in objectively comparing and communicating different design scenarios in a structured work flow to make robust implementation or funding decisions. Used during early design stages, it can promote district concepts with high energy and climate performance and resilience and reduce reservations about the architectural quality of solar and greening systems and their integration in sensitive urban environments.

So far, users can easily understand and apply the rather simple calculation procedure and adjust weighting factors according to their preferences. This involves the risk that inputs are tuned to achieve the desired result. Moreover, translating qualitative estimations into numerical scores pretends high accuracy and objectivity that is not achievable due to the subjective input of the user. Perspectives, a more sophisticated MCDA method like the Analytic Hierarchy Process (AHP) or outranking techniques such as the Preference Ranking Organization Method for Enrichment of Evaluations (PROMETHEE) will be applied in order to use the full potential of MCDA to model and display various stakeholder perspectives as default option, and a sensitivity analysis will be conducted. This refinement is supposed to be developed and validated in the framework of a case study.

Acknowledgement

This research is a product of the research project Cleanvelope which is sponsored by the Bavarian Ministry of Science and the Arts in the context of Bavarian Climate Research Network (bayklif)

References

- Andes, L. (2019). Methodensammlung zur Nachhaltigkeitsbewertung: Grundlagen, Indikatoren, Hilfsmittel.
- Berardi, U. (2015). Sustainability assessments of buildings, communities, and cities. In J. J. Klemeš (Ed.), *Environmental science, engineering and technology. Assessing and measuring environmental impact and sustainability* (pp. 497–545). Butterworth-Heinemann.
- Brohmann, B., Buchert, M., Bunke, D., Fischer, C., Hesse, T., Schütte, S., & Weber, M. (2020). Handlungsempfehlungen für eine nachhaltige und integrierte Quartiersentwicklung – Erkenntnisse aus dem Forschungsprojekt TRASIQ: Öko-Institut Working Paper 1/2020. Freiburg.
- Cinelli, M., Kadziński, M., Gonzalez, M., & Stowiński, R. (2020). How to support the application of multiple criteria decision analysis? Let us start with a comprehensive taxonomy. *Omega*, 96, 102261. <https://doi.org/10.1016/j.omega.2020.102261>
- Deutsche Gesellschaft für Nachhaltiges Bauen e.V. (Ed.). (2020). DGNB System - Kriterienkatalog Quartiere: Version 2020.
- Dhar, S., Desgain, D., & Narkeviciute, R. (2015). Identifying and prioritising technologies for mitigation: A hands on guidance to multi-criteria analysis (MCA).
- Foster, N. (2010). Swiss solar prize 2010: Solar Architecture. In *Solar agentur Schweiz* (Ed.), 20. Schweizer Solarpreis: 20e Prix Solaire Suisse.
- Geldermann, J., & Lerche, N. (2014). Leitfaden zur Anwendung von Methoden der multikriteriellen Entscheidungsunterstützung: Methode: PROMETHEE. Georg-August-Universität, Göttingen.
- Geldermann, J., & Rentz, O. (2005). Multicriteria Analysis for Technique Assessment: Case Study from Industrial Coating. *Journal of Industrial Ecology*, 9(3). <https://doi.org/10.1162/1088198054821591>
- Hermann, B. G., Kroeze, C., & Jawjit, W. (2007). Assessing environmental performance by combining life cycle assessment, multi-criteria analysis and environmental performance indicators. *Journal of Cleaner Production*, 15(18), 1787–1796. <https://doi.org/10.1016/j.jclepro.2006.04.004>
- Kaan, H., & Reijenga, T. (2004). Photovoltaics in an architectural context. *Progress in Photovoltaics: Research and Applications*.
- Kühnapfel, J. B. (2019). *Nutzwertanalysen in Marketing und Vertrieb*. Springer Fachmedien Wiesbaden. <https://doi.org/10.1007/978-3-658-25164-2>
- Lizana, J., Barrios-Padura, J., Molina-Huelva, M., & Chacartegui, R. (2016). Multi-criteria assessment for the effective decision management in residential energy retrofitting. *Energy and Buildings*, 129, 284–307. <https://doi.org/10.1016/j.enbuild.2016.07.043>
- Moghtadernejad, S., Chouinard, L. E., & Mirza, M. S. (2020). Design strategies using multi-criteria decision-making tools to enhance the performance of building façades. *Journal of Building Engineering*, 30, 101274. <https://doi.org/10.1016/j.jobe.2020.101274>
- Munari Probst, M. C., & Roecker, C. (2007). Towards an improved architectural quality of building integrated solar thermal systems (BIST). *Solar Energy*, 81(9), 1104–1116. <https://doi.org/10.1016/j.solener.2007.02.009>
- Munari Probst, M. C., & Roecker, C. (2012). Criteria for Architectural Integration of Active Solar Systems IEA Task 41, Subtask A. *Energy Procedia*, 30, 1195–1204. <https://doi.org/10.1016/j.egypro.2012.11.132>

- Munari Probst, M. C., & Roecker, C. (2016). Solar Energy Promotion and Urban Context Protection: LESO-QSV-Quality-Site Visibility-Method.
- Rosasco, P., & Perini, K. (2019). Selection of (Green) Roof Systems: A Sustainability-Based Multi-Criteria Analysis. *Buildings*, 9(5), 134.
- Schuetze, T., Willkomm, W., & Roos, M. (2015). Development of a Holistic Evaluation System for BIPV Façades. *Energies*, 8(6), 6135–6152. <https://doi.org/10.3390/en8066135>
- Trærup, S. L. M., & Bakkegaard, R. K. (2015). Evaluating and prioritizing technologies for adaptation to climate change. A hands on guidance to multi criteria analysis (MCA) and the identification and assessment of related criteria.
- Vullo, P., Passera, A., Lollini, R., Prada, A., & Gasparella, A. (2018). Implementation of a multi-criteria and performance-based procurement procedure for energy retrofitting of façades during early design. *Sustainable Cities and Society*, 36, 363–377. <https://doi.org/10.1016/j.scs.2017.09.029>
- Wilkens, I. (2012). Multikriterielle Analyse zur Nachhaltigkeitsbewertung von Energiesystemen – Von der Theorie zur praktischen Anwendung [Dissertation]. Technische Universität Berlin, Berlin.

Design Model for Dry-Stacked and Demountable Masonry Blocks

Gelen Gael Chewe Ngapeya¹, Danièle Waldmann¹

1 University of Luxembourg, 6 Avenue de la Fonte, L-4364 Esch/Alzette, (+352) 46 66 44 5279, danièle.waldmann@uni.lu

Abstract

The construction industry around the world produces a large part of inert wastes mainly coming from building demolitions. Facing to this environmental challenge and considering the new policy initiatives supporting the designing of sustainable buildings, dry-stacked masonry comes forward as a promising solution since components can be dismantled, saved in a component bank and reassembled on new sites. The speedy growth of the construction industry, the increasing importance given to the complete life cycle of buildings and the evolution of construction techniques have led to the development of dry-stacked masonry structures. Mortarless masonry structures minimise skilled labour requirements and improve construction productivity. However, despite these advantages, there are no design standards providing guidelines to assess the load-bearing capacity of dry-stacked masonry block, which therefore limits its use in construction. In an attempt to fill this lack, the current paper investigates the load-bearing capacity of dry-stacked masonry and its influencing parameters. The effects of the geometric imperfections such as height imperfections and bed-joint roughness have been analysed as well as a mitigation strategy. Then, based on experimental evidence, a design method has been proposed for dry-stacked masonry solicited by axial compression. The developed design methodology provided promising results, with 93% of accuracy in the prediction of the dry-stacked masonry's' load-bearing capacity.

Keywords

Dry-stacked masonry, Load-bearing capacity, Geometric imperfections

1 INTRODUCTION

In the last decades, large-scale demolition and reconstruction of old urban areas have been observed, producing a significant part of inert waste materials around the world. During deconstruction or at the end of life, traditional mortared masonry walls offer limited recycling paths. Following the demolition, either they are used as basement in road construction or they are simply landfilled. Conversely, demountable construction systems like dry-stacked masonry bring forward twofold main assets: (i) the ease and speed of execution, which directly affects the construction cost; and (ii) the demountability, which positively affects the ecological impact by offering a second life to masonry blocks. (Bari, Abdullah, Yusuff, Ismail, & Jaapar, 2012) and (Anand & Ramamurthy, 2003) investigated the effectiveness of the dry-stacked masonry system in the construction productivity. They evidenced that the use of a dry-stacked masonry system leads to an enhancement of the productivity by 80 to 100% compared to a traditional mortared masonry system. The measurement made by (Anand & Ramamurthy, 2003) regarding the net output of 1 m² of wall per productive hour while using different masonry systems is reported as a radar in Fig. 1. They evidenced that dry-stacked systems are more effective than a traditional system in terms of productivity.

In view of this productivity performance, researchers have made intensive efforts for developing dry-stacked masonry systems to make masonry construction more affordable and sustainable. Thus, several dry-stacked masonry blocks have been designed worldwide with different interlocking mechanisms (Abang Ali, 1987; Agaajani, Waldmann, Scholzen, & Louge, 2016; Ben Ayed, Limam, Aidi, & Jelidi, 2016; Cetholic, 1988; Haener, 1984; Sturm, Ramos, & Lourenço, 2015; Thallon R, 1983; W. A. Thanoon et al., 2004). The interlocking mechanism improves the vertical and horizontal alignment of walls and provides a certain out-of-plane resistance to walls in the absence of the mortar layer.

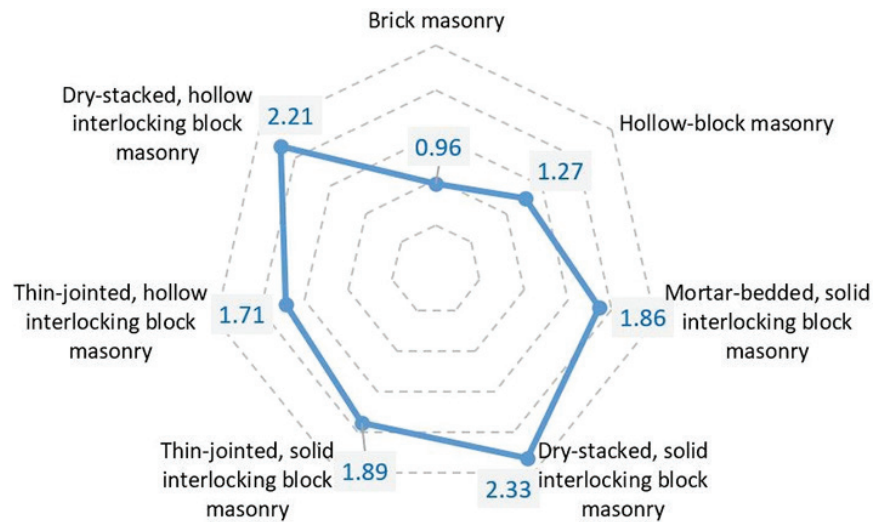


FIG. 1 Construction net output of 1 m² of wall per productive hour for different masonry systems (figure made using the data of (Anand & Ramamurthy, 2003))

Nonetheless, although the dry-stacked masonry system offers attractive interests, its extensive use is still hindered by (i) the premature cracking of wall which is related to the effect of the block geometric imperfections; and (ii) the lack of appropriate design standards for safely predicting its load-bearing capacity. In the current state-of-art, a couple of investigations first characterised the geometric imperfections of dry-stacked blocks as being the height difference and bed-joint

roughness (Agaajani et al., 2016; Allaoui, Rekik, Gasser, Blond, & Andreev, 2018; Andreev et al., 2012; Gelen Gaël Chewe Ngapeya & Waldmann, 2020; Gasser, Terny-Rebeyrotte, & Boisse, 2004; Mohd Saleh Jaafar; Ahmed Alwathaf; Waleed Thanoon; J. Noorzaei; M. R. Abdulkadir, 2006). Then, the authors measured the imperfections using different techniques like the matrix-based tactile surface sensors, the Fuji film strips, the carbon footprint paper, the digital image correlation and the standard displacement sensors. From the different measurements, it emerged that the height difference between dry-stacked masonry blocks varies between +/- 0,25 and 2 mm, while the height of the asperities in the bed-joint roughness falls between 0,03 and 0,25 mm.

The lack of mortar layers in the horizontal joints of interlocking masonry walls combined to geometric imperfections of blocks lead to structural behaviour fundamentally different from conventional masonry walls under axial compression. (Bigoni & Noselli, 2010a) carried out investigations on dry-stacked masonry under axial compression. Upon the loading, they captured the actual load percolation system using the photo-elasticity transmission technique. They evidenced a tree-like load percolation system occurring in a dry-stacked masonry wall. They also revealed that the load transfer from course to course occurs in the middle and the edge sections of blocks, which results in high-stress peaks in dry-stacked masonry walls. The authors also observed that the highly localised stress percolation system observed in the first stages of the loading gradually tends towards a wider stress distribution in the last loading stages, a result of the increase of the contact surfaces in the wall as demonstrated by (Gelen Gael Chewe Ngapeya & Waldmann, 2020; Zahra & Dhanasekar, 2018). In further investigations, the authors (Bigoni & Noselli, 2010b) proposed a simple analytical model for determining the intensity of loads transmitted on blocks as a function of a predefined load transmission mechanism in the dry-stacked masonry wall.

(W. A. M. Thanoon, Alwathaf, Noorzaei, Jaafar, & Abdulkadir, 2008) performed numerical and experimental investigations on a 3-course dry-stacked masonry prism for discussing the mechanical behaviour under axial compression. First, they constructed a dry-stacked masonry prism in the lab and measured its stress-deformation response under axial compression. They observed (i) a non-linear stress-deformation curve with a flat part related to the closure of gaps in the bed-joints, (ii) a progressive inflexion of the measured curve related both to the crushing of the asperities and the increase of the actual contact, and (iii) a flat and oblique curve part related to the achievement of the maximum contact stiffness in the bed-joints. Then, they computed the corresponding contact stiffness of the bed-joints, which they imported in their finite element model for indirectly consider the effect of the bed-joint roughness on the overall mechanical behaviour of the masonry prism. After running their numerical model, they found that under compression dry-stacked masonry suffers from asymmetric stress distribution in the face-shells of blocks. In addition, they demonstrated that dry-stacked masonry suffers from surface roughness related stress concentration, which strongly reduces its load-bearing capacity. Their results confirm the findings of (Ben Ayed et al., 2016; Kang-Ho Oh; Harry G. Harries; Ahmed A. Hamid, 1995; Lourenço, Oliveira, Roca, & Orduña, 2005; Lourenço & Ramos, 2004). In an attempt to guide the prediction of the load-bearing capacity of dry-stacked masonry walls, several other authors developed correlations between block strength and masonry wallet/prism strength (Jaafar, Thanoon, Najm, Abdulkadir, & Ali, 2006; Silva et al., 2015; Sturm et al., 2015). A review of the proposed correlations revealed that the prism/wallet to block strength ratio varies between 0,21 and 0,70. Although being of significant value, the strength correlations cannot be directly used for designing dry-stacked masonry walls since the influence of the block imperfections strongly varies with the size of both blocks and walls.

The present investigation has a twofold perspective of (1) settling a design model for dry-stacked masonry and (2) assessing a mitigation strategy to overcome the impact of the geometric imperfections of block units on the load-bearing capacity of walls.

2 METHODOLOGY

In the framework of this investigation, the methodology adopted to set up a design model for dry-stacked masonry was organised in three stages. In the first stage, experimental tests were carried out on wallets with a dual purpose: (i) to assess the effectiveness of the mitigation strategy for improving the load-bearing capacity of dry-stacked masonry and (ii) to constitute an experimental database useful for developing a reliable design model. In the second stage, the results of the experimental tests were combined with a statistical modelling of the impact of the geometrical imperfections of block units to settle down a design model for dry-stacked and demountable masonry. In the third and last stage, a design model was implemented to compute the load-bearing capacity of dry-stacked masonry walls and to compare the findings to the test results found in literature.

2.1 RAW DRY-STACKED MASONRY

The investigations on the load-bearing capacity of dry-stacked masonry and the influence of the geometric imperfections of the block units have been carried out on a block delivered by a local producer. The used masonry block was made of two load-bearing face-shells with a net cross-section of 22.000 mm², interconnected by two webs (Fig. 2). The masonry block has a nominal height, length and thickness of 200 mm, 500 mm and 200 mm respectively, with a self-weight of 20 kg. In the first stage of the experimental analysis, following the provisions of the British Standards EN 772-1 (BS EN 772-1:2000, Methods of test for masonry units – Part 1: Determination of compressive strength, n.d.), uni-axial compressive tests have been realised on 10 randomly selected masonry blocks for the purpose of mechanical characterisation. The masonry blocks exhibited a mean compressive strength of 13 MPa.



FIG. 2 Masonry block (Gelen Gaél Chewe Ngapeya & Waldmann, 2020)

2.2 IMPROVED DRY-STACKED MASONRY

In the framework of the development of a design model for dry-stacked and demountable masonry, a mitigation strategy was also analysed for overcoming the curtailing effect of the geometric imperfections of blocks on the overall load-bearing capacity of walls. Indeed, (Zahra & Dhanasekar, 2018) have evidenced that the strong stress peaks generally observed in dry-stacked masonry systems can be partially relieved effortlessly by embedding a compressible material in the contact interfaces. As a mitigation strategy, a 10 mm layer of soft material was applied on the top faces of the

block face-shells, with the aim to dampen or level the geometric imperfections of raw dry-stacked masonry blocks. The definition of the thickness of the additional layer was mainly based on the works of (Tang, 2012) who studied the effect of mortar thickness on the compressive strength of brick masonry. In fact, the author demonstrated that the optimum mortar thickness leading to the least effect on the masonry's strength is 10 mm.

For applying the additional material layer, the hardened masonry blocks were re-moulded in formworks heightened by 10 mm around the block face-shells. The empty space precasted on the face-shells was then filled by hand with fresh mixed and purposely selected materials, before being slightly vibrated. The improved dry-stacked masonry blocks were then stored 28 days for hardening purpose.

3 EXPERIMENTAL ANALYSIS OF THE CONTACT NETWORK AND THE LOAD-BEARING CAPACITY OF MASONRY WALLS

3.1 MATERIALS OF THE ADDITIONAL LAYER

(Vasconcelos & Lourenço, 2009) carried out experimental characterisations of stone masonry in shear and compression and revealed that the bed-joint closure in dry-stacked masonry is proportional to the contacting material stiffness. The closure of the bed-joint strongly relates to the rate of the actual contact in the contact interfaces while the ultimate resistance of dry-stacked masonry still closely relates to the rate of the actual contact in the contact interfaces (Gelen Gael Chew Ngapeya, Waldmann, & Scholzen, 2018). The selection of the material for the additional layer was of high significance. Indeed, four materials of different mechanical properties have been chosen. Three materials of a relatively common strength but of decreasing Young's modulus (Mix A, Mix B and Mix C) were compared to a very low strength material (Mix D). Low strength materials are known to induce significant lateral tensile stresses in dry-stacked masonry, which might limit the overall ultimate load-bearing capacity of walls. Despite that, it has been chosen for its possible high expectation of levelling capacity of block imperfections. On the other hand, although they might lead to less levelling of block imperfections, medium strength materials have been chosen as they are known to induce less lateral tensile stresses and higher load-bearing capacity in mortared masonry (Mohamad, Fonseca, Vermeltfoort, Martens, & Lourenço, 2017; Zucchini & Lourenço, 2007).

The compressive strength of the four mixes used for the additional layer was determined on prism samples of 4 x 4 x 16 cm following the recommendations of the British standard EN 1015-11, the stress-strain behaviour has been captured as well. The results of the experimental tests are summarised in Table 1.

MIXTURE	MEAN COMPRESSIVE STRENGTH (N/MM ²)	YOUNG'S MODULUS (MPA)
Mix A	37,0	11500
Mix B	34,0	10500
Mix C	38,0	7000
Mix D	5,2	3000

TABLE 1 Compressive strength and Young's Modulus of different variations of the additional layer

3.2 TEST DESIGN ON MASONRY WALL AND PRISM.

The experimental program sought to investigate the impact of the different materials of the additional layer on the levelling of the bed-joint imperfections and ultimately on the load-bearing capacity of dry-stacked masonry walls. The following questions were raised:

- Which mixes of the additional layer achieve a high actual contact in the bed-joint?
- To what extent the load-bearing capacity of a dry-stacked masonry wall with improved blocks can be increased with respect to a similar one with raw dry-stacked masonry blocks?

For the purpose of answering these questions, two test series have been designed. In the first series, 25 masonry prisms constituted each of a dry-stacking of three blocks were investigated to singularly analyse the impact of the bed-joint roughness on the actual contact. The actual contact in the bed-joints was captured using Fuji film strips. Indeed, Fuji film strips are a type of sensors able to record the footprint and the intensity of the contact at the interface between solids. The Fuji film strips were inserted at the interface between the masonry blocks during the prism erection. Afterwards, the prism specimens were axially compressed to failure using a couple of six hydraulic pistons as showed in Fig. 3. Thereafter, the Fuji film strips were retrieved, digitalised and processed on MATLAB for computing the maximum rate of the actual contact recorded in the bed-joints. In the second series, 20 masonry wallets of 0,8 m height and 1,0 m length were tested (Fig. 3). Indeed, masonry wallets were investigated because they better depict the behaviour of dry-stacked masonry, since they include effects of both bed-joint roughness and height difference of blocks. Like for the masonry prisms, the wallets were also axially compressed to failure. The ultimate load was monitored. In addition, cameras were used to record and further analyse the failure mechanism of the wallets.

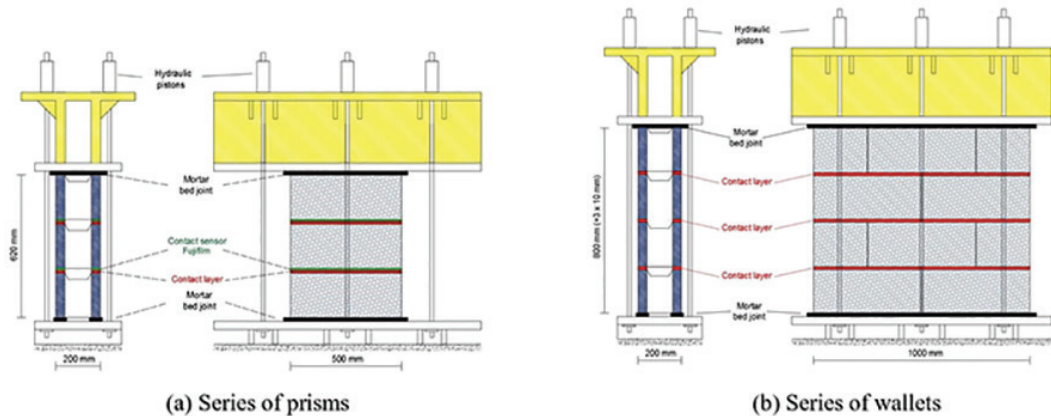


FIG. 3 Design of the experimental tests on (a) prisms and (b) masonry wallets (Gelen Gaël Chew Ngapeya & Waldmann, 2020)

3.3 RESULTS

The mean rates of the actual contact measured in the bed-joints of the masonry prisms are summarized in Table 2. A huge reduction of the nominal contact section has been observed in the masonry prisms with raw blocks (group I), with only 23% of actual contact. This could have been foreseen since the parts of the masonry blocks coming into contact exhibit a same and high stiffness, which results in a very low deformation of the asperities at the interface and ultimately a very low contact. Regarding the masonry prisms with blocks improved with Mix A and Mix B (group II and group III respectively), a significant improvement was observed about the actual contact. Indeed,

the actual contact has been doubled and achieved up to 50%, thanks to a higher deformation and crushing of the asperities at the interfaces. A similar tendency was observed for the masonry prisms with blocks improved with Mix C (group IV). In this case, the low Young's Modulus of Mix C even still allowed to slightly increase the actual contact to 55%. In the last case where the blocks of the masonry prisms were improved with Mix D (Group V), although this material of the contact layer had the lowest Young's Modulus, the resulting actual contact was just about 40%. This performance was better than the one of group I but still less than the ones of group II, III and IV. The default of higher performance of the masonry prisms of group II, III and IV was due to the reduction of the load-bearing capacity related the significant lateral tensile stresses induced in the masonry prisms.

As a summary of the tendency observed from prisms with raw blocks to prisms with improved blocks, it can be stated that the lower the stiffness of the parts coming into contact, the higher the resulting actual contact in the interface, which lines up with the finding of (Vasconcelos & Lourenço, 2009).

MIXTURE	NUMBER OF PRISMS TESTED	MEAN RATE OF THE ACTUAL CONTACT	COEF. OF VARIATION
Group I – prisms with raw blocks (no additional layer)	5	23%	4%
Group II – prisms with blocks improved using Mix A	5	50%	7%
Group III – prisms with blocks improved using Mix B	5	50%	8%
Group IV – prisms with blocks improved using Mix C	5	55%	8%
Group V – prisms with blocks improved using Mix D	5	40%	7%

TABLE 2 Compressive strength and Young's Modulus of different variations of the additional layer

The load-bearing capacity of the tested wallets is summarised in Table 3. The wallets of group I made with raw dry-stacked masonry blocks showed a load bearing capacity of about 3,66 N/mm². In the wallets of group II and III, it was only improved by 1,0% and 6,1% respectively, which is not relevant for engineering purposes. The impact of the additional layer was balanced between the positive aspect related to the increase of the actual contact, hence the better stress distribution, and the negative aspect related to the induction of lateral tensile stress in lateral masonry block walls, leading to a premature cracking of the webs. A considerable structural improvement could be observed for the wallets of group IV, with an increase of the load-bearing capacity of 31,9%. This largely results from the high levelling capacity of the additional layer material. Both block height difference and bed-joint roughness were significantly overcome. In the last group, the load-bearing capacity was diminished 41,3%, due to the significant lateral tensile stress induced by the low strength material Mix D in the wallets.

MIXTURE	NUMBER OF WALLETS TESTED	MEAN LOAD-BEARING CAPACITY P_{ij} (N/mm ²)	IMPROVEMENT
Group I – prisms with raw blocks (no additional layer)	4	3,66	-
Group II – prisms with blocks improved using Mix A	4	3,70	+1,0%
Group III – prisms with blocks improved using Mix B	4	3,88	+6,1%

>>>

Group IV – prisms with blocks improved using Mix C	4	4,83	+31,9%
Group V – prisms with blocks improved using Mix D	4	2,15	-41,3%

TABLE 3 Load-bearing capacity of the wallets

Throughout the experimental campaign, three damage mechanisms have been observed prior to the wall collapse. Consecutively, it was first the face-shells splitting due to the height difference between the blocks and occurring around 17% to 92% of the load-bearing capacity. Then, it was the spalling of some sections of the face-shells near the bed-joints, due to the high-stress concentration resulting from the tree-like load percolation system (Gelen Gael Chewe Ngapeya et al., 2018). This damage mechanism occurred generally after 70% of the load-bearing capacity. The third and last damage mechanism occurring near the failure was the cracking at the interface between the face-shells and the webs of blocks. This latter one was mainly due to the development of significant lateral tensile stress in the masonry blocks.

4 DESIGN MODEL

To date, the standards for the design of masonry structures only provide guidelines for traditional and thin-mortared masonry. As shown in equation (1) recommended by EN 1996-1-1(EN1996-1-1), the compressive strength of mortared masonry is calculated while considering exclusively the safety factor γ_M , the slenderness effect ϕ , the masonry block thickness t , the normalised compressive strength of blocks f_b , the mortar compressive strength f_m and a coefficient K , which depends on the block material (concrete, clay, brick, etc.). In equation (1), for thin mortared masonry $\alpha = 0.85$ and $\beta = 0$, while for traditional mortared masonry $\alpha = 0.7$ and $\beta = 0.3$.

$$N_{Rd, EN1996-1-1} = \frac{1}{\gamma_M} (\phi t K f_b^\alpha f_m^\beta) \quad (1)$$

For developing a design model for dry-stacked masonry, the proposal of equation (1) was exploited and extended by including two new factors involving the impact of the geometric imperfections of blocks on the overall compressive strength of walls. Equation (2) stands for dry-stacked masonry walls with raw blocks, whereas equation (3) stands for walls with improved blocks. Moreover, in these proposals, δ_h and δ_r stand for the reduction factor due to the height variation and the reduction factor due to the bed-joint roughness respectively. Given that in a wall the effects of the two geometric imperfections are coupled, each design model was defined to fit the best with the experimental results and this was then validated with the results of former experiments collected in literature.

$$N_{Rd, proposed} = \frac{1}{\gamma_M} (\phi t K f_b^{0.95}) \delta_h^{0.85(1-\delta_r)} \quad (2)$$

$$N_{Rd, proposed} = \frac{1}{\gamma_M} (\phi t K f_b^{0.85} f_m^{0.2}) \delta_h^{0.85(1-\delta_r)} \quad (3)$$

4.1 FACTOR δ_r

Standing for the impact of the bed-joint roughness, the factor δ_r is defined as being the ratio between the maximum surface of actual contact achieved in a bed-joint and the nominal contact surface.

Hence, the impact of the bed-joint roughness was indirectly measured during the experimental tests on the masonry prisms. The mean rate of the actual contact defined in Table 2 is here considered as being the factor δ_r for each type of masonry blocks.

4.2 FACTOR δ_h

The determination of factor δ_h standing for the impact of the height difference between masonry blocks is mainly based on a developed deterministic model. Indeed, δ_h depicts the overall reduction of the useful section of a wall due to a reduction of the contact surface due to imperfections. As demonstrated in several investigations (Agaajani et al., 2016; Bigoni & Noselli, 2010a; Gelen Gaël Chewe Ngapeya et al., 2018), the height difference between dry-stacked masonry blocks strongly impacts the contact network and systematically leads to a major tree-like ramification through which the load percolates. Concisely, for a given wall, factor δ_h was defined as being the ratio between the total actual contact through which the load percolates and the total nominal contact sections of the wall. However, since the load percolation system might vary from one wall to another according to a random distribution of blocks, the factor δ_h might also vary from one wall to another of same geometry. To consider this, n-walls different walls have been analysed within a deterministic model. With a number $n = 1000$ a quasi-steady value of δ_h for a given wall geometry has been found.

For engineering purposes, a designer's diagram was developed using a MATLAB code for determining the factor δ_h . More details are provided in (Gelen Gaël Chewe Ngapeya & Waldmann, 2020). The designer's diagram is here presented in Fig. 4.

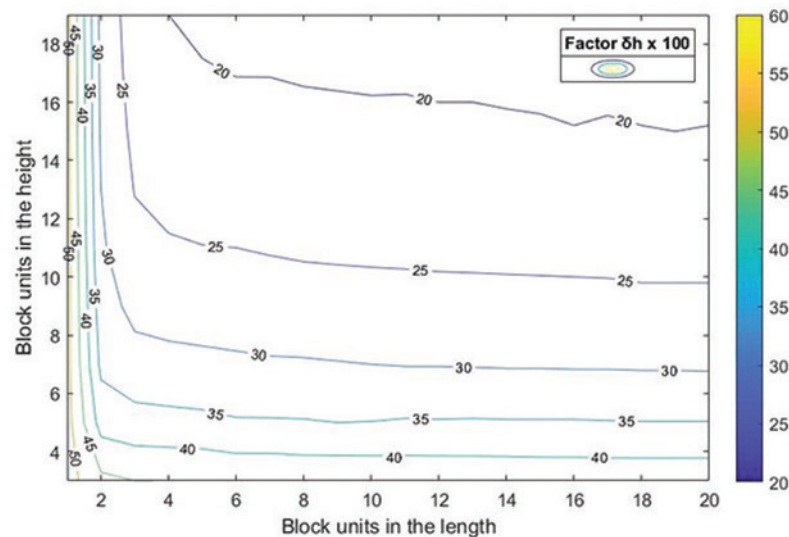


FIG. 4 Designer's diagram for the determination of δ_h (Gelen Gaël Chewe Ngapeya & Waldmann, 2020)

4.3 IMPLEMENTATION

In the present sub-section, the load-bearing capacity of dry-stacked masonry walls are computed using the proposed design model and the results of the implementation ($P_{u,DM}$) are compared to the experimental results ($P_{u,EXP}$) collected in literature. Likewise, the load-bearing capacity of the same walls are computed using the provisions of EN 1996-1-1 for thin mortared masonry structures ($P_{u,C6}$). The shape factor and the coefficient K related to the block material have been defined

following the provisions of EN 1996-1-1. The brief summary of the parameters used for the implementation of the design model, the results of the experimental tests collected in literature and the load-bearing capacity computed with both approaches are all gathered in Table 4. Upon the computation of the load-bearing capacity of the masonry walls, the safety factor of the concrete material γ_M was set equal to 1.0, since the results of the prediction were intended to be compared to the experimental results.

At the analysis of the results, it is found that the proposed design model is conservative. Indeed, a ratio between the prediction $P_{u,DM}$ and the experimental results $P_{u,EXP}$ respectively for each wall gives a mean value of 93%, which means that the proposed design model estimates the actual load-bearing capacity of dry-stacked masonry walls with a satisfactory accuracy. This is of course due to the capacity of the design model to include the negative impact of the geometric imperfections on the overall wall resistance. Indeed, it has been demonstrated that the block imperfections act against the development of the load-bearing capacity of dry-stacked masonry wall by strongly reducing the contact behaviour in walls.

At the same time, the provisions of EN 1996-1-1 for thin-mortared masonry structures overestimate the load-bearing capacity of dry-stacked masonry walls. When the predictions $P_{u,EC6}$ of EN 1996-1-1 are compared to the experimental results $P_{u,EXP}$ respectively for each wall, a mean ratio of 131% is found, which means that the load-bearing capacity is overestimated by roughly 31%. This trend could have been expected, as the impacts of block imperfections on the load-bearing capacity of dry-stacked masonry walls are not considered in the current standards. Indeed, the provisions of EN 1996-1-1 are set up for mortared masonry where block imperfections are directly levelled by a mortar layer.

AUTHORS IN LITERATURE	δ_v	δ_h	SHAPE FACTOR	K	HEIGHT (mm)	THICKNESS (mm)	BLOCK STRENGTH (N/mm ²)	$P_{u,EXP}$ EXPERIMENTAL (N/mm ²)	$P_{u,EC6}$ EN 1996-1-1 (N/mm ²)	$P_{u,DM}$ DESIGN MODEL (N/mm ²)	ACCURACY OF THE DESIGN MODEL IN %
Silva et al. (2015)	0,23	0,52	0,9	0,75	500	140	8,8	3,30	3,68	2,95	89%
Silva et al. (2015)	0,23	0,52	0,9	0,75	500	140	12	4,60	4,61	3,95	86%
Sturm et al. (2015)	0,23	0,30	0,9	0,75	810	140	1,96	0,53	1,02	0,50	94%
Drysdale et al. (1991)	0,23	0,52	1,15	0,65	812	203	10,30	3,90	4,72	3,93	101%
Jaafar et al. (2006)	0,23	0,37	1,25	0,65	1200	150	15,20	5,90	6,56	4,56	77%
Thanoon et al (2007, 2014)	0,23	0,27	1,25	0,65	3000	150	17,20	3,89	5,67	3,02	78%
Agajani et al. (2015)	0,23	0,37	1,25	0,65	1250	200	26,30	5,35	8,40	5,64	105%

TABLE 4 Heat pipe inclinations in correlation with various slat dimensions.

5 CONCLUSION

The present research focuses on the assessment of a mitigation strategy to overcome the impact of the geometric imperfections of blocks on the load-bearing capacity of dry-stacked masonry walls and the development of a design model proper to such walls. Experimental tests were performed on masonry wallets and prisms to evidence the efficiency of an additional layer made of well-defined properties to improve the load-bearing capacity of dry-stacked masonry walls. Furthermore, the experimental results were combined with a deterministic statistical model for developing a design

model. The efficiency of the design model was discussed in terms of accuracy in the prediction of the load-bearing capacity with respect to the actual value obtained following experiments. In a nutshell, it was found that:

- For engineering purpose, the most relevant improvement of the load-bearing capacity of dry-stacked masonry walls was obtained with the blocks having an additional layer made with a mixture which has a Young's Modulus of 7000 MPa and a mean compressive strength of 38 MPa. They provided up to 31,9% of additional load carrying capacity.
- The design model exhibited an accuracy varying between 77 and 105%, with a mean of 93% in the prediction of the load-bearing capacity of dry-stacked masonry walls.

Worldwide, the design of façades is directed towards the optimisation of the environmental quality and the minimisation of used resources. The development of construction components like dry-stacked and demountable masonry delivers smart and sustainable structural façade elements. The results of this research work can be used for extending the use of dry-stacked masonry as structural façade elements in buildings, while ensuring the structural stability with a robust and reliable design method.

Acknowledgements

The authors wholeheartedly thank "Contern - Lëtzebuurger Beton" for the financial support throughout this project. The authors also acknowledge the laboratory technicians of the University of Luxembourg for their commitment during the designing and execution of the experimental tests.

References

- Abang Ali, A. K. (1987). Strength properties and structural performance of interlocking hollow block walls. *J. Inst. Jurutera Malya*, 53, 25–35.
- Agaajani, S., Waldmann, D., Scholzen, F., & Louge, A. (2016). Numerical analysis for the determination of stress percolation in dry-stacked wall systems. *Masonry International*, 29(2), 27–38.
- Allaoui, S., Rekik, A., Gasser, A., Blond, E., & Andreev, K. (2018). Digital Image Correlation measurements of mortarless joint closure in refractory masonries. *Construction and Building Materials*, 162, 334–344. <https://doi.org/10.1016/j.conbuildmat.2017.12.055>
- Anand, K. B., & Ramamurthy, K. (2003). Laboratory-Based Productivity Study on Alternative Masonry Systems. *Journal of Construction Engineering and Management*, 129(3), 237–242. [https://doi.org/10.1061/\(asce\)0733-9364\(2003\)129:3\(237\)](https://doi.org/10.1061/(asce)0733-9364(2003)129:3(237))
- Andreev, K., Sinnema, S., Rekik, A., Allaoui, S., Blond, E., & Gasser, A. (2012). Compressive behaviour of dry joints in refractory ceramic masonry. *Construction and Building Materials*, 34, 402–408. <https://doi.org/10.1016/j.conbuildmat.2012.02.024>
- Bari, N. A. A., Abdullah, N. A., Yusuff, R., Ismail, N., & Jaapar, A. (2012). Environmental Awareness and Benefits of Industrialized Building Systems (IBS). *Procedia - Social and Behavioral Sciences*, 50(July), 392–404. <https://doi.org/10.1016/j.sbspro.2012.08.044>
- Ben Ayed, H., Limam, O., Aidi, M., & Jelidi, A. (2016). Experimental and numerical study of Interlocking Stabilized Earth Blocks mechanical behavior. *Journal of Building Engineering*, 7, 207–216. <https://doi.org/10.1016/j.job.2016.06.012>
- Bigoni, D., & Noselli, G. (2010a). Localized stress percolation through dry masonry walls. Part I - Experiments. *European Journal of Mechanics, A/Solids*, 29(3), 291–298. <https://doi.org/10.1016/j.euromechsol.2009.10.009>
- Bigoni, D., & Noselli, G. (2010b). Localized stress percolation through dry masonry walls. Part II - Modelling. *European Journal of Mechanics, A/Solids*, 29(3), 299–307. <https://doi.org/10.1016/j.euromechsol.2009.10.013>
- BS EN 772-1:2000, Methods of test for masonry units – Part 1: Determination of compressive strength.
- Cetholic. (1988). Mortarless Masonry - The Mecano System. *Housing Science*, 12(2), 145–157.
- Chewe Ngapeya, Gelen Gael, & Waldmann, D. (2020). Overcome of bed-joint imperfections and improvement of actual contact in dry-stacked masonry. *Construction and Building Materials*, 233, 117173. <https://doi.org/10.1016/j.conbuildmat.2019.117173>
- Chewe Ngapeya, Gelen Gael, & Waldmann, D. (2020). Experimental and analytical analysis of the load-bearing capacity P_u of improved dry-stacked masonry. *Journal of Building Engineering*, 27(May 2019). <https://doi.org/10.1016/j.job.2019.100927>
- Chewe Ngapeya, Gelen Gael, Waldmann, D., & Scholzen, F. (2018). Impact of the height imperfections of masonry blocks on the load bearing capacity of dry-stack masonry walls. *Construction and Building Materials*, 165, 898–913. <https://doi.org/10.1016/j.conbuildmat.2017.12.183>
- Gasser, A., Terny-Rebeyrotte, K., & Boisse, P. (2004). Modelling of joint effects on refractory lining behaviour. *Proceedings of the Institution of Mechanical Engineers, Part L: Journal of Materials: Design and Applications*, 218(1), 19–28. <https://doi.org/10.1243/146442004322849881>
- Haener. (1984). Stacking Mortarless Block System. *Engineering Design Manual*.

- Jaafar, M. S., Thanoon, W. A., Najm, A. M. S., Abdulkadir, M. R., & Ali, A. A. A. (2006). Strength correlation between individual block, prism and basic wall panel for load bearing interlocking mortarless hollow block masonry. *Construction and Building Materials*, 20(7), 492–498. <https://doi.org/10.1016/j.conbuildmat.2005.01.046>
- Kang-Ho Oh; Harry G. Harries; Ahmed A. Hamid. (1995). Behavior of Interlocking Mortarless Masonry Under Compressive Loads. *Seventh Canadian Masonry Symposium*, 340–352.
- Lourenço, P. B., Oliveira, D. V., Roca, P., & Orduña, A. (2005). Dry Joint Stone Masonry Walls Subjected to In-Plane Combined Loading. *Journal of Structural Engineering*, 131(11), 1665–1673. [https://doi.org/10.1061/\(asce\)0733-9445\(2005\)131:11\(1665\)](https://doi.org/10.1061/(asce)0733-9445(2005)131:11(1665))
- Lourenço, P. B., & Ramos, L. F. (2004). Characterization of Cyclic Behavior of Dry Masonry Joints. *Journal of Structural Engineering*, 130(5), 779–786. [https://doi.org/10.1061/\(asce\)0733-9445\(2004\)130:5\(779\)](https://doi.org/10.1061/(asce)0733-9445(2004)130:5(779))
- Mohamad, G., Fonseca, F. S., Vermeltfoort, A. T., Martens, D. R. W., & Lourenço, P. B. (2017). Strength, behavior, and failure mode of hollow concrete masonry constructed with mortars of different strengths. *Construction and Building Materials*, 134, 489–496. <https://doi.org/10.1016/j.conbuildmat.2016.12.112>
- Mohd Saleh Jaafar; Ahmed Alwathaf; Waleed Thanoon; J. Noorzaei; M. R. Abdulkadir. (2006). Behaviour of interlocking mortarless block masonry. *Construction Materials*, 159, 111–117.
- Silva, R. A., Soares, E., Oliveira, D. V., Miranda, T., Cristelo, N. M., & Leitão, D. (2015). Mechanical characterisation of dry-stack masonry made of CEBs stabilised with alkaline activation. *Construction and Building Materials*, 75, 349–358. <https://doi.org/10.1016/j.conbuildmat.2014.11.038>
- Sturm, T., Ramos, L. F., & Lourenço, P. B. (2015). Characterization of dry-stack interlocking compressed earth blocks. *Materials and Structures/Materiaux et Constructions*, 48(9), 3059–3074. <https://doi.org/10.1617/s11527-014-0379-3>
- Tang, F. (2012). Effect of mortar joint thickness on the compressive strength of autoclaved flyash-lime brick masonry. *Applied Mechanics and Materials*, 190–191, 462–466.
- Thallon R. (1983). Dry-Stack Block. *Fine Homebuilding Magazine*, 50–57.
- Thanoon, W. A., Jaafar, M. S., Abdul Kadir, M. R., Abang Ali, A. A., Trikha, D. N., & Najm, A. M. S. (2004). Development of an innovative interlocking load bearing hollow block system in Malaysia. *Construction and Building Materials*, 18(6), 445–454. <https://doi.org/10.1016/j.conbuildmat.2004.03.013>
- Thanoon, W. A. M., Alwathaf, A. H., Noorzaei, J., Jaafar, M. S., & Abdulkadir, M. R. (2008). Finite element analysis of interlocking mortarless hollow block masonry prism. *Computers and Structures*, 86(6), 520–528. <https://doi.org/10.1016/j.compstruc.2007.05.022>
- Vasconcelos, G., & Lourenço, P. B. (2009). Experimental characterization of stone masonry in shear and compression. *Construction and Building Materials*, 23(11), 3337–3345. <https://doi.org/10.1016/j.conbuildmat.2009.06.045>
- Zahra, T., & Dhanasekar, M. (2018). Characterisation and strategies for mitigation of the contact surface unevenness in dry-stack masonry. *Construction and Building Materials*, 169, 612–628. <https://doi.org/10.1016/j.conbuildmat.2018.03.002>
- Zucchini, A., & Lourenço, P. B. (2007). Mechanics of masonry in compression: Results from a homogenisation approach. *Computers and Structures*, 85(3–4), 193–204. <https://doi.org/10.1016/j.compstruc.2006.08.054>

Eco-Construction for Sustainable Development: Concept of a Material and Component Bank

Laddu Bhagya Jayasinghe¹, Daniele Waldmann¹

¹ University of Luxembourg, 6 Avenue de la Fonte, L-4364 Esch/Alzette, bhagya.jayasinghe@uni.lu

Abstract

The European Commission has recently promulgated the concept of Circular Economy as a new pathway towards sustainability, in particular through new policy initiatives such as the Circular Economy Action Plan (CEAP). Since the environmental impact of the construction industry with the depletion of natural resources and the raising CO₂ emissions will have to be reduced in the future, the need of recycling and even reusing entire building components supporting the principles of circular economy have been identified. The direct reuse of components extracted from old deconstructed buildings presents an energy-efficient and environmental-friendly solution. However, the reuse of components can be hindered by e.g. the lack of information on the availability of decommissioned structural components and uncertainties on the warranty of structural components. To handle this process an additional independent institution acting as Material and Component (M&C) Bank is needed. This entity assures activities such as e.g. the identification of reusable components in buildings which are proposed for selective dismantling; the condition assessment; the data management and the data transfer from a previously deconstructed building to a new building; and finally, an official certification of the components' conformity for another service life in a new application. In the current paper, a concept for such a M&C bank is presented. This study investigates the potential of a M&C bank in the framework of circular economy concepts for the planning of sustainable and circular buildings with a reduced eco-footprint by focusing on the reuse of decommissioned structural components. The concept, main businesses and work operation of the bank are discussed. Furthermore, a digital representation of the bank as BIM-based M&C bank needed to publicize the availability of the reusable components to the market and to enable circular business models by showing their circular pathways are described.

Keywords

Sustainability, construction and demolition waste, material and component bank, reuse, building information modelling

1 INTRODUCTION

The construction sector has a significant negative impact on the environment, and buildings consume large amount of global resources and generate vast amount of construction and demolition (C&D) waste such as concrete, bricks, steel, wood, glass, plastic materials, excavated soil, etc. (Poon, Yu, Wong, & Cheung, 2004). As a result, sustainability principles continue to grow within the construction industry to adopt environmentally friendly construction methods and waste management methods.

Sustainable development is most widely defined as the development that meets the needs of the present without compromising future generations (Brundtland, 1987). The European Commission noted that circular economy systems have huge benefit for sustainable development and adopted new policy initiatives such as the Circular Economy Action Plan (CEAP) to encourage policy makers, academia and industry towards sustainability (COM, 2020). It includes everything from production to consumption, repair, manufacturing and waste management. The circular economy is a fundamental shift from a linear economy, which is based on take, make and dispose to a more sustainable model that reduces the extracting of raw materials from finite natural resources and stops producing the waste at the other end. It transforms the linear approach into a closed loop, which is very much dependent on the use of secondary raw materials. The circular economy contributes to a sustainable development in the construction sector, as it eliminates systematic physical degradation of natural resources, amount of waste produced by construction and the volume of raw materials extracted from earth.

In circular economy, reuse and recycling are the key strategies to maximize the use of materials through moving materials from one application and producing new materials out of waste, respectively (Pan, et al., 2015). Although recycling of materials is a common practice, direct reuse is a more beneficial use of building materials at the end of a service life. This is because recycling requires more energy usage as compared to the energy needed for material reuse (Addis, 2006). Furthermore, the reuse of structural components from old buildings would provide many benefits for the environment and for energy and resource saving (Aye, Ngo, Crawford, Gammampila, & Mendis, 2012). Kummatti housing estate rehabilitation project in Raahe in Finland during 2008-2010 showed that 36% of savings in construction cost when reuse of concrete wall panels (Huuhka, Kaasalainen, Hakanen, & Lahdensivu, 2015). In German, precast concrete elements were reused in a new housing project in Mehrow and resulted in 30% reduction in cost (Stacey, 2011). A unique recent BAMB project (BAMB, 2020) explored the view of buildings as material banks within which components are retained at high value for future reuse. Several pilot projects presented which can be incorporated circular economy in such a development (e.g. BRIC building and new office building).

The recent research has proven that the development of the Building Information Modelling (BIM) based on sustainable tools for estimating the energy and environmental performances of buildings (e.g. Salvage performance, life cycle assessment regarding energy consumption, CO₂ emission, waste generation) during the early design stages would be beneficial in adopting circular economy principles in the construction industry (Akanbi, et al., 2018; Ghisellini, Ripa, & Ulgiati, 2018). Akanbi et al. developed a BIM-based building salvage performance estimator to evaluate the salvage performance of structural components of buildings during their useful life and found that building design with steel structures, demountable connections and prefabricated assemblies are mostly reusable (Akanbi, et al., 2018). Bilal et al. discussed the potential of BIM-based waste prediction in the construction industry and identified twelve (12) critical features that can be implemented in BIM-based tools for construction waste prediction and minimization (Bilal, et al., 2015). Galic et al. adopted a BIM-based approach to identify instabilities when deconstruction of a steel structure for further reuse or relocation (Galic, Dolacek-Alduk, Cerovecki, Glick, & Abramovic, 2014). Honic

et al. presented a BIM-based Material Passport, which acts as an optimization tool in early design stages and an inventory at the end of the life-cycle of a single building (Honic, Kovacic, Sibenik, & Rechberger, 2019).

However, there is no circular economy market that supports the reuse of whole structural components (Waldmann, 2017). In order to bridge this gap, a new circular economy strategy, which is called Material and Component (M&C) bank, has been developed within the EU funded Eco-Construction for Sustainable Development (ECON4SD) project. It paves the way to increase sustainability of construction by effectively managing the reuse of structural components and recycling of materials (Cai & Waldmann, 2019). The authors propose and develop a BIM-based tool as a digital representation of the bank, which allows to store information of the materials and components of buildings preparing them for an application in circular economy perspective (Jayasinghe & Waldmann, 2020).

As part of the ECON4SD project, this paper discusses the concept, key businesses and work operation of the M&C bank, as well as a broader framework of a BIM-based tool that will be able to assess recycling and reuse potential of materials and components.

2 OVERVIEW OF RESEARCH

Reuse is recognized as a better practice in the construction industry to recover the value of building materials. However, the lack of data standardization to identify potentially reusable components as well as to re-certificate the decommissioned components providing a guarantee of their future structural reliability are the major obstacles for reusing structural components. Recently, there are few projects such as e.g. the project BAMB (BAMB, 2020) which try to provide related tools to increase the value of building materials for recovery and reuse. Certainty in material properties and manufacturing data are important to provide the quality assurance and warranty of reusable components as well as professional indemnity insurance for the designers. There is currently limited information available about how to reuse structural components. Therefore, an additional institution is needed playing the role of a living Material Bank, which organizes the transfer of components for reuse extracted from old deconstructed buildings to a new structure including condition assessment, conditioning, management of the related BIM data and certification of these components.

Fig. 1 demonstrates the concept of the M&C bank, which is closely linked with Design for Deconstruction (DfD). In Fig. 1, the dashed line shows the core business of the bank that permits to establish the circular economy in construction. DfD helps to increase the useful life of components of a structure by making them available as material stocks for the future (Tingley & Davison, 2011). Structures with DfD can easily reach high level of circular economy in the construction sector. DfD should be introduced in the planning phase to improve the technical usability of structural components of structures. Crowther (Crowther, 2005) produced a list of general concepts and principles for deconstruction. For the structures without DfD, some smart demolition technologies are needed to separate the part of the components, which can be reused in new structures, from the C&D waste (Cai & Waldmann, 2019). As shown in Fig. 1, through the M&C bank the information on the disassembly and reuse potential for structural components can be provided for the next utilization. However, new deconstruction strategies and set of processes such as (i) designing reasonable demountable connections with reasonable mechanical properties and durability, (ii) assessing residual performance and (iii) evaluating the possibility of reassembly must be developed to facilitate the disassembly of structural components after a life-cycle of a building (Waldmann, 2017).

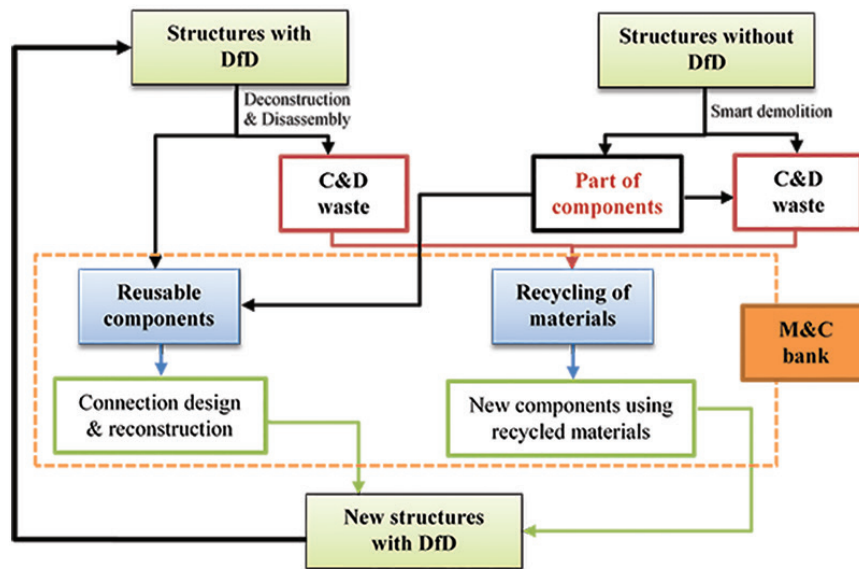


FIG. 1 Concept of M&C bank. The figure is modified from (Cai & Waldmann, 2019)

The role of the M&C bank on the transfer of decommissioned components from the old structures to the new structures is illustrated in Fig. 2. The key functions of the bank are identified as follows:

- **Database** – The bank must be able to extract and store the characteristics of materials and components in existing buildings. Thus, a detailed database that contains material specifications, design relevant parameters, dis- and re-assembly details, connection details, load-bearing capacities, aging and deterioration and suppliers' information must be established. This means that the database will provide all kind of information on the components in a building to allow their reuse in a context of circular economy. These data can be effectively used to identify the recyclable and reusable potentials of the materials and then, separate the recyclable and reusable materials from the waste. Since BIM contains all the information about materials and components with numerous life-cycle related data, such as material properties, geographic information, quantities, function, life, composition and cost (Kensek, 2015), a BIM-coupled database promises a solution to the digital representation of the bank. Producing appropriately categorized and detailed information about components will help contractors and designers to easily identify the (future) availability of reusable components as well as their condition.
- **Assessment and conditioning** – Uncertainties on the condition of the structural components for reuse is one of the main barriers for the reuse of disassembled components. The bank is responsible to conduct a condition assessment of components by forecasting their future condition considering the time-dependent impacts and material degradation. Once the structural components that will be decommissioned for reuse are identified, an adequate plan for structural condition assessment and the determination of the remaining load-bearing capacity and the service life of the structural components has to be done. In addition, with the help of the bank and by considering the chemical properties of the materials and specification of recyclable materials, environmental and human risk assessments can be adapted to separate the toxic and hazardous materials from the recyclable materials in order to improve the efficiency of recycling as well as economic value of recovered recyclable materials.
- **Certification and storage** – The reuse of structural components can be hindered by the lack of the certification for the reuse. Thus, with the help of the bank, after the condition assessment of the components is done, the certification of the materials and components can be formalized with the support from Government politics to provide the guarantee on the components to reuse after the first lifespan. For that, the data from the M&C bank

can be directly linked to the relevant certification systems. It is the most crucial process that the bank has to perform (Cai & Waldmann, 2019). Furthermore, it is not very likely that the decommissioned components can immediately go from a deconstructed site to a new construction site. Thus, the reusable components have to be stored for a certain time before re-use. Hence, another prime consideration of the bank should be to provide safe and reasonable storage strategies to avoid local damage of components during storage.

- **Production of new components** – Another important role of the bank is to cooperate with designers and contractors to promote the production of new components using recycled materials. In addition, solutions for detachable connections between different components have to be found in order to enable further reuse in the next application.
- **Monitoring and tracking** – After implemented reuse components or new components produced by recycled materials in a new structure, the bank will keep in touch with the owner/users of structure and will closely monitor the structure. For that, the bank will propose a proper monitoring concept and will provide some suggestions and recommendations for repairing and strengthening of the structures any degradation occurs. In the future, new structures could be leased by the building owners. These owners will have to closely monitor the buildings with elaborated monitoring concepts. The data provided by the monitoring will be fed into the BIM model and so, be available at any time. The flowchart in Fig. 3 identifies the methodology and major tasks that can be undertaken in an investigation before rehabilitation. Such an investigation could be initiated at different stages of life-span of a structure such as an anticipated change in use, at the end of design working life, structural deterioration due to time-dependent actions and structural damage by accidental actions.

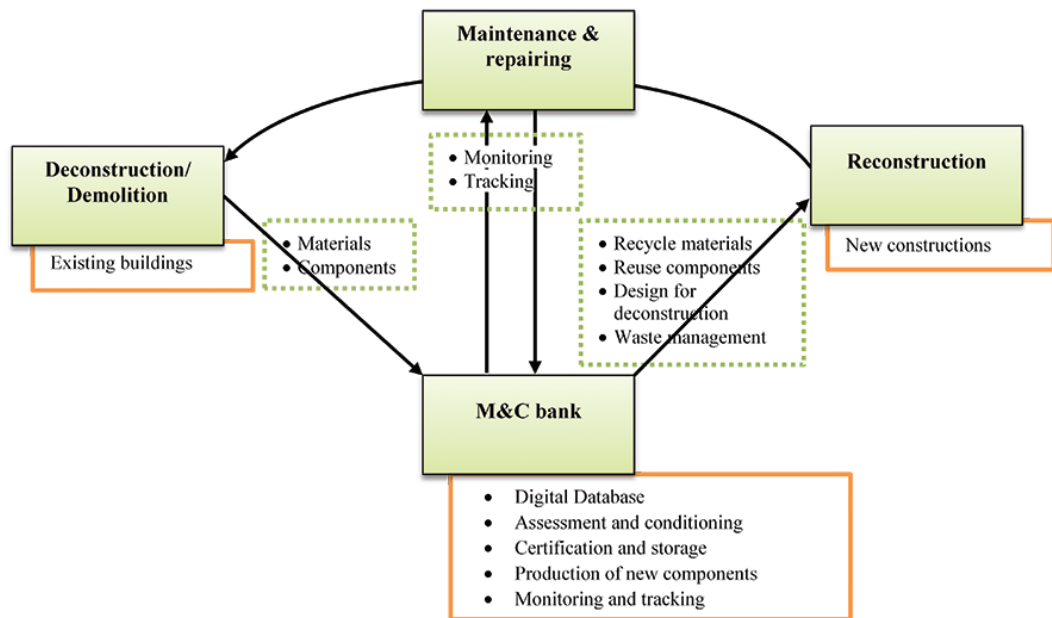


FIG. 2 Role of the M&C bank. The figure is modified from (Jayasinghe & Waldmann, 2020)

Several challenges exist on the implementation of the M&C bank in practical. A major challenge is that the majority of buildings are not designed for the reuse of components due to the lack of market for them. On the other hand, if the buildings are designed for deconstruction/reuse, the initial construction cost of the buildings could be high compared to conventional construction. Other concerns are related to feasibility to extract building components from old buildings at the end of their service life and to determination of their remaining value for reuse in future buildings. Thus, the M&C bank should be a company or institution in large scale which have managers, engineers,

researchers, technicians, market analysts etc. to be able to address above-mentioned challenges (Cai & Waldmann, 2019). Such an organization of the bank will increase its effectiveness for the recovering of the materials and components during the deconstruction. Since the reuse of building components involves several suppliers at the end, the entire market will be often not owned by a single company. Therefore, it is needed to have an intensive collaboration between other construction companies in order to maintain the circular economy to related leasing activities. Indeed, the logistic sector has to be linked to cover the transportation and storage operations related to the reuse of building components. In addition, the bank must evaluate the market potential and value of the recyclable materials and reusable components in order to promote high-level sustainability in the construction industry. Moreover, the bank has to maintain a strong collaboration with the government bodies in order to standardize the data and re-certify the components for reusing. The bank can act as an independent bank, which is responsible for the clients, or as a dependent bank which is strongly dependent on the main contractor and responsible for the contractor, but not for the client directly (Cai & Waldmann, 2019). The independent bank as a chance for a greater collaboration between different parties in the construction industry, while the dependent bank will only connect with the contractor for the supply of materials and components or exchange the related information of the project.

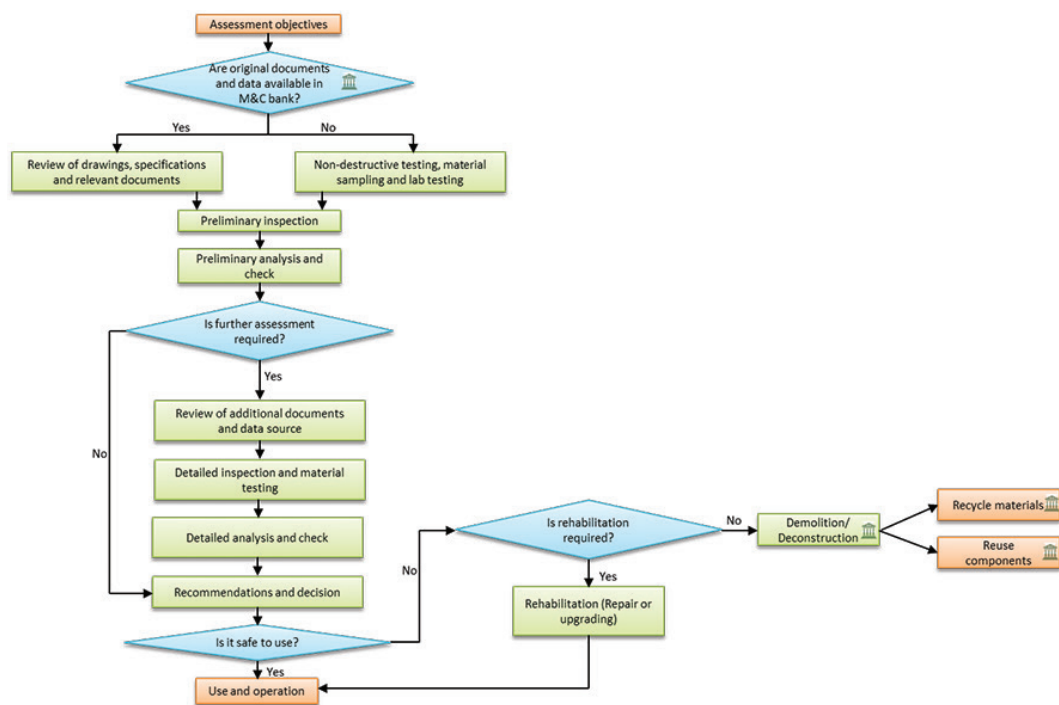


FIG. 3 Methodology in an investigation

3 BIM-TO-MATERIAL BANK WORK FLOW

These days, a growing number of architects, engineers and contractors are using BIM, which is an intelligent model-based process that connect all the professionals in the construction industry, ultimately helping them to efficiently plan, design, construct and operate buildings and structures. With BIM, designers can create digital 3D models that include detailed geometric information and semantic information of components in a building. BIM can also facilitate the data management

that is useful to identify recyclable and reusable components in advance and to identify cost and risk in the waste disposal at the deconstruction stage of a building (Liu, Osmani, Demian, & Baldwin, 2015; Volk, Stengel, & Schultmann, 2014; Wang, Wang, Wang, Yung, & Jun, 2013). This information, which provide information for decision-making calculation, could be used by the M&C bank to reduce the intensive work of collecting data about building components. Since the transparency and accessibility on information will be increased through BIM, having a BIM-coupled digital representation of the materials and components in a structure will expand the reusable M&C market. The representation of the BIM-coupled digital M&C bank is illustrated in Fig. 4.

As illustrated in Fig. 4, it is expected that the BIM models for future buildings are available. However, BIM models may not be available for some existing structures. In this case, the digitization of the physical structure can be done through the use of BIM, adopting the existing information and specifications as well as collected information from a real evaluation of the structures during the deconstruction phase. Since the BIM includes quantities and properties of building components, the developed BIM model can more accurately estimate the amount and type of waste and identify the recyclable and reusable potentials of building materials.

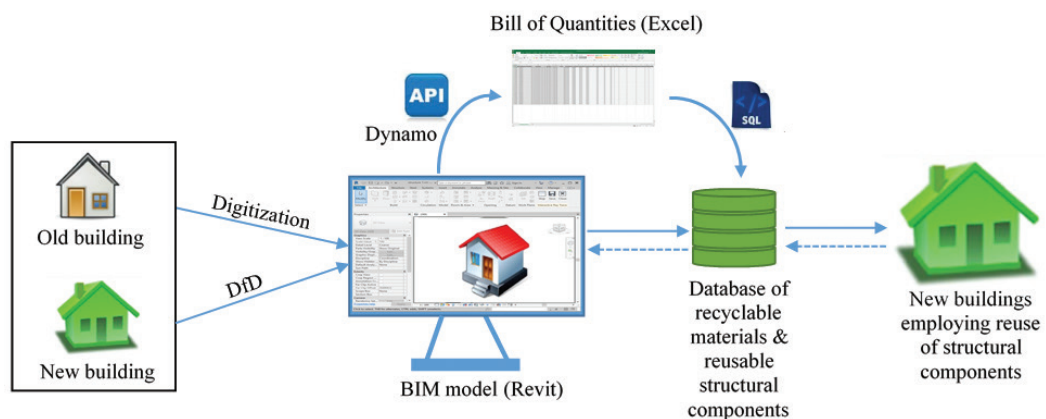


FIG. 4 The representation of BIM-coupled digital M&C bank

There are different strategies which exist for the development of an interoperable work flow and algorithm that integrate the relevant information in the BIM model to the database. In this paper, the data flow from the BIM model to the database or vice versa is achieved by developing a script using a visual programming language DYNAMO, as shown in Fig. 4. The DYNAMO script can be used to access the data structure in the Revit BIM model and obtain information from it, and then insert it into an Excel sheet. The Dynamo script can be divided into four parts that have different functionalities such as (i) element take-off, (ii) database reading, (iii) calculation and (iv) export of data to Excel. All the relevant geometrical and material properties of structural elements (such as slabs, beams, columns, walls) are extracted and then, the mathematical approach based calculation takes under the consideration of material and element type to identify the reusable and recyclable materials as well as to predict the total volume of demolition waste. This spreadsheet could be used to be automatically added to the chosen database, MYSQL.

To make it possible to assess the recyclability of materials and reusability of components, some newly created parameters have to be added into the BIM model in the form of shared parameters. Some of the identified important information which is incorporated into the BIM model is shown in Fig. 5. This information can be used for various purposes. For example, structural properties in

function of time are helpful for structural assessments to determine whether the components can be reused, while design properties of the components provide instructions on how to reuse them in a new structure. Chemical properties and thermal properties are needed to conduct environmental and energy assessments, respectively.

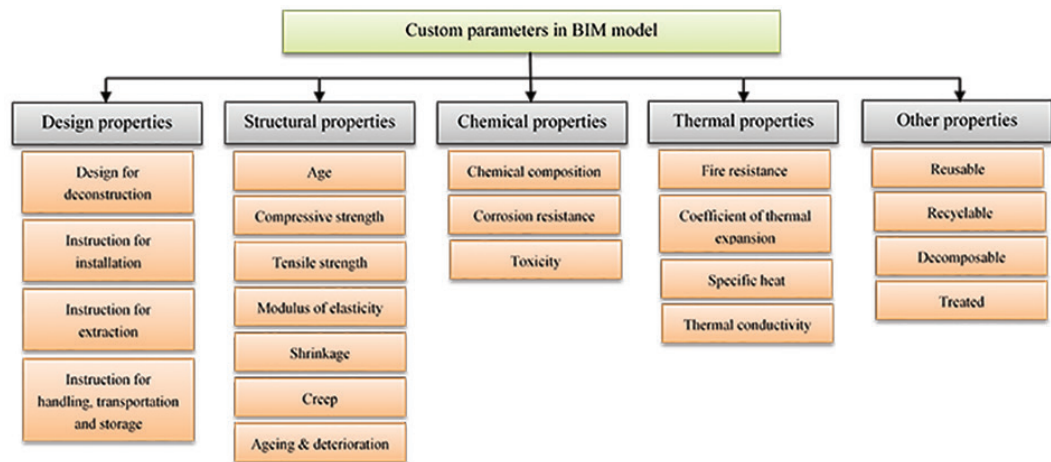


FIG. 5 Custom parameters to be incorporated in BIM model

4 THE DIGITAL REPRESENTATION OF THE BANK

A digital representation of the bank is needed to publicize the available recyclable materials and reusable components to the market. The proposed digital system for the bank consists of a repository database, a server, a web application and end user terminals, as shown in Fig. 6. The database management system is created using a SQL server, and MYSQL is used for the database connection. It stores all information related to the BIM model elements. The connection of the MYSQL database is made directly to the BIM model, by writing parameters to the database. In MYSQL database, several tables are created according the type of element (i.e. column, beam, slab and wall) and type of material (i.e. concrete, steel, wood and masonry). Each table has a set of values that uniquely identifies the row. Two rows cannot be identical and no repeating groups of data are allowed when writing to the database. A unique ID for the element is kept for each element in the database and the BIM model to serve a permanent link between the M&C bank and BIM model. Three specific types of relationships (i.e. one-to-one relationship, one-to-many relationship and many-to-many relationship) are used to define the logical connection between the records in two or more tables.

Database Management System (DBMS) is the only way to access to the information in the database. DBMS is a collection of programs which control and manage the database system. A web application is developed using PHP and MYSQL which allows end users (e.g. designers and planners, suppliers, contractors, government and client) to access the information in database and to perform project-based modifications of the database by e.g. adding data or changing the retrieval of data. It contains, a set of web pages including the project database, the material database, the components database and the assessments database in addition to the log-in and home pages. It is developed to upload the generated excel file using DYNAMO script, described above, so that the data will be automatically added and stored in the database. The amount of C&D waste are automatically calculated. In addition, reusable and recyclable materials are automatically identified and separated from the C&D waste. The information of each element is summarized in an appropriate list so that users can easily check

the properties of all the elements. This will help users to easily identify the availability of reusable components and their condition. More details can be found in ref. (Jayasinghe & Waldmann, 2020).

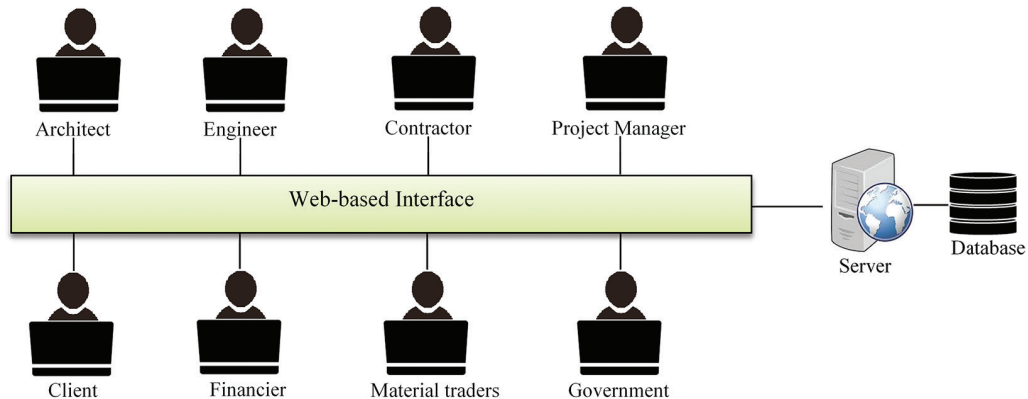


FIG. 6 The system architecture

As described above, the M&C bank should be able to keep available all kind of information on the materials and components extracted from several buildings for a long time throughout the whole life span of the buildings. This is performed by establishing a centralized database that could built a vast number of elements for future market of reuse components and recycle materials. The buildings recently built usually have BIM, sometimes, coupled with material passports (Luscuere, 2017) and life cycle assessment (LCA) software (Eleftheriadis, Duffour, & Mumovic, 2018). Therefore, automate the integration of information in BIM models into database makes it easier to collect and update the data. However, the information previously identified for reuse is needed to incorporate into the BIM model in the form of shared parameters. The accessibility and the interoperability of the BIM-to-Bank work flow throughout the whole life span of the buildings is a major concern because the maintenance of the software during such a long period will be not feasible (Bertin, Mesnil, Jaeger, Feraille, & Le Roy, 2020). Link of the bank to the material directory databases, which provide the data on material composition, recycling potentials, reusability and LCA data, will provide the required information on the bank for taking reliable and sustainable decisions. However, lack of adequate data on the construction and deconstruction processes as well as reusability and recycling potentials of materials available in the existing material directories is a big issue to identify and separate the reusable and recyclable materials from the C&D waste. On the other hand, the values on database have to be regularly updated, even if such a material directory exist and link to the database.

5 CONCLUSIONS

In this paper, the proposed concept of a Material and Component Bank which has been developed within the research project "Eco-Construction for Sustainable Development" is presented. The proposed bank will promote a circular economy in the construction industry by effectively managing the recyclable and reusable materials and components extracted from old buildings to new ones. The key businesses and roles are also introduced. In addition, a BIM-coupled system is discussed which is a digital representation of the bank and which allows to increase the transparency and accessibility of the bank. Since it provides information on disassembly of the components and the reuse and recycle potential for materials and components, it promotes the design for deconstruction leading to a high level of sustainability in the construction sector. The developed BIM-based web tool can facilitate the data management which allows designers of future buildings to easily identify the availability and the condition of the recyclable materials and

reusable components in advance which could be useful for a further application. The BIM-based web tool will also be helpful to identify the cost and risk in waste disposal at the deconstruction stage by using the volume details by material type which could provide more detailed information on the waste. This information will help contractors to calculate waste disposal fees and decision-makers to make adequate decisions for minimization and sustainable management of C&D waste. However, the accuracy of the results depends on the accuracy on the precision of the database, which is again depending on the precision of the BIM model and the accuracy of the data takeoff. Thus, it is recommended to check the BIM model using a control tool, in order to be error-free, before transferring the information from the BIM model to the bank.

Acknowledgements

This paper was developed within the framework of the European project "Eco-Construction for Sustainable Development (ECON4SD) " financed by Fonds européen de développement régional (FEDER) (Grant No.:2017-02-015-15).

References

- Addis, B. (2006). *Building with reclaimed components and materials: A design hand book for reuse and recycling*. London: Earthscan.
- Akanbi, L. A., Oyedele, L. O., Akinade, O. O., Ajayi, A. O., Delgado, M. D., Bilal, M., & Bello, S. A. (2018). Salvaging building materials in a circular economy: a BIM based whole-life performance estimator. *Resources, Conservation and Recycling*, 129, 175-186.
- Aye, L., Ngo, T., Crawford, R. H., Gammampila, R., & Mendis, P. (2012). Life cycle greenhouse gas emissions and energy analysis of prefabricated reusable building modules. *Energy and Buildings*, 47, 159-168.
- BAMB. (2020). *Buildings As Material Banks*. Retrieved June 2020, from <https://www.bamb2020.eu/>
- Bertin, I., Mesnil, R., Jaeger, J.-M., Feraille, A., & Le Roy, R. (2020). A BIM-based framework and databank for reusing load-bearing structural elements. *Sustainability*, 12, 3147.
- Bilal, M., Oyedele, L. O., Qadir, J., Munir, K., Akinade, O. O., Ajayi, S. O., . . . Owolabi, H. A. (2015). Analysis of critical features and evaluation of BIM software: towards a plug-in for construction waste minimization using big data. *International Journal of Sustainable Building Technology and Urban Development*, 6(4), 211-228.
- Brundtland, G. H. (1987). Our common future: report of the world commission on environment. *Medicine and War*, 4(1), 300.
- Cai, G., & Waldmann, D. (2019). A material and component bank to facilitate material recycling and component reuse for a sustainable construction industry: concept and preliminary study. *Clean Technologies and Environmental Policy*, 21, 2015-2032.
- COM. (2020, March 11). *EU Circular Economy Action Plan*. Retrieved from European Commission. Environment: https://eur-lex.europa.eu/resource.html?uri=cellar:9903b325-6388-11ea-b735-01aa75ed71a1.0017.02/DOC_1&format=PDF
- Crowther, P. (2005). *Design for disassembly themes and principles*. RAIA/BDP Environmental Design Guide.
- Eleftheriadis, S., Duffour, P., & Mumovic, D. (2018). BIM-embedded life cycle carbon assessment of RC buildings using optimised structural design alternatives. *Energy and Buildings*, 173, 587-600.
- Galic, M., Dolacek-Alduk, Z., Cerovecki, A., Glick, D., & Abramovic, M. (2014). BIM in planning deconstruction projects. *eWork and eBusiness in Architecture, Engineering and Construction: ECPPM 2014*. Vienna, Austria.
- Ghisellini, P., Ripa, M., & Ulgiati, S. (2018). Exploring environmental and economic costs and benefits of a circular economy approach to the construction and demolition sector. A literature review. *Journal of Cleaner Production*, 178, 618-643.
- Honic, M., Kovacic, I., Sibenik, G., & Rechberger, H. (2019). Data- and stakeholder management framework for the implementation of BIM-based Material Passports. *Journal of Building Engineering*, 23, 341-350.
- Huuhka, S., Kaasalainen, T., Hakanen, J. H., & Lahdensivu, J. (2015). Reusing concrete panels from buildings for building: Potential in Finnish 1970s mass housing. *Resources Conservation and Recycling*, 101, 105-121.
- Iacoboaia, C., Aldea, M., & Petrescu, F. (2019). Construction and demolition waste - A challenge for the European Union? *Theoretical and Empirical Researches in Urban Management*, 14(1), 30-52.
- Jayasinghe, L. B., & Waldmann, D. (2020). Development of a BIM-based web tool as a material and component bank for a sustainable construction industry. *Sustainability*, 12(5), 1766.
- Kensek, K. (2015). BIM guidelines inform facilities management databases: a case study over time. *Buildings*, 5, 899-916.
- Liu, Z., Osmani, M., Demian, P., & Baldwin, A. (2015). A BIM-aided construction waste minimisation framework. *Automation in Construction*, 59, 1-23.
- Luscuere, L. M. (2017). *Materials Passports: Optimising value recovery from materials*. *Proceedings of the Institution of Civil Engineers – Waste and Resource Management*, 170(1), pp. 25-28.
- Pan, S.-Y., Du, M. A., Huang, I.-T., Liu, I.-H., Chang, E.-E., & Chiang, P.-C. (2015). Strategies on implementation of waste-to-energy (WTE) supply chain for circular economy system: a review. *Journal of Cleaner Production*, 108, 409-421.
- Poon, C. S., Yu, A. T., Wong, S. W., & Cheung, E. (2004). Management of construction waste in public housing projects in Hong Kong. *Construction Management and Economics*, 22(7), 675-689.
- Stacey, M. (2011). *Concrete: a studio design guide*. London: RIBA.
- Teo, M. M., & Loosemore, M. (2001). A theory of waste behaviour in the construction industry. *Construction, Management and Economics*, 19(7), 741-751.
- Tingley, D. D., & Davison, B. (2011). Design for deconstruction and material reuse. *Proceedings of the Institution of Civil Engineers – Energy*, (pp. 195-204).

- Volk, R., Stengel, J., & Schultmann, F. (2014). Building Information Modelling (BIM) for existing buildings - literature review and future needs. *Automation in Construction*, 38, 109-127.
- Waldmann, D. (2017). Demountable construction enables structural diversity. *Open Access Gov.*, 212-213.
- Wang, Y., Wang, X., Wang, J., Yung, P., & Jun, G. (2013). Engagement of facilities management in design. *Advances in Civil Engineering*, 2013, 189105.

A Definition of Essential Characteristics for a Method to Measure Circularity Potential in Architectural Design

Charlotte Heesbeen¹, Magdalena Zabek², Linda Hildebrand²

- 1 Department of Architectural Engineering and Technology; Faculty of Architecture and the Built Environment, Delft University of Technology, 2628 BL Delft, The Netherlands, c.heesbeen@tudelft.nl
- 2 Juniorprofessorship of Reuse in Architecture, Faculty of Architecture, RWTH Aachen University, Templergraben 83, 52064 Aachen, Germany, magdalena.zabek@rwth-aachen.de

Abstract

Circularity potential in the construction sector, a quality that quantifies the contribution to carbon and resource neutrality, is to be standardised in Europe yet. In order to do so, a harmonised definition and method of calculation that offers transparency is crucial. Simplicity in construction methods, a low-tech approach, and a limited variety and pure use of materials support the development of innovation towards a Circular Economy (CE). The state-of-the-art in architecture features both simple and complex constructions, which need to be quantified with respect to their circular performance in light of the European norm. A clear European standardised method and accompanying tool(s) to assess the circularity potential of a building or element will encourage designers to use secondary material, to limit waste production, and to enable multiple life cycles of buildings and elements to preserve primary natural resources.

In order to meet the target of a successful CE, firstly, a method to quantify success and inform the architectural design process have to be developed and adopted across Europe. Subsequently, the development of practical assessment tools to measure the circularity potential of building components is an essential step towards the implementation of CE. As a matter of fact, several methods are ready or under development, but none has reached the level to be implemented as a European standard. This study aims to provide answers on what characteristics a harmonised method and practical design tool should contain.

Two assessment metrics for circularity, one from Germany and one from the Netherlands, are reviewed to compare their applicability in the design process and point out opportunities for a harmonised European method. Five case studies, comprising prefabricated concrete façade elements, are assessed using both metrics. The results will be used to analyse the metrics' transparencies and abilities to holistically measure the amount of reused and recycled material in a building's substance and quantify the recyclability of building products in light of their intended recycling path in the future. The third aspect that is integrally analysed is, therefore, applicability in a design process.

Keywords

Circular Economy, circularity potential, architectural design, circularity assessment method, prefabricated concrete

1 INTRODUCTION

The evident contribution of the building sector to climate change fills the architectural discussion with ways to improve the architectural practice. Until now, the energy consumed during the use phase of buildings has been the focus of sustainable development ever since policymakers implemented energy efficiency restrictions in the 70'ies of the last century (Hildebrand et al., 2009), resulting in energy efficiency for the use phase of a building. On the other hand, little progress was made in the physical production and deconstruction of a building.

Still, the building industry consumes 40 - 50 % of the global resources, produces 60 % of the global waste and 33% of the global CO₂ emissions (UNEP, 2012). Consequently, it is the moral obligation of this industry to preserve resources and balance the industries impact on the environment. Although authorities set regulations to save natural resources and increase recycling rates, the linear economy is still dominant (Zabek et al., 2017). The European Commission introduced the EU Waste Directive in 2018 that requires all new construction to have a recycling rate of 70% by mass by 2020 (Commission, 2013). The gap between political directions and practice puts architects and planners in charge to bring principles of the Circular Economy (CE) into practice.

The ones who are willing to integrate the strategies of a CE on material level are facing different challenges: uncertainties within the closed-loop systems of products, an increased amount of information during design, lack of experienced stakeholders and different political regulations (Mackenbach et al., 2020). There are several ways to achieve circularity like a Low-Tech approach of construction method, detachable components, the use of reused and recycled material (EMF, 2017; TransitieteamCirculaireEconomy, 2018). But the key to practice is the ability to compare the environmental impact of design alternatives. Several characteristics of a method to measure circularity have been introduced on the market, such as the Circularity Indicators from the McArthur Foundation (Foundation; et al., 2015), which assesses, rates and reports on how well a product or company performs in the context of CE. Based on this method, the company Madaster uses the circularity indicators (Madaster, 2020) to assign a circularity score of buildings with the data being registered on their platform. Besides, several more methods are under development (Ebert et al., 2020) or available (Rosen, 2019) but none has reached a level to be implemented as a European standard tool yet (Rahla et al., 2019; wbcSD, 2018). This calls for a harmonised definition of the essential characteristics for methods to assess circularity during design. Hence, this paper reviews two circularity potential metrics for construction, one from Germany and one from the Netherlands by assessing five case studies to evaluate the metrics ability for standardisation with regard to their applicability in design, transparency and holistic perspective. The first metric has been selected due to its user-friendliness proved during student courses, and the second due to its integrity into a mandatory Dutch environmental impact assessment tool and focused approach to measure demountability as an indicator for circularity. The results are used to point out what characteristics a European harmonised method to measure circularity potential and practical tools should contain.

2 METHODOLOGY

Two metrics are introduced, and their parameters and calculation method are described based on publications. Both metrics are used to assess the circularity potential of five case study of a prefabricated façade element using the same input data, namely a bill of materials (BoM). Metric A assesses circularity including the reuse and recycling content in addition to the suitability for further use. Metric B focuses on the disassembly potential of building components and their composition. The metrics are compared in three categories, with a focus on the use in an architectural design process, in order to improve the design in regard to future reusability and generate a circular design.

Doing so, the reliability of the metrics was assumed to be a fact, and this fundamental requirement was excluded from the assessment. The categories include:

- 1 Applicability to Design: a method that is applicable in design should be supportive of the design process. It generates information that can be used to improve the design in an ongoing process (Saidani et al., 2017; wbcasd, 2018).
- 2 Transparency: a transparent method enables the user to learn from the design consequences and third parties to understand and reconstruct the design and calculation process (Linder et al., 2017).
- 3 Holistic perspective: a holistic view integrates all aspects of circular design, including closed life cycles through product longevity (high value/performance), life extension (material input) and disassembly (material output) (Ness et al., 2017). The weighting of results by mass and GWP (CO2 equivalent). A holistic method, including the quantification of resource guarantees that a complete representation of the design task is part of the calculation (wbcasd, 2018).

The method leads to the following research step: the specific and shared characteristics of metrics A and B contribute to the categories identified and summarised as essential characteristics for a harmonised method.

2.1 METRIC A: ADVISORY METRIC OF MATERIAL IN- AND OUTPUT

This metric has been developed at the Chair of Reuse in Architecture at the RWTH Aachen University in 2017 and was first published in 2018. According to the authors (Hildebrand et al., 2018), the main goal is to provide information on the environmental benefit related to the design task and to distinguish the benefit that is potentially accessible after the buildings use phase. In relation to that (Hildebrand et al., 2019) the metric consists of two parts; 1) "input" which shows the use of (I) reused, (II) recycled and (III) renewable material and its future recycling path as 2) "potential output" with fractions that show different potential for further application. Both criteria are expressed in percentage of the Global Warming Potential GWP (CO2 equivalent) or mass (kg).

2.1.1 Input

The materials that are planned to be part of the building substances are divided into four indicators:

- re: reused material
- rc: recycled material
- rw: renewable material
- pw: primary non-renewable material.

In the first step of the analysis, the items on the BoM are identified using data in "Ökobaudat", the Germany Sustainable Construction Information Portal (Kerz, 2012). Then, each layer is classified into four indicators listed above (re,rc,rw,rp). The calculation of the amount of material (input) used in one object for one indicator is:

Reused materials (re):

$$V_{re} = \frac{\sum_i M_i + M_{re}}{\sum_i M_i}$$

Recycled materials (rc):

$$V_{rc} = \frac{\sum_i M_i + M_{rc}}{\sum_i M_i}$$

Renewable materials (rw):

$$V_{rw} = \frac{\sum_i M_i + M_{rw}}{\sum_i M_i}$$

Primary materials (pw):

$$V_{pw} = \frac{\sum_i M_i + M_{pw}}{\sum_i M_i}$$

- M_i = Mass or GWP of an object or sub-object (i),
- M_{rx} = Percentage by mass or GWP of reused (re) / recycled (rc) / renewable (rw) / primary (pw) material input in a component,
- V_{rx} = Reused (re) / recycled (rc) / renewable (rw) / primary (pw) materials input as a percentage of a total component.

2.1.2 Potential Output

The future recycling path of a building component is mostly based on the component's connectivity, material family and potential hazardous substances. In order to display the building substance's reuse or recycling potential, the output is assessed based on the future material flow categorised into four different fractions (a,b,c,d):

- A deconstructable, without damage, pure material with high potential for reuse
- B deconstructable, with damage, pure material with high potential for recycling
- C dismountable, with damage, mixed material with low potential for high-value recycling
- D critical material with hazardous substances used for landfill.

The calculation of the potential output in one object of one indicator is:

$$\begin{array}{llll}
 \text{Fraction a:} & \text{Fraction b:} & \text{Fraction c:} & \text{Fraction d:} \\
 V_a = \sum_i M_i * M_a / \sum_i M_i & V_b = \sum_i M_i * M_b / \sum_i M_i & V_c = \sum_i M_i * M_c / \sum_i M_i & V_d = \sum_i M_i * M_d / \sum_i M_i
 \end{array}$$

- M_i = Mass or GWP of an object or sub-object (i),
- M_x = Percentage by mass or GWP of fraction (a) / (b) / (c) / (d) materials output in a component,
- V_x = Fraction (a)/(b)/(c)/(d) materials output as a percentage of a total component.

2.2 METRIC B: ASSESSMENT OF DISASSEMBLY POTENTIAL

The Dutch government aims for a CE in 2050 and pro-actively stimulates innovation towards that direction (TransitieteamCirculaireEconomy, 2018). In the slipstream of this ambition, several initiatives have been launched to speed up the transition. One of which is the development of a metric proposal for disassembly potential in constructions (Vliet, 2019), which is called Metric B in this publication. The degree of disassembly of buildings determines the probability of successful reuse of their parts. The scenarios in the 10-R model (Cramer, 2015) are used to express the degree of value retention through disassembly. A nationally adopted coding system, NL/SfB (BNA, 2005), is used to define the scale on which the assessment takes place. As such, the metric can be integrated in the mandatory Dutch environmental impact assessment system MilieuPrestatie van Gebouwen (MPG) in the near future. The MPG is an indicator of sustainable building based on LCA using data from a national database for environmental impact for construction (RVO, 2020)

The potential to detach an element from the building depends both on the connection of the element to another and the composition of it. Metric B is used to calculate the disassembly potential. The disassembly potential of an element (LIn) is therefore equally composed of the disassembly potential of the object itself (LIcn) and the disassembly potential with other objects (LIsn). Four factors are used to rate this, detailed definitions are found in the method (Vliet, 2019). The result is subsequently normalised using a ratio of the object's and building's MPG.

- TV_n = Object n connection type
- ToV_n = Accessibility of object n connection
- DK_n = Degree of integration of object n with other objects
- VIn = Shape of integration of element n

$$LIC_n = \frac{LIC_n + LIS_n}{2}, \quad LIC_n = \frac{TV_n + ToV_n}{2}, \quad LIS_n = \frac{DK_n + VIn}{2}$$

3 CASE STUDIES

The five case studies are variations on one functional unit, namely a 20 m² load-bearing prefabricated façade element (Figure 1 Case study context). The variation is created in material selection, deconstruction principle and end-of-life (Table 1 Case study design variants). The designs were developed for a residential highrise building of approximately 70m and a footprint of 47 x 16 meters. They have a similar load-bearing capacity for comparability. Other building components than the façade elements are excluded from the calculations. Furthermore, the alternative designs represent the state-of-the-art in prefabricated concrete construction.

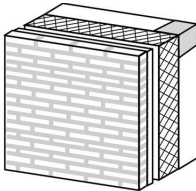
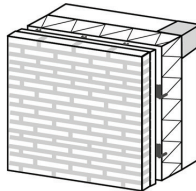
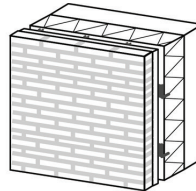
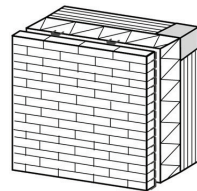
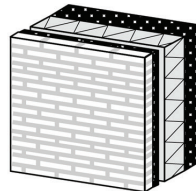
1	2	3	4	5
				
Dfx Reuse	Dfx Dissassembly	Dfx Upgradability	Dfx Biological cycle	Dfx Life extension
Construction material Concrete – PIR – Brick and mortar	Construction material Concrete – Mineral wool – Brick and mortar	Construction material Concrete – Mineral wool – Brick and mortar	Construction material Cross-laminated timber – Mineral wool – Brick and backing system	Construction material Recycled concrete – Mineral wool – Brick and recycled mortar

TABLE 1 Case study design variants.

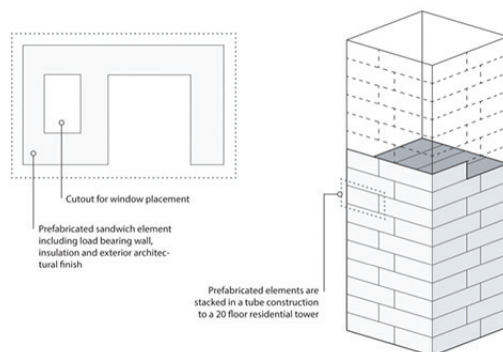


FIG. 1 Case study context

In order to achieve various life cycles of a product with high quality, the maintenance in its original format and the material purity play an important role. Mechanical connections improve

the detachability of a component, and therefore its material can be rated with a higher reuse potential. Connections with high connectivity that can only be detached with heavy machinery, like plaster, must be rated with a low reuse potential. In this regard, element 4 has the highest performance achieved using both metrics (Fraction a=86%, Lin=0.55), although its design intention was a high amount of renewable material (Mrw=59.57%, Tab.1) presented in Table 2. Element 1 and 5 has the highest potential to end up as landfill (Fraction d=0.4, Tab.2) or be recycled with a low quality (Fraction b=89%, Tab.2) and therefore has the most inferior performance. Similar results are achieved with metric B (Lin= 0,1). Element 2 performs slightly better than Element 3 using both methods.

	METRIC A (proportions explained in Chapter 2.1.2)				METRIC B (proportions explained in Chapter 2.2)
	FRACTION A	FRACTION B	FRACTION C	FRACTION D	DISASSEMBLY POTENTIAL (Lin)
ELEMENT 1	0.46	10.1	89.02	0.42	0.18
ELEMENT 2	15.1	84.9	0.59	0	0.46
ELEMENT 3	0.45	82.9	16.64	0	0.33
ELEMENT 4	86.72	12.94	0	0	0.55
ELEMENT 5	0.46	9.43	89.68	0.43	0.15

TABLE 2 Case Study Circularity Potential derived from calculation in chapter 2.

Per element, one single score is generated from the calculation in metric B. A score between 0.4 and 0.6 is considered low, between 0.6 and 0.8 average, above 0.8 high. Scores below 0.4 are not labelled, although they can occur in theory and do in the calculation made in this research. Three elements are considered below par, and two elements score low, a meagre overall score which could indicate, based on the state-of-the-art techniques used in the case study, that this method yields a strict rating.

In comparison to metric A, metric B does not consider the input material as an indicator for circularity. Therefore, the results are not presented, although it is part of the calculation of metric A.

4 RESULTS

In order to achieve CE in the building industry, products must be designed with a high potential to be reused as well as containing a reduced amount of primary resources and kept at their highest level of utility and value at all times (EMF, 2017). A harmonised assessment method can inform circular design across Europe. This method should be 1) applicable to a design process from an early design stage, 2) transparent, and 3) apply a holistic perspective. These three categories are used to analyse the results presented in paragraph 3, created with the two presented metrics in paragraph 2, and essential characteristics have been developed in Tab.3.

CATEGORY	ESSENTIAL CHARACTERISTIC	METRIC A	METRIC B	NOTES
APPLICABLE TO DESIGN	Benchmark comparison	0	+	A: is missing a benchmark
	Readability of results	+	++	A: result consists of 8 categories B: result consists of a single score
	Offers insight to improve the design	++	+	A: separate categories allow the planner to improve the design within a specific category B: one score result shows little insight into derivation
	Level of additional knowledge needed to use the method and to improve the design	+	0	A: requires knowledge of material substances and connections B: requires detailed technical knowledge on the execution of the project
	Compatibility with sustainability assessment tools	+	++	A: LCA B: LCA, MPG, NL/SfB
TRANSPARENCY	Open-access data and pre-defined data sources	+	+	A: data from (www.oekobaudat.de, 06.06.2020) B: calculation is based on an MPG calculation, derived from an open-access or purchased tool
	Rating and concept definition	+	++	A: criteria are shortly explained in publications. B: criteria are clearly explained in the method's guideline
	Pre-defined assessment options	+	++	A: Connectivity level/future recycling path and materials substance is divided into 8 general categories B: 30 prescribed options for connectivity level
HOLISTIC PERSPECTIVE	Encourage designers to design according to CE objectives	++	0	A: includes a more holistic view due to the assessment of material in- and output B: only assesses the output material connectivity
	Complete life cycle data	++	++	A: is assessed based on GWP B: is assessed based on GWP
	Applicable to the entire design process (concept to detail) in order to influence circularity at an early design phase	+	+	A: applicable with detailed information about materials substance and connectivity B: applicable with detailed information about materials connectivity
	Relevant environmental indicators	++	++	A: Volume and GWP is used as indicators B is based on GWP and other indicators
	Assessment of materials flow and potential hazardous substance	++	+	A: assesses potential hazardous substances and future recycling path B: includes integration of various materials

TABLE 3 Characteristics of metrics A & B - (++) very good performance, (+) good performance, (0) poor performance

5 DISCUSSION

In the transition towards a CE in the built environment, there are several aspects that need to be faced, such as the lack of harmonised assessment methods for circularity. Authorities cannot implement restrictions on the usage of resources if a reliable method to measure circularity in construction is not available. In this research, two metrics for circularity potential have been evaluated in regard to applicability in the design process, transparency and their holistic perspective. Based on the observations, the following essential characteristics of a method have been identified:

Applicability to Design:

- Insight in improving the design for circularity during use of the method

- Definition of a realistic benchmark creates insight in the improvement of circularity potential and design quality
- Clear relation and compatibility with regulations and existing methods and tools
- Correlation with the average sustainability and circularity knowledge level of architects and engineers

Transparency:

- Detailed pre-defined options for assessment
- A readable, though nuanced score that indicates the circularity potential
- Based on open-access data and tools
- Applicability during concept design to detailed and execution design in order to improve the design according to CE principles
- Clear definitions of concepts and rating
- Clear and openly available guideline for use

Holistic perspective:

- A weighted contribution of materials to the final score, for instance, based on mass and CO2 emissions
- A holistic system perspective including input and potential output material
- Include the effort of reprocessing and recycling, contamination risk and hazardous materials rate

6 CONCLUSION

Measuring and rating the circularity of buildings results to be an intricate objective due the complex notion of a building as a conglomerate of different products and materials and uncertain lifespans (Rahla et al., 2019). In the past, several metrics had been developed, and two of them have been evaluated in this review. The path towards CE is dynamic and can be shaped with an integral and harmonised assessment method that should be implemented on a European level. The list of essential characteristics in this publication should be used as a starting point for the development of a systematic method and provides interpretation for other metrics in order to move towards an environmentally and technically high-performance building industry based on CE principles.

Acknowledgements

This collaboration has been supported by the Short-Term Scientific Mission (STSM) grant of the Cost Action group CA17133 - Implementing nature-based solutions for creating a resourceful circular city - funded by the Horizon 2020 Framework Programme of the European Union. The data that support the findings of this study are available from the corresponding authors, [CH, MZ], upon reasonable request.

References

- BNA. (2005). NL/SfB Tabellen. In: BNA.
- Commission, E. (2013). Directive 2008/98/EC on waste (Waste Framework Directive). In European Parliament and the Council of the European Union (Vol. 2008/98). Brussels: Official Journal of the European Union.
- Cramer, J. (2015). Strategische Verkenning: 'Op weg naar Cirkelregio Utrecht'. Retrieved from Utrecht Sustainability Institute: <https://www.usi.nl/nl/circulaire-economie/cirkelregio-utrecht>
- Ebert, S., Ott, S., Krause, K., Hafner, A., & Krechel, M. (2020). Model for the recyclability of building components. doi:<https://doi.org/10.1002/bate.201900109>
- EMF. (2017). Concept. Retrieved from <https://www.ellenmacarthurfoundation.org/circular-economy/concept>
- Foundation, E. M., & Design, G. (2015). Circularity Indicators - An approach to measuring circularity - Methodology. Retrieved from https://www.ellenmacarthurfoundation.org/assets/downloads/insight/Circularity-Indicators_Project-Overview_May2015.pdf
- Hildebrand, & Knaack. (2009). Bewertung von Fassaden auf dem Hintergrund Grauer Energie. Ernst & Sohn Special, 5/2009.

- Hildebrand, L., Schwan, P., Vollpracht, A., Brell-Cokcan, S., & Zabek, M. (2018). Methodology to evaluate secondary resources regarding their ability for deconstruction. *Creativity game - Theory and Practice of Spatial Planning*. doi:10.15292/IU-CG.2017.05.020-032
- Hildebrand, L., & Wemmer, A. (2019). Circular tectonic thinking : Life cycle assessment for building elements. *Circular Construction - Materials Architecture Tectonics (CINARK)*, 72-84.
- Kerz, N. (2012). Nachhaltiges Bauen / Baustoff- und Gebäudedaten/ Ökobaudat. Retrieved from <http://www.nachhaltigesbauen.de/baustoff-und-gebaeuedaten/oekobaudat.html>
- Linder, M., Sarasini, S., & van Loon, P. (2017). A Metric for Quantifying Product-Level Circularity. *Journal of Industrial Ecology*, 21(3), 545-558. doi:10.1111/jiec.12552
- Mackenbach, S., Vossenkuhl, C., Zeller, J., & Osebold, R. (2020). Circularity in the German Construction Industry. doi:10.18154/RWTH-2020-05724.
- Madaster. (2020). Madaster Circularity Indicator explained. (Madaster Services B.V.).
- Ness, D. A., & Xing, K. (2017). Toward a Resource-Efficient Built Environment: A Literature Review and Conceptual Model. *Journal of Industrial Ecology*, 21(3), 572-592. doi:10.1111/jiec.12586
- Rahla, K., Bragança, L., & Mateus, R. (2019). Obstacles and barriers for measuring building's circularity. *IOP Conference Series: Earth and Environmental Science*, 225.
- Rosen, A. (2019). Assessment of Loop Potential. *Manual of Recycling*, 114-117.
- RVO. (2020). MilieuPrestatie Gebouwen - MPG. Retrieved from <https://www.rvo.nl/onderwerpen/duurzaam-ondernemen/gebouwen/wetten-en-regels/nieuwbouw/milieuprestatie-gebouwen>
- Saidani, M., Yannou, B., Leroy, Y., & Cluzel, F. (2017). How to Assess Product Performance in the Circular Economy? Proposed Requirements for the Design of a Circularity Measurement Framework. *Recycling*, 2(1). doi:10.3390/recycling2010006
- TransitieTeamCirculaireEconomy. (2018). Transitieagenda Circulaire Economy. Retrieved from <https://www.rijksoverheid.nl/documenten/rapporten/2018/01/15/bijlage-4-transitieagenda-bouw>.
- UNEP. (2012). *Building Design and Construction: Forging Resource Efficiency and Sustainable Development*.
- Vliet, M. v. G., J. van; Teunizen, J. (2019). Circular Buildings Meetmethodiek Losmaakbaarheid. Retrieved from <https://www.dgbc.nl/publicaties/circular-buildings-eeen-meeetmethodiek-voor-losmaakbaarheid-26>
- wbcsd, W. B. C. f. S. D. (2018). *Circular Metrics Landscape Analysis*. www.oekobaudat.de. (06.06.2020).
- Zabek, M., Hildebrand, L., & Brell-Cokcan, S. (2017). Used building materials as secondary resource- Identification of valuable building materials and automatised deconstruction. *Journal of Façade Design and Engineering*.

Sustainability in Façade Design: Approaches and Outlooks from Design Practitioners

Alejandro Prieto*¹, Mimi Oldenhave²

* Corresponding author

- 1 Delft University of Technology, Faculty of Architecture and the Built Environment, Department of Architectural Engineering + Technology, Architectural Façades & Products Research Group, Julianalaan 134, 2628BL Delft, Netherlands, +31(0)618189151, A.I.PrietoHoces@tudelft.nl.
- 2 Delft University of Technology, Faculty of Architecture and the Built Environment, Department of Architectural Engineering + Technology, Julianalaan 134, 2628BL Delft, Netherlands, M.M.Oldenhave@tudelft.nl / mmoldenhave@gmail.com

Abstract

The concept of sustainability has risen in the last three decades, as a vehicle to guide our efforts to overcome major environmental and societal challenges such as global warming and environmental degradation. The built environment is responsible for about 40% of the global CO2 emissions, a fact that has led to countless debates, approaches, and new technologies for the design of our buildings, and especially, the building envelope. The goal of this paper is to explore the current role and the impact that sustainability has in the design of the building façade, based on the insights from practicing architects with relevant experience in the field. While we know of countless theoretical approaches and design theories to deal with sustainability, the point of view from practitioners has hardly been in the spotlight. So, the input for the assessment was obtained through a series of interviews with designers, representing 34 different architectural firms in the Netherlands, between January and April of 2020. The 34 interviews followed a semi-structured questionnaire comprising open-ended questions, structured around different themes concerning their façade design process. The present document showcases and discusses the results from the following questions: what is the role of sustainability in your façade design process? How does it influence the result?

The exploration of the gathered information shows that within the broader scope of sustainability, circularity is the most mentioned set of aspects that currently have a clear impact on façade design, closely followed by energy related aspects, and further below issues related to the user, nature inclusion, and val. Furthermore, it is possible to identify different and sometimes clashing approaches derived from different notions of sustainability: some interviewees believe in permanence and timeless buildings, which leads to massive structures and detailing focused on ageing and durability; while for others it mainly revolves around using less raw materials and re-use/recycling potential of building components; which leads to light structures, with focus on connections aiming for total disassembly and material recovery. These, among others, should be regarded as possibilities to choose from a set of potential approaches, whose suitability should be carefully assessed to match each project brief, under the larger aim to design and build sustainable façades, buildings and cities.

Keywords

Façade design, sustainability, design process

1 INTRODUCTION

The concept of sustainability has risen in the last three decades, as a vehicle to guide our efforts to overcome major environmental and societal challenges such as global warming and environmental degradation. The built environment is responsible for 39% of the global CO₂ emissions (UNEP, 2019), a fact that has led to countless debates, approaches, and new technologies for the design of our buildings, and especially, the building envelope. The façade is arguably the most complex system in any building, having to deal with a myriad of requirements ranging from technical to symbolic, in its dual condition of interface between inside and outside and literal face and expression of the building. Therefore, it is there where said approaches and technologies collide during the design process. Nevertheless, while we know of countless theoretical approaches and design theories to tackle the issue, the point of view from practitioners has hardly been in the spotlight.

Architects are the main professionals in charge of putting sustainable measures in place within our built environment, adding them to the inherent complexity behind the design of our buildings and their façades. Understanding how they deal with these challenges in their design process is regarded as a key issue if we seriously strive to make a sustainable built environment a reality. New challenges will undoubtedly impact the design choices of said architects, thus indirectly defining the performance, construction and aesthetics of building façades. However, it is not always clear what these challenges entail, nor what is exactly being asked from a sustainable design. So, what do architects understand under the broad term of sustainability when it comes to façade design? How do they apply this in their practice?

The goal of this paper is to explore the role and the impact that sustainability has in the design of the building façade, based on the insights from practicing architects with relevant experience in the field. This entails a dual purpose, aiming to identify certain concepts underlying the notions of sustainability that are currently understood by a sample of practitioners; while aiming to understand their façade design choices and the approaches they currently follow in the name of sustainability. Hopefully this knowledge will provide relevant insights to the practical application of sustainable measures in façade design, from the perspective of architectural designers.

2 METHODOLOGY

The study follows the qualitative evaluation of primary information by means of content analysis techniques. The input for the assessment was obtained through a series of interviews with designers, representing 34 different architectural firms in the Netherlands (based in Amsterdam, Rotterdam, The Hague and Delft), between January and April of 2020. The 34 interviews followed a semi-structured questionnaire comprising open-ended questions, structured around four themes: (I) General design approach, (II) Façade design elements and intentions (III) Aesthetic perception of façades, and (IV) Sustainability in façade design. The present document focuses on the results from the last theme, which circled around two related questions: What is the role of sustainability in your façade design process? How does it influence the result?

The architectural firms that participated in the study mostly comprise small-sized companies, having between 10 and 49 employees (47%); being followed by medium ones (41%). Within the latter, a sub-distinction is made, between medium-sized companies with less than 100 employees (10 firms / 29%) and medium-large-sized companies employing 100-250 people (4 firms / 12%). Lastly, 4 micro-sized companies (less than 10 employees) also took part in the study (12%). About the interviewees, the vast majority holds a Partner position in the firm (85%, considering 9 Partners and 20 Founding Partners); while roughly a third of the group has had between 10 to 19 years of

experience in architectural design (32%), and another third has been designing for 30-39 years (32%). The remaining third is composed of professionals with 20-29 years of experience (18%) and others with more than 40 years in design (15%).

Figure 1 shows the complete sample in terms of their declared years of experience and the size of the firm they represent. The graph shows a high dispersion in the years of experience declared by the interviewees, evidencing an heterogeneous sample. Furthermore, this wide range of experience is reflected across the different categories of company sizes. Moreover, the graph distinguishes between the interviewees who stated to have more experience working on residential projects (housing and mixed-use buildings), and who declared to have more experience with non-residential buildings (commercial, cultural, educational and public buildings, among others).

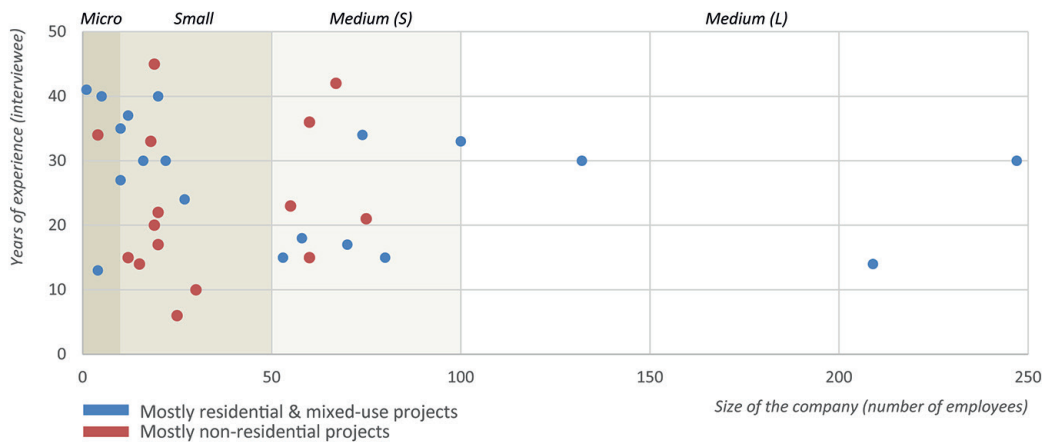


FIG. 1 Years of experience declared by the interviewees vs. the size of the company they represent

3 RESEARCH

3.1 CONTENT ANALYSIS AND CODING OF THE RESPONSES

The interviews were recorded and transcribed; to be then coded for the assessment using the software ATLAS.ti, resulting in a database in Microsoft Excel to allow for the qualitative and quantitative analysis of the gathered information. By coding the responses, it was possible to identify 27 distinctive keywords, depicted in a word cloud in Figure 2. The word sizes reflect the frequency of each keyword within the pool of responses.



FIG. 2 Word cloud of identified aspects (keywords)

An initial exploration of the keywords showed that the consideration of passive strategies is the aspect most mentioned by the sample (n=14), being addressed by almost half of the interviewees; followed by material durability (n=12); permanence (n=12); and recycling & reuse (n=10). As a second step in the assessment, the keywords were grouped into larger themes, categorising the gathered information for a better understanding of the responses. Based on the 27 keywords, 5 main themes were identified: (I) energy, (II) circularity, (III) user, (IV) nature and (V) value (Fig. 3).

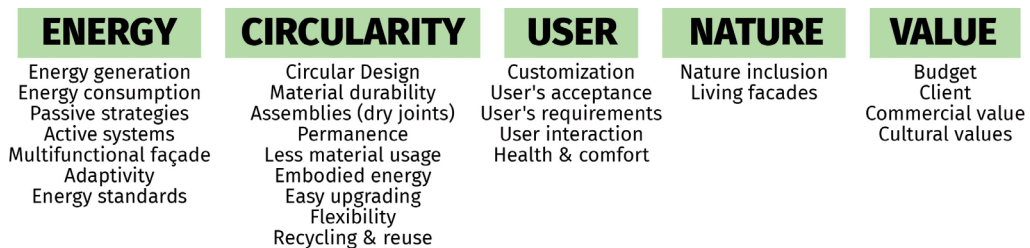


FIG. 3 Identified themes across the mentioned aspects

The keywords grouped under energy consist of aspects related to the energy flows required for the successful operation of our buildings. The mentions by the interviewees consider energy consumption (n=8) and energy generation (n=9), as central aspects for the design of nearly zero energy buildings (NZEB), establishing demands and limitations for the design of their envelopes. Likewise, in this group belong mentions of passive strategies (n=14) that may be applied as part of the design of the envelope, such as the use of louvres or insulation; or the potential integration of active systems and new technologies (n=6) to improve the energy efficiency of the overall building, such as heat storage components or decentral ventilation units. The explicit mentions of the multiple functions that façades need to increasingly accommodate were gathered within the keyword multifunctional façade (n=2), making a distinction against mentions for the need for adaptive façades (n=5), understood as façade systems that are “able to change its functions, features, or behaviour over time in response to transient performance requirements and boundary conditions, with the aim of improving the overall building performances” (Loonen et al., 2015). Lastly, this group also considers mentions of energy standards and building regulations, due to their direct impact on design decisions (n=7).

The second group, dubbed circularity, considers first of all general mentions of circular design (n=6), plus other aspects related to the efficient use of material flows and resources in the building construction. Among them, there is a relevant number of mentions of material durability (n=12) and overall material usage (n=4), alongside concerns for the embodied energy of materials and components (n=9). Regarding the direct impact of these concerns on the design of façades, the group gathers diverging approaches on the matter. On the one hand, it is possible to identify permanence (n=12) as a relevant concept posed by interviewees advocating for long-lasting buildings that can pass the test of time, by means of durable materials and a timeless design. On the other hand, the conception of buildings as assemblies was posed by a section of the sample, with emphasis on the design of construction details under dry connections (n=9), which allow for the easy disassembly of the building and/or its components. Other mentions in the group refer to the recycling & reuse of building components (n=10), either allowing the reuse of new components by ensuring an easy disassembly, or incorporating reclaimed materials into a new design. Lastly, the ability of the façade to accommodate changes during the lifetime of the building was reflected in mentions of the need for more flexibility (n=7) and the easy upgrading of its components (n=5).

The third identified theme revolves around the user and groups aspects that were declared to have a role in the design of sustainable façades, such as users' requirements in general (n=3), where health & comfort requirements were identified as distinctive aspects (n=4); and users' acceptance (n=2) was explicitly mentioned in a couple of cases. Here the distinction refers to the pragmatic nature of answering to general and various functional requirements stated during the design process, while acceptance speaks of the approval of the result, appealing to personal preferences. Single mentions within the theme referred to user interaction (n=1), and the potential for customisation (n=1).

The fourth theme, nature, focuses on the use of nature-based solutions as a resource for the design of façades, with the aim to benefit biodiversity in our cities. Within this theme, two keywords were grouped: living façades (n=7) and nature inclusion (n=4). The former refers to the integration of greenery in the building envelope, either as green façades, where climbers are attached to building surfaces; or living walls, where plants directly grow on fertile modular panels (Perini et al., 2011). Nature inclusion is a broader concept that explicitly tackles the aim of restoring the urban ecosystem, which not also includes the use of vegetation, but also promotes biodiversity by actively attracting bees and birds into urban areas.

Lastly, mentions of budget constraints (n=5), the relation with the client (n=4), and the commercial value of the façade (n=2) were grouped under a theme labelled value. These mentions mostly tackle practical aspects and difficulties of implementing sustainable measures in the design of the building envelope, asking the designers for inventive solutions to keep projects on the agreed budget; and constantly advocating for these measures in talks with the clients, trying to convince them by means of quantifying the potential returns that these could have in the long run. Also within this group it was considered a mention for cultural values (n=1), in the case of the renovation of heritage buildings, broadening the scope of what value refers to in the application of sustainable measures. The fact that these practical aspects appeared in the study shows the relevance of considering practitioners' point of view, being the ones dealing with practical matters in the name of sustainability.

4 RESULTS AND DISCUSSION

4.1 FREQUENCY OF MENTIONS AND IDENTIFICATION OF RELEVANT ASPECTS AND THEMES

The frequency of the mentions per identified aspect, and the total amount of mentions per theme/group are shown in figure 4, arranged from higher to lower frequency for an easier understanding. It is important to point out that the quantitative assessment of the responses serves an illustrative purpose, to discuss the relative perceived relevance of these aspects within the interviewed sample. Hence, these results must be understood as merely referential, needing further research to unequivocally judge their overall importance. With this in mind, passive design strategies have the higher mentions, their application being regarded as the most clear impact that concerns for sustainability have in the design of the building envelope. Nonetheless, the energy group comes second after the circularity group, which gathers most mentions, by being addressed by 30 out of the 34 interviewed professionals (88% of the sample). These two themes (energy and circularity) were by far the most associated to sustainability in façade design by the interviewees, not just by the number of mentions, but also by the number of distinguishable aspects identified in their responses and their level of detail, which will be discussed in the following paragraphs.

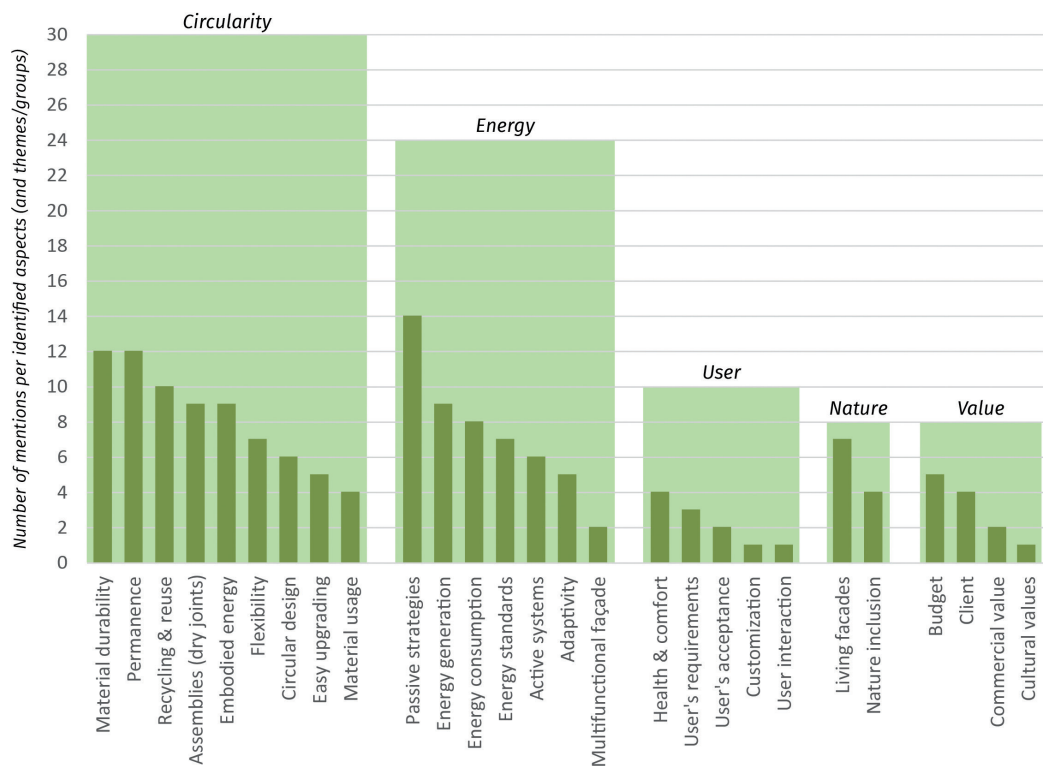


FIG. 4 Frequency of mentions for each identified aspect and total mentions per theme

The fact that circularity, as a group, scored the highest comes as no surprise, given the current attention and interest around such concepts. Notwithstanding, it is refreshing to see how embedded it already is in Dutch designers' practice and their concerns about the future. When answering, several interviewees stated concerns about the lack of information and validated tools to assess the impact of circularity on building construction. Moreover, and directly related to the previous

statement, there does not seem to be a unified strategy to incorporate these concerns into architectural design. Hence, based on the gathered responses, it is possible to see that the firms have adopted particular approaches that suit their work flow and design views, as a way to wrap their heads around circularity themes, aiming to stay ahead of regulations on the matter that they know will come sooner rather than later. This issue will be expanded upon in section 4.2.

After circularity, energy appears as a major issue, although it is the authors' opinion that the fact that energy appears second might be explained by the early internalisation of energy requirements in their daily practice. Thus, it seems to be taken for granted, skewing the number of mentions and making it seem like it is a secondary issue (although the number of mentions correctly reflect the fact that right now, circularity seems to be the major issue that Dutch architects are trying to wrap their heads around). This statement is backed by the tone of some responses when stating that "obviously, one aspect is the technical one. If you have to make an energy neutral building there will be a lot of let's say limitation or demands on the façade", or "it starts always with insulation and sun and all of that, in order to try and make sure it (the building) performs energetically as well as we can".

One of the major concerns declared in relation to energy aspects, refers to the impact stringent regulations have on the final design, mostly regarding daylight availability and the decrease of transparency in buildings. Thus, some interviewees stated as a relevant issue in their daily practice, to find the balance between energy performance and daylight access when it comes to defining window-to-wall ratios and window position in their façade projects. Moreover, some interviewees expressed concern about the impact that increasing temperatures will have on Dutch buildings, which is not considered in current regulations and building guidelines ("there is a sort of strange contradiction between the fact that we insulate like hell and the climate is becoming warmer"). Another relevant concern expressed within this theme was related to energy generation and its role in energy neutral buildings. It was explicitly stated by some interviewees that the need for energy neutrality in the built environment will make the integration of PV panels in façades more common over time, due to the lack of roof space, which will bring completely different aesthetics. While some interviewees merely referred to PV integration in buildings (BIPV) as a fact that architects will have to increasingly deal with, others took a strong stand against the need for building integration, arguing "why should architecture be defined by PV panels?! Come on! We should find another way and take it away from the buildings. What do we do with all this technical stuff in about 10-20 years?"

The user and nature groups, while less mentioned, are regarded as emerging themes. About a third of the sample mentioned at least one user-related aspect, and several aspects were distinguished within the group, which shows the multiple facets of an issue that is nowadays getting increasing attention. Similarly, the application of nature-based solutions in the built environment has been heavily promoted by the European Union in the last years, being defined as "solutions that are inspired and supported by nature, which are cost-effective, simultaneously provide environmental, social and economic benefits and help build resilience. Such solutions bring more, and more diverse, nature and natural features and processes into cities, landscapes and seascapes, through locally adapted, resource-efficient and systemic interventions" (European Commission, 2015). When it comes to the building façade, nature-based solutions mostly refer to green façades or living walls, as the responses showed; however other strategies for nature inclusion are also attracting attention, evidenced by the integration of "bee hotels" and nesting zones in projects declared by the interviewees. The fact that about a fourth of the sample mentioned these aspects is regarded as a promising sign of their ongoing application, which is expected to increase in the coming years based on their active promotion.

Lastly, value related aspects were mentioned as the most practical impact derived from the application of sustainable measures, evidenced by statements referring to the return of initial investments (“budget versus how much money the building can generate once it’s finished”), or maintenance costs associated to complex measures (“we had a complex double façade with solar shades in between, ventilation and openable windows... the maintenance costs were constantly a discussion”). Nonetheless, while budget issues are of course central for the implementation of sustainable measures, the same interviewees that declared this also stated that they have seen an ongoing change on the clients’ wishes and willingness to implement sustainable measures, which greatly facilitates the process.

4.2 RELATION BETWEEN THEMES/ASPECTS AND IDENTIFICATION OF TRENDS

Sustainability is a multi-variable concept, which tackles multiple areas of knowledge and practical applications. Thus, the responses of the interviewees usually considered mentions of multiple aspects, touching upon more than one of the previously discussed themes. The average number of identified mentions per interviewee was 4.8; divided across 2.4 themes in average. Because of that, these cross-mentions were explored as a second part of the assessment, aiming to show the interviewees’ understanding of sustainability in façade design, not only considering isolated mentions of certain aspects but also potential relations between them.

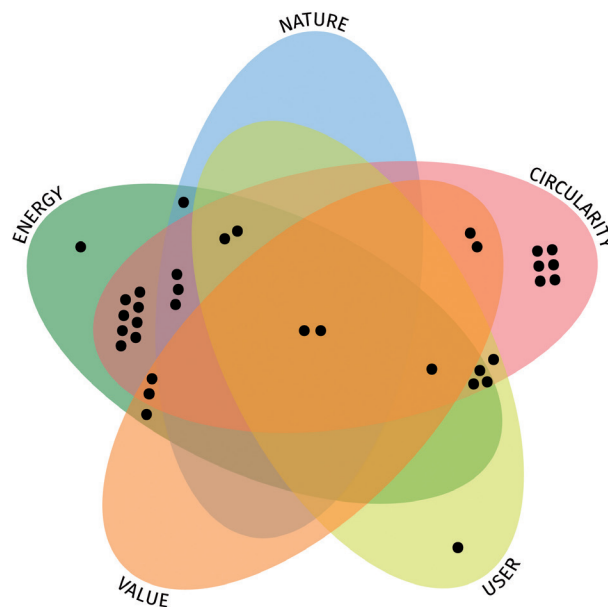


FIG. 5 Position of the interviewees’ responses based on the themes they tackled

Figure 5 shows a 5-way Venn graph showing all responses in relation to the themes they tackled (using the online tool developed by Bardou et al., 2014). So, each dot represents a different interviewee, and its position shows which themes shape their understanding of sustainability. As discussed earlier in the text, circularity aspects were mentioned by 88% of the sample, while energy aspects were mentioned by 71%. Moreover, interviewees that mention aspects contained in either one or both of them add up to almost the total sample (97%); cementing their position as the themes most commonly associated to sustainability when it comes to façade design. Only one interviewee did not explicitly mention any aspect within those themes, placing the focus on users’ behaviour and their interaction with the building envelope in order to control or at least modify their

comfort. Nonetheless, this posture does not negate the relevance of the aforementioned themes, but simply chooses to actively place the focus somewhere else (the user).

As another layer in the assessment of the responses, an effort was made to identify trends based on potentially distinguishable relations between groups of aspects, that would allow to identify different approaches to the topic of sustainability; and then compare these trends against basic characteristics of the surveyed sample, in an attempt to check for the existence of potential designers' profiles when it comes to following these approaches. This, of course, as an exploratory exercise constrained within the boundaries of the sample size considered in the study.

Given the multi-variable nature of the overall concept of sustainability, in general there were no discernible patterns or trends. Nonetheless, two clashing approaches were distinguished when it comes to circularity: (a) permanence; and (b) design for disassembly. Figure 6 shows a 4-way Venn diagram depicting the relations between these aspects from the interviewees' responses; where it is possible to see on the one hand that mentions of permanence and material durability are highly correlated; while on the other hand, fairly distinct from the first group, there is also some correlation between mentions of assembly and material usage.

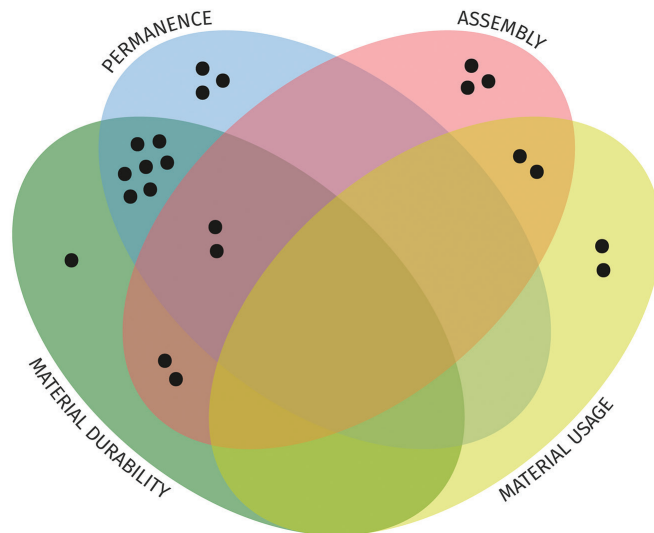


FIG. 6 Interviewees' responses related to selected aspects within the circularity theme

A more detailed overview of the responses effectively shows that designers who declared permanence as one of the aspects related to sustainability, also mentioned to strive for timeless buildings; besides a predilection for the use of "real" materials such as natural stone or concrete, over steel or aluminium, based on how well the former sustain the passage of time. Therefore, in these cases, the design of the envelope follows massiveness as a guide, with façade detailing focused on improving the durability and aesthetics of the building surfaces over time. The reasoning behind this approach entails that long-lasting buildings make a more efficient use of the material and energy resources embedded into their design and construction, aiming to keep these on-site by prolonging the operation phase for as long as possible (Foster, 2020). Consequently, besides massiveness and the use of materials that do not require major maintenance; a key aspect in the design of façades within this approach is an embedded flexibility and resilience, that allows the façade – and the building behind it – to accommodate to changes that will occur along its lifetime.

On the other hand, reviewing the responses that contain mentions of façade design as an assembly of components, it is possible to see assembly-related aspects along concerns for the recycling and reuse of such components and materials. Moreover, the responses also referred to the need to use less raw materials; which of course circles back to the reuse of already processed building materials and components, but also entails the design of slender structures and lightweight façades, where material usage has been optimised for their particular performance. If the first approach was based on permanence and usage flexibility to achieve a 'never-ending building'; thinking of buildings in terms of assemblies focuses instead on their components' lifecycle, under the assumption that buildings do not need to last forever, but their parts and components need to be designed to allow for their reuse in other buildings under a smart output approach (Heesbeen & Prieto, 2020). Consequently, a key aspect in this is the design of the interfaces between components, based on dry connections and mono-material components, striving for total disassembly and material recovery.

When comparing the mention of these approaches against other responses from the interviewees, no clear correlations were found. This means that the predilection for either approach does not seem to follow any discernible pattern that could help defining designers' profiles. This holds true when comparing the responses against basic sample descriptors such as their declared years of experience, the size of the firms they represented, or their particular expertise in either newly built projects or renovations; and also other responses from the questionnaire such as their understanding of the main role of façades, the role of façade design within their building design work flow, or aesthetic preferences when it comes to façades. The only exception to this, would be a faint relation encountered between the mention of these approaches and the declared main experience of the interviewees in terms of either residential or non-residential projects. Hence, it was found that designers who mentioned permanence and durability as aspects related to sustainability, tended to be the ones who declared to have more experience with residential projects; while the mentions for assembly were almost equally divided among the ones who declared to have mostly worked in residential and non-residential projects, slightly favouring the latter (Fig.7). This fact seems to make sense, considering the different nature of both types of projects (arguably, housing is generally meant to last and blend with the urban layout; while the usually iconic aspect of non-residential buildings means that they are subjected to more changes during their lifetime); nevertheless, although this fact is worth mentioning within the exploratory aims of the study, further research activities with a larger sample are needed in order to test and fully corroborate this finding.

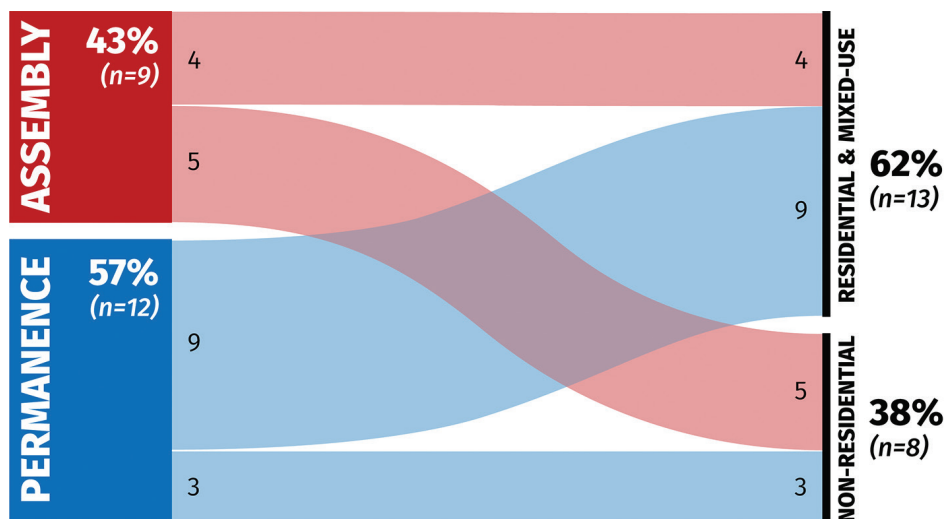


FIG. 7 Relation between mentions of the identified approaches and the main experience of the interviewees

5 CONCLUSIONS

The paper aimed to explore the role and the impact that sustainability has in façade design, through the analysis of gathered responses from several interviews with experienced architects, from 34 architectural firms based in The Netherlands. Based on the responses, it was possible to identify several aspects that have an impact on the design process, which were categorised in 5 distinct themes: energy, circularity, user, nature and value. Energy and circularity themes clustered most aspects, and received the highest amount of total mentions. As an isolated aspect, the integration of passive design strategies was singled out to be the most mentioned; while the highest total mentions of the circularity theme are regarded as evidence of the current interest around these issues in architectural design.

The fact that the interviewees mentioned multiple aspects across different themes within their responses; perfectly shows the multi-variable nature behind the concept of sustainability, tackling multiple challenges that respond to diverse areas of knowledge and practical applications. It is this multitude of aspects, that need to be considered at once, which makes the application of sustainable measures a complex matter. The interviewees acknowledged the fact that more information and tools for a comprehensive evaluation of these measures are needed, to assist them throughout the design process. Also, particularly in the case of circularity, it was possible to identify certain approaches that architects have adopted to navigate through these issues, aiming to incorporate them in their daily practice.

Therefore, when it comes to circular design, it was found that some believe in permanence and timeless buildings, which leads to massive structures and detailing focused on ageing and durability; while for others it mainly revolves around using less raw materials and the reuse/recycling potential of building components; which leads to light structures, with focus on connections aiming for total disassembly and material recovery. The identification of such strategies helps gathering a set of potential responses, which should of course follow the particularities of each case. Thus, it would be wrong to declare one strategy as generally better than the other; instead, they should be seen as possible approaches, whose suitability will be assessed after a careful consideration of the context and brief. This of course, circles back to the need for tools for the assessment of these or other approaches in terms of their response to a given set of requirements.

The exploration of the façade design process and the new challenges that sustainability brings to it, directly from the practitioners' experience; is regarded as a key issue to promote further application of sustainable measures in the built environment under a grounded discussion that includes both theory and practice. Hopefully the identification of diverse strategies and approaches, along with similarities and differences across various points of view; will help designing a common vocabulary for the understanding of sustainability in façade design, which enhances synergies between the different stakeholders responsible for the design and construction of a sustainable future.

Acknowledgement

This paper is part of the project PrettyFace – Exploration of aesthetics in façade design, aimed at exploring the façade design processes and aesthetic preferences of architectural designers, to gather insights from their practical experience. The project was funded by The Dutch Research Council (NWO) through their programme Creative Industry - Knowledge Innovation Mapping (KIEM), under the dossier number KI.18.037. The consortium behind the project comprises Delft University of Technology, KAAN Architecten, BARCODE Architects, Thijs Asselbergs architectuurcentrale and ArchDaily.

The authors wish to acknowledge the architectural firms that took part in the study (in alphabetical order): Architecten van Mourik, Arconiko, Thijs Asselbergs architectuurcentrale, Atelier Kempe Thill, BARCODE Architects, Benthem Crouwel Architects, Braaksma & Roos Architecten, Cepezed architectenbureau, De Nijl Architecten, Dok Architecten, DUS Architects, Ector Hoogstad Architecten, Gaaga, Gortemaker Algra Feenstra, Heren5 Architects, Hulshof Architects, KAAN Architecten, KCAP Architects&Planners, Kraaijvanger Architects, MECANOO, mei architects and planners, Moedersheim Moonen Architects, Mollink Soeters PPHP,

MVRDV, MVSA Architects, NEXT Architects, ORANGE Architects, OZ Architects, Paul de Ruiter Architects, Team V Architectuur, UN Studio, V8 Architects, VanSchagen Architecten, and WDJ Architecten.

References

- Bardou, P., Mariette, J., Escudié, F., Djemiel, C., & Klopp, C. (2014). jvenn: an interactive Venn diagram viewer. *BMC Bioinformatics*, 15:293 doi:10.1186/1471-2105-15-293
- European Commission (2015). Towards an EU Research and Innovation policy agenda for Nature-Based Solutions & Re-Naturing Cities. Final Report of the Horizon 2020 Expert Group on 'Nature-Based Solutions and Re-Naturing Cities'. Directorate-General for Research and Innovation - Climate Action, Environment, Resource Efficiency and Raw Materials.
- Foster, G. (2020). Circular economy strategies for adaptive reuse of cultural heritage buildings to reduce environmental impacts. *Resources, Conservation and Recycling*, 152. doi:10.1016/j.resconrec.2019.104507
- Heesbeen, C., & Prieto, A. (2020). Archetypical CBMs in Construction and a Translation to Industrialized Manufacture. *Sustainability*, 12(4). doi:10.3390/su12041572
- Loonen, R.C.G.M., Rico-Martinez, J.M., Favoino, F., Brzezicki, M., Menezes, C., La Ferla, G., & Aelenei, L. (2015). Design for façade adaptability – Towards a unified and systematic characterization. *Proceedings of the 10th Conference on Advanced Building Skins*, Bern, Switzerland, pp.1284-1294
- Perini, K., Ottelé, M., Haas, E.M., Raiteri, R. (2011). Greening the building envelope, façade greening and living wall systems. UNEP - Global Alliance for Buildings and Construction, International Energy Agency and the United Nations Environment Programme (2019): 2019 global status report for buildings and construction: Towards a zero-emission, efficient and resilient buildings and construction sector

Fibrous Interfaces for Indoor Temperature Modulation Based on Phase Change Materials

Iva Rešetar¹, Christiane Sauer²

- 1 Humboldt-Universität zu Berlin, Cluster of Excellence 'Matters of Activity, Image Space Material', Unter den Linden 6, 10099 Berlin, +49 30 209366140, iva.resetar@hu-berlin.de
- 2 Kunsthochschule Berlin Weißensee, Cluster of Excellence 'Matters of Activity, Image Space Material', Bühringstraße 20, 13086 Berlin, +49 30 47705281, sauer@kh-berlin.de

Abstract

This paper investigates strategies for passive indoor cooling with novel fibrous structures based on Phase Change Materials (PCMs). The project approaches PCMs from a design perspective and introduces local temperature modulation into an interior space by using exposed, mobile, and changeable structures that can be installed and adapted by users. The aim of the research is to develop design concepts and production processes for integrating PCMs into various interior interfaces - façade screens, spatial dividers and ceiling elements. We present three case studies with novel PCM elements focusing on their exposure in the interior space and embedding the logic of material assembly and disassembly into the design. These interventions are particularly suitable for retrofitting buildings to address critical thermal loads and different programmatic scenarios. More broadly, they extend the concept of static building elements towards material-based cooling devices that allow greater flexibility in use and remain adaptable throughout their lifespan.

Keywords

Phase change materials, passive cooling, retrofitting, fibrous systems, adaptive use, textile technology

1 INTRODUCTION

Growing demand for cooling of buildings requires rethinking of technologies for climate control as one of the main sources of energy consumption in buildings. In efforts to transform building energy practices, current approaches are oriented towards passive cooling and retrofitting measures to prevent overheating and improve the performance of existing buildings (Directive 2010/31/EU of the European Parliament and of the Council on the Energy Performance of Buildings, 2010). Passive cooling with phase-change materials (PCMs) has been widely investigated over the last decades as a promising method for material-based thermal regulation and has proven effective in reducing dependence on air-conditioning and improving thermal comfort (Kośny, 2015).

The integration of PCMs into building elements brings with it the challenge of resolving multiple, often conflicting performance requirements within standardized, built-in components. Building applications with PCMs have thus been largely driven by integration techniques leading to developments in the field of composite materials, often involving difficulties in monitoring, replacing, and recycling of these systems. This paper discusses an approach to PCM structures that allows greater flexibility in use and a way of integrating PCMs that makes adaptation, disassembly, material separation, and reuse possible.

1.1 STATE OF THE ART

PCMs are materials capable of storing, absorbing and releasing energy in the form of latent heat during melting and solidification at a certain, predictable temperature, which makes them suitable for managing thermal environments in architecture. Although early precedents in the built environment can be found in vernacular igloo architecture, the first application of latent heat thermal energy storage as a technology for achieving thermal comfort in buildings was documented in the Dover Sun House in 1948 (Kośny, 2015). The applications of PCMs in buildings have since been the subject of extensive research, and more recently, many studies have provided an overview of PCM classification and properties, encapsulation methods, performance factors and applications (Mavrigiannaki & Ampatzi, 2016). A variety of components that have been investigated for building applications mostly relate to the context of building technology and are rarely design-oriented.

The range of currently available PCM-based building elements includes micro-encapsulated PCMs integrated to conventional building materials, such as gypsum, plaster or concrete, or macro-encapsulated PCMs in the form of pouches, capsule strips or panels located in building cavities, e.g. behind walls or suspended ceilings (de Gracia & Cabeza, 2015). These solutions increase the heat storage capacity of lightweight structures and operate passively or in combination with automated active systems for forced ventilation and removal of the absorbed heat from PCMs (VDI, 2016). Crucial for the passive performance of PCM elements is that they are exposed to night ventilation and placed in zones with the highest heat input and temperature fluctuations, such as the façade. While some notable examples in the field of responsive building elements have highlighted this potential (GLASSX AG; Perino & Serra, 2015; Weinlaeder et al., 2011), visible elements that can be installed or adapted by building occupants are still under-represented. Our study addresses this aspect in the design of novel PCM macro-encapsulations to enable their exposure in the indoor space as well as their placement close to the façade and, importantly, within the sight and reach of the user.

Among the strategies for functional integration of PCMs outside the building industry, advances have been made in the field of technical textiles for climate regulation. PCMs have been embedded in textiles at the fibre level or through micro-capsules in non-woven fabrics developed for the clothing industry and other close-to-body applications. Existing functional textiles, therefore, face similar difficulties as other PCM composites in separating and recycling the small and bound component

materials. As they are tailored for small-scale use, their heat storage capacity would not be sufficient for building scale (e.g. products like Outlast®, schoeller®-PCM™). However, they offer an interesting possibility of flexible, dynamic and local temperature compensation in close correlation to the human scale, which we propose to transfer to the building context in this paper.

Rethinking PCMs in buildings from the perspective of textiles can introduce a different logic of temperature modulation into interior space by using exposed, mobile and interchangeable structures that can be installed and adapted by users to meet different programmatic scenarios. Despite the existing range of solutions for PCM-enhanced textiles, the processes of scaling textile logic in an architectural context require a specific approach to create customized PCM elements. Starting from the fibre as a basic lightweight element with the potential for multi-scale PCM integration, our study translates fibrous systems to the building scale, placing the criteria of circularity and dismantlability at the centre of investigations.

2 METHODOLOGY

Practice-based design research involving experimental prototyping is a basis for this project. The design potential of PCM elements is explored through three case studies that use novel design and production methods to upscale fibrous structures into tangible and adaptable interfaces in an architectural context. The experiments investigate the integration of PCMs into various fibre-shaped elements using manufacturing processes such as textile or glass making to create larger interior structures.

The case studies draw on the understanding of the integrative possibilities of fibrous structures on different scales: linear elements filled with PCMs are interconnected to form larger material systems with adaptable configurations. Fibres as elongated structural elements are not only found in natural systems to provide specific functions in plants, muscles or in various vascular tissues, but also in engineered environments. Reinforcement by linear tensioned elements like steel rods or carbon fibres is common in architecture – as are tubular structures for storing and transporting media for cooling or heating. In exploring tubular structures as material-based cooling devices, both the design and technological aspects are considered in the case studies.

Three experimental settings were explored for the implementation of thermally responsive elements in the interior space: (1) flexible PCM tubing – Strands, up-scaled into a surface, (2) rigid linear PCM tubing – Bars, connected by flexible binding, and (3) rigid glass PCM tubing – Dendrites with branching configuration. Strands and Bars were worked into flexible surfaces using textile manufacturing technologies and were investigated qualitatively. Key design and production parameters, a phase-change transition of PCM elements – from opaque, translucent to transparent, as well as the texture, density and haptics of the structures are documented in the studies. The dendritic structures were produced in glass using the lamp-working technique and were taken to the further test phase in the experimental set-up for thermal analysis. An overview of experimental settings with all material components and processes is shown in Table 1.

CASE STUDY	PROTO-TYPE	PCM PROD-UCT	PCM MELTING TEMPERATURE	ENCAP-SULATION MATERIAL	PRODUCTION TECHNIQUE	TYPE OF APPLICA-TION	EFFECT/TYPE OF ANALYSIS
1	Strands	Bound granular	26-28 °C	PE non-woven textile, PE foil, PES monofilament	Kemafil® technology	Vertical screen	Cooling, shading, dividing / qualitative analysis

>>>

2	Bars	Paraffinic	27-29 °C	Acrylic tube	Coarse warp-knitting	Vertical screen	Cooling, shading, dividing / qualitative analysis
3	Dendrites	Bio-based	24 °C	Glass tube	Lamp-working	Ceiling	Cooling / quantitative analysis

TABLE 1 Overview of experimental settings

With the aim to improve the cooling effect of PCMs, various material-specific strategies have been pursued in design and production to maximize the exposure of PCMs to the surroundings and positively affect the heat exchange and the indoor temperature reduction. Compared to built-in surface components like PCM-enhanced boards, panels or pouches, tubular containments have a better surface-to-volume ratio and the potential to improve convective heat transfer through their indoor exposure, geometry and spacing. Following the guidelines on the effective thickness of PCM, which supports full melting and solidification (VDI, 2016), the design decision was made to dimension the tubular elements to a diameter of 20 mm and to create configurations that allow natural air circulation around the containments and good contact of the material with the surrounding air.

3 EXPERIMENT / RESEARCH - CASE STUDIES

The design potential of fibre shaped PCM elements for passive cooling is investigated on examples of tangible, lightweight structures that reduce temperature peaks in indoor spaces. In three case studies, we develop design strategies and processes for integrating PCMs into different interior interfaces - façade screens, spatial dividers and ceiling elements. A common element in all case studies is PCM tubing – an up-scaled “fibre” that builds different configurations of PCM strands, bars and dendrites. These “soft” interventions are particularly suitable for retrofitting buildings to address critical thermal loads and different scenarios of use, as the elements can be easily installed, handled and adapted on-site, in the occupancy phase and according to the specific cooling demand.

3.1 PCM STRANDS

Since window areas and large glass surfaces in particular provide additional heat input into buildings, temperature-modulating screens in the interior can be a suitable measure in addition to the external sun protection. To create thermally effective “curtains”, PCMs were filled into tubular structures, which were further processed with textile technology: Kemafil® and coarse warp knitting. The Kemafil® technology is used in the field of technical textiles for the sheathing of longitudinally oriented, strand-shaped loose core materials - mainly for the production of rope and strand-like structures. Coarse warp knitting allows for the integration of flexible or even stiff linear elements with a diameter of up to 30 mm. The resulting curtain-like textile screens can be used in front of windows or freely suspended as room divisions. These flexible PCM elements store heat during the day and release it back into the environment with a time delay when cooled down at night. Compared to existing PCM-coated fibres, which are commonly used to produce functional textiles, a significant increase in effectiveness can be expected due to the greater amount of active material incorporated.

The first case study deals with façade elements and spatial dividers produced with oversized PCM yarns. The volume of the incorporated PCM determines the degree of effectiveness of the overall surface. Using approximately 20 mm thick PCM-filled yarns enables a relatively large, effective mass of material to be introduced into a room. PCMs require a dense casing in which the liquid or granular material can be contained. This should not be absorbent, otherwise, the PCM would “wander” into the

envelope. A transparent polyethylene (PE) plastic tubular film (material thickness 0.15 mm, width 30 mm) was chosen for creating the flexible yarn filled with granular PCM that acts as a dry PCM system. The PCM changes between solid and soft inside of its granular structure. Initially, braided textile tubes were also examined as wrapping material, but these were discarded because of the risk of the granulate “trickling through”.



FIG. 8 PCM Strands close-up with Kemafil® casing (left); Yarn processing on coarse warp knitting machine (right) © Christiane Sauer

After initial tests on the machine, the PE tube formed kinks in the radii in an uncontrollable manner and led to an unsatisfactory overall appearance. This problem was significantly improved by additionally covering the hose with a fine fleece and a transparent filament in the Kemafil® process (Fig 1). The additional wrapping and binding made the hose more flexible and evenly bendable. The aesthetics of the surface also improved decisively. Technically, haptically and optically, the textile-coated hose with granular PCM represented a very promising first result (Fig. 2).

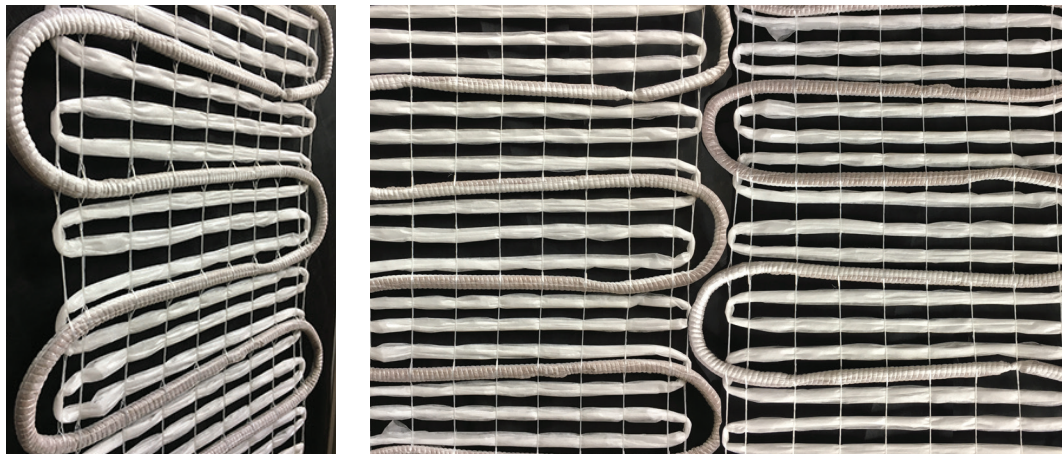


FIG. 9 An experimental PCM Strand prototype processed into a flexible textile surface © Christiane Sauer

3.2 PCM BARS

Based on the same type of application as the previous experiment, the second case study implements transparent bars filled with pure PCM connected into the construction of a coarse warp knitted fabric. Acrylic glass tubes with a length of 700 mm, a diameter of 20 mm and a wall thickness of 2 mm were chosen as containers for the material. After filling, these were tightly closed with conical cork

connectors. As in the previous example, the 20 mm diameter allows integration of relevant quantities of PCM, while at the same time enabling complete melting and solidification.

To find a technically and visually suitable variation for this PCM surface, the spacing of the bars was first tested with empty tubes. This was done in increasing steps of placing them at one additional warp stitch each time. The tubes, which were connected by a fine filament, represent a filigree solution with an appealing design (Fig. 3). When being processed with the warp knitting machine, the empty acrylic glass tubes posed a technical challenge because the rollers, which keep the material under tension in the process, exert great pressure on the working piece. During the first tests, the tubes were destroyed by this pressure. The rollers were therefore loosened in further tests, and the necessary tension had to be applied by manual tensioning.

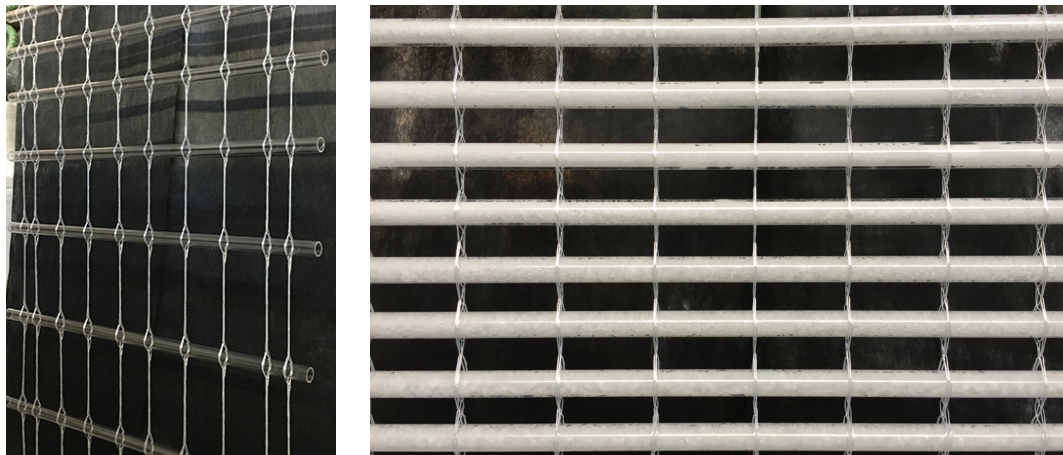


FIG. 10 PCM Bars - rigid tubing interconnected into a flexible structure by warp-knitted binding with testing various bar spacings (left) and a regular 7,5 cm vertical grid spacing with filled-in PCM (right) © Christiane Sauer

In the next step, the tubes were filled with the PCM and integrated into the surface. The waxy, pure PCM is delivered in solid state in canisters. For processing, it must first be heated so that it can be decanted in a liquid/viscous state. The resulting elements are transparent when exposed to sunlight and become milky translucent when the temperature drops at night. The waxy state provides visual protection at night, while the liquid state allows transparency without obstructing the view and natural light during the day. The visible phase change between liquid and solid is a feature that makes the climatic function of PCM an active element in the space (Fig. 5). The advantage of the PCM bar construction is that, depending on the climatic room requirements, the number of tubes can be selected from widely spaced to a closed surface in order to adjust to desired technical parameters and the amount of material.

3.3 PCM DENDRITES

The third case study, situated between practice-based design research and engineering, explores a cooling ceiling system with novel, bio-based PCMs. Taking a design approach to a cooling technology with PCMs, the study combined the design possibilities offered by digital technologies with a production technique of glass making. Large-scale test cells were built for this experiment to install and analyse customized glass containments on an architectural scale. The methodological framework included the digital design of macro-encapsulations, their manufacturing in glass and thermal cycling in test cells to determine their cooling effect. The design focused on the three-dimensional dendritic geometry of encapsulations as a strategy to increase the exchange surface between PCMs and the surrounding air and to improve the cooling capacity of PCMs. The project

builds on previous studies of tubular and dendritic structures with a large surface area that were experimentally and numerically tested on a smaller scale and proved to be a suitable concept for passive in-door cooling (Rešetar & Palz, 2018, Rešetar et al., 2021).

Dendritic typologies can be described as branching structures found in various natural systems and processes such as growth and crystal solidification, whose geometry evolves and self-organizes under a defined set of constraints, often forming efficient transport and exchange networks. The branching structures with interconnected linear elements have been studied for solving various problems of heat exchange in thermal engineering applications (Bejan, 2000). Drawing on the principles of these structures, the dendritic encapsulations in this experiment were digitally designed in Rhinoceros and Grasshopper around the logic of shortest paths and the large exchange surface area. Design criteria included: a) fitting the structure into the available space underneath the ceiling in the test cell to correspond to the window openings and night ventilation flows; b) adequate thickness of tubular elements that ensures structural robustness, as well as full melting and solidification of PCMs; c) branching angle of elements close to the horizontal for more uniform melting and solidification; d) material is placed into a configuration that allows for air circulation and natural convection; e) consideration of constraints from the glass production in terms of complexity and size of elements.

The modules were crafted by a lamp-working technique in borosilicate glass, which is commonly used for the manufacturing of laboratory equipment. Following the conclusions of previous experiments and recommendations on the thickness of PCM elements (VDI, 2016), the chosen standard glass tube had a diameter of 20 mm, with a wall thickness of 1,8 mm. The amount of material for filling the prototypes was calculated in the digital model, based on the amounts reported in PCM ceiling studies and maximized to fit the available space. The prototypes occupied a space 300 mm beneath the ceiling construction in the proximity and the “extension” of the window opening, thus taking full advantage of the night ventilation.

PROPERTY	VALUES
Melting temperature	24 °C
Crystallization temperature	21 °C
Latent heat	183 kJ/kg
Specific heat capacity solid / liquid	2.4 / 1.7 kJ/(kg K)
Thermal conductivity solid / liquid	0.29 / 0.16 W/(m K)
Density solid / liquid	949 / 842 kg/m ³

TABLE 2 Physical properties of bio-based PCM.

The eight dendritic elements occupied the central part of the ceiling and were able to store approx. 4.5 kg/m² of room area of PCM. According to the guidelines for calculating PCM mass (VDI, 2016), with a total melting enthalpy of the bio-based PCM in the effective temperature range (52.5 Wh/kg) and a high projected thermal load per room area, the amount of PCMs was less than required but proved effective in the measurements with a halogen lamp of 750W as a heat source over a six-hour heating cycle.

Important criteria for the choice of the PCM for indoor temperature regulation is that the melting range of the PCMs corresponds to the daily temperature fluctuations that allow the material to melt and solidify. In this case, the selected PCM had a melting temperature of 24 °C, with the physical properties given in Table 2.



FIG. 11 Experimental set-up for thermal cycling of dendritic prototypes showing twin test cells (left), placement of measurement probes (middle) and dendritic structure (right)

In the experimental set-up of test cells, which was developed for thermal cycling, the material system was exposed to thermal excitation and natural ventilation overnight (Fig. 4). Two identical, neighbouring test cells (1.45 x 3.10 x 3.06 m) were built using lightweight wood construction with an 80 mm thick insulation infill and a 6 mm thick removable acrylic glass front. The ambient temperature of the room at the beginning of the measurements was approx. 19 °C and, after six hours of heating, the heaters were switched off, and the test cells were left to cool down to reach 19 °C again in the morning after a period of natural night ventilation. Although various scenarios have been tested, the experimental results presented in this paper refer to the heat source of halogen lamps of 750 W placed one in each cell. The measurement probes Pt-100 were capturing ambient temperature in both test cells and in the room, as well as the temperature of PCMs in a one-minute interval.

4 RESULTS

4.1 PCM STRANDS / BARS FOR TEXTILE SCREENS

Textiles screens are lightweight, flexible structures, which can be customized “off the roll” to any desired length and geometry, and are easy to transport, store and install. The described climate devices based on PCM Strands and Bars create a moveable thermal boundary in the space that can be positioned, slid aside or removed like a curtain. The elements can thus be adapted for changes in use, as well as for technical or individual preferences.

Presented experiments were carried out as a design study of up-scaling textile elements and production techniques to architectural scale. The flexible PCM Strands were produced using Kemafil® technology. The Bars were made on the coarse warp-knitting machine, with the weft of acrylic glass tubes held by the stitches during the production process and the warp knit forming the vertical stitches at a modular spacing of 40 mm in the stretched state. The possibilities for customizing these adaptive building components were explored through different layouts and spacing patterns.

Both tubing systems had a diameter of 20 mm, which is recommended as the effective thickness in guidelines for PCM storage systems in buildings (VDI, 2016). The elongated shape of PCM elements maximized the surface exposure and thus heat exchange. The performance can be further programmed through textile technology by densifying the pattern and applying more material to the given surface area. Depending on the cooling requirements and size of the room, the arrangement and spacing of the Strands and Bars can be altered while maintaining the view to the outside or to an adjacent space.

In the case of the PCM Strands, the improvement in flexibility would result in smaller edge turning radii of the weft and, therefore, a denser configuration. This allowed for a higher total length of PCM strands per unit and, therefore, more active material to be implemented in a given surface area. The bulk density of the PCM granulate of 0.8 kg/litre results in approx. 0.25 kg of granular PCM per meter of strand. The approx. 700 mm wide textile screen demonstrator (Fig. 2) therefore contains a total of 1.25 kg of granular PCM per meter with the current spacing, which can be densified by adjusting the textile pattern.

In the PCM Bars prototype, the number of elements can simply be added into the available vertical warp stitches. A maximum number of bars would result in a closed but soft surface with a bar implemented in every warp stitch that acts as a flexible joint. The acrylic tubes with an outer diameter of 20 mm and an inner diameter of 16mm can hold approx. 0.215 kg of PCM per meter. Thus, a 700 mm wide and 1000 mm long screen surface can contain a total of approx. 7.5 kg of PCM if bars are inserted densely in every stitch row. The surface area of such a screen is 2.2 m², whereas a comparable flat board surface would be only 1.4 m². The surface area of a tubular screen significantly enhances the contact surface between PCM and surrounding air in comparison to the conventional panel geometry. In the demonstrator shown in Fig. 5, bars are inserted in every second row. This screen holds approx. 3.75 kg of PCM per meter while still providing good visual transparency and high flexibility.

The phase transition from solid to liquid of the PCM is perceived as a fascinating process of thermal adaptation. This visible technology can be implemented both in living and working areas. The principle is also applicable to large glass façade areas, which can be easily retrofitted with sliding PCM screens. As textile screens, these interfaces can improve the indoor climate and reduce the operation of existing cooling technology, therefore lowering the energy consumption of existing buildings.

Due to the short project duration, the focus was on the knowledge transfer between textile technology and architectural design and the experimental prototyping of PCM structures. Further investigations will include the analysis of the cooling performance of prototypes which will follow in the next research steps.

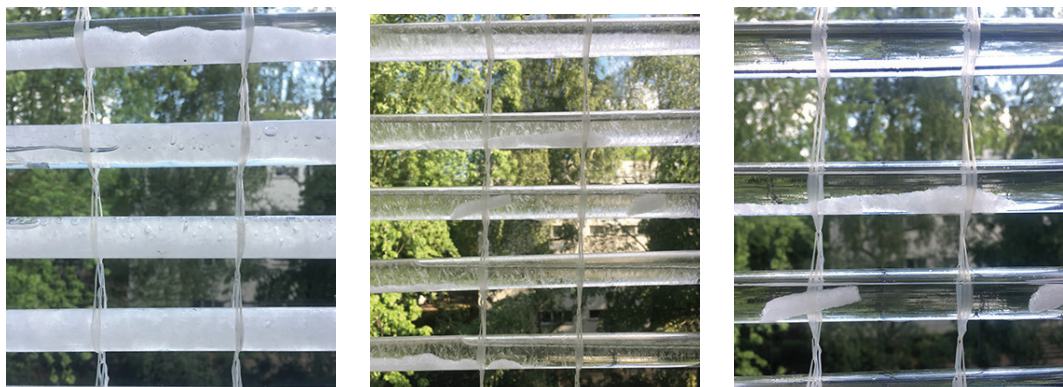


FIG. 12 Melting and solidification effect of PCM textile screens made from transparent tubular bars with textile warp knitted binding

4.2 PCM DENDRITES FOR CEILING ELEMENTS

The experiment showed that the cooling ceiling with dendritic encapsulations can contribute to temperature reduction in test cells in the periods of excessive heat. Starting from the ambient

temperature of approx. 19 °C, the temperature in the test cells rose to approx. 27 °C in the PCM test cell and to 29.5 °C in the reference cell (Fig. 6), leading to the temperature difference between test cells and a cooling effect of PCM ceiling of approx. 2.5 °C. The PCMs were able to melt completely during six hours of heating (Fig. 7) and solidify over-night with the help of night ventilation.

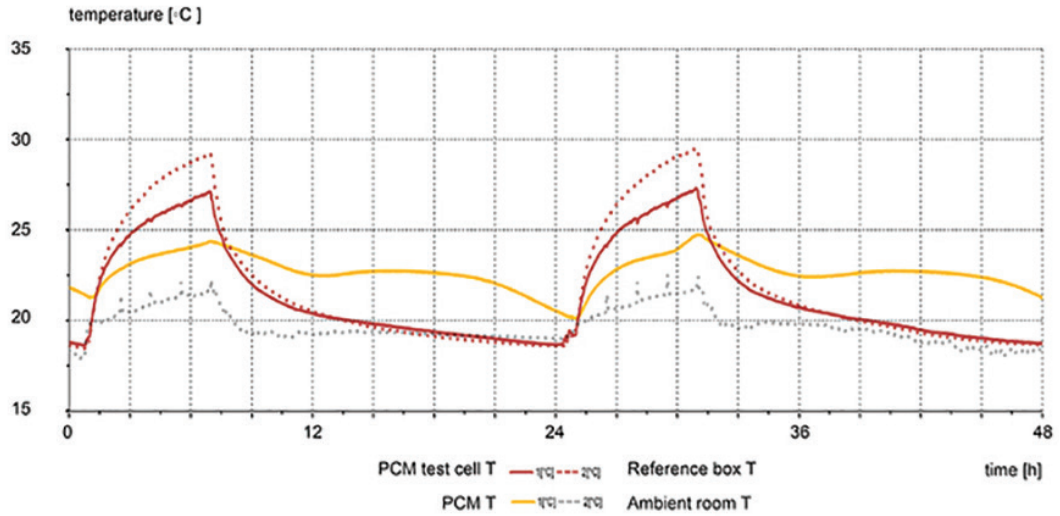


FIG. 13 Impact of PCM on indoor temperature reduction



FIG. 14 Melting process showing the PCM transition from opaque to transparent in dendritic structure

5 CONCLUSIONS

The design potential of PCM elements was explored in three case studies using novel design and production methods for up-scaling fibrous structures in an architectural context. Our experimental investigations combined practice-based design research and engineering, demonstrating PCM integration in examples of façade screens, spatial dividers and ceiling elements – all with thin, tubular elements with a large surface that enhance the thermal behaviour of PCMs.

The presented design strategies show an alternative mode of PCM implementation for retrofitting interiors of buildings. In the case studies, the design and technological considerations were addressed equally in order to achieve visibility and higher user acceptance of PCM elements. Rather than being concealed in layers of the building structure, passive cooling technology appears as a tangible element of the interior space. The component-based PCM structures were designed to adapt to changing needs during the occupancy of the building – one can add, maintain or remove the PCM elements, and customize the PCM quantity and the thermal performance by modifying the layout, spacing and clustering of the functional components.

With the idea of advancing an “analogue” and material character of environmental systems in architecture, the project offers a new perspective on PCM applications to engage occupants in adjusting the comfort levels of their thermal environment. This dynamic temperature modulation in close correlation to the human scale can extend the concept of static building elements towards material-based cooling devices that remain flexible in use throughout their lifespan.

The simplicity of the interventions is reflected in the logic of material assembly and disassembly embedded in the production process: the structures are created by filling granular or liquid PCM into tubular elements, which enables separation into the initial components after their life cycle. This is a major advantage over conventional built-in PCM components, where the materials are permanently integrated into the building structures and bonded together. All case studies showed novel, sustainable ways to combine PCMs with other materials while addressing critical aspects of circularity and dismantlability through design.

Finally, the experiments show that PCM-based temperature modulation can effectively reduce temperature peaks and provide an alternative to energy-intensive conditioning of buildings. The exposed PCM elements operate locally and in close relation to the climate to dynamically respond to the available thermal energy and accommodate daily temperature fluctuations. The design approach suggests a shift from current practices of climate control to thermally responsive elements that can invite an active engagement with the material and thermal environments.

Acknowledgements

The research on PCM Strands and Bars received support from Fritz und Trude Fortmann-Stiftung für Baukultur und Material. PCM Dendrites were developed at the Berlin University of the Arts as a part of a doctoral thesis under the supervision of Prof. Dr Palz. This project has received funding from the European Union’s Horizon 2020 research and innovation programme under the Marie Skłodowska-Curie grant agreement No. 642328. In the joint publication, authors acknowledge the support of the Cluster of Excellence “Matters of Activity, Image Space Material” funded by the Deutsche Forschungsgemeinschaft (DFG, German Research Foundation) under Germany’s Excellence Strategy – EXC 2025 – 390648296.

References

- Bejan, A. (2000). *Shape and structure, from engineering to nature*. Cambridge Univ. Press.
- de Gracia, A., & Cabeza, L. F. (2015). Phase change materials and thermal energy storage for buildings. *Energy and Buildings*, 103, pp. 414–419. <https://doi.org/10.1016/j.enbuild.2015.06.007>
- Directive 2010/31/EU of the European Parliament and of the Council on the energy performance of buildings. (2010). 23. GLASSX AG. Retrieved 19 June 2018, from <http://glassx.ch/index.php>
- Mavrigiannaki, A., & Ampatzi, E. (2016). Latent heat storage in building elements: A systematic review on properties and contextual performance factors. *Renewable and Sustainable Energy Reviews*, 60, pp. 852–866. <https://doi.org/10.1016/j.rser.2016.01.115>
- Košný, J. (2015). *PCM-enhanced building components: An application of phase change materials in building envelopes and internal structures*. Springer.
- Perino, M., & Serra, V. (2015). Switching from static to adaptable and dynamic building envelopes: A paradigm shift for the energy efficiency in buildings. *Journal of Façade Design and Engineering*, 3(2), pp. 143–163. <https://doi.org/10.3233/FDE-150039>
- Rešetar, I., Jurtz, N., Böhm, L., Kraume, M., & Palz, N. (2021). Integrated Framework for Digital Design and Thermal Analysis of PCM Macro-encapsulations for Passive Indoor Cooling. *Sustainable Cities and Society*, 66. <https://doi.org/10.1016/j.scs.2020.102536>
- Rešetar, I. and Palz, N. (2018). Passive Cooling with Phase Change Materials: Integrative Method for Design of Dendritic Encapsulation Prototype. *Proceedings of the 34th International Conference on Passive and Low Energy Architecture*, pp. 145-150.

VDI. (2016). VDI 2164, PCM energy storage systems in building services. Verein Deutscher Ingenieure.
Weinlaeder, H., Koerner, W., & Heidenfelder, M. (2011). Monitoring results of an interior sun protection system with integrated latent heat storage. *Energy and Buildings*, 43(9), pp. 2468–2475. <https://doi.org/10.1016/j.enbuild.2011.06.007>

Mono-Material Wood Wall: Digital Fabrication of Performative Wood Envelopes



Oliver Bucklin^{*1}, Prof. Achim Menges², Oliver Krieg³, Hans Drexler⁴, Angela Rohr⁵

* Corresponding author

1 Research Associate: University of Stuttgart Institute for Computational Design and Construction, Stuttgart, Germany. oliver.bucklin@icd.uni-stuttgart.de

2 Institute Director: University of Stuttgart Institute for Computational Design and Construction, Stuttgart, Germany.

3 Research Associate: University of Stuttgart Institute for Computational Design and Construction, Stuttgart, Germany.

4 Assistant Professor: Jade University of Applied Sciences: Department of Architecture, Oldenburg Germany.

5 Research Associate: Jade University of Applied Sciences: Department of Architecture, Oldenburg Germany

Abstract

The project seeks to create a building envelope that functions as structure, enclosure, and insulation, which is assembled from one solid timber construction element type. Wood has clear environmental benefits when compared to other standard construction materials such as steel and concrete, a good strength-to-weight ratio, relatively high thermal insulation, and low production costs. This research seeks to leverage these characteristics to simultaneously reduce the number of material layers in timber building envelopes while improving the building physics performance. Thus, the environmental impact of buildings can be reduced during planning, construction, operation, and disposal. The project proposes a system that reduces material layers and improves envelope performance by combining contemporary fabrication technologies with traditional woodworking techniques. Design tools should allow for compelling formal opportunities and facilitate fabrication and construction. The system manifests as a free-form, curvilinear log-cabin. Solid timber beams are used to minimise binders and fillers found in composite wood products, and the entire primary construction is achieved with pure wood joinery. CNC machining allows for the precise joining of members to achieve robust, easy-to-assemble, structural and airtight façades. By sawing deep slits into solid timber beams, the resulting air chambers improve thermal insulation values up to 30% compared to comparable solid wood assemblies while also relieving naturally occurring internal stresses. Computational design algorithms generate toolpaths and construction data directly from simple input curves, enabling direct coordination of architects, engineers, and contractors. To evaluate the system, multiple prototypes are fabricated to test constructability, thermal conductance, and airtightness, including a demonstrator building to test full-scale implementation. Laboratory tests and the successful completion of the IBA: Timber Prototype House demonstrates the potential for this renewable material to fulfil the requirements of contemporary building envelopes and opens the door for the development of all-wood multi-storey façades.

Keywords

Computational design, timber, digital fabrication, layer-reduced construction, wood, façade, envelope

DOI 10.7480/jfde.2021.1.5398

Exploring the Possibility of Using Bioreceptive Concrete in Building Façades



M. Veeger^{1*}, A. Prieto², M. Ottel ³

* Corresponding author

1 TU Delft, Faculty of Architecture and the Built Environment, Department of Architectural Engineering and Technology, maxveeger@hotmail.com

2 TU Delft, Faculty of Architecture and the Built Environment, Department of Architectural Engineering and Technology

3 TU Delft, Faculty of Civil Engineering and Geosciences, Department of Materials, Mechanics, Management & Design (3Md)

Abstract

Bioreceptive materials allow for biological content (biofilms) to grow on it, without necessarily affecting the material itself. If a bioreceptive concrete could therefore be integrated into a building façade, it could lead to green façades that do not need additional technical systems. As part of previous research by the authors, a promising bioreceptive concrete mixture was formulated. The aim of this research is to take this development, by using this previously developed mixture to create a bioreceptive concrete façade panel prototype, made using commonly available materials, that can direct where the biological growth takes place. The latter is done by combining the bioreceptive concrete with a non-bioreceptive (UHPC-based) one in the same panel, through a two-stage pouring process. A biofilm was developed on this prototype panel and results show that full coverage of the bioreceptive parts of the panel can be achieved within two weeks under optimal growing conditions and biological growth can be directed. However, exterior survivability is an issue for now. The concept of bioreceptive façades therefore shows promise, yet further investigation into improving exterior survivability is necessary, as well as further research into the underlying ecology, material, economics and climate effects is necessary.

Keywords

Bioreceptivity, biofilm, concrete, façade, panel

DOI 10.7480/jfde.2021.1.5527

State of the Art and Potentials of Additive Manufactured Earth (AME)

Elisabeth Endres¹, Jan Mehnert¹, Linda Hildebrand², Marcel Schweiker², Eike Roswag-Klinge³, Ulrich Knaack^{4, 5}

- 1 TU Braunschweig, Mühlenpfordtstr. 23, 38106 Braunschweig, +49 (531) 391 3555, e.endres@tu-braunschweig.de, j.mehnert@tu-braunschweig.de
- 2 RWTH Aachen University, Templergraben 55, 52062 Aachen, mschweiker@ukaachen.de, lhildebrand@rb.arch.rwth-aachen.de
- 3 TU Berlin, Strasse des 17. Juni 152, Sek. A44, 10623 Berlin, +49 30 31421883, ros wag-klinge@tu-berlin.de
- 4 TU Darmstadt, Franziska-Braun-Strasse 3, 64287 Darmstadt, knaack@ismd.tu-darmstadt.de
- 5 TU Delft, Julianalaan 134, 2628 BL Delft, u.knaack@tudelft.nl

Abstract

Additive production techniques such as 3D printing and robotics enable new production methods and possible uses for earth, as one of the most ancient building materials in the building industry. This study examines the potential of different building elements and components and their possible combinations made of or containing earthen building products. In addition to the 3D printing of lightweight, highly insulating external and heavy internal wall elements and load-bearing rammed earth walls for use as inner and outside walls are compared. Furthermore, the activation of the walls with water-based heating and cooling elements is taken into consideration. In particular, the sensitivity of earth to humidity and water has a positive effect on all life cycle phases from production through operation as a low-tech building to the end of use, i.e. the reuse as well as the possible return to natural cycles. The focus of the study is to assess the building material earth in light of modern production methodologies, the impact on indoor comfort and indoor air quality as well its life cycle assessment.

Keywords

Earth construction, circularity, indoor environmental quality, user satisfaction, user health, additive manufacturing

1 INTRODUCTION

As an estimation, 30% of all houses worldwide are built from earth (Keefe, 2012). Besides regions in which earth as a building material is the only available resource, in Europe, the number of buildings made from earth is increasing slowly. This essentially does not result from earth as the only available resource but from demands of sustainable, healthy and comfortable living (Minke, 2017). Not only from an indoor environmental quality (IEQ) point of view but also from technical aspects, earth has a high potential of minimizing the energy demand which is used for the operation of buildings. Buildings from earth not only positively affect the human well-being inside the building but also have a positive impact on the outdoors, contributing to the resilience of cities against heat stress (Santamouris, 2013). This is already well understood in warmer climates (e.g. street canyons in arid climate), but considering global warming, the consideration makes increasing sense in colder climates and dense cities.

Earth as a building material still has a low market share in European regions which could be caused by lost knowledge from construction companies that are not familiar with the building techniques (Minke, 2017). Furthermore, buildings from earth can only be cost-effective when the building process is (semi) automated (Kloft et al., 2019). The structure of building elements from earth are usually rammed earth, blocks, dry boards or plasters, whereas supportive additive manufacturing processes could enhance not only the production process itself but also indoor environmental qualities.

Historically, earth is used with different techniques in form of earth blocks and rammed earth as a solid construction or as fillings in wattle-and-daub buildings. In different cultures, earth is used in a variety of techniques and designs as a cladding material, mostly as plaster but also as dry earth boards. Due to its climate-controlling and ecological potential, earth is gaining increasing attention as a building material. In Germany, the standardization of earth building products has been progressed intensively in recent years. Standards for earth blocks (DIN 18945), earth mortar (DIN 18946), earth plaster (DIN 18947) and earth dry boards (DIN 18948) have been introduced.

Due to the small market, the use of earth is still very artisan. New manufacturing technologies such as 3D printing and robotics will unlock the potential for optimizing the use of earth in the construction industry and are expected to contribute to the further spread of earth buildings.

In order to develop the full potential of products from additive manufactured earth, the advantages of earth construction need to be maintained. Therefore, the objective of this article is a multi-dimensional discussion of the main relevant capacities, which are here considered as indoor environmental quality, user satisfaction, and the circularity against the background of evolving technologies to assess the potential of the new technologies.

2 METHODOLOGY

In this article, the potentials of earth products are described and classified from different perspectives. Firstly, the technology with the latest developments in additive manufactured earth products is introduced. Secondly, the state of the art of the most relevant capacities (indoor environmental quality, user satisfaction and circularity) is summarized. In the discussion, the status quo is outlined, and the potential of additive manufactured earth products to improve the market share and the application within moderate climate zones is discussed. Subsequently, the assessments are overlaid with each other to reflect the status quo of AM earth products, demonstrating the potentials for the application in the building industry.

While the potential of additive manufactured earth products is discussed based on the technology and the relevant capacities on an abstract level, the findings presented below are based on a literature review, experiences from practice and from small size produced prototypes by the authors. The section on user satisfaction is based on a literature search in web of science and sciencedirect, using search terms including "rammed earth", "earth building" or "earth plaster" in combination with "comfort", "well-being", and others, which revealed 37 journal articles of which only 11 were suitable for this article after reviewing their content in detail.

3 ADDITIVE MANUFACTURING TECHNOLOGIES

In general, AM technologies will be distinguished by the nature of the raw material and the methods used to produce the different layers of the structure, as well as by the joining phase of the layer differences. Before the material is processed, there is a digital planning process in which the object to be created is digitally created in three dimensions and then broken down into layers so that the corresponding additive manufacturing process can process it.

The usual technologies currently in use are Selective Laser Melting (SLM), Direct Metal Laser Sintering (DMLS) and Selective Laser Sintering (SLS), all three processes in which a thin layer of powder is melted using an energy source at the points where volume is to be created. In a next layer, the same process is repeated in a higher layer until a corresponding volume is created. The Fused Deposition Modelling (FDM) and Fused Filament Fabrication (FFF) processes work differently in principle: the material is extruded from a nozzle, and individual layers are created by controlling the nozzle or the carrier platform, which then produce the desired volume according to the digital control (Lim et al.; Knaack et al. 2010; Knaack et al. 2016). Other technologies like stereo-lithography (SLA) or Laminated Object Manufacturing (LOM) are alternative methods of additive manufacturing, but technologies do not currently appear to make much sense for use in earth.

Earth consists of sand, silt and clay. Depending on the corn size distribution, it can be used for different purposes in construction. By optimizing the mineral composition and adding natural fibres, for example, the properties can be optimized according to its purpose. Additive production techniques such as 3D printing and robotics enable new production methods and possible uses for earth, as one of the most ancient building materials in the building industry. This chapter introduces the most relevant techniques.

3.1 AUTOMATED RAMMED EARTH

Based on one of the traditional production methods for components made of earth, the rammed earth technique, automated rammed earth technologies have been developed. In a first step, the material is penetrated by means of automation and then automatically compacted. In this process, components can be produced both on-site and as finished parts that are subsequently transported (Heringer, Blair Howe, Rausch; Djahanschah, Auer, Kaufmann;). This process has already been tested several times and is currently being used in the construction industry for limited and individual projects. In a further development step, the automated rammed earth technologies can be developed towards an automated control of the formwork, which offers the principle advantage of free control of the form. This process has so far only been investigated experimentally (Kloft et al.).

3.2 DIGITALLY CONTROLLED BUILDING ELEMENT EXTRUSION

Following the system of the FDM Technology there is the possibility to create large-sized building elements and structures on-site by means of extrusion. In this case, a cord of earth is placed on the

underlying cord by means of extrusion and thus creates the volume. The process allows the creation of large volumes relatively quickly and is currently being investigated experimentally at various institutes in the USA and Europe. Semi-industrial production is active in Italy (WASP).

3.3 DIGITALLY CONTROLLED COMPONENT EXTRUSION

Also based on the extrusion, small components as parts of building elements can be purchased for the first time, which are developed for complex geometric situations or additional functions and can then be produced by means of digitally controlled extrusion and transported after drying. The principal technology of digitally controlling the extrusion of earth is being investigated by various institutes in Spain, Hong Kong, the Netherlands and Germany, but up to now, it has always been followed by a firing process to produce a brick as a special shape from the component (Knaack et al., 2010; Knaack et al., 2016). Next to the individualized volume itself, the surface of the object can be designed to improve its performance.

4 INDOOR COMFORT

Certainly, the best-understood fact is that earth buildings have a high thermal capacity so that heat can be buffered to times with lower temperatures and thereby shifting temperature peaks and reducing active cooling to a minimum. Due to the fact that the heat transfer is driven by the temperature difference between surface and adjacent air one can speak of a self-regulating effect since the heat flow from or into a building element depends on the temperature difference (BINE, 2007). Combined with materials having lower densities, an insulating building material can be produced, making earth as a building material likewise interesting for colder climates using porous mineral aggregates (e.g. foamed glass). If the wall structure is built from 100% reusable materials, a minimum of embodied energy content is achieved if structural or insulating elements are built from wood or straw.

In addition to other mineral materials earth is porous and has the capability to buffer also large amounts of humidity from the air. This hygroscopic behaviour can be described as the sorption of humidity. The measurement procedures of sorption processes are standardized. During a constant air temperature of 23°C and a rise in relative humidity from 50 to 80% is induced while the control volume is weighted continuously to identify the absorption of water during at least 12 hours (DIN 18945-18948). Under laboratory conditions, a wall made from earth which is exposed from both sides to a rise in relative humidity the ability to absorb water from the air is described as nine times higher compared to a wall made from concrete (Minke, 2017). Considering real-life operating conditions, the ability of humidity sorption from the air into earth dry boards is 3-5 times higher compared to plasterboards made of gypsum (Klinge, 2016). Here 100 g/m² of humidity is absorbed by the earthen product with a thickness of 20 mm after 12 hours compared to 20 g/m² absorption by the gypsum board. It can reasonably be concluded that the self-regulating effect of the air temperature is also applicable to self-regulation in relative humidity (Lan et al. 2017).

Considering the local climate during the design process, the hygrothermal properties (thermal capacity, insulation, humidity buffering) of earth provides the potential to reduce the demand of technical equipment (Djahanschah, et al., 2020). In the example the risk of mould (in bathrooms) due to peak-loads of moist can be compensated by the ability to absorb humidity quickly (McGregor et al., 2016). Hence, ventilation rates of peak loads can be reduced. Two residential buildings, which are operated within German climate conditions where one is built from conventional materials and the other is built from natural materials shows a significant difference in humidity levels (Klinge, 2016). The building which is made from natural materials shows that humidity levels range almost

between 50% - 60% which is a spectrum providing healthy conditions whereat buildings made of conventional materials show lower rates in relative humidity with higher alterations. To achieve those healthy conditions, it can be discussed that active humidification and hence an air conditioning system is obsolete if the building is designed with proper materials.

On the basis of AM technologies and automated construction techniques, the surface texture itself can be optimized. This could be achieved with an increase in surface area through a roughened texture of the surface by for example digitally controlled component extrusion. This could result in a higher transfer of humidity and heat flow between the air and the building element. As another potential, the inner characteristics of building elements from earth could be adjusted during the additive manufacturing process so that modified thermal masses and insulating properties are made from one homogeneous material.

Furthermore, the material can be equipped with functions by the material itself (e.g. openings for ventilation, cavities) or with technology. Chilled walls with earth as a material base that could be plastered cooling systems as well as prefabricated earthen dry wall systems with embedded cooling system have the benefit of reducing the risk of condensation leading to the possibility of lower supply temperatures; hence, higher cooling rates are possible. The fact that peaks of the relative humidity can be buffered and flattened the opposite is valid for cases in which dehumidification is necessary. With a chilled ceiling or a thermo-activated building system, dehumidification is thinkable.

5 USER SATISFACTION AND HEALTH

From the viewpoint of human comfort, satisfaction and health, lower indoor temperatures and humidity levels, due to above-described characteristics of earth, reduce the thermal strain and increase the level of satisfaction under warm summer conditions (Parsons, 2014). In addition, respiratory health effects during wintertime are caused by rather low relative humidity levels (Mäkinen et al., 2009), potentially reduced with earth materials regulating humidity levels.

However, studies looking specifically at the effect of earth materials on user satisfaction and health are scarce. Furthermore, when considering rigorous scientific methods (i.e., meaningful sample sizes and controlled experiments), nearly all of these studies cannot draw conclusions on systematic cause-effect relations. At the same time, their findings are useful for formulating research questions and hypothesis for future research.

A first group of studies looks at direct effects. Li et al. (2013) compared traditional Chinese Tulou buildings made of rammed earth in a wooden framework with close by "normal rural buildings". They obtained 139 questionnaires from six Tulou buildings and 97 responses from an undefined number of normal buildings and performed additional IEQ measurements. They observed higher thermal satisfaction with the Chinese Tulou buildings compared to normal rural buildings, but no differences in the perception of the luminous and indoor air quality environment. However, their study cannot reveal whether the observed differences are due to different building materials or the differences in architecture and style of buildings. Fernandes et al. (2019) base their conclusion on a single rammed earth building in Portugal with measurements and subjective votes of five respondents. Thermal performance was satisfactory during summer, but heating was required in winter. Beckett et al. (2017) compared one building with traditional solid rammed earth walls with one other building with rammed earth walls including an insulating polystyrene core in Australia. Both buildings led to high thermal satisfaction in winter and summer, with only short periods with heating demand in winter. Noteworthy, occupants' ratings were more positive than predicted by calculated satisfaction indices. These examples confirm the focus on thermal aspects when dealing

with earthen constructions, while additional direct effects due to the application of above-described technologies can be envisioned. These effects include the potential of earth plaster optimizing acoustic properties while keeping thermal mass activated; increased satisfaction with the indoor air quality due to lower temperatures and the known effect of cooler air perceived as more fresh (Fang et al., 1998); and an improved visual environment through enhanced visual properties of the surface minimizing glare.

Compared to such direct effects, indirect effects mentioned in the literature are even more difficult to be assigned solely to the application of earth as building material. Deuble and de Dear (2012) found that occupants in green buildings tended to forgive their buildings IEQ conditions outside classical comfort ranges more likely than occupants in conventional buildings. Again, the evidence is based on case studies partly contradictory and not systematically assessed. For example, Taylor et al. (2008) found no difference in occupants perception with respect to thermal, visual, and acoustic aspects comparing one rammed earth building with one other conventional building. Supporting the existence of such an effect, Sant'Anna et al. (2018), Leaman and Bordass (2007) and others found strong positive effects of green buildings on user satisfaction compared to conventional buildings. Due to small sample sizes and the large variety in human perception and preferences, the debate is still ongoing and further well-designed research required.

In this context, the notion and importance of perceived control is a crucial aspect to be considered. Evidence from studies not addressing earth buildings suggest positive effects of perceived control on user satisfaction (e.g. Brager et al. 2004, Schweiker et al. 2016). Keeping buildings simple will help their users understanding their behaviour. At the same time, a buildings' capability of self-regulation should not reduce control opportunities for individual comfort.

A final note shall be given on the effect of building with earth and "feeling earth" on human health. Based on an experimental study with 36 Chinese adult participants, Wong & Au (2019) concluded that participants who created earth work using their bare hands improved significantly in positive mood and well-being immediately after the session, compared to those wearing gloves. Nan and Ho (2017) reported a positive effect of earth art therapy compared to visual art therapy on emotion regulation and other aspects of mental health in adults with depression based on an experimental study with 106 participants. These studies reveal interesting potential side-effects of building with earth.

6 CIRCULARITY

Circularity is a strategy that aims in balancing human needs for resources and environmental concerns by designing circular flows. In the context of the building industry, different levels can be considered like the flow of finances or the flow of information. The environmental impact is related to the material or resource flow which is considered in the following.

Resources in the building context are used to operate the building as gas or oil for heating, cooling and electricity. Furthermore, resources are used to form the building substance - its construction materials. Due to high insulating building envelopes and efficient technology, which provide growing shares of renewable energy, the relevance for resources in the building context is growing.

In order to evaluate the extent of circularity of construction materials, two categories are distinguished: 1) the material which is or is becoming part of the construction (input) and 2) its after-use potential (or potential output). Different methods by different stakeholders like the Dutch platform CB23 (CB'23, 2019; Foundation; & Design, 2015), institutions like most relevant the Ellen Macarther Foundation, universities e.g. RWTH Aachen (Hildebrand, Schwan, Vollpracht, Brell-Cokcan,

& Zabek, 2018) or architects and engineers (Hillebrandt, Riegler-Floors, Rosen, & Seggewies, 2018) are available with the attempt to evaluate design decisions and quantify circularity.

In order to discuss the circularity of earth products and additive manufactured earth products the two categories input and potential output are used.

Input. Earth products are most commonly used in near proximity and often manually processed. Hence, only little energy and emissions are linked to the transport and the processing of earth products. This results in low values for primary energy not renewable ranging from 0,07 to 1,05 MJ/kg and for global warming potential 0,004 to 0,06 kg CO₂eq/kg (Schröder, 2019). In comparison with other building materials, the thickness needs to be considered. While solid construction from bricks, limestone or concrete with insulation typically result in thicknesses from 25-40 cm, a wall with the same functionality from earth will need 40-70 cm. Even with the increased material amount, the earth wall, if produced with low-tech measures, will result in significantly lower values.

For additive manufactured earth products, the machine work is highly relevant. Studies on this aspect are not available. Environmental data on automated processes were investigated in a study on deconstruction of façades (Hildebrand, Schwan, Vollpracht, Brell-Cokcan, & Zabek, 2018). The processes are comparable to producing rammed earth; the findings show that the effort for cutting and lifting are as energy-intensive as processing the construction again. Furthermore, a wide variety of machine efficiency can be found; older machines use more energy. When renewable energy is used, the environmental impact can be reduced significantly. In respect of the printing process, different results can be expected as no lifting of bigger pieces is involved. Additionally, only necessary material is placed, which can potentially reduce the overall resource spent on a construction.

The deconstruction of earth products is manually and mechanically doable. The material can be processed (in order to provide homogeneous material) and used in a different construction like it was done with the earliest earth products, documented for 8000 B.C. in Afrasiab (today Samarkand), which were isolated from a building context, processed and used as a recycled building product in a new building. When grade purity is provided, the material keeps its recyclability endlessly.

For additive manufactured earth products, especially for printed construction, the ingredients can vary. Additives and aggregates are used in order to impact the viscosity during the printing process and limit the shrinkage while drying. Fibres from vegetables, animals or minerals can be added to support the material strength. Additives can be hexametaphosphate (HMP), ash or enzymes. Experiments from IACC document the interdependencies between the material properties and the construction geometry in which the printing pattern follows the material strength and provides an original shape. Schröder (2019) distinguishes additives that impact the chemical properties of earth products and additives that do not. While the first group has no effect on the circularity of the material, the latter has; since the additives cannot be sorted out, the product is impure and limited in its application. Recycling is no longer possible. Examples here for are cement, chalk or fly ash.

7 SYNOPSIS OF POTENTIALS

Even if earthen construction is one of the oldest construction techniques known to mankind, the scientifically proven knowledge of this building technique is limited. Although the hygric capabilities, i.e. moist sorption and desorption of the material, can be demonstrated using the earth building standard (DIN Norm), the basics of the hygrothermal behaviour, for example, in relation to potentials in heat protection or dynamic behaviour is missing. There are also limited methods to model the

hygrothermal behaviour of heterogeneous structures in order to be able to validate the empirically determined performance and thus support the design process of earthen structures leading to higher market shares. The answer to the potential of earth as a high-performance building material which could reduce or even replace technical building equipment is still open. The well-being of the users in earthen buildings, which is often mentioned, has also only been examined to a very limited extent and requires further research. In the holistic view of sustainability, the material can do very well if it is left "pure" and not mixed with cement or chemical substances, i.e. reused endlessly in the life cycle or returned to nature at the possible end of life. Based on the knowledge which additives result in a weak environmental performance, those compositions that shown potential need to be exploited regarding their different applications. It offers potential to substitute common building materials which are made from non-renewable resources or cannot be reused or recycled to serve the same function. While earth products are increasingly available, the information on the physical properties of the products needs to grow in order to become easily integrated into the planning process.

The great potential of this material with regard to the physical properties of the building and the resulting possibilities to reduce building technology, especially ventilation and cooling technology, can only be reached with further research on the material level. The experiences with AM produced building elements and associated components made of earth are not yet very extensive and tend to be at the level of prototype development.

Partly automated prefabrication in the field of rammed earth construction, such as Martin Rauch e.g. practiced in the projects Ricola Kräuterzentrum and the Alnatura Arbeitswelt (Djahanschah, Auer, Kaufmann, 2020) is continued in the automation of rammed earth technology, which will open up greater efficiency in processing and new design options in free forms. After the first prototypical steps, further research is necessary.

The AM technology in the form of FDM technology opens up completely new potentials for designing solid earth wall components. While using different raw materials, eventually additives and aggregates and producing new spatial formations new wall systems are possible. The arrangement of air chambers enables the thermal resistance of the earth building materials to be optimized for winter performance. By designing the surface, in addition to the visual impression, the acoustic but also the hygrothermal effect of the elements can be improved.

Thanks to their structural design and the additives, AM earth elements (AME) enable a construction that is precisely tailored to the requirements. In this way, external and internal walls can react to different criteria of acoustic and sound insulation as well as to thermal and hygric ones. In connection with digital planning processes, customized elements and buildings can be manufactured.

The limitation of earth building materials lies in their load-bearing capacity. In Germany, solid earth buildings with up to two storeys are possible. There is great potential here in the connection to additively produced, optimized wooden structures. These are optimized for the statically necessary cross-section and enable new types of connections and automated production techniques in timber construction (Menges, Knippers, Wagner, Zechmeister, 2020).

In connection with wooden skeleton structures, AME can also find its way into multi-storey buildings. The combination of wood and earth was traditionally used in wattle and daub construction and is already known there for its good physical properties. The potential of both technologies can be joined by combining AME and automated timber construction. So far, the wood and earth construction has only been carried out by hand. Additive manufacturing techniques are suitable for components

such as prefabricating complete walls in the workshops in the future and avoiding costly construction site production.

Through their further development until they are ready for the market, new types of construction elements are created which, on the one hand, can react precisely to new requirements such as climate change and, on the other hand, enable an economical construction method and thus distribution on the market.

8 CONCLUSIONS

In view of the interdisciplinary potential for sustainable architecture described above, it seems sensible to work on the topic of AME in greater depth. In particular the potential of complete individualization and the possibility of optimally adapting the structural design to the functional requirements with regard to load-bearing behaviour, climate, well-being and deconstructability promises to have a special influence on the performance of components and buildings. Furthermore, a targeted development of strategies for the transfer to the building industry is required, also against the background of the lack of experience with the combination of the technology, the lack of standards and the necessary exemplary application in order to create confidence in the technology.

References

- Asimakopoulos, D.; Santamouris, M. (2013): *Passive Cooling of Buildings*. Hoboken: Taylor and Francis
- Beckett, C. T. S., Cardell-Oliver, R., Ciancio, D., & Huebner, C. (2017). Measured and simulated thermal behaviour in rammed earth houses in a hot-arid climate. Part B: Comfort. *Journal of Building Engineering*, 13, 146–158. doi:10.1016/j.jobee.2017.07.013
- BINE: Thermo-active building systems. (2017). Online available at http://www.bine.info/fileadmin/content/Publikationen/Englische_Infos/themeninfo_I07_engl_internetx.pdf
- Brager, G., Paliaga, G., & De Dear, R. (2004). Operable windows, personal control and occupant comfort.
- Deuble, M. P., & de Dear, R. J. (2012). Green occupants for green buildings: the missing link?. *Building and Environment*, 56, 21–27.
- Djahanschah, S.; Auer, T.; Kaufmann, H. (2020). *Gewerbebauten aus Lehm und Holz*, DBU Bauband 3 (2020)
- Fang, L., Clausen, G., & Fanger, P. O. (1998). Impact of temperature and humidity on the perception of indoor air quality. *Indoor air*, 8(2), 80–90.
- Fernandes, J., Mateus, R., Gervásio, H., Silva, S. M., & Bragança, L. (2019). Passive strategies used in Southern Portugal vernacular rammed earth buildings and their influence in thermal performance. *Renewable Energy*, 142, 345–363. doi:10.1016/j.renene.2019.04.098
- Heringer, Anna; Blair Howe, Lindsay; Rausch, Martin: *UPSCALING EARTH - MATERIAL, PROCESS, CATALYST*; gta Verlag, ETH Zürich (2019)
- Keefe, L (2012): *Earth building: methods and materials, repair and conservation*. Routledge
- Klinge, A., Roswag-Klinge, E., Fontana, P., Hoppe, J, Richter, M., Sjöström, C. (2016): Reduktion von Lüftungstechnik durch den Einsatz klimasteuernder Naturbaustoffe – Ergebnisse aus dem EU Forschungsvorhaben H-House und der Baupraxis. In: LEHM. Kloft H-, Oechsler J., Loccarini F., Gosslar J., Delille C. (2019). *Robotische Fabrikation von Bauteilen aus Stampflehm*. Deutsche Bauzeitschrift.
- Knaack, U; Klein, T; Bilow, M; De Witte, D; Mohsen, A; Tessmann, O: *Imagine 10 – rapids 2.0: 2016* Rotterdam, 010 publisher
- Knaack, U; Klein, T; Bilow, M; Strauss, H: *Imagine 04 – rapids: 2010* Rotterdam, 010 publisher
- Lan, Haoran; Jing, Zhenzi; Li, Jian; Miao, Jiajun; Chen, Yuqian (2017): Influence of pore dimensions of materials on humidity self-regulating performances. In: *Materials Letters* 204, S. 23–26. DOI: 10.1016/j.matlet.2017.05.095.
- Lim, S., Buswell, R. A., Le, T. T., Austin, S. A., Gibb, G. F., Thorpe, T. (2012). Development in Construction-Scale Additive Manufacturing Processes. *Automation in Construction*. (2012).
- McGregor F. Heath A., Maskell D., Fabbri A.; Morel, J.-C. (2016): A review on the buffering capacity of earth building materials. In: *Proceedings of the Institution of Civil Engineers - Construction Materials* 169 (5), S. 241–251. DOI: 10.1680/jcoma.15.00035.
- Minke, G. (2017): *Handbuch Lehm- und Baustoffkunde, Techniken, Lehmarchitektur*. 9. Auflage. Stauf bei Freiburg: ökobuch.
- Minke, G. (2013): *Building with earth. Design and technology of a sustainable architecture*. Third and revised edition. Basel, Switzerland: Birkhäuser.
- Leaman, A. & Bordass, B. (2007). Are users more tolerant of 'green' buildings?. *Building Research & Information*, 35:6, 662–673, doi: 10.1080/09613210701529518
- Li, Q., You, R., Chen, C., & Yang, X. (2013). A field investigation and comparative study of indoor environmental quality in heritage Chinese rural buildings with thick rammed earth wall. *Energy and Buildings*, 62, 286–293. doi: 10.1016/j.enbuild.2013.02.057
- Mäkinen, T. M., Juvonen, R., Jokelainen, J., Harju, T. H., Peitso, A., Bloigu, A., ... & Hassi, J. (2009). Cold temperature and low humidity are associated with increased occurrence of respiratory tract infections. *Respiratory medicine*, 103(3), 456–462.

- Menges, A., Knippers, J., Wagne, H., Zechmeiste, C. (2020). Pilotprojekte für ein Integratives Computerbasiertes Planen und Bauen-
Beitrag in: Baustatik – Baupraxis 14, Universität Stuttgart ISBN: 978-3-00-064639-3
- Nan, JKM, Ho, RTH (2017). Effects of clay art therapy on adults outpatients with major depressive disorder: A randomized controlled trial. *Journal of Affective Disorders*, 217, 237-245. doi: 10.1016/j.jad.2017.04.013.
- Parsons, K. (2014). *Human thermal environments: the effects of hot, moderate, and cold environments on human health, comfort, and performance*. CRC press.
- Sant'Anna, D.O., Dos Santos, P.H., Vianna, N.S., Romero, M.A. (2018). Indoor environmental quality perception and users' satisfaction of conventional and green buildings in Brazil. *Sustainable Cities and Society*, 43, 95-110, doi: 10.1016/j.scs.2018.08.027
- Schweiker, M., Hawighorst, M., & Wagner, A. (2016). The influence of personality traits on occupant behavioural patterns. *Energy and Buildings*, 131, 63-75. doi: 10.1016/j.enbuild.2016.09.019
- Taylor, P., Fuller, R. J., & Luther, M. B. (2008). Energy use and thermal comfort in a rammed earth office building. *Energy and Buildings*, 40(5), 793-800. doi:10.1016/j.enbuild.2007.05.013
- Wong, Antonio Ngok Tung & Au, Wing Tung (2019). Effects of Tactile Experience During Clay Work Creation in Improving Psychological Well-Being, *Art Therapy*, 36:4, 192-199, doi: 10.1080/07421656.2019.1645501
- The World's Advanced Saing Project (WASP): <https://www.3dwasp.com/en/about-us/#manifesto>

Carbon Conscious! The Impact of Embodied Emissions on Design Decisions for Building Envelopes

Tania Cortes Vargas¹, Linda Hildebrand², Lisa Rammig³, Andrea Zani⁴

- 1 Eckersley O'Callaghan, 450 Geary Street, Suite 500, +1 415 813 3810, tania@eocengineers.com
- 2 RWTH Aachen, TBC, lhildebrand@rb.arch.rwth-aachen.de
- 3 Delft University of Technology / Eckersley O'Callaghan, 450 Geary Street, Suite 500, +1 415 813 3810, lisa@eocengineers.com
- 4 Eckersley O'Callaghan, 450 Geary Street, Suite 500, +1 415 813 3810, andrea@eocengineers.com

Abstract

A focus on embodied emissions in building materials has been notorious in the last years, mostly due to high improvements in optimisation of operational energy in buildings. The environmental impact of building materials reflected in embodied energy and potential (re) life options that stimulate circular flows has become the focus of discussion. During the design process, designers and engineers are confronted with different decisions that might impact the embodied emissions (EE) of a façade system. This paper focuses on the EE of different curtain wall configurations whilst applying the Kit-of-Parts approach in a case study in California. The study was carried out under the LCA methodology applied from the A1 to A4 stages and limited to five main parameters: façade typology, span and grid size, different LCA phases, material choice, and supply chain. The results are compared against each other to understand the relevance of each parameter and level of impact of each parameter.

Keywords

Kit of parts, embodied emissions, façades, life cycle assessment

1 INTRODUCTION

For many years, due to more stringent building codes, local energy guidelines and regulations a focus on reducing operational energy of buildings and reaching zero energy targets could be observed. More recently, as the efficiency in operational energy use has increased significantly, the focus is moving towards the environmental impact of building materials, primarily reflected in the embodied energy and emissions and the potential (re)life options that allow circular material flows. Façade systems typically represent between 25 and 30% of a building's total embodied energy; however, designers and façade engineers are confronted with several design parameters that affect the environmental impact to a varying extent (Hartwell, R, Overend, M, 2020). The environmental relevance of design decisions is discussed in the literature on an abstract level; how light-weight constructions are favoured over solid assemblies, wood products over metal products, local materials over materials sourced from overseas. In real practice, parameters mix, which leads to higher complexity in answering the questions of design, performance, costs, and environmental concerns into consideration.

This paper addresses embodied emissions (EE) in different curtain wall configurations and presents the results of a case study conducted in the San Francisco Bay Area in California that investigates the application of a Kit-of-Parts approach to curtain wall systems. The goal of this study is to evaluate the relevance and impact of different design parameters on EE that derive from the design process such as façade typology, the span and grid size, the different life cycle phases, material choice, and the supply chain. The study is based on four different typical configurations of curtain wall units with a varying grid based upon standard sizes in the US.

2 METHODOLOGY

The study investigates a façade system that provides different configuration options. For each configuration, the environmental impact is investigated by quantifying the emissions through a life cycle assessment method (LCA) for a façade on an office building located in the San Francisco South Bay, US. The LCA methodology yields information about the embodied energy or embodied greenhouse gases, indicating the environmental impact of materials. The data used originates from German Ökobaudat and Environmental Product Declaration (EPD). Design alternatives are assessed with LCA and compared against each other. Additionally, the different production routes are analysed using the database Ecotransit, which calculates emissions due to transport means. Parallel, a financial calculation was conducted to see the economic dimension of reducing distances. In the end, all alternatives are compared against each other, and their relative share of potential for improvement is evaluated for this case study.

While part of the methodology relies on LCA databases to understand the environmental impact of materials, it also included the collaboration of local partners to assess the supply chain and the typical curtain wall units and configurations (as they are based on typical US sizes). The research aims to go beyond the materials' database standard values and understand a real-life scenario that, besides material impact, also considers logistics and design processes.

3 EXPERIMENT / RESEARCH

The research initiates with a literature review about façade typologies, from which the results direct towards curtain walls. Collaboration with local manufacturers pointed towards typical curtain wall configurations in the Bay Area. Thus, the experiment is limited to four different

curtain wall configurations with dissimilar construction, which further derives into four different sizes per configuration.

In addition to the varying sizes, a cradle-to-gate assessment (A1-A3) is conducted to compare each phase and determine the relevance of the production phase. Additionally, the same cradle-to-gate assessment is carried out to understand the environmental impact of curtain walls' typical infill materials. The system boundary is further expanded to A4 to analyse different baselines for transport scenarios. The results are then evaluated and compared to each other to determine each parameter's level of impact.

3.1 FAÇADE TYPOLOGY

In a first analysis of the façade system, the façade typology was considered regarding two aspects: the environmental impact of materials calculated with LCA and the construction typology with its suitability for de-construction.

According to (Hildebrand, 2014), the façade typology predefines the range of environmental impact; while double skin façades can be lighter compared to solid façades, their embodied energy is significantly higher. Curtain walls fall into the typology with the lowest environmental impact when compared to solid and double skin envelopes. This is due to the low weight that results from a lighter construction required for only one layer (compared to double skin) and the skeleton structure (compared to solid façades). Figure 1 shows the result of different case studies analysed by Hildebrand (2004), where different typologies fall into cluster-like arrangements, indicating the embodied emissions per weight. As Figure 1 depicts, curtain wall envelopes have lower embodied emissions, followed by solid façades/punched windows and, finally, double skin façades.

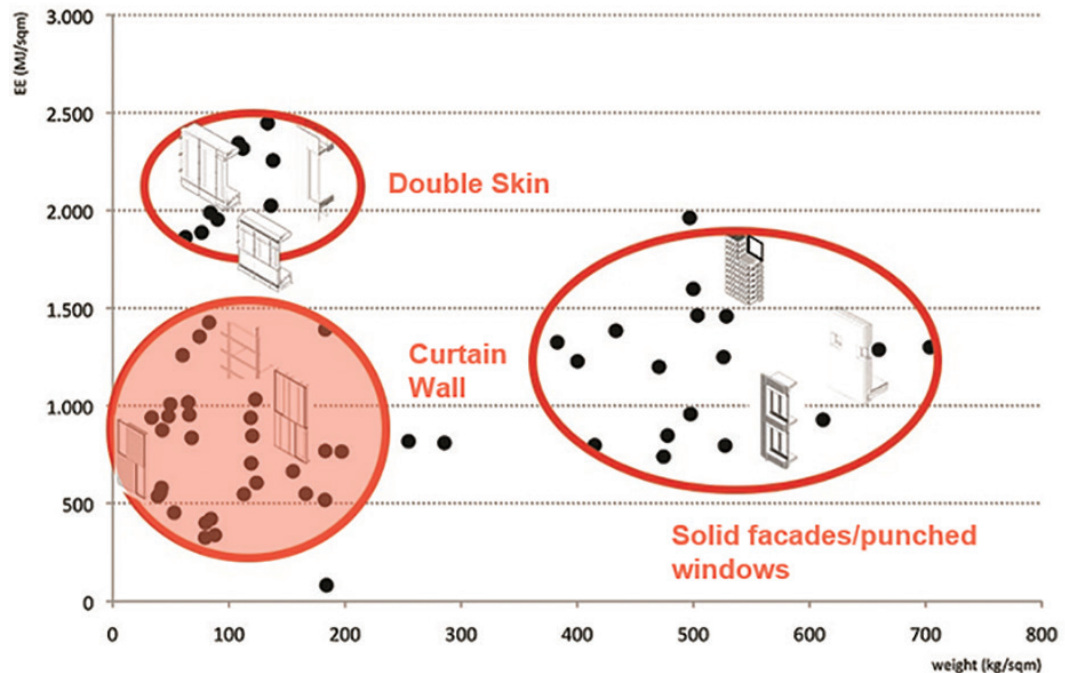


FIG. 1 Curtain walls are relatively low in weight and embodied emissions. Image by Hildebrand (2004)

In addition to their light-weight nature, curtain walls are more suitable for deconstruction compared to solid façades due to their joining technique. In comparison to a traditional brick or block wall, mortar bonds take higher mechanical forces to separate bricks or blocks from one another. Mortar typically remains on the brick, which will lead to a recycling scenario rather than reuse of the material. Curtain wall construction is based on mechanical connections, where components are screwed or clamped with each other, and they can be easily separated. Even where bonded connections are used, surfaces are clean, so silicone bonds can easily be cut off. This helps to deconstruct with little effort, which has proven to be a driver of ease of reuse or recycling, therefore, stimulating a circular flow of materials.

3.2 SPAN/GRID SIZE

To understand the impact of unit sizes and common metrics like window-to-wall ratio on the EE of the components, a variation of unit sizes was assessed. As the size of curtain wall units has a considerable impact on cost as well as transport and installation efficiencies, it was considered important to understand the impact of sizes and framing ratios on the EE, as it would help negotiate performance, cost and environmental impact.

Four different unit configurations were assessed to analyse the impact of the curtain wall's span/grid size: glazing panel and shadow box, glazing panel and bottomless shadow box, full-height aluminium panel (opaque), and a full-height shadow box unit (opaque). Each configuration then derives into four different variations to study the impact of span/grid size, where the following sizes are studied: 5' x 14', 5' x 16', 7.5' x 14', 7.5 x 16', summarised as follows:

- Unit A - Curtain wall unit with glazing panel and shadow box
- Unit B - Curtain wall unit with glazing panel and bottomless shadow box
- Unit C - Curtain wall with full-height aluminium panel
- Unit D - Curtain wall with full-height shadow box unit

The number, followed by the letter indicating the configuration, corresponds to the panel's dimensions according to two variations in width (5' or 7.5') and (14' or 16'). This results in four different sizes for each of the four configurations, a total of sixteen variations.

- Size 1 - 5' x 14'
- Size 2 - 5' x 16'
- Size 3 - 7.5' x 14'
- Size 4 - 7.5 x 16'

Additionally, due to the varying dimensions, different glass sizes are required. Depending on the panel size, three different types of glass build-up are used. The built-up glass dimensions are expressed as: outer lite — spacer — inner lite. Laminated lites are expressed as a sum in brackets.

- Glass I: 5/16" — 1/2" — 5/16"
- Glass II: 3/8" — 1/2" — 3/8"
- Glass III: [1/4" + 1/4"] — 1/2" — [1/4" + 1/4"]

Figure. 2 illustrates the different unit configurations, sizes, and glass build-up.

	UNIT A				UNIT B				UNIT C				UNIT D			
	A1	A2	A3	A4	B1	B2	B3	B4	C1	C2	C3	C4	D1	D2	D3	D4
UNIT WIDTH	5	5	7.5	7.5	5	5	7.5	7.5	5	5	7.5	7.5	5	5	7.5	7.5
UNIT HEIGHT	14	16	14	16	14	16	14	16	14	16	14	16	14	16	14	16
SHADOW BOX HEIGHT	3	3	3	3	1.5	1.5	1.5	1.5	1.5	1.5	1.5	1.5	3	3	3	3
GLASS TYPE	I	I	II	III	I	I	III	III	-	-	-	-	I	I	III	III

TABLE 1 Summary of the different unit configurations, panel sizes, and glass build-up. All dimensions in feet.

Each unit and its corresponding variations were assessed according to the established LCA methodology as a cradle-to-gate assessment (A1-A3). Figure 2 shows the results.

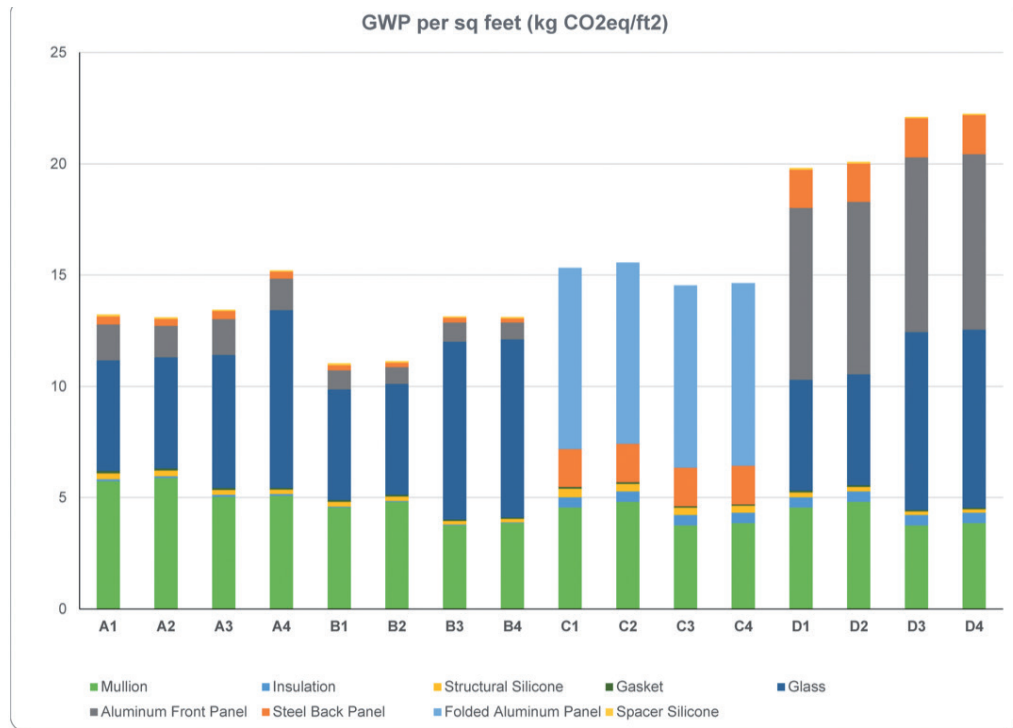


FIG. 2 Results of A1-A3 assessment for the different unit configurations described in Table 1.

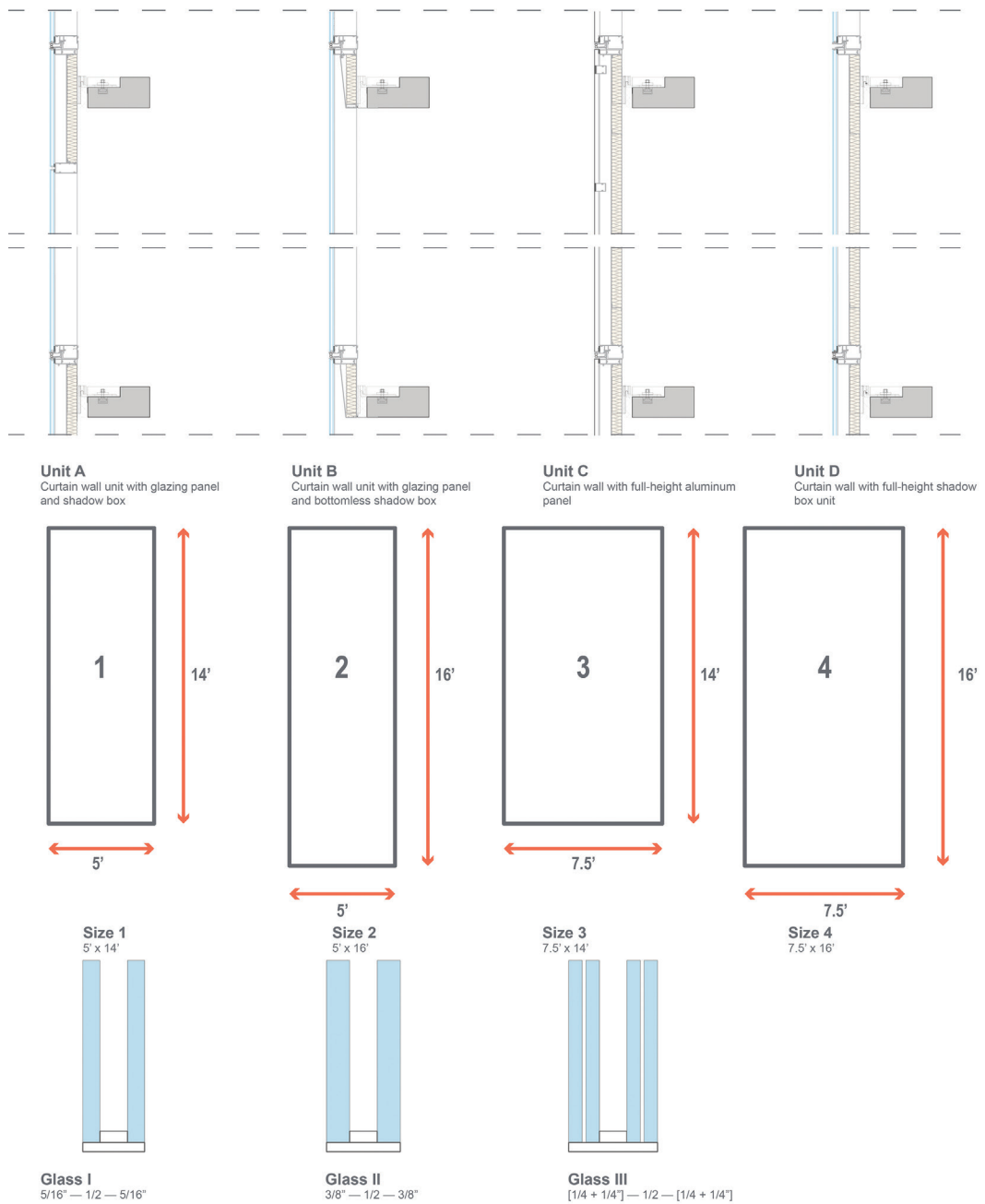


FIG. 3 Diagram showing the different unit configurations described in Table 1.

The results' overall trend shows similar GWP output in Units A and B, along with its corresponding variations. Unit C has slightly higher results, where the highest contribution is from aluminium panels. A significant increase in GWP is shown in unit D, mostly due to its construction nature. Since this is a shadow box unit, it uses both glass and aluminium panels, meaning that it uses all the materials from the previous configurations, making it the most material-intensive unit of all four. The increment in GWP for A4, B3, B4, D3, and D4 is because they require a thicker glass build-up, due to the larger panel size.

3.3 LIFE CYCLE PHASES

The system boundary was established as cradle-to-gate, referring to the A1 – A3 production phases. Four different glass types were compared: clear float glass, clear laminated glass, clear coated glass, and tinted coated glass. Figure 4 shows the percentage of energy corresponding to each production phase (A1 to A3). While the effort to supply raw materials and transport them is comparably low, production emissions are the most significant. Such is the case for other building materials, especially if intensive treatment is involved. It shows the relevance of the energy source. Operating a production plant with renewable energy helps essentially to reduce the overall environmental impact.

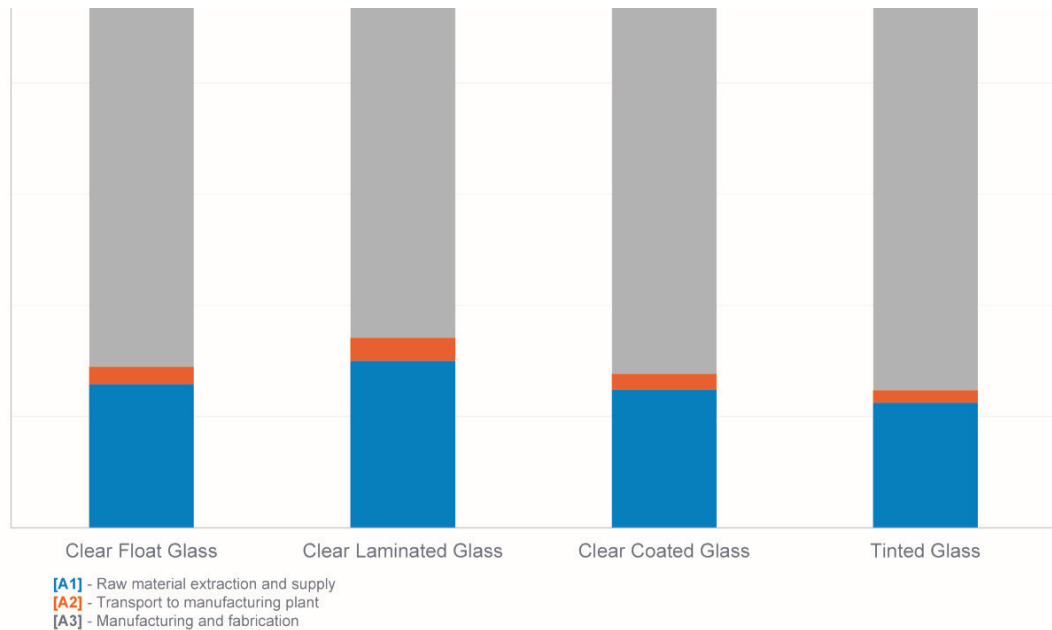


FIG. 4 Results of cradle-to-gate assessment showing a breakdown of embodied emissions for the A1 - A3 phases.

The comparison of the three different stages, Raw material extraction and supply (A1), Transport to manufacturing plant (A2), and Manufacturing and fabrication (A3), shows that from these three, the highest impact comes from the manufacturing process. This is highly related to the nature of the process itself, as mining and transporting material is less energy-intensive.

3.4 INFILL MATERIALS

To further understand the environmental impact of different materials, several infill materials commonly used in curtain walls are assessed in a cradle-to-gate system boundary for Unit C, the opaque façade element. The objective is to compare the results of units with the same configuration, but with different infill materials and varying thickness. The assessed materials are natural stone, aluminium panel, meshed metal baffle, fibre cement, wood fibreboard, and gypsum board. Figure 5 shows the results of the assessments applied to Unit C and its corresponding four variations.

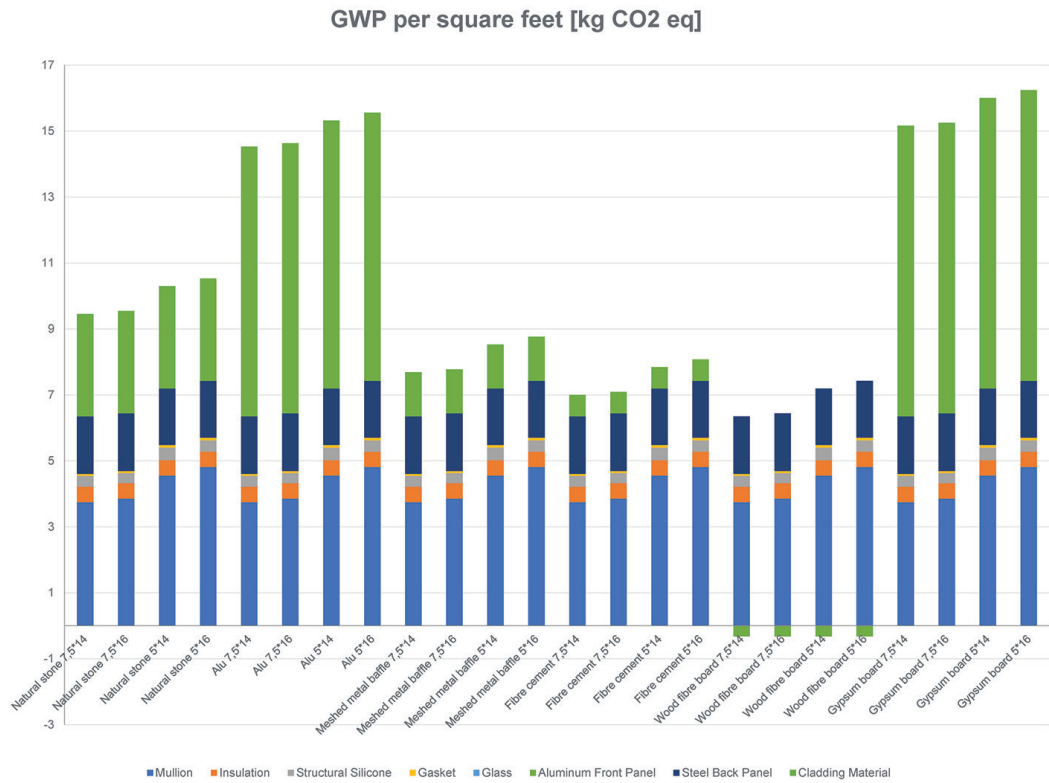


FIG. 5 Results of cradle-to-gate assessment comparing different infill materials and varying thickness

The results for different infill panels show that each material’s production process has a significant impact on the embodied emissions. The results show that the wood fibreboard cladding has the lowest GWP per square feet, followed by fibre cement, meshed metal baffle, and natural stone. Both the aluminium and gypsum board panels have the highest embodied emissions.

3.5 SUPPLY CHAIN

The supply chain cost analysis focuses on understanding how much percentage accounts for transportation. Therefore, the system boundary was expanded by adding the A4 transport stage. Three scenarios with different international baselines were analysed: Italy, Vietnam, and Thailand. Table 2 summarises the baselines for each international scenario.

BASELINE - ITALY	BASELINE - VIETNAM	BASELINE - THAILAND
Glass is sourced from Germany and taken to Italy.	Glass is sourced from Germany.	Glass is sourced from Germany.
Components are assembled in the factory in Italy.	Aluminium is extruded in Vietnam.	Aluminium is extruded in Thailand.
Components are transported by ship to Oakland, and then to the SF Bay Area by truck	Components are shipped to Bangkok to be assembled in the factory, transported by ship to Oakland, and then to the SF Bay Area by truck.	Components are assembled in Thailand, transported by ship to Oakland, and then to the SF Bay Area by truck.

TABLE 2 — Comparison of international scenarios

To have a domestic comparison, three different North America baselines are analysed, where production took place on the East coast of the US and then transported to the West coast. The following table summarises each domestic scenario.

DOMESTIC (1)	DOMESTIC (2)	DOMESTIC (3)
Glass is sourced from Minnesota, US. Aluminium is extruded in New York, US. Components are shipped to Quebec, CA, where they are assembled. Assembled units are distributed from Quebec, CA to the SF Bay Area by truck.	Glass is sourced from Minnesota, US. Aluminium is extruded in New York, US. Components are shipped to Connecticut US, Where they are assembled. Assembled units are distributed from Connecticut US to the SF Bay Area by truck.	Glass is sourced from Massachusetts, US. Aluminium is extruded in New York, US. Components are sent to California by truck to be assembled close to the construction site in the SF Bay Area.

TABLE 3 — Comparison of domestic baseline scenarios

The results indicate that several parameters within the baselines play a role, such as the country of origin, the source of primary energy in each country, and the shipping method. When comparing the results between the international baseline and the domestic scenarios, it can be observed that shipping from Europe to Asia can be in the same range or lower compared to trucking from the East to the West coast of the US. Electrically operated transportation, such as train or even shipping, but mostly by avoiding trucking. As trains within the US are primarily diesel operated however, the use of trains has limited effect on the improvement of shipping impact within the US. Additionally, a financial assessment was carried out to determine if the domestic scenarios are cost-competitive compared to international baselines. The results indicated that both domestic and international baselines yield very similar costs.

4 DISCUSSION OF RESULTS

According to the results, the highest impact parameters are façade typology, life cycle phases, infill materials, and supply chain. For the first parameter, Façade typology, literature results show that curtain wall façades average 50% less embodied emissions than double-skin façades, and roughly 20% - 25% compared to solid façades. Therefore, it is determined that the overall impact of façade typology is high.

The second parameter, different spans/grid sizes, shows only a small deviation when comparing one configuration to the other. The increase in GWP for the panels that require a larger built-up is no more than 15%. Overall, it is concluded that varying the width and height of façade panels does not have a significant impact.

The third studied parameter, life cycle phases, shows the relevance of the energy source used in the factory, as, on average, 75% of the embodied emissions are produced by the manufacturing stage. If the energy used for manufacturing relied on a renewable source, a significant GWP reduction would be possible. Therefore, it is concluded that the impact of the life cycle phases, particularly concerning the A3 stage, is high.

The fourth parameter of the research, infill materials, shows that aluminium and gypsum board panels have the highest emissions. If we compare an aluminium panel of 5" x 16" against a wood fibreboard panel of the same size, the aluminium panel has roughly 50% more embodied emissions. The result shows the importance the selected material has not only due to the required energy for mining but also for production, as previously discussed. Hence, it is concluded that the impact of infill materials is high.

The last studied parameter, supply chain, indicates that transportation accounts for 3% to 10% of the total embodied emissions in an A1 – A4 system boundary, as shown in Table 4.

	BASELINE - ITALY	BASELINE - VIETNAM	BASELINE - THAILAND
Account for transport	6%	3%	3%

	Domestic (1)	Domestic (2)	Domestic (3)
Account for transport	6%	10%	3%

TABLE 4 — Results of the international and domestic scenarios

The supply chain results indicate that transportation accounts between 3% to 10% of the total embodied emissions in an A1-A4 system boundary. Potentially, if the procurement and fabrication occur close to the construction site and its neighbouring states, the reduction in embodied emissions is also significant, as shown in Domestic (3). Therefore, it is concluded that the impact of the supply chain is high.

While the parameters were studied independently, they are also related to each other, such as the case of the life cycle phases and the infill materials. Some infill materials have a higher GWP closely related to the manufacturing phase. Several infill materials that are opaque have lower embodied emissions, and thus selecting them might reduce the GWP per square feet in a façade system. This is also cross-referenced to the results in the varying span/grid size. As observed in the results from Span/Grid size, Unit D had the highest embodied emissions from all configurations. This is because it uses both glass and aluminium panels, meaning that it is more material-intensive by design. Using spandrel panels (as observed in Unit C) instead of shadow boxes can significantly decrease roughly 35%, where such reduction is strongly related to the infill materials. To achieve additional reduction, an important recommendation would be to carefully select the adequate window to wall ratio, as results also showed that glass has higher embodied emissions. However, while glass is a material that is not easily replaced, opaque infill materials have the potential of offering a wider variety of options, where lower GWP is preferred. Therefore, having a correct window to wall ratio, where opaque materials have low embodied emissions, can also be a strategy that can lower the embodied emissions of a façade system.

Additionally, it was proven that while transportation does not account for more than 10%, a significant reduction is possible when trucking is avoided. This was mainly observed in the domestic baseline scenarios, where trucking from the East to the West coast of the US was comparable to shipping from Europe to Asia. Container shipping does not only show lower embodied emissions, but it also allows us to ship more components at once. Table 5 summarises the results of each parameter while highlighting its impact level.

PARAMETER	LEVEL OF IMPACT	EXPLANATION
Façade typology	High	Assessment documented in academia shows that façade typology influences environmental impact; double-skin façades with high glass share the highest contribution, followed by solid façades with punched windows. Curtain wall systems belong to the group with the lowest environmental impact.
Span/grid size	Low	Assuming a fully glazed system, the ratio of glass and aluminium per square feet varies, which leads to a small deviation.

>>>

Life cycle phases (A1-A4)	High	Comparing A1, A2 and A3, the production (A3) indicates the highest impact with 66-75%. This suggests that the location of production should be assessed carefully for every project.
Infill material	High	The choice of the infill material impacts the environmental performance significantly. Many opaque materials perform better environmentally than glass, depending on the chosen fabrication.
Supply chain	High	By using aluminium with recycled content, the GWP of the entire façade can be reduced by approximately 25%. Using locally sourced materials and optimising transport can contribute up to 15%.

TABLE 5 — Summary of the studied parameters and their impact level.

5 CONCLUSIONS

The research conducted presents results that apply to curtain walls, with five different parameters assessed and compared to determine their level of impact, respectively. The study shows that the parameters with the highest level of impact are façade typology, life cycle phases, infill material and supply chain. The only parameter that did not show a significant level of impact was the span/grid size, as only a small deviation is observed. The different parameters aimed to study an approach that changes while looking not only at design decisions but also at logistics and processes that involve manufacturers and local supply chains. It is also important to consider that the level of impact of these parameters is limited to curtain walls, and it would need to be reassessed for other typologies. Most likely, it would need to be incorporated into a specific LCA separately to determine the level of impact of each parameter when applied to a new typology. The same applies to the supply chain, as each part would need to be incorporated with a specific LCA separately.

In addition, the results of the research show that there are several design decisions that can be taken into consideration to lower embodied emissions, such as selecting an adequate window-to-wall ratio, infill materials with low GWP, and selecting to assemble components close to the construction site whilst avoiding trucking. Additionally, regarding the different life cycle phases, the results showed the relevance of the production phase, where it was observed that the source of energy used in the factory had a significant impact. If materials are manufactured with renewable energy, the embodied emissions are significantly lower. Overall, it is concluded that the embodied emissions in curtain wall envelopes can be significantly reduced when these parameters are considered. However, it is still to be determined how these parameters relate to financial feasibility, which is also a main driver in construction and design decisions.

References

- Hildebrand, L. (2014). Strategic investment of embodied energy during the architectural planning process. Retrieved from <http://abe.tudelft.nl/index.php/faculty-architecture/article/view/Hildebrand>
- Hartwell, R, Overend, M. (2020). End-of-life Challenges in Façade Design: A disassembly framework for assessing the environmental reclamation potential of façade systems. Façade Technics World Congress.

PART 3 // ENERGY

Holistic Design Explorations Building Envelopes Supported by Machine Learning



Federico Bertagna¹, Pierluigi D'Acunto¹, Ole Patrick Ohlbrock¹, Vahid Moosavi²

* Corresponding author

1 ETH Zurich, Institute of Technology in Architecture, Chair of Structural Design, Stefano-Franscini-Platz 1, 8093 Zurich (Switzerland) bertagna@arch.ethz.ch

2 ETH Zurich, Institute of Technology in Architecture, Chair of Digital Architectonics, Stefano-Franscini-Platz 1, 8093 Zurich (Switzerland)

Abstract

The design of building envelopes requires a negotiation between qualitative and quantitative aspects belonging to different disciplines, such as architecture, structural design, and building physics. In contrast to hierarchical linear approaches in which various design aspects are considered and conceived sequentially, holistic frameworks allow such aspects to be taken into consideration simultaneously. However, these multi-disciplinary approaches often lead to the formulation of complex high-dimensional design spaces of solutions that are generally not easy to handle manually. Computational optimisation techniques may offer a solution to this problem; however, they mainly focus on quantitative aspects, not always guaranteeing the flexibility and interactive responsiveness designers need in the early design stage. The use of intuitive geometry-based generative tools, in combination with machine learning algorithms, is a way to overcome the issues that arise when dealing with multi-dimensional design spaces without necessarily replacing the designer with the machine. The presented research follows a human-centred design framework in which the machine assists the human designer in generating, evaluating, and clustering large sets of design options. Through a case study, this paper suggests ways of making use of interactive tools that do not overlook the performance criteria or personal preferences of the designer while preserving the simplicity and flexibility needed in the early design stage.

Keywords

Photovoltaic / thermal systems, radiant cooling, building-integrated photovoltaic, façade, solar cooling

DOI 10.7480/jfde.2021.1.5423

Simple versus Complex: Comparing the Accuracy of Cooling Energy Demands for Complex Fenestration Systems using BSDF and SHGC

Christiane Wermke¹, Brian Cody²

- 1 Graz University of Technology, Rechbauerstraße 12, 8010 Graz/AT, christiane.wermke@tugraz.at
- 2 Graz University of Technology, Rechbauerstraße 12, 8010 Graz/AT

Abstract

Although technologically advanced glasses exist on the market, external shading devices can be an easy to integrate design feature for existing buildings as well as new developments. External shading devices are designed to help control and reduce the impact of excessive solar gains emanating from solar radiation. The assessment of the energy performance of a fenestration system requires properties of both, the window and the shading device. It is common practice to use solar heat gain coefficients (or g -value) to represent energy flows through the window to the inside of a building. Another method is to use angular-dependent properties such as transmittance and reflectance in the form of a BSDF file (bi-directional scattering distribution function). On one hand, standardised descriptions for windows such as solar heat gain coefficient (SHGC) do not accurately represent the angular dependency of windows with external shadings such as Venetian blinds. On the other hand, approaches that use angular-dependent transmission and reflection to calculate energy flows through the façade more accurately are not always available during early planning stages of a shading design. The present work compares the differences in cooling energy demands using three ways to describe the property of a double glazing unit (DGU) with external Venetian blinds, which are: a) BSDF data, b) an annual solar heat gain coefficient (anSHGC), calculated for normal incidence) and c) a climate-based SHGC (cbSHGC) which is calculated for actual solar angles dependent on the geographic location. Not only do the energy results differ in precision, but the effort taken in determining the input parameters for BSDF, annual SHGC and climate-based SHGC also varies. A lower precision in energy results may be acceptable during early planning stages, but high accuracy is required to proof code compliance.

Keywords

Bi-directional Scattering Distribution Function, solar shading, Venetian blinds, cooling energy, g -value, solar heat gain coefficient, climate

1 INTRODUCTION

The building envelope is a central part of a building design; it separates the indoor from the outdoor conditions and is therefore crucial for the aesthetic and architectural appearance of the building but also fundamental to achieve occupant's comfort and energy goals (Kuhn et al. 2011). The transparent portion of the building skin is of particular interest in terms of achieving energy goals. Undesirable, excessive solar gains may cause indoor overheating and may result in unnecessary high cooling energy as well as undesirable glare (Kuhn et al. 2011). This circumstance highlights the importance of effective shading designs. With climate change at the forefront of many individuals and organisations around the world, there is an ever-growing need of efficient building envelope design. However, there is a distinct lack of simple and easy to use tools using physical properties that architects and building designers can use in early stages of the façade design process to quickly and accurately assess its effect on the energy demands of the building. Complex fenestration systems (CFS), such as a glazing with external shading devices, are the focus of many iconic praised building designs. These CFS can be categorised as either static or as adaptable. The assessment of their energy performance is often undertaken by engineering and façade experts. The amount of desired and undesired solar gains is not only dependent on the building orientation and surrounding objects (adjacent buildings, trees etc.) but also rely on the façade properties, namely glazing and shading properties, as well as the overall size of the transparent part of the façade (Kuhn et al. 2011). Besides an efficient envelope design, the optimal control strategy i.e. opening and closing of Venetian blinds, changing the tilt angle of horizontal slats of external blinds) of the façade will significantly influence both the user's comfort as well as the energy demand.

It is common to measure or calculate optical properties for windows such as solar heat gain coefficient (SHGC) at normal incidence (0°) of the incoming solar radiation on the window (Curcija et al. 2018). This practice does not reflect the angle-dependency of the CFS and is insufficient for the performance evaluation (Curcija et al. 2018). Ideally, angle-dependent properties are determined through measurements. However, for innovative designs, these are not available during the early-design stages and are expensive (Kuhn et al., 2011). Assessments through computational simulations are precise but slow (Kohler, Shukla, and Rawal 2017). The costly assessment of angular properties of a glazing with shading contradicts the notion of early design stage evaluation where an extensive analysis of the façade performance is not suitable, but fast and approximate results are required. This fact constitutes an enormous challenge for building designers not knowing their design's properties and unable to check its performance in a fast but reliable manner. Knowing the façade properties of a window with shading within a specific climatic context should be the first step to evaluate a design towards its performance. It does not, however, replace a thorough analysis of energy flows through the façade, including direct and diffuse radiation considering surroundings and ground reflections for most accurate results.

There have been various efforts to design and build tools with high and low complexity to determine optical properties of transparent façades with shading devices (Berkeley 2019; van Dijk and Oversloot 2003; EQUA 2013; Kohler, Shukla, and Rawal 2017; Petersen et al. 2018; Wall and Bülow-Hübe 2001; Wall, Wall, and Bülow-Hübe 2003). Openly available tools such as ParaSol (Hellström et al. 2007; Wall and Bülow-Hübe 2001; Wall, Wall, and Bülow-Hübe 2003), COMFEN (Robin Mitchell, Mehry Yazdanian, Charlie Curcija, Ling Zhu 2019), WIS (van Dijk and Oversloot 2003) and ES-SO ESBO-Light (EQUA 2013) are all able to calculate the g-value (or SHGC) of a window with shading. The predefined selection options are restricted to a limited number of shading designs as well as locations and therefore may not be useful for an innovative shading design in a designated location.

Kohler et al. (Kohler, Shukla, and Rawal 2017) developed an algorithm for COMFEN (Robin Mitchell, Mehry Yazdanian, Charlie Curcija, Ling Zhu 2019) that builds upon existing calculation methods

to calculate an aSHGC (adjusted Solar Heat Gain Coefficient) for windows with fixed shadings i.e. awnings or overhangs as well as a seasonal or weighted SHGC (for direct and diffuse radiation), which is dependent on the geographic and climatic location of the fenestration system as well as its orientation to the sun angle. COMFEN is limited to windows with awnings and cannot calculate a combined SHGC for windows with Venetian blinds or other shading devices that are planar to the window surface.

Other efforts to accurately calculate solar heat gains include Petersen (Petersen et al. 2018), who defined an algorithm to account for direct and diffuse radiation from the sky and the ground, including reflections from external surfaces (Petersen et al., 2018). Fener is a tool conceived by Fraunhofer (Bueno et al. 2015; Bueno, Cejudo-Lopez, and Kuhn 2017; Fraunhofer 2018) that uses BSDF (bi-directional scattering distribution function) datasets (see section 2.2 for details) and includes direct and diffuse (sky and ground) radiation and reflections, respectively. (Kuhn et al. 2011) proposed an approach to compute g_{total} by means of hourly direct and diffuse solar radiation using the Perez-Model from weather data for hours of the year with direct solar radiation. Using transmittance and reflectance (that are represented by a BSDF file) for optical properties of the fenestration system give most accurate energy results. Tools for building performance simulation that support BSDF include EnergyPlus (US Department of Energy 2013). However, using BSDF data in thermal building simulations are costly (Kohler, Shukla, and Rawal 2017; Petersen et al. 2018) and not suitable for fast design evaluations.

This paper will first discuss the current state-of-the-art, focusing on the representation of façade properties that are linked to solar heat gain. This work analyses contradictions between low and high complex performance assessment approaches and their impact on cooling energy results on the example study of an office room with a double glazing unit and external horizontal Venetian blinds.

2 STATE-OF-THE-ART

2.1 SOLAR HEAT GAIN COEFFICIENT

External environmental impacts such as solar gains on the transparent portion of the façade greatly influence the energy demand, particularly for cooling but also heating (Kharchi et al. 2012). Undesirable indoor over-heating caused by solar heat gains may cause occupant's discomfort (Marino, Nucara, and Pietrafesa 2017).

The solar heat gain coefficient (SHGC) of a simple glass pane is defined as the total fraction of incident solar energy that is transmitted through a transparent façade component. The incident solar radiation that enters a space is composed of the solar transmittance (T_{sol}), the solar absorptance and the inward flowing fraction of the absorbed radiation (ASHRAE 2013).

The solar heat gain coefficient is the ratio of solar heat gains through a window (and/or window with shading) in relation to the angle of incident solar radiation and is dependent on the angle of incidence and the wave-length of the radiation (Berkeley 2019). Standardised calorimetric measurements and computational evaluations of solar heat gain coefficient (SHGC) take place at normal incidence (0°) (Berkeley 2019). This approach neglects two important factors,

- 1 The solar incidence angle on the façade changes during the day and throughout the year and is almost never at 0° when the solar radiation is fairly low,

- 2 the SHGC for unshaded double glazing is quite high at 0° (Table 1) and drops very slowly until an altitude of 45° but drops significantly between an incidence angle of 45° to 90° (Kohler, Shukla, and Rawal 2017).

A climate-based SHGC (or directional SHGC) takes different solar angles into account that greatly vary depending on the location. The SHGC calculation method in this work is based on ISO 15099 (Standard 2006) using LBNL's WINDOW 7.7 software. High SHGC may result in higher cooling energy demands in the summer, whereas low SHGC lead to smaller amounts of cooling energy demands.

Considering the aforementioned angle-dependency of optical properties of CFS, it is clear that the SHGC at normal incidence (0°) of the fenestration system is not precise and will hence lead to inaccurate energy simulation results (US Department of Energy 2013). The SHGC is not the most accurate indicator for windows with shading but maybe be sufficient for first performance estimations at the beginning of the design process. More precise results for solar transmissions through fenestration systems are obtained by using transmittance and reflectance properties of all incoming incident angles of solar radiation (US Department of Energy 2013). This is achieved, for example, by using BSDF data (bidirectional scattering distribution function).

ANGLE	0	10	20	30	40	50	60	70	80	90	hem
SHGC	0.764	0.763	0.761	0.756	0.743	0.713	0.645	0.502	0.259	0	0.665

TABLE 1 Angle-dependent and hemispheric SHGC for DGU with argon filling (without shading)

2.2 BI-DIRECTIONAL SCATTERING DISTRIBUTION FUNCTION

Bi-directional scattering distribution function (BSDF) was first mentioned by (Nicodemus 1965) and describes the angular dependency of solar properties (transmission and reflection) of a complex fenestration system (Asmail 1991). BSDF are represented by a matrix of reflectance and transmittance coefficients for incident and outgoing directions (McNeil 2011). A matrix that is commonly used was established by Klems et al. (Klems 1993, 1994). The 'Klems' coordinate system (see Fig. 2) divides a hemisphere into 145 'patches' for 145 incoming and 145 outgoing directions (McNeil 2011).

LBNL WINDOW 7.7 (Berkeley 2019) has implemented the Klems' coordinate system combined with matrix entries for transmission and reflection (Ward, Kurt, and Bonneel 2012). The hemispherical basis of Klems' coordinate system and the indexing scheme of the individual patches can be seen in Fig. 1 and Fig. 2.

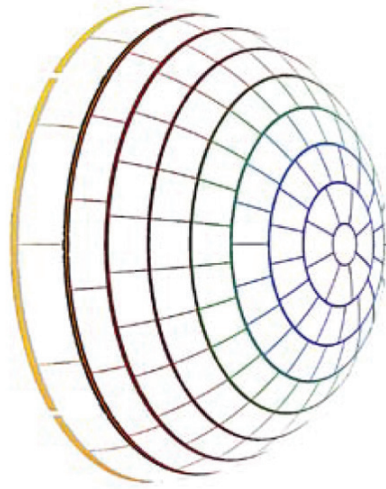


FIG. 1 Klems' Coordinate System 3D view (Ward, Kurt, and Bonneel 2012)

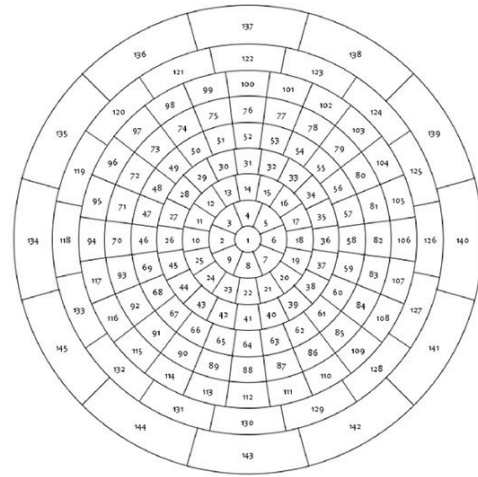


FIG. 2 Klems' Coordinate System plan view (outgoing directions) (Curcija et al. 2018)

Spectral data of a glazing such as transmission and reflection change with the number of layers, coatings etc. (US Department of Energy 2013). Products that are characterised by the same SGHC can have different angular properties Reference and Calculations 2013), which may result in large errors for energy results (US Department of Energy 2013). Although the use of BSDF during building simulation will lead to more accurate results (i.e. energy demand), the implementation of BSDF is not common in most BPS tools and simulation run time is slow (Kohler, Shukla, and Rawal 2017). Programmes that support BSDF file formats include LBNL WINDOW 7.7 and EnergyPlus and others.

2.3 BUILDING PERFORMANCE SIMULATION TOOLS

Current capabilities of building simulation software to accurately assess the performance of Venetian blinds are limited. The angular dependency of optical properties of CFS is applied in a very simplified way and different slat angles of i.e. horizontal external blinds are not taken into consideration (Kuhn et al. 2011). Accurate simulations of various shading options that account for angle dependency are too costly (Kuhn 2006). This is why simplified calculation methods (direct beam at normal incidence angle) are used by manufacturers to proof building code compliances which neglects realistic control strategies, angle dependency and diffuse radiation (Kuhn 2006).

Performance evaluation of innovative shading designs is costly and limited by current software capabilities; i.e. EnergyPlus has two options to simulate windows:

- 1 Simple window model, where one value for SHGC (at 0°) is used. The angle-dependency is calculated by applying the Fresnel approach (azimuth 0°, altitude 0°-90°). This approach is fast but precision is low. (US Department of Energy 2013)
- 2 Detailed layer-by-layer calculation makes use of transmittance and reflectance from BSDF data. This method is expensive and slow but give more accurate energy results (US Department of Energy 2013).

3 GLAZING AND SHADING PROPERTIES

3.1 GLAZING AND SHADING PARAMETERS

The WINDOW 7.7 software by Lawrence Berkeley National Laboratory (LBNL) was chosen for the following reasons:

- Open source software
- Regularly updated database for glazing, shading and shading materials
- Possibility to add customised data like BSDF data for an innovative shading design that needs to be evaluated
- Ease of use (user-friendly interface)

The calculations for SHGC as well as all BSDF using within the present study were undertaken in LBNL WINDOW version 7.7. (Berkeley 2019) using environmental conditions described in ISO 15099 (see Table 2) (centre-of-glazing calculation). LBNL WINDOW allows centre-of-glass calculations of SHGC at normal incidence as well as angle-dependent SHGC according to the BSDF matrix (Berkeley 2019). The window properties are based on beam incident radiation only which is transmitted and reflected diffusely.

	SOLAR RADIATION	EXTERNAL TEMPERATURE	INTERNAL TEMPERATURE
ISO 15099	500 W/m ²	30°C	25°C

TABLE 2 Environmental conditions according to ISO 15099 for SHGC calculations

It is possible in WINDOW to generate SHGC for direct radiation at incidence angles ranging from 0° to 90° (at 10° increment angle) and at 0° azimuth angle. LBNL WINDOW cannot calculate the combined value for direct and diffuse solar radiation but a hemispherical SHGC is given for diffuse radiation (Petersen et al. 2018). There are no energy flows through the window and shading system calculated which reduce the accuracy of the SHGC values but makes it a fast method for establishing SHGC.

LBNL WINDOW consists of a glazing and shading database which has been used for this work. It allows the calculation of SHGC for any chosen combination of glazing and shading from the IGDB (International Glazing Database (International Glazing Database n.d.)).

3.2 ANGLE-DEPENDENCY IN LBNL WINDOW

Furthermore, LBNL WINDOW can calculate BSDF data for glazing only or for glazing with shadings. The SHGC is an angular-dependent property of a CFS, and the value for SHGC greatly depends on both the altitude and the azimuth of the sun vector reaching the fenestration system. This complex approach has been described by Klems' 145 patches ((Klems 1993),(Klems 1994)) organised hemispherically onto the glazing surface. This method has been adopted by LBNL WINDOW to calculate 145 values for SHGC for outgoing directions for every patch of Klems' 145 patches (Robin Mitchell, Christian Kohler, Joe Klems, Mike Rubin 2008).

4 SIMULATION SET-UP

4.1 OFFICE ROOM SPECIFICATIONS

The performance evaluations of the window with Venetian blinds were undertaken to calculate cooling energy for an office room of the size of 6m x 6m and 3m high. The office room consists of one façade with a WWR (window-to-wall ratio) of 90% and external horizontal Venetian blinds with a tilt angle of 45°. All other walls are internal partitions and are considered adiabatic. Three façade orientations were studied, namely east, south and west façade. To get an idea of the impact in diverse climates, six European cities were chosen, ranging from cold to hot locations (Helsinki, London, Berlin, Rome, Madrid and Athens). Helsinki and Athens describe the coldest and hottest location studied in the experiment.

All energy simulations were done with EnergyPlus (US Department of Energy 2013) using Honeybee (Roudsari 2020) for Grasshopper/Rhinoceros (McNeel 2020).

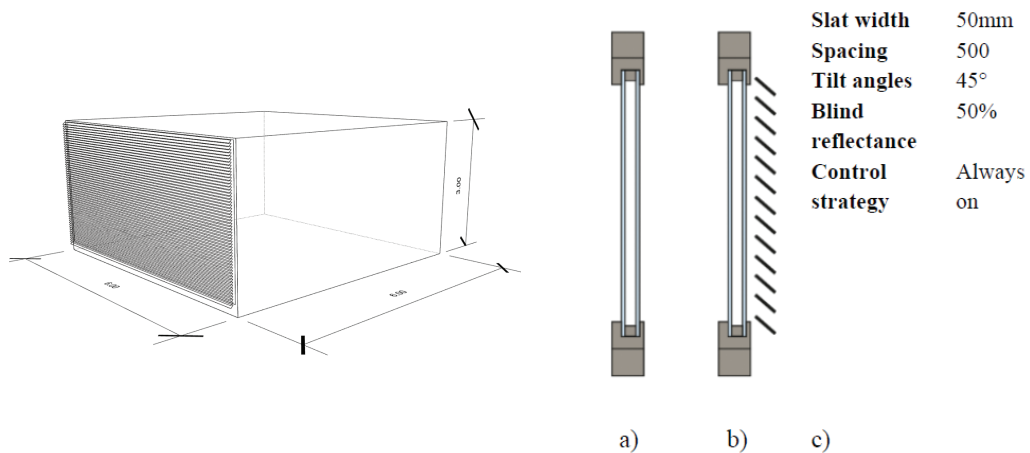


FIG. 3 Office room

FIG. 4 a) DGU with argon filling and b) DGU with external Venetian blinds and c) blind specification

4.2 SIMULATION PARAMETERS

The properties of the CFS that are used for the simulations are produced using LBNL's WINDOW 7.7 software. WINDOW 7.7 consists of an extensive glazing and shading database that is used to produce the properties of the CFS. For this case study, a double glazing unit (DGU) with argon filling and the same DGU combined with an external Venetian blind with horizontal slats was chosen. The annual SHGC (anSHGC) was calculated with WINDOW under ISO 15099 environmental conditions (see Table 2). The software further enables the export of BSDF data and directional SHGC for all 145 patches according to Klems. These values were used to determine climate-based (directional) SHGC for all studied locations. Climate data for the solar altitude and azimuth have been extracted from an epw-file using Ladybug for Grasshopper (Rhinoceros) for six European climates. Climate and BSDF data were used to calculate a seasonal SHGC (summer and winter) as well as a mean annual, monthly (August) and weekly (first week of August) value. The annual SHGC is calculated at normal incidence Fig. 6 a) whereas the climate-based SHGC is derived WINDOW's directional SHGC an associated with actual solar angles in the chosen locations (compare Fig. 6 b) and c). An overview of the annual and climate-based SHGC is shown in Table 3 for a whole year as well as the cooling season (21.3.-22.9.), a typical summer month (August) and a very hot week during the summer (1.8.-

7.8.). Table 3 illustrates the differences in values for anSHGC and cbSHGC that were used for the energy simulations. The BSDF data used in the study are represented by a matrix of 145x145 (21,025) values for transmittance and reflectance.

		ANNUAL			SEASONAL (21.3.-22.9.)			MONTHLY (1.8.-31.8.)			WEEKLY (1.8.-7.8.)		
		East	South	West	East	South	West	East	South	West	East	South	West
HEL	anSHGC	0.34	0.34	0.34	0.34	0.34	0.34	0.34	0.34	0.34	0.34	0.34	0.34
	cbSHGC	0.10	0.18	0.10	0.07	0.13	0.07	0.07	0.13	0.07	0.17	0.12	0.17
ATH	anSHGC	0.34	0.34	0.34	0.34	0.34	0.34	0.34	0.34	0.34	0.34	0.34	0.34
	cbSHGC	0.08	0.13	0.08	0.06	0.11	0.06	0.06	0.12	0.06	0.16	0.10	0.16

TABLE 3 Annual (anSHGC) and climate-based (cbSHGC) solar heat gain coefficients for Helsinki and Athens for DGU with external Venetian blinds at 45°

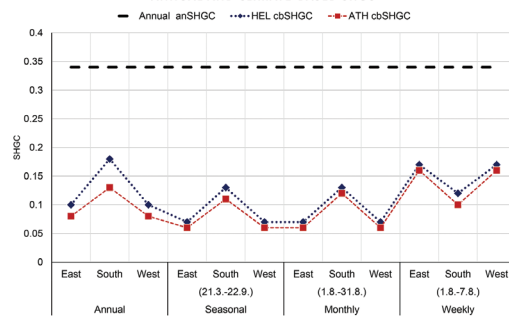


FIG. 5 Annual SHGC compared to Climate-based SHGC for Helsinki and Athens

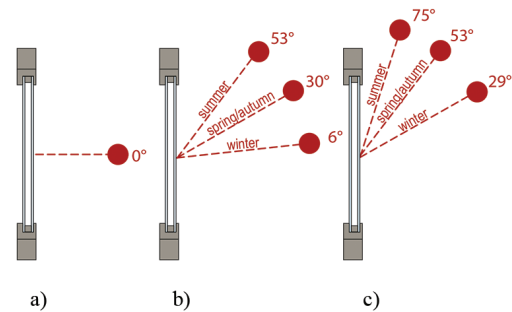


FIG. 6 Angle of incidence for solar radiation for a) at 0° (normal incidence) for product (standardised) measurements and actual incidence angle for b) Helsinki and c) Athens for different seasons of the year

5 RESULTS

The results of cooling energy demands for Helsinki and Athens are found in Fig. 7 for three façade orientations and for four time-steps, namely yearly, seasonal, monthly and weekly. The diagrams show an expected increase in cooling energy for Athens compared to Helsinki. Generally, using the BSDF for the simulations result in the lowest cooling energy demand for all cases. Though the use of anSHGC and cbSHGC increase the cooling energy demand. In the case of annual cooling energy, the discrepancy between BSDF and SHGC is greater for the east and west façade as opposed to the south façade. This is particularly the case for Athens.

Fig. 9 visualises the cooling demand for all cities for the period from 21st March to 22nd September for a south façade. Energy results are the farthest off from the BSDF results for Helsinki (145%), followed by Berlin (88%) and London (87%). The results for cooling are still between 36% and 60% higher for Rome, Madrid and Athens compared to BSDF results. Though the results are still quite high for cbSHGC (between 32%- 60%) for the cooler locations of Helsinki, Berlin and London, the results for the warm places are much closer to the BSDF results and are 6% to 17% larger.

Looking at the discrepancy between the two SHGC methods and the BSDF in Fig. 8 it is obvious that results for anSHGC are much greater in comparison to cbSHGC. The largest differences can be seen for Helsinki, where results are up to 150% higher than for BSDF for the south façade. On the contrary, the results are closest to BSDF for the exact same location when using cbSHGC during the

simulations (Helsinki: seasonal/east, monthly/east/west and weekly/west). The results for Athens for the cbSHGC are often underestimated and up to 14% lower than the BSDF results.

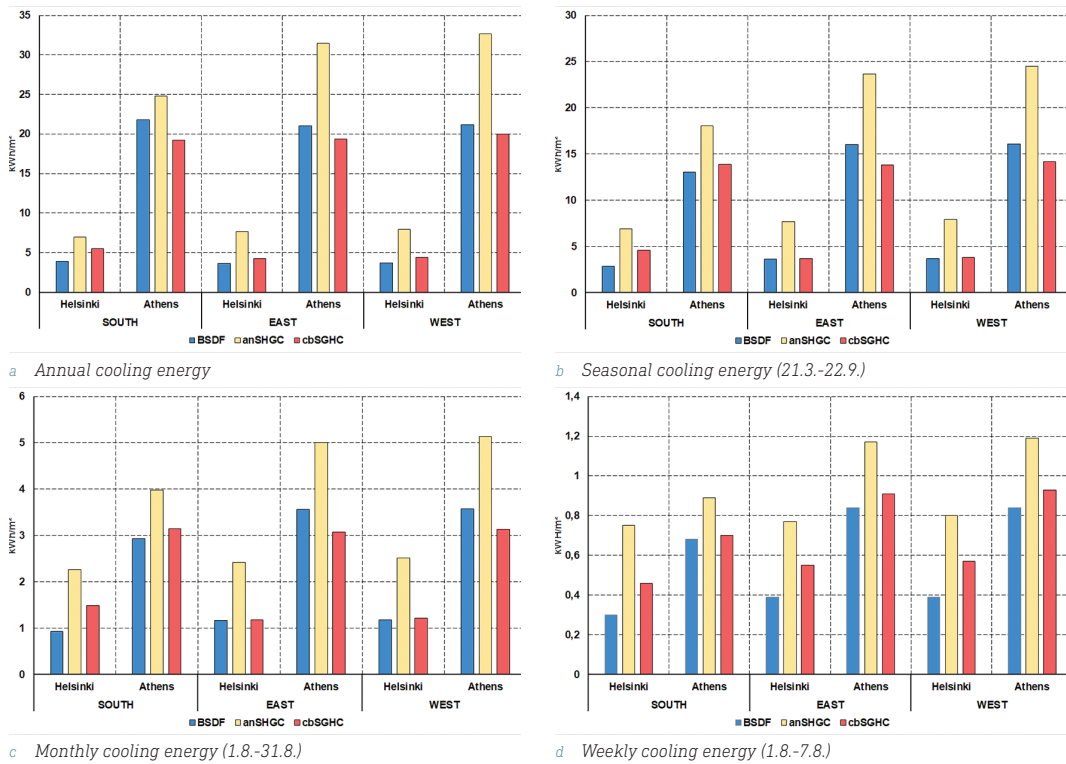


FIG. 7 Results for a) annual, b) summer, c) monthly and d) weekly cooling energy for Helsinki and Athens for East, South and West façade

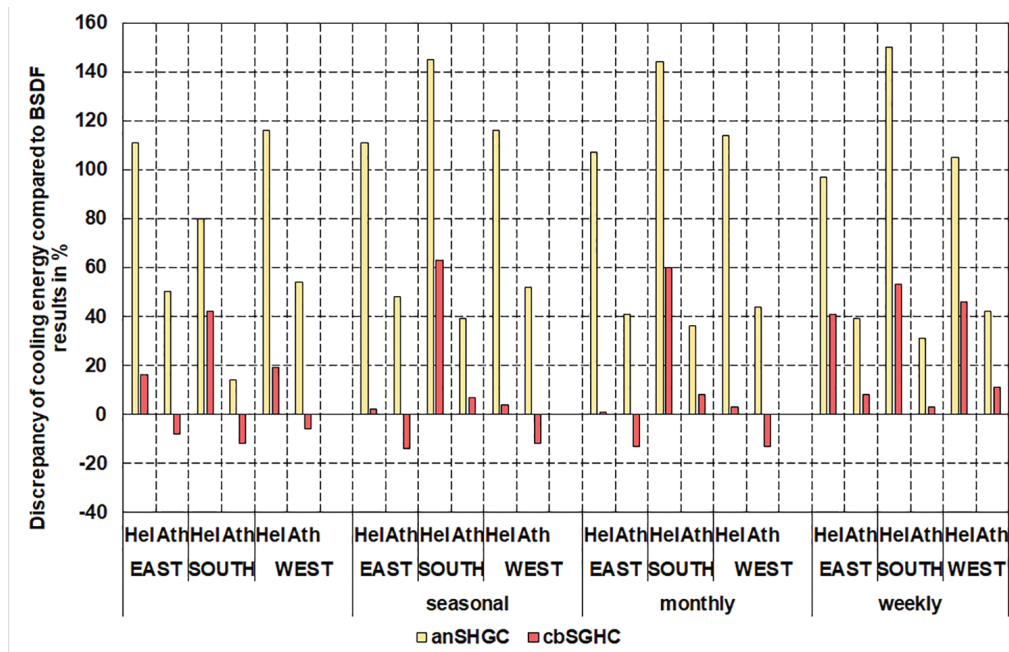


FIG. 8 Discrepancy of annual cooling energy results compared with results using BSDF for the complex fenestration system for three façade orientations (east, south and west) for Helsinki and Athens

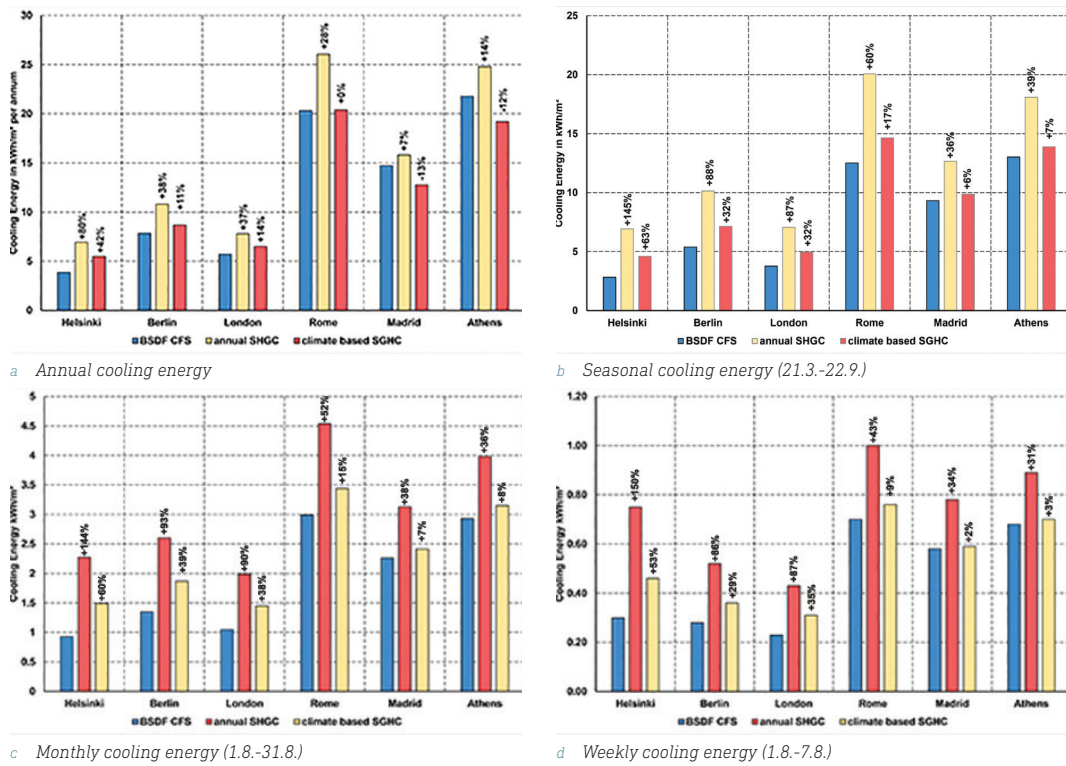


FIG. 9 Cooling energy for the south façade for six European cities comparing results for BPDF, annual SHGC and climate-based SHGC

Table 4 compares the disparities of cooling energy for an eastern and a western façade for annual, seasonal, monthly and weekly energy simulations for six European cities. The largest differences in annual energy results compared to BPDF results can be found for the west façade using a single value for SHGC (anSHGC). The results are farthest off from BPDF results for Helsinki (+116%) and closest for Athens (+54%). The lowest differences for the west façade can be found for weekly energy results (Helsinki: 105% and Athens: +42%). The discrepancy of anSHGC for the east façade are marginally lower for annual results: Helsinki +111% / Athens +48% and weekly cooling energy: Helsinki +97% / Athens +39%. One noticeable finding is that the annual SHGC overestimates the cooling energy between 50% to 100%. Besides, the results are consistent, with Helsinki being the farthest and Athens the closest to BPDF results.

On the contrary, the cbSHGC does both; it underestimates and overestimates the cooling energy for the considered time-steps (yearly, seasonal, monthly, weekly). Here, results are not as consistent as opposed to the anSHGC results. The yearly and weekly cooling energy demand is largest for Helsinki and the lowest for seasonal and monthly demands on the east façade. The lowest energy requirements can be found for Berlin (annual), Helsinki (seasonal and monthly) and Madrid/ Athens (weekly) on the east side.

A similar phenomenon can be found on the west façade, where the smallest differences in results can be stated for Madrid (annual), Helsinki (seasonal and monthly) and Athens (weekly). The greatest discrepancy, however, can be found in Helsinki (annual), Madrid (seasonal and monthly) as well as London (weekly).

		Annual						Seasonal					
		Hel	Ber	Lon	Rom	Mad	Ath	Hel	Ber	Lon	Rom	Mad	Ath
East	BSDF	3.65	7.7	5.4	19.51	14.36	21.04	3.64	7.03	4.88	15.5	11.78	16.01
	anSHGC	7.69	13.46	10.47	30.56	22.71	31.48	7.67	12.64	9.43	24.06	18.5	23.68
	*(an)	+111	+75	+94	+57	+58	+50	+111	+80	+93	+55	+57	+48
	cbSHGC	4.25	7.65	6	18.42	12.96	19.36	3.7	6.34	4.72	14.06	9.83	13.8
	*(cb)	+16	-1	+11	-6	-10	-8	+2	-10	-3	-9	-17	-14
West	BSDF	3.69	7.57	5.49	19.69	14.37	21.21	3.68	7.13	4.96	15.61	11.77	16.11
	anSHGC	7.97	14.03	11.06	31.65	23.65	32.69	7.94	13.18	9.97	24.79	19.19	24.47
	*(an)	+116	+85	+101	+61	+65	+54	+116	+85	+101	+59	+63	+52
	cbSHGC	4.4	8	6.07	18.95	12.97	20	3.82	6.67	5.02	14	9.84	14.2
	*(cb)	+19	+6	+11	-4	-10	-6	+4	-6	+1	-10	-16	-12
		Monthly						Weekly					
		Hel	Ber	Lon	Rom	Mad	Ath	Hel	Ber	Lon	Rom	Mad	Ath
East	BSDF	1.17	1.75	1.36	3.56	2.84	3.56	0.39	0.36	0.3	0.83	0.73	0.84
	anSHGC	2.42	3.11	2.61	5.13	4.33	5.01	0.77	0.65	0.58	1.17	1.1	1.17
	*(an)	+107	+78	+92	+44	+52	+41	+97	+81	+93	+41	+51	+39
	cbSHGC	1.18	1.57	1.31	3.3	2.38	3.08	0.55	0.49	0.41	0.91	0.79	0.91
	*(cb)	+1	-10	-4	-7	-16	-13	+41	+36	+37	+10	+8	+8
West	BSDF	1.18	1.78	1.38	3.58	2.83	3.58	0.39	0.37	0.3	0.84	0.73	0.84
	anSHGC	2.52	3.27	2.77	5.25	4.43	5.14	0.8	0.69	0.61	1.21	1.1	1.19
	*(an)	+114	+84	+101	+47	+57	+44	+105	+86	+103	+44	+51	+42
	cbSHGC	1.22	1.66	1.34	3.18	2.36	3.13	0.57	0.5	0.45	0.94	0.83	0.93
	*(cb)	+3	-7	-3	-11	-17	-13	+46	+35	+50	+12	+14	+11

* Discrepancy to BSDF results in

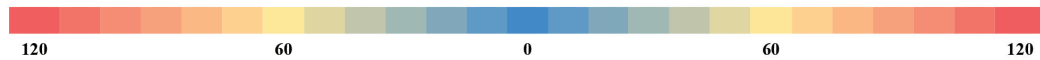


TABLE 4 Comparing the difference of cooling energy results of anSHGC and cbSHGC to BSDF results

6 CONCLUSIONS

External solar shading can help reduce negative impacts of solar gains on a building façade and hence contribute to reducing cooling energy to achieve internal comfort. To quantify the performance of innovative shading designs by means of building performance simulations, precise façade parameters are required for both static and adaptive shading devices.

This work compared three approaches to represent properties of CFS (complex fenestration systems) and their impact on cooling energy results, ranging from simple (single value SHGC or annual SHGC) to more complex interpretation of angular properties (BSDF data). Another method was introduced with a complexity in between annual SHGC and BSDF, which is called climate-based SHGC, and can be derived for any hour of the year for particular solar altitudes and azimuths of a given geographic location. It is possible to establish values for cbSHGC for time-steps as small as hourly values (or more detailed if more detailed data for sun positions are available).

The analysis in this paper showed that cooling energy results for the annual SHGC are up to 2.5 times larger compared to energy demands using BSDF data. The maximum deviation of cbSHGC

results are 1.6 times greater when comparing to BSDF results. Considering that using SHGC for thermal building performance simulation is common practice, the cooling energy results differ significantly from those using transmittance and reflectance (BSDF) to describe the angular properties of a façade system.

This should be borne in mind when the design goal is a zero-energy building. Nonetheless, future building design and performance assessment must be simple yet accurate for designers with non-engineering backgrounds. The present work highlighted the high accuracy of simulation results when using angular-sensitive transmittance and reflectance data. BSDF data are not always available, and may need expert level skills to retrieve necessary information on the shading design. Further, some conventional BPS (building performance software) do not (yet) support the implementation of BSDF files during simulations. On the other hand, relying on SHGC that are measured or calculated at normal incidence (0°) will inevitably lead to energy demands (cooling) that are more than double than what they should be.

The third analysed input parameter was the climate-based SHGC. This value is similar to the conventional SHGC, which is widely used in thermal building simulations. The difference, however, is that it takes other angles than 0° (normal incidence) into account and actually uses solar angles present in the location of interest. Even though the cooling energy results for climate-based SHGC are higher than for BSDF, the errors are much lower as opposed to annual SHGC. Interestingly, the differences in all studied cases are much lower using climate-based SHGC as opposed to results using the annual SHGC at normal incidence in comparison to the BSDF results. This approach may be of help for planners during the early planning stages when high energy standards must be fulfilled, and specialist engineers are not yet involved.

It is important to find ways to quickly assess the performance of a shading design during the early stages of the planning process. Directional and climate-based SHGC may be a sufficient alternative for early design stage performance analyses, despite the differences in cooling energy demands.

Further research shall investigate the suitability of all mentioned methods to assess the energy performance of adaptive shading and to find appropriate shading control strategies. Table 5 summarises typical qualities of the analysed methods to describe parameters for windows with external shadings.

	BSDF	CLIMATE-BASED SHGC	ANNUAL SHGC
COMPLEXITY	high	medium	low
CHARACTERISTICS	+ Most accurate energy results - Advanced user experience to generate BSDF data and to implement BSDF matrix into simulation software	+ multiple values per year + multiple solar angles taken into account +/- medium advanced user skills needed	- single value (at 0° = normal incidence) per annum defines energy flows through the window with shading - neglects realistic solar altitudes and azimuths at a given geographic location + no advanced user skills required
PRECISION OF ENERGY RESULTS	high	medium	low

TABLE 5 Comparison of BSDF, climate-based SHGC and annual SHGC

References

- ASHRAE (2013). 2013. "ASHRAE (2013) ANSI/ASHRAE Standard 55-2013- Chapter 15 - Fenestration."
- Asmail, C. 1991. "Bidirectional Scattering Distribution Function (BSDF): A Systematized Bibliography." *Journal of Research of the National Institute of Standards and Technology* 96(2): 215.
- Berkeley, Lawrence. 2019. "WINDOW 7 User Manual." (March).
- Bueno, Bruno, Jose M. Cejudo-Lopez, and Tilmann E. Kuhn. 2017. "A General Method to Evaluate the Thermal Impact of Complex Fenestration Systems in Building Zones." *Energy and Buildings* 155: 43–53. <https://doi.org/10.1016/j.enbuild.2017.08.055>.
- Bueno, Bruno, Jan Wienold, Angelina Katsifaraki, and Tilmann E Kuhn. 2015. "Fener : A Radiance-Based Modelling Approach to Assess the Thermal and Daylighting Performance of Complex Fenestration Systems in Office Spaces." *Energy & Buildings* 94: 10–20. <http://dx.doi.org/10.1016/j.enbuild.2015.02.038>.
- Curcija, Charlie et al. 2018. "WINDOW Technical Documentation." Windows and Envelope Materials Group, Lawrence Berkeley National Laboratory.
- van Dijk, H.A.L., and H. Oversloot. 2003. "WIS, the European Tool to Calculate Thermal and Solar Properties of Windows and Window Components." *Proceedings of Building Simulation 3*: 259–266. http://www.inive.org/members_area/medias/pdf/Inive%5CIBPSA%5CUFSC885.pdf.
- EQUA. 2013. "IDA Early Stage Building Optimization (ESBO) User Guide." (April): 1–74.
- Fraunhofer. 2018. "FENER." <https://www.ise.fraunhofer.de/de/geschaeftsfelder/gebaeudeenergietechnik/gebaeudehuelle/licht-technik/fener.html> (December 14, 2018).
- Hellström, Bengt, Hasse Kvist, Håkan Håkansson, and Helena Bülow-Hübe. 2007. "Description of ParaSol v3.0 and Comparison with Measurements." *Energy and Buildings* 39(3): 279–83.
- "International Glazing Database." <https://windows.lbl.gov/software/cgdb> (5th November, 2019).
- Kharchi, R. et al. 2012. "The Effect of Solar Heating Gain on Energetic Thermal Consumption of Housing." *Procedia Engineering* 33: 485–91. <http://dx.doi.org/10.1016/j.proeng.2012.01.1228>.
- Klems, J. H. 1993. "A New Method for Predicting the Solar Heat Gain of Complex Fenestration Systems I. Overview and Derivation of the Matrix Layer Calculation."
- . 1994. "New Method for Predicting the Solar Heat Gain of Complex Fenestration Systems - 2. Detailed Description of the Matrix Layer Calculation." *ASHRAE Transactions* 100(1): 1073–86.
- Kohler, Christian, Yash Shukla, and Rajan Rawal. 2017. "Calculating the Effect of External Shading on the Solar Heat Gain Coefficient of Windows." *IBPSA 2017 - International Building Performance Simulation Association*: 8.
- Kuhn, Tilmann E. 2006. "Solar Control : A General Evaluation Method for Façades with Venetian Blinds or Other Solar Control Systems." 38: 648–60.
- . 2011. "Solar Control : A General Method for Modelling of Solar Gains through Complex Façades in Building Simulation Programs." *Energy & Buildings* 43(1): 19–27. <http://dx.doi.org/10.1016/j.enbuild.2010.07.015>.
- Marino, Concettina, Antonino Nucara, and Matilde Pietrafesa. 2017. "Thermal Comfort in Indoor Environment: Effect of the Solar Radiation on the Radiant Temperature Asymmetry." *Solar Energy* 144: 295–309. <http://dx.doi.org/10.1016/j.solener.2017.01.014>.
- McNeel. 2020. "Rhino 6." <https://www.rhino3d.com/de/6/new/grasshopper/>.
- McNeil, Andrew. 2011. "On the Sensitivity of Daylight Simulations to the Resolution of the Hemispherical Basis Used to Define Bidirectional Scattering Distribution Functions." : 1–19.
- Nicodemus, Fred E. 1965. Directional Reflectance and e Missivity of an Opaque Surface.
- Petersen, Steffen, Thea Broholt, Louise Christensen, and Pil Brix Purup. 2018. "Thermal Performance Simulation of Complex Fenestration Systems in the Early Design Stage." *BSO2018 papers* (September): 11–12.
- Robin Mitchell, Christian Kohler, Joe Klems, Mike Rubin, Dariush Arasteh. 2008. University of California WINDOW 6.2/THERM 6.2 Research Version User Manual. Berkeley.
- Robin Mitchell, Mehry Yazdani, Charlie Curcija, Ling Zhu, Stephen Czarnecki. 2019. "COMFEN5- Program for Calculating the Energy Demand and Comfort Impacts."
- Roudsari, M. S. 2020. "Honeybee." <https://www.food4rhino.com/app/ladybug-tools>.
- Standard, International. 2006. "ISO 15099." 2006.
- US Department of Energy. 2013. "EnergyPlus Engineering Reference The Reference to EnergyPlus Calculations."
- Wall, Maria, and Helena Bülow-hübe. 2001. Report TABK--01/3060 Solar Protection in Buildings -01/3060. Lund.
- Wall, Maria, and Helena Bülow-Hübe. 2001. "Solar Protection in Buildings." *Building Design*: 192.
- Wall, Maria, Maria Wall, and Helena Bülow-Hübe. 2003. Solar Protection in Buildings. Report EBD. Lund: Lund University.
- Ward, G., M. Kurt, and N. Bonneel. 2012. "A Practical Framework for Sharing and Rendering Real-World Bidirectional Scattering Distribution Functions." (September): 24.

Comparison of BSDF, Climate-based SHGC and Annual SHGC

Deepak Singh Dhama¹, Daniel Arzmann²

- 1 Technische Hochschule Ostwestfalen-Lippe, Emiliestraße 45, 32756 Detmold; +49 1782103167; deepaksinghdhama2002@gmail.com
- 2 Schüco International KG, Karolinenstraße 1-15, 33609 Bielefeld, +49 15119528237; darzmann@schueco.com

Abstract

The global direct and indirect CO₂ emission contributed by the building and construction sector amounts to 40% (GlobalABC, IEA & United Nations, 2019). It is again responsible for 36% of the global energy consumption (IEA, 1974). One of the main reasons is that the building uses artificial climatization systems to achieve human comfort, i.e. thermal comfort. Another comfort related factor is the quality of air inside the building, which is crucial for human health, productivity and for reducing the risk of Sick Building Syndrome. It is estimated that an average citizen spends about 90% of the day inside a building (ENERGY STAR, 2007). In comparison, air-conditioned buildings show a higher prevalence ranging from 30-200% of sick building syndrome (SBS) symptoms as compared to the naturally ventilated ones (Seppanen & Fisk, 2002). In addition to that, natural ventilation is one of the most common technique to reduce the energy consumption of buildings with a reduction up to 10-30% (Walker, 2016). Mechanical systems are consistently being outperformed by natural ventilation systems (NVS) in terms of SBS and associated symptoms (Krtati, 2018).

This research focuses on the design and performance evaluation of an optimized ventilation panel for unitized façades with adjustable air inlet openings to control natural ventilation and air distribution. It outlines the basic principles, considerations and concepts adopted for the design and simultaneously addresses the effectiveness of different ways of ventilation and standards. Additionally, this study also describes the major classification of a ventilation system based on natural forces. The optimized ventilation panel is a double layer system integrated into one unit. The outer unit acts as a solar protection device with adjustable ventilation openings, controlled by sensors and actuators that optimizes the wind volume and velocity for natural ventilation purposes. To evaluate the system's ventilation performance, a room of standard size (Bhatia, 2014) for the wind simulations has been taken with maximum fin opening and three varying internal air inlet designs i.e. with no window, side operable and parallel projecting. The unit has been analysed through virtual wind tunnel simulation using RWIND software. The proposed fin design concept is capable of capturing wind flow successfully. The 45° fin inclination to the façade provides maximum fresh air intake with balanced solar shading fin depth. All the options provide enough air velocity inside the room for cross-ventilation utilizing the Venturi effect. The third option with a parallel projecting window is the most suitable and preferable in terms of air velocity and distribution.

Keywords

CO₂ emission, sick building syndrome (SBS), natural ventilation system (NVS), optimized ventilation panel, façade design, RWIND

1 INTRODUCTION

1.1 BACKGROUND

These days it is common to see buildings that have artificial climatization systems, which in many cases could be avoided. HVAC systems are often installed in buildings where good natural ventilation would have been sufficient to obtain a comfortable indoor climate and good air quality. The comfort standards vary as per the type of building i.e. residential or commercial (Prinsegate Chartered Surveyors, 2018). Sick Building Syndrome and associated symptoms are the major demerits of using artificial climatization systems. The acceptable thermal comfort for buildings with standard mechanical HVAC systems is significantly lower than the buildings with natural ventilation systems (Dear & Brager, 2002). It can provide convective and evaporative cooling of the human body. The sweat evaporation rate is higher if the speed of air ventilating a space increases. A comfort level of 27°C can be achieved with air movement of 1m/s through a space at 30°C. In general, an airspeed of 3 m/s is enough to ventilate the space comfortably. The upper recommended air velocity in offices is 1.5 m/s. Natural ventilation due to thermal difference allows a significant air exchange rate (5-25 arc/h) for heat removal with minimal operation costs (Guedes, 2013). Usage benefits of natural ventilation include:

- 1 Fresh air introduction for odour and carbon dioxide dissipation
- 2 Fire control/ smoke clearance
- 3 Heat dissipation/ cooling
- 4 Provision of oxygen for fuel-burning devices
- 5 Control of inner humidity (Inside the space)

A theoretical case study of an existing office building in Wolfsburg, Germany, is developed in order to prove the concept. The entire research process has been divided into two phases: design and evaluation. The first part involves redesigning of existing façade considering sustainable development using all possible passive measures. This paper focuses mainly on utilizing wind for natural ventilation using an optimized ventilation panel for unitized façades.

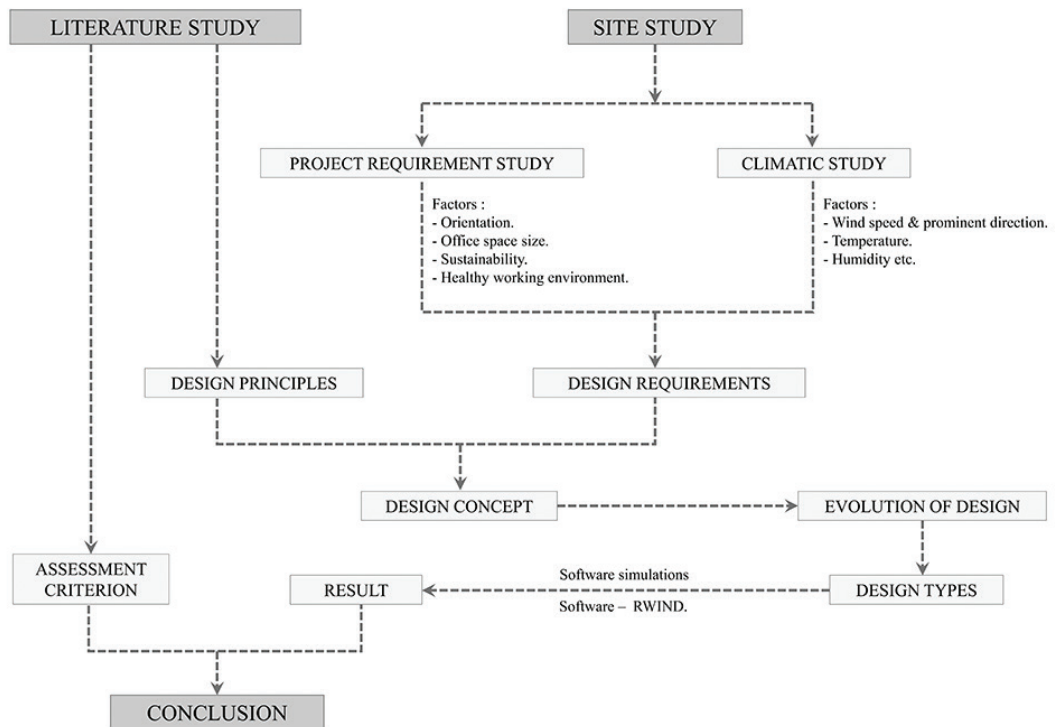


FIG. 1 Schematic research process

1.2 LIMITATION

- 1 The optimized ventilation panel has been proposed for areas with higher wind speeds (Refer to section 5.1).
- 2 All the simulations have been done using the maximum wind speed of the area i.e. 25 m/s. Case 1 has also been tested for a basic wind speed of 1m/s.
- 3 The simulations do not take into account the air movement due to temperature difference between the internal and external environment.

2 LITERATURE REVIEW

2.1 HUMAN COMFORT

The main human comfort categorization is thermal comfort, visual comfort, auditory comfort, olfactory comfort and hygienic comfort. Temperature is a key component to the experience of comfort in a space. The internal metabolic processes in human beings operate on a temperature range much smaller than outer temperatures. The dissipation of heat in this process due to human body metabolism must be released to surroundings. It varies from person to person, and it depends on various factors like genetics, sex, seasonality, diet etc. People may feel more overheated or warm, and this process becomes more difficult when the external temperature is high. A balanced external temperature in relation to the human body is required for a smooth heat release. Various other factors which add up to thermal comfort include room temperature, relative humidity, air velocity, cloth insulation and colour of the space (Warren & Boduch, 2009) (Attila, 2019).

Human perception of thermal comfort depends on other aspects rather than just air temperature. The mean radiant temperature entails averaging the temperatures of each surface in the room. Combined with the air temperature, this produces an overall measure, the mean operative temperature. In addition to this, the closeness of the human body to a particular surface also affects the overall experience. If the temperature of a ceiling hikes by 5 °C than the rest of the surfaces in a room, a person feels warmer, and if it goes down by 14 °C, then it feels colder. Similarly, if the temperature of a wall increases by 23 °C than the other surfaces, a person feels warmer, and if it drops by 10 °C then it feels colder. A sense of discomfort can be felt with the difference in temperature within a room or across the human body. As seen in Figure 2-A, a vertical air temperature difference from our feet to our head shouldn't exceed 3 °C, otherwise the high temperature gradient highlights one part of the body as feeling notably warmer or colder than the other.

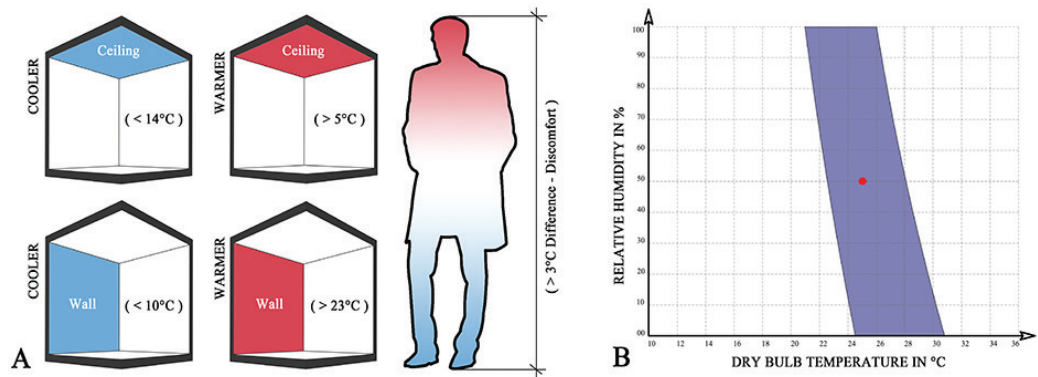


FIG. 2 A – Allowable temperature variances (Warren & Boduch, 2009) & B – Human comfort zone (Attila, 2019).

Relative humidity plays a large part in conjunction with temperature to provide a sense of discomfort. High levels of relative humidity can work against the evaporative cooling effects of sweating and leave the body prone to overheating. Further, high levels of relative humidity in inclement winter weather produce a greater sense of cold. The human body cannot perceive differences in relative humidity levels within the range of 25% and 60%, which is the primary reason that this range is often cited as the baseline. When the humidity is too high, the moisture from the skin does not evaporate, and it gives an uncomfortable feeling. In case the humidity is too low, skin and mucous surfaces become drier, leading to complaints about dry nose, throat, eyes, and skin. It exacerbates the situation of eye strain due to working in an office with a computer.

Air velocity also plays an important role in the perception of temperature. It helps the human body through evaporative cooling. Mechanisms of convection can further move the heat generated by metabolic processes from the skin into the surrounding air. This leads to continued cooling, and the process is more effective at higher air velocity. Generally, airflow slower than 100 feet per minute (0.5 m/s) feels either pleasant or goes unnoticed. The flow of air higher than that within an enclosed space can provoke distraction (up to 200 fpm or 1 m/s) and annoyance (above 200 fpm).

In terms of colour perception, experiments have revealed that the rooms painted in hues between blue or green can feel colder than rooms with red or orange walls by as much as 3 °C (Warren & Boduch, 2009).

2.2 NATURAL VENTILATION.

It is the process of exchanging air between the outside and inside of a building. This can broadly be classified into two categories depending on the type of natural forces. Wind-driven ventilation & stack effect, the former is created by the pressure difference around the building and the latter is governed by the principle of temperature difference (Efficient Windows Collaborative, 2000). Figure 3 shows the various ways in which ventilation through a space can happen. Table 1 shows the efficiency of opening for each case. Table 1 shows the efficiency of opening for each case.

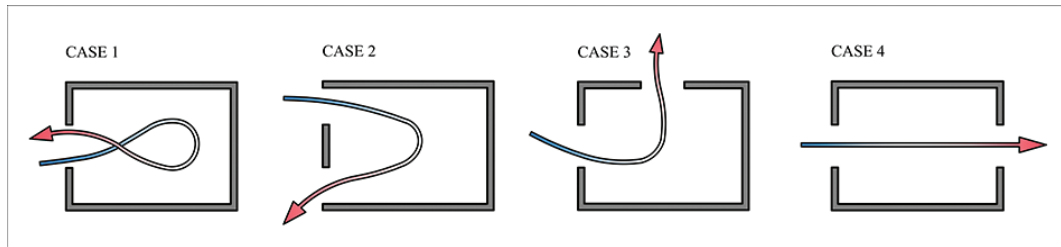


FIG. 3 Types of cross-ventilation possibilities (Efficient Windows Collaborative, 2000)

OPENING HEIGHT AS A FRACTION OF WALL HEIGHT		1/3		
OPENING WIDTH AS A FRACTION OF WALL HEIGHT		1/3	2/3	3/3
Case 1	Single opening	12-14%	13-17%	16-23%
Case 2	Two openings in the same wall	-	22%	23%
Case 3	Two openings in adjacent walls	37-45%	37-45%	40-51%
Case 4	Two openings in opposite walls	35-42%	37-51%	47-65%

TABLE 1 Natural ventilation efficiency of openings (Efficient Windows Collaborative, 2000)

Table 1 describes the natural ventilation efficiency of opening proportions as a fraction of wall height and width in terms of its most probable position on different walls. The opening height has been taken consistently as one third, and it has been correlated with three opening width proportions. This provides an understanding of opening efficiency under each size and type.

Natural ventilation achieved through temperature difference can reach the human comfort level when the inside temperature is higher than the outer temperature, and the external diurnal temperature fluctuates by 10 °C or less (Guedes, 2013).

2.3 ABOUT RWIND

RWIND is a virtual wind tunnel software for product designers, engineers and architects. The parent company is Dlubal Software. It models the airflow around design concepts to help test ideas early in the development stage with precision. This software supports .stl and .vtp file formats as input. It is a powerful CFD simulation tool that reads minute openings. It automatically does meshing for the input 3D finite volume. It uses Open-FOAM numerical solver and it is widely used for CFD simulation (Dlubal Software GmbH, 2020). The software can be learned with the manual given on the software and website. A demo version of this software for 30 days is available on the Dlubal website. They don't provide a student version.

3 METHODOLOGY

3.1 SITE STUDY AND DESIGN REQUIREMENTS.

The project presents the case study of an office building in Wolfsburg, Germany, whose front façade faces south. The project basically focuses on renovating the entire façade using a unitized façade system. The prominent wind direction for the location is west. An ample share of office buildings faces prominent wind direction, and it has the potential of using natural ventilation for reducing HVAC loads. The site falls in wind zone 2 with a basic wind speed and velocity pressure of 25m/s and 0.39 kN/m², respectively (Dlupal, 1987). The office depth in wind direction on the second floor is around 17.5 m. The office aims at providing a healthy working environment to workers, and at the same time, it also emphasizes the sustainability aspects. The minimum and maximum temperature for the location is -7°C (December) and 27°C (July). The average humidity of the area is 75% which can be considered on higher side (World Weather Online, 2020). The south façade receives the maximum solar radiation, whereas the west façade takes the second position. The optimized unitized ventilated panel needs to be designed in such a way that it cuts solar radiation, and at the same time, it also allows fresh air movement for natural ventilation.

3.2 CRUCIAL DESIGN CONSIDERATIONS AND ASSESSMENT CRITERION.

The entire designing process needs a set of guidelines that could help to reach an optimal solution. The following are the standards:

- 1 In general, 5% of the floor area of the space is required for natural ventilation.
- 2 Cross ventilation is the best effective way which yields an efficiency up to 65% (Efficient Windows Collaborative, 2000).
- 3 The volume of airflow is maximum when it hits the façade at 90 degrees.
- 4 The coefficient of effectiveness depends on the wind angle and the relative size of entry and exit openings. It ranges from about 0.4 for wind hitting opening at 45° of incidence to 0.8 for winds hitting directly at 90° angle (Walker, 2016).
- 5 For offices (open-plan offices or private office), required outdoor air supply ranges from 8.5 - 10 L/s (ASHRAE Standard 62-2001, 2003) (NCBI, 1988).
- 6 For effective cross ventilation, the depth of the room should not exceed five times the height of the room (Bhatia, 2014).
- 7 Preferable room height is 2.7 m (WindowMaster, 1990).

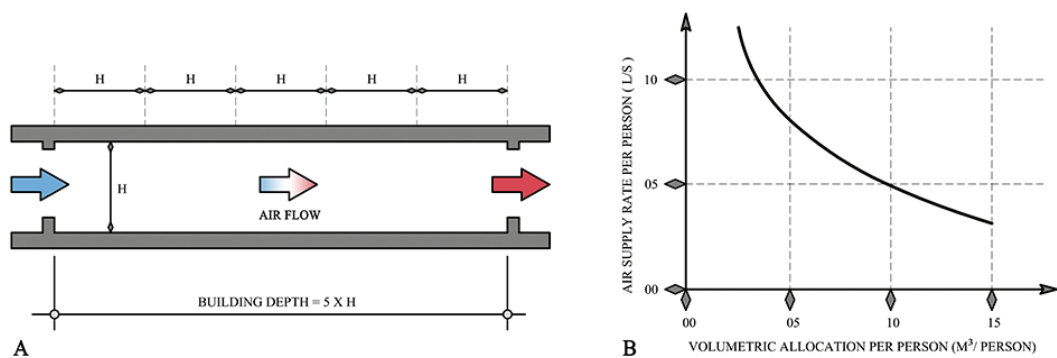


FIG. 4 A – Standard for cross ventilation; B – Air supply rate for odour removal

3.3 DESIGN CONCEPT

The panel consists of glazed unit and automated projecting fin. Figure 5 (A) shows the position of the fin (plan) in the closed and open position. The fin acts as a kinetic façade with actuators helping it to close and open. The forward movement of fins results in increased length, thus creating a larger shadow on the glass panel, and it also allows air to flow inside the space at the same time. An operable window has been placed inside the fin for controlling the air movement (second barrier). It could be a standard, sliding, bottom-hung or parallel projecting window.

The fin has a dual function. Figure 5 (B) shows the relationship between the catchment area of air and the solar shading length of the vertical fin. The 45° inclination of the fin to the façade provides an ideal or balanced condition where the catchment width is equal to the solar shading depth of the fin.

In terms of detailing, the complete fin is an external identity that can be fitted to the unitized panel once the panel is installed on-site. The unitized panel leaves necessary supporting members so that the entire unit of automated fin could be fitted later in the construction stage. The whole fin module consists of 7 vertical fins/louvres, which have been designed for smooth interlocking. Three fins out of 7 don't move, and they have been placed as on the vertices of an isosceles triangle. They have been fixed to a specially designed triangulated base plate having channels for fins to slide with the help of rollers. The three fixed fins basically provide stability to the structure, thus it makes the installation of the fin unit quite easy and precise. The actuators have been attached to the top and bottom for uniform movement controlled by a central operating device and sensors.

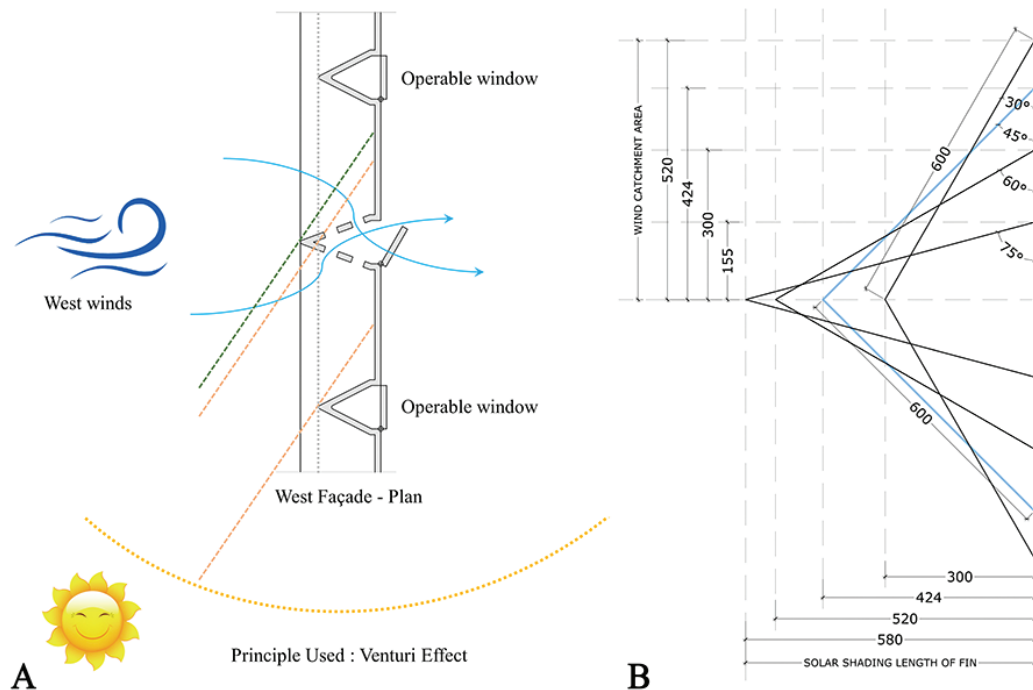


FIG. 5 A – Fin concept; B – Fin inclination optimization

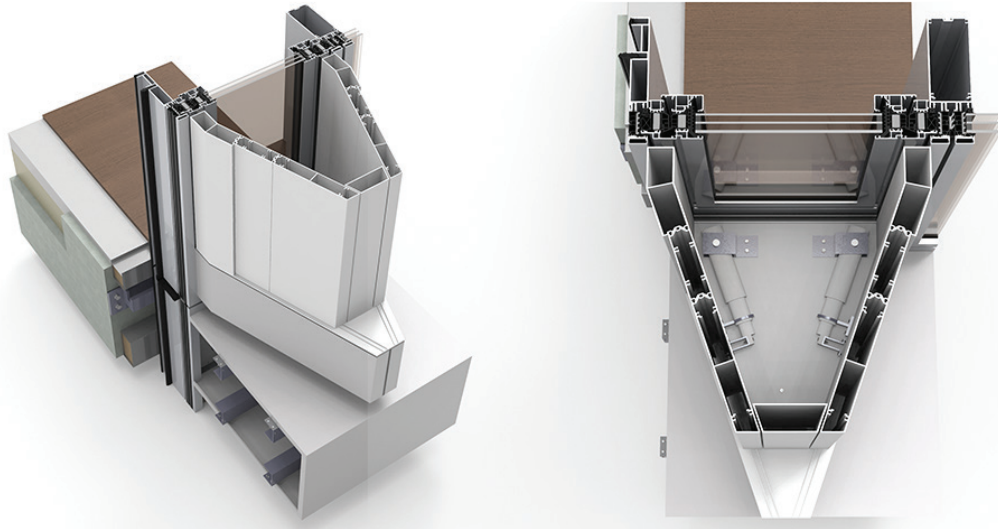


FIG. 6 3D views - Optimized ventilation unitized panel with internal adjustable opening

4 EXPERIMENT

4.1 MODEL DIMENSION – IDEAL ROOM SIZE FOR WIND SIMULATION

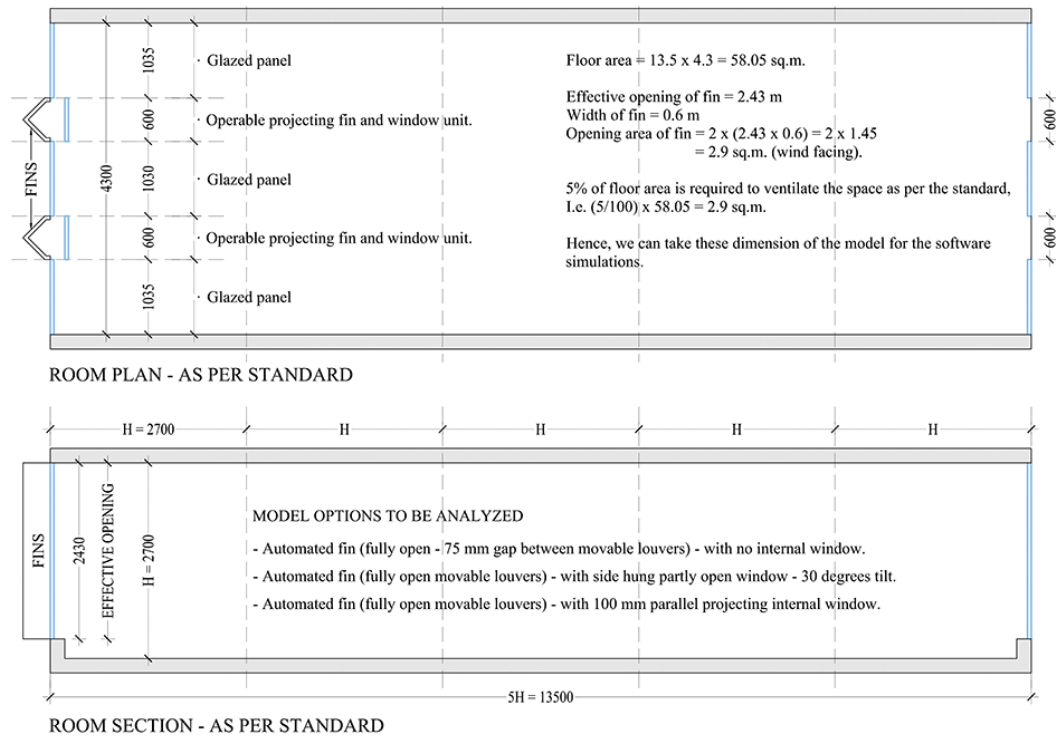


FIG. 7 Ideal room size for wind simulation concerning natural ventilation as per standards

The room size has been designed, keeping in mind the natural cross-ventilation design considerations. The maximum allowable depth of the room can go up to five times the height of the space, and the openings for ventilation should be 5% of the total floor area of the space.

The opening type falls under case 4 of natural ventilation efficiency. It does not follow the same proportions given in Table 1 as the simulation proportions have been derived from the design intent. If we compare the actual opening size of the model to the proportions given in the table, then it falls approximately between the second and third width proportion category. The natural ventilation efficiency of the reference model should lie in the range of 37-65 %.

4.2 SOFTWARE CONSIDERATIONS FOR WIND SIMULATION

The software used for the simulation is RWIND by Dlubal Software, and the main motive of the entire process is to analyse wind distribution and wind speed inside standard space by varying opening of fins and using different types of internal windows. The model will be analysed in a virtual wind tunnel setup, and the following figures show the size of the wind tunnel in relation to the model (as per the default setting of the software).

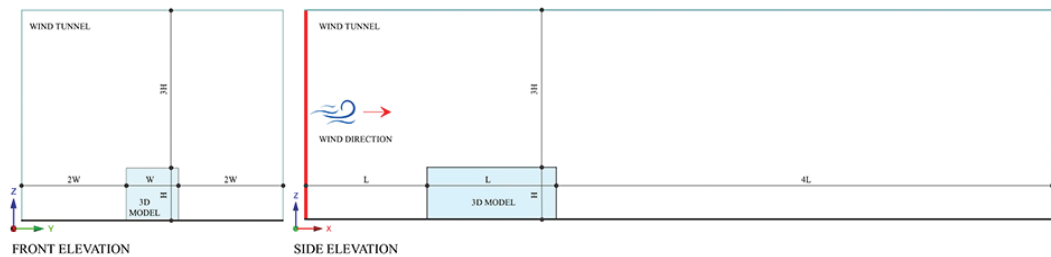


FIG. 8 Wind tunnel proportions with respect to the 3D model to be analysed

5 RESULTS

5.1 AUTOMATED FIN (FULLY OPEN – 75MM GAP BETWEEN MOVABLE LOUVRES) - WITH NO INTERNAL WINDOW

The fully open fins allow a good amount of air to come in, and the air rushes through the slits. Figure 9-A shows the occurrence of the Venturi effect as a hike in air velocity can be noticed when it passes through the narrow spaces in the vertical fins. A hike of 11 units from 13 m/s can be noticed in that area. The approaching wind loses its velocity from 25 m/s to 13 m/s as it hits the façade or obstruction. This results in increase in wind pressure on the façade as per the conservation of energy and Bernoulli's principle (NASA, 2010). The façade face line is the point where two physical phenomena occur i.e. the first is the decrease of wind velocity, and the second is the Venturi effect. The air from both sides of the fin converges and it increases the velocity of air up-to approximately 14 m/s (maximum for the mid interior volume). The wind speed drastically drops as it reaches the façade, and it results in an increase in wind pressure. This analysis has been done for the basic wind speed that the façade receives i.e. 25 m/s. The analysis shows an upsurge in the direction of the air movement as it travels through the interior space. The outlet velocity of the air in this case is 12 m/s. It is quite high, and air speed can indeed be controlled by varying the fin openings. The façade certainly needs an inner control system which could help to regulate the velocity of the air coming

inside from the external fins. The design works successfully in terms of air circulation and cross ventilation. All the simulations have been carried out by keeping the standard 3D room model at ground level. The maximum indoor and exit velocity for 1m/s basic wind speed is 0.76 m/s and 0.48 m/s, respectively. The mid interior space attains an air velocity of 0.47 m/s, which is almost similar to the velocity of air leaving the space from the opposite direction.

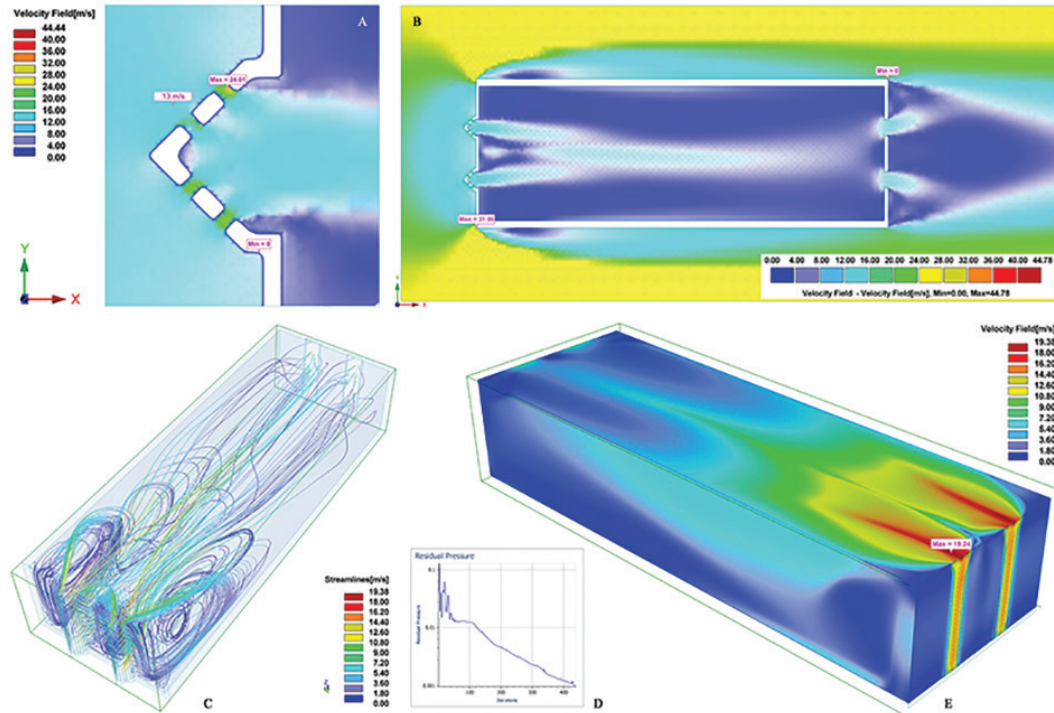


FIG. 9 A – Venturi effect; B – Velocity field diagram at 2 m height; C – Streamlines representation of wind flow; D – Residual pressure graph & E – Volumetric velocity field representation with maximum internal value

5.2 AUTOMATED FIN (FULLY OPEN) - WITH SIDE HUNG INTERNAL WINDOW - 30° TILT

The side-hung internal window diverges the airflow in one direction, thus creating a bulk stream of air movement on one side. This creates a narrow stream of air movement with higher air velocity, which could significantly disturb the interior in terms of air movement. The velocity of air for mid-volume of the interiors is approximately 16 m/s, and it shows an average velocity of around 12 m/s even for the rear quarter portion of the interior volume. This option does not provide the desired distribution of air movement for the interiors.

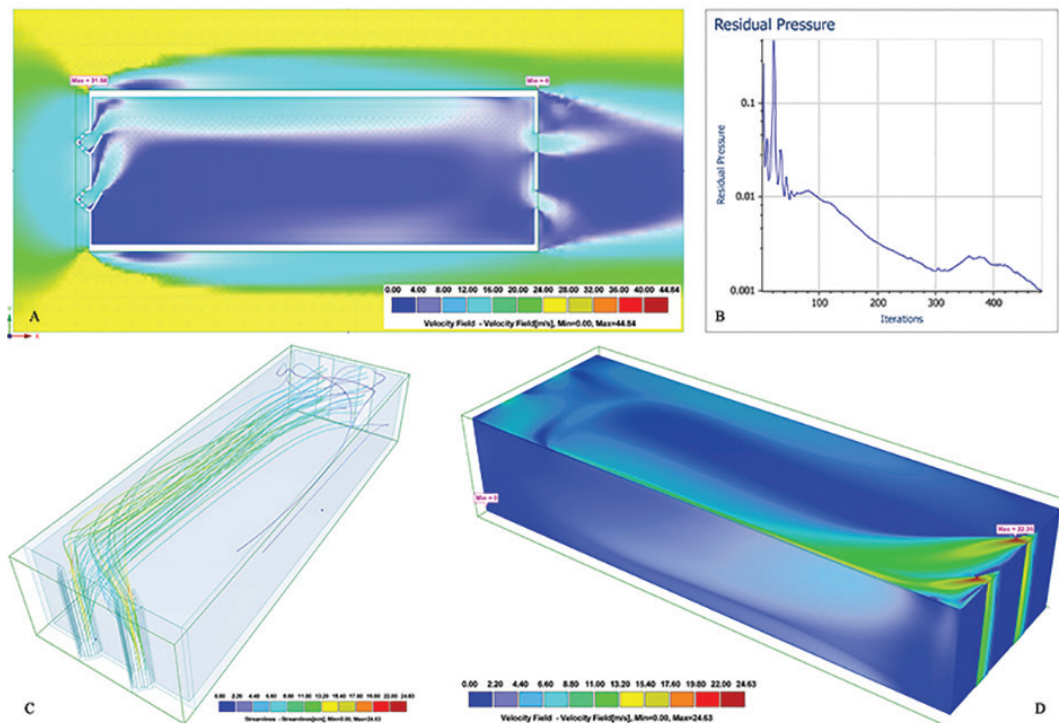


FIG. 10 A - Velocity field diagram at 2 m height; B - Residual pressure graph; C - Streamlines representation of wind flow & D - Volumetric velocity field representation with maximum internal value

5.3 AUTOMATED FIN (FULLY OPEN) - WITH PARALLEL PROJECTING INTERNAL WINDOW – 100MM (CLEAR DISTANCE)

The parallel projecting internal window diverges the airflow sideways in both directions, thus distributing the pressure equally on either side. Figure 12-A shows the three-way distribution of air by two window modules. The air from both the windows merges at the centre, and this effect helps in minimizing higher wind speed due to the Venturi effect. It avoids the direct flow of air into the interiors. The mid interior volume receives a maximum velocity of 12 m/s, but it exists on the upper level of the interior space. The distribution of air is even as compared to the previous options. There is a slight turbulence near the window, which can be controlled by regulating the opening of external fins and adjusting the projection of the internal window. The outlet air velocity, in this case, is 9 m/s. The residual pressure in this case reaches the desired value of 0.001 after approximately 450 iterations.

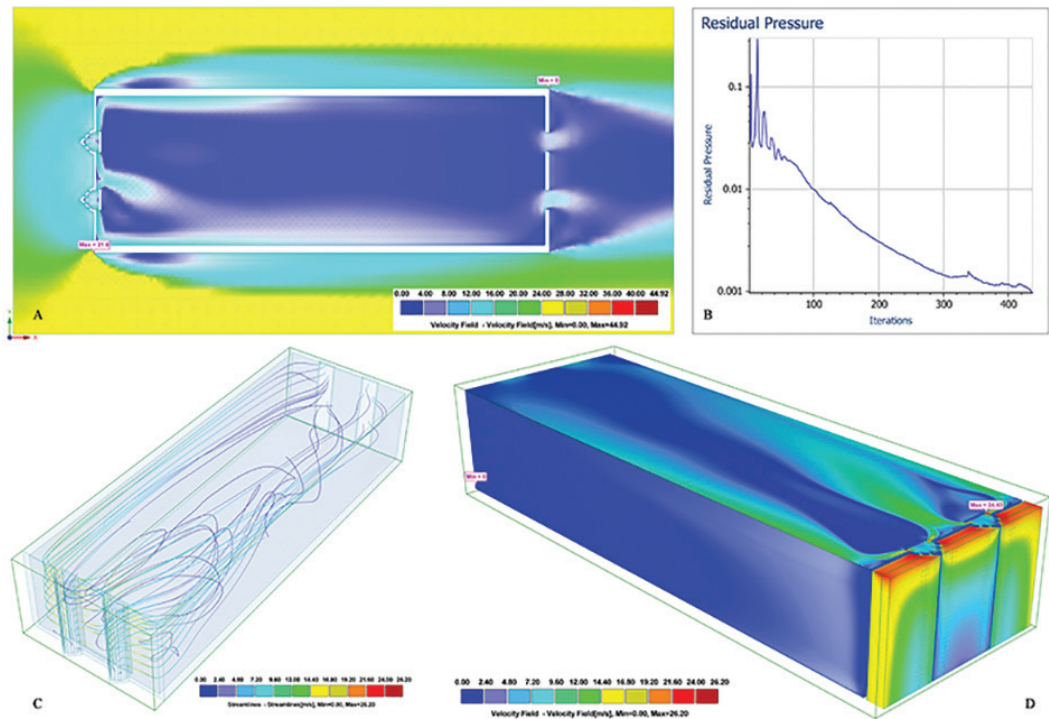


FIG. 11 A - Velocity field diagram at 2 m height; B - Residual pressure graph; C - Streamlines representation of air movement & D - Volumetric velocity field representation with maximum internal value

6 CONCLUSIONS

The proposed optimized ventilation panel design concept for unitized façade shows successful results in terms of capturing the wind flow. The 45° fin inclination to the façade provides the maximum intake possibilities of fresh air with a balanced solar shading depth of vertical fins. The wind velocity drops considerably as it strikes the façade, which results in an increase in wind pressure. The movement of air particles from larger space (outside) to the office interior through narrow space between the fins help to maintain the consistency of air velocity (Venturi effect). The velocity in the fin gaps rises to compensate for the external air pressure. All the options provide enough air velocity inside the room for cross-ventilation. The third option with a parallel projecting window is the most suitable and preferable in terms of air velocity and distribution.

The entire experiment leaves a scope of exploring the airflow inside the standard space using all possible window types like top hung, bottom-hung etc. It would also be interesting to know the effect of wind when it strikes the façade with some incident angle (perpendicular in this case). In addition to this, the efficiency of the proposed system could also be analysed in terms of all four possibilities of natural ventilation. Apart from that, mechanical simulation software can also be deployed to analyse the capacity of actuators needed for smooth fin movement under allowable wind loads. Furthermore, it can also be analysed from the perspective of acoustics as it may produce noise due to air movement at higher wind speed through narrow fin openings. It also leaves an opportunity to explore the lower limit of wind velocity up to which the system works effectively. Lastly, the entire panel can also be evaluated for structural stability under different live loads.

Acknowledgements

Alvaro Balderrama, Prem Singh Dhami, Nisha Dhami, Stefan Hoffmann (Dlupal Software)

References

- ASHRAE Standard 62-2001. (2003). Ventilation for Acceptable Indoor Air Quality. Atlanta: Standing Standard Project Committee. Retrieved on 18. July 2020 von https://www.ashrae.org/File%20Library/Technical%20Resources/Standards%20and%20Guidelines/Standards%20Addenda/62-2001/62-2001_Addendum-n.pdf
- Attila, F. (06. June 2019). Where to Place Ventilation for Maximum Comfort in a Building. Retrieved on 12. July 2020 from SIMS-CALE: <https://www.simscale.com/blog/2017/10/ventilation-for-maximum-comfort/>
- Bhatia, A. (2014). HVAC – Natural Ventilation Principles. Createspace Independent Pub. Retrieved on 08. July 2020 from <https://www.cedengineering.com/userfiles/HVAC%20-%20Natural%20Ventilation%20Principles%20.pdf>
- Dear, R. J., & Brager, G. S. (2002). Thermal comfort in naturally ventilated buildings: revisions to ASHRAE Standard 55. *Energy and Buildings*, 34, 549–561. Retrieved on 04. July 2020 from https://www.sysecol2.ethz.ch/OptiControl/LiteratureOC/Dear_02_EB_34_549.pdf
- Dlupal. (1987). WIND LOAD | EN 1991-1-4 | DIN EN 1991-1-4. Retrieved on 25. July 2020 von Dlupal: Structural Analysis and Design Software: <https://www.dlupal.com/en/load-zones-for-snow-wind-earthquake/wind-din-en-1991-1-4.html#¢er=52.54308206403791,10.720628131250018&zoom=6&marker=52.4226503,10.7865461>
- Dlupal Software GmbH. (2020). RWIND Simulation. Generation of Wind - Induced Loads on General. Tiefenbach, Germany: Dlupal. Retrieved on 25. July 2020 von <https://www.dlupal.com/-/media/B8828DD3F8ED48FDAA7BB9F82681B724.ashx?mld=B-8828DD3F8ED48FDAA7BB9F82681B724>
- Efficient Windows Collaborative. (2000). Design Considerations: Provide Fresh Air (Improving Ventilation). Retrieved on 14. July 2020 from Efficient Windows Collaborative: https://www.efficientwindows.org/design_ventilation.php
- ENERGY STAR. (2007). Mechanical Ventilation: Breathe Easy with Fresh Air in the Home. ENERGY STAR® A US Environmental Protection Agency. Retrieved on 20. July 2020 von https://www.energystar.gov/ia/new_homes/features/MechVent_062906.pdf
- GlobalABC, IEA & United Nations. (2019). 2019 global status report for buildings and construction: Towards a zero-emission, efficient and resilient buildings and construction sector. IEA and the United Nations Environment Programme. Retrieved on 17. July 2020 from <https://wedocs.unep.org/bitstream/handle/20.500.11822/30950/2019GSR.pdf?sequence=1&isAllowed=y>
- Guedes, M. C. (2013). Sustainability, Energy and Architecture: Case Studies in Realizing Green Buildings. Academic Press. Retrieved on 04. November 2020 from <https://www.sciencedirect.com/topics/engineering/natural-ventilation>
- IEA. (1974). Buildings: A source of enormous untapped efficiency potential. Retrieved on 20. May 2020 from IEA: The International Energy Agency: <https://www.iea.org/topics/buildings>
- Krarti, M. (2018). Natural Ventilation. In M. Krarti, Optimal Design and Retrofit of Energy Efficient Buildings, Communities, and Urban Centers. Elsevier Science. Retrieved on 18. July 2020 from <https://www.sciencedirect.com/topics/engineering/natural-ventilation>
- NASA. (2010). Principles of flight: Bernoulli's Principle. MUSEUM IN A BOX. NASA. Retrieved on 03. November 2020 from https://www.nasa.gov/sites/default/files/atoms/files/bernoulli_principle_k-4.pdf
- NCBI. (04. November 1988). Basic concept of ventilation flow rate. Retrieved on 20. July 2020 from NCBI: <https://www.ncbi.nlm.nih.gov/books/NBK143289/>
- Prinsegate Chartered Surveyors. (14. December 2018). Mechanical ventilation: Essential in commercial buildings? Retrieved on 03. July 2020 from Prinsegate Chartered Surveyors: <https://prinsegate.com/blog/mechanical-ventilation-essential-in-commercial-buildings/>
- Seppanen, O., & Fisk, W. J. (June 2002). Association of ventilation system type with SBS symptoms in office workers. Retrieved on 01. July 2020 from NCBI: National Centre for Biotechnology Information: <https://www.ncbi.nlm.nih.gov/pubmed/12216473>
- Walker, A. (08. February 2016). Natural Ventilation. Retrieved on 17. July 2020 from WBDG: Whole Building Design Guide: <https://www.wbdg.org/resources/natural-ventilation>
- Warren, F., & Boduch, M. (2009). Standards of human comfort: relative and absolute. Austin: The University of Texas at Austin. Retrieved on 08. July 2020 from <https://repositories.lib.utexas.edu/handle/2152/13980>
- WindowMaster. (1990). How to Design for Natural ventilation : Geometry of space. Retrieved on 20. July 2020 von WindowMaster: <https://www.windowmaster.com/solutions/natural-ventilation/natural-ventilation-design-guidelines>
- World Weather Online. (2020). Wolfsburg Monthly Climate Averages: Cloud and Humidity. Retrieved on 16. July 2020 from World Weather Online: <https://www.worldweatheronline.com/wolfsburg-weather-averages/niedersachsen/de.aspx>

Effects of Phase Change Materials on Heat Flows Through Double Skin Façades



Thomas Wüest*¹, Lars O. Grobe¹, Andreas Luible¹

* Corresponding author, thomas.wueest@hslu.ch

¹ Lucerne University of Applied Sciences and Arts, Institute of Civil Engineering IBI, Switzerland

Abstract

The potential of exemplary organic and inorganic Phase Change Materials (PCMs) as façade integrated storage is tested. The impact of two PCMs on heat flows is assessed in comparison with water and concrete. The simulation study employs a transient Modelica simulation model of a test cell featuring the Solar Energy Balanced Façade (SEBF). It is shown that, when compared to water, PCMs of identical volume change the seasonal energy balance in winter and summer by only $\pm 4\%$. Other than water, the PCMs maintain this effect even if the storage volume decreases. Due to spatial constraints, this can support the integration of thermal storage in façade design considerably. Preliminary results indicate that designing thermal storage in façades with PCMs must not only consider the latent heat storage capacity, but also take into account the combined effects of latent heat capacity, melting point, conductivity, and dead load. The application of PCMs promises to foster the integration of the technology of SEBF into façades, but the necessary deliberate selection of, and design with, PCMs requires further research.

Keywords

Thermal storage, passive solar façade, Trombe wall, phase change materials, solar-energy balanced façade

DOI 10.7480/jfde.2021.1.5408

Effects of Heat Transfer Systems on Comfort and Energy Demand

David Bewersdorff¹, Carina da Silva², Ulrich Knaack³

- 1 TU Darmstadt Germany, Martinstr. 46, 64285 Darmstadt, +496151/3926216, +496151/1623010 DavidBwd@online.de
- 2 TU Darmstadt Germany, Conrad-Rehrich-Str. 3, 64850 Schaaheim, +491778474277, +496151/1623010, dasilva@ismd.tu-darmstadt.de
- 3 TU Darmstadt Germany, Franziska-Braun-Straße 3, 64287 Darmstadt, +496151/1623013, +496151/1623010, knaack@ismd.tu-darmstadt.de

Abstract

The evaluation of different façade qualities and conditioning concepts combined in an early stage requires realistic and holistic building inputs in simulation programs. Energy demand values need to be estimated, the comfort for building users should be simulated, and refurbishment measures can be planned. This paper shows different depths of evaluation by variable use of simulation techniques to minimise the necessary simulation effort. As a result, reference points for combinations of façade qualities and heat transfer strategies are given.

Keywords

CFD, energetic simulation, early-stage simulation, heat transfer systems, façade qualities, conditioning systems

1 INTRODUCTION

Fast and accurate estimation of energy requirements is crucial for a successful and satisfying planning process. Climate simulations can be used to determine consumptions realistically and test energy-efficient buildings with comprehensive technology concepts. This requires extensive and time-consuming input of detailed data. In plant engineering, there is often a lack of more precise inventory data. Their input into the model for each zone is very complex. Especially for the heat transfer systems in the zone, the orientation, power output and size must be modelled exactly, which has an effect on the demand values. It is also questionable how realistic the default values of standards are and which energetic difference a variation would make.

The effects of different conditioning strategies and their influence on energy demand are often in question. The aim is to simplify and increase the realism of quick estimations of energy demand and their influence on the user comfort. It is of enormous importance to understand the interrelationships and interactions between conditioning systems (heating), façades and the building user.

Since an estimation of the energy demand is of great importance, it must be investigated whether a detailed and thus time-consuming input of individual transfer strategies is necessary in order to estimate the energy demand and to improve user comfort.

Usually, energetic demands are calculated via normative static calculations. Comfort is just measured by minimal values for heat transfer coefficients. These calculation methods often do not justify innovative façade and transfer concepts in particular, since calculation approaches and characteristic values rarely exist for them. Additionally, both components are becoming increasingly dynamic and technical. Already in today's standardisation, for example, simulation calculations of the summer thermal behaviour of double façades are provided in the standards, but this represents only a small part of the normative building certificates for the time being. Other evaluations are often static like the German DIN 18599 (DIN, 2018) and are known to deliver certain deviations of the requirement values. (Knissel & Loga, 2006) They also don't fit today's planning processes anymore, especially regarding BIM implementation and holistic approaches. For the preparation of the design planning, most of the people involved in the planning process already require extensive information about the envelope quality and the planned plants, although many concepts are still being considered in this phase. A simulation with consolidated assumptions at a low level of detail can provide a good start to the design process and will evolve over time.

2 METHODOLOGY

The basic goal is a simulation of a whole project within the software IDA ICE from EQUA. It is capable of evaluating energetic and comfort-oriented benchmarks in one run. For an easy start in every project, the influence of different façade standards, room placements in the building, orientation in the room and their dependence are examined in IDA ICE.

Comfort factors are used according to DIN EN ISO 7730 (E. I. DIN 2006) after investigations of Ole Fanger (Fanger 1972) established evaluation system. For this purpose, two quantities are used for evaluation, whereby the PMV (Predicted Mean Vote) is a temperature evaluation between cold (- 3) and hot (+ 3). A zero-rating is thermally optimal, even though, according to Mayer (Mayer 1998), the comfortable optimum is + 0.4. From the PMV, a percentage can be derived, which considers the general dissatisfaction with the considered thermal state, the PPD (Predicted Percentage of Dissatisfied). The general dissatisfaction is at least 5 %, with some sources assuming values of

up to 16 %. This type allows evaluating special room situations for a certain time and specific room-position. It is suitable for special analysis but no good representation for a quick evaluation. Classification of the thermal indoor climate as a function of the outside air temperature adaptation is also possible according to DIN EN 15251 (E. DIN 2007), by which the thermal state of the room over the course of the year can be evaluated and represented both optically and numerically. The latter is possible by using different comfort categories and evaluating the fulfilled hours over the simulated annual course, as shown in Figure 1.

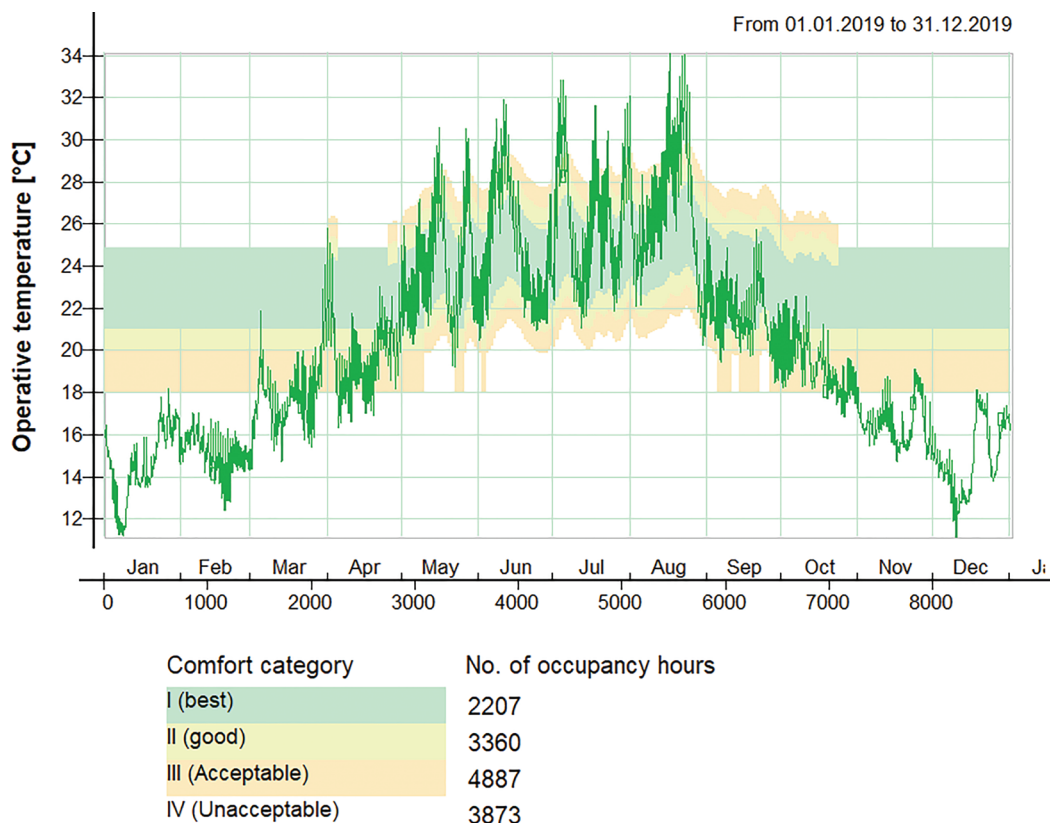


FIG. 1 Evaluation of the operative temperature curve according to DIN EN 15251 (E. DIN 2007)

Therefore, the following five heating transfer types are implemented: 1. Ideal heating element, 2. Floor heating, 3. Ceiling heating, 4. Ventilation heating and 5. Water-guided radiators with different room positions.

To validate these findings, comfort-influences are evaluated with the software "Autodesk CFD 2019". This closer look at the different heat transfer strategies allows conclusions of the detailed heat distribution in the room and is not typical in a usual planning process. Therefore, various positions and combinations of heating transfer types are analysed with different façade qualities.

The analysis is limited to the parameter temperature and its distribution and expansion in the room. In addition, the above-mentioned systems are evaluated for different insulation standards. Those were exemplarily created with characteristic values for the passive house, the EnEV 2014, the DIN 4108-2 and an old building-standard.

All strategies are also analysed with regard to the influence of room size. Here, the options "standard room according to DIN 13791 (geometry B)" and to evaluate a huge difference "open-plan office

for 7 to 8 people” are considered. Based on this, a total of 32 strategies were identified that had to be examined. DIN 13791 also contains the specifications for walls, including the density, thermal conductivity and thickness of each layer of the wall.

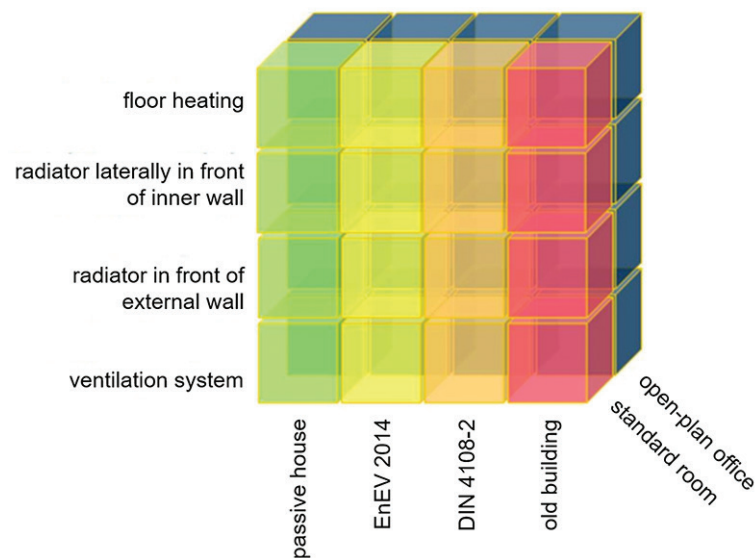


FIG. 2 Parameters for identifying the strategies to be analysed

3 EXPERIMENT / RESEARCH

3.1 SIMULATIONS IN IDA ICE

The dimensioning of the individual heat transfer systems are done iteratively on the basis of standards or presets of the simulation software IDA ICE from EQUA. For each transfer, as much energy is provided as it requires to realise the specified control setpoints for the average room temperature of 21 °C.

In addition to the input of the individual room cubature and the corresponding transfers, numerous other building-specifics ($UA= 1.36 \text{ (W/m}^2\text{K)}$, $UW= 2.13 \text{ (W/m}^2\text{K)}$) and zone-specific influences, such as weather data or user locations, plant-specific boundary conditions and structural conditions are considered in the simulation, and all are similar for the different versions.

The simulation of the various conditioning strategies is carried out dynamically for the different rooms shown in Figure 3. The first set is simulated in a low standard building because of the strong influence of the façade. The results of the entire year 2018 are considered, as well as those of a cold design day (22 January 2018) for a closer examination.

With regard to the energetic evaluation, the final energy requirements and especially the heating requirements of the different variants are compared.

The selection of the first three simulation rooms is based on their location within the building and orientation. The fourth simulation room was defined on the basis of DIN EN ISO 13791 Chapter 8.3.



FIG. 3 Floor plan with positioning of the selected rooms (Bewersdorff & Glanzner, 2018)

3.2 SIMULATIONS IN AUTODESK CFD 2019

The identified strategies described in chapter 2 are now examined with regard to thermal comfort, considering certain influencing factors.

Determination of comfort results – standard room:

For each of the 32 configurations, the results were shown using two evaluation options:

- via the cumulative distribution of temperatures and its representation in cumulative curves
- about the comfort volume, which has been visualised using the isovolumic tool

Figure 4 describes the comfort volume as an example for the scenario "Radiators in front of the outer wall in a standard room with an insulation standard according to DIN 4108-2". The darker shade of green represents the limits of the lower temperature limit (15.97 °C), and the light green/yellowish shade represents the limits of the upper-temperature limit (20.97 °C). The volume between these two limits represents the volume of comfort.

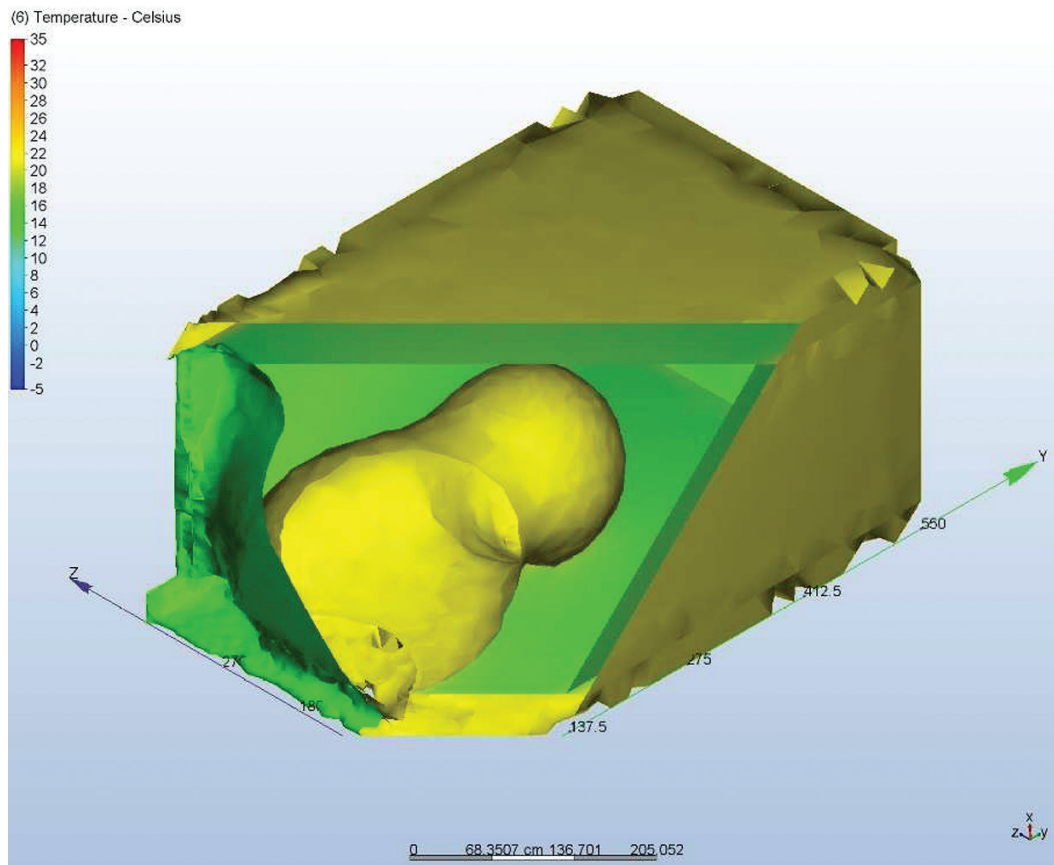


FIG. 4 Exemplary comfort volume

Determination of comfort results - open-plan office:

In general, the values for the comfort volume in an open-plan office are higher than in a standard room. One reason is the influence of the window is lower than in the standard room compared to the room volume. On the other hand, the open-plan office has a relatively larger area that acts as a wall to heated interiors. Similar to the principle of underfloor heating, a constant temperature is maintained by the surrounding surfaces from the initial stage. A less decisive but nevertheless existing reason for the higher comfort volumes is the air heated directly around the person in the room takes up less space in relative terms than in a standard room due to its own heat flow. (Bewersdorff, Silva, Gappisch, Goad, & Hannemann, 2019)

4 RESULTS

4.1 RESULTS OF IDA ICE

Air heating is energetically advantageous in almost all room constellations, as the average air temperature is quickly reached without significantly warming the surrounding surfaces. That also indicates its lack of comfort because of the cold surfaces.

ENERGY DEMAND	ROOM A CORNER ROOM (N)	ROOM B MIDDLE ROOM (W)	ROOM C CORNER ROOM (S)	ROOM D STANDARD ROOM (W)
low	4	4	4	2
	5a, 5c	1	5b, 5c	4
	5b	5a	5a	1
	1	5b, 5c	1	5a, 5b, 5c
	2	2	2	3
high	3	3	3	-

1. Ideal heating 2. Floor heating 3. Ceiling heating 4. Ventilation heating 5a. Water-guided radiators 5b. Water-guided radiators 5c. Water-guided radiators

TABLE 1 Differences in final energy demand of different heat transfer systems in a low standard building

The ideal heating element is located in the middle of the demand assessment like the radiators, whereby their positioning in the room plays a subordinate role. Surface heating has no advantages in terms of energy efficiency as opposed to comfort. Just in the case of very small wall areas, underfloor heating in existing buildings can have a low demand.

COMFORT EVALUATION	ROOM A CORNER ROOM (N)	ROOM B MIDDLE ROOM (W)	ROOM C CORNER ROOM (S)	ROOM D STANDARD ROOM (W)
low	2 (11.5 %)	5a (12.8 %)	2 (11.56 %)	5a (11.9 %)
	3 (11.8 %)	3 (12.5 %)	3 (11.7 %)	5b (12.1 %)
	5b (18.5 %)	2 (12.9 %)	5a (17.3 %)	5c (12.2 %)
	5c (18.5 %)	5b (13.3 %)	1 (19.5 %)	3 (12.8 %)
	5a (19.2 %)	5c (13.4 %)	5b (20.1 %)	2 (13.4 %)
	1 (19.4 %)	1 (15.5 %)	5c (20.2 %)	1 (14.4 %)
high	4 (23.7 %)	4 (16.5 %)	4 (23.8 %)	4 (14.9 %)

1. Ideal heating 2. Floor heating 3. Ceiling heating 4. Ventilation heating 5a. Water-guided radiators 5b. Water-guided radiators 5c. Water-guided radiators

TABLE 2 Differences in comfort evaluation of different heat transfer systems in a low standard building

Comfort-wise, surface heating systems and radiators are assumed to be beneficial. In a standard room with large windows on one side, radiators are beneficial on the comfort side. Otherwise, surface transfer systems are always more advantageous if the surface can introduce sufficient energy. The ideal heating system usually receives a medium rating, while air heating consistently receives the worst rating because it mainly heats the air but only slightly the surfaces.

A closer look at the energetic influences, as shown in Figure 5 for the critical northern corner room in winter confirms the previous results. In percentage terms, the values flatten slightly. Still, they have similar tendencies, whereby the absolute values show a higher demand for area transfer systems and, in this case, also an increase for radiators. Air heating is always below the ideal heating element.

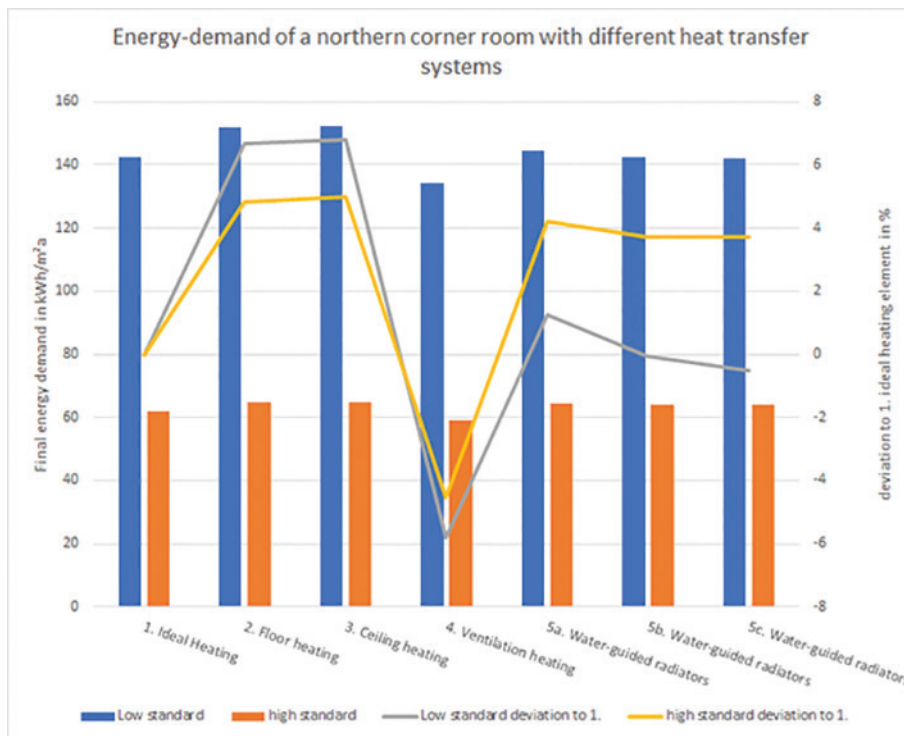


FIG. 5 Energy demand deviations of different heat transfer systems in a northern corner room with different hull standards

4.2 RESULTS OF AUTODESK

Standard room - factor insulation standard

In terms of the insulation standard, it can be concluded first that the better the insulation standard, the more consistent the temperatures are. This is also plausible with increasing insulation standard, on the one hand, the temperatures at the window are higher, and on the other hand, the required temperature level of the heating system is lower. The passive house, therefore, comes off best: The comfort volume is the highest for each heating variant. If the insulation standard is reduced, the values of the comfort volume also decrease in principle. There are, however, a few exceptions to this:

- Underfloor heating and ventilation: The comfort volume for the insulation standard according to DIN 4108 is lower than the old buildings.
- Radiators on the outside wall: The comfort volume for the insulation standard according to EnEV is lower than for the insulation standard according to DIN 4108.

Standard room - factor heat transfer type

Looking now at the heating system, it is clearly visible that the ventilation system works most effectively in terms of a constant temperature profile; it consistently has the highest values for comfort volume.

The next best heating systems are underfloor heating and the radiator directly in front of the window. The idea of installing the radiator in front of the window or the external wall is based on the fact that the heat from the radiator can be transferred to the air with the low temperatures of the outside air directly at the point of origin so that no cold front can penetrate into the depth of the room. The fact that this concept ensures better comfort than a radiator in a separate place is also shown in the

overview. The radiator in front of the window even performs slightly better than the underfloor heating in the passive house variant, but the values of the comfort volume break down relatively strongly in relation to the old building. In a passive house, neither the low temperatures behind the outer wall have a major influence, nor does more heat from the radiator escape to the outside due to the high insulation standard. Accordingly, the heat from the radiator can compensate the low temperatures from the outside relatively well. The radiator on the sidewall has very low comfort values, which can be explained by the fact that there are very large temperature differences due to the arrangement of the outer wall and radiator in the room: the cold window front on one side and the hot radiator separates it in the middle of the sidewall.

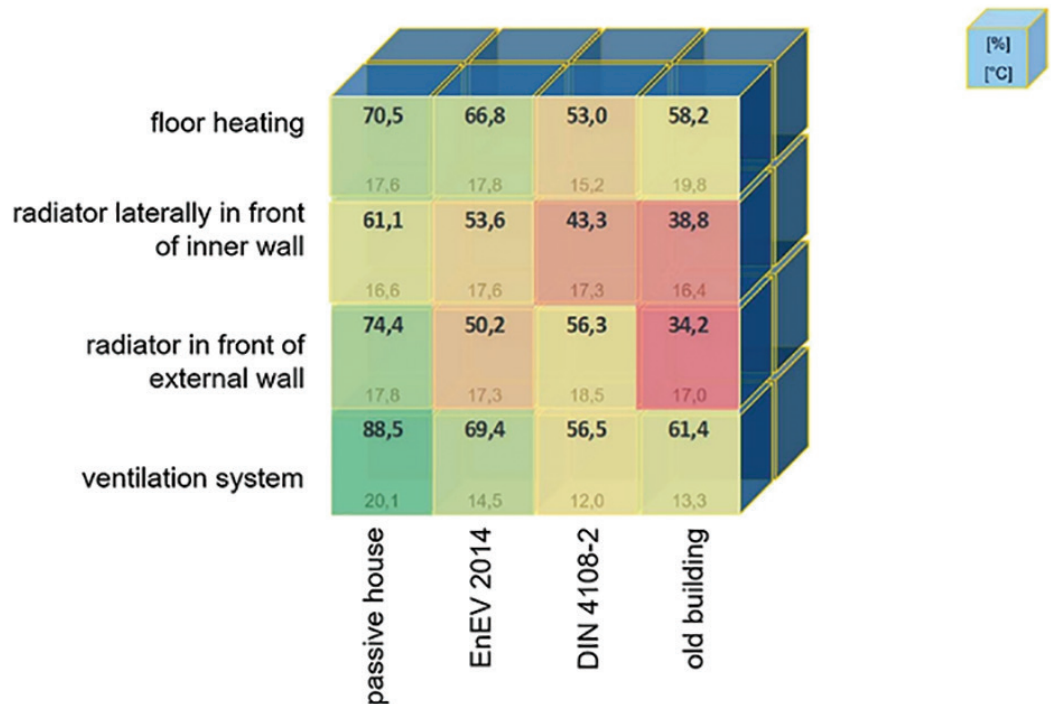


FIG. 6 Overview of comfort volumes with associated average temperatures (standard room)

Open-plan office - factor insulation standard and heat transfer type:

With regard to the insulation standard, the higher the insulation standard, the more balanced are the room temperatures. In this case, the form of heating has changed in such a way that ventilation is no longer the most suitable method of heat supply but rather underfloor heating. The fact that ventilation is no longer performing so effectively is primarily due to the fact that the airflow can no longer fill the entire room evenly - especially not with the requirement to limit airspeeds to a level suitable for human wellbeing. Therefore, the variant with a radiator on the outer wall also performs better than the ventilation variant. The variant with a radiator installed on the side of the room takes last place.

Optimisation strategies

The standard variants described above were supplemented by further optimisation variants. These included in particular

- the installation density of the underfloor heating
- the variation of the surface heating and
- the infrared heating approach.

Optimisation strategy - installation density of underfloor heating

Typical pipes of underfloor heating systems require a certain distance from each other. Capillary tube mats are an alternative; they have a small diameter and minimal distance between the pipes. This improves comfort due to the higher density of heat transfer.

Capillary tube mats consist of capillary tubes with a small tube diameter and are made of thermal plastic (mostly polyethylene). The main advantage of this system is to only need low temperatures (approx. 30 °C) to heat the room. This means the room's temperature asymmetry is low and has no unpleasant effects on the users (more moderate temperatures and, therefore, more comfort). Furthermore, renewable heat sources such as geothermal or solar thermal energy are particularly suitable for achieving the low flow temperatures. Coupling them with a heat pump would make the renewable heat sources even more reliable and would also allow cooling in summer. Due to the low installation height (approx. 4 to 5 mm), this type of surface heating is also suitable for installation in plaster - it can therefore be installed on walls as well as in floors and can also be retrofitted.

The different effects of the different pipe diameters and installation densities are clearly visible. The conventional pipes need much higher temperatures; these are restricting the comfort volume, why they are left out in the iso volume. In the case of capillary tube mats, the tubes don't show a major contribution to the level of discomfort. This also reflects the values of the comfort volumes: while the version with conventional tubes has a value of 78% by volume, the alternative with capillary tube mats has a value of almost 85% by volume, which is significantly higher.

The following surfaces were examined with regard to the location of the surface heating:

- Strategy 1: Outer wall
- Strategy 2: Floor + ceiling
- Strategy 3: Room half floor
- Strategy 4: Room half floor + wall
- Strategy 5: Room half floor + wall + ceiling

The main focus to create the variants was to identify the most effective position of the surface heating system in terms of thermal comfort. In the comfort volumes, there is a clear tendency for the heated surfaces to be oriented towards the window in order to achieve the highest comfort:

- The "room half floor" variant with the orientation of the surfaces on the outer wall results in a comfort volume of just under 68% of the room volume, while the variant with a complementary heated floor half has a comfort volume of just 51%.
- The "room half-floor + wall" variant shows similar values: the orientation towards the outer wall provides a comfort volume of 70 vol.%, the opposite orientation provides 52 vol.%.

All five variants mentioned above perform better than underfloor heating alone in the basic simulation. This confirms the objectives of achieving the largest possible surface area and locating the surfaces as close as possible to the outer wall are suitable to improve comfort. The most advantageous variant is number 4 ("room half-floor + wall"), with a comfort volume of 70 %. Here, the compromise of a large surface area proportion and a suitable alignment to the outer wall at the same time works best. The fact that ceiling heating - as a further increase in surface area - does not lead to better comfort because heat rises upwards, so the heat from the heated ceiling would only accumulate in the upper part of the room and could not contribute to a pleasant temperature distribution.

If it's not possible or desired to install surface heating in the room, infrared heating can be an alternative to conventional radiators. Infrared heating is an electric heating system that emits infrared rays, i.e. electromagnetic waves in a wavelength from 3 to 50 μm . Pure heat radiation is emitted so that all bodies in the room are heated equally - even over a long distance. Infrared heaters can directly heat the room surfaces through the heat radiation, which reduces the percentage of warm rising air. Infrared heating has a comfort volume of 68.6 % and thus performs significantly better than conventional heating systems with a comfort volume of only 50.2 %. With regard to energy consumption, it should be noted that infrared heating is operated as direct electric heating. It, therefore, requires the highest form of energy and can't be operated with decentralised renewable heat, such as near-surface geothermal energy.

5 CONCLUSIONS

IDA ICE

The transfer technology with higher efficiency is not always the most comfortable. By controlling the transfer units on the basis of the average room temperature and not the operative temperature, the air heating system has the lowest final energy requirement despite the poor surface temperatures of the enveloping surfaces. As the air heating solely heats surfaces to a limited extent, only little energy is lost in this way. The surface transfers show exactly the opposite effect and, in both cases, also behave inversely. In the case of large, unrenovated enveloping surface areas, an unrealistically large surface area is necessary to compensate for the losses. For this purpose, a simplified simulation (ideal heating element) for air heating systems in old buildings can be assumed to yield savings of up to - 6 %. For surface transfer systems, up to + 7 % should be added to the ideal calculation.

Autodesk

In conclusion, the simulative analysis described above states underfloor heating and ventilation are the most effective and efficient ways of heating. At low necessary temperature differences, ventilation is optimal, suitable for a passive house or a very small room with a low heating load. Under other conditions, the aim is to achieve a high heating load through low-temperature differences and high volume flows, and, consequently, draughts can be expected. In these cases, underfloor heating is more suitable.

If underfloor or surface heating is chosen, variants with partial wall and floor equipped surface heating elements close to the window are particularly recommended. It is important to make the areas as large as possible.

If no wall heating is desired because appliances or pictures are to be installed in this area as well, underfloor heating can be used again, with the sufficient use of half of the floor area close to the window. So, material and installation costs could be minimised. However, this arrangement requires the other walls to be warm internal walls.

References

- Bewersdorff, D., & Glanzner, A.-K. (2018). Auswirkung von Übergabeeinrichtungen auf Simulationsergebnisse energetischer Simulationen (Bachelor Bachelor-Thesis). Technische Universität Darmstadt, "unveröffentlicht".
- Bewersdorff, D., Silva, C. d., Gappisch, J., Goad, N., & Hannemann, L. (2019). Innovative Raumtemperierungsmethoden (Interdisziplinäres Energieprojekt). Technische Universität Darmstadt, "unveröffentlicht".

- DIN, E. I. (2006). DIN EN ISO 7730 (2006-05): Ergonomie der thermischen Umgebung-Analytische Bestimmung und Interpretation der thermischen Behaglichkeit durch Berechnung des PMV- und des PPD-Indexes und Kriterien der lokalen thermischen Behaglichkeit. In: Berlin: Beuth-Verlag GmbH.
- DIN, V. (2018). 18599-1 2018-09: Energetische Bewertung von Gebäuden-Berechnung des Nutz-, End- und Primärenergiebedarfs für Heizung, Kühlung, Lüftung, Trinkwarmwasser und Beleuchtung-Teil 1: Allgemeine Bilanzierungsverfahren, Begriffe, Zonierung und Bewertung der Energieträger. In (Vol. 1), Berlin: Beuth.
- Fanger, P. O. (1972). Thermal comfort, analysis and application in environmental engineering. In: McGraw Hill, New York.
- Knissel, J., & Loga, T. (2006). Vereinfachte Ermittlung von Primärenergiekennwerten. Bauphysik, 28(4), 270-276.
- Mayer, Edmund (1998), 'Ist die bisherige Zuordnung von PMV und PPD noch richtig?', KI. Luft- und Kältetechnik, 34 (12), 575-77.

Robust Renovation of Buildings: Enhancing Energy Efficiency and Flexibility

Martin Gabriel¹, Manuel de-Borja-Torrejon²

- 1 Technical University of Munich, Arcisstrasse 21, 80333 Munich, +49 89 289 23990, martin.gabriel@tum.de
- 2 Technical University of Munich, Arcisstrasse 21, 80333 Munich, +49 89 289 23823, manuel.de-borja-torrejon@tum.de

Abstract

Buildings are expected to play a key role in the decarbonisation context by reducing their energy consumption and flexibly managing their demand. Existing studies on strategies for achieving a robust performance in buildings focus on energy conservation. Findings showing that the applied measures also affect a building's demand-side management potential, and call for the study of strategies considering both energy conservation and flexibility. This offers the possibility of identifying alternatives that minimise the level of intervention in façades while enhancing the overall building performance. The aim of this study is to explore renovation alternatives for the German residential building stock to save energy and increase its demand-side management potential whilst ensuring a good performance of buildings under uncertain conditions. A representative multi-family home located in Munich is used as a case study. A full-factorial robust optimisation is conducted to analyse multiple combinations based on several design parameters and seven uncertainty scenarios, including climate change. The resulting renovation variants are assessed according to robustness and simplicity through over 200.000 simulations using TRNSYS/TRNLizard. The results show that an optimised renovation strategy aiming for robustness could increase demand-side management potential up to 122% and simultaneously reduce energy consumption by 56%, compared to a non-optimised variant. This maximum performance improvement could be achieved in non-insulated buildings by integrating into the façade an insulation layer of 4cm, installing double-glazed windows, and replacing the heating system with under-floor heating. Skipping the additional insulation would reduce energy consumption less (35%), but it would increase the building's demand-side management potential (129%). In contrast to the implementation of additional efforts to meet the highest energy efficiency, this would offer an alternative for the renovation of buildings in which a passive upgrade of their constructive envelope is constrained (e.g. listed buildings) to boost decarbonisation through a more simple but robust refurbishment.

Keywords

Building renovation, energy conservation, demand-side management, robust optimisation

1 INTRODUCTION

At the 2015 climate conference, a decision was reached to reduce global greenhouse gas emissions to a naturally degradable level until 2050. To this end, Germany aims to contribute with ambitious climate goals for 2030, including reducing its emissions by 55%, compared to 1990 (BMU 2019). However, Germany's reduction of emissions has been stagnating in the last years, putting at risk the ability to meet emission goals for 2030. Therefore, there is a need for developing further strategies able to unlock potentials for reducing additional emissions.

The building sector is one of the key contributors to greenhouse gas emissions. Thus, buildings are expected to play a key role in the decarbonisation context by reducing their energy consumption and flexibly managing their demand. According to (BMU 2019), about 30% of carbon emissions in Germany are due to the operation of buildings. Even though a significant 44% reduction in emissions has been achieved in Germany between 1990 and 2018, a further reduction of 67% is required to meet its climate goals by 2030. To this effect, savings may be primarily achieved through the renovation of the existing building stock rather than from new buildings, as around two-thirds of the existing German buildings are still lowly insulated.

1.1 ROBUSTNESS OPTIMISATION AND ENERGY CONSERVATION

Robustness is defined as *a building's ability to perform well under a wide range of uncertain conditions* (Chalupnik, Wynn, & Clarkson 2013; Olewnik et al. 2004). Robust optimisation (RO) analysis can be used to study renovation strategies for enhancing a building's robust performance.

A literature review based on a selection of ten studies (Table 1) shows that RO analyses commonly address the potential optimising effect of upgrading the constructive envelope as a basic passive means and its optimum combination with active systems. Thus, nine of the reviewed studies consider wall insulation as a variable for their parameter analysis, while all of them include the windows. In addition, seven studies evaluate the effect of unexpected user behaviour and the impacts of climate change. With regard to the analysis method, a full-factorial optimisation approach is applied in eight of the ten studies. This approach consists of analysing all possible combinations of the selected design parameters and their defined values (Chlela et al. 2007). Furthermore, RO studies mainly focus on energy conservation and use the energy demand of the building as a metric to assess the optimisation of the building performance. In half of the reviewed studies, some additional optimisation objective (comfort, costs, CO₂) is also considered, using a Pareto-front or a weighted objective function to identify the optimum parameter combinations.

The outcomes of the studies suggest a high impact of usage and climate scenarios on the optimisation objectives. These studies also show that performing RO contributes to significantly reduce the performance gap. In most studies, simplicity outperformed high-tech solutions due to their higher robustness towards changing conditions.

1.2 ROBUSTNESS OPTIMISATION AND ENERGY FLEXIBILITY

In addition to developing robust renovation strategies for energy conservation, there is an increasing call for energy flexibility in the building sector. Energy flexibility of buildings can be defined as *"the ability to manage its demand and generation according to local climate conditions, user needs and grid requirements"* (Jensen et al., 2017). The expansion of renewable energies increases the demand for short-term balancing power. Buildings can provide this balancing power by flexibly managing their demand. Aligning demand to the volatile energy generation can minimise the required amount of residual load and can therefore contribute to reducing carbon emissions (Hausladen et al. 2014).

(Hausladen et al. 2014) analyse the potential of the German building stock for flexibly managing its energy demand to participate in demand-side management (DSM) actions in the power grid without compromising the thermal comfort of building users. DSM potentials are identified in residential- and office buildings. Heavy constructions with thermal systems of high inertia show the maximum levels of DSM potential. Differences are shown between existing and new buildings. While existing buildings can provide high DSM potentials but only for a short period of time (< 2 hours), new buildings tend to have lower DSM potentials, but these potentials can be used during longer periods of time (> 24 hours in some cases). This suggests that especially existing buildings may be able to support the mitigation of peak loads, while new buildings could be suitable for shifting loads on a multi-day timescale. Based on these results (Auer et al. 2017) addresses the coupling of the German building stock with the power sector by studying the impact of the electrification of the thermal demand of buildings and thereby the use of their DSM potentials on the future development of the national power system. Their results show that buildings acting as thermal storage components of the power system (based on the use of the thermal mass of buildings and electricity-driven thermal systems, e.g. heat pumps) could enable the integration of a higher share of renewable energies in the grid and the reduction of CO² emissions.

1.3 RESEARCH GAP

As mentioned above, studies have shown that robust optimisation can support reducing the performance gap in buildings. However, current studies in RO mainly focus on basic passive means aiming at energy conservation. The results of the cited studies on DSM of buildings indicate that these measures also affect a building's DSM potential. This calls for the study of refurbishment strategies considering both energy conservation and flexibility in robust optimisation, aiming to address decarbonisation of the building stock and the power sector. Furthermore, it can be hypothesised that this holistic approach, in turn, offers the possibility of identifying renovation alternatives that minimise the level of intervention in façades while enhancing the overall building performance.

Thus, this study performs a RO on an exemplary case study to analyse renovation strategies for the German residential building stock aiming to save energy while increasing its DSM potential. Moreover, options for buildings where the renovation of their envelope is limited or highly complex are identified.

SOURCE	OPTIMISATION OBJECTIVE	DESIGN PARAMETERS	UNCERTAINTY SCENARIOS
(Auer & Endres 2017)	Comfort	a b c d e _	1 _ _ _ _
(Maderspacher 2017) (Buso et al. 2015)	Energy demand, Costs	a _ _ d _ f	_ _ 3 _ 5
(Endres et al. 2019)	Energy demand	_ b _ d _ f	_ 2 _ _ _
(Auer et al. 2013)	Energy demand	a _ _ d e _	_ _ 3 _ _
(Chinazzo, Rastogi, & Andersen 2015)	Energy demand, CO2	a _ _ d e _	1 2 3 4 _
(Kotireddy, Hoes, & Hensen 2015)	Energy demand	a b _ d _ f	_ _ 3 _ _
(Van Gelder, Janssen, & Roels 2014)	Energy demand, Comfort	a _ c d e f	1 2 3 _ _
(Kotireddy, Hoes, & Hensen 2017)	Energy demand, Costs	a _ c d _ f	_ 2 _ _ _
(Kotireddy, Hoes, & Hensen 2019)	Energy demand, Comfort	a b c d e _	1 2 3 _ _

a: Insulation; b: Thermal Mass; c: Ventilation; d: Glazing; e: Geometry; f: Shading
1: Usage; 2: Occupancy; 3: Climate; 4: Technology; 5: Policy

TABLE 1 Literature analysis of studies that performed a robust optimisation in building performance simulation

2 METHODOLOGY

A parametric simulation study is conducted to examine the robust optimisation potential of refurbishment measures. A representative multi-family home located in Munich is modelled as a case study using TRNSYS and TRNLizard. TRNSYS is a transient simulation tool for thermal systems widely used to evaluate the performance of buildings. TRNLizard is a tool that allows combining the use of TRNSYS and the parametrisation features of the Grasshopper environment (Frenzel & Hiller 2014). The focus of the parametric study lies on the heating period, represented by four "type days" to simplify simulation efforts. A full-factorial robust optimisation for energy consumption and DSM potential is performed, covering the most influential design parameters under seven uncertainty scenarios.

2.1 CASE STUDY AND ANALYSIS PERIOD

The model's geometry, orientation, and boundary conditions are adopted from (Auer et al. 2017). The chosen zone represents a typical flat in an apartment block, with windows at the Eastern, Western and Southern façade. Ceiling, floor and Northern wall are considered adiabatic. A typical floor area of 110 m² and a window-to-wall ratio of 14 % are selected for this residential typology (Auer et al. 2017; Loga et al. 2015). Radiators are considered as the thermal system of the base case, due to their predominant use in the residential building stock (Auer et al. 2017). Nonetheless, for the studied variants in the RO, the integration of underfloor heating is set as a required refurbishment measure to activate the buildings' thermal mass. This is based on the results of (Hausladen et al. 2014), showing that the highly-inertial thermal systems in combination with the building mass leads to higher levels of DSM potential. Since cooling systems only account for 0.9% of the energy consumption in the German residential building stock (Graichen et al. 2011), this study focuses on the heating period, considering that it provides a sufficient estimation of the annual potential.

Four "type days" are selected from the typical meteorological year (TMY) to represent the heating period in order to simplify simulation efforts. Each type day corresponds to a typical daily climatic profile based on average weather conditions. Thus, the selected type day "very cold" represents days with mean ambient temperature less than -5 °C; "cold" -5 - 0 °C, "cool" 0 - 4.5 °C, and "moderate" 4.5 - 13 °C. The solar radiation profile is also considered in the selection. Based on this, the heating period is assumed as a succession of these type days, in which each consecutive day from the TMY is replaced by the corresponding type day according to the mean ambient temperature.

The model has been checked for plausibility by assessing the annual specific energy demand of different building age classes' simulation results and comparing them to literature data. The results lie within the expected range and indicate a properly-working model.

2.2 UNCERTAINTY SCENARIOS AND ROBUSTNESS INDICATOR

In addition to design parameters (e.g. insulation), the robustness concept includes uncertainties in operation as well as external uncertainties. The RO approach seeks to find an optimum setup, which performs well over a wide range of future scenarios. In this study, a full-factorial RO based on seven uncertainty scenarios (S1-7) and several design parameters (see 3.1) is conducted by simulating all possible combinations as shown in section 3.2. The base case described above is used to compare the new performance of each building variant after applying the different combinations, in order to assess their robustness.

The assumed uncertainty scenarios are classified into “user”, “building use”, “climate” and “planning”, being implemented as follows:

- User: Represents the impact of the building user. Building performance is highly sensitive to the user’s ventilation behaviour. Hence, two different ventilation-patterns are introduced as user scenarios, varying from the minimum value of provision of fresh air in the base case: (S1) user who does not ventilate at all; (S2) user who is continuously tilting the window, causing a constant air change rate of 1.5 h⁻¹.
- Building use: Represents a different usage from the original building use. Thus, (S3) conversion of the residential into an office space is considered through a rise in the model’s internal gains by 20 W/m², resembling the gains of a densely populated office.
- Climate: Represents changes in the external climatic conditions. Therefore, climate change is taken into account over the typical lifespan of a residential building by implementing climate scenarios for (S4) 2050 and (S5) 2080. These weather files are generated based on a methodology developed in (Jentsch, Bahaj, & James 2008), using a morphing approach to convert EnergyPlus Weather (EPW) files of current conditions to future scenarios based on the International Panel for Climate Change’s medium-high emission scenario (Nakicenovic & Swart 2000).
- Planning: Represents uncertainties in the planning, construction and renovation of a building. As mentioned above, DSM potential is especially sensitive to the available building’s thermal mass. Historical preservation regulations or refurbishment constraints may require internal instead of external insulation, causing a significant decrease in the available thermal mass. Thus, different positions of the wall insulation are used to exemplify planning uncertainty: (S6) at external surface and (S7) at internal surface.

In the RO approach, each variant’s quality is assessed by a performance indicator through an optimisation goal function. In each implemented scenario, this function integrates the individual variant’s performance values associated with the considered optimisation objectives (energy demand and DSM potential in this study) into one single indicator. In this study, the minmax-regret indicator is used, which corresponds to a performance-oriented method. To obtain this indicator, the difference between the local best case is calculated for each variant in each scenario. The resulting performance difference (performance regret) is then summed up over all scenarios. The variant with the lowest performance regret is selected as a robust optimum. Thus, the minmax-regret approach aims at minimising the maximum performance regret to perform close to the optimum in all scenarios (Averbakh, 2000).

2.3 DSM ESTIMATION

DSM consists of controlling the energy demand to shift loads over certain periods. Aligning the demand to the volatile energy generation can minimise the required amount of residual load (Hausladen et al. 2014). In this sense, electrical loads can be shifted to operate during peak generation hours, and to reduce the demand during low generation periods. Load management can therefore allow for efficient use of the available production and grid infrastructure and maximises utilisation of renewable technologies.

In this study, the method in (Hausladen et al. 2014) for estimating DSM potentials is implemented. This method examines DSM potential of buildings taking both thermal storage and installed power into account. A transient thermal dynamic simulation is used for modelling the system due to the complex physical processes. DSM is assessed as the electrical load that can be shifted when switching the thermal systems on or off. To ensure thermal comfort, the fluctuation of the indoor temperature is limited within a comfort band of 20°C to 24°C (based on EN 16798-1’s Indoor Thermal Environment Category II, normal level of expectation). Thus, a base simulation with constant heating

setpoint (22°C) is respectively compared to a full-load operation and a deactivation of the heating system. For each case (activation and deactivation), the DSM potentials are the integral of the power between the base simulation and DSM simulation for the period during which the temperature stays within the comfort band.

3 EXPERIMENT

In this study TRNLizard is used for the parametric simulation using TRNSYS. TRNLizard is an interface between TRNSYS and the graphic programming environment Grasshopper (Frenzel & Hiller 2014). TRNLizard allows transferring input data related to geometry and other parameters to the TRNSYS simulation engine by creating simulation files based on predefined templates. The pre-written simulation files are launched via a command-line argument. TRNLizard's components can be adapted and extended due to its open-source configuration, written in the programming language Python. In this study, various adaptations have been implemented in order to perform the robust optimisation study.

3.1 DESIGN PARAMETERS

For the parametric analysis, a pre-selection of the most sensitive design parameters for a building's robust performance is conducted, to simplify simulation efforts. A preliminary estimation of parameter sensitivity is conducted by a one-at-a-time (OAT) analysis. The OAT analysis is a local sensitivity analysis method often used in building energy simulation (Wei 2013). In OAT, a single parameter is varied for a set of discrete steps. For each parameter, the former adaptations are reset, thus providing comparable conditions. The impact on one or more objectives is recorded to determine the sensitivity of each parameter. Although OAT is limited in providing accurate sensitivity data, it is time-efficient and provides enough level of detail to screen the parameters that will later be used in the RO. The parameters are selected according to the following constraints: (a) Comparable to the studies of (Auer et al. 2017; Hausladen et al. 2014); (b) Influenceable in the planning process, (c) Compatible with the DSM calculation method, (d) Compatible with the framework of the case study.

The parameter step values are selected to cover the majority of building standards present in the German residential building stock. Values are selected according to the different age classes identified in (Loga et al. 2015). The parameters in Table 2 are assessed in the parameter screening. Fig. 1 shows the cumulative normalised sensitivity of the parameters on energy demand and DSM potential derived from the OAT study. "Wall construction" is most influential, having a significant impact on energy demand. This parameter is followed by "screed thickness", and "coverage" (position of pipes within the active layer with respect to the surface facing the room), the impacts of which are more pronounced on DSM potential. The impact of "window constructions" mostly affects energy demand. All other examined parameters are considered to have a minor impact (cumulated normalised sensitivity below 0.5) and are therefore excluded from the RO.

PARAMETER	VALUE 1	VALUE 2	VALUE 3	VALUE 4
External wall insulation	0 cm [$U_{EW} = 1.2$]	4 cm [$U_{EW} = 0.6$]	14 cm [$U_{EW} = 0.238$]	28 cm [$U_{EW} = 0.12$]
Window construction	Single pane glazing [$U_w = 2.2$]	Double pane glazing [$U_w = 1.2$]	Double pane thermal glazing [$U_w = 0.9$]	Triple pane thermal glazing [$U_w = 0.6$]
Screed thickness	5 cm	8 cm	11 cm	15 cm
Active-layer coverage	3 cm	5 cm	8 cm	11 cm
External shading	0 %	25 %	50 %	75 %
Internal shading	0 %	25 %	50 %	75 %

>>>

Infiltration	0.42	0.39	0.21	0.15
Heat recovery	0 %	25 %	50 %	75 %

TABLE 2 Assessed parameters in the study. Selected parameters are highlighted

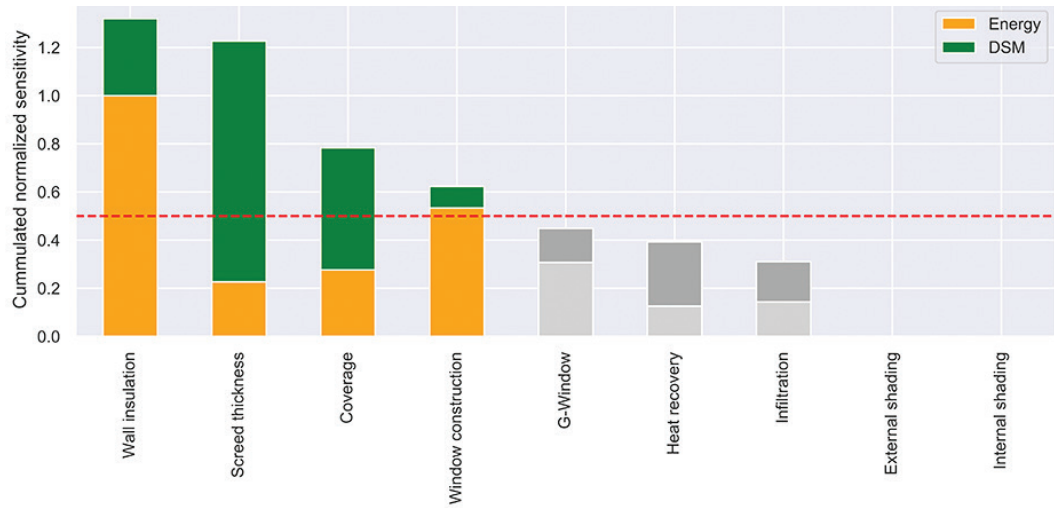


FIG. 1 Parameter sensitivity to energy consumption and DSM potential. Parameter selection is highlighted.

3.2 FULL-FACTORIAL STUDY

A full-factorial study is performed for the parameters and values selected in section 3.1. A set of values is defined for each design parameter and all combinations across the defined parameters and values are computed. Hence, if there are n values for x stages, nx runs are conducted (Chlela et al. 2007). In this study, four discrete steps are assessed for each parameter, resulting in a total of 256 parameter combinations. Infeasible variants are sorted out to simplify simulation efforts, resulting in a total of 160 parameter combinations. The scenarios described in section 2.2. are used in the RO to represent uncertainty. Thus, seven scenarios (S1-7) are combined with the 160 parameter combinations.

After setting up all variations, the calculation of DSM potential is integrated as the last step into the full-factorial RO. DSM potential is assessed individually for each time step and requires separate simulations for the deactivation and activation of the heating system. An hourly time resolution is chosen for this study, resulting in 48 DSM simulations for one type day. For each scenario up to 193 simulations (including a base simulation and the activation/deactivation simulations) were required. All in all, a total of 216.160 simulations were conducted for the RO study, taking into account all parameter combinations, scenarios and DSM simulations. Even though a full-factorial study is time-intensive, its general applicability and self-verifying nature enable it to be the best fit for the RO of energy demand and DSM potential.

3.3 SIMULATION

Initial estimations suggested a required simulation time as high as 35 days for all 216.160 variants. Therefore, a parallelisation method (Figure 2) for the use of TRNYS and TRNlizard was developed to be able to reduce the simulation time in the study by more than 80% on an eight-core PC, compared to standard TRNLizard-TRNSYS simulations. This method consists of a custom library programmed in Python. By using this method, TRNlizard generates the simulation templates and provides the

instructions to the Python program, which then writes the simulation files according to predefined instructions. To read and write TRNSYS simulation files, the developed python library allows working with TRNSYS .d18 and .b18 files (respectively "input" and "building description" files) in Python as well as starting TRNSYS simulations via command-line arguments. The library is designed to find and replace certain passages in the base TRNSYS files and thereby modify the specification of each simulation according to predefined instructions.

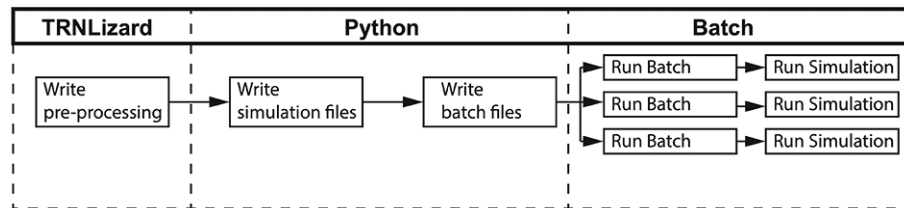


FIG. 2 Parallelisation methodology

3.4 POST-PROCESSING

After the simulation phase, post-processing of the results is automated using Python. The main post-processing steps are: (1) calculation of the final-energy demand; (2) extrapolation of the annual DSM potential; (3) calculation of the performance indicator (minmax-regret indicator); and (4) the selection of the optima.

- Step 1: The assessment of the final energy demand is based on the calculation of the electricity consumption for heating required from a heat pump. To this end, a COP curve for the heat pump (Wolf 2016) is used to convert the useful-energy demand to final-energy demand. Inlet temperatures of 55°C for radiators and 35°C for underfloor heating systems are adopted.
- Step 2: For the post-processing of the DSM potential, all simulated hourly potentials are aggregated to a single metric to enable interpretation and enhance the applicability of the resulting data. Thus, for each type day an average DSM potential is calculated first (encompassing both activation and deactivation potential). After that, an annual DSM potential is extrapolated by multiplying each daily aggregation by its yearly occurrence (proportion of type days, see section 2.1).
- Step 3: The minmax-regret indicator (see section 2.2.) is calculated in the post-processing by assessing both the final-energy demand and the annual DSM potential in each scenario. Based on this, a single metric is generated by normalising the minmax-regret indicator of energy demand and DSM potential and joining them in a weighted function.
- Step 4: The optimal variants of the resulting set are identified by computing a Pareto-front of the performance indicators for energy demand and DSM potential. A Pareto-front is a form of multi-criteria optimisation, where a set of optima is output, being the non-dominated solutions (variants where one optimisation objective cannot be improved without impairing the other; see e.g. Fig. 3). Non-optimised variants are calculated for each energy standard to evaluate the improvements. The configuration of these variants is according to the building-age classes. The classes are derived from a survey of the German residential building stock, subdividing it into eleven age-classes (Loga et al. 2015). In a previous study, these have been grouped into four energy standards (Auer et al. 2017): (R1) buildings built before 1978, (R2) buildings built after 1978 according to the former German thermal protection regulation (Wärmeschutzverordnung), (R3) buildings built according to the current German energy standard (EnEV), (R4) Passivhaus standard.

4 RESULTS

For each considered building-age class, specific optimised refurbishment strategies are generated. These strategies include up to three refurbishment measures, considered as a part of a three-step intervention: (M1) replacement of the thermal system; (M2) replacement of windows; and (M3) addition of insulation to the external wall. The simulation results on the building performance resulting from the strategies are shown for each intervention step in Fig. 3-5, respectively. Each subsequent intervention step in the strategy incorporates the previous implemented measure.

The representation on Fig. 3-5 consists of scatter plots, which visualise the performance of each variant with regard to annual electricity demand for activation-based and deactivation-based DSM potential. Pareto-optimal solutions are marked in the scatter plot and define the Pareto-front (red line). These variants correspond to the non-dominated solutions. The colour scale indicates the robustness of each optimised variant. A small indicator value indicates high robustness in all scenarios. The points in black in the scatter plots represent the non-optimised case (base case) for each building-age class (R1-R4). These cases are compared to their resulting optimised variants (A-D), which offer the highest robustness under consideration of climate change and the other assumed uncertainties. Non-optimised and optimised cases are represented in the images in the form of house symbols. The colours of the wall and windows represent the respective constructive energy standards listed in the legend. The legend also includes a reference to the underfloor heating system. The amount of grey surface represents the screed thickness, while the position of the yellow surfaces shows the coverage of the pipes within the floor.

Thus, the resulting specific measures M1 to M3 from the RO analysis, which constitute the renovation strategies of each building-age class to achieve their optimised variants A-D are:

- M1: Variant A-D: screed thickness of 14cm and a coverage of 11cm
- M2: Variant A: double-pane thermal-protection glazing; B-D: triple-pane thermal-protection glazing
- M3: Variant A: 4cm external insulation; B: 14cm external insulation; C-D 28cm external insulation

The optimisation results under refurbishment through M1 (Fig. 3) show that replacing radiators with an optimised heat transfer system improves DSM up to 124% (R1→A) and reduce energy consumption by a maximum of 28% (R4→D). Results also show that DSM improvements lower with declining building age (or rather with higher energy-efficient building standard). Thus, the cases of a building of EnEV (R3→C) and Passivhaus standard (R4→D) respectively achieve a 41% and 45% lower improvement than non-insulated buildings. In contrast to this, all building-age classes show a uniform reduction in energy demand by about one fourth. This is due to the increment in annual COP by using lower inlet temperatures. An optimum heat transfer system configuration has been identified for underfloor heating at a screed thickness of 14cm and coverage of 11cm.

The optimisation results under refurbishment through M1+M2 (Fig. 4) show that replacing the windows alongside the heat transfer system would increase DSM potential up to 129% and simultaneously reduce energy consumption by 35% (R1→A). In line with the previous findings in Fig. 3, the maximum DSM improvement can be achieved in non-insulated buildings. Higher energy-efficiency standards achieve fewer improvements in DSM potential (up to 44 % in case R3→C). Improvements in energy consumption decrease with higher energy-efficiency too. EnEV standard buildings achieve 6% less energy reduction than non-insulated buildings (R3→C vs. R1→A). In case M1+M2, the highest refurbishment efficiency is achieved in non-insulated buildings by installing an underfloor heating system with a 14cm-thickness screed and coverage of 11cm, and double-paned thermal-protection windows.

The optimisation results under refurbishment through M1+M2+M3 (Fig. 5) show that a deep-renovation of the building envelope (insulation + windows) alongside the incorporation of an underfloor heating system would increase DSM potential up to 122% and simultaneously reduce energy consumption by 56% (R1→A). In line with previous findings in Fig. 4, renovated non-insulated buildings achieve the highest DSM improvements. Buildings with higher energy efficiency improve their DSM potential to a lower extent after renovation (up to 51% in case R2→B). This also applies with regard to energy consumption. The highest reduction of 56% is achievable in non-insulated buildings, while buildings with better energy standards achieve only half of this energy reduction by simultaneously using more than three times as much insulation material. Therefore, the highest refurbishment efficiency can be achieved in non-insulated buildings by integrating an underfloor heating system with a screed thickness of 14cm and coverage of 11cm, installing double-glazed thermal-protection windows, and adding a 4cm -layer of external insulation.

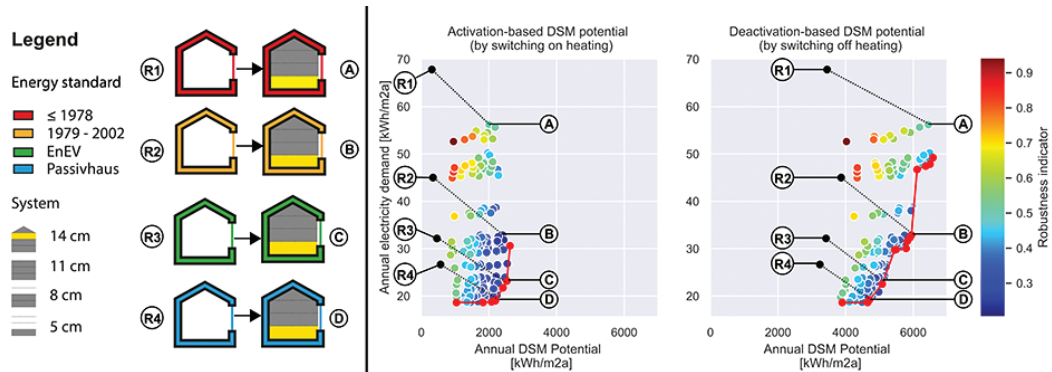


FIG. 3 Robust renovation step 1 (heating upgrade). R1-4: reference variants with radiators. A-D: optimum renovated variants with underfloor heating (screed thickness 14cm and coverage 11cm in all four energy standards).

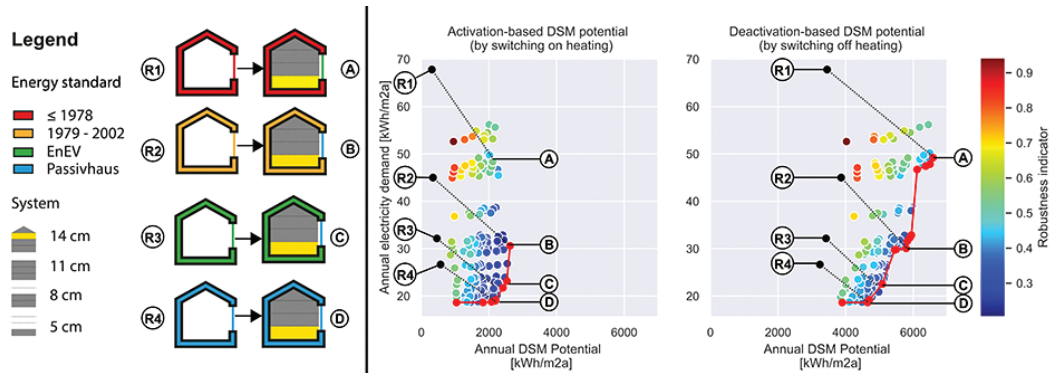


FIG. 4 Robust optimisation step 2 (heating & window upgrade). R1-4: reference variants with radiators. A-D: optimum renovated variants with underfloor heating (screed thickness 14cm, coverage 11cm) and replaced windows (A: double-pane thermal glazing, B-D: triple-pane thermal glazing).

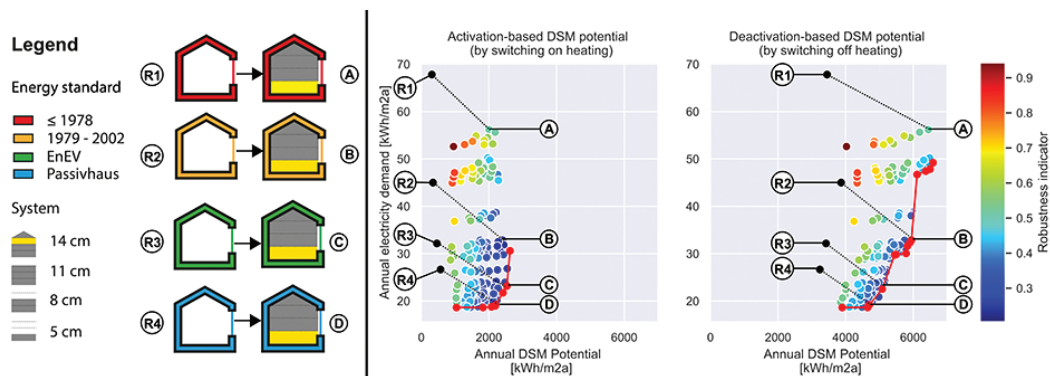


FIG. 5 Robust optimisation step 3 (heating, window & insulation upgrade). R1-4: reference variants with radiators. A-D: optimised variants with underfloor heating (screed thickness 14cm, coverage 11cm) and upgraded envelope (A: 4cm insulation on external walls and double-pane windows, B: 14 cm insulation on external walls and double-pane thermal windows, C-D: 28 cm insulation on external walls and triple-pane thermal windows).

5 CONCLUSION

In this study, a full-factorial robust optimisation focused on enhancing energy efficiency and flexibility was performed on the case of a representative multi-family home located in Munich. Several extensions have been developed for TRNLizard (TRNSYS' Grasshopper interface), integrating an advanced parallelisation methodology, which reduced simulation time for the 216.160 variants by 82%. Four different efficiency standards, according to building-age classes, were considered as base cases for the definition of optimum renovation strategies in each situation, aiming for robust building performance.

The highest improvement potential resulted from the refurbishment of buildings classified as non-insulated (built before 1978). Thus, upgrading their envelope with an insulation layer of 4cm and double-glazed windows, and exchanging the heating system by underfloor heating, showed an improvement of DSM potential of 122% and simultaneous reduction of energy consumption by 56%. Skipping the additional insulation would reduce energy consumption less (35%), but it would increase the building's DSM potential (129%), offering an alternative for the renovation of buildings in which a passive upgrade of their constructive envelope is constrained (e.g. listed buildings).

In addition, the analysis showed that the achievable improvements in energy demand and DSM potential diminish when renovating a base case towards higher energy-efficiency standards, despite additional renovation efforts (more insulation, triple glazing). These results suggest that simple refurbishment actions based on moderate efforts in existing buildings could contribute the most to the goal of decarbonising the building stock.

Acknowledgements

The authors would like to thank Dr C.P. Harris for the assistance as a native speaker in the revision of this manuscript.

References

- Auer, T., T. Hamacher, U. Wagner, and D. Atabay. 2017. "Gebäude Als Intelligenter Baustein Im Energiesystem. Lastmanagement-Potenziale von Gebäuden Im Kontext Der Zukünftigen Energieversorgungsstruktur In."
- Auer, Thomas, and Maria-Elisabeth Endres. 2017. "Parameterstudie Low-Tech Bürogebäude."
- Auer, Thomas, Laura Franke, Hermann Kaufmann, Stefan Winter, Stephan Ott, Marco Krechel, Christoph Gehlen, and Charlotte Thiel. 2013. "Einfach Bauen." Einfach Bauen.

- Averbakh, Igor. 2000. "Minmax Regret Solutions for Minimax Optimization Problems with Uncertainty." *Operations Research Letters*.
- BMU. 2019. "Klimaschutz in Zahlen : Der Sektor Gebäude." 150.
- Buso, Tiziana, Valentina Fabi, Rune K. Andersen, and Stefano P. Corngati. 2015. "Occupant Behaviour and Robustness of Building Design." *Building and Environment*.
- Chalupnik, Marek J., David C. Wynn, and P. John Clarkson. 2013. "Comparison of Metrics for Protection against Uncertainty in System Design." *Journal of Engineering Design*.
- Chinazzo, Giorgia, Parag Rastogi, and Marilyn Andersen. 2015. "Assessing Robustness Regarding Weather Uncertainties for Energy-Efficiency-Driven Building Refurbishments." in *Energy Procedia*.
- Chlela, Fadi, Ahmad Husaunndee, Peter Riederer, and Christian Inard. 2007. "A Statistical Method to Improve the Energy Efficiency of an Office Building." Pp. 1756–64 in *IBPSA 2007 - International Building Performance Simulation Association 2007*.
- Endres, Maria-Elisabeth, Laura Franke, Mark Sen Dong, and Lisa Neubert. 2019. "Parameters to Design Low-Tech Strategies." *JANUARY 17TH 2019 – MUNICH POWERSKIN CONFERENCE | PROCEEDINGS*, 1–11.
- Frenzel, C., and M. Hiller. 2014. "TRNSYSLIZARD – Open Source Tool Für Rhinoceros – Grasshopper." *Fifth German-Austrian IBPSA Conference* 490–96.
- Van Gelder, Liesje, Hans Janssen, and Staf Roels. 2014. "Probabilistic Design and Analysis of Building Performances: Methodology and Application Example." *Energy and Buildings* 79:202–11.
- Graichen, Verena, Sabine Gores, Gerhard Penninger, Wiebke Zimmer, Vanessa Cook, Barbara Schломann, Tobias Fleiter, Adrian Strigel, Wolfgang Eichhammer, and Hans-Joachim Ziesing. 2011. "Energieeffizienz in Zahlen." *Endbericht. Dessau-Roßlau: Umweltbundesamt*.
- Hausladen, Gerhard, Thomas Auer, Jakob Schneegans, Klaus Klimke, and Hana Riemer. 2014. "Lastverhalten von Gebäuden Unter Berücksichtigung Unterschiedlicher Bauweisen Und Technischer Systeme Speicher- Und Lastmanagementpotenziale in Gebäuden." 113.
- Jentsch, Mark F., Abu Bakr S. Bahaj, and Patrick A. B. James. 2008. "Climate Change Future Proofing of Buildings-Generation and Assessment of Building Simulation Weather Files." *Energy and Buildings* 40(12):2148–68.
- Kotireddy, R., P. Hoes, and Jan L. M. Hensen. 2017. "Simulation-Based Comparison of Robustness Assessment Methods to Identify Robust Low Energy Building Designs." *Proceedings of 15th IBPSA Conference, San Francisco, CA, USA (Proceedings of 15th IBPSA conference, Sanfransisco, USA):892–901*.
- Kotireddy, Rajesh, Pieter Jan Hoes, and Jan L. M. Hensen. 2015. "Optimal Balance between Energy Demand and Onsite Energy Generation for Robust Net Zero Energy Buildings Considering Future Scenarios." Pp. 1970–77 in *14th International Conference of IBPSA - Building Simulation 2015, BS 2015, Conference Proceedings*.
- Kotireddy, Rajesh, Pieter Jan Hoes, and Jan L. M. Hensen. 2019. "Integrating Robustness Indicators into Multi-Objective Optimization to Find Robust Optimal Low-Energy Building Designs." *Journal of Building Performance Simulation* 12(5):546–65.
- Loga, Tobias, Britta Stein, Nikolaus Diefenbach, and Rolf Born. 2015. *Deutsche Wohngebäudetypologie - Beispielhafte Maßnahmen Zur Verbesserung Der Energieeffizienz von Typischen Wohngebäuden*.
- Maderspacher, Johannes. 2017. "Robuste Optimierung in Der Gebäudesimulation: Entwicklung Einer Methode Zur Robusten Optimierung Für Die Energetische Sanierung von Gebäuden Unter Unsicheren Randbedingungen."
- Nakicenovic, Nebojsa, and Robert Swart. 2000. "Emission Scenarios. IPCC Special Report on Emission Scenarios."
- Olewnik, Andrew, Trevor Brauen, Scott Ferguson, and Kemper Lewis. 2004. "A Framework for Flexible Systems and Its Implementation in Multiattribute Decision Making." *Journal of Mechanical Design, Transactions of the ASME*.
- Wei, Tian. 2013. "A Review of Sensitivity Analysis Methods in Building Energy Analysis." *Renewable and Sustainable Energy Reviews* 20:411–19.
- Wolf. 2016. *Hocheffizienz-Wärmepumpen*.

Potential of Façade-Integrated PVT with Radiant Heating and Cooling Panel Supported by a Thermal Storage for Temperature Stability and Energy Efficiency



Mohannad Bayoumi*¹

* Corresponding author

¹ Assoc. Prof. Mohannad Bayoumi, Faculty of Architecture and Planning, King Abdulaziz University, Saudi Arabia

Abstract

Hybrid photovoltaic/thermal (PVT) systems combine electric and thermal energy generation and provide noiseless operation and space-saving features. As the efficiency of photovoltaic (PV) panels increases at low surface temperatures, this paper suggests combining the PVT panel with a radiant cooling and heating panel in one system. A thermal storage tank fluidly connects the heat-exchanging pipes at the back of the PVT system and radiant panel. The upper portion of the tank feeds the radiant panel and the lower portion of the tank is connected to the PVT system. The proposed device is expected to function in connection with a heat pump that feeds the thermal storage. Using the dynamic thermal simulation software Polysun, the performance of the proposed façade-integrated device was investigated while considering the surface temperatures and energy production in the moderate climatic condition of the city of Munich. The results indicate a substantial impact on the efficiency of the PV module with an increase of up to 35% in the electricity production of the PV due to the lowered surface temperature. The obtained results contribute to façade-supported cooling/heating and electricity generation through the novel coupling and integration of PV, PVT, and radiant cooling elements.

Keywords

Photovoltaic/thermal systems, radiant cooling, building-integrated photovoltaic, façade, solar cooling

DOI 10.7480/jfde.2021.1.5442

Simplicity and Performance | Area-Efficient Super- Insulating Façades

David Schenke, Dipl. Ing. LEED AP

Drees & Sommer Façade engineering, Obere Waldplätze 11, 70569 Stuttgart, +49 (0)172 799 50 20, david.schenke@dreso.com

Abstract

Abstract: Using conventional engineering solutions, the rising performance requirements for building envelopes lead to ever increasing thickness of façade build-ups consuming valuable floor area. For the new office building development 'Obere Waldplätze 12' (OWP 12) on the outskirts of Stuttgart, in direct vicinity to a highly frequented 4-lane feeder road, the boundary conditions require high noise insulation and a very effective thermal envelope. Adopting a standard design strategy, sound insulation is achieved by adding weight to the exterior building parts. For this office building a light and slim, highly insulating building skin has been developed using engineering principles of a different approach. The resulting façade system is surprisingly simple yet highly effective. In laboratory testing its prototype elements are showing significant improvement in performance of several properties in comparison to conventional solutions. The elements are slim, can be applied in high-rise curtain walls and show an insulation quality unprecedented in lightweight façade construction. This paper is outlining the project boundary conditions for the system development from target definition, engineering concept and material research to trial and design proofing phase. For this light-house project, the first adoption of this state-of-the-art high-performance façade is currently being manufactured. Installation is starting early 2021 and the building will go into operation by the end of the same year.

Keywords

Super-slim façade, area efficient curtain wall, energy efficient façade, simplified envelope build-up, design for disassembly, Super-insulating façade, sound absorption with innovative material properties, vacuum insulation panels (VIP) elements in multi-layer configuration

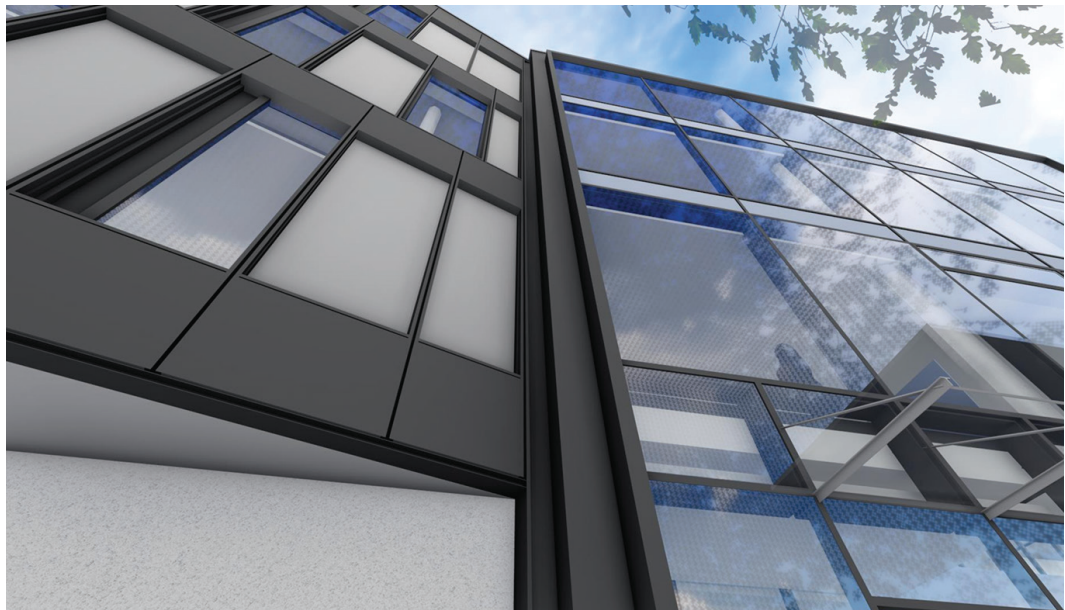


FIG. 1 Visualization of the project 'Obere Waldplätze 12' (OWP12), Stuttgart: new office building façade with first adaptation of an ultra-insulating curtain wall

1 INTRODUCTION

1.1 RELEVANT PARAMETERS OF ENVELOPE PERFORMANCE

Modern building envelope designs are faced with numerous requirements such as thermal insulation, sound insulation, fire resistance or daylighting, which are increasingly difficult to combine without drastically increasing the build-up thickness of the façade construction. The national energy efficiency ordinance of Germany 'Energieeinsparverordnung EnEV' (Bundesregierung, 2013), with its latest version of 2014 is making steps to further decrease the energy usage of buildings. The next stage of this development is the 2021 replacement of the EnEV by a European-wide standard for low energy buildings in new construction, which poses even stricter requirements for new building construction. Consequently, the heat transfer coefficient U_{cw} through the exterior building skin has become a key parameter to meet the energy efficiency standards. U_{cw} -values of 0,5 W/m²K or lower for the overall façade performance are now common in the mission books for construction projects.

Another parameter of increasing importance for the quality of an envelope system is the insulation from exterior airborne noise. The market need for optimized noise control of building skins is caused by two tendencies of the real estate business, namely building sites of residential developments, which are more commonly situated in city areas that are exposed to high levels of traffic or commercial noise sources. At the same time, this inner-city residential construction is often using the typology of high-rise buildings, which - for the purpose of an economic construction process - is demanding modular, light-weight curtain wall façades. A well-known example of noise-exposed urban residential developments is the Hafencity in Hamburg, where luxury apartment towers face the noisy activity of Germany's largest container terminal at night.

Looking at the noise emission charts issued by German municipalities for building projects, sound levels of 65 dB to 75 dB (see fig. 2) during night-time are a frequently occurring boundary condition for the envelope design. Noise impact on residents is not simply a question of higher or lower living comfort in their homes. It has been identified as a medical cause for irreversible cardiovascular damage of residents when exposed to its source for an extended period as for example it is stated in the 'Hamburger Leitfaden Lärm in der Bauleitplanung 2010' (Behörde für Stadtentwicklung und Umwelt, Freie Hansestadt Hamburg, 2010)

1.2 THE ENERGY-NOISE PERFORMANCE CONFLICT

Noise reduction capability of a building envelope is conventionally achieved by adding mass to the building parts – a characteristic which is ironically directly opposed to the necessity of achieving a low heat conductivity within the façade construction. Thermal insulation layers characteristically are low-density panels or boards and require airy, light materials like wools or foams with the capability of encasing resting air cushions inside their micro-cavities (Sprengard, Treml, & Holm, 2014).

To combine the thermal and acoustic insulation in a building façade, the standard engineering design approach is to fulfil every requirement (structural, thermal, acoustical) in separate layers, which are then only added together. The result of this non-integrated approach is commonly a façade build-up of 450 mm thickness or more - using up valuable floor area.

1.3 INNOVATION GAP

Using light-weight materials, conventional curtain wall façades are slim but do not exceed 45 dB – 46 dB noise reduction levels installed on site. Double skin façades with technical enhancements of the cavity can go up to 48 dB – 50 dB, but they are complex, expensive, and less suited for use in residential buildings. Alternative or more innovative solutions are not available on the market; thus, a façade system that fulfils all challenges of insulation integrated in a single functional layer could, if developed, find demand from the building industry.

2 INTEGRATED SOLUTION

In 2016 the German project management firm Drees & Sommer decided to acquire and develop the plot 'Obere Waldplätze 12' (project name later referred to as OWP12) in the vicinity of its Stuttgart head-quarter office campus and construct a new building with offices, functional spaces for public receptions, conference, and meetings. The building plot is a narrow stretch bordering to the South the 4-lane Autobahn 81, one of the main feeder roads for Stuttgart's commuter traffic. The long south façade is facing high noise emission levels (LrT) of up to 75 dB (see fig. 2). Noise control through the façade was, therefore a key requirement in the design of the building.

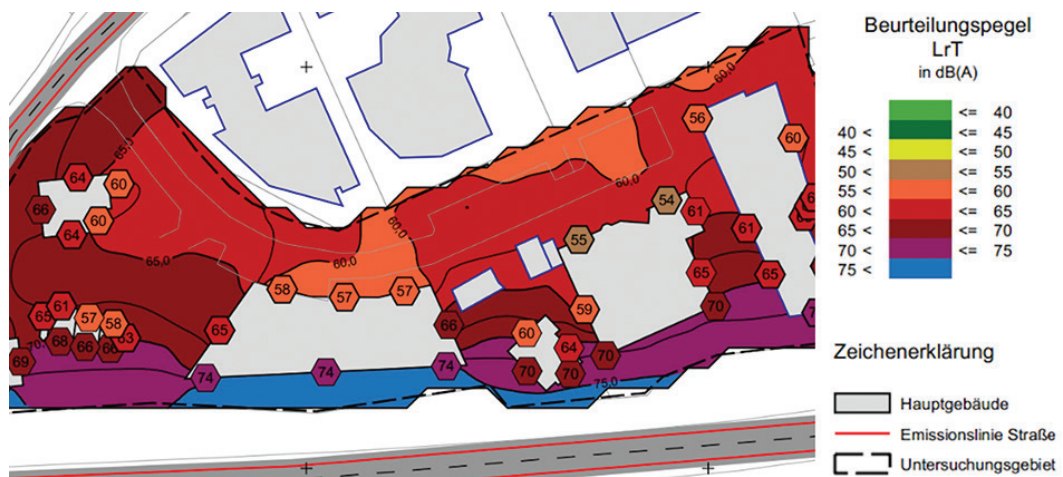


FIG. 2 Plot of the Obere Waldplätze 12 (OWP12) office building project with noise emission levels along the Autobahn 81 south of the plot, (source: OWP12 emission noise concept design documentation)

With a client coming from the building engineering industry, the project is aimed at creating a reference building of applied technological innovation, using new design and construction methods. The design goals, including development targets for the building façades are therefore defined by the investor and the engineering teams as below:

- High sound insulation of up to 48 dB for the façade with regards to user comfort and healthy building design
- High energy efficiency of the façade to achieve the plus-energy target of the project
- Building-integrated photovoltaics in the façade surfaces for green electricity to contribute to the plus-energy target
- Fully modular construction and prefabrication, façade installation without external scaffolding
- Usage of design for disassembly principles and Cradle to Cradle guidelines for non-toxic material content

- Slim and light façade construction as economic solution with regards to area efficiency and construction cost
- Simple but innovative technical solutions as prototypes that are ready for a wider market application
- Engineering design which is applicable for high-rise façade construction using only 'A'-rated fire resistance insulation layers
- Fully digital twin modelling and BIM application during planning and execution

The design team must adopt an integrated approach for the engineering solution, with early involvement of material science and technology, material testing, façade technology and manufacturing, building physics and façade engineering to deliver timely results. Looking at a construction deadline and budgetary goals of an actual building site, the systematic choices for the engineering development of the façade have to consider market availability of materials and buildability of the design, aiming at simplified technical solutions and using as many standardized parts as possible.

Although numerical simulation of sound insulation for material samples is possible with specialized software, it is determined that for sufficient accuracy and reliable design proofing of façade parts in the OWP12 project, laboratory testing of physical mock-ups is inevitable and must include time and resources for repeat-testing of alternative configurations. Quality gates for testing are hierarchically defined as: fire performance rating, thermal insulation, sound attenuation and others (e.g. standard façade testing such as dynamic waterproof testing).

The façade production costs are consequently defined as a parameter that is continuously monitored during the design development. The cost target is set at an average of below 900 Euro/m² for manufacturing and installation, including integrated equipment such as sun-shading blinds. For cost control, the total number of parts, the number of different parts, the number of materials and the overall system complexity are continuously reduced and simplified in the process.

3 DEVELOPMENT OF THE ENGINEERING SOLUTION

During a one-year research process, the engineering team evaluated innovative façade technologies and material combinations for a promising, integrated solution. It is intended to gain valuable know-how early in the engineering process by involving the curtain-wall industry. Inside an industry-partnering model, the client and the engineering team invited several manufacturers to further develop preliminary engineering concepts for an ultra-slim curtain wall façade. Finally, a prototype system of the R&D laboratory of FKN façades GmbH, Neuenstein was identified as a promising technological basis and selected for full development into a functional, modular façade of the OWP12 office building project.

3.1 INSULATION MATERIAL CHOICE

Early research in insulation technology clearly showed that the usage of vacuum insulation panels (VIP) in the façade provided the best possibility for a drastically effective reduction of the thermal layer. Although VIP panels have been readily available on the market for years, the focus of their application in building construction today is based purely on the thermal performance characteristics. However, the principle of evacuated cavities as a noise barrier is very intriguing, as sound waves do not travel through a vacuum.

Research on custom made elements tested with 'low' vacuum conditions (100 kPa to 3 kPa) shows that with an increase of the vacuum to values above 80% in relation to the atmospheric pressure

(pressure at sea-level = 0% vacuum), the sound insulation of the panel starts to rise exponentially (Dance & Walters, 2014).

Studies on VIP panel's airborne noise transmission properties in 2007 by experimental testing reveals that the 'naked' panels show continuously rising sound attenuation up to a frequency of 1000 Hz. The sound transfer reduction then drastically drops to a minimum at approx. 3100 Hz. Combined with different material boards into multi-layered configurations, however, the sound attenuation of the hybrids continuously rises with an only insignificant drop at approx. 2000 Hz (Gudelji, 2007, p. 18 Fig 28); (Maysenhölder, 2009, p. 6 ff).

Therefore, one key factor for higher noise insulation of elements with VIP panel inlays is clearly the combination of the VIP with other actively contributing materials into multi-layered configurations. Several material properties such as thickness and density, elasticity, the connection between the layers as well as the influence of framing and supports need to be considered as well.

3.2 PRELIMINARY ENGINEERING CONCEPT

The preliminary engineering concept is developed by using non-proprietary façade components, which allows any standard profile system to be used in the further development. The relevant multi-layered insulation barriers are designed inside a 90 mm aluminium frame. It can be fabricated into a fully unitized curtain wall by using standard tools and connectors. The layers between the profile frames are made up from a combination of different high-performance insulation materials with a preliminary configuration of the panel, as listed in Table 1.

LAYER DESCRIPTION	BUILD-UP THICKNESS (mm)
Cover layer: HT safety glass	6
Mineral insulation material, silicon dioxide board → thermal transfer value λ (design value) = 0,021 W/(mK)	30
VIP insulation material, evacuated silica block → λ (peak) = 0.007 W/(mK) → λ (condensate min.) = 0.020 W/(mK)	30
Mineral insulation material, silicon dioxide board → thermal transfer value λ (design value) = 0.021 W/(mK)	20
Gypsum fibre panel	9.5
Cover layer: Aluminium sheet metal panel, powder-coated	3

TABLE 1 Regular element panel build-up – preliminary calculation model

The preliminary façade panel configuration is used for simulation models as well as for the first performance test mock-ups. These small material mock-ups are sent to undergo the milestone tests of fire safety at the laboratory of the Rosenheim Institute of Window Technology IfT Rosenheim (IfT Rosenheim, 2018) and material fire behaviour classification as per DIN EN 13501-1:2010-01 at the Braunschweig University of Technology building material institute (iBMB, TU Braunschweig, 2018). The test reports of both institutes result in a material fire rating classification regarding combustion (A2 = no contribution to combustion), smoke development (s1 = low smoke development), melting or dripping (d0 = no dripping of burning particles) of the combined panel:

A2-s1,d0

This classification is important for the further development of the system, from a prototype into a market-ready façade application. The usage of curtain wall façades is especially viable in high-rise construction where all economic advantages of a modular façade can be used and fire regulations require the installation of fire-rated 'A'-class materials solely. Any other rating result

of this innovative panel configuration could not be accepted for lack of market readiness of the curtain wall system.

3.3 CONSOLIDATED SYSTEM DESIGN - THERMAL PERFORMANCE

The preliminary panel configuration is further developed into a customized technical façade design for the office building project 'Obere Waldplätze 12', Stuttgart (OWP12). In the process, a market available profile system is specified to be used in the execution design, and tools and processes are adapted to it (here: Schüco USC Façade, type no 331980).

The technical description of the fully functional façade is as follows:

- Fully unitized façade system based on a 90 mm system profile with thermally broken frames
- System with structurally enhanced mullion to the exterior which also serves as the guiding rail for sun shading system and support of the integrated photovoltaic (PV) panels
- Element size with connectors at split mullion every 2.700 mm, structural mullion every 1.350 mm (see Fig. 3)
- Element height 4.050 mm (see Fig. 4)
- Each element is divided into one opaque half (1.350 mm) manufactured as a highly insulating panel and one half (1.350 mm) with room high, transparent fixed glazing (see fig. 3)
- Triple insulating glass with $U_g = \text{approx. } 0,7 \text{ W/m}^2\text{K}$ with fall protection requirements
- Selected elements are equipped with an opaque panel opening sash for comfort ventilation, approx. 250 mm wide x 2.050 mm high (see Fig. 3)
- Spandrel section with opaque glazing elements at the exterior, connected at the interior to the concrete floor-slab and fully filled with mineral fibre insulation
- Elements are fixed at 3 points by adjustable bracket consoles on the concrete slab of the superstructure
- South facing façade parts are equipped with integrated photovoltaic panels with anti-reflective surface structure
- Glazed element parts are equipped with a highly effective exterior sun shading system using motorized Venetian blinds

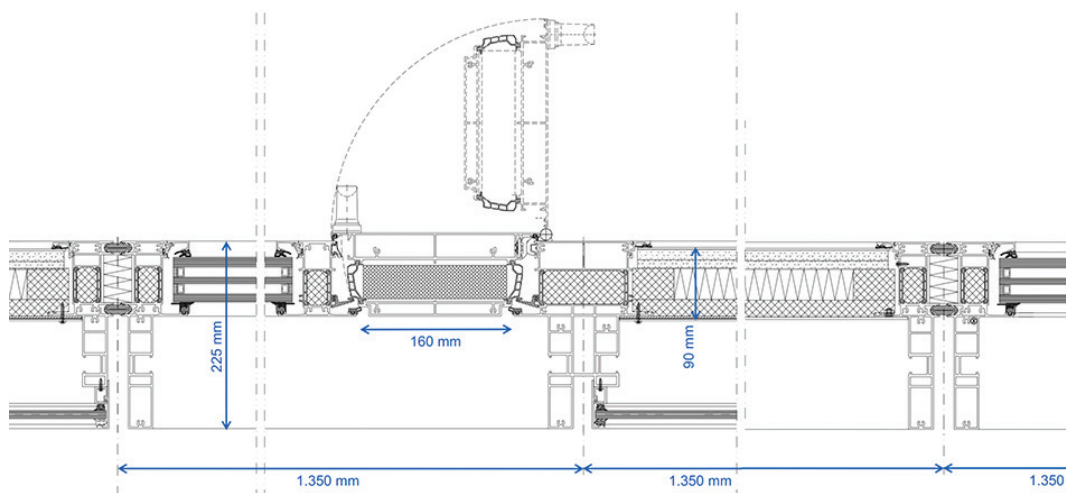


FIG. 3 Façade with BIPV horizontal section | fixed glazing with opening sash (left) – specific panel build-up (right)

During the technical design process within the engineering development of FKN Façade GmbH, Neuenstein, the specific project requirement values are adapted, and a consolidated façade build-up is defined for the OWP12 project to the following layer configuration:

LAYER DESCRIPTION	BUILD-UP THICKNESS (mm)
Exterior cover layer: Aluminium sheet metal panel, powder-coated	2
2 nd cover layer: flat steel panel, galvanized	3
Mineral insulation material, silicon dioxide board → thermal transfer value λ (design value)	20
VIP insulation material, evacuated silica block → λ (peak) = 0.007 W/(mK) → λ (condensate min.) = 0.020 W/(mK)	30
Gypsum fibre panels 10 mm + 15 mm	25
Interior cover layer: Aluminium sheet metal panel, powder-coated	2.5

TABLE 2 Regular element panel build-up – specific façade model for OWP12 project

This consolidated, specific façade build-up is further used for simulation of thermal bridges and calculation of the overall thermal system performance as per DIN EN ISO 10077-1:2018 and DIN EN 12631:2018. For the Ucw calculation, several different façade sections of the specific project are selected as described in tables 3.

NUMBER, ELEMENT TYPE DESCRIPTION	U-VALUE CALCULATED (W/m ² K)
N1, combination element panel and glass, width = 2.700 mm	0.53
N2, glass element, width 1.350 mm	0.73
N3, panel element, width 1.350 mm	0.33
N4, glass element with opening sash panel, width 1.350 mm	0.82
S1, combination element panel and glass, width = 2.700 mm	0.52
S2, glass element, width 1.350 mm	0.72
S3, panel element, width 1.350 mm	0.32

TABLE 3 U-value calculation for different sections of the specific façade configuration

From the above-listed sections, the calculation results of N1 and S1 best represent the overall system performance with a window to wall ratio of approx. 50% glazed elements and 50% panels. The thermal transfer value of this specific build-up can be defined at approx. 0.52 W/m²K (FKN Fassaden Neuenstein, 2020).

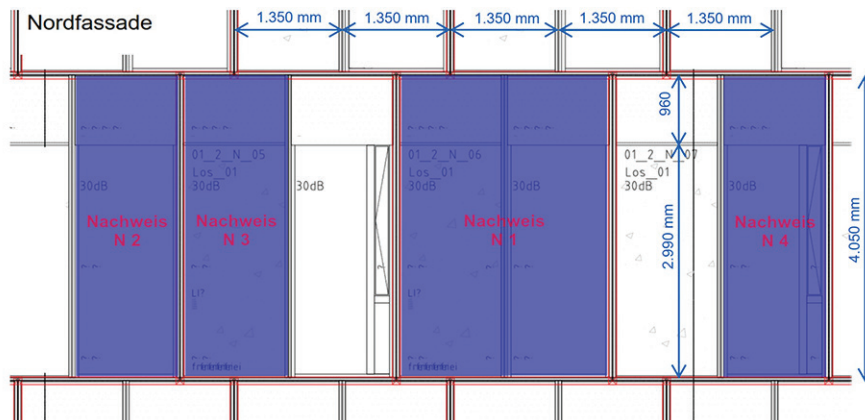


FIG. 4 Simulation model (extract) for different façade types and situation in the project OWP12

The system, as applied for the office building project OWP12, has not been designed to reach its full potential since the requirements of energy efficiency for this building project are already over-achieved. When making full use of every layer inside the 90 mm frame system, the overall thermal transfer value can be further decreased to as low as $U_{cw} = 0,41 \text{ W/m}^2\text{K}$ (FKN Fassaden Neuenstein, 2020). In comparison, a conventional insulation layer made from mineral fibre, would need to be at least 250 mm thick.

3.4 SOUND INSULATION FROM AIRBORNE NOISE

In mechanical engineering, VIP panels have been used successfully for sound attenuation purpose, for example, for noise reduction in medical equipment. However, this usage of VIP in building construction is not common practice. Theoretical data shows that a reduction of the internal pressure in a test element cavity to 10% of the atmospheric pressure or 10.13 kPa (90% relative vacuum) already yields significant improvement of the sound attenuation above 250 Hz. A 'high' vacuum as per physical definition below 100 mPa internal pressure is not necessary for an effective usage of VIP elements in noise control for building parts (Maysen-Hölder, 2009). Market available VIP elements that comply with the regulatory approval no Z-23.11-1662 of the DIBT (Deutsches Institut für Bautechnik) must not exceed an internal pressure of 0.5 kPa at the time of delivery, equalling per definition a 'medium' vacuum at 3 kPa to 100 mPa (DIBT Deutsches Institut für Bautechnik, 2017). Their degree of evacuation or relative vacuum is as high as 99.5% and therefore fully effective for sound attenuation purposes in the OWP12 ultra-slim façade.

The technical solution for the noise transfer reduction is based on the principle of mass-spring-mass acoustic absorption. The multi-layer panel configuration is using a compensation strategy for weak links within the resonant frequencies of its combined material layers. As every construction material has its individual resonance frequency depending on its weight, a balanced combination of different masses, separated by acoustically weak materials or adhesive layers omits the performance fall-off that homogeneous constructions typically show at a specific frequency (see Fig 5). Regarding the improvement of sound insulation within deep frequencies like traffic noise, the sound transfer between adjacent material shells can be reduced to an optimized level without adding weight to the system. An 'asymmetrical' configuration of the layers is found to be best performing, also the order in which materials with different elasticity characteristics are mounted has an influence on the overall performance in testing.

Resulting from this research, the specific façade build-up as shown in table 2) is developed into a façade prototype element for performance testing in the laboratories of the Testing Centre for Building Parts, Traunstein (PfB Prüfzentrum für Bauelemente, 2020). Several different acoustic performance parameters are checked, but the relevant method for design proofing of this innovative development is based on airborne sound reduction tests performed as per standard DIN EN ISO 10140-2 : 2010-12 and DIN EN ISO 717-1 : 2013-06.

Testing sample build-up for 1-axis elements (only panel part) and 2-axis testing (combined panel and glass)

- 1-axis: total surface area of curtain wall section: 6.05 m², width: 1.55 m, height: 3.9 m
- 2-axis: total surface area of curtain wall section: 11.31 m², width: 2.9 m, height: 3.9 m
- Simulation of the floor connection, no simulation of the ceiling connection
- Fixed glazing part with Triple insulating glass build-up:
Laminated safety glass (LSG) 66.2 SI/SPACER 14 mm/Float 6 mm/SPACER 14 mm/ LSG 66.2 SI
- Simulated PV module mounted at the exterior with glass build-up:
Laminated safety glass (LSG) from 2x 6 mm Float and 1.52 mm PVB-lamination foil

- Panel build-up as per specific façade design seen in Table 2)

EMISSION FREQUENCY (Hz)	SOUND REDUCTION LEVEL (dB) 2-AXIS ELEMENT (COMBINED PANEL AND GLASS)	SOUND REDUCTION LEVEL (dB) 1-AXIS ELEMENT (PANEL)
400	45.9	52.1
500	48.0	53.4
630	49.6	54.2
800	50.1	55.5
1000	51.0	55.3
1250	51.8	55.7
1600	52.1	58.2
2000	51.0	59.5
2500	51.7	60.5
3150	54.9	63.3

TABLE 4 Testing results (extract) for 2-axis elements and 1-axis elements

Consolidated testing result for 2-axis element (combined panel and glass):

$$R_w (C; Ctr) = 50 (-1; -5) \text{ dB}$$

Consolidated testing result for 1-axis element (panel):

$$R_w (C; Ctr) = 55 (-1; -5) \text{ dB}$$

The test of the isolated panel section in the performance mock-up shows high measurement results for the selected configuration of materials inside the profile spacing. Conventional panels made from light-weight materials are often the weak link in the sound transfer reduction, having a lower performance than acoustic insulating glass.

This innovative panel combination, however, proves to test at levels of 55 dB for noise reduction (R_w). This is due to the multi-layered combination of plate and panel materials which, in a mass-spring-system, compensates their individual acoustic weakness caused by the typical resonance frequency of each panel. The test results confirm the theoretically expected improved sound insulation, particularly in the low-frequency range (PfB Prüfzentrum für Bauelemente, 2020).

Considering a panel thickness of only 90 mm, the potential of this engineering solution becomes evident: Compared to a conventional façade with similar noise reduction capabilities (for example: 220 mm concrete wall for a 53 dB reduction installed on site), this high-performance panel achieves a 60% reduction in building parts thickness and a 75% reduction of material weight (500 kg/m² for a concrete wall in comparison to approx. 110 kg/m² average weight for the ultra-slim façade, see Fig. 6)

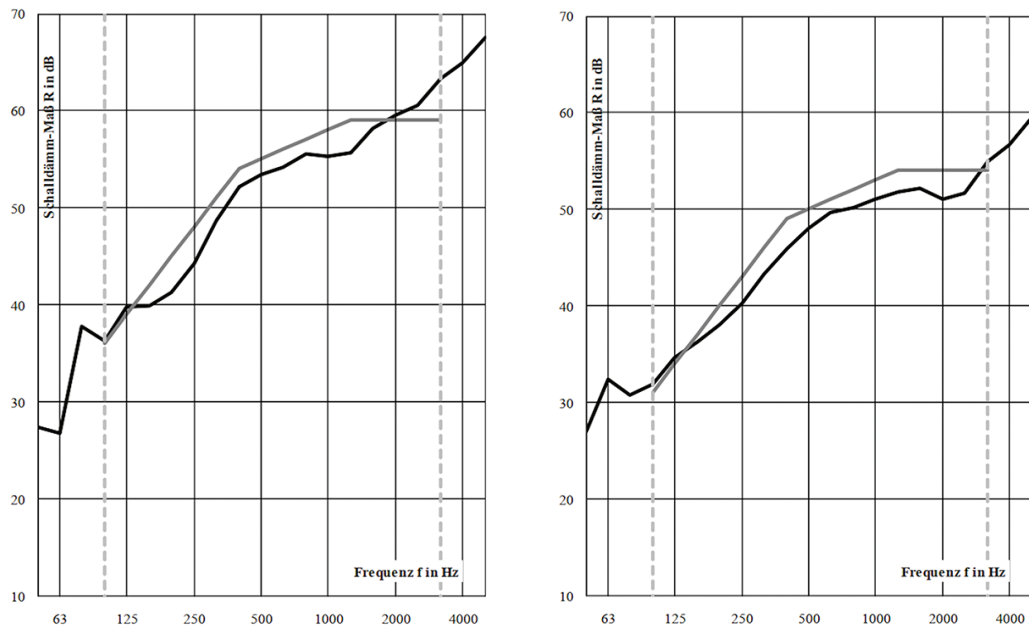


FIG. 5 Testing results (graph) for sound transfer reduction [dB] in relation to the frequency [Hz]
left: 1-axis system, right: 2-axis system

For the specific project OWP12, the laboratory test result of 50 dB as a combination of fixed glazing and opaque panel is fully compliant with the project goals (requirement 48 dB installed on-site).

4 RESULTS

While conventional curtain wall façades with single glass layer configuration are not exceeding 45 dB-46 dB sound level reduction installed on-site, the prototype configuration of this ultra-slim curtain wall is showing to reach 48 dB to 50 dB. With further optimization e.g. better sound insulation glazing or an adjusted window to wall ratio, even performance values of 52 dB noise reduction are plausible – all of which can be achieved based on a 90 mm façade profile section. The 6 dB-7 dB difference equal a reduction in sound energy by 50% compared to the performance of a conventional curtain wall skin. This is a huge step of improvement for this ultra-slim façade which provides new freedom and opportunity for designers and investors alike.

Any conventional façade achieving the same qualities would be in comparison approx. 500 mm deep. This new system requires merely 90 mm for the insulation layers + 120 mm for structural stiffener – totally 210 mm – 250 mm total façade build-up. This equals a reduction of 55% for the façade construction area. On a typical floor plan, this area gained along the façade parameter amounts up to 25 m² per floor or 250 m²-400 m² for an average high-rise building development. The area gained directly generates additional revenue and represents a noticeable economic offset in the first investment as well as in operation and energy costs alike – added value for developers and building owners.

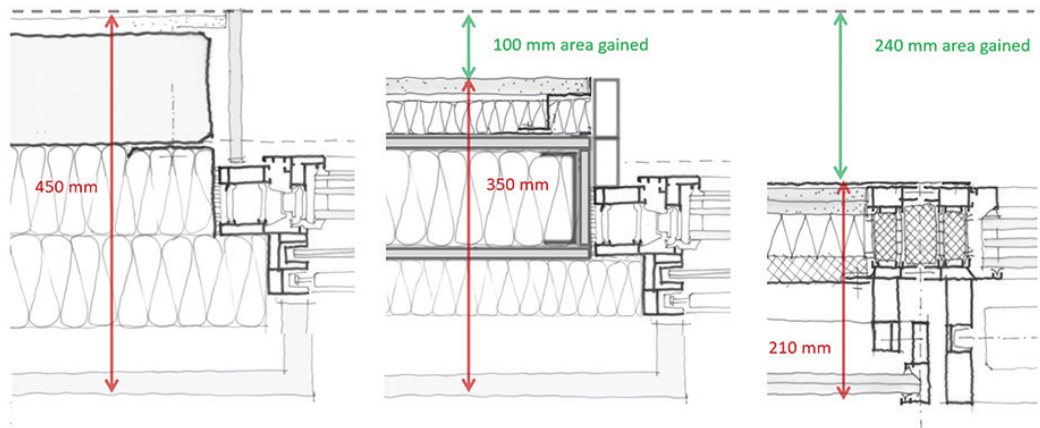


FIG. 6 Comparison of the net floor area gain (green arrow) by the application of ultra-slim façade systems

left: concrete window wall
 $U_{cw} = 0.7 \text{ W/m}^2\text{K}$

middle: lightweight exterior wall
 $U_{cw} = 0.7 \text{ W/m}^2\text{K}$

right: ultra-slim façade
 $U_{cw} = 0.4\text{-}0.5 \text{ W/m}^2\text{K}$

5 CONCLUSIONS AND OUTLOOK

In simulation and testing this state-of-the-art prototype façade is showing unprecedented performance results considering its ultra-slim configuration. The target costs of the façade development, as stated in the methodology part, have been met and first elements are currently being produced by FKN façades GmbH Neuenstein, Germany. Installation on site will start at the beginning of 2021. Testing and optimization of the curtain wall system will continue during the first years of operation and the production feedback as well as the long-term operation experience will influence further development steps of the system.

The usage of VIP insulation in modular façade construction will be further developed as the prefabrication process of façade manufacturers provides an appropriate framework of precision, quality control and customization that are necessary for handling and installation of the relatively delicate vacuum elements. Although the system is simple and very slim, this innovative curtain wall façade sets new standards for thermal and acoustic insulation, simply by applying an optimized combination of material characteristics.

Simplicity and performance – in this ultra-slim modular system, the two qualities are not opposing characteristics but - in combination - make this façade a trendsetting economic innovation for the building industry.

Acknowledgements

FKN façade GmbH, Neuenstein, IfT Rosenheim, PfB GmbH Traunstein, SCD architects, Stuttgart, Drees & Sommer SE project management, Drees & Sommer building physics, Stuttgart

References

- Behörde für Stadtentwicklung und Umwelt, Freie Hansestadt Hamburg. (Januar 2010). Hamburger Leitfaden Lärm in der Bauleitplanung 2010. Hamburg: Freie Hansestadt Hamburg.
- Bundesregierung, D. (11 2013). Bundesgesetzblatt Jahrgang 2013 Teil 1 Nr.67. Energieeinsparverordnung EnEV 2014. Bonn: Bundesanzeiger-Verlag.
- Dance, S., & Walters, S. (2014). InterNoise 2014. Development of vacuum isolating panels for noise control applications (S. 10). London: London South Bank University.

- DIBt Deutsches Institut für Bautechnik. (11. 05 2017). Allgemein bauaufsichtliche Zulassung Z-23.11-1662. Vakuum-Wärmedämmplatten aus Kieselsäure. Berlin: Zulassungsstelle für Bauprodukte und Bauarten.
- DIBt Deutsches Institut für Bautechnik. (14. 02 2020). Allgemein bauaufsichtliche Zulassung Z-23.11-2103. Mehrschichtige Wärmedämmplatten CT Paneel Multi. Berlin: Zulassungsstelle für Bauprodukte und Bauarten.
- FKN Fassaden Neuenstein. (2020). Wärmeschutznachweis Ucw EL-Fassade 19005 OWP12. Neuenstein: FKN Fassaden.
- Gudelji, Z. (2007). Schalldämmung von Vakuum-Isolier-Bauteilen. Diplomarbeit. Stuttgart : Lehrstuhl für Bauphysik Universität Stuttgart .
- iBMB, TU Braunschweig. (2018). Klassifizierungsbericht zum Brandverhalten nach DIN EN 13501-1:2010-01. Braunschweig: iBMB Institut für Baustoffe Massivbau und Brandschutz MPA TU Braunschweig im Auftrag von FKN Fassaden Neuenstein.
- IfT Rosenheim . (2018). CT-Paneel MULTI Kleinbrandprüfung. Rosenheim : IfT im Auftrag FKN Fassaden R&D.
- Maysenhölder, W. (2009). Schallschutz mit Vakuumisolationspaneelen. Stuttgart: Fraunhofer IRB Verlag.
- PfB Prüfzentrum für Bauelemente. (2020). Prüfbericht Nr. 2020-05-0138-B1 Messung der Luftschalldämmung nach DIN EN ISO 10140-2:2020-12. Traunstein: PfB im Auftrag FKN Fassaden Neuenstein.
- Sprengard, C., Tremel, S., & Holm, A. (2014). Technologien und Techniken zur Verbesserung der Energieeffizienz von Gebäuden durch Wärmedämmstoffe . Stuttgart: Fraunhofer IRB Verlag.

Effect of Energy Management and Influencing Parameters in Local PV Use

Lea Bogischef¹, Manuel de-Borja-Torrejon², Claudia Hemmerle³

- 1 Technical University of Munich, Arcisstrasse 21, 80333 Munich, +49 89 289 23980, lea.bogischef@tum.de
- 2 Technical University of Munich, Arcisstrasse 21, 80333 Munich, +49 89 289 23823, manuel.de-borja-torrejon@tum.de
- 3 Technical University of Munich, Arcisstrasse 21, 80333 Munich, +49 89 289 22964, claudia.hemmerle@tum.de

Abstract

Aiming at a climate-neutral energy system, the need for on-site supply and consumption of renewable energy is becoming increasingly relevant. Sector-coupling energy management utilising heat pumps and optimised control can enhance the local consumption of decentral renewable electricity. This study evaluates the potential of energy management on that enhancement in multi-family buildings and how much impact different parameters have on this potential. To this end, a case study consisting of two exemplary residential apartments with different orientation located in Potsdam (Germany) is simulated for the month of October, an optimisation algorithm for energy management is implemented, and results are evaluated based on two main indicators for energy management potential: one representing the relative difference in autarky between fix setpoint and optimised operation and the other, analogue, the relative difference in self-consumption. Among the examined parameters, the analysis suggests a high relevance of the constructive standard and its resulting heating demand. This is based upon a change in the indicator values regarding self-consumption and autarky from respectively 24 and 17 % in a base case scenario with an original building state to 0 % for both indicators in a variant with a passive house standard. Limiting the envelope area used for PV to the roof area results in a relevant reduction of the energy management potential revealed by a decrease of the self-consumption and autarky indicator to 16 and 5 %. Moreover, only a small difference in the energy management potential was identified when the control definition of the prediction horizon was changed from 48 to 24 hours, meaning that most of the flexibility from the heating operation can be exploited within a one-day horizon. The detailed results presented can potentially support decision making and economic estimations in projects related to building renovation and integration of PV technology at a local level.

Keywords

Sector coupling, building mass, photovoltaic power, energy management, energy flexibility

1 INTRODUCTION

With the goal of a fossil-free energy system, balancing energy supply and demand at a local scale with high on-site renewable production gains more and more importance. All components of the local energy system with the capacity to regulate loads are suitable to be considered for that balance. These components are not limited to the electricity sector but extend to the heating sector via sector-coupling devices such as heat pumps. Thus, the sector interaction has increased attention to the building stock from electricity suppliers and network operators (Zander et al. 2017).

The building sector in Germany is responsible for a large part of the national energy consumption and related carbon emissions (Umweltbundesamt n.d). Besides renovation actions, the integration of renewable energies accounts for means to decarbonise the built environment. Studies addressing the load-management capacity of buildings have shown considerable potential for achieving flexibility for a renewable energy-based system through the building stock (Hausladen et al. 2014; Auer et al. 2017). This potential is based on the electrification of the heating demand in buildings and the use of their thermal mass as an energy storage component. Combining such potential with the goal of a local near-zero energy balance gives rise to the need for further researching energy management and control in buildings for the successful use of locally produced photovoltaic (PV) power.

This topic has been addressed in a number of studies focussing on single-family houses (Weniger et al. 2015, Beer et al. 2016, Kramer et al. 2017). In order to complement this research, the present study deals with the case of residential multi-family buildings, for which there is still a need for more investigation as a promising study case with a relatively large PV surface. The objective includes, on the one hand, knowing the magnitude of the effect of energy management in this type of buildings through an optimised operation of their thermal systems to enhance the consumption of locally produced photovoltaic energy. On the other hand, it is strived to gain more insight into the relevance of different parameters influencing the mentioned effect by energy management.

Influencing parameters can range from passive aspects to active systems and control definitions. With regard to the first category, Hausladen et al. (2014) show that the constructive characteristics of the building and the level of insulation of the envelope influence the load-management potential of the building. In the field of indoor thermal comfort, broader thermal comfort bands have shown potential for energy savings (Dear und Brager 2002), influencing the energy performance of buildings. These findings suggest that the limits of the indoor temperature can potentially have an impact on the effect of energy management, too. Thus, the expectations of users in terms of indoor environmental conditions could play a significant role in the use of the building mass as a resource for energy storage, as the shifting heating loads results in changing indoor temperatures.

In relation to parameters linked to active systems, the study by Weniger et al. (2015) identifies heat pump-related loads in addition to household loads (e.g. lighting and home appliances) amongst the factors influencing autarky and self-consumption of solar energy. Moreover, the study *e-Mobilie* has identified a high shifting potential by the batteries of an electric vehicle, complementary to the flexibility offered by heat pumps, by using integrated energy management. The control of the heat-pump and the loading of the battery is implemented according to the performance of the installed photovoltaic system. This study shows that energy management is able to increase in single-family houses their self-consumption rate of renewable energy produced on-site (Beer et al. 2016).

Optimised control strategies for energy management aim to predict fluctuating renewable power generation and accordingly adapt flexible demand. To this end, the defined time horizon for specifying the prediction period can have an impact on the energy management potential.

To study optimised control strategies in a system with multiple components and the integration of building mass as storage, Kramer et al. (2017) implement a distributed model predictive control approach in order to manage the residual load of multiple buildings. This approach differs from the one implemented for single houses, in which the management of energy relates to only one residential unit.

In this framework, the present study quantifies how much impact different features have on the potential for enhancing the consumption of locally produced photovoltaic power by means of energy management. To carry out the analysis in a holistic manner, parameters of the three mentioned categories are addressed. In addition to the objectives described above, this work aims to contribute valuable data and findings to support the decision making in the development of future studies and the application of energy management in real cases.

2 METHODOLOGY

To address the objective of the study, a parametric analysis using simulation models is conducted. Two residential apartments located in Potsdam, Germany, modelled as single thermal zones are used as a case study (see section 3). A base model is compared to a number of variants, each corresponding to a change of one of the analysed parameters included in the base model. Simulation results are evaluated according to predefined indicators. This section explains the overall modelling approach and its different constituent parts. The selected parameters considered in this study are described as well. Furthermore, the simulation variants are shown, and the parametric analysis is introduced. Finally, the indicators defined for the evaluation of results are presented, followed by an explanation of the implementation of the optimised energy management in the simulations.

2.1 OVERALL MODEL STRUCTURE

The overall modelling approach developed within the project Cleanvelope is applied for this analysis (Bogischef et al. 2019). This approach consists of the articulation of two models integrated into one consistent work flow: a micro-climate model and a district-wide energy system and its optimisation. The latter model includes all relevant aspects required for the present analysis, which are integrated through a newly scripted python-code in the following three layers: (i) consumption, (ii) production, (iii) control. These three layers relate to the above mentioned key categories addressed by the selected parameters. Thus, the program is able to model different types of consumers and producers and uses optimisation methods for coupling these two sides. The script enables modelling a system at a district scale and is hence suitable for this study on two representative thermal zones (see case study in section 3). The reduced magnitude of the two-zone model allows for taking advantage of a shorter required computation time compared to more complex cases. Figure 1 gives an overview of the model components, which are explained in more detail below.

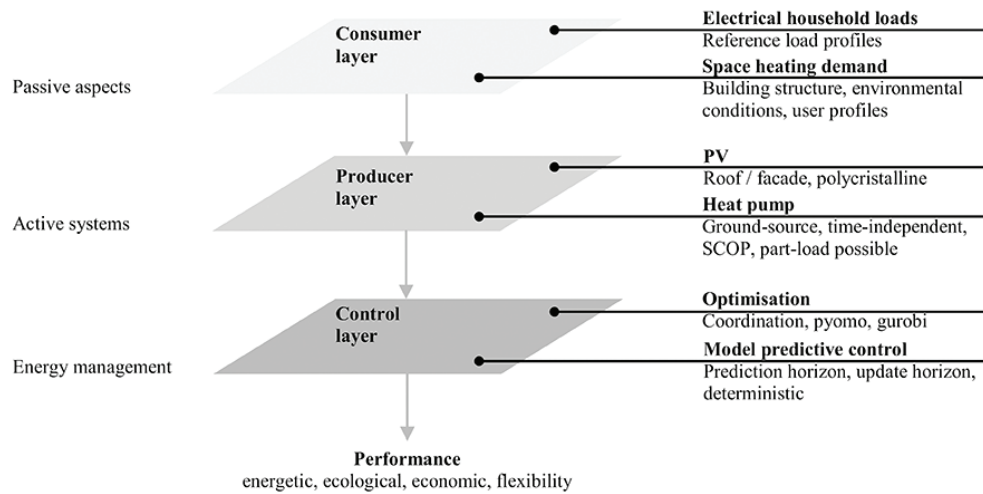


FIG. 1 Model components

Consumers: This model part covers the representation of both the thermal behaviour (space heating) and the electrical load profiles. The thermal behaviour of each thermal zone is represented via a Resistance-Capacitance model (RC model) (Fig. 2). The topology approach of the RC-model and its parametrisation are based on the procedure described in VDI 6007-1:2015-06 with two relevant capacitances: one representing the sum of external building components and the non-adiabatic internal components; and the other representing the internal components. Deviating from the original VDI approach, the model represents a whole apartment instead of a room as a thermal zone. It is regarded as a necessary simplification in order to reduce the total number of model instances as well as an adequate compromise between modelling a whole building as a single zone and a room-wise approach (Hausladen et al. 2014). The implementation of the RC-model builds upon the continuous time-state-space formulation of its dynamic equations that is discretised by applying the *cont2discrete* function of the *signal* package (Virtanen et al. 2020). This results in a discrete system description for each thermal zone i and time instance k (Equation 1). This description features the MPC-typical distinction between uncontrollable inputs, also named disturbances, and controllable variables. The disturbance vector (Equation 2) consists, on the one hand, of the heating loads such as internal gains by people, machines and solar gains (sorted and summed into parameters reflecting the location where they become effective within the RC-model). On the other hand, this disturbance vector also includes the equivalent outdoor temperature (air temperature altered by longwave and shortwave radiation effects) and the ventilation air temperature. The controllable variables are considered in vector u_i (Equation 3) and correspond to the heating and cooling demand. Moreover, x_i represents the state vector (Equation 4), which consists of the temperatures of the summed external and the summed internal building components (walls, windows, floor and ceiling) at the respective locations in Figure 2, and the zone air temperature (T_z). Finally, A_i , B_i and C_i are matrices based on the parametrisation of the RC-model (see VDI 6007-1:2015-06 for more detail). The developed RC model has been validated based on the examples attached to VDI 6007-1:2015-06, which this norm provides for that purpose.

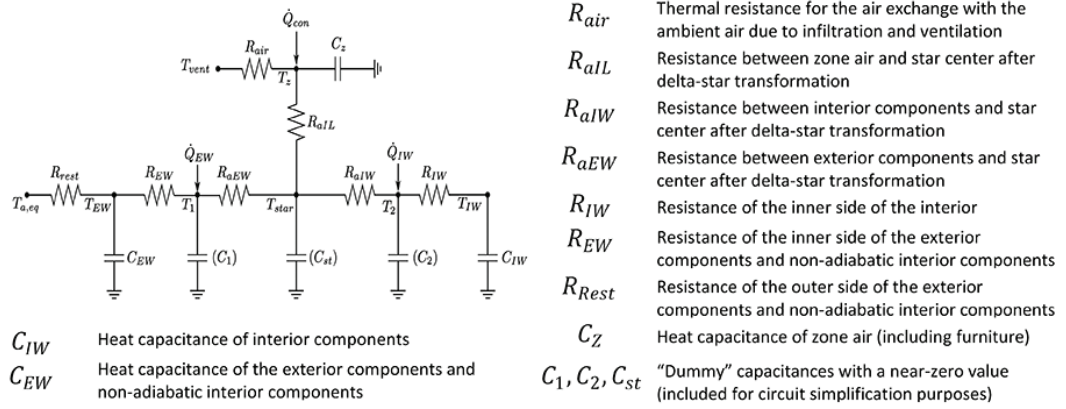


FIG. 2 RC-model of a thermal zone

$$x_i(k+1) = A_i x_i(k) + B_i u_i(k) + C_i d_i(k) \quad (1)$$

$$d_i = [Q_{EW,fix}(k), Q_{IW,fix}(k), Q_{con,fix}(k), T_{aeq}(k), T_{vent}(k)]^T \quad (2)$$

$$u_i = [Q_h, Q_c]^T \quad (3)$$

$$x_i = [T_{EW}(k), T_{IW}(k), T_z(k), T_1(k), T_2(k)]^T \quad (4)$$

The energy demand calculated by the thermal model is translated into an electrical load profile by modelling the operation of a heat pump (see below, Producers). This profile is extended by taking into account a total electrical load profile from lighting and appliances representative for households. This complementary profile is modelled following the norm VDI 4655-1:2019-09. According to this guideline, the load profile for a household is dependent on the annual demand, which the norm suggests to be set to 3000 kWh/household for multi-family buildings independent from the number of inhabitants, and the parameters climate zone, outdoor temperature (defining the season), cloudiness and day of the week. It should be highlighted that this method results in identical load profiles for both apartments because the climate and total annual demand are the same.

Producers: Besides local renewable electricity production via photovoltaic panels installed at the building envelope, a heat pump is considered in the model serving as a monovalent heat producer and as the element that is enabling sector-coupling. The PV generation is calculated externally in TRNSYS using Type-190d (Klein et al. 2017, S. 119–132), whereas the heat pump performance is implemented as a part of the model. With the aim of simplification, the representation chosen for the ground-source heat pump is a time-independent efficiency factor, taken as the Seasonal Coefficient of Performance (SCOP). Thus, possible time lags resulting from capacities or further supply-side losses between generator and usage are neglected. Furthermore, the system is not aiming at autarky and therefore, electricity import from the grid is allowed without any power limit.

Control: The control feature consists of an optimisation that employs the prediction of inputs known as model predictive control (MPC). It does not aim at a global optimisation of the whole time period simulated but at an optimal operation that considers a limited amount of future time steps N_p . This optimisation is then repeated with a defined update horizon t_{update} which results in a so-called receding horizon, which is characteristic of the MPC approach. Thus, only the values within this update horizon are implemented. The values for the remaining time steps within the prediction horizon located outside the update interval are part of the current optimisation run, but they are not

fixed prior to the respective iteration. This reflects the fact that uncertainty is included in predictions and is reduced in near future compared to time steps further ahead. Within the study at hand, uncertainty is not a focus. Therefore, inputs and model outputs are assumed to be deterministic, and time resolution Δt is set to 1 h. The optimisation is executed utilising the python packages of *Pyomo* (Hart et al. 2011), and *Gurobi* (Gurobi Optimization 2020) is set as the solver. An objective function and constraints are required for the implementation of the optimisation. The ones implemented in this study are described in section 2.5.

2.2 ANALYSED PARAMETERS

For the parametric analysis performed in this study, a total of six parameters (P1-P6), covering the three key categories mentioned above (Passive aspects; Active systems; Control definitions) are selected. The relevance of these parameters for the purpose of this study has been identified according to the literature on this topic cited in the introduction. For each parameter, two alternative configurations are taken into account:

- **P1 - Building age/state:** original and new/renovated. This parameter is considered to study the effect of the energy demand profile of different building efficiency standards and the corresponding constructive composition of the building envelope and available thermal mass. Thus, original is represented by a constructive standard corresponding to a German building built between 1958 and 1968, and new/renovated a passive-house building as representative of a nearly-zero energy standard (see details in section 3).
- **P2 - User profile:** normal and moderate level of expectation. This parameter is selected to evaluate the influence of different user preferences in terms of thermal comfort and shiftable loads from a varying operation of the set- point temperatures of the heating system. Hence, normal and moderate level of expectation are respectively based on the indoor environment categories II and III according to the current European standard EN 16798-1. The former is represented by an acceptable range of indoor temperatures for heating between 20 and 25 °C, while users related to the latter would accept a wider range from 18 to 25 °C.
- **P3 - Heating power:** 100 % and 50 % of the total installed heating capacity of the heat pump required to cover the heating demand of the case study. This parameter and its two configurations are used as a simplified representation and comparison of the load profile of a monovalent and a bivalent operation of a heat pump. The installed heating capacity for monovalent and bivalent is respectively set to 45 and 23 W/m² based on a calculation of the design heat load using the above considered building age/state original.
- **P4 - PV panel surface:** roof and southern façade, and roof-only. These alternatives represent different extents of envelope usage for PV power production and are defined to study their different opportunities for energy flexibility. For the case study used in this analysis roof and southern façade corresponds to a total PV panel surface of 39.2 m² and an installed peak power of 5.9 kW_p per zone, while 20 m² and 3 kW_p per zone are considered for roof-only.
- **P5 - Time horizon:** 24 and 48 hours. This parameter represents the period of time in the future that the optimisation algorithm takes into account during the processing of forecast information (e.g. climate conditions or expected energy demand and PV power production) in order to regulate the operation of the heating systems. These two configurations are selected to analyse the impact of their resulting optimisation controls.
- **P6 - Optimisation mode:** collective and individual optimisation. The analysis of this parameter aims at evaluating the impact of a regulation of the heating system in the residential units (and in turn their energy consumption) as a part of a centralised strategy in comparison to a case, in which the energy management strategies are separately defined and implemented in each unit.

2.3 VARIANTS AND PARAMETRIC ANALYSIS

Table 2 shows the scenario variants analysed in this study. V0 corresponds to the base case scenario. The other variants are defined by taking the base case and changing the configuration of one focus parameter. Important to mention is that each scenario is twofold simulated: without energy management by considering a constant setpoint temperature for the heating system of 22.5 °C (named *fixed* in the result tables); and with energy management (named *opti* in the result tables), which results in a varying setpoint temperature of the heating system by the optimisation. The regulation of the set temperature is allowed only within the limits of the comfort band defined by the two configurations of parameter P2 as specified in each variant.

CATEGORIES		PASSIVE ASPECTS			ACTIVE SYSTEMS		CONTROL DEFINITIONS	
PARAMETERS		P1		P2	P3	P4	P5	P6
BASE CASE		BUILDING AGE/STATE UNIT 1	UNIT 2	USER PROFILE	HEATING POWER	PV PANEL SURFACE	TIME HORIZON	OPTIMISATION
V0		Original	Original	Normal expectation	100%	Roof % + Façade S	48 h	Collective
Variants	Focus	Parameter change compared to base case						
V1	P1	=	Renovated	=	=	=	=	=
V2	P2	Renovated	Renovated	=	=	=	=	=
V3	P3	=	=	Moderate expectation	=	=	=	=
V4	P4	=	=	=	50 %	=	=	=
V5	P5	=	=	=	=	Roof	=	=
V6	P6	=	=	=	=	=	24 h	=
V7	P7	=	=	=	=	=	=	Individual

TABLE 1 Simulated variants. Each scenario is simulated without and with energy management: constant 22.5 °C (*fixed*) and varying Tset heating (*opti*), respectively.

2.4 INDICATORS

To evaluate the effect of energy management and the influence of the selected parameters on the use of on-site photovoltaic energy, the indicators autarky and self-consumption are used (Equations 5 to 14). Autarky refers to the ratio of consumed photovoltaic energy to total electricity consumption. Self-consumption represents the ratio of used photovoltaic energy to total on-site power production. Both indicators are calculated upon summed energy values for the whole of the simulation time period with N time steps. These indicators are considered to be useful as a reference for economic (energy costs) and ecological (carbon emissions) considerations.

$$selfconsumption = \frac{(W_{gen,PV} - W_{surplus})}{W_{gen,PV}} \times 100 \quad [\%] \quad (6)$$

$$W_{import} = \sum_{k=1}^N (W_{consumpt,total}(k) - W_{gen,PV}(k)) \quad [kWh] \quad (7)$$

$$W_{consumpt,total} = \sum_{k=1}^N (W_{consumpt,HeatPump}(k) + W_{consumpt,addelec}(k)) \quad [kWh] \quad (8)$$

$$W_{consumpt,HeatPump}(k) = \sum_{i=1}^2 Q_{heating,i}(k) / SCOP_{HeatPump} \quad [kWh] \quad (9)$$

$$W_{consumpt,addelec}(k) = \sum_{i=1}^2 W_{consumpt,Lighting+Appliances,i}(k) \quad [kWh] \quad (10)$$

$$W_{surplus} = \sum_{k=1}^N (W_{gen,PV}(k) + W_{import}(k) - W_{consumpt,total}(k)) \quad [kWh] \quad (11)$$

The potential of energy management is then quantified by comparing a simulation implementing energy management to a simulation using a fixed set temperature for each variant. Thus, the difference in autarky and self-consumption is set in relation to the values of the simulation using the fixed set temperature, and this relative difference is used as a measure for energy management potential.

$$EM\ potential_{autarky} = \frac{autarky_{opti} - autarky_{fix}}{autarky_{fix}} \times 100 \quad [\%] \quad (13)$$

$$EM\ potential_{selfconsumption} = \frac{selfconsumpt_{opti} - selfconsumpt_{fix}}{selfconsumpt_{fix}} \times 100 \quad [\%] \quad (14)$$

2.5 IMPLEMENTATION OF THE OPTIMISATION: OBJECTIVE AND CONSTRAINTS

To implement the optimised energy management in the simulated variants, an objective function is defined (equation 15). Thus, the objective of each iteration of the optimisation is set to minimising the use of electricity from the grid, W_{import} , which in turn corresponds to maximising the indicator autarky described above. Excluding multi-objective optimisation based on its more complex character that is not regarded as necessary in the context of this study, the other option left, is setting the objective on self-consumption. The reason for the decision against this option lies in a non-trivial implementation, also here, because additional terms in the objective function would have been required to prohibit not-desirable excess heating from surplus PV energy. The objective function is further subject to defined constraints, of which the most important ones, regarding comfort criteria, are shown below.

$$\min \sum_{k=1}^{N_p} W_{import}(k) \quad (15)$$

The first constraint (Equation 16) ensures that the electrical balance of the system is respected at each time step. This equation is supplemented by a binary variable which additionally ensures that only one of $W_{import}(k)$ and $W_{surplus}(k)$ can take a non-zero value in a given time step. The second and third constraint (Equation 17,18) serve the purpose to prevent discomfort due to rapid zone temperature changes by limiting temperature drifts to a maximum of $\Delta T_{max} = 2$ K/h (based on DIN EN ISO 7730:2006). Finally, the fourth and fifth constraint set a minimum value for the average zone temperature $T_{z,avg}$ of all time steps N_p within the prediction horizon (Equation 19,20). This is based

on the aim of not causing a better performance of optimised variants by just lowering the zone temperatures. This last constraint comes in two forms: considering past temperatures and including the temperature to be implemented in the current update time step; and considering the predicted temperatures for future time steps of the current optimisation horizon. The reason for this set up is that applying only the last consideration does not ensure the defined limited average temperature is kept. In addition, the second consideration is a valuable extension for the first one in order to not create a schedule with too low temperatures that cannot be counterbalanced by later above-average temperatures, which would lead to simulation errors.

$$W_{consumpt,total}(k) = W_{gen,PV}(k) + W_{import}(k) - W_{surplus}(k) \quad \forall k \leq N_p \quad (16)$$

$$T_{Z,i}(k+1) - T_{Z,i}(k) \leq \Delta T_{max} \quad \forall k \leq N_p, i \in [1,2] \quad (17)$$

$$T_{Z,i}(k+1) - T_{Z,i}(k) \geq -\Delta T_{max} \quad \forall k \leq N_p, i \in [1,2] \quad (18)$$

$$\sum_{k=1}^{N_p} T_{Z,i}(k) / N_p \geq T_{Z,avg} \quad \forall i \in [1,2] \quad (19)$$

$$\sum_{k=-N_p+t_{update}}^{t_{update}} T_{Z,i}(k) / N_p \geq T_{Z,avg} \quad \forall i \in [1,2] \quad (20)$$

3 EXPERIMENT / RESEARCH

This section gives details on the configuration of the case study of the present parametric analysis. The case study consists of two thermal zones as a representation of two typical residential units of a multi-family apartment building. Table 1, and figures 3 and 4 summarise the boundary conditions assumed.

The case study is considered to be located in Potsdam, Germany. This location has been selected in line with the criteria of the German Meteorological Service (DWD), which sets the climate of Potsdam as the reference in energy efficiency certificates for buildings in Germany (DWD n.d.). Thus, the climate profile corresponding to the DWD Test Reference Year Normal of this city is implemented in the simulations. Moreover, the analysis is carried out on the shoulder season (October), during which exists a combination of heating demand and a relevant level of solar radiation and, therefore, photovoltaic power production. The potential of energy management aiming at high autarky and self-consumption is therefore highest in this season and the effect of single parameters can be observed.

ELEMENT	STANDARD 1958-68	PASSIVE HOUSE STANDARD
External wall	Plaster + Brick + Plaster; U_{EW} : 1.2 W/m ² K Window-to-wall ratio 14 %	Plaster + Brick + Ext. insulation + Plaster U_{EW} : 0.12 W/m ² K Window-to-wall ratio 14 %
Windows	Double glazing; U_g 2.65 W/m ² K; g : 0.65 Frame fraction: 30 %; U_f : 2 W/m ² K	Triple glazing; U_g : 0.72 W/m ² K; g : 0.5 Frame fraction: 30 %; U_f : 0.8 W/m ² K
Thermal bridges	0.10 W/m ² K	0.02 W/m ² K
Infiltration	0.42 h ⁻¹	0.15 h ⁻¹
Ventilation	Natural; hygienic ACR 0.47 h ⁻¹	Mechanical; hygienic ACR 0.47 h ⁻¹
Heat recovery	-	75 % efficiency
Floor / ceiling	Flooring + Screed + Sound insulation + Concrete + Plaster; $U_{F,C}$: 0.98 W/m ² K; UIC: 1.14 W/m ² K	
Internal walls	Plaster + Brick + Plaster; U_{IW} : 1.6 W/m ² K	

>>>

Internal gains	People: 5 W/m ² ; Appliances: 3 W/m ² ; Lighting: 4.5 W/m ² ; Weighted schedules in Fig. 4
Heating system	Geothermal heat pump (SCOP = 3.7) + Radiators (55/45 as inlet/outlet temperatures)
PV system	Polycrystalline panels (module efficiency 15.46 %), inclination/orientation: roof: 30 °/S; façade: 90 °/ façade orientation
Climate	Potsdam (Germany) - DWD Test Reference Year Normal

TABLE 2 Boundary conditions in case study

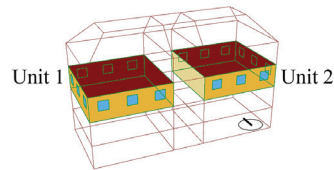


FIG. 3 Case study layout

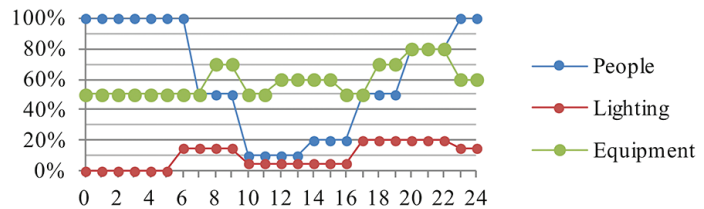


FIG. 4 Weighted schedule per hour for internal gains (EN 16798-1)

The study by Auer et al. (2017) is used as a basis for the geometrical and constructive specification of the units. As mentioned in section 2.2 (Selected parameters), for the original state of the units a representative standard related to a building age 1958-68 is assumed (P1a). This configuration is applied for the base case, while an upgrade to passive house standard is assumed as an approximation for a renovation to a nearly-zero energy building in one of the simulated variants (see 2.3 Variants and parametric analysis). Hence, each unit is represented in the simulation model as a single zone with 110 m² floor surface and 286 m³ room volume. Unit 1 and unit 2 are respectively oriented to West- North-South and East-North-South to take into account differences in terms of solar gains and, thus, their possible impact on the energy management plan of each apartment. Internal walls are also modelled and their thermal capacitance (kJ/K) is added to the zones to take them into account as a part of the available building mass. The thermal capacitance (kJ/K) of the room air and furniture is additionally taken into account as a part of the internal masses by multiplying the room volume (in m³) by a factor of 12. This assumption is based on the values reported by Lizana et al. (2019), Klein et al. (2017) and Johra & Heiselberg (2017). Internal gains are represented based on specific values and schedules for residential apartments, according to DIN EN 16789-1:2015-07. As this norm requires a detailed calculation of the internal gains due to lighting and therefore does not provide a specific value, a simplified assumption for this type of heat gains is made based on the German norm EnEV (DIN V 4108-6:2003-06), which approximates the total internal gains to 5 W/m². Therefore, the assumed specific values for internal gains in W/m² floor area are 5 for people, 3 for appliances, and 4.5 for lighting. These values are implemented following the corresponding weighted schedules represented in figure 4. The resulting daily average of internal gains is 5.25 W/m², lying around the cited value from EnEV. With regard to active systems, mechanical ventilation with heat recovery (75 % efficiency) is considered in the renovated state, whereas for the original state natural ventilation is assumed. In both cases, the ventilation rate has been set to 0.47 h⁻¹ as the minimum amount of fresh air to be provided based on DIN 1946-6. Considering that infiltration rates (set to 0.42 and 0.15 h⁻¹ respectively) already provide part of the required air change, only the remaining part is supplied via mechanical or natural ventilation. A combination of a geothermal heat pump (SCOP = 3.7) with radiators (55/45 as inlet/outlet temperatures) is considered as heating system, representing the link between the electric and the thermal sides. As a photovoltaic system, standard polycrystalline panels covering 80 % of the focus surface (external southern wall and/or roof according to the above defined parameter settings P4a and P4b) are assumed. The attribution of the roof area to the zones is done by equally

dividing a typical total roof area of the selected building typology of 500 m² by its total number of apartments (20 apartments).

The thermal model of the case study has been checked for plausibility. For this, two exemplary values of annual heating consumption of a building with same typology and age group (MFH_E 1958-68) from the TABULA study by (Loga et al. 2015, p. 87, 113, 120) were used as a reference: one of them considering the performance of the building under a generic climate profile for Germany (based on DIN V 18599-10:2018-09 and DIN V 4108-6:2003-06, and with similar characteristics as the one adopted in this analysis for Potsdam); and a second one applying the climate profile of Mannheim. These values were respectively compared to the results of annual energy demand for heating of the base case using the RC model and the DWD climate profiles for Potsdam and Mannheim. In both cases, the heating values laid close to each by approximately 11 %, with the simulated values being higher. This deviation may be due to slight differences in the assumed boundary conditions (e.g. internal gains, or the rate of outdoor surface to floor surface).

4 RESULTS

The results of this study are shown in figure 5, structured in the following way: On the upper left side, the energy management potential is quantified for each variant. This potential is based on the difference in self-consumption and autarky values between fix set point and optimised heating as described in section 2.4 (see Equations 13,14), relative to fix set-point values (100 %). These relative values are supplemented by the upper right graph, where the outcome of the optimised versions is shown separately in order to give insight into the level of autarky and self-consumption reached in each variant. The bottom graphs highlight the effect of changing the parameters in the variants by giving the results as relative to the base case for each upper graph, respectively.

Regarding the quantification of energy management potential, the top-left graph in figure 5 shows that all variants offer potential through energy management with the exception of V2 (setting the building standard of both apartments to a renovated state). This potential ranges between 5 and 17 % based on autarky as an indicator and between 15 and 24 % based on self-consumption. The graph further shows that all of the parameter variations lead to equal or lower potentials compared to the base case meaning that the parameter set of the base case constitutes the most promising conditions for energy management among the simulated cases. Moreover, the parameters differ in whether they result in a higher effect on autarky or on self-consumption, which underpins the additional value of examining both indicators.

The results in the top-right graph in figure 5 give additional information on the levels of autarky and self-consumption reached in each variant. All of the studied variants lie within the range 35 to 89 % regarding self-consumption and a more compact range in case of autarky values, spanning from 32 to 51 %. It should be mentioned that self-consumption in the base case is already high, with 70 % compared to single-family buildings without heat pumps or electric vehicles where typical annual values lie within 30-40 %.

Results on the effect of the single influencing parameters are based upon the top-left graph of figure 5 and described and discussed in the following.

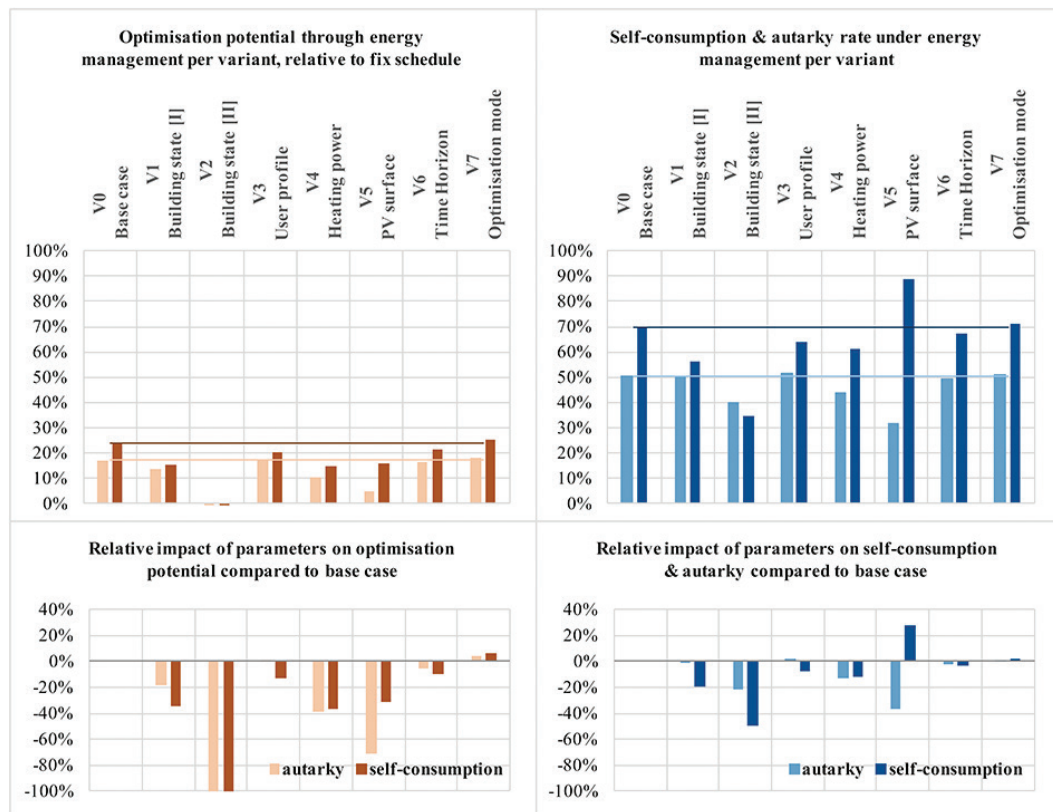


FIG. 5 Results. Note: relative values in the bottom graphs are calculated using the base case values in the respective upper graph as the references. The references are represented in the upper graphs through horizontal lines.

The parameter building state has a high impact on the optimisation potential of the energy management, which matches the expectations. The effect on self-consumption is more pronounced if compared to the other variants. Comparing the values of V1 and V2 to the base case reveals that a higher decrease takes place when also the second zone is renovated. Hence, the flexibility that is made available by one apartment of the original building state procures a higher share of self-consumption and autarky improvement. Under the boundary conditions of this case study, the conclusion can be drawn that surplus PV energy from the attributed PV surface area of two apartments can already be exploited to a high extent by energy management of one apartment with original building state. Furthermore, optimisation potential is reduced to zero when both apartments feature a renovated building standard because there is no heat demand, thus no shifting potential, in October (see results of V2 in Table 3).

The second parameter analysed, the user profile, leads to less optimisation potential and self-consumption than in the base case. Only autarky increases by 1 %. This is counter-intuitive because the comfort band in V3 is broader, and expectations are that this opens up higher opportunities for energy management. An explanation for this can be the lower total amount of consumed heating energy because of the 1 °C lower average temperature. A second reason can be identified by a detailed analysis of the variables' time series that reveals the zone temperature never goes down to its lower limit. An explanation could be that the constraints for the minimum average temperature are set too tight, i.e. that the time horizon for the average is too short relative to the time the thermal mass takes to cool down from the point in time where the upper zone temperature level was reached. Close attention should therefore be paid to the limiting conditions of a strict minimum average temperature, and it has to be checked in further simulations whether another time horizon for the average or lower average values deliver further insights.

Changing the parameter heating power of the heat pump to 50 % of its value in the base case has a negative impact on both self-consumption and autarky optimisation potential but not in the same relative magnitude as the nominal power of the heat pump is reduced in variant V4. It can be concluded that other factors lead to a limit in the optimisation potential prior to the power limit of the heat pump during the major part of the time. Nevertheless, the conclusion to be drawn from this parameter variation is that by choosing a bivalent system instead of a monovalent heat pump as heat producer the energy management potential decreases.

Expectations on the effect of the parameter PV surface are met by the results. The PV surface directly affects the available energy for local usage and thus also the quantities that the relative values refer to. In V5 with only roof-installed PV, self-consumption of PV reaches 89 % just by supplying the household electricity demand, and as a consequence, little energy is left for the exploitation via heat demand flexibility. The high value of self-consumption goes hand in hand with a low value of optimisation potential of 16 %. Improving autarky by energy management even decreases to 5 %. The effect of the PV area on the results is valuable as a benchmark for the other parameters and, additionally, delivers the quantitative basis for how much more relevant energy management becomes when more than just roof areas of the building envelope are used for PV.

Considering the prediction horizon, the shortening from 48 h to 24 h (V6) reveals the expected tendency to less energy management potential than in the base case, but the effect is not very pronounced. The value decreases from 24 % in the base case to 21 % in V6, regarding self-consumption, and for autarky, an even smaller difference can be observed. The results here suggest that most of the potential can be exploited by shifting the heat demand only within the time-period of 24 hours, which is a valuable finding for future simulations with similar boundary conditions because limiting the prediction horizon to 24 h reduces the computation time.

The last parameter variation analysed, regarding the optimisation mode, leads to slightly higher resulting indicator values in a separate optimisation mode than in the base case with cooperation. This can be explained by choosing to use two rather identical zones combined with the effect of a higher total heating demand. Findings may be different if the diversity of the zones is more pronounced. Diversity effects could result from individual household electricity profiles, different comfort band limits or disturbance profiles like solar irradiation.

By basing all of these findings on indicators chosen to be relative values, it has to be mentioned that some of the optimised variants result in a higher absolute heating demand $Q_{heating}$ (see V4, V5, V7 in table 3 in the appendix). This is regarded as a side-effect that has to be kept in mind, but the indicators are still suitable when focusing on high local consumption of local renewable energy and little grid imported electricity consumption. Moreover, within this study minimising electricity import from the grid in order to maximise autarky was set as the only objective and reason to support energy management. A more holistic approach has to extend this goal by other complementary goals of energy management like grid support which can lead to a higher relevance of energy management measures.

5 CONCLUSIONS

In this study, the potential of energy management via utilisation of the building mass as storage for local PV gains and the impact of different parameters on this potential were analysed. A case study consisting of two exemplary residential apartments with different orientation located in Potsdam was simulated for the month of October, an optimisation algorithm for energy management was implemented, and results were evaluated based on the indicators autarky and self-consumption. All the simulated variants revealed optimisation potential through energy management ranging from 5 to 24 %, relative to autarky and self-consumption values of the simulation with fix setpoint

temperatures (the only exception being the variant with the building state of both apartments set to renovated). Besides the quantification of the energy management potential, the study analysed the impact of different parameters on this potential. An interesting finding is that the difference in energy management potential with a prediction horizon of 48 h compared to one of 24 h is small, and thus the shifting of the heating demand is mainly beneficial within 24 h. Another finding is that implementing energy management in one of two unrenovated apartments with PV surfaces already exploits a major part of the potential. This study is seen as the first step of identifying promising use cases for energy management and next steps include gaining more insights by adding further indicators from the economic and ecological domain.

Acknowledgements

This research is a product of the research project Cleanvelope which is sponsored by the Bavarian Ministry of Science and the Arts in the context of Bavarian Climate Research Network (bayklif)

References

- Auer, Thomas; Hamacher, Thomas; Wagner, Ulrich; Atabay, Dennis; De-Borja-Torrejón, Manuel; Dornmair, Rita et al. (2017): Gebäude als intelligenter Baustein im Energiesystem. Lastmanagement-Potenziale von Gebäuden im Kontext der zukünftigen Energieversorgungsstruktur in Deutschland: Abschlussbericht. Stuttgart: Fraunhofer IRB Verlag (Forschungsinitiative Zukunft Bau, F 3054).
- Beer, Michael; Beistler, Detlef; Chelly, Haythem; Hemmerle, Claudia; Höhle, Christian; Honold, Johannes (2016): Abschlussbericht zum Förderprojekt "Energieautarke Elektromobilität im Smart-Micro-Grid vom Einfamilienhaus bis zum intelligenten Parkhaus". Unter Mitarbeit von TIB-Technische Informationsbibliothek Universität Hannover und Technische Informationsbibliothek (TIB).
- Bogischef, Lea; De-Borja-Torrejón, Manuel; Fassbender, Elisabeth; Jambagi, Akhila; Hemmerle, Claudia (2019): Solar activated envelopes in district context – energy modelling tasks. In: Thomas Hamacher (Hg.): Shaping a Sustainable Energy Future. 9th Colloquium of the Munich School of Engineering, Garching, 01.08.2019, S. 16.
- Dear, Richard J. de; Brager, Gail S. (2002): Thermal comfort in naturally ventilated buildings: revisions to ASHRAE Standard 55. In: *Energy and Buildings* 34 (6), S. 549–561. DOI: 10.1016/S0378-7788(02)00005-1.
- Gurobi Optimization, L.L.C. (2020): Gurobi Optimizer Reference Manual. Online verfügbar unter <http://www.gurobi.com>, last updated 2020.
- Hart, William E.; Watson, Jean-Paul; Woodruff, David L. (2011): Pyomo: modelling and solving mathematical programs in Python. In: *Math. Prog. Comp.* 3 (3), S. 219–260. DOI: 10.1007/s12532-011-0026-8.
- Hausladen, Gerhard; Auer, Thomas; Schneegans, Jakob; Klimke, Klaus; Riemer, Hana; Trojer, Barbara et al. (2014): Lastverhalten von Gebäuden unter Berücksichtigung unterschiedlicher Bauweisen und technischer Systeme - Speicher- und Lastmanagementpotenziale in Gebäuden. Endbericht. Stuttgart: Fraunhofer IRB Verlag (Forschungsinitiative Zukunft Bau, F 2920). Online verfügbar unter <http://www.irbnet.de/daten/rswb/14109008253.pdf>.
- Johra, Hicham; Heiselberg, Per (2017): Influence of internal thermal mass on the indoor thermal dynamics and integration of phase change materials in furniture for building energy storage: A review. In: *Renewable and Sustainable Energy Reviews* 69, S. 19–32. DOI: 10.1016/j.rser.2016.11.145.
- Klein, S. A.; Beckman, W. A.; Mitchell, J. W.; Duffie, J. A.; Duffie, N. A.; Freeman, T. L. et al. (2017): TRNSYS 18 a TRaNsient SYstem Simulation program. Volume 4. Mathematical Reference.
- Kramer, Michael; Jambagi, Akhila; Cheng, Vicky (2017): Distributed Model Predictive Control for Building Energy Systems in Distribution Grids. In: 2017 IEEE PES Innovative Smart Grid Technologies Conference Europe (ISGT-Europe). Torino, Italy, 26–29 September 2017 : conference proceedings. IEEE PES Innovative Smart Grid Technologies Conference Europe; Institute of Electrical and Electronics Engineers; IEEE Power & Energy Society; ISGT-Europe. Piscataway, NJ: IEEE.
- Lizana, Jesus; de-Borja-Torrejón, Manuel; Barrios-Padura, Angela; Auer, Thomas; Chacartegui, Ricardo (2019): Passive cooling through phase change materials in buildings. A critical study of implementation alternatives. In: *Applied Energy* 254, S. 113658. DOI: 10.1016/j.apenergy.2019.113658.
- Loga, Tobias; Stein, Britta; Diefenbach, Nikolaus; Born, Rolf (2015): Deutsche Wohngebäudetypologie. Beispielhafte Maßnahmen zur Verbesserung der Energieeffizienz von typischen Wohngebäuden ; erarbeitet im Rahmen der EU-Projekte TABULA - "Typology approach for building stock energy assessment", EPISCOPE - "Energy performance indicator tracking schemes for the continuous optimisation of refurbishment processes in European housing stocks". 2., erw. Aufl. Darmstadt: IWU. Online available at http://www.building-typology.eu/downloads/public/docs/brochure/DE_TABULA_TypologyBrochure_IWU.pdf.
- Virtanen, Pauli; Gommers, Ralf; Oliphant, Travis E.; Haberland, Matt; Reddy, Tyler; Cournapeau, David et al. (2020): SciPy 1.0: fundamental algorithms for scientific computing in Python. In: *Nature methods* 17 (3), S. 261–272. DOI: 10.1038/s41592-019-0686-2.
- Weniger, Johannes; Bergner, Joseph; Tjaden, Tjarko; Quaschnig, Volker (2015): Dezentrale Solarstromspeicher für die Energiewende. Berlin: Berliner Wissenschafts-Verlag. Online available at <http://pvspeicher.htw-berlin.de>.
- Zander, Wolfgang; Lemkens, Stephan; Macharey, Uwe; Langrock, Thomas; Nailis, Dominic; Zdrallek, Markus et al. (2017): dena-Netzflexstudie - Optimierter Einsatz von Speichern für Netz und Marktanwendungen in der Stromversorgung. Hg. v. dena. Online available at <https://www.dena.de/themen-projekte/projekte/energiesysteme/netzflexstudie/>, last checked on 02.01.2020.

APPENDIX A TABLE 3: RESULTS OF THE SIMULATED VARIANTS

	V0 FIXED [KWH]	V0 OPTI [KWH]	V0 DIFF [%]	-	-	V1 FIXED [KWH]	V1 OPTI [KWH]	V1 DIFF [%]	V1vsV0 OPTI-OPTI [%]	V1vsV0 DIFF-DIFF [%]
Q _{heating}	1091	1088	-0.3	-	-	547	534	-2.4	-50.9	-
W _{consumpt.HeatPump}	295	294	-0.3	-	-	148	144	-2.4	-50.9	-
W _{consumpt.addelec}	514	514	0.0	-	-	514	514	0.0	0.0	-
W _{consumpt.total}	809	808	-0.1	-	-	662	658	-0.5	-18.5	-
W _{gen.PV}	586	586	0.0	-	-	586	586	0.0	0.0	-
W _{import}	539	400	-25.9	-	-	424	330	-22.2	-17.5	-
W _{surplus}	316	177	-43.9	-	-	348	257	-26.1	45%	-
self-consumption	46%	70%	24%	-	-	41%	56%	15%	-20%	-35%
autarky	33%	51%	17%	-	-	36%	50%	14%	-1%	-19%
	V2 FIXED [KWH]	V2 OPTI [KWH]	V2 DIFF [%]	V2vsV0 OPTI-OPTI [%]	V2vsV0 DIFF-DIFF [%]	V3 FIXED [KWH]	V3 OPTI [KWH]	V3 DIFF [%]	V3vsV0 OPTI-OPTI [%]	V3vsV0 DIFF-DIFF [%]
Q _{heating}	4	0	-95.8	-100.0	-	869	802	-7.7	-26.2	-
W _{consumpt.HeatPump}	1	0	-95.8	-100.0	-	235	217	-7.7	-26.2	-
W _{consumpt.addelec}	514	514	0.0	0.0	-	514	514	0.0	0.0	-
W _{consumpt.total}	515	514	-0.2	-36.4	-	749	731	-2.4	-9.5	-
W _{gen.PV}	586	586	0.0	0.0	-	586	586	0.0	0.0	-
W _{import}	310	309	-0.1	-22.6	-	493	355	-28.0	-11.1	-
W _{surplus}	380	381	0.2	115%	-	330	210	-36.4	18%	-
self-consumption	35%	35%	0%	-50%	-101%	44%	64%	20%	-8%	-14%
autarky	40%	40%	0%	-21%	-100%	34%	51%	17%	2%	0%
	V4 FIXED [KWH]	V4 OPTI [KWH]	V4 DIFF [%]	V4vsV0 OPTI-OPTI [%]	V4vsV0 DIFF-DIFF [%]	V5 FIXED [KWH]	V5 OPTI [KWH]	V5 DIFF [%]	V5vsV0 OPTI-OPTI [%]	V5vsV0 DIFF-DIFF [%]
Q _{heating}	1091	1119	2.6	2.9	-	1091	1177	7.9	8.2	-
W _{consumpt.HeatPump}	295	302	2.6	2.9	-	295	318	7.9	8.2	-
W _{consumpt.addelec}	514	514	0.0	0.0	-	514	514	0.0	0.0	-
W _{consumpt.total}	809	817	0.9	1.0	-	809	832	2.9	3.0	-
W _{gen.PV}	586	586	0.0	0.0	-	298	298	0.0	-49.1	-
W _{import}	539	458	-15.0	14.7	-	592	567	-4.2	41.9	-
W _{surplus}	316	228	-28.0	28%	-	81	33	-59.5	-81%	-
self-consumption	46%	61%	15%	-12%	-36%	73%	89%	16%	28%	-32%
autarky	33%	44%	11%	-13%	-39%	27%	32%	5%	-37%	-71%
	V6 FIXED [KWH]	V6 OPTI [KWH]	V6 DIFF [%]	V6vsV0 OPTI-OPTI [%]	V6vsV0 DIFF-DIFF [%]	V7 FIXED [KWH]	V7 OPTI [KWH]	V7 DIFF [%]	V7vsV0 OPTI-OPTI [%]	V7vsV0 DIFF-DIFF [%]
Q _{heating}	1091	1044	-4.3	-4.0	-	1091	1112	1.9	2.2	-
W _{consumpt.HeatPump}	295	282	-4.3	-4.0	-	295	300	1.9	2.2	-
W _{consumpt.addelec}	514	514	0.0	0.0	-	514	514	0.0	0.0	-
W _{consumpt.total}	809	796	-1.6	-1.5	-	809	815	0.7	0.8	-
W _{gen.PV}	586	586	0.0	0.0	-	586	586	0.0	0.0	-
W _{import}	539	402	-25.6	0.5	-	540	398	-26.3	-0.5	-
W _{surplus}	316	191	-39.6	8%	-	317	169	-46.6	-5%	-
self-consumption	46%	67%	21%	-3%	-10%	46%	71%	25%	2%	6%
autarky	33%	50%	16%	-2%	-6%	33%	51%	18%	1%	4%

Internal Shading Systems Analysis for High-Performance Façades – Do More With Less

Alessandro Baldini¹, Anna Ioannidou-Kati²

- 1 Eckersley O'Callaghan, 236 Gray's Inn rd, +44 20 7354 5402, alessandro@eocengineers.com
- 2 Eckersley O'Callaghan, 236 Gray's Inn rd, +44 20 7354 5402, anna@eocengineers.com

Abstract

Among a number of passive solar control solutions, internal shading systems can be considered as a "simple" one, as buildings often see these being fitted for glare control or privacy reasons. Although these systems are typically regarded to have a limited effect in the reduction of building solar gains and are often neglected by the building energy modellers, recent product development showed that a good level of performance can actually be provided by internal blinds when carefully selected and specified in combination with the glazing. The initial review work carried out identified the complexity of the physics involved, highlighting a number of simulation limitations among some common whole-building energy modelling software. As a result, an alternative design work flow approach is proposed as part of the current research. This is based on combining detailed internal shading simulations to ISO 15099 with the whole-building energy model, aiming to increase the accuracy of the final results as well as to allow the required flexibility to the envelope designers to explore optimal solutions. This shift in the approach to internal shading design aims to relocate the scope of these systems from the internal fit-out package to the external performing envelope, leading to holistic building skin solutions engineered that work as effectively as possible by using readily available technologies, in line with the dogma: "Do more with less". Further collaboration by façade, sustainability and MEP engineers as well as software developers and product manufacturers is also encouraged towards this aim.

Keywords

Façade engineering, building envelope design, energy modelling, energy performance, solar heat gain coefficient, total solar transmittance, blinds, internal shading, reference glazing, switchable glazing, IES VE, EnergyPlus, Honeybee, Grasshopper, ISO 15099, EN 14501, EN ISO 52022

1 INTRODUCTION

A growing architectural interest towards highly transparent building envelopes developed over the past decades across major global countries. However, recent energy policies are imposing increasingly tighter performance limits, particularly in those regions where mitigation of solar gains is of key importance to target carbon emission reductions, which pose serious challenges to the realisation of fully glazed buildings in the way these have been conceived up to the current times. This calls for a holistically coordinated building skin design approach implemented early on projects, one that allows efficient façade solutions to be developed for designs that would otherwise have never reach compliance.

The benefits of passive solar control design measures are well recognised within the industry by both designers and investors; however, these might sometimes limit the design possibilities by strongly affecting the appearance of the building or by introducing additional complexity to the envelope package, possibly leading to increased capital and maintenance costs. Among all the passive solar control solutions, internal blind systems can be considered as a “simple” one, as buildings often see these being fitted for glare control or privacy reasons. Although these systems are typically regarded to have a limited effect in the reduction of building solar gains and are often neglected by the building energy modellers, recent product development showed that a good level of performance could actually be provided by these systems when carefully selected and specified in combination with the glazing.

In an effort to seek simple but effective design solutions that make use of already available resources towards increased performance, internal shading system are attracting the attention of designers, who can rely on them to achieve energy-efficient buildings with reduced compromises on exterior aesthetics and glass clarity as well as sometimes limiting impact on capital.

The object of this research is to encourage a shift in the approach to internal shading design, aiming to relocate its scope from the internal fit-out package to the external performing envelope. This would result in holistic building skin solutions engineered to work as effectively as possible by using readily available technologies, in line with the dogma: “Do more with less”.

2 BACKGROUND

2.1 INTERNAL BLINDS MODELLING

Currently in the UK, glass and blind performance are not typically specified together. Blinds tend to get specified independently from the glazing in varying ways depending on the modelling software used by the MEP engineer.

For glazed elements, the most common metric used in consideration of the energy analysis of a building is the total solar energy transmission (g-value) or Solar Heat Gain Coefficient (SHGC). SHGC defines the ratio of the internal heat gain passing through the building component and the incident solar radiation. The solar heat gain inside the room is the combination of the transmitted incident radiation passing through a fenestration system and a percentage of the absorbed solar radiation that is re-emitted inside the room. This percentage is also referred to as ‘inward flowing fraction’. The solar heat gain coefficient of a transparent or semi-transparent element of a building is calculated as (Kohler, Shukla & Rawal, 2017):

$$SHGC = T_s + N * A_s \quad (1)$$

Where:

- T_s Solar transmission
- A_s Solar absorption
- N Inward flowing fraction

On the other hand, a fenestration system that combines two layers of protection against solar radiation, such as a glazing construction with internal blinds, can be more complex to calculate due to the physical interactions between the layers. Depending on the colour, surface finish and geometry of the blind, some percentage of radiation is reflected back out from the blind hitting the glass again with a part of it being transmitted directly to the outside. The phenomenon of returning a portion of the beam radiation back to its source is called retro-reflection and can be an important factor when calculating the performance of internal blinds, as heat reflected back from the glass leads to increased indoor heat gain (Yunyang, Peng, Jiachen & Ying, 2015). The solar radiation absorbed by the blind causes the blind to heat up, and part of it is re-emitted inside the room by convection and longwave radiation. The longwave radiation can also be trapped between the glass and the internal shade and heat the air within this space.

For the purpose of blind specification and characterisation of performance, BS EN ISO 52022-3:2017 and ISO 15099 standards describe a methodology for estimating the g_{tot} or τ_s , respectively, meaning the total solar energy transmittance of a system that combines a glazing construction and a shading device (external, internal or interstitial). These standards cover all types of solar protection devices parallel to the glass ($\pm 15^\circ$), such as louvres, Venetian blinds and roller blinds. The methodology is based on normal incidence of radiation but does not consider an angular dependence of transmittance and reflectance of the materials.

According to ISO 15099, the total solar energy transmittance, τ_s , is calculated by the difference between the net heat flow rate into the indoor environment with and without radiation. The net heat flow depends on the thermo-optical interaction between the layers of the system (glass and blind), meaning that the layers exchange heat with each other and the indoor environment by conduction, convection and thermal radiation, and they absorb, transmit and reflect solar radiation. Other parameters that affect the net heat flow rate are openings of the blind or gaps on the perimeter that cause airflow between the blind cavity and the indoor environment. The calculation of the net heat flow density is an iterative process and is described in more detail in ISO 15099.

There is a variety of simulation tools on the market that are certified to comply with the above standards. For compliance with BS EN ISO 52022, WinSLT and VITRAGES DÉCISION are available on the market. For compliance with ISO 15099, Berkeley Lab WINDOW and ES-SO ESBO Light are also available.

From a whole-building performance standpoint, established energy simulation tools, such as IES VE (Integrated Environmental Solutions Virtual Environment) and EnergyPlus, consider the effect of internal blinds based on the interaction of the transmitted short-wave and longwave (re-emitted) radiation with the internal room surfaces. IES VE is a widely used simulation tool for building energy calculations and it is accredited in several countries for energy certifications. Internal shading devices are considered by specifying a Shading Coefficient (SC) and a Short-Wave Radiant Fraction (SWRF) factor for the blind. According to IES technical manual and clarification from the IES development team, the SC factor specifies the reduction of the short-wave component of solar radiation passing through the glazing construction. This means that a blind with SC factor of 1 provides no shading, while a value of 0 defines perfect shading. The SWRF factor specifies the

percentage of the room heat gain that passes through the glass and blind constructions as short-wave radiation. For homogeneous diffusing roller blinds, IES VE Constructions Database User Guide recommends calculating these factors as follows:

$$SC=T+0.87 * A \quad (2)$$

$$SWRF=T / SC \quad (3)$$

Where:

- T Solar transmittance of the blind
- A Solar absorptance of the blind

The suggested formulas are only based on properties of the blind, suggesting that the phenomenon of the retro-reflection between glass and blind might not be considered. Further to this, the internal blind is not considered to affect the longwave radiation and convective heat transfer from the glazing to the room. This can lead to inaccurate assessments in the calculation of the blind performance, especially in the case of high-performance reflective blinds.

On the other hand, the software appears to manage the internal re-emission phenomenon more accurately. Experimental measurements (Klems & Kelley, 1995) found that the inward flowing fraction depends on the temperature of the blind and the surrounding surfaces and the temperature and state of motion of the adjacent air cavity. Inward flowing fraction for a double-glazing system with an internal (non-metallic) blind was measured at 0.85 ± 0.01 and for a double-glazing system with an internal Venetian blind at 0.86 ± 0.06 . This explains the suggested value of 0.87 in (3).

2.2 SENSITIVITY CHECKS

As part of the initial background research, the total solar energy transmittance through a system with double glazing and an internal blind was calculated firstly following the methodology described in IES VE technical manual (as an example of a whole building energy modelling tool) and then to ISO 15099 (using the tool WINDOW7.7). This was aimed at comparing the effects of the different approaches for calculating the solar heat gain inside a room.

A window of 1x1m was assumed with a blind 50mm behind the glass and 10mm gaps on the perimeter of the blind (top, bottom, left and right). Since IES VE and WINDOW 7.7 calculate the effect of internal blinds in different ways, in both cases, this comparison assumes a theoretical surface right behind the internal shading device. In this way, we can calculate the total solar radiation that is transmitted through the system before it passes through the theoretical surface and hits the internal surfaces of the room.

BLIND NAME	Ts	Rs (front & back)	E (front & back)	OPENNESS FACTOR
White blind	0.171	0.727	0.784	0.030
Charcoal blind	0.040	0.041	0.804	0.030
Golden low-e blind	0.062	0.409	0.147	0.059

TABLE 1 Blind properties

Table 2 gives the total solar energy transmission through the glass and blind system assuming incident radiation as per reference conditions of BS EN ISO 52022-3. Glass properties according to reference Glass C of BS EN 14501:2005.

BLIND NAME	IES VE METHODOLOGY	ISO 15099 (WINDOW LBNL)	DISCREPANCY
White blind	68.2	91.8	35%
Charcoal blind	153.4	164.4	7%
Golden low-e blind	106.8	132.3	24%

TABLE 2 Total solar energy transmission (W/m^2)

Results show that the more reflective the blind is, the larger the error of the total solar energy transmission calculated with these two methods. The white blind is highly reflective, which means that the phenomenon of retro-reflection has a larger effect on the total solar energy transmission compared with the charcoal blind, which mainly reduces solar heat gains through absorption rather than reflection.

A separate assessment was also carried out to investigate the correlation between g_{tot} results (calculated to ISO 15099) and cavity ventilation. The analysis is based on a combination of a low-e IGU and a white blind and involves two scenarios: Unvented cavity (no gaps to the perimeter); Vented cavity (20mm gap around perimeter).

COMBINATION	UNVENTED CAVITY	VENTED CAVITY	DEVIATION
Low-e & white blind	0.267	0.292	9.4%

TABLE 3 g_{tot} for unvented and vented cavities

Results show that the vented cavity yields higher g_{tot} values. This can be explained due to the higher internal convective heat transfer coefficient caused by the air velocity, which increases the amount of heat dissipated towards the inner space. To conclude, gaps on the perimeter of the blind can be important for the g_{tot} calculation of the blind system. It is thus important that calculations done by the supplier and the engineer are consistent in terms of cavity ventilation state.

3 PROPOSED WORK FLOW APPROACH

From the background research carried out, it emerged that there is a risk for the current whole building energy modelling tools to provide a number of limitations that would not allow the right flexibility for exploring internal blinds design solutions in a detailed manner.

An alternative work flow approach is investigated where blinds are instead modelled in combination with glazing constructions separately by Façade Engineering experts and then introduced into the energy model calculations (by the MEP engineer) as simplified profiles.

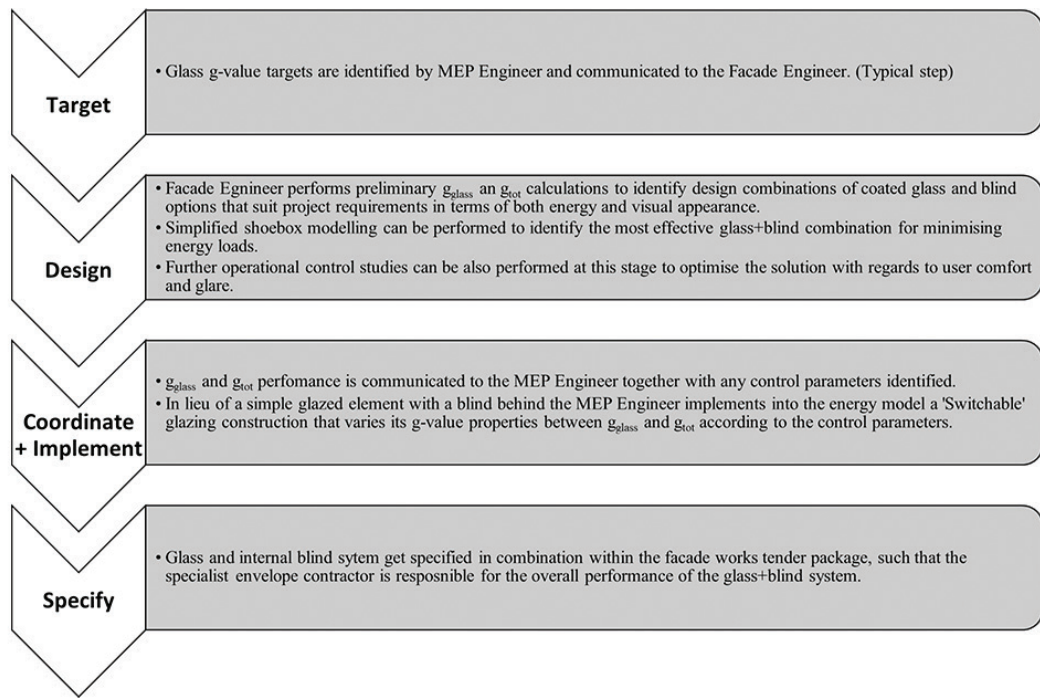


FIG. 1 Work flow outline

4 ANALYSIS

4.1 g_{tot} CALCULATION METHOD

The g_{tot} of a glass and blind construction can be either preliminarily assessed based on a set of reference glazing types (A, B, C and D) from EN 14501, or calculated in detail for the project-specific build-up through modelling tools based on ISO 15099 equations.

European blind suppliers typically provide g_{tot} performance of their products in association with the standard glazing types according to EN 14501. Suppliers also typically provide a set shading factors F_c for each EN 14501 glazing type; This is a metric that shows the efficiency of the blind towards a glazing construction:

$$F_c = \frac{g_{\text{tot}}}{g(\text{glass})} \quad (4)$$

A series of g_{tot} calculations were performed on two different blind products to assess whether the F_c values provided by the manufacturer (based on standardised glazing) do vary according to the different coating products that might be considered for a project.

A glazing construction of 3m (high) x 1.5m (wide) has been assumed. Glazing constructions have the following build-up: 6mm clear glass – 16mm Argon gas EN 673 – 6mm clear glass. This study considers a range of both low-e and high-performance glass coatings to compare them against standard glazing C and D, representing respectively a low-e coated IGU and a High Performance coated IGU. The blind is located 50mm behind the glass and allows no gaps at top and bottom,

only 10mm on the left and right side, allowing limited amount of ventilation through the cavity. Calculations have been performed with WINDOW 7.7. Boundary conditions for internal and external temperatures, convective heat transfer coefficients and incident radiation flow rate are according to BS EN ISO 52022-3 (reference conditions). Results are compared for two blind products (a white reflective blind and a dark charcoal blind, - properties as per Table 1) in combination with the standard glazing types C & D and with a set of coatings available on the market.

A dashed line was plotted in each graph aimed at representing the performance of the blind across a wider g-value range. This means that the inclination of this line is equal to the Fc factor relative to the standard glazing type for each case considered.

COMBINATION	g_{glass} (EN 14501)	g_{tot} (ISO 15099)	Fc
1. Glass C & white blind	0.59	0.28	0.48
2. Glass D & white blind	0.32	0.11	0.35
3. Glass C & charcoal blind	0.59	0.51	0.87
4. Glass D & charcoal blind	0.32	0.31	0.94

TABLE 4 Glass and blind combinations

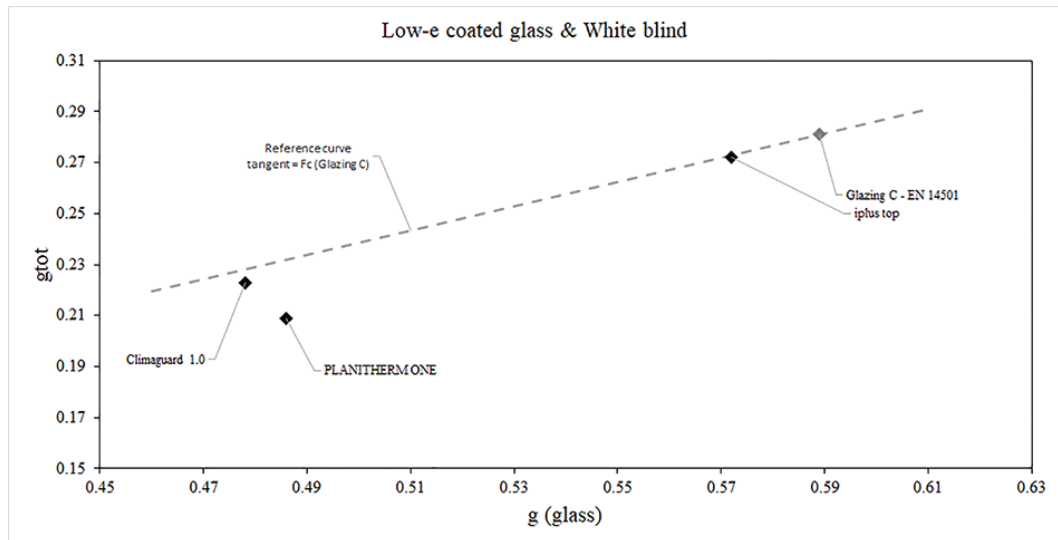


FIG. 2 g_{tot} vs g_{glass} graph for a white blind in combination with low-e coatings

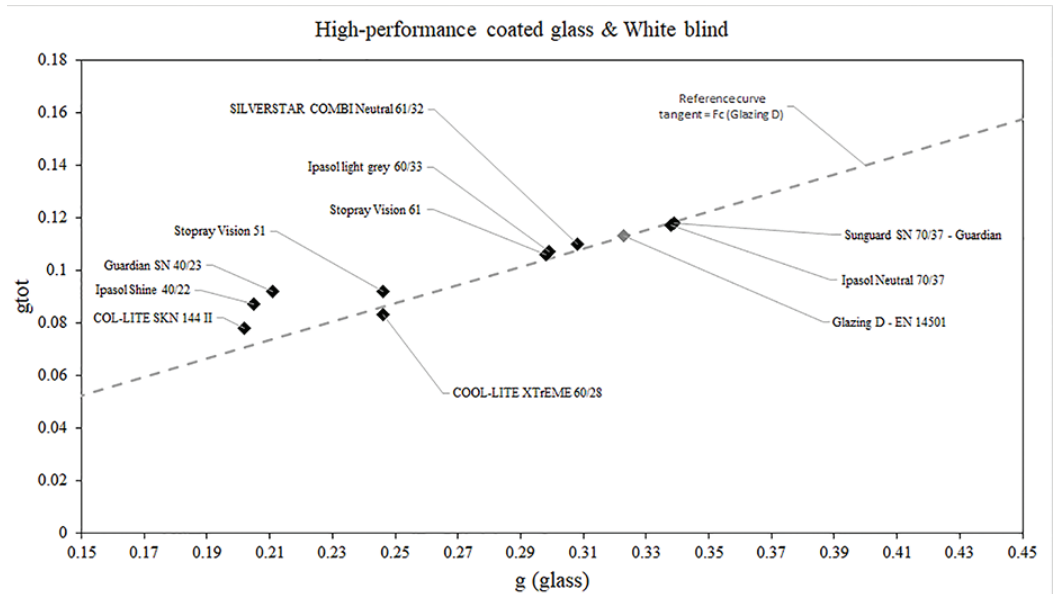


FIG. 3 g_{tot} vs g_{glass} graph for a white blind in combination with high-performance coatings

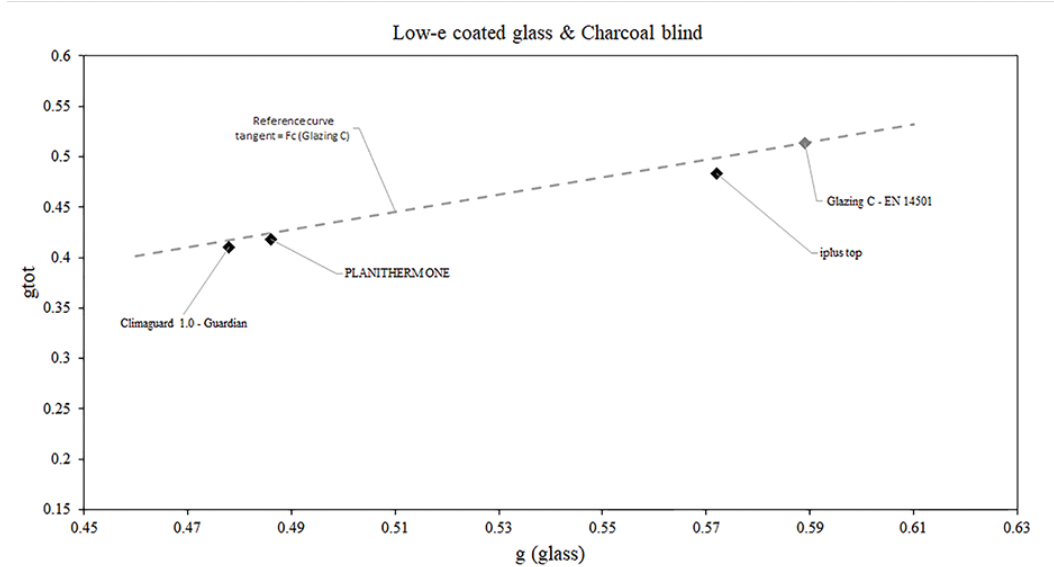


FIG. 4 g_{tot} vs g_{glass} graph for a charcoal blind in combination with low-e coatings

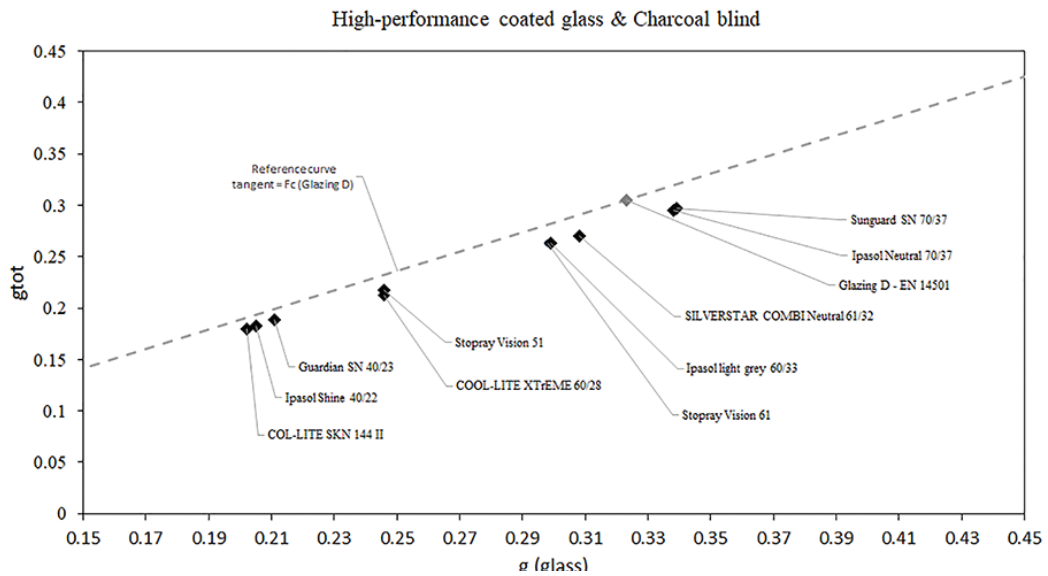


FIG. 5 g_{tot} vs g_{glass} graph for a charcoal blind in combination with high-performance coatings

A general good correlation of the various coating products to the reference dashed lines was found, particularly for higher g-value ranges. A greater difference was observed in Combination 1 and 2 (White blind), where, at the lower end of the g-value range, the g_{tot} calculated for the specific coating combinations appeared to diverge from the dashed reference line by a maximum of 18%. This is believed to be due to the complex reflection interaction between the white blind and the coating, which might vary depending on the specific spectral properties of the glass. This phenomenon was less influential in the dark blind calculations due to their lower reflectivity.

Analysis results show that reference glazing F_c lines values can be a useful tool during preliminary design exercises for predicting the performance of the blind+glass system. However, it should be bared in mind that these do not take into account any ventilation phenomenon and might require further detailed calculations, particularly for lower g-value glass products.

4.2 ENERGY MODELLING APPROACH

The traditional way of modelling internal blinds is by setting the glazing g-value and modelling internal shading separately by specifying its optical properties (transmittance, reflectance and emissivity). A simplified case study was conducted in a Rhino+Grasshopper environment by using Honeybee v0.065 plug-in (EnergyPlus based simulation engine) to compare energy simulation results from the traditional modelling approach against the 'Switchable' glazing approach, as described in the proposed work flow approach (Section 3). In one case, blind components were added to the model in the traditional way (Method A); In the other case (Method B), the effect of the blind was simulated by using a fictional 'Switchable' glazing construction with a g-value varying between g_{glass} (i.e. blind raised) and g_{tot} (i.e. blind lowered). Both cases assumed blinds to be deployed (or glass properties to be switched) in case of incident radiation > 350KW/m². The model consisted of a single thermal zone, 6m wide, 9m deep and 4.1m high. The façade comprises 3m high double glazing and an opaque spandrel panel at the top of 1.1m height. Glass properties are according to reference glazing C (refer to Table 3). Glass framing is assumed to cover 5% of the total glazing area. Spandrel panel U-value is assumed at 0.5 W/m²K. Adiabatic properties are attributed to all faces of the box except for the externally exposed façade surface.

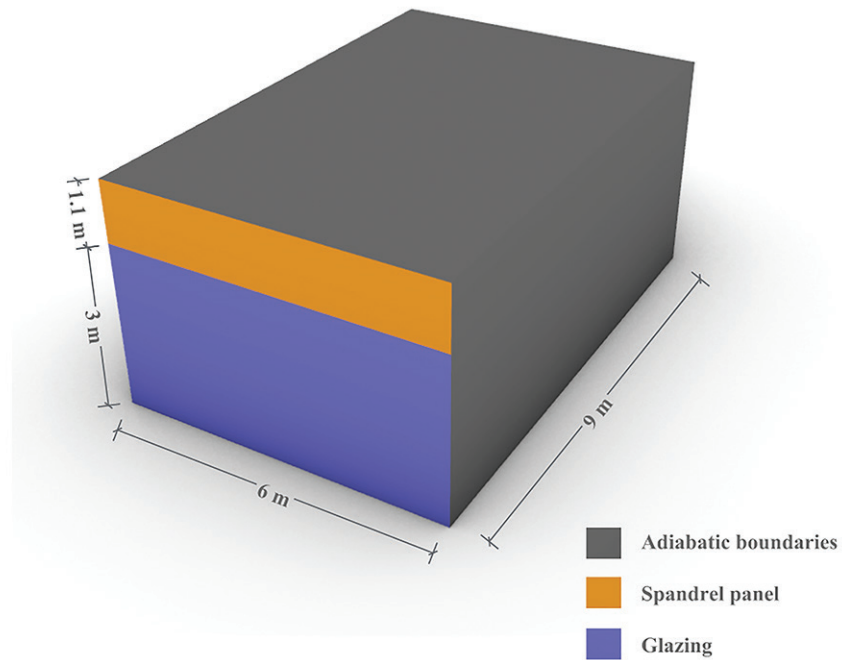


FIG. 6 Shoebox model

The energy model is run for a South orientated façade using IWEC EPW weather file 037760, which represents a typical year at London Gatwick airport based on measured climate data. Cooling loads are calculated as ideal air loads with fixed ventilation. The modelling parameters of the shoe box simulation are based on guidance for typical office space conditions, such as CIBSE Guide A. The assumptions are given below.

PARAMETER	VALUE	SCHEDULE
Cooling setpoint	24°C	Monday to Friday 8am to 6pm
Façade air infiltration	0.15 ACH	Constant
Mechanical ventilation	10 L/s per person	Monday to Friday 7am to 7pm
Occupant density	0.1 m ² per person	Monday to Friday 7am to 7pm

TABLE 5 Energy model assumptions

The analysis is performed for white and charcoal blind colours with properties as per Table 1. The g_{tot} value that represents the closed state of the switchable glazing is calculated with WINDOW 7.7:

STATE	g_{tot}
Open (or light) state	0.59
Closed (or dark) state - white blind	0.28
Closed (or dark) state - charcoal blind	0.51

TABLE 6 Switchable glazing inputs

Cooling loads are extracted and compared for a summer period starting from 15th May and up until 15th September.

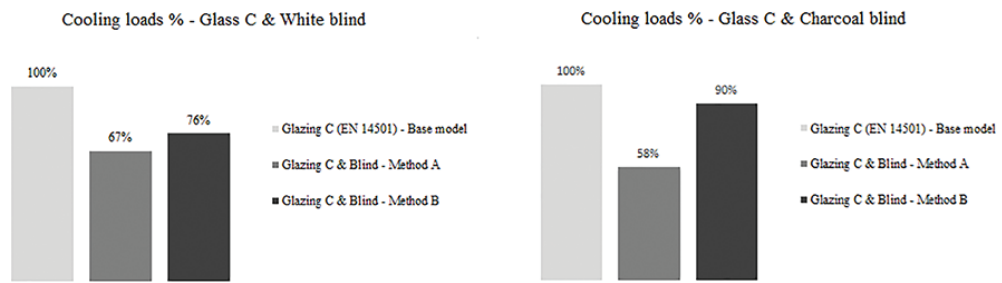


FIG. 7 Summer cooling load according to Methods A & B

Results from Method A calculations show greater cooling load reductions being achieved by both the blind types compared to Method B. Additionally, it is noted that simulations carried out based on Method A show a greater cooling load reduction for the charcoal blind compared to the white blind, despite a higher g_{tot} value (0.51 vs 0.28). On the other hand, results from Method B show a greater cooling load reduction offered by the white blind compared to the charcoal blind (24% vs 10%, respectively), which appears consistent with the difference in the g_{tot} values of the two blind types analysed.

EnergyPlus accounts for inter-reflections between the interior shades and the glass (EnergyPlus, 2015), a fact which explains the difference in results observed between Methods A and B for the white blind. However, when looking at the inward flowing portion of the short-wave radiation that is absorbed by the blind, EnergyPlus assumes that all absorbed energy by the blind immediately flows inside the room through a convection mechanism (Winkelmann, 2001). Hence there might be no portion of the absorbed radiation that is re-radiated from the blind as longwave radiation. This potentially shows a weakness of Method A to capture the inward flowing heat distribution inside the room and could explain the reason the charcoal blind shows greater cooling load reduction compared with the white blind.

Limitations have been identified with the traditional method (Method A) to capture the effect of internal blinds on the cooling loads, particularly for highly absorbent elements. On the other hand, the 'Switchable' glazing method (Method B) yields more consistent results that could be used both for preliminary shoebox modelling studies as well as MEP whole building energy calculations.

4.3 CONCLUSIONS AND FUTURE OUTLOOKS

Internal shading systems are identified as an opportunity to bring additional performance from an already available "simple" resource that often forms part of the building envelope but is not designed/specified to contribute to its efficiency. The findings of this study showed a number of limitations to the approach to internal blinds modelling within traditional whole building energy modelling tools, which might risk not allow designers the flexibility to explore comprehensive, high-performance design solutions.

Further work will have to be considered to: Carry out detailed methodology validation tests; Conduct physical testing on internal shading systems to reduce performance simulation gap; Refine the building energy modelling coordination process; Investigate ways of implementing glare reduction parameters and detailed operational controls; Carry out comparative assessments against complex solar control façade solutions (e.g. CCF) considering performance, embodied carbon and cost. Further collaboration by Façade, Sustainability and MEP engineers, as well as software developers and product manufacturers, should be pursued in a jointed effort towards increasingly holistic building skin design solutions that use the available resources and technologies responsibly and effectively,

believed to lead the industry to develop further system technologies towards a competitive market, encouraging investors to consider their integration within the project base façade specification.

References

- Kohler, C., Shukla, Y., & Rawal, R. (2017). Calculating the effect of external shading on the solar heat gain coefficient of windows. Proceedings of Building Simulation 2017.
- Klems, J H., & Kelley, G O. (1995). Calorimetric measurements of inward-flowing fraction for complex glazing and shading systems. United States.
- Yunyang, Y., Peng, X., Jiachen, M., & Ying, J. (2015). Experimental study on the effectiveness of internal shading devices. Energy and Buildings, 111, pp.154–163
- Winkelmann, F C. (2001). Modelling Windows in EnergyPlus. Proceedings of IBPSA, Building Simulation 2001, Riode Janeiro.
- British Standard. (2005). Blinds and shutters - Thermal and visual comfort - Performance characteristics and classification. (BS EN Standard No. 14501:2005)
- British Standard. (2017). Energy performance of buildings - Thermal, solar and daylight properties of building components and elements. Part 1: Simplified calculation method of the solar and daylight characteristics for solar protection devices combined with glazing. (BS EN Standard No. 52022-1:2017)
- British Standard. (2017). Energy performance of buildings - Thermal, solar and daylight properties of building components and elements. Part 3: Detailed calculation method of the solar and daylight characteristics for solar protection devices combined with glazing. (BS EN Standard No. 52022-3:2017)
- International Organization for Standardization. (2003). Thermal performance of windows, doors and shading devices - Detailed calculations. (ISO Standard No. 15099:2003)
- Chartered Institution of Building Services Engineers. (2015). CIBSE Guide A: Environmental design.
- EnergyPlus™ Documentation. (2015). Engineering Reference The Reference to EnergyPlus Calculations.

Photovoltaic Warm Façades with Phase Change Materials in European Climates



Christian Popp^{*1}, Dirk Weiß², Katja Tribulowski², Bernhard Weller¹

* Corresponding author

1 Technische Universität Dresden, Institute of Building Construction, Dresden, Germany, christian.popp1@tu-dresden.de

2 Technische Universität Dresden, Institute of Building Climatology, Dresden, Germany

Abstract

Since façade-integrated photovoltaic (PV) modules heat up strong, which reduces the efficiency of the PV, façade panels with PV and phase change materials (PCM) were developed. PCMs absorb a significant amount of thermal energy during the phase transition from solid to liquid, while maintaining a specific melting temperature. This cools down the PV and increases the electrical yield. Numerical studies on PV-PCM warm façades without rear-ventilation have been missing so far. Therefore, a thermal and an electrical simulation model for PV-PCM warm façades were developed and validated. They were then used to analyse the yield increase of two PCM-types and -quantities in PV warm façades facing east, south and west in Athens, Potsdam and Helsinki. An annual yield increase of 1.2% to 8.5% for mono-crystalline PV modules was determined. The maximum monthly yield increase is 8.0% in Helsinki, 11.4% in Potsdam and 11.3% in Athens. The study shows that a case-specific selection of the appropriate type and quantity of PCM is necessary. Using the models, a design tool for PV-PCM warm façades will be developed. It will be validated with real monitoring data from PV-PCM façade test rigs at the Technische Universität Dresden and the National Technical University of Athens.

Keywords

Building-integrated photovoltaics, efficiency increase, phase change materials, thermal simulation, yield simulation

DOI 10.7480/jfde.2021.1.5513

Design of Moveable Façade Elements for Energy Harvesting and Vibration Control of Super Slender Tall Buildings under Wind Excitation

Yangwen Zhang¹, Thomas Schauer², Laurenz Wernicke², Apostolos Vrontos², Michael Engelmann³, Wulf Wulff¹, Achim Bleicher¹

- 1 Brandenburg University of Technology, Chair of Hybrid Structures - Structural Concrete, 03046 Cottbus, Germany, (e-mail: bleicher@b-tu.de)
- 2 Technische Universität Berlin, Control Systems Group, 10587 Berlin, Germany, (e-mail: schauer@control.tu-berlin.de)
- 3 Josef Gartner GmbH, 89423 Gundelfingen, Germany, (e-mail: m.engelmann@permasteelisagroup.com)

Abstract

Tall buildings are increasingly built worldwide due to significant economic benefits in dense urban land use. But super-slender tall buildings are very susceptible to wind excitation. Tuned Mass Damper (TMD) and distributed-Multiple Tuned Mass Damper (d-MTMD) have been widely investigated passively and actively and proven to be efficient solutions to mitigate the structure vibration. However, they both need additional mass and huge installation space near the top of the building. In this contribution, a new semi-active distributed-Multiple Tuned Façade Damper (d-MTFD) is investigated that employs the mass of the outer skin of a Double-Skin Façade (DSF) as damping mass. The outer skin of DSF at the upper storeys of the building are parallel moveable to the inner skin fixed on the primary structure. A design criterion besides the damping of the primary structure vibration is that the relative displacement of the outer skin with respect to the inner skin fixed on the primary structure should not be too large. Otherwise, it makes the occupants feel uncomfortable and imposes too high constructional demands. Therefore, on-off ground-hook control is investigated, where the two control objectives are optimized using genetic algorithms. One control objective is to minimize the peak top floor acceleration, and the other control objective is to reduce the maximum peak relative displacement of all the moveable outer skins. This multi-objective optimization results in a Pareto Front, which allows choosing controller settings that yield a good trade-off between both objectives. The approach has been first validated in a simulation with a 306 m benchmark building for a wind speed of 13,5 m/s at 10 m above ground level with a return period of 10 years. Acceptable peak top floor accelerations for hotel usage and a maximal displacement between the primary structure and the moveable outer skin less than ± 0.5 m could be achieved despite the presence of rolling friction. The variable damping coefficients for the on-off ground-hook control can be realized by means of a stepper motor in each moveable DSF element which acts as a generator using customized power electronics for energy harvesting. An open research question is if the harvested energy will be sufficient for enabling a self-sustainable operation of the embedded control system and power electronics. Further validations will be carried out in Hardware-in-the-Loop (HiL) simulations in which a currently built prototype of one moveable DSF element will be physically connected to the simulation of the benchmark building.

Keywords

Moveable façade, double-skin façade (DSF), energy harvesting, wind-induced vibration, semi-active vibration control, super-slender tall building, distributed-Multiple Tuned Façade Damper (d-MTFD), multi-objective optimization, Genetic Algorithm (GA), ground-hook control

1 INTRODUCTION

With our limited ground space and always increasing population in big cities, high-rise buildings give us a solution, which can provide more living space on a fixed amount of land. More and more super-slender tall buildings have been built around the world. Slender structures are very susceptible to dynamic wind excitation. Different methods have been proposed to mitigate the wind-induced motion, see e.g. (Altay, Annika, & Klinkel, 2017), (Jafari & Alipour, 2020). Tuned Liquid Damper (TLD) and Liquid Tuned Mass Damper (TMD) have been proven to be very effective for reducing structural vibrations. However, large additional mass and huge installation space are required. A new concept using fully active vibration control without any additional mass is investigated by the research group from the University of Stuttgart (Weidner, Steffen, & Sobek, 2019). Wind loads can be compensated by parallel actuation of actuator-incorporated columns, thus reducing the overall wind-induced structural deflection. This concept is quite suitable for lightweight structures, but continuous operating energy supply for the actuators is needed for vibration control. In this paper, the existing mass of Double-Skin Façade (DSF) is used as damping mass instead of the additional mass for traditional TMD, and semi-active control is implemented to reduce not only the structural vibration but also the façade vibration. The energy harvesting technique is used to convert the vibrational energy to electrical energy as the power source for semi-active control.

The DSF is an efficient solution for tall buildings, which allows for natural ventilation and natural lightening. By using DSF, air-conditioning energy usage can be significantly reduced (Oldfield, Trabucco, & Wood, 2009). DSF reduce also the additional heating requirement in winter and cooling requirement in summer largely (Weller, Fahrion, Horn, & Pfuhl, 2014). The advantage of energy saving has been greatly explored. Its structural potential also has been studied for the use of vibration control. Kareem first proposed an approach of using moveable building claddings to isolate dynamic wind loads from the structural system, which is similar to the concept of base isolation for buildings under earthquake excitation (Kareem, 1994). Moon further developed this approach by using DSF (Moon, 2009) and the TMD/DSF damping (DSFD) interaction system (Moon, 2016). We also investigated the energy harvesting potential of this approach (Zhang, Schauer, & Bleicher, 2019). In Moon's approach, wind loads act on the moveable façade and are transferred to the primary structure via springs and dampers. However, if the moveable façades are perpendicularly connected and the system is under seismic load, the seismic loads will act directly on the primary structure and be transferred to the moveable façades. This system is called d-MTMD, where the moveable façade mass functions as damping mass. For d-MTMD under seismic excitation, the tuning of the connection is different from that of the façade isolation. Many studies have been carried out to investigate and optimize the vibration mitigation performance of d-MTMD with perpendicularly moveable façades (Barone, Palmeri, & Khetawat, 2015), (Fu & Zhang, 2016), (Pipitone, Barone, & Palmeri, 2018).

Distributed-Multiple Tuned Façade Damping System (d-MTFD) with innovative parallel moveable connections is proposed by (Zhang, Schauer, Wernicke, Wulff, & Bleicher, 2020), and its performance for reducing wind-induced oscillation has been intensively studied. Using parallel connection, the façade is fixed in the direction perpendicular to the primary structure but moveable in the direction parallel to the primary structure. The wind-induced structure vibration causes the parallel moveable façades to vibrate, which in turn damp the structure motion. Therefore, a d-MTFD system under wind excitation behaves like a d-MTMD system under seismic excitation (Rahmani & Könke, 2019). By Moon's approach using a perpendicular connection, the moveable DSF's outer skin begins to oscillate first; then the oscillation transmits to the primary structure, so making the transmission as small as possible is the design objective. The difference between parallel and perpendicular connection of DSFs is illustrated in Fig. 1. The treatment of the corner is also conceptually presented.

In the approach of parallel connection, the movement of the outer skin is covered at the corners, as shown in Fig. 1.

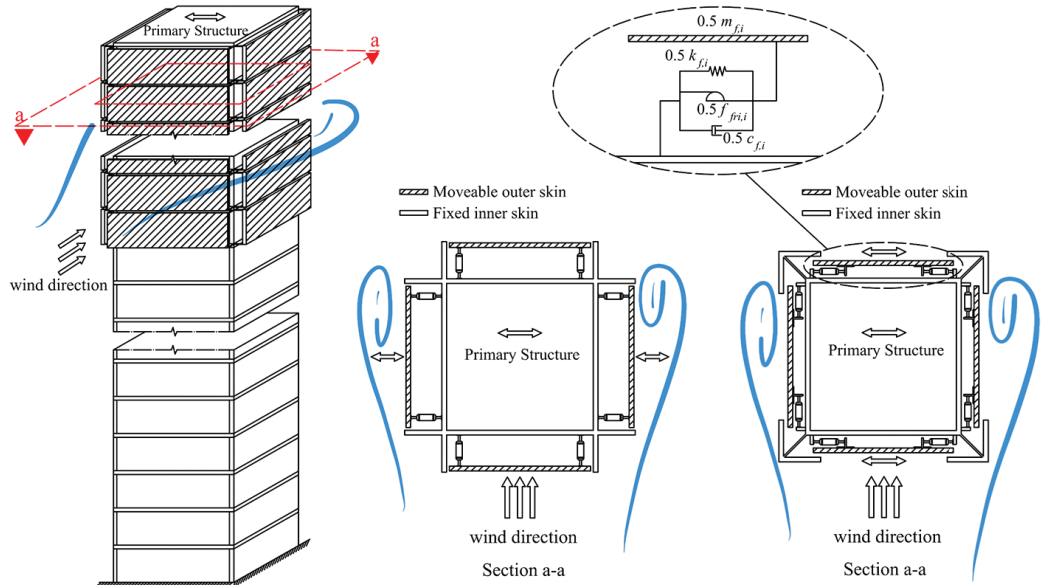


FIG. 1 Concept of the moveable DSF using a perpendicular connection (left section) and a parallel connection (right section)

In this paper, the proposed d-MTFD system with parallel moveable connections is further developed and investigated. To realize that the façade's outer skin is parallel moveable, it is mounted on a guide rail system which brings primarily rolling friction to the system. The sliding friction can be neglected compared with the rolling friction. So, the inevitable rolling friction $f_{fri,i}$ between the moveable façade's outer skin and fixed inner skin is considered in this paper, as shown in Fig. 1. With consideration of the rolling friction, the d-MTFD system is further optimized with multi-objective Genetic Algorithms (GA) based on two defined optimization objectives: reducing the peak top floor acceleration and controlling the maximum peak relative displacement of all the moveable outer skins (cf. Section 3). On-off ground-hook control is implemented as one form of semi-active control. The variable damping coefficients for the on-off ground-hook control can be realized by means of stepper motors which act as generators using customized power electronics for energy harvesting. Its energy harvesting potential is estimated by a moveable façade element equipped with a stepper motor and electronic system at the top floor of the building. The investigation of this system is based on a wind direction perpendicular to the front of the building, which only activates the moveable façade element on the windward and leeward sides of the building. When the wind blows at different angles towards the building, it can be decomposed to be perpendicular to the building façade in two directions, which activates all the moveable façade elements. However, investigation in one direction is sufficient for the focus of our research questions.

2 SYSTEM MODELLING

As shown in Fig. 1, the weight of the parallel moveable DSF's outer skins on each side of different storeys is $0.5 m_{fi,i}$, and the connection is modelled by introducing the façade connection stiffness $0.5 k_{fi,i}$, the façade connection damping coefficient $0.5 c_{fi,i}$ and the rolling friction $0.5 f_{fri,i}$, where the subscript i is used to distinguish different storeys installed with moveable DSF's outer skin. Therefore, the outer skin weight at different storeys is $m_{fi,i}$, and the connection is modelled as $k_{fi,i}$, $c_{fi,i}$ and $f_{fri,i}$, where $i=1,2,\dots,n_f$. The upper n_f storeys are installed with the parallel moveable outer skin. Fig.

2 illustrates the model of a n storey high building with its upper n_f storeys using parallel moveable outer skin. m_1, m_2, \dots, m_n are the weights of the building storeys and $f_{w,1}, f_{w,2}, \dots, f_{w,n}$ are the across-wind loads due to vortex shedding. x_i ($i=1,2,\dots,n$) and $x_{f,i}$ ($i=1,2,\dots,n_f$) indicates respectively the absolute structural displacement of different storeys and absolute façade displacement of the upper n_f storeys. The model equations given in (Zhang, Schauer, Wernicke, Wulff, & Bleicher, 2020) have been extended by considering the rolling friction.

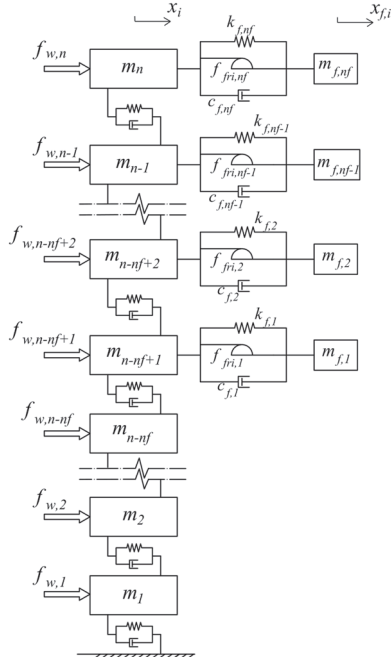


FIG. 2 d-MTFD system modelling with rolling friction

A Coulomb friction model is assumed for the rolling friction, which can be written in the form of Eq. (1) as follows:

$$\begin{cases} f_{fr,i} = -\text{sgn}(\dot{x}_{fr,i})\mu_r N & (i = 1, 2, \dots, n_f) \\ \dot{x}_{fr,i} = \dot{x}_{f,i} - \dot{x}_{n-n_f+i} \end{cases} \quad (1),$$

where μ_r is the coefficient of rolling friction and $N = m_i g$ is the normal contact force. In the rolling case, Coulomb's law only considers the direction of the relative velocity of the façade at each floor $x_{fr,i}$, not its magnitude. The rolling friction is opposite the direction of the relative velocity $x_{fr,i}$. Modal reduction (Zhang, Schauer, Wernicke, Wulff, & Bleicher, 2020) is carried out to reduce the model complexity, which speeds up the optimization of the system introduced in the next section. Wind loads only excite the lower modes, mainly the first mode, because of the phenomenon of lock-in in vortex-induced vibration. Therefore, cutting off the higher modes in modal space can save a lot of simulation time without much loss in the results' accuracy.

3 MULTI-OBJECTIVE GA OPTIMIZED SEMI-ACTIVE CONTROL

The d-MTFD system is optimized using a multi-objective Genetic Algorithm (GA). GA is based on the biological principle of optimization through natural selection. This method relies on genetic operations such as elitism, replication, crossover, and mutation. In GA, a population consisting

of many system solutions with different parameter values compete to minimize the defined fitness functions (two defined objectives), and the successful parameter values are propagated to the next generations through a set of genetic rules. For multi-objective optimization, there is a trade-off between the defined objectives. Therefore, a Pareto Front will be generated, which plots all non-inferior results. The multi-objective GA optimization is integrated into the optimization toolbox of MATLAB.

Two objectives are defined in the fitness function to optimize the d-MTFD system. The first objective is to minimize the peak top floor acceleration, i.e. $\min(\|\ddot{x}_n\|_\infty)$, which is an important design criterion for high-rise building to ensure its serviceability under strong wind excitation. The limits for the perceptible acceleration based on different use of the building can be found in (Sarkisian, 2016). For a ten year return wind period, the limited acceleration for the use of an apartment is 0.118-0.147 m/s²; for a hotel, it is 0.147-0.196 m/s²; and for an office, it is 0.196-0.245 m/s². The second objective is to minimize the peak relative displacement of moveable façades and primary structure at the upper n_f storeys, i.e. $\min(\|x_{t,1}, x_{t,2}, \dots, x_{t,n_f}\|^T \|_\infty)$. There are still no regulations for the limitation of the required parallel movement of the movable outer skin. However, out of consideration of construction difficulty and the comfort of the occupants, it is desirable to keep the façade parallel movement as small as possible. As a remark, design codes like ETAG 002, DIN 18008 and EN 13830 need to be considered for the detailed design of the façade elements. These further structural-physical requirements must be further ensured but are not the focus of the current research.

The optimization parameters for the semi-active d-MTFD system need to be defined before running the algorithm. In a semi-active d-MTFD system, the parameters, which can be optimized, are the constant stiffness coefficients $k_{t,i}$, the varying damping coefficients $c_{t,i}$ of the connections and the number n_f of upper storeys that are equipped with parallel moveable façade. The rolling friction $f_{t,i}$ is related to the rolling friction coefficient μ_r , which depends on the material of the contact surface and the radius of the roller. In this paper, the system is investigated by considering $\mu_r = 0$, and reasonable values $\mu_r = 0.005$ and $\mu_r = 0.01$. As the wind load excite primary the first mode of the system, the entire façade connections can be tuned to the first natural frequency of the primary structure. Hence, the stiffness coefficients at all the storeys can be calculated as:

$$k_{f,i} = m_{f,i} \cdot \omega_1^2 \quad (i = 1, 2, \dots, n_f) \quad (2),$$

in which ω_1 is the first natural angular frequency of the primary structure and $m_{t,i}$ is the moveable DSF outer skin mass at storey i , which can be estimated by its area $A_{t,i}$ (both sides) and area density ρ_A .

Ground-hook semi-active control is implemented by using a stepper motor as a variable damper. The ground-hook control is altered from the original skyhook control. Skyhook control is developed to reduce the vibration of the so-called sprung mass, i.e. the damping mass. Therefore, skyhook control can be implied to reduce the response of vehicles, but it is not suitable for motion control of high-rise buildings. The ground-hook control is thus developed which aims to reduce the vibration of the so-called unsprung mass, i.e. the building structure (Demetriou, Nikitas, & Tsavdaridis, 2016). For a simple TMD system, ground-hook control has been applied to reduce the structural response (Koo, Ahmadian, Setareh, & Murray, 2004). In this paper, Velocity Based Ground-hook (VBG) control is implied in the d-TMFD system. The on-off VBG control logic can be summarized in the following equations:

$$\begin{aligned} &\text{if } \dot{x}_{n-n_f+i} \cdot \dot{x}_{f_r,i} \geq 0, \text{ then } c_{f,i} = c_{low,i} \\ &\text{if } \dot{x}_{n-n_f+i} \cdot \dot{x}_{f_r,i} < 0, \text{ then } c_{f,i} = c_{high,i} \end{aligned} \quad (3)$$

The corresponding on-off façade damping coefficients can be calculated as:

$$c_{f,i} = \begin{cases} c_{low,i} = 2\xi_{low,i}\sqrt{m_{f,i}k_{f,i}} & \text{off state} \\ c_{high,i} = 2\xi_{high,i}\sqrt{m_{f,i}k_{f,i}} & \text{on state} \end{cases} \quad i = (1, 2, \dots, n_f) \quad (4)$$

The on-off damping ratio $\xi_{low,1}$ and $\xi_{high,1}$ at the lowest floor, the on-off damping ratio ξ_{low,n_f} and ξ_{high,n_f} at the highest floor and the on-off damping ratios of three evenly distributed floors in between are selected as the optimization parameters of GA. The searching scope of the damping ratio is set up based on the reference optimum damping ratio ξ_{ref} of a single TMD system (Den Hartog, 1985). The upper and lower boundary of the searching scope also considers whether the damping coefficients can be practically achieved by stepper motors later. Piecewise linear interpolation is used respectively to determine the on-off damping ratios of floors between the selected optimized damping ratio. The upper n_f floors installed with moveable façade is also used as a parameter. There is a total of eleven optimization parameters in the GA, as shown in Fig. 3.

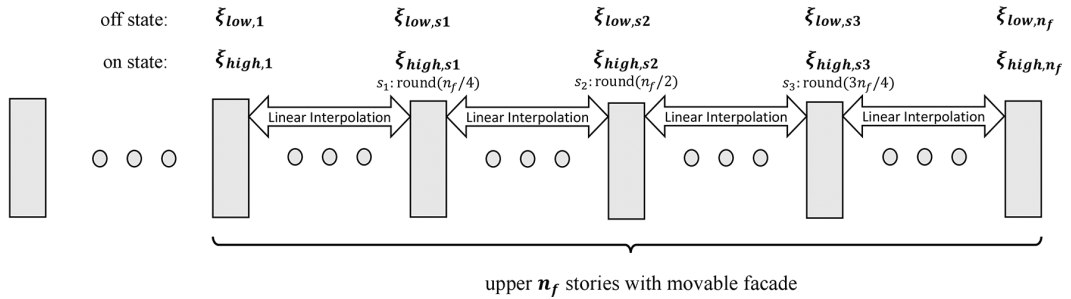


FIG. 3 Optimization parameters of semi-active d-MTFD system

4 RESULTS FOR BENCHMARK BUILDING

In this paper, the model of a 76-storey 306m high benchmark building with an aspect ratio of 7.3 is installed with the parallel moveable façades in the upper storeys for analysis. Yang et al. described all the details and the mathematical model of this benchmark building (Yang, Agrawal, Samali, & Wu, 2004). The first five natural frequencies of this building are 0.160, 0.765, 1.992, 3.790 and 6.395 Hz. The structure damping ratio has been taken from the benchmark building using Rayleigh's approach and is 0.01 for the first five modes. Its slenderness makes the building sensitive to wind excitation. The across-wind loads acting on this benchmark building are measured from the wind tunnel test based on a scaled model (Samali, Kwok, Wood, & Yang, 2004). The referenced mean wind velocity of 13.5m/s at 10 m above ground level with a return period of 10 years represents the serviceability level winds at which occupant's comfort is an important design criterion.

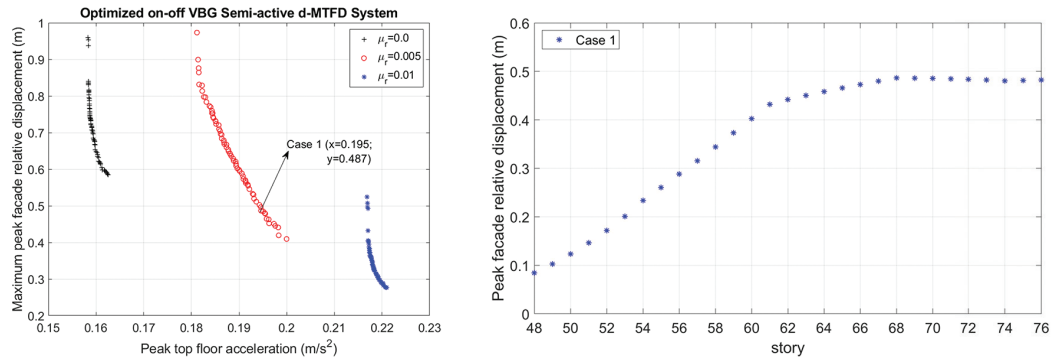


FIG. 4 Pareto Front of multi-objective GA optimized on-off VBG semi-active d-MTFD system with different rolling friction coefficient (left); Peak façade relative displacement at different storeys for Case 1 (right)

The upper n_f storeys of this benchmark model are installed with the parallel moveable DSF. The searching scope of n_f is set between 5 and 30. The weight of 50 moveable DSF's outer skin elements (25 elements coupled on each side) of each storey is 30 t, calculated in Section 5. As all these connections at upper n_f storeys are tuned to the structure's first natural frequency $\omega_1=0.16$, all the stiffness coefficient can be calculated based on the Eq. (2). The reference façade damping ratio ξ_{ref} can be calculated as 0.055 when the upper 30 storeys are installed with d-MTFD system. The searching scope of all the selected damping ratio to be optimized is set between 0.004 and 0.15. The population size of the GA is set to 150 and then evolved for 50 generations. The optimized results of a semi-active d-MTFD system with a rolling friction ratio of 0.0, 0.005 and 0.01 are presented in the Pareto Front, as shown in Fig. 4 (left). As observed from the plotted Pareto Front, a trade-off between these two objectives always exists. The inevitable rolling friction has a big influence on this system. A large rolling friction coefficient can result in a weakened function of reducing peak floor acceleration.

Case 1 with the rolling friction ration of 0.005 is chosen for further analysis, as shown in Fig. 4 (left). There are no regulations for the movable outer skin about the maximum allowable parallel movement. ± 0.5 m maximum façade displacement is selected as the limitation. Case 1 has satisfied this limitation. The peak façade relative displacement at different storeys of Case 1 is plotted in Fig. 4 (right). Due to the existence of the rolling friction, the moveable façades at lower storeys have difficulties to overcome the friction. Therefore, the lower storeys have a smaller contribution to damp the structural motion. By adding the upper n_f storeys with moveable parameter as an optimization parameter, non-functional or less functional lower storeys can be automatically deleted during the optimization. In the optimized Case 1 with $n_f=29$, the peak façade relative displacements at upper storeys are optimized to almost the same value, proving that using piecewise linear interpolation is reasonable.

The uncontrolled benchmark building with a fixed façade under the same wind excitation is compared to Case 1. The (1) peak top floor displacement $\|x_{76}\|_{\infty}$, (2) Root Mean Square (RMS) value of top floor displacement x_{76}^{rms} , (3) peak top floor acceleration $\|\ddot{x}_{76}\|_{\infty}$ (4) RMS value of top floor acceleration \ddot{x}_{76}^{rms} , (5) peak top floor façade relative displacement $\|x_{fr,rf}\|_{\infty}$, and (6) RMS value of top floor façade relative displacement $x_{fr,rf}^{rms}$ are listed in Table 1.

SYSTEM	FIXED FAÇADE	VBG (CASE 1)
$\ x_{76}\ _{\infty}$ (m)	0.346	0.321 (-7.23%)
x_{76}^{rms} (m)	0.116	0.087 (-25.00%)

>>>

$\ \ddot{\mathbf{x}}_{76}\ _{\infty}$ (m/s ²)	0.269	0.195 (-27.51%)
$\ddot{\mathbf{x}}_{76}^{rms}$ (m/s ²)	0.104	0.068 (-34.62%)
$\ x_{H,n}\ _{\infty}$ (m)	/	0.483
$x_{H,n}^{rms}$ (m)	/	0.139

TABLE 1 Comparison of structure with Fixed façade and VBG (Case 1)

As shown in Table 1, compared with the uncontrolled structure with fixed façade, Case 1 has better vibration damping performance. For top floor displacement and acceleration, the reduction percentage compared with the structure with fixed façade are also listed in Table 1. For the top floor displacement, the design requirement $h/500$ ($h = 306$ m is the height of the building) is easy to meet even without an extra damping system. Therefore, the top floor displacement is not chosen as an optimization objective. The top floor acceleration becomes more dominant in the design of tall buildings under wind excitation. The structure with a fixed façade does not meet the design requirement; with VBG semi-active control, Case 1 is on the edge of the design limit as a hotel.

To estimate whether autonomous operation of the semi-active control is possible, the average dissipated power in the damper units (stepper motors) for the entire building is calculated based on Eq. (5):

$$P_{diss} = \frac{\sum_{i=1}^{n_f} \int_0^T c_{f,i} \dot{x}_{fr,i}^2 dt}{T} \quad (5),$$

where T is the total simulation time of 10 minutes. For the selected Case 1, the average dissipated power is 1.09 kW with consideration of rolling friction. About 40% of the dissipated power can be estimated to be harvested with consideration of the energy harvesting circuit consumption, copper loss and parasitic damping loss (Shen, Zhu, Xu, & Zhu, 2018). Therefore, the average harvested power is estimated at 0.436 kW. An open research question is if this limited energy output will be sufficient for enabling a self-sustainable operation of the embedded control system and power electronics.

5 MOVEABLE DOUBLE-SKIN FAÇADE ELEMENT AND DEVELOPMENT OF A PROTOTYPE

After different possible methods of integrating all the mechatronic components in a moveable double-skin façade element have been investigated, the preferred solution is proposed and developed together with Josef Gartner GmbH. The detailed section is shown in Fig. 5. The fixed inner skin of the proposed system, which is made of an aluminium unitized element, is mounted to the floor ceiling. The movable outer skin is connected to the fixed inner skin using smooth-running guide rails at the top and bottom. The damper unit, which means the stepper motor with corresponding control and energy harvesting circuit, and the blind are in the cavity and mounted to the fixed inner skin. The moveable double-skin façade element is to be completely pre-assembled in the factory and then mounted as a unit.

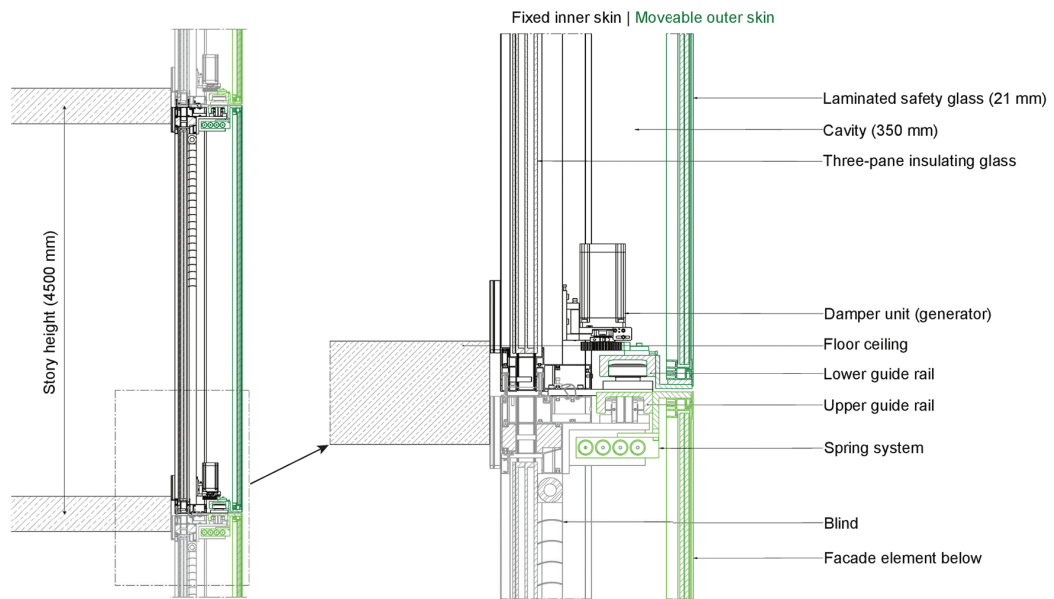


FIG. 5 Details of the proposed moveable double-skin façade element

Based on this proposed solution, a prototype is developed to test the d-MTFD system. A rendering of the current prototype is shown in Fig. 6. In the benchmark building, the height of the DSF element at the top floor is 4.5 m. However, considering the possibility of transport and installation in the lab at BTU Cottbus - Senftenberg, a façade element with a height of 2.8 m and a width of 2.6 m was designed, which corresponds to a 4.5 m × 1.6 m same area sized façade element at the top floor of the benchmark building. If the corners of the benchmark building are not cut, each side of the benchmark building is 42 m long. This results in 25 elements with a width of 1.6 m on each side and 50 elements in total on each storey. The total length of the moveable façade elements at one side is then 40m leaving 1m space at each corner of the building for the unhindered façade movement.

The weight of the moveable outer skin of the prototype, including the weight of the guide rail system, is approximately 600 kg. This 600 kg element is taken out of the building simulation as hardware-in-the-loop (HiL). On the top floor, the remaining 49 moveable façade elements are still running in the simulation. Details about HiL are given in Section 6.

The prototype consists of a base frame and a building frame, as shown in Fig. 6. The building frame can slide on the base frame through rollers with low friction. The building actuator works together with the building spring system to ensure that the motion of the building frame reproduces the motion of the top floor of the 76-storey high benchmark building under wind excitation precisely. The fixed inner skin of the DSF is mounted on the building frame, and the moveable outer skin is connected to the fixed inner skin through smooth-running lower and upper guide rails. Therefore, the outer skin is parallel moveable, and its motion is limited to ±500 mm. The damper unit, which consists of the stepper motor with corresponding power electronics, is installed in the connection to realize energy harvesting and semi-active control. The stiffness of the spring system in the connection is determined using Eq. (2), but is based on the real mass of the moveable outer skin. The stepper motor is the core element in the damper unit, which works as a generator to harvest energy and as a variable damper to realize semi-active control. The components of the damper unit for semi-active control are illustrated in Fig. 7. The relative movement of the outer skin is transmitted to the stepper motor through motion transmission and converter (rack and pinion). Through an encoder, the relative movement of the outer skin is measured. The building movement is measured by the inertial sensor. Based on the measured information from the encoder and the

inertial sensor, the ground-hook semi-active control algorithm in the embedded system can adapt the control signals of the power electronics so that the optimized, time-varying damping coefficient can be realized by the stepper motor. The force sensor in the motion transmission is only used for testing the prototype using hardware-in-the-loop simulation (cf. Section 6). A great advantage of this implemented control concept is that each façade element is an independent mechatronic vibration damper with control and sensors. No information exchange between the façade elements is required for efficient damping.

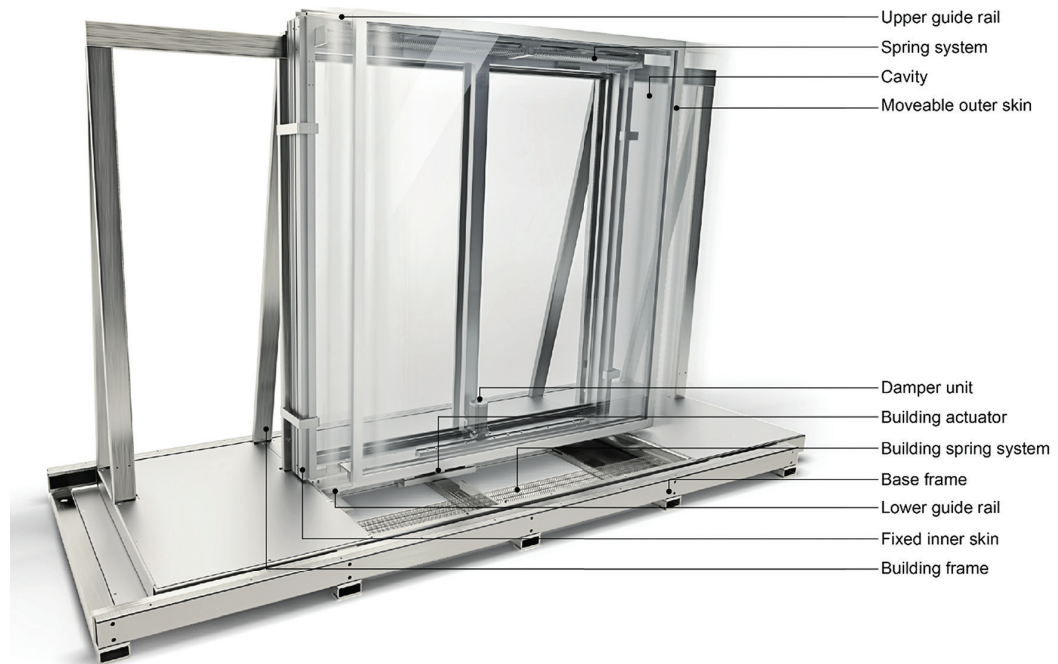


FIG. 6 Rendering of the developed prototype to test the system

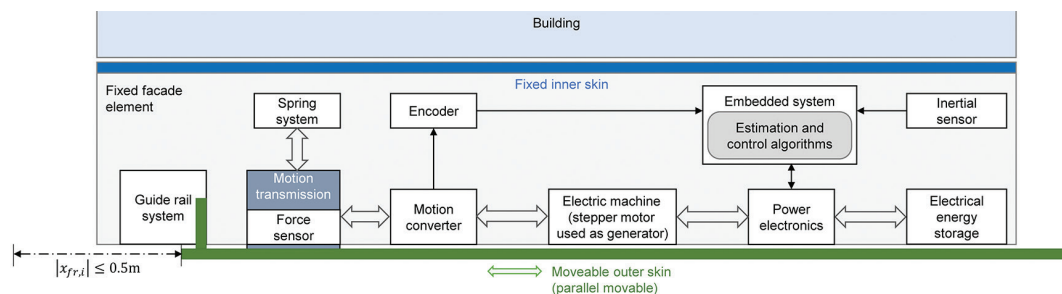


FIG. 7 Components of the damper unit

6 HARDWARE-IN-THE-LOOP CONCEPT

After production, the prototype will be tested using hardware-in-the-loop (HiL) simulations. The 76-storey high benchmark building under wind excitation will be completely simulated with one missing façade element. This missing 600 kg façade element mounted on the moving building frame will be physically presented as this prototype (i.e. hardware), as described in Section 5. The diagram

of the HiL simulation is illustrated in Fig. 8. The hardware part (prototype) in this illustration is a top view. To consider the influence of the moveable outer skin on the simulated building dynamics, the interaction force between the moveable outer skin and the fixed inner skin need to be measured using a force sensor and will be fed back to the simulation model. To make the motion of the building frame similar to the top floor motion of the benchmark building in the simulation, a linear–quadratic regulator (LQR) controller with rolling friction compensation will be used to control the building actuator.

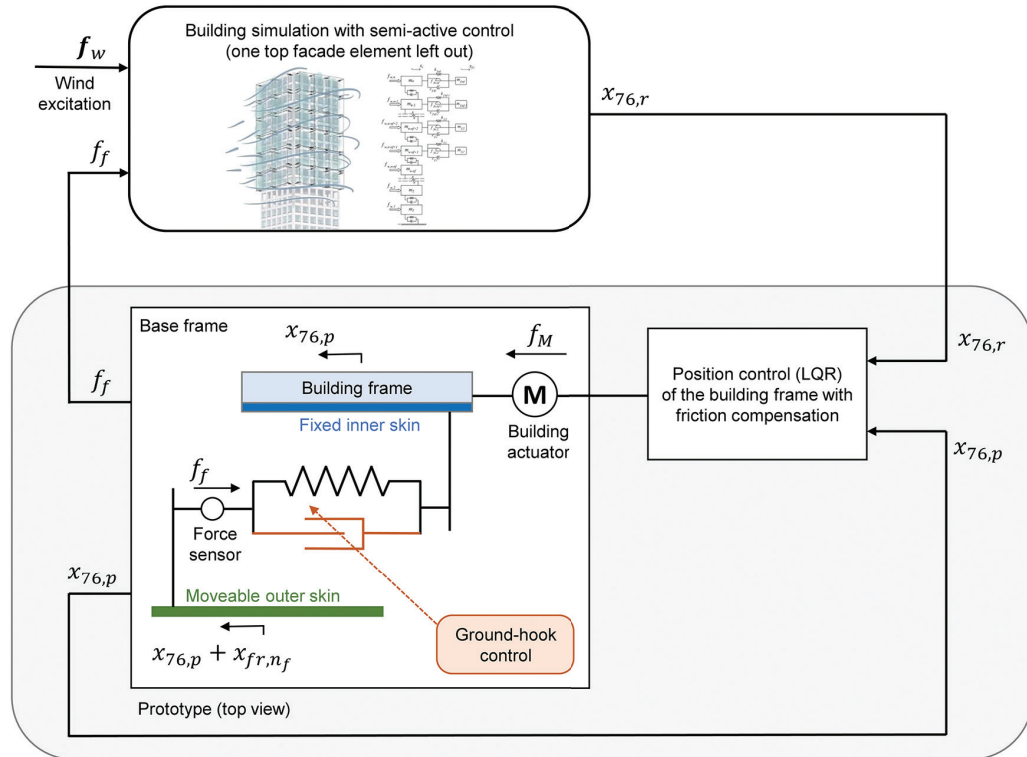


FIG. 8 Hardware in the Loop (HiL) simulation

7 DISCUSSION AND CONCLUSIONS

In this paper, the innovative d-MTFD with consideration of rolling friction is studied using optimized on-off ground-hook semi-active control. Multi-objective GA is used to find the optimum parameters to reduce the building acceleration and to reduce the maximum relative displacement of the entire parallel moveable outer skin, which ensures the serviceability of the system. By implementing the optimized VBG semi-active control, despite the presence of rolling friction, acceptable peak top floor accelerations for hotel usage and a maximal displacement between the structure and the moveable outer skin of less than ± 0.5 m can be achieved. The prototype for the d-MTFD system and the planned HiL simulation based on the built prototype are introduced. The energy harvesting performance and vibration damping performance will be validated based on the real prototype after production using HiL simulation. Autonomous semi-active control is foreseen.

Acknowledgements

This work was funded by the Graduate Research School (GRS) of the Brandenburg University of Technology Cottbus-Senftenberg with the support of the Federal State Government of Brandenburg based on the Postgraduate Scholarship Regulations (GradV) and the research initiative "Future Building" of the Federal Ministry of the Interior, Building and Community, Germany (BMI), (project number: 10.08.18.7-18.22). We also thank Therese Schmidt (Chair of Hybrid Structures - Structural Concrete, Brandenburg University of Technology) for rendering the developed prototype in Fig. 6.

References

- Altay, O., Annika, B., & Klinkel, S. (2017). Wirkung von semi-aktiven Schwingungsdämpfern bei böenerregten Zufallsschwingungen. 15. D-A-CH - Tagung 2017 Erdbebeningenieurwesen und Baudynamik. Weimar.
- Barone, G., Palmeri, A., & Khetawat, A. (2015). Passive control of building structures using double-skin façades as vibration absorbers. In Kruijs, J., Tsompanakis, Y., & Topping, B.H.V. (Hrsg.), Proceedings of the Fifteenth International Conference on Civil, Structural and Environmental Engineering Computing, (S. 94). Prague.
- Demetriou, D., Nikitas, N., & Tsavdaridis, K. D. (2016). Performance of fixed parameter control algorithms on high-rise structures equipped with semi-active tuned mass dampers. *The Structural Design of Tall and Special Buildings*, 25(7), S. 340-354.
- Den Hartog, J. P. (1985). *Mechanical vibrations*. Courier Corporation.
- Fu, T., & Zhang, R. (2016). Integrating Double-Skin Façades and Mass Dampers for Structural Safety and Energy Efficiency. *Journal of Architectural Engineering*.
- Jafari, M., & Alipour, A. (2020). Methodologies to mitigate wind-induced vibration of tall buildings: A state-of-the-art review. *Journal of Building Engineering*, 101582.
- Kareem, A. (1994). Methods to control wind-induced building motions. In *Structures Congress XII*. ASCE., S. 654-659.
- Moon, S. K. (2009). Tall Building Motion Control Using Double Skin Façades. *Journal of Architectural Engineering*.
- Moon, S. K. (2016). Integrated damping systems for tall buildings: tuned mass damper/double skin façade damping interaction system. *The Structural Design of Tall and Special Buildings*, S. 232-244.
- Oldfield, P., Trabucco, D., & Wood, A. (October 2009). Five energy generations of tall buildings: A historical analysis of energy consumption in high rise buildings. *The Journal of Architecture*, 14(5), S. 591-613. doi:10.1080/13602360903119405
- Pipitone, G., Barone, G., & Palmeri, A. (2018). Optimal design of double-skin façades as vibration absorbers. *Structural Control and Health Monitoring*.
- Rahmani, H. R., & Könke, C. (2019). Seismic control of tall buildings using distributed multiple tuned mass dampers. *Advances in Civil Engineering*.
- Samali, B., Kwok, K., Wood, G., & Yang, J. (2004). Wind tunnel tests for wind-excited benchmark building. *Journal of Engineering Mechanics*, 130(4), S. 447-450.
- Sarkisian, M. (2016). *Designing tall buildings: structure as architecture*. Routledge.
- Shen, W., Zhu, S., Xu, Y., & Zhu, H. (2018). Energy regenerative tuned mass dampers in high-rise buildings. *Structural Control and Health Monitoring*, 25(2).
- Weidner, S., Steffen, S., & Sobek, W. (2019). The integration of adaptive elements into high-rise structures. *International Journal of High-Rise Buildings*, 8(2), 95-100.
- Weller, B., Fahrion, M. S., Horn, S., & Pfuhl, A. M. (2014). Doppelfassaden im Zeichen des Klimawandels. *Bauphysik*, 36, S. 68-73. doi:10.1002/bapi.201410018
- Yang, J. N., Agrawal, A. K., Samali, B., & Wu, J. C. (2004). Benchmark problem for response control of wind-excited tall buildings. *Journal of Engineering*, 130(4), S. 437-446.
- Zhang, Y., Schauer, T., & Bleicher, A. (2019). Assessment of wind-induced vibration suppression and energy harvesting using façades. In *20th CONGRESS OF IABSE New York City 2019 - The Evolving Metropolis*. (S. 352-356).
- Zhang, Y., Schauer, T., Wernicke, L., Wulff, W., & Bleicher, A. (2020). Façade-Integrated Semi-Active Vibration Control for Wind-Excited Super-Slender Tall Buildings. *IFAC World Congress Berlin 2020*.

POWERSKIN CONFERENCE

HOSTED BY



SPONSORED BY

